SOCIO-ECOLOGY OF MICROBES IN A CHANGING OCEAN

EDITED BY: Matthias Wietz, Stanley C. Lau and Tilmann Harder
PUBLISHED IN: Frontiers in Marine Science and Frontiers in Microbiology

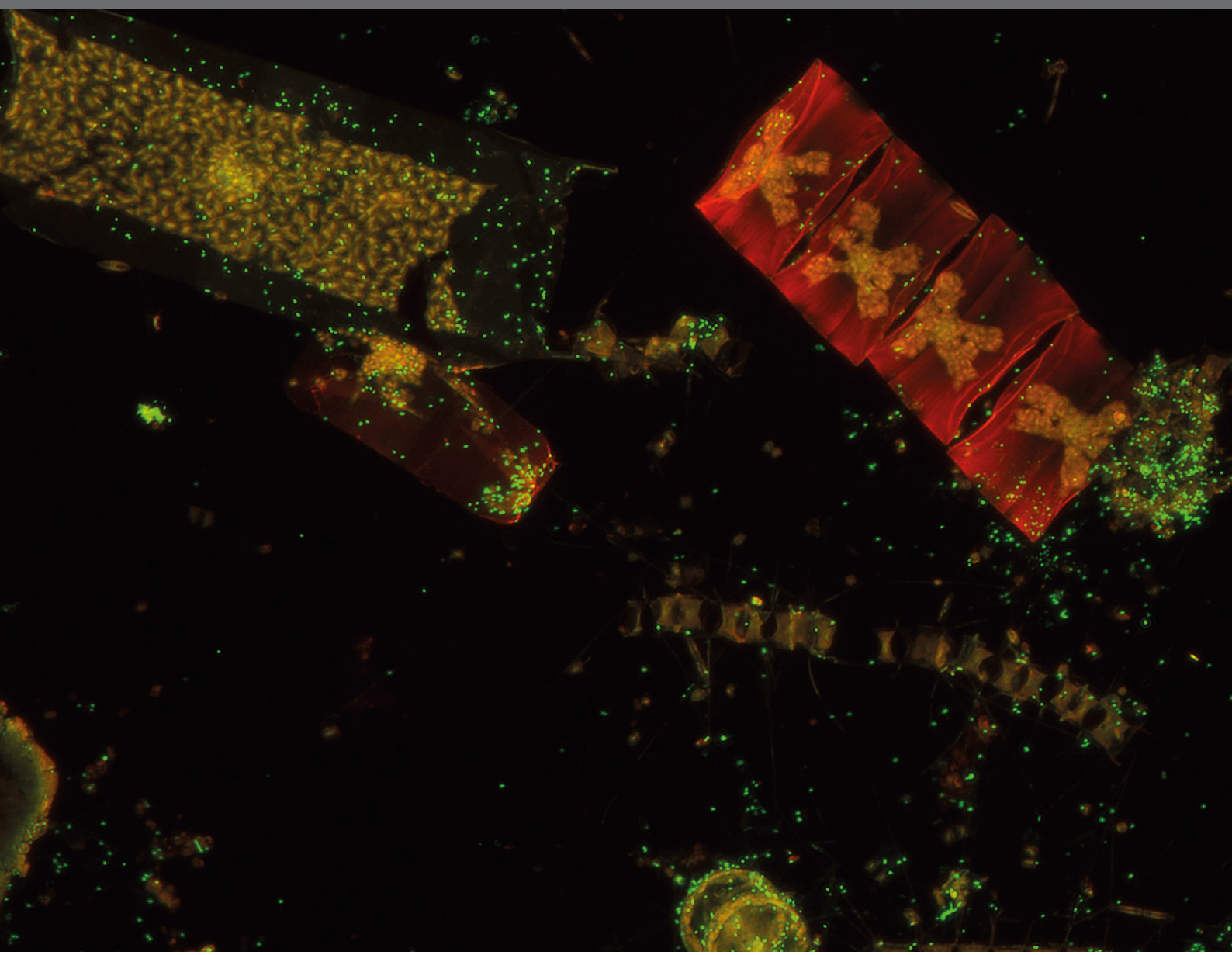

frontiers Research Topics

frontiers

ISSN 1664-8714
ISBN 978-2-88945-908-7
DOI 10.3389/978-2-88945-908-7

About Frontiers

Frontiers is more than just an open-access publisher of scholarly articles: it is a pioneering approach to the world of academia, radically improving the way scholarly research is managed. The grand vision of Frontiers is a world where all people have an equal opportunity to seek, share and generate knowledge. Frontiers provides immediate and permanent online open access to all its publications, but this alone is not enough to realize our grand goals.

Frontiers Journal Series

The Frontiers Journal Series is a multi-tier and interdisciplinary set of open-access, online journals, promising a paradigm shift from the current review, selection and dissemination processes in academic publishing. All Frontiers journals are driven by researchers for researchers; therefore, they constitute a service to the scholarly community. At the same time, the Frontiers Journal Series operates on a revolutionary invention, the tiered publishing system, initially addressing specific communities of scholars, and gradually climbing up to broader public understanding, thus serving the interests of the lay society, too.

Dedication to Quality

Each Frontiers article is a landmark of the highest quality, thanks to genuinely collaborative interactions between authors and review editors, who include some of the world's best academicians. Research must be certified by peers before entering a stream of knowledge that may eventually reach the public - and shape society; therefore, Frontiers only applies the most rigorous and unbiased reviews.
Frontiers revolutionizes research publishing by freely delivering the most outstanding research, evaluated with no bias from both the academic and social point of view. By applying the most advanced information technologies, Frontiers is catapulting scholarly publishing into a new generation.

What are Frontiers Research Topics?

Frontiers Research Topics are very popular trademarks of the Frontiers Journals Series: they are collections of at least ten articles, all centered on a particular subject. With their unique mix of varied contributions from Original Research to Review Articles, Frontiers Research Topics unify the most influential researchers, the latest key findings and historical advances in a hot research area! Find out more on how to host your own Frontiers Research Topic or contribute to one as an author by contacting the Frontiers Editorial Office: researchtopics@frontiersin.org

SOCIO-ECOLOGY OF MICROBES IN A CHANGING OCEAN

Topic Editors:
Matthias Wietz, University of Oldenburg, Germany
Stanley C. Lau, Hong Kong University of Science and Technology, Hong Kong
Tilmann Harder, University of Bremen, Germany

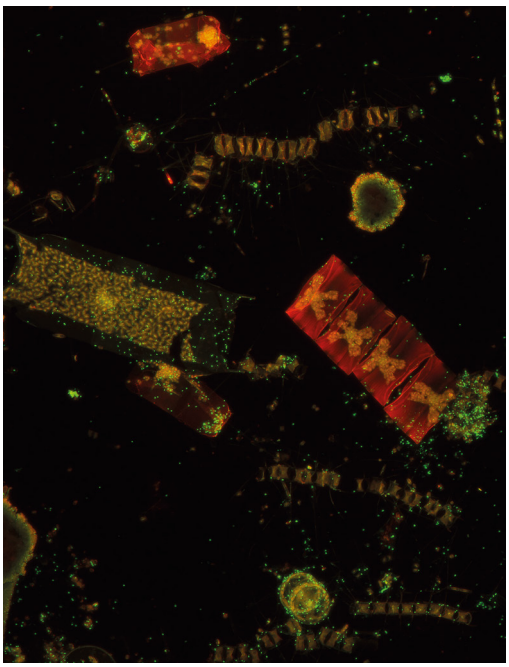

Phytoplankton and associated bacteria from the North Sea
Image by Insa Bakenhus

Socio-ecological interactions between microbes and associated organisms are integral elements of marine ecosystem dynamics. This Research Topic combines sixteen papers on interactions across the major domains of marine life, including prokaryotes, phytoplankton, macroalgae, cnidarians, viruses and fungi. These studies offer exciting insights into microbial cooperation and competition, holobiont ecology, interkingdom signaling, chemical microdiversity, and biogeography. Understanding such network processes is essential for the interpretation of ecosystem functioning and biogeochemical events, particularly in the wake of climate change.

Citation: Wietz, M., Lau, S. C., Harder, T., eds. (2019). Socio-Ecology of Microbes in a Changing Ocean. Lausanne: Frontiers Media. doi: 10.3389/978-2-88945-908-7

Table of Contents

frontiers in Marine Science

EDITORIAL
published: 16 April 2019
doi: 10.3389/fmars.2019.00190

Editorial: Socio-Ecology of Microbes in a Changing Ocean

Matthias Wietz[1]*, *Stanley C. Lau*[2] and *Tilmann Harder*[1,3]

[1] Alfred Wegener Institute Helmholtz Centre for Polar and Marine Research, Bremerhaven, Germany, [2] Division of Life Science, The Hong Kong University of Science and Technology, Clear Water Bay, Hong Kong, [3] Faculty of Biology and Chemistry, University of Bremen, Bremen, Germany

Keywords: symbioses, microbe-host interactions, phytoplankton, marine bacteria, microbial networks, holobiont ecology, climate change

Editorial on the Research Topic

Socio-Ecology of Microbes in a Changing Ocean

Marine microbes live in complex socio-ecological networks with diverse microbial and macrobial neighbors. These networks operate on different scales, spanning the single-cell level to microhabitats and (meta)communities to entire phytoplankton blooms (Faust and Raes, 2012; Teeling et al., 2012; Cordero and Datta, 2016). Boosted by recent advances in next-generation sequencing and high-resolution chemical analyses, the scientific community begins to unveil the complexity of microbial relationships and how these interactions influence biological dynamics and holobiont functioning (Pita et al., 2018; Van De Water et al., 2018). Ultimately, the elucidation of microbial network processes helps with the interpretation of large-scale ecological and biogeochemical events (Strom, 2008; Fuhrman et al., 2015).

The Frontiers Research Topic Socio-Ecology of Microbes in a Changing Ocean invited contributions on microbial signaling and communication, the effect of microbial interactions on microhabitat structuring, the function of secondary metabolites in bacterial antagonism and microbe-host interactions, the conversion and cross-feeding of nutrients, microbial physiology and gene regulation in response to co-occurring organisms, as well as metabolic exchange in diverse communities. Special emphasis was placed on socio-ecological dynamics under a changing climate, addressing the biological effects of ocean acidification and warming and the increasing spread of invasive species.

The Research Topic encompasses 16 papers on diverse aspects of microbial cooperation and competition, such as bacterial interactions with phytoplankton, macroalgae and invertebrates, chemical microdiversity, interkingdom signaling, viral infections of macroalgae, as well as the distribution of archaea and fungi in relation to environmental parameters. In addition, one Review and one Perspective article offer exciting views on coral disease and phytoplankton multicellularity.

BACTERIA-ALGAE INTERACTIONS

Interactions between bacteria and algae are a major focus of the Research Topic, reflecting the pivotal role of micro- and macroalgae in marine carbon fluxes (Falkowski and Woodhead, 1992; Field et al., 1998) and associated microbial dynamics (Amin et al., 2012; Martin et al., 2014; Seymour et al., 2017). Contributed papers highlight the importance of bacteria for algae and vice versa, describing the composition and function of associated microbiota, interdependencies by metabolite exchange, and how these interactions can vary under changing environmental conditions.

In their paper "Bacterial Communities of Diatoms Display Strong Conservation Across Strains and Time," Behringer et al. show that the diatoms *Asterionellopsis glacialis* and *Nitzschia longissima* harbor conserved microbiota that remain stable over 1 year of co-existence. These distinct and

OPEN ACCESS

Edited by:
Hongyue Dang,
Xiamen University, China

Reviewed by:
Gian Marco Luna,
Italian National Research Council (CNR), Italy
Michael Joseph Behrenfeld,
Oregon State University, United States

***Correspondence:**
Matthias Wietz
matthias.wietz@awi.de

Specialty section:
This article was submitted to Aquatic Microbiology, a section of the journal Frontiers in Marine Science

Received: *22 December 2018*
Accepted: *26 March 2019*
Published: *16 April 2019*

Citation:
Wietz M, Lau SC and Harder T (2019) Editorial: Socio-Ecology of Microbes in a Changing Ocean. Front. Mar. Sci. 6:190. doi: 10.3389/fmars.2019.00190

consistent temporal associations are linked to a range of bacterial processes that enhance diatom growth. The concept of specific associations between bacteria and microalgae is supported by Crenn et al. in their paper "Bacterial Epibiotic Communities of Ubiquitous and Abundant Marine Diatoms Are Distinct in Short- and Long-Term Associations." Here, screening of single *Thalassiosira* and *Chaetoceros* cells demonstrates that laboratory experiments select for specific diatom microbiota adapted to long-term associations, whereas environmental diatoms harbor different bacterial associates. A step toward deciphering the molecular mechanisms behind such interactions is made by Torres-Monroy and Ullrich in their paper "Identification of Bacterial Genes Expressed During Diatom-Bacteria Interactions Using an *in vivo* Expression Technology Approach." Here, bacterial gene expression is studied in response to the diatom *Thalassiosira weissflogii*, revealing specific expression of bacterial promoters during interactions with *T. weissflogii*. These observations correspond to specific regulation of bacterial attachment, nitrogen metabolism and heavy metal resistance. Interactions between algae and bacteria also include the exchange of ecologically relevant metabolites, as demonstrated by Wienhausen et al. in "The Exometabolome of Two Model Strains of the *Roseobacter* Group: A Marketplace of Microbial Metabolites." Here, ultrahigh-resolution mass spectrometry reveals diverse exometabolites secreted by the bacteria *Phaeobacter inhibens* and *Dinoroseobacter shibae*, including plant auxins and precursors of different B vitamins that may benefit co-occurring auxotrophs. A related scenario is presented in "The B-Vitamin Mutualism Between the Dinoflagellate *Lingulodinium polyedrum* and the Bacterium *Dinoroseobacter shibae*" by Cruz-López et al. who describe that *D. shibae* is dependent on vitamin B_7 produced by *L. polyedrum* while in turn providing vitamins B_1 and B_{12} to the eukaryotic partner. Yarimizu et al. describe another type of bacterial interaction with this dinoflagellate species in their paper "Iron and Harmful Algae Blooms: Potential Algal-Bacterial Mutualism Between *Lingulodinium polyedrum* and *Marinobacter algicola*." Here, *M. algicola* is shown as essential for dinoflagellate growth by supplying bioavailable iron via the siderophore vibrioferrin. As *L. polyedrum* can be a major cause of harmful algal blooms, bacteria-algae interactions can hence also have detrimental ecological and economic consequences. This alternative perspective is also addressed by Bramucci et al. in "The Bacterial Symbiont *Phaeobacter inhibens* Shapes the Life History of Its Algal Host *Emiliania huxleyi*." During long-term co-cultivation, *P. inhibens* selectively kills calcifying and flagellated types of the coccolithophore *Emiliania huxleyi*, whereas non-calcifying *E. huxleyi* remain unaffected. This differential pathogenesis may alter the composition of *E. huxleyi* blooms, with probable consequences for marine primary production.

The section on bacteria-algae interactions also includes two papers on macroalgae and associated microbes. Macroalgae are important primary producers in coastal environments and have central functions as habitat formers and nutrient source, but are threatened by environmental stressors (Steneck and Erlandson, 2002; Krumhansl et al., 2016). In their paper "Novel ssDNA Viruses Detected in the Virome of Bleached, Habitat-Forming Kelp *Ecklonia radiata*," Beattie et al. shotgun-sequenced viral particles isolated from healthy and diseased phenotypes of the kelp *Ecklonia radiata*. This approach identified novel ssDNA viruses restricted to bleached kelp, indicating that stress-induced viral infections may affect coastal primary production. The view on macroalgae-associated microbes is complemented by the paper "Exploring the Cultivable *Ectocarpus* Microbiome," where KleinJan et al. isolated over 300 bacterial strains associated with the brown macroalga *Ectocarpus subulatus*. This first step toward a model system for functional studies of algae–bacteria interactions during abiotic stress is highly relevant for future-ocean scenarios in the wake of climate change.

The collection of papers related to bacteria and algae concludes with a Perspective article raising thought-provoking concepts about "Multicellular Features of Phytoplankton." Here, Abada and Segev propose that microalgal populations often display the characteristics of a multicellular-like community; representing an evolutionary intermediate between single cells and aggregates that communicate and cooperate. By combining evidence on coccolithophores and diatoms, two key phytoplankton groups, the authors discuss exciting aspects such as coordinated behavior and programmed cell death in a multicellular context.

BACTERIA-CNIDARIA INTERACTIONS

Studies on functional interactions between cnidarian hosts and microbes are receiving continued interest, particularly owing to ecological threats connected to climate change, for instance coral bleaching (Pandolfi et al., 2003; Bourne et al., 2016). This Research Topic includes four related papers, including the Review "Responses of Coral-Associated Bacterial Communities to Local and Global Stressors." Here, McDevitt-Irvin et al. summarize 45 recent studies to show that coral health can be strongly influenced by microbiome composition, illustrating that stress-related shifts in bacterial diversity may have important ecological consequences. A second coral-related contribution, "Quorum Sensing Interference and Structural Variation of Quorum Sensing Mimics in Australian Soft Coral" by Freckelton et al. describes how coral-derived metabolites mimic bacterial signaling molecules and hence influence cell-cell communication. The finding of chemical crosstalk between soft corals and their associated bacteria is important considering the ecological network within the coral holobiont. Another type of cnidarian, the sea anemone *Nematostella*, is investigated in the paper "Predicted Bacterial Interactions Affect *in vivo* Microbial Colonization Dynamics in *Nematostella*" by Domin et al. Through bacterial cultivation and co-occurrence networks, bacteria–bacteria interactions are shown to change according to the host's developmental stage. Predicted competitive bacteria influence community structure for a short period of time but are soon replaced, indicating a high degree of resilience within the bacterial community. In their paper "Stimulated Respiration and Net Photosynthesis in *Cassiopeia* sp. during Glucose Enrichment Suggests *in hospite* CO_2 Limitation of Algal

Endosymbionts," Rädecker et al. show that glucose enrichment stimulates respiration and photosynthesis in the holobiont of upside-down jellyfish, likely resulting from bacterial activity that subsequently stimulates primary production by algal symbionts through increased CO_2 availability.

EFFECTS OF ENVIRONMENTAL PARAMETERS ON MICROBIAL DISTRIBUTION

The third section of the Research Topic includes two papers on the distribution of microbes in relation to environmental parameters (Hanson et al., 2012; Sunagawa et al., 2015). Whereas biogeographical patterns are comparatively well-studied for bacteria, Müller et al. focus on archaea by resolving "Spatiotemporal Dynamics of Ammonia-Oxidizing Thaumarchaeota in Distinct Arctic Water Masses." The authors describe distributional patterns of Thaumarchaeota genotypes in specific water masses in the Arctic-Atlantic boundary, a region under special threat from climate change. Considering the thaumarchaeotal contribution to ammonia oxidation, these findings have implications for nitrogen cycling. Finally, the paper "Spatiotemporal Distribution and Assemblages of Planktonic Fungi in the Coastal Waters of the Bohai Sea" by Wang et al. illustrates regional and temporal changes in the abundance and diversity of fungi, a so-far largely unexplored group of marine microbes. Differential distribution of *Ascomycota* and *Basidiomycota* between coastal habitats was related to riverine inputs and phytoplankton detritus, providing insights into the ecology of fungi in marine systems.

CONCLUSIONS AND PERSPECTIVES

As evidenced by the contributions to this Research Topic, the socio-ecology of microbes is a growing field of research that substantially benefits from cross-disciplinary approaches. The diverse Topic contributions showcase that the field is clearly moving from merely descriptive analyses of "who-is-associated-with-whom" to functional studies of diversity and phenotypic traits within metaorganisms, which harbor a network of associates from all domains of life. Holistic perspectives and systemic analyses, which acknowledge the complexity and linkages within biological systems, are fundamental for the comprehensive understanding of ecological and biogeochemical processes, particularly in the wake of climate change.

AUTHOR CONTRIBUTIONS

This editorial was co-authored by the Topic Editors MW, SL, and TH.

REFERENCES

Amin, S. A., Parker, M. S., and Armbrust, E. V. (2012). Interactions between diatoms and bacteria. *Microbiol. Mol. Biol. Rev.* 76, 667–684. doi: 10.1128/MMBR.00007-12

Bourne, D. G., Morrow, K. M., and Webster, N. S. (2016). Insights into the coral microbiome: underpinning the health and resilience of reef ecosystems. *Annu. Rev. Microbiol.* 70, 317–340. doi: 10.1146/annurev-micro-102215-095440

Cordero, O. X., and Datta, M. S. (2016). Microbial interactions and community assembly at microscales. *Curr. Opin. Microbiol.* 31, 227–234. doi: 10.1016/j.mib.2016.03.015

Falkowski, P. G., and Woodhead, A. D. (1992). *Primary Productivity and Biogeochemical Cycles in the Sea*. New York, NY: Plenum Press.

Faust, K., and Raes, J. (2012). Microbial interactions: from networks to models. *Nat. Rev. Microbiol.* 10, 538–550. doi: 10.1038/nrmicro2832

Field, C. B., Behrenfeld, M. J., Randerson, J. T., and Falkowski, P. (1998). Primary production of the biosphere: integrating terrestrial and oceanic components. *Science* 281, 237–240. doi: 10.1126/science.281.5374.237

Fuhrman, J. A., Cram, J. A., and Needham, D. M. (2015). Marine microbial community dynamics and their ecological interpretation. *Nat. Rev. Microbiol.* 13, 133–146. doi: 10.1038/nrmicro3417

Hanson, C. A., Fuhrman, J. A., Horner-Devine, M. C., and Martiny, J. B. H. (2012). Beyond biogeographic patterns: processes shaping the microbial landscape. *Nat. Rev. Microbiol.* 10, 497–507. doi: 10.1038/nrmicro2795

Krumhansl, K. A., Okamoto, D. K., Rassweiler, A., Novak, M., Bolton, J. J., Cavanaugh, K. C., et al. (2016). Global patterns of kelp forest change over the past half-century. *Proc. Natl. Acad. Sci. U.S.A.* 113, 13785–13790. doi: 10.1073/pnas.1606102113

Martin, M., Portetelle, D., Michel, G., and Vandenbol, M. (2014). Microorganisms living on macroalgae: diversity, interactions, and biotechnological applications. *Appl. Microbiol. Biotechnol.* 98, 2917–2935. doi: 10.1007/s00253-014-5557-2

Pandolfi, J. M., Bradbury, R. H., Sala, E., Hughes, T. P., Bjorndal, K. A., Cooke, R. G., et al. (2003). Global trajectories of the long-term decline of coral reef ecosystems. *Science* 301, 955–958. doi: 10.1126/science.1085706

Pita, L., Rix, L., Slaby, B. M., Franke, A., and Hentschel, U. (2018). The sponge holobiont in a changing ocean: from microbes to ecosystems. *Microbiome* 6:46. doi: 10.1186/s40168-018-0428-1

Seymour, J. R., Amin, S. A., Raina, J. B., and Stocker, R. (2017). Zooming in on the phycosphere: the ecological interface for phytoplankton-bacteria relationships. *Nat. Microbiol.* 2, 17065. doi: 10.1038/nmicrobiol.2017.65

Steneck, R., and Erlandson, J. M. (2002). Kelp forest ecosystems: biodiversity, stability, resilience and future. *Environ. Conserv.* 29, 436–459. doi: 10.1017/S0376892902000322

Strom, S. L. (2008). Microbial ecology of ocean biogeochemistry: a community perspective. *Science* 320, 1043–1045. doi: 10.1126/science.1153527

Sunagawa, S., Coelho, L. P., Chaffron, S., Kultima, J. R., Labadie, K., Salazar, G., et al. (2015). Structure and function of the global ocean microbiome. *Science* 348:1261359. doi: 10.1126/science.1261359

Teeling, H., Fuchs, B. M., Becher, D., Klockow, C., Gardebrecht, A., Bennke, C. M., et al. (2012). Substrate-controlled succession of marine bacterioplankton populations induced by a phytoplankton bloom. *Science* 336, 608–611. doi: 10.1126/science.1218344

Van De Water, J. A. J. M., Allemand, D., and Ferrier-Pagès, C. (2018). Host-microbe interactions in octocoral holobionts - recent advances and perspectives. *Microbiome* 6:64. doi: 10.1186/s40168-018-0431-6

Conflict of Interest Statement: The authors declare that the research was conducted in the absence of any commercial or financial relationships that could be construed as a potential conflict of interest.

frontiers in Microbiology

ORIGINAL RESEARCH
published: 06 April 2018
doi: 10.3389/fmicb.2018.00659

Bacterial Communities of Diatoms Display Strong Conservation Across Strains and Time

*Gregory Behringer[1], Michael A. Ochsenkühn[1], Cong Fei[1,2], Jhamal Fanning[1], Julie A. Koester[3] and Shady A. Amin[1]**

[1] Marine Microbial Ecology Lab, Biology Program, New York University Abu Dhabi, Abu Dhabi, United Arab Emirates, [2] College of Resources and Environmental Science, Nanjing Agriculture University, Nanjing, China, [3] Department of Biology and Marine Biology, University of North Carolina at Wilmington, Wilmington, NC, United States

OPEN ACCESS

Edited by:
Matthias Wietz,
University of Oldenburg, Germany

Reviewed by:
Marine Landa,
University of California, Santa Cruz, United States
Matthias S. Ullrich,
Jacobs University Bremen, Germany
Christian Jeanthon,
Station Biologique de Roscoff (CNRS), France

***Correspondence:**
Shady A. Amin
samin@nyu.edu

Specialty section:
This article was submitted to Aquatic Microbiology, a section of the journal Frontiers in Microbiology

Received: 13 December 2017
Accepted: 21 March 2018
Published: 06 April 2018

Citation:
Behringer G, Ochsenkühn MA, Fei C, Fanning J, Koester JA and Amin SA (2018) Bacterial Communities of Diatoms Display Strong Conservation Across Strains and Time. Front. Microbiol. 9:659. doi: 10.3389/fmicb.2018.00659

Interactions between phytoplankton and bacteria play important roles in shaping the microenvironment surrounding these organisms and in turn influence global biogeochemical cycles. This microenvironment, known as the phycosphere, is presumed to shape the bacterial diversity around phytoplankton and thus stimulate a diverse array of interactions between both groups. Although many studies have attempted to characterize bacterial communities that associate and interact with phytoplankton, bias in bacterial cultivation and consistency and persistence of bacterial communities across phytoplankton isolates likely impede the understanding of these microbial associations. Here, we isolate four strains of the diatom *Asterionellopsis glacialis* and three strains of the diatom *Nitzschia longissima* and show through metabarcoding of the bacterial 16S rDNA gene that though each species possesses a unique bacterial community, the bacterial composition across strains from the same species are highly conserved at the genus level. Cultivation of all seven strains in the laboratory for longer than 1 year resulted in only small changes to the bacterial composition, suggesting that despite strong pressures from laboratory culturing conditions associations between these diatoms and their bacterial communities are robust. Specific operational taxonomic units (OTUs) belonging to the Roseobacter-clade appear to be conserved across all strains and time, suggesting their importance to diatoms. In addition, we isolate a range of cultivable bacteria from one of these cultures, *A. glacialis* strain A3, including several strains of *Shimia marina* and *Nautella* sp. that appear closely related to OTUs conserved across all strains and times. Coculturing of A3 with some of its cultivable bacteria as well as other diatom-associated bacteria shows a wide range of responses that include enhancing diatom growth. Cumulatively, these findings suggest that phytoplankton possess unique microbiomes that are consistent across strains and temporal scales.

Keywords: phytoplankton–bacteria interactions, diatoms, microbial interactions, phytoplankton microbiome, marine microbial ecology, microalgae

INTRODUCTION

Interactions between phytoplankton and bacteria are some of the most important relationships in aquatic environments (Cole, 1982; Azam and Malfatti, 2007; Seymour et al., 2017). Bacteria are inherently dependent on the photosynthetic phytoplankton to acquire organic carbon needed to sustain their growth (Field et al., 1998; Falkowski et al., 2008); in turn phytoplankton rely on bacteria to remineralize organic matter back to inorganic substituents that ultimately support algal growth (Cho and Azam, 1988; Worden et al., 2015). More recent research has shown that interactions between both groups are complex, involving the exchange of cofactors, micronutrients, macronutrients, proteins, and signaling molecules. These exchanges result in mutualistic, commensal, competitive, and antagonistic interactions that can lead to the demise or success of interacting species (Amin et al., 2012; Kazamia et al., 2016; Seymour et al., 2017). For example, more than 170 microalgal species out of 326 tested species cannot synthesize vitamins B_1, B_7, and B_{12}, yet require it to grow (Croft et al., 2005; Tang et al., 2010). Many bacteria fulfill this requirement by synthesizing vitamins in exchange for algal photosynthates. The ubiquitous marine bacterium *Ruegeria pomeroyi* alleviates vitamin B_{12} limitation of the diatom *Thalassiosira pseudonana* in exchange for organic carbon and sulfur metabolites (Durham et al., 2015, 2017). Some marine bacteria increase the bioavailability of iron, a major limiting element in the open ocean (Martin and Fitzwater, 1988), to their algal partners by producing photolabile iron-binding chelates (Amin et al., 2009). Phytoplankton–bacteria interactions can also involve cell cycle manipulations. For example, bacteria belonging to the *Roseobacter* clade convert tryptophan secreted by phytoplankton to the hormone indole-3-acetic acid (IAA). In turn, IAA enhances the cell division of algal cells, its photosynthetic machinery, and potentially its carbon output to the bacteria (Amin et al., 2015; Segev et al., 2016). Other bacteria manipulate algal growth by producing proteins that lyse algal cells or unknown factors that arrest algal cell division (Paul and Pohnert, 2011, 2013; Seyedsayamdost et al., 2011; van Tol et al., 2017).

Algal–bacterial interactions are hypothesized to occur in the microenvironment surrounding algal cells known as the phycosphere (Bell and Mitchell, 1972; Amin et al., 2012; Seymour et al., 2017), the aquatic analog of the rhizosphere in plants (Mendes et al., 2011). The phycosphere is a region characterized by relatively high concentrations of organic molecules released by algal cells relative to bulk seawater (Biddanda and Benner, 1997). Bacteria colonize the phycosphere either using chemotaxis, random encounter with algal cells or via vertical transmission (Seymour et al., 2017). It is becoming apparent that though these interactions occur at the scale of individual cells, they have major implications at the ecosystem level. Understanding the mechanisms of these interactions and the major players (bacteria and phytoplankton) that mediate these relationships is essential to modeling and predicting changes to the marine environment.

In order to understand interactions in the phycosphere, we must first determine the types of bacteria that associate with different species of phytoplankton and their abundance. Most studies examining bacterial association with phytoplankton rely mostly on cultivation of bacteria from algal cultures or algal blooms and on metagenomic sequencing of algal blooms. For example, marine bacteria that have been consistently isolated from diatom cultures and diatom-dominated blooms belong to a small number of genera relative to total bacterial genera found in seawater (Sapp et al., 2007; Amin et al., 2012; Baker and Kemp, 2014). Similar examples have been shown in other phytoplankton lineages (Biegala et al., 2002; Green et al., 2004; Hasegawa et al., 2007; Eigemann et al., 2013). For example, two coccolithophore species have also been shown to harbor specific types of bacteria across several cultures (Green et al., 2015) while specific bacteria have been shown to associate with certain dinoflagellate species (Green et al., 2004; Bolch et al., 2011). Blooms of the colonial cyanobacterium *Trichodesmium* appear to also harbor a core microbiome (Frischkorn et al., 2017). However, some microalgal species do not appear to harbor a core set of bacteria. For example, 13 different cultures of the green alga *Ostreococcus tauri* contain varying bacteria with no apparent microbiome at the genus level (Abby et al., 2014). Cumulatively, these studies demonstrate that although there is a general tendency to find specific species of bacteria that associate with phytoplankton, more work is needed to truly define phytoplankton microbiomes.

Unlike plants or mammals, defining the microbiome of phytoplankton is difficult given that they are unicellular organisms that grow in aquatic, dilute environments. Cultivation studies are inherently biased since most marine bacteria cannot be isolated and maintained through existing culturing techniques (Rappé and Giovannoni, 2003). Isolation and culturing of microalgae and their associated bacteria in the laboratory for prolonged periods before identification of bacteria is also problematic as it is hypothesized that under nutrient-rich laboratory conditions, the microbiome may undergo major changes in composition. Metagenomic sequencing of algal blooms also poses a problem since other bacteria in seawater could be misidentified as algal-associated.

Although previous studies have highlighted important taxa that interact with many phytoplankton species, our knowledge of the abundance and persistence of these bacterial taxa with their algal host either in the environment or in laboratory cultures is lacking. In addition, the occurrence of specific species of bacteria across strains of the same phytoplankton species, which would suggest 'intimate' associations between an alga and its 'microbiome,' has been largely unexamined. To address some of these limitations, we isolated multiple strains of the same species of phytoplankton and cultured them in the laboratory in order to compare the microbial communities across strains and time. We isolated single cells of the diatoms *Asterionellopsis glacialis* and *Nitzschia longissima* from different locations in the Arabian Gulf around the coastline of Abu Dhabi. Shortly after isolation, we characterized the microbiomes of all diatom isolates and continued to monitor changes to these microbiomes over the course of one year. Using *A. glacialis* as a model for studying algal–bacterial interactions, we cultivated bacteria from this diatom and cocultured them to find if these

bacteria play any role in the physiology or life cycle of the diatom.

MATERIALS AND METHODS

Diatom Isolation, Maintenance, and Identification

Single diatom cells (or chains) were isolated in October 2015 and July 2016 from different locations in the Arabian Gulf near the Abu Dhabi Coast, United Arab Emirates by dilution of a small volume (<0.2–0.5 μL) in sterile f/2+Si medium (Ryther and Guillard, 1962). Volumes isolated from seawater were observed using light microscopy prior to dilution with sterile media to ensure a single diatom cell/chain was present in the sample. Isolates were identified using light microscopy (Leica DM IL LED, Wetzlar, Germany) and scanning electron microscopy (SEM) using a 5-kV beam and the secondary electron detector for platinum-palladium coated (12 nm) samples (Phillips XL 30S FEG SEM, FEI Inc., Hillsboro, OR, United States). Putative taxonomic identities were assigned based on morphological characteristics as well as partial sequencing of the 18S rDNA and the partial sequencing of both internal transcribed spacer (ITS) regions and 5.8S rDNA.

Batch cultures were maintained in sterile borosilicate culture tubes (Fisher, Hampton, NH, United States) containing 25-mL of sterile f/2+Si media. All diatom cultures were grown in semi-continuous batch cultures (Brand et al., 1981) in algal growth chambers (Percival AL-30L2 and AL-36L4) at 22°C, 125 μE m^{-2} s^{-1}, and 12:12 light/dark cycle. All cultures were transferred approximately every 7 days by inoculating 25 mL fresh media with 50 μL of culture. Although the growth rate of each culture varied over the course of the experiment, on average cultures were transferred 30 times between each time point for bacterial profiling. Light flux was measured using a QSL-2100 PAR Sensor (Biospherical Instruments Inc., San Diego, CA, United States). Diatom growth was monitored initially by direct cell counts using a Sedgwick rafter (Pyser-SGI Ltd., Kent, United Kingdom) and once a linear relationship between cell number and *in vivo* fluorescence was established, by measuring relative fluorescence units (RFUs) using a 10-AU fluorimeter (Turner Designs, San Jose, CA, United States). Specific growth rates (μ) were calculated from the linear regression of the natural log of *in vivo* fluorescence versus time during the exponential growth phase of cultures. Standard deviation of μ was calculated using μ values from biological replicates ($n = 6$ unless otherwise indicated) over the exponential growth period.

Diatom DNA Isolation and Phylogeny

For DNA isolation, log-phase diatom cultures were vacuum filtered onto a 47 mm 3-μm cyclopore membrane filters (Whatman) and flash frozen in liquid nitrogen. Subsequently, DNA was extracted either with the PureLink Plant Total DNA Purification kit (Invitrogen, Life Technologies) directly or cells were lysed by repeated freeze/thaw cycles in liquid nitrogen, incubation at ∼90°C in a water bath followed by pulsed bead beating (BioSpec, Bartlesville, OK, United States) with zirconium ceramic oxide bulk beads (Thermo Fisher Scientific) in "Nuclei Lysis Buffer" (Promega, Madison, WI, United States). The resulting lysate was processed via the Wizard genomic DNA Purification Kit using the plant tissue protocol (Promega). Targeted DNA loci were then amplified using Q5 High-Fidelity 2X Master Mix (New England Biolabs, Ipswich, MA, United States) and the primer pair ITS1-FWD TCCGTAGGTGAACCTGCGG, and ITS4-REV TCCTCCGCTTATTGATATGC (White et al., 1990) and 18S primers A: AACCTGGTTGATCCTGCCAGT and B: TGATCCTTCTGCAGGTTCACCTAC (Medlin et al., 1988). PCR cycle conditions for ITS were as follows: an initial 94°C for 1 min followed by 94°C for 1 min, 51°C for 1 min, 72°C for 1 min for 35 cycles, and a final incubation at 72°C for 8 min. PCR cycle conditions for 18S rDNA were as follows: an initial 94°C for 2 min followed by 95°C for 1 min, 58°C for 45 s, 72°C for 1 min for 35 cycles, and a final incubation at 72°C for 5 min. ITS products were size-selected using gel electrophoresis on a 1% agarose gel, and excised bands were purified with the Wizard SV Gel and PCR Clean-Up kit (Promega). DNA was stored at −20°C until Sanger sequenced (GENEWIZ, South Plainfield, NJ, United States). For 18S sequencing, PCR reactions were cleaned with ExoSAP (Applied Biosystems) and Sanger sequenced (NC State University, Genome Sciences Laboratory, Raleigh, NC, United States). The NCBI BLASTn suite[1] (Altschul et al., 1990) was used to assign taxonomy to all consensus contigs.

Consensus sequences for ITS were aligned in MAFFT version 7 (Katoh and Standley, 2013). Alignments were then exported to BEAUti (Bayesian Evolutionary Analysis Utility Version v1.8.4) (Drummond et al., 2012). The Markov chain Monte Carlo (MCMC) was set in BEAUti with 100,000,000 generations. Resulting XML files were analyzed by BEAST (Bayesian Evolutionary Analysis Sampling Trees Version v1.8.4) (Drummond et al., 2012) and post chain termination Markov Chain convergence was assessed using Tracer (MCMC Trace Analysis Tool Version v1.6.0). Consensus trees were analyzed using FigTree v1.4.3. A supplemental maximum-likelihood (ML) inference was also run for diatom loci using RAxML 7.3.0 (Stamatakis, 2006) to complement the findings of the above Bayes analysis, as the two can sometimes conflict (Beerli, 2006). A partitioned dataset was run under the model parameter "GTRGAMMA," and rapid bootstrap analysis (Stamatakis et al., 2008) was performed with 1,000 bootstraps.

Bacterial DNA Isolation

Twenty days after isolation, 10 mL of each culture with RFU ∼12–16 (mid-to-late exponential phase) were gently vacuum filtered onto a 25 mm 0.2-μm polycarbonate membrane filters (Whatman, NJ, United States). All filters were flash frozen and stored at −80°C for later processing. This process was repeated approximately every 6 months (200 days and 400 days) with cultures at the same cell densities as the original filtration mainly to avoid variations of the bacterial community as a function of culture density. For bacterial DNA isolation, 25% of each filter was excised using sterile

[1] https://blast.ncbi.nlm.nih.gov/Blast.cgi

scissors and DNA was isolated using E.Z.N.A. bacterial DNA kit (OMEGA Bio-tek, Norcross, GA, United States) according to the manufacturer's protocol. DNA was stored at −80°C until further processing.

16S rDNA Profiling of Bacteria

All samples were amplified and sequenced by the University of Illinois's Roy J. Carver High-Throughput Sequencing and Genotyping Unit (Urbana, IL, United States). In brief, DNA concentrations were measured via a Qubit instrument (Thermo Fisher) and diluted to a final concentration of 2 ng/μl. Reaction mixes contained the Fast Start High Fidelity PCR System (Roche, Basel, Switzerland) and 20x Access Array loading reagents (Fluidigm, San Francisco, CA, United States) per the manufacturer's protocol. For 16S rDNA amplification, the following bacterial primers were used: 515FB-FWD: GTGYCAGCMGCCGCGGTAA and 806RB-REV: GGACTACNVGGGTWTCTAAT. PCR was performed using standard conditions (Parada et al., 2016). PCR amplicons were size selected on a 2% agarose E-gel (Thermo Fisher) and purified via a gel extraction kit (Qiagen, Hilden, Germany). Amplicon sizes were then verified post purification using a Bioanalyzer (Agilent, Santa Clara, CA, United States). Illumina reads of the bacterial communities from all samples were deposited in the short read archive (Accession No. SRP132349).

Recovery of Archaeal amplicons from filtrate samples was also attempted using the same method as for bacteria except for the Fluidigm protocol, the following primer pairs were used: Arch349F (5′-GYGCASCAGKCGMGAAW-3′) and Arch806R (5′-GGACTACVSGGGTATCTAAT-3′) (Takai and Horikoshi, 2000). No archaeal amplicons were recovered using this protocol.

Phylogenetic Analysis of Bacteria

For Illumina sequencing, samples were denatured and spiked with a 20% non-indexed PhiX control library (Illumina) and loaded onto a MiSeq V2 flowcell at a final concentration of 8 pM. Libraries were then paired-end sequenced (2x250 bp). Generated *.bcl files were converted into demultiplexed compressed FASTQ files. The "FastX-Toolkit" (Hannon Lab[2]) was employed for quality checks and other metrics. Sequences were analyzed using the Mothur platform (Schloss et al., 2009). After contig alignment and trimming, identical sequences were merged using the 'unique.seqs' command to save computation time, and the command 'count.seqs' was used to keep a count of the number of sequences over samples represented by the remaining representative sequence. Rare sequence reads were removed ($n < 10$) and the remaining sequences were aligned against the SILVA database (release 128) (Quast et al., 2012). Chimeric sequences were removed using UCHIME as implemented in MOTHUR (Schloss et al., 2009). Chloroplast, mitochondrial, eukaryotic, and unknown reads were also removed. Sequences were classified against Greengenes using bootstrapping of 60, and the sample compositions were compared on the family level (Caporaso et al., 2010). For further analyses, a 97% similarity cut-off level was chosen to obtain operational taxonomic units (OTUs) after trimming, singleton and chimera removal and chloroplast filtering.

Both Bayesian Markov chain Monte Carlo (MCMC) and ML analysis methods were used to analyze phylogeny of bacterial isolates. MRBAYES 3.1.2 (Ronquist and Huelsenbeck, 2003) was used for Bayesian MCMC analysis of 16S rDNA with the GTR model (Lanave et al., 1984). The ML analysis was performed using PhyML 3.0 (Guindon et al., 2010) and an automatic model was selected by SMS (Lefort et al., 2017).

Isolation of Cultivable Bacteria From *A. glacialis*

To isolate individual bacterial colonies, several non-axenic A3 cultures in the exponential growth phase were serially diluted, and plated (75–100 μL aliquots) onto four different seawater agar plates (15.0 g/L agar in 0.2-μm filtered seawater) that contained either 2.0g/L casamino acids (Thermo Fisher), 2.0g/L dibasic sodium succinate (Sigma-Aldrich), 3.0 g/L D-(+)-glucose (Sigma-Aldrich), or plain seawater. In addition, Marine Broth 2216 (HIMEDIA, Mumbai, India) dissolved in MQ-H_2O was also used as an additional culturing plate. Plates were incubated at 25°C and single colonies were picked with sterile toothpicks and cultured in the respective liquid media types. Liquid cultures were grown overnight in a Stuart Orbital SI 600 shaker at 25°C and a glycerol stock was preserved for later experiments and bacterial identification. For bacterial identification, 16S rDNA gene was amplified using universal primers (27F, 1492R) as previously described (Amin et al., 2015). Amplicons were Sanger sequenced (GENEWIZ, South Plainfield, NJ, United States). All Sanger sequences of bacterial 16S rDNA were deposited in GenBank (Accession Nos. MG488233–MG488271).

Axenic *A. glacialis* Culture Generation

Axenic cultures were generated as described previously (Shishlyannikov et al., 2011) with some modifications. In brief, approximately 25 ml of a late-exponential phase growing diatom culture was gravity filtered onto 0.65 μm pore-size polycarbonate membrane filter (Millipore). Cells were quickly rinsed with sterile f/2+Si media. Using sterile tweezers, the filter was carefully removed from the filtration unit and washed for ∼1 min in sterile media containing 20 mg/ml Triton X-100 detergent to remove surface-attached bacteria. The filter was discarded after re-suspension of cells by gentle shaking in sterile detergent-free media. Cells were again gravity filtered onto a fresh 0.65-μm pore-size polycarbonate membrane filter and rinsed with sterile media. Subsequently, cells were washed off the filter by gentle shaking into sterile media containing a suite of antibiotics (per milliliter: 50 μg streptomycin, 66.6 μg gentamycin, 20 μg ciprofloxacin, 2.2 μg chloramphenicol, and 100 μg ampicillin). Cells were incubated in antibiotic-containing media for 48 h under regular growth conditions. Finally, 0.5–1.0 mL of antibiotics-treated cells were transferred to antibiotic-free media. Cultures were regularly monitored for bacterial contamination by checking for bacterial growth

[2]http://hannonlab.cshl.edu/fastx_toolkit/index.html

in Zobell marine broth (ZoBell, 1941) in addition to filtering 2–3 mL of exponential-phase growing culture and using Sybr Green I (Invitrogen) staining and epifluorescence microscopy (Nikon Eclipse 80i) as described previously (Lunau et al., 2005).

Coculture Experiments

Bacterial isolates were plated before each experiment on marine agar and were grown from single colonies in marine broth overnight (30°C, 150 rpm). Bacteria were centrifuged (3,500 × *g* for 5 min), washed twice with sterile f/2+Si, and inoculated into sterile, fresh 25-mL tubes containing f/2+Si media at a final cell density of $\sim 1 \times 10^4$ cells/mL. Axenic diatom cultures were acclimated for at least three transfers using semi-continuous batch cultures (Brand et al., 1981). Cultures were considered acclimated if the growth rate of three consecutive transfers of triplicate cultures did not vary by more than 15%. Subsequently, cultures were inoculated into the same tubes at a final concentration of ∼5,000 cells/mL. Cocultures were incubated as described above for diatoms. Statistical analysis of coculture growth rates were performed using omnibus ANOVA testing and *post hoc*, pairwise comparisons were generated from Tukey Honest Significance Difference tests.

RESULTS

Diatom Isolation

To examine the bacterial composition of diatoms, the persistence of these microbiomes over culturing time in the laboratory and their conservation across different strains of the same species, we isolated four single-cell isolates of a putative *Asterionellopsis* sp. (A1, A2, A3, and A4) and three isolates of a putative *Nitzschia* sp. (N1, N2, and N3). To confirm the identities of these diatoms, the 18S rDNA gene was Sanger sequenced. 18S rDNA sequences from *Asterionellopsis* spp. showed the strongest similarity to the *A. glacialis* CCAP 1009/3 (FR865485) 18S rDNA gene in NCBI. *A. glacialis* sensu lato has been shown to possess a wide cryptic diversity that encompasses at least five separate species, *A. glacialis*, *A. tropicalis*, *A. guyunusae, A. maritima*, *A. lenisilicea,* and *A. thurstonii*, using ITS1, 5.8S rRNA, and ITS2 sequences (Franco et al., 2016). To confirm that our isolates were indeed *A. glacialis* we further sequenced the ITS1, 5.8S rRNA, and ITS2 regions of all four *Asterionellopsis* isolates. Phylogeny based on these sequences showed that indeed all four isolates belonged to the *A. glacialis* clade (**Figure 1**).

Like *Asterionellopsis*, the taxonomic status of *N. longissima* remains unclear due to variation in species descriptions (Kaczmarska et al., 2007). The 18S rDNA sequences from our *Nitzschia* spp. showed the strongest similarity to *N. longissima* (AY881968). Analysis of the ITS regions and 5.8S rRNA sequence of N1, N2, and N3 failed to unequivocally show that these isolates belong to *N. longissima* since NCBI contains no ITS sequences from this species. Therefore, we relied on morphological evidence using SEM to provisionally assign our *Nitzschia* sp. isolates to *N. longissima* (**Figure 2**). Cells were lanceolate in shape with pronounced tapering at the ends (**Figure 2A**) and each contained two elongated chloroplasts. The morphological characteristics determined from SEM include an average of 15 ± 0.63 (SD) fibulae and 51.75 ± 1.28 striae per 10 μm (N = 6 and 8 valves, respectively) (**Figures 2B–E**). These characteristics corroborate that N1–N3 likely belong to *N. longissima* (Kaczmarska et al., 2007).

To characterize the bacterial communities of these isolates and assess their stability over laboratory culturing time, non-axenic diatoms were filtered at different time points, DNA was extracted and the bacterial 16S rDNA was amplified and partially sequenced using the Illumina MiSeq platform as described in the Materials and Methods. For *A. glacialis*, cultures A2 and A3 were sampled at 20, 200, and 400 days after isolation while cultures A1 and A4 were sampled only at 20 and 200 days after isolation. All *N. longissima* cultures (N1–N3) were sampled at 20, 200, and 400 days after isolation (**Table 1**).

A. glacialis Bacterial Community

Despite differences in the timing of sampling and isolation of the *A. glacialis* strains, all four strains displayed strong conservation of their microbiome across cultures and time with small differences at the genus level. Twenty days after isolation, the microbiome of all four strains were dominated by unclassified Rhodobacteraceae, an important member of diatom and phytoplankton microbiomes (Mayali et al., 2008; Geng and Belas, 2010; Amin et al., 2012; Goecke et al., 2013), comprising on average ∼60% of all reads (**Figure 3A**). The second most abundant group of bacteria belonged to the *Neptuniibacter* genus, comprising on average ∼20% of all reads. Other genera present include *Mesorhizobium* (Phyllobacteriaceae), a group of rhizobacteria, *Jannaschia* (Rhodobacteraceae), *Pedobacter* (Sphingobacteriaceae) and unclassified Flavobacteriaceae. All cultures were characterized by relatively a small number of OTUs (≤11) (**Table 1** and **Figure 3A**).

As the cultures were propagated in the laboratory, minor differences in the composition of the microbiome were observed. There was a modest reduction in the number of Rhodobacteraceae reads over time in A2, A3, and A4 coupled with an increase in *Neptuniibacter* reads (**Figure 3A**). In general, more significant changes were observed after 400 days relative to 200 days. Mainly, as cultures aged in the laboratory new genera were detected at relatively small percentage of reads (<10%). For example, at 400 days the A2 microbiome included <5% Jannaschia while the A3 microbiome included unclassified Flavobacteriaceae (**Figure 3A**). In addition, at 200 days the A4 microbiome included *Pedobacter* and unclassified Flavobacteriaceae. The variability of some genera over time likely stems from their low abundance in the sample.

N. longissima Bacterial Community

N1–N3 microbiomes contained more diversity at the genus level relative to *A. glacialis* with some genera being conserved between both species. Remarkably, the microbiomes of all isolates had strong similarities to each other at 20 days, suggesting that *N. longissima*, like *A. glacialis*, possesses a core microbiome. N1–N3 reads were dominated by unclassified Rhodobacteraceae

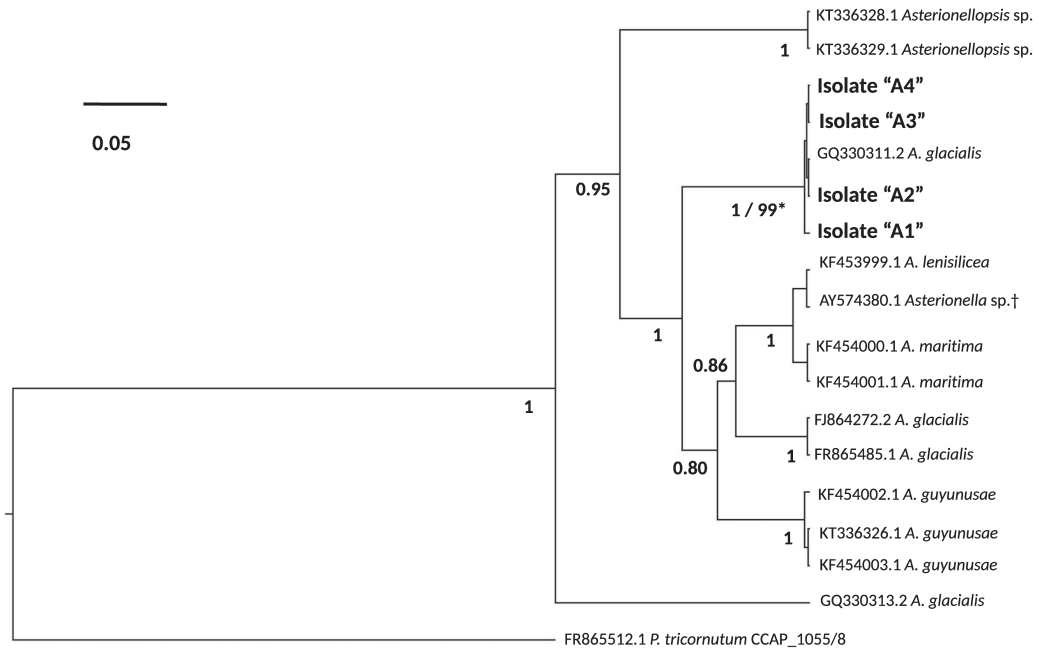

FIGURE 1 | Phylogeny of the diatoms *Asterionellopsis glacialis. A. glacialis* Bayesian phylogeny was constructed using internal transcribed spacer 1 (ITS1), 5.8S rRNA gene and internal transcribed spacer 2 (ITS2) of four isolates (A1–A4). Main nodes are labeled with posterior probability values (0.0–1.0) and clade for our isolates is also supported by a maximum-likelihood (ML) bootstrap value (0–100). Scale bar represents nucleotide substitutions per site. †Current NCBI nomenclature. However, recent literature suggests erroneous naming in NCBI and prescribes assignment to the *Asterionellopsis* genus (Moniz and Kaczmarska, 2011).

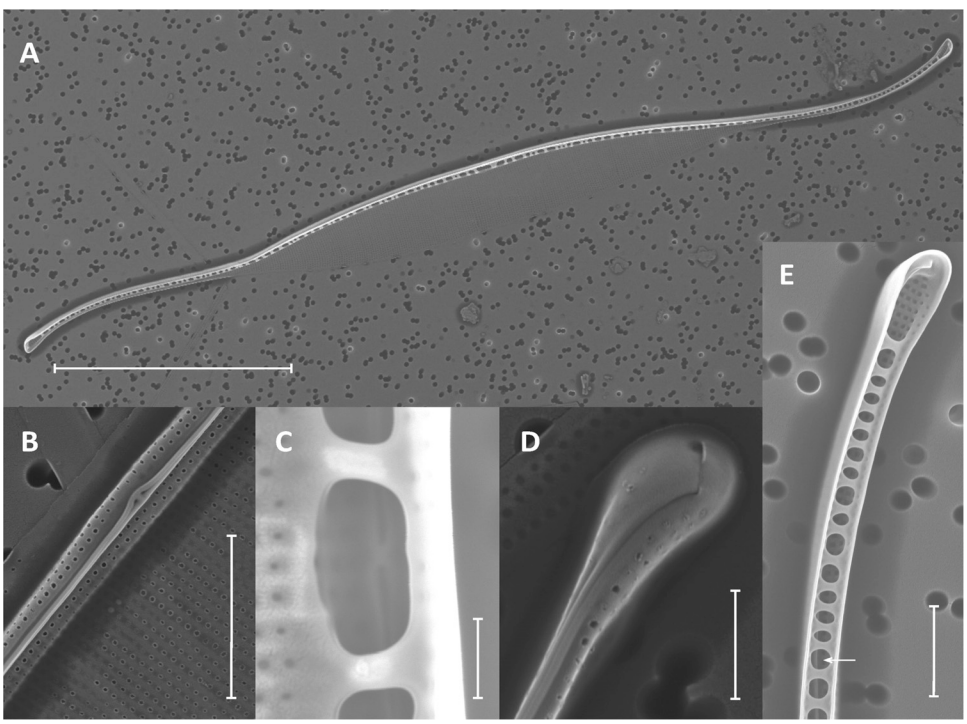

FIGURE 2 | Morphological identification of *Nitzschia longissima* using SEM. **(A)** Interior of a single valve with eccentrically placed, rib-like fibulae and lanceolate ends; scale bar = 20 μm. **(B)** Exterior of the elevated and eccentrically placed raphe and raphe ends at the midpoint of the valve (main body of valve is collapsed); scale bar = 2 μm. **(C)** Interior raphe canal and ends between and behind two fibulae; scale bar = 500 nm. **(D)** Exterior of the apical end of the valve and terminal raphe fissure; scale bar = 1 μm. **(E)** Interior view of raphe canal (arrow) and helictoglossa (terminal end of valve canal) with fused fibulae; scale bar = 2 μm.

TABLE 1 | Overview of Illumina MiSeq reads and OTUs recovered from each diatom culture.

Species	Sample name	Site of isolation	Isolation date	Time in culture (days)	Total reads	Number unique OTUs
A. glacialis	A1	Lat: 24.5177	10/2015	20	158,213	9
		Long: 54.3383		200	192,670	8
	A2	Lat: 24.5941	10/2015	20	167,785	8
		Long: 54.4501		200	306,132	11
				400	133,910	8
	A3	Lat: 24.5941	10/2015	20	158,512	9
		Long: 54.4501		200	157,125	7
				400	171,932	9
	A4	Lat: 24.5970	6/2016	20	97,633	9
		Long: 54.4940		200	114,888	8
N. longissima	N1	Lat: 24.5941	10/2015	20	114,142	10
		Long: 54.4501		200	108,087	8
				400	148,584	7
	N2	Lat: 24.5177	10/2015	20	167,651	8
		Long: 54.3383		200	223,772	12
				400	300,069	8
	N3	Lat: 24.5177	10/2015	20	126,532	8
		Long: 54.3383		200	216,973	10
				400	139,197	6

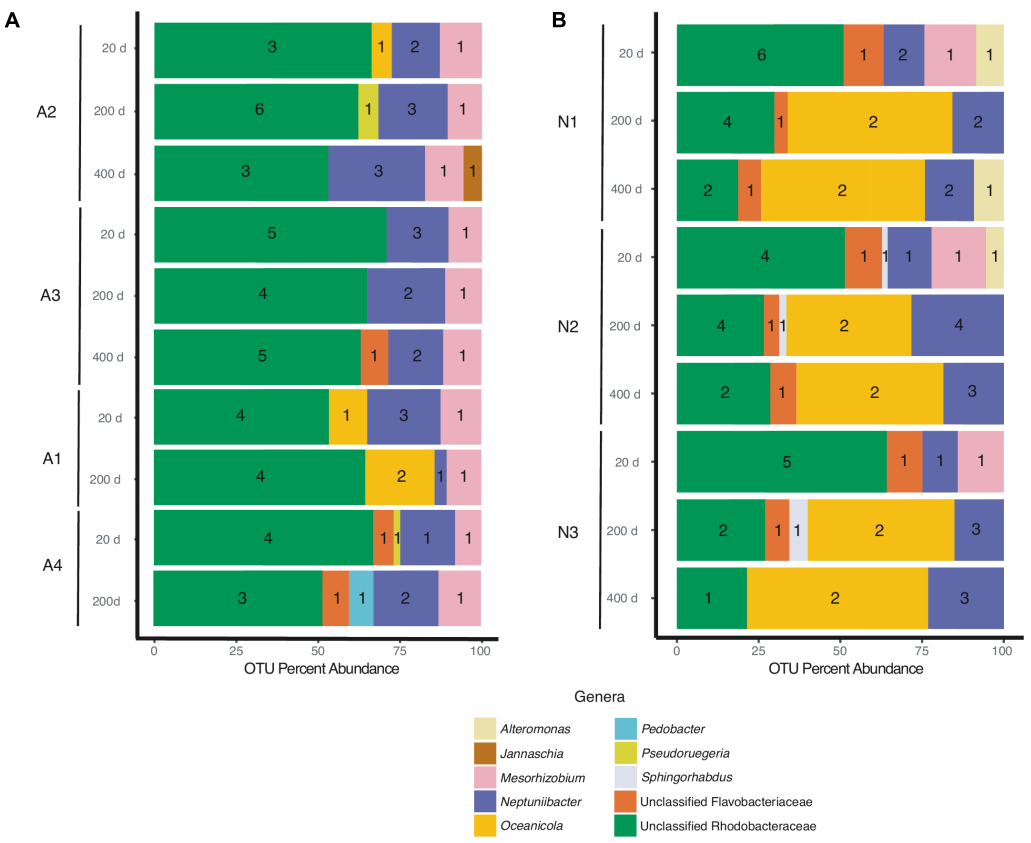

FIGURE 3 | Bacterial composition of **(A)** *A. glacialis* (A1, A2, A3, and A4) and **(B)** *N. longissima* (N1, N2, and N3) across culturing time in the laboratory at the genus level. Numbers inside colored bars represents unique number of OTUs for a specific genus.

(∼55% total OTU abundance) followed by *Neptuniibacter* and *Mesorhizobium* (**Figure 3B**). In addition to genera observed in *A. glacialis*, N1 included *Alteromonas* (Alteromonadaceae) and unclassified Flavobacteriaceae, while N2 and N3 included these two and *Sphingorhabdus* (Sphingomonadaceae) (**Figure 3B**). As seen in *A. glacialis* cultures, percent abundance of some genera changed over time albeit with more drastic changes. For example, *Mesorhizobium* disappeared altogether from all three cultures at 200 days. Rhodobacteraceae in all cultures increased in abundance at 200 days but then decreased again at 400 days with an overall increase when compared to the 20-day time point. Similar to *A. glacialis*, all strains throughout time exhibited relatively low diversity (≤12 OTUs per sample) (**Table 1** and **Figure 3B**). In general, the *A. glacialis* community appeared to decrease in diversity over time while the *N. longissima* community appeared to increase in diversity over the same time frame (**Figure 3B**).

Since Rhodobacteraceae represented the majority of reads from all strains at all time points, further analysis examining the taxonomic relationship between Rhodobacteraceae OTUs and samples were examined. Most OTUs were specific to either *A. glacialis* or *N. longissima* with some variability in their distribution across strains and time (**Figure 4A**). Interestingly, five OTUs were found in both diatoms and two of which (Rhodobacteraceae_otu A and Rhodobacteraceae_otu B) were consistently found across all strains at 20 days and persisted over time for the most part (**Figure 4**). Rhodobacteraceae_otu A is a distant relative of *Pseudoruegeria marinistellae* strain SF-16 and *Shimia biformata* strain CC-AMW-C while Rhodobacteraceae_otu B is a distant relative of *Loktanella koreensis* strain GA2-M3.

Isolation of Cultivable Bacteria and Coculturing

In addition to sequencing, we isolated and identified 17 bacteria from the A3 culture at the 20-day time point. In general, cultivable bacterial diversity was low compared to other studies isolating bacteria from diatom cultures (reviewed in Amin et al., 2012). The cultivable bacteria that were recovered belonged to the Alteromonadaceae (*Alteromonas macleodii*, >99% 16S rDNA identity; and *A. marina*, >92% 16S rDNA identity) and Rhodobacteraceae (*Shimia marina*, ≥99% 16S rDNA identity; *Nautella* sp., >97%) representing all isolates (**Figure 5**). Interestingly, the 16S rDNA gene of strains AGSF28, AGSF2, AGSF11, and AGSF4 (**Figure 5**) displayed >95% nucleotide identity to Rhodobacteraceae_otu A (**Figure 4A**), suggesting this OTU may represent a close relative of *Shimia* bacteria in the A3 culture. *Alteromonadaceae* did not represent an important group in the sequencing data highlighting the inherent bias of bacterial cultivation from algal cultures, which has been used in the past to study bacterial association with phytoplankton.

To examine potential interactions between *A. glacialis* and some of its bacterial consortium members, we first monitored the growth of A3 and its complete microbial consortium. Because the media used for growth, f/2+Si, lack organic carbon besides background organic carbon in seawater (Guillard, 1975), we anticipated that bacterial growth would be dependent on organic exudate excretion from the diatom. Indeed, as A3 grew bacterial cell densities increased from 5.9×10^4 to 3.3×10^6 cells mL^{-1} over the course of 10 days relative to controls without the diatom (**Figure 6**). To examine how different cultivable bacteria influence the growth of *A. glacialis*, A3 was made axenic as described in the Section "Materials and Methods" using a cocktail of antibiotics. Cocultures of A3 and six representative members from **Figure 5** were set up and the growth of the diatom was monitored. When cocultured with *Alteromonas* strains AGSF3, AGSF20 and AGSF23, A3 did not exhibit a significant change in growth rate relative to axenic cultures; however, coculture with *A. macleodii* strain AGSF14 caused a modest increase in growth rate of 5% (**Figure 7** and **Table 2**). Coculture with *S. marina* strains AGSF11 and AGSF28 did not show a significant change in growth rate relative to controls; however, a statistically significant growth enhancement was observed when A3 was cocultured with *Nautella* sp. AGSF5 (**Table 2** and **Figure 7**).

To test whether *A. glacialis* responds to other bacteria associated with other diatoms, we cocultured A3 with several strains of bacteria that were previously isolated from other diatoms: *Sulfitobacter* sp. SA11 and *Ruegeria* sp. AGSA97 both belong to Rhodobacteraceae and were previously isolated from the diatoms *Pseudo-nitzschia multiseries* and *Asterionella* sp., respectively. Both bacteria enhanced the growth rate of A3 by 19 and 15%, respectively, relative to axenic A3 (**Figures 8A,B** and **Table 2**). *Croceibacter atlanticus* strain SA60, a bacterium that was isolated from the diatom *P. multiseries* (Amin et al., 2015), was also cocultured with A3 and inhibited its growth relative to axenic controls (**Figure 8C** and **Table 2**).

DISCUSSION

Research examining interactions between phytoplankton and bacteria typically relies on isolation of bacteria from microalgal cultures that have been maintained in the laboratory for years; however, the relevance of such bacteria to natural bacterial populations encountered by phytoplankton in the environment is not clear. Our study shows that two diatom species possess a microbiome dominated by a relatively small number of unique OTUs (**Table 1**) and that the diatoms maintain high conservation of these microbiomes shortly after isolation from the field and up to more than 1 year in culture under typical laboratory conditions. These results provide preliminary evidence that diatom microbiomes may be similar in composition and do not undergo major changes when cultured in the laboratory. Although analysis of the microbiomes of four *A. glacialis* and three *N. longissima* isolates show small changes particularly after one year of cultivation, overall most of the dominant groups of bacteria persisted beyond 1 year (**Figure 3**). In general, bacterial diversity of the *A. glacialis* strains exhibited a reduction over time while the opposite trend was observed with *N. longissima*, suggesting a fundamental difference between the two diatoms. This difference may be due to differences in the composition of organic carbon molecules produced by each species that can support different groups of bacteria.

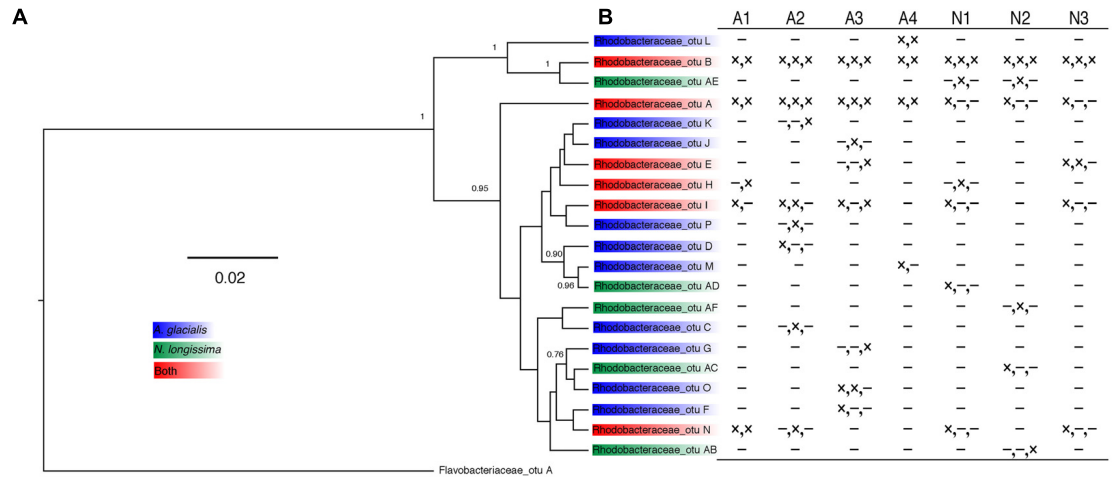

FIGURE 4 | Analysis of Rhodobacteraceae OTUs from *A. glacialis* and *N. longissima*. **(A)** Phylogram showing the relationship between different Rhodobacteraceae OTUs in both diatoms. Posterior probabilities >50 are indicated at the branching points. **(B)** Table showing the distribution of OTUs across samples. Columns represent different strains of each diatom. Rows represent different OTUs with presence (×) or absence (–) indicated for 20 days, 200 days, and 400 days, respectively.

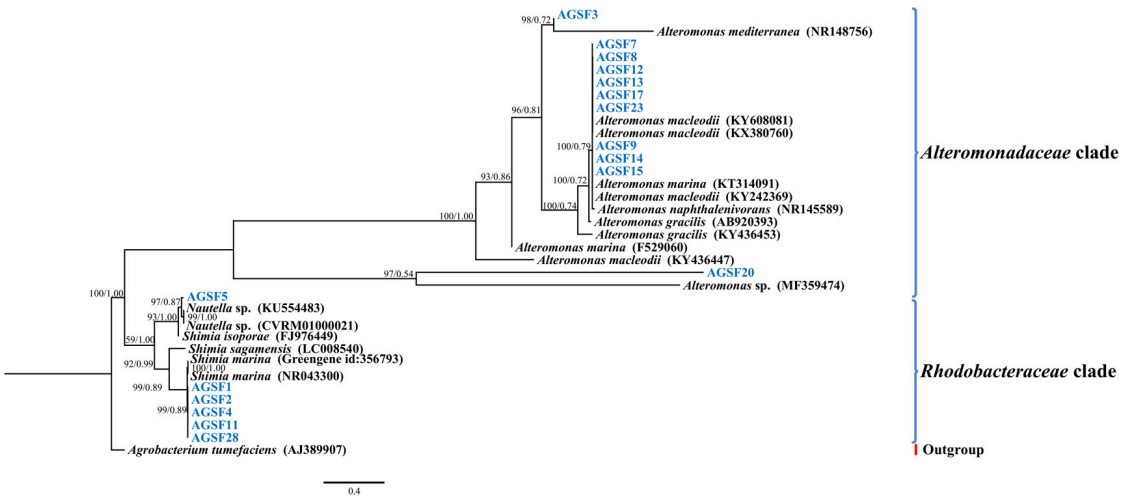

FIGURE 5 | Bayesian phylogenetic tree for the A3 cultivable bacterial 16S rDNA gene. Bacteria isolated from A3 are highlighted in blue. Accession numbers of GenBank sequences are included in parentheses. Family of different clades are indicated on the right. Posterior probabilities and ML bootstrap values are listed next to branches.

The identity of bacteria co-existing with both diatoms belonged to genera that are often recognized as generally microalgal, and specifically diatom, associated. The most dominant bacterial group with all seven diatom strains reported here was the Roseobacter-clade (Rhodobacteraceae). Members of the Rhodobacteraceae have been shown to associate with diatoms in culture and in the field (Grossart et al., 2005; Guannel et al., 2011; Sison-Mangus et al., 2014; Baker and Kemp, 2014; Amin et al., 2015). In addition, they have also been shown to interact in a variety of ways with phytoplankton. For example, *Sulfitobacter* sp. SA11 has been shown to enhance the growth of the diatom *P. multiseries* by converting diatom-derived tryptophan to the hormone IAA. SA11 also provides ammonia to the diatom in exchange for organosulfur compounds such as taurine and dimethylsulfoniopropionate (DMSP). These interactions appear to increase photosynthesis and carbon fixation by the diatom, which may benefit the bacterium (Amin et al., 2015). *Ruegeria pomeroyi* DSS-3 alleviates vitamin B_{12} limitation of the diatom *T. pseudonana* in exchange for organosulfur compounds such as 2,3-dihydroxypropane-1-sulfonate and *N*-acetyltaurine (Durham et al., 2015). The interaction between both species appears to involve a range of genes involved in response to external stimuli, lipid and chitin biosynthesis in the diatom (Durham et al., 2017). *Phaeobacter inhibens* attaches to the coccolithophore *Emiliania huxleyi* and initially promotes its growth by converting algal-derived tryptophan to IAA (Segev

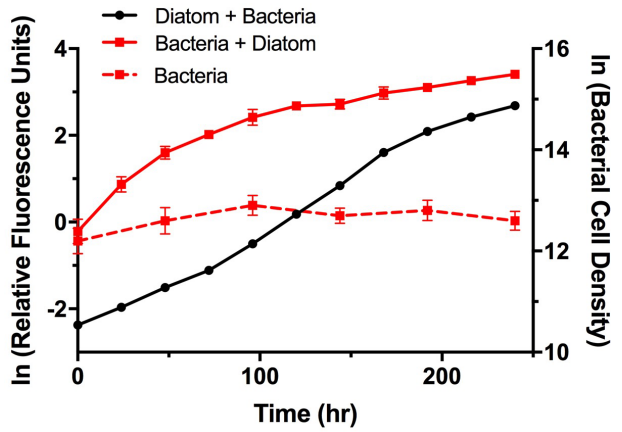

FIGURE 6 | Growth of A3 and its microbiome. Cultures were acclimated as described in the Section "Materials and Methods." Diatom growth (black circles) with its microbiome was monitored using relative fluorescence and bacterial growth with the diatom (red squares, solid line) or without the diatom (red squares, dashed line) was monitored using microscopy counts of Sybr Green I stained cells. Error bars represent standard deviation (SD) of six cultures.

et al., 2016). However, *P. inhibens* proceeds to kill *E. huxleyi* during later phases of growth by producing the algicidal molecules roseobacticides (Seyedsayamdost et al., 2011). In contrast, *Roseobacter* sp. DG874 significantly inhibits the growth of the dinoflagellate *Gymnodinium catenatum* potentially due to the bacterial ability to lyse algal cells (Bolch et al., 2017).

Analysis of the 21 Rhodobacteraceae OTUs found with both diatoms shows that only five were common to both diatoms (**Figure 4A**). Most OTUs exhibited variation across strains and time of culturing in the laboratory (**Figure 4B**), despite being highly conserved at the genus level. Such variations at the OTU level likely reflects different metabolic potential for these bacteria and it is not clear how these variations are reflected in interactions with the diatom. It is noteworthy that cocultures of A3 with two *Alteromonas* spp. that have near identical 16S rDNA gene (AGSF14, AGSF23) have different effects on the growth rate of A3 (**Table 2** and **Figure 7**). Interestingly, two OTUs were found consistently with all seven strains and across time. Of these, Rhodobacteraceae_otu A showed strong nucleotide identity to *Shimia* and *Nautella* species, including four strains that we isolated from *A. glacialis*. These findings suggest that our *Shimia* and *Nautella* isolates may represent a good model to examine diatom–bacteria interactions given that they are closely related to an OTU that was found consistently with two diatom species across seven strains. Interestingly, two *S. marina* strains (AGSF11, AGSF28) showed no effect on the growth rate of A3 while a *Nautella* strain (AGSF5) enhanced the growth rate of A3 relative to axenic control (**Table 2** and **Figure 7**). Given that these cocultures were conducted in optimal media under no nutrient limitations it is likely that these bacteria interact with the diatom under special conditions (i.e., nutrient limitation or environmental disturbance).

A. glacialis and *N. longissima* isolates also harbored a significant number of reads that belonged to *Neptuniibacter* (**Figure 3**), a genus of γ-proteobacteria that has been shown to be a major player in response to phytoplankton-derived organic matter during blooms (Beier et al., 2014). *Neptuniibacter* reads have also been detected in cultures of toxigenic diatoms (Guannel et al., 2011) and close relatives have been shown to significantly contribute to vitamin B_{12} production in the Southern Ocean sea ice edge where diatom communities dominate (Bertrand et al., 2015). Members of the same family have also been shown to closely associate with blooms of the haptophyte *Phaeocystis antarctica* where they appear to also contribute to vitamin biosynthesis (Delmont et al., 2015).

Other notable OTUs found in both diatoms were unclassified Flavobacteriaceae (**Figure 3**), which contain several members that have been shown to be algicidal to diatoms (Paul and Pohnert, 2011; van Tol et al., 2017). All cultures at 20 days contained one single OTU that belonged to *Mesorhizobium*, which persisted over time in *A. glacialis* but disappeared after 20 days in *N. longissima* (**Figure 3**). *Mesorhizobium* are nitrogen-fixing rhizobial symbionts that provide ammonia to legumes in exchange for organic carbon. Interactions between both taxa involve the production of IAA by the bacterium to facilitate engulfment of bacterial colonies by the plant root hairs (Laranjo et al., 2014). Two members of *Mesorhizobium* have been previously recovered from single-cell diatom isolates from station ALOHA (Baker and Kemp, 2014), suggesting they may be an overlooked components of diatom consortia. It remains to be seen whether these bacteria also fix nitrogen in seawater and whether their interactions with diatoms resemble interactions with plants in soil environments. It is noteworthy that in our sequencing efforts, we attempted to amplify 16S rDNA of archaea; however, we were not able to detect any genuine archaeal sequences suggesting no archaea associate with either diatoms.

A. glacialis is a blooming, cosmopolitan diatom that has been isolated from the coastal regions of every continent, including tropical, subtropical and temperate zones (Körner, 1970; Rao, 1969; Choudhury and Panigrahy, 1989). Several studies highlight its dominance in surf zones, where *A. glacialis* is believed to be a major producer of dissolved organic carbon (Lewin and Norris, 1970; Karentz and Smayda, 1984; Du Preez et al., 1989). Several studies also report that bacteria exhibit chemotaxis toward *A. glacialis* exudates (Riquelme and Ishida, 1988) and that some *A. glacialis* strains cannot be grown without specific bacteria (Riquelm et al., 1988). Together, these observations suggest that *A. glacialis* is an important phytoplankton species that interacts with bacteria and likely plays an important role in carbon cycling. Therefore, we focused further efforts on examining whether *A. glacialis* growth is controlled by bacteria.

The varied response of *A. glacialis* A3 to different bacterial isolates highlights the complexity of algal–bacterial interactions. We were only able to cultivate bacteria that belonged to the *Alteromonadaceae* and *Rhodobacteraceae* families (*Alteromonas*, *Shimia*, and *Nautella*) (**Figure 5**). Most *Alteromonas* isolates had no significant effect on A3 with the exception of *A. macleodii*

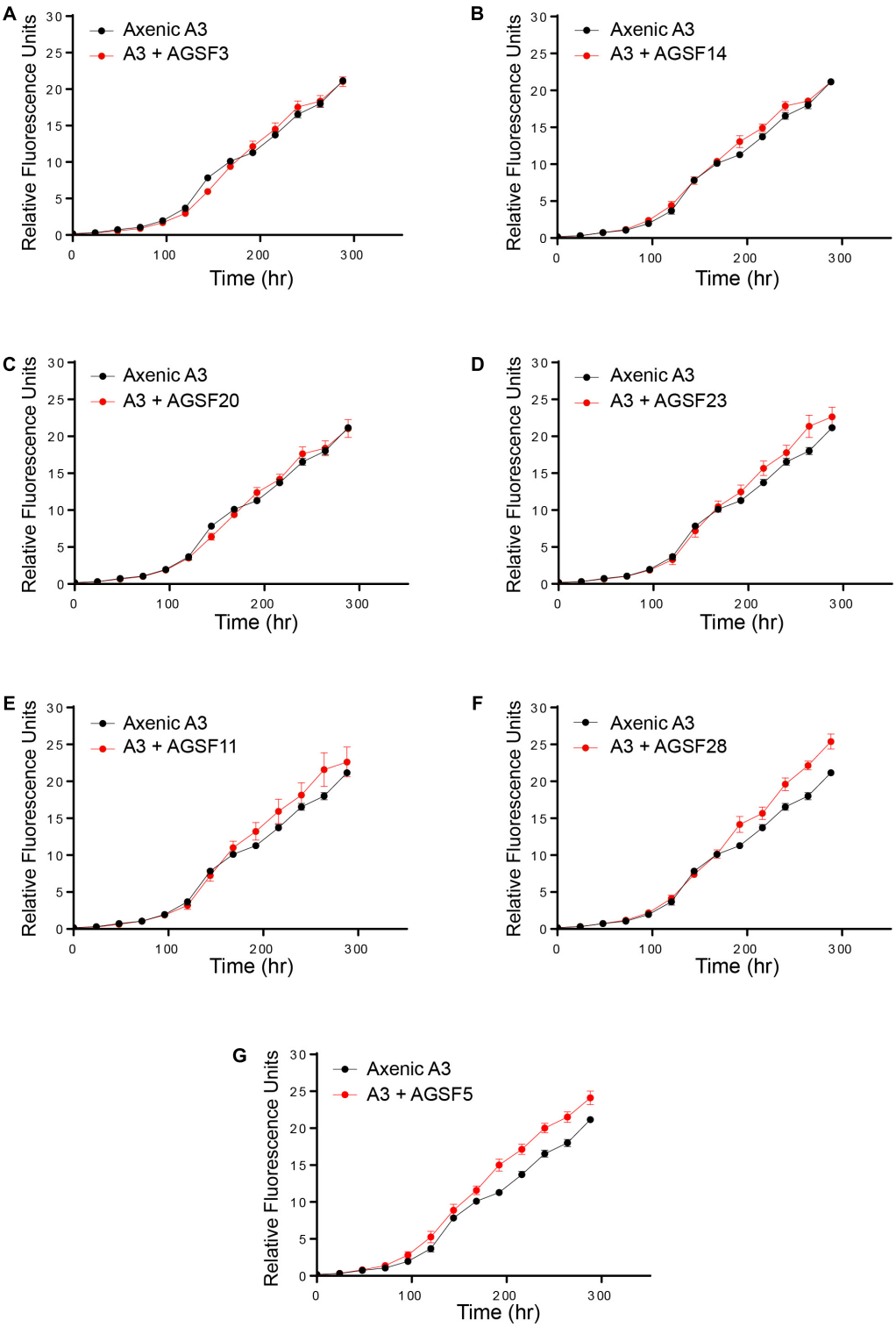

FIGURE 7 | Cocultures of A3 with cultivable bacterial representatives from its microbiome show varying effects of bacterial isolates on the diatom. **(A,C)** Coculture of A3 with two *Alteromonas* sp. isolates. **(B,D)** Coculture of A3 with two *A. macleodii* strains. **(E,F)** Coculture of A3 with two *S. marina* strains. **(G)** Coculture of A3 with a *Nautella* sp. isolate. Error bars represent SD of six cultures.

TABLE 2 | Change in A3 growth rate (μ) as a function of coculture with different bacteria relative to axenic growth.

Bacterial genus	Name	$\mu_{axenic} \pm SD$	$\mu_{co-culture} \pm SD$	% Change in μ
Alteromonas				
	AGSF14	0.61 ± 0.02	0.65 ± 0.02	5.3**
	AGSF3	0.61 ± 0.02	0.60 ± 0.01	2.8
	AGSF20	0.61 ± 0.02	0.60 ± 0.01	−0.2
	AGSF23	0.61 ± 0.02	0.60 ± 0.01	−1.7
Nautella				
	AGSF5	0.61 ± 0.02	0.66 ± 0.02	7.4*
Ruegeria				
	AGSA97†	0.72 ± 0.02	0.84 ± 0.03	17*
Shimia				
	AGSF11	0.61 ± 0.02	0.63 ± 0.02	2.6
	AGSF28	0.61 ± 0.02	0.61 ± 0.01	−0.2
Sulfitobacter				
	SA11†	0.72 ± 0.02	0.88 ± 0.1	22*
Croceibacter				
	SA60†	0.72 ± 0.02	0.57 ± 0.03	−14*

*Standard deviations (SDs) were calculated from six cultures. †Bacteria previously isolated from other diatom cultures. *$p < 0.01$ (ANOVA); **$p < 0.05$ (ANOVA).*

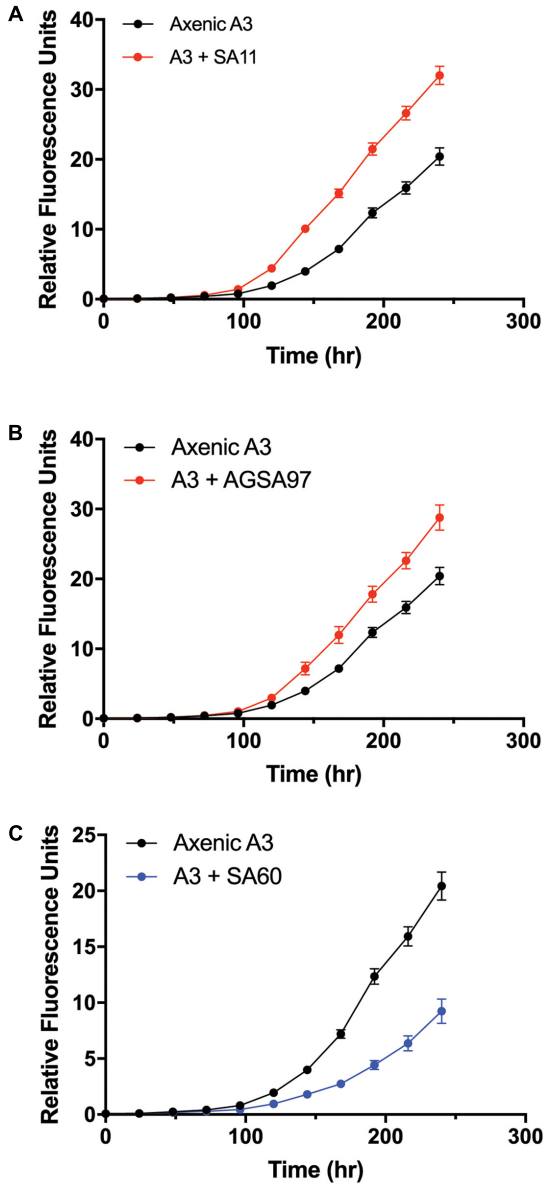

FIGURE 8 | Cocultures of A3 with cultivable bacterial representatives isolated from the diatoms *P. multiseries* and *Asterionella* sp. show either growth enhancement or inhibition on the diatom. **(A)** Coculture of A3 with *Sulfitobacter* sp. SA11 isolated from the pennate diatom *P. multiseries*. **(B)** Coculture of A3 with *Ruegeria* sp. AGSA97 isolated from the pennate diatom *Asterionella* sp. **(C)** Coculture of A3 with *Croceibacter atlanticus* SA60 isolated from *P. multiseries*. Error bars represent SD of six cultures.

strain AGSF14. Variable responses between diatoms and bacteria across strains has been documented before (Amin et al., 2015), though the mechanisms of why these variations occur are not understood. *Nautella* sp. AGSF5 also enhanced the growth rate of A3 (**Figure 7G**). Bacteria belonging to *Nautella* have been shown to confer resistance to the diatom *Chaetoceros tenuissimus* against viral infection, suggesting they may have a role in algal health and growth (Kimura and Tomaru, 2014).

The consistent growth response of axenic A3 to several bacteria that were previously isolated from other pennate diatoms suggests that the mechanisms of interactions between these bacteria and their original diatom hosts are similar to their interactions with A3. These observations may suggest that diatoms and bacteria interact using common sets of genes and molecules that can be complemented with different hosts or bacteria. For example, *Sulfitobacter* sp. SA11 enhances the growth rate of *P. multiseries* by 19–35% by producing the hormone IAA (Amin et al., 2015). In cocultures reported here, *Sulfitobacter* sp. SA11 enhances the growth rate of A3 by 22% relative to axenic control (**Figure 8A** and **Table 1**), in line with experiments with *P. multiseries*. This observation also suggests that other growth enhancing bacteria, e.g., *Ruegeria* sp. AGSA97 (**Figure 8B**) may use the same mechanism to enhance diatom growth. Likewise, *C. atlanticus* SA60 inhibits the growth of several diatoms including its original host, *P. multiseries*, by ≥ 53%, *P. fraudulenta* by 34%, *T. oceanica* by 15% and *T. pseudonana* by 33% (van Tol et al., 2017). In cocultures reported here, *C. atlanticus* SA60 inhibits the growth rate of A3 by 14% (**Figure 8C** and **Table 1**). The mechanisms of inhibition in A3 may be similar to those reported previously.

Our results suggest that diatoms maintain a stable microbiome even under laboratory culturing conditions and that members of their microbiomes are consistent across different diatom isolates from the same species. These findings strengthen approaches that aim to isolate bacteria from old algal cultures and study their interactions with their algal host. One important caveat to our approach is that the diatom microbiomes were characterized 20 days after isolation. During this time, there may have been changes to the microbiome relative to what was isolated from seawater. Further work is needed to close this gap in knowledge.

Since algal-associated bacteria can enhance or inhibit algal growth, these interactions may play an important role in carbon and nutrient cycling. Further work is needed to examine the bacterial diversity across a wide range of phytoplankton species and elucidate their importance to biogeochemistry.

AUTHOR CONTRIBUTIONS

GB, MO, and SA designed the experiments. GB, MO, JF, CF, and JK carried out the experiments. GB isolated and identified the diatoms and along with MO characterized their microbial communities. GB, JF, and CF isolated and identified bacteria and conducted coculture experiments. JK conducted the SEM analysis. All authors were involved in writing and reviewing the manuscript.

FUNDING

The study was supported by the NYU Abu Dhabi Research Fund AD179 to SA.

ACKNOWLEDGMENTS

The authors would like to thank the NYU Abu Dhabi Core Technology Platforms for support and the UNC Wilmington Microscopy Facilities.

REFERENCES

Abby, S. S., Touchon, M., De Jode, A., Grimsley, N., and Piganeau, G. (2014). Bacteria in *Ostreococcus tauri* cultures - friends, foes or hitchhikers? *Front. Microbiol.* 5:505. doi: 10.3389/fmicb.2014.00505

Altschul, S. F., Gish, W., Miller, W., Myers, E. W., and Lipman, D. J. (1990). Basic local alignment search tool. *J. Mol. Biol.* 215, 403–410. doi: 10.1016/S0022-2836(05)80360-2

Amin, S. A., Green, D. H., Hart, M. C., Küpper, F. C., Sunda, W. G., and Carrano, C. J. (2009). Photolysis of iron-siderophore chelates promotes bacterial-algal mutualism. *Proc. Natl. Acad. Sci. U.S.A.* 106, 17071–17076. doi: 10.1073/pnas.0905512106

Amin, S. A., Hmelo, L. R., van Tol, H. M., Durham, B. P., Carlson, L. T., Heal, K. R., et al. (2015). Interaction and signalling between a cosmopolitan phytoplankton and associated bacteria. *Nat. Microbiol.* 522, 98–101. doi: 10.1038/nature14488

Amin, S. A., Parker, M. S., and Armbrust, E. V. (2012). Interactions between diatoms and bacteria. *Microbiol. Mol. Biol. Rev.* 76, 667–684. doi: 10.1128/MMBR.00007-12

Azam, F., and Malfatti, F. (2007). Microbial structuring of marine ecosystems. *Nat. Rev. Microbiol.* 5, 782–791. doi: 10.1038/nrmicro1747

Baker, L. J., and Kemp, P. F. (2014). Exploring bacteria–diatom associations using single-cell whole genome amplification. *Aquat. Microb. Ecol.* 72, 73–88. doi: 10.3354/ame01686

Beerli, P. (2006). Comparison of Bayesian and maximum-likelihood inference of population genetic parameters. *Bioinformatics* 22, 341–345. doi: 10.1093/bioinformatics/bti803

Beier, S., Rivers, A. R., Moran, M. A., and Obernosterer, I. (2014). The transcriptional response of prokaryotes to phytoplankton-derived dissolved organic matter in seawater. *Environ. Microbiol.* 17, 3466–3480. doi: 10.1111/1462-2920.12434

Bell, W., and Mitchell, R. (1972). Chemotactic and growth responses of marine bacteria to algal extracellular products. *Biol. Bull.* 143, 265–277. doi: 10.2307/1540052

Bertrand, E. M., McCrow, J. P., Moustafa, A., Zheng, H., McQuaid, J. B., Delmont, T. O., et al. (2015). Phytoplankton-bacterial interactions mediate micronutrient colimitation at the coastal Antarctic sea ice edge. *Proc. Natl. Acad. Sci. U.S.A.* 112, 9938–9943. doi: 10.1073/pnas.1501615112

Biddanda, B., and Benner, R. (1997). Carbon, nitrogen, and carbohydrate fluxes during the production of particulate and dissolved organic matter by marine phytoplankton. *Limnol. Oceanogr.* 42, 506–518. doi: 10.4319/lo.1997.42.3.0506

Biegala, I. C., Kennaway, G., Alverca, E., Lennon, J.-F., Vaulot, D., and Simon, N. (2002). Identification of bacteria associated with dinoflagellates (Dinophyceae) Alexandrium spp. using tyramide signal amplification-fluorescent *in situ* hybridization and confocal microscopy. *J. Phycol.* 38, 404–411. doi: 10.1046/j.1529-8817.2002.01045.x

Bolch, C. J. S., Bejoy, T. A., and Green, D. H. (2017). Bacterial associates modify growth dynamics of the dinoflagellate *Gymnodinium catenatum*. *Front. Microbiol.* 8:670. doi: 10.3389/fmicb.2017.00670

Bolch, C. J. S., Subramanian, T. A., and Green, D. H. (2011). The toxic dinoflagellate *Gymnodinium catenatum* (Dinophyceae) requires marine bacteria for growth. *J. Phycol.* 47, 1009–1022. doi: 10.1111/j.1529-8817.2011.01043.x

Brand, L. E., Guillard, R. R. L., and Murphy, L. S. (1981). A method for the rapid and precise determination of acclimated phytoplankton reproduction rates. *J. Plankton Res.* 3, 193–201. doi: 10.1093/plankt/3.2.193

Caporaso, J. G., Kuczynski, J., Stombaugh, J., Bittinger, K., Bushman, F. D., Costello, E. K., et al. (2010). QIIME allows analysis of high-throughput community sequencing data. *Nat. Methods* 7, 335–336. doi: 10.1038/nmeth.f.303

Cho, B. C., and Azam, F. (1988). Major role of bacteria in biogeochemical fluxes in the ocean's interior. *Nat. Microbiol.* 332, 441–443. doi: 10.1038/332441a0

Choudhury, S. B., and Panigrahy, R. C. (1989). Occurrence of bloom of diatom *Asterionella glacialis* in nearshore waters of Gopalpur, Bay of Bengal. *Indian J. Mar. Sci.* 18, 204–206.

Cole, J. J. (1982). Interactions between bacteria and algae in aquatic ecosystems. *Annu. Rev. Ecol. Evol. Syst.* 13, 291–314. doi: 10.1146/annurev.es.13.110182.001451

Croft, M. T., Lawrence, A. D., Raux-Deery, E., Warren, M. J., and Smith, A. G. (2005). Algae acquire vitamin B12 through a symbiotic relationship with bacteria. *Nat. Microbiol.* 438, 90–93. doi: 10.1038/nature04056

Delmont, T. O., Eren, A. M., Vineis, J. H., and Post, A. F. (2015). Genome reconstructions indicate the partitioning of ecological functions inside a phytoplankton bloom in the Amundsen Sea, Antarctica. *Front. Microbiol.* 6:1090. doi: 10.3389/fmicb.2015.01090

Drummond, A. J., Suchard, M. A., Xie, D., and Rambaut, A. (2012). Bayesian phylogenetics with BEAUti and the BEAST 1.7. *Mol. Biol. Evol.* 29, 1969–1973. doi: 10.1093/molbev/mss075

Du Preez, D. R., Campbell, E. E., and Bate, G. C. (1989). First recorded bloom of the diatom *Asterionella glacialis* Castracane in the surf-zone of the Sundays River Beach. *Bot. Mar.* 32, 503–504. doi: 10.1515/botm.1989.32.6.503

Durham, B. P., Dearth, S. P., Sharma, S., Amin, S. A., Smith, C. B., Campagna, S. R., et al. (2017). Recognition cascade and metabolite transfer in a marine bacteria-phytoplankton model system. *Environ. Microbiol.* 21, 2104–2114. doi: 10.1111/1462-2920.13834

Durham, B. P., Sharma, S., Luo, H., Smith, C. B., Amin, S. A., Bender, S. J., et al. (2015). Cryptic carbon and sulfur cycling between surface ocean plankton. *Proc. Natl. Acad. Sci. U.S.A.* 112, 453–457. doi: 10.1073/pnas.1413137112

Eigemann, F., Hilt, S., Salka, I., and Grossart, H.-P. (2013). Bacterial community composition associated with freshwater algae: species specificity vs. dependency on environmental conditions and source community. *FEMS Microbiol. Ecol.* 83, 650–663. doi: 10.1111/1574-6941.12022

Falkowski, P. G., Fenchel, T., and Delong, E. F. (2008). The microbial engines that drive earth's biogeochemical cycles. *Science* 320, 1034–1039. doi: 10.1126/science.1153213

Field, C., Behrenfeld, M., Randerson, J., and Falkowski, P. (1998). Primary production of the biosphere: integrating terrestrial and oceanic components. *Science* 281, 237–240. doi: 10.1126/science.281.5374.237

Franco, A. O., They, N. H., Canani, L. G., Maggioni, R., and Odebrecht, C. (2016). *Asterionellopsis tropicalis* (Bacillariophyceae): a new tropical species found in diatom accumulations. *J. Phycol.* 52, 888–895. doi: 10.1111/jpy.12435

Frischkorn, K. R., Rouco, M., Van Mooy, B. A., and Dyhrman, S. T. (2017). Epibionts dominate metabolic functional potential of *Trichodesmium* colonies from the oligotrophic ocean. *ISME J.* 180, 1–12. doi: 10.1038/ismej.2017.74

Geng, H., and Belas, R. (2010). Molecular mechanisms underlying roseobacter-phytoplankton symbioses. *Curr. Opin. Biotechnol.* 21, 332–338. doi: 10.1016/j.copbio.2010.03.013

Goecke, F., Thiel, V., Wiese, J., Labes, A., and Imhoff, J. F. (2013). Algae as an important environment for bacteria – phylogenetic relationships among new bacterial species isolated from algae. *Phycologia* 52, 14–24. doi: 10.2216/12-24.1

Green, D. H., Echavarri-Bravo, V., Brennan, D., and Hart, M. C. (2015). Bacterial diversity associated with the coccolithophorid algae *Emiliania huxleyi* and *Coccolithus pelagicus* f. *braarudii*. *Biomed. Res. Int.* 2015:194540. doi: 10.1155/2015/194540

Green, D. H., Llewellyn, L. E., Negri, A. P., Blackburn, S. I., and Bolch, C. J. S. (2004). Phylogenetic and functional diversity of the cultivable bacterial community associated with the paralytic shellfish poisoning dinoflagellate *Gymnodinium catenatum*. *FEMS Microbiol. Ecol.* 47, 345–357. doi: 10.1016/S0168-6496(03)00298-8

Grossart, H.-P., Levold, F., Allgaier, M., Simon, M., and Brinkhoff, T. (2005). Marine diatom species harbour distinct bacterial communities. *Environ. Microbiol.* 7, 860–873. doi: 10.1111/j.1462-2920.2005.00759.x

Guannel, M. L., Horner-Devine, M., and Rocap, G. (2011). Bacterial community composition differs with species and toxigenicity of the diatom Pseudo-nitzschia. *Aquat. Microb. Ecol.* 64, 117–133. doi: 10.3354/ame01513

Guillard, R. R. L. (1975). "Culture of phytoplankton for feeding marine invertebrates," in *Culture of Marine Invertebrate Animals*, eds W. L. Smith and M. H. Chanley (Boston, MA: Springer), 29–60. doi: 10.1007/978-1-4615-8714-9_3

Guindon, S., Dufayard, J.-F., Lefort, V., Anisimova, M., Hordijk, W., and Gascuel, O. (2010). New algorithms and methods to estimate maximum-likelihood phylogenies: assessing the performance of PhyML 3.0. *Syst. Biol.* 59, 307–321. doi: 10.1093/sysbio/syq010

Hasegawa, Y., Martin, J. L., Giewat, M. W., and Rooney-Varga, J. N. (2007). Microbial community diversity in the phycosphere of natural populations of the toxic alga, *Alexandrium fundyense*. *Environ. Microbiol.* 9, 3108–3121. doi: 10.1111/j.1462-2920.2007.01421.x

Kaczmarska, I., Davidovich, N. A., and Ehrman, J. M. (2007). Sex cells and reproduction in the diatom *Nitzschia longissima* (Bacillariophyta): discovery of siliceous scales in gamete cell walls and novel elements of the perizonium. *Phycologia* 46, 726–737. doi: 10.2216/07-04.1

Karentz, D., and Smayda, T. J. (1984). Temperature and seasonal occurrence patterns of 30 dominant phytoplankton species in Narragansett Bay over a 22-year period (1959–1980). *Mar. Ecol. Prog. Ser.* 18, 277–293. doi: 10.3354/meps018277

Katoh, K., and Standley, D. M. (2013). MAFFT multiple Sequence alignment software version 7: improvements in performance and usability. *Mol. Biol. Evol.* 30, 772–780. doi: 10.1093/molbev/mst010

Kazamia, E., Helliwell, K. E., Purton, S., and Smith, A. G. (2016). How mutualisms arise in phytoplankton communities: building eco-evolutionary principles for aquatic microbes. *Ecol. Lett.* 19, 810–822. doi: 10.1111/ele.12615

Kimura, K., and Tomaru, Y. (2014). Coculture with marine bacteria confers resistance to complete viral lysis of diatom cultures. *Aquat. Microb. Ecol.* 73, 69–80. doi: 10.3354/ame01705

Körner, H. (1970). Morphologie und Taxonomie der Diatomeengattung Asterionella. Nova Hedwigia 20, 557–723.

Lanave, C., Preparata, G., Sacone, C., and Serio, G. (1984). A new method for calculating evolutionary substitution rates. *J. Mol. Evol.* 20, 86–93. doi: 10.1007/BF02101990

Laranjo, M., Alexandre, A., and Oliveira, S. (2014). Legume growth-promoting rhizobia: an overview on the *Mesorhizobium* genus. *Microbiol. Res.* 169, 2–17. doi: 10.1016/j.micres.2013.09.012

Lefort, V., Longueville, J.-E., and Gascuel, O. (2017). SMS: smart model selection in PhyML. *Mol. Biol. Evol.* 34, 2422–2424. doi: 10.1093/molbev/msx149

Lewin, J., and Norris, R. E. (1970). Surf-zone diatoms of the coasts of Washington and New Zealand (*Chaetoceros armatum* T. West and *Asterionella* spp.). *Phycologia* 9, 143–149. doi: 10.2216/i0031-8884-9-2-143.1

Lunau, M., Lemke, A., Walther, K., Martens-Habbena, W., and Simon, M. (2005). An improved method for counting bacteria from sediments and turbid environments by epifluorescence microscopy. *Environ. Microbiol.* 7, 961–968. doi: 10.1111/j.1462-2920.2005.00767.x

Martin, J. H., and Fitzwater, S. E. (1988). Iron deficiency limits phytoplankton growth in the north-east Pacific subarctic. *Nature* 331, 341–343. doi: 10.1038/331341a0

Mayali, X., Franks, P. J. S., and Azam, F. (2008). Cultivation and ecosystem role of a marine *Roseobacter* clade-affiliated cluster bacterium. *Appl. Environ. Microbiol.* 74, 2595–2603. doi: 10.1128/aem.02191-07

Medlin, L., Elwood, H. J., Stickel, S., and Sogin, M. L. (1988). The characterization of enzymatically amplified eukaryotic 16S-like rRNA-coding regions. *Gene* 71, 491–499. doi: 10.1016/0378-1119(88)90066-2

Mendes, R., Kruijt, M., de Bruijn, I., Dekkers, E., van der Voort, M., Schneider, J. H. M., et al. (2011). Deciphering the rhizosphere microbiome for disease-suppressive bacteria. *Science* 332, 1097–1100. doi: 10.1126/science.1203980

Moniz, M. B., and Kaczmarska, I. (2010). Barcoding of diatoms: nuclear encoded ITS revisited. *Protist* 161, 7–34. doi: 10.1016/j.protis.2009.07.001

Parada, A. E., Needham, D. M., and Fuhrman, J. A. (2016). Every base matters: assessing small subunit rRNA primers for marine microbiomes with mock communities, time series and global field samples. *Environ. Microbiol.* 18, 1403–1414. doi: 10.1111/1462-2920.13023

Paul, C., and Pohnert, G. (2011). Interactions of the algicidal bacterium *Kordia algicida* with diatoms: regulated protease excretion for specific algal lysis. *PLoS One* 6:e21032. doi: 10.1371/journal.pone.0021032

Paul, C., and Pohnert, G. (2013). Induction of protease release of the resistant diatom *Chaetoceros didymus* in response to lytic enzymes from an algicidal bacterium. *PLoS One* 8:e57577. doi: 10.1371/journal.pone.0057577

Quast, C., Pruesse, E., Yilmaz, P., Gerken, J., Schweer, T., Yarza, P., et al. (2012). The SILVA ribosomal RNA gene database project: improved data processing and web-based tools. *Nucleic Acids Res.* 41, D590–D596. doi: 10.1093/nar/gks1219

Rao, D. V. S. (1969). *Asterionella japonica* bloom and discoloration off Waltair, Bay of Bengal. *Limnol. Oceanogr.* 14, 632–634. doi: 10.4319/lo.1969.14.4.0632

Rappé, M. S., and Giovannoni, S. J. (2003). The uncultured microbial majority. *Annu. Rev. Microbiol.* 57, 369–394. doi: 10.1146/annurev.micro.57.030502.090759

Riquelm, C. E., Fukami, K., and Ishida, Y. (1988). Effects of bacteria on the growth of a marine diatom, *Asterionella glacialis*. *Bull. Jpn. Soc. Microb. Ecol.* 3, 29–34. doi: 10.1264/microbes1986.3.29

Riquelme, C. E., and Ishida, Y. (1988). Chemotaxis of bacteria to extracellular products of marine bloom algae. *J. Gen. Appl. Microbiol.* 34, 417–423. doi: 10.2323/jgam.34.417

Ronquist, F., and Huelsenbeck, J. P. (2003). MrBayes 3: Bayesian phylogenetic inference under mixed models. *Bioinformatics* 19, 1572–1574. doi: 10.1093/bioinformatics/btg180

Ryther, J. H., and Guillard, R. (1962). Studies of marine planktonic diatoms:II. Use of *Cyclotella nana* Hustedt for assays of vitamin B_{12} in sea water. *Can. J. Microbiol.* 8, 437–445. doi: 10.1128/AEM.02380-14

Sapp, M., Schwaderer, A., Wiltshire, K., Hoppe, H.-G., Gerdts, G., and Wichels, A. (2007). Species-specific bacterial communities in the phycosphere of microalgae? *Microb. Ecol.* 53, 683–699. doi: 10.1007/s00248-006-9162-5

Schloss, P. D., Westcott, S. L., Ryabin, T., Hall, J. R., Hartmann, M., Hollister, E. B., et al. (2009). Introducing mothur: open-source, platform-independent, community-supported software for describing and comparing microbial communities. *Appl. Environ. Microbiol.* 75, 7537–7541. doi: 10.1128/AEM.01541-09

Segev, E., Wyche, T. P., Kim, K. H., Petersen, J., Ellebrandt, C., Vlamakis, H., et al. (2016). Dynamic metabolic exchange governs a marine algal-bacterial interaction. *Elife* 5:e17473. doi: 10.7554/eLife.17473

Seyedsayamdost, M. R., Case, R. J., Kolter, R., and Clardy, J. (2011). The Jekyll-and-Hyde chemistry of *Phaeobacter gallaeciensis*. *Nat. Chem.* 3, 331–335. doi: 10.1038/nchem.1002

Seymour, J. R., Amin, S. A., Raina, J.-B., and Stocker, R. (2017). Zooming in on the phycosphere: the ecological interface for phytoplankton-bacteria relationships. *Nat. Microbiol.* 2:17065. doi: 10.1038/nmicrobiol.2017.65

Shishlyannikov, S. M., Zakharova, Y. R., Volokitina, N. A., Mikhailov, I. S., Petrova, D. P., and Likhoshway, Y. V. (2011). A procedure for establishing an axenic culture of the diatom *Synedra acus* subsp. *radians* (Kütz.) Skabibitsch. from Lake Baikal. *Limnol. Oceanogr. Methods* 9, 478–484. doi: 10.4319/lom.2011.9.478

Sison-Mangus, M. P., Jiang, S., Tran, K. N., and Kudela, R. M. (2014). Host-specific adaptation governs the interaction of the marine diatom, Pseudo-nitzschia and their microbiota. *ISME J* 8, 63–76. doi: 10.1038/ismej.2013.138

Stamatakis, A. (2006). RAxML-VI-HPC: maximum likelihood-based phylogenetic analyses with thousands of taxa and mixed models. *Bioinformatics* 22, 2688–2690. doi: 10.1093/bioinformatics/btl446

Stamatakis, A., Hoover, P., Rougemont, J., and Renner, S. (2008). A rapid Bootstrap Algorithm for the RAxML Web Servers. *Syst. Biol.* 57, 758–771. doi: 10.1080/10635150802429642

Takai, K., and Horikoshi, K. (2000). Rapid detection and quantification of members of the archaeal community by quantitative PCR using fluorogenic probes. *Appl. Environ. Microbiol.* 66, 5066–5072. doi: 10.1128/AEM.66.11.5066-5072.2000

Tang, Y.-Z., Koch, F., and Gobler, C. J. (2010). Most harmful algal bloom species are vitamin B_1 and B_{12} auxotrophs. *Proc. Natl. Acad. Sci. U.S.A.* 107, 20756–20761. doi: 10.1073/pnas.1009566107

van Tol, H. M., Amin, S. A., and Armbrust, E. V. (2017). Ubiquitous marine bacterium inhibits diatom cell division. *ISME J.* 11, 31–42. doi: 10.1038/ismej.2016.112

White, T. J., Bruns, T., Lee, S., and Taylor, J. W. (1990). "Amplification and direct sequencing of fungal ribosomal RNA genes for phylogenetics," in *PCR Protocols: A Guide to Methods and Applications*, eds M. A. Innis, D. H. Gelfand, J. J. Sninsky, and T. J. White (New York: Academic Press Inc.), 315–322.

Worden, A. Z., Follows, M. J., Giovannoni, S. J., Wilken, S., Zimmerman, A. E., and Keeling, P. J. (2015). Environmental science. Rethinking the marine carbon cycle: factoring in the multifarious lifestyles of microbes. *Science* 347:1257594. doi: 10.1126/science.1257594

ZoBell, C. E. (1941). Studies on marine bacteria. I. The cultural requirements of heterotrophic aerobes. *J. Mar. Res.* 4, 42–75.

Conflict of Interest Statement: The authors declare that the research was conducted in the absence of any commercial or financial relationships that could be construed as a potential conflict of interest.

frontiers in Microbiology

ORIGINAL RESEARCH
published: 04 December 2018
doi: 10.3389/fmicb.2018.02879

Bacterial Epibiotic Communities of Ubiquitous and Abundant Marine Diatoms Are Distinct in Short- and Long-Term Associations

*Klervi Crenn, Delphine Duffieux and Christian Jeanthon**

CNRS, Sorbonne Université, Station Biologique de Roscoff, Adaptation et Diversité en Milieu Marin, Roscoff, France

Interactions between phytoplankton and bacteria play a central role in mediating biogeochemical cycling and food web structure in the ocean. The cosmopolitan diatoms *Thalassiosira* and *Chaetoceros* often dominate phytoplankton communities in marine systems. Past studies of diatom-bacterial associations have employed community-level methods and culture-based or natural diatom populations. Although bacterial assemblages attached to individual diatoms represents tight associations little is known on their makeup or interactions. Here, we examined the epibiotic bacteria of 436 *Thalassiosira* and 329 *Chaetoceros* single cells isolated from natural samples and collection cultures, regarded here as short- and long-term associations, respectively. Epibiotic microbiota of single diatom hosts was analyzed by cultivation and by cloning-sequencing of 16S rRNA genes obtained from whole-genome amplification products. The prevalence of epibiotic bacteria was higher in cultures and dependent of the host species. Culture approaches demonstrated that both diatoms carry distinct bacterial communities in short- and long-term associations. Bacterial epibonts, commonly associated with phytoplankton, were repeatedly isolated from cells of diatom collection cultures but were not recovered from environmental cells. Our results suggest that in controlled laboratory culture conditions bacterial–diatom and bacterial–bacterial interactions select for a simplified, but specific, epibiotic microbiota shaped and adapted for long-term associations.

Keywords: diversity, heterotrophic bacteria, interactions, diatoms, *Thalassiosira*, *Chaetoceros*, microbiome, Western English Channel

OPEN ACCESS

Edited by:
Matthias Wietz,
Alfred Wegener Institut, Germany

Reviewed by:
Lydia Jeanne Baker,
Cornell University, United States
Bryndan Paige Durham,
University of Washington,
United States

****Correspondence:***
Christian Jeanthon
jeanthon@sb-roscoff.fr

Specialty section:
This article was submitted to Microbial Symbioses, a section of the journal Frontiers in Microbiology

Received: *27 February 2018*
Accepted: *09 November 2018*
Published: *04 December 2018*

Citation:
Crenn K, Duffieux D and Jeanthon C (2018) Bacterial Epibiotic Communities of Ubiquitous and Abundant Marine Diatoms Are Distinct in Short- and Long-Term Associations. Front. Microbiol. 9:2879. doi: 10.3389/fmicb.2018.02879

INTRODUCTION

Bacteria eukaryotic microalgae are the major components of the plankton in the upper and ocean layers and their metabolism largely controls pelagic energy flow and nutrient cycling (Falkowski et al., 2008). Determining how they interact is therefore essential to strengthen the understanding of these groups and how they impact marine biogeochemical cycles.

While heterotrophic prokaryotes and phytoplankton are known to interact through complex mechanisms (Azam and Malfatti, 2007), it is expected that they are very closely related in the planktonic environment. The immediate environment of marine phytoplankton cells or phycosphere (Bell and Mitchell, 1972) is considered as physically and chemically distinct from

the surrounding seawater, which promote the growth of specific microbial taxa, thus creating a dynamic of interactions which can help to explain the complexity of marine food webs (Seymour et al., 2017 and references therein). The use of rRNA gene sequencing and barcoding approaches allowed establishing links between phytoplankton and bacterial community dynamics in natural communities (Rooney-Varga et al., 2005; Teeling et al., 2012) and culture collections (Schäfer et al., 2002; Jasti et al., 2005; Sapp et al., 2007). These partners often co-occur which lead to beneficial, neutral or parasitic interactions (Amin et al., 2012; Cooper and Smith, 2015; Seymour et al., 2017).

Diatoms are a large component of marine biomass and produce about 25% of the total C fixed on Earth (Nelson et al., 1995; Field et al., 1998). These key ecological players of the modern ocean have been described as the most diverse group of phytoplankton (Armbrust, 2009). Their ecological success is mainly due to their numerous metabolic properties and to their silicified cell wall (Raven and Waite, 2004). Most of their evolutionary adaptations are due to the acquisition of genes from their endosymbiotic ancestors, and by indisputable horizontal gene transfers from marine bacteria, which are rarely documented in other eukaryotic organisms (Armbrust et al., 2004; Bowler et al., 2008). The co-occurrence of bacteria and diatoms in common habitats for more than 200 million years and their intimate associations likely played a major role in the ecological success and species diversification of diatoms (Amin et al., 2012).

Although few reports of diatom–bacterial interactions have used natural diatom populations (Kaczmarska et al., 2005; Rooney-Varga et al., 2005; Amin et al., 2012), most studies were performed using cultures (Grossart, 1999; Schäfer et al., 2002; Grossart et al., 2005; Kaczmarska et al., 2005; Grossart and Simon, 2007; Sapp et al., 2007; Behringer et al., 2018). Consistent associations between specific bacterial and diatom taxa have been found (Schäfer et al., 2002; Amin et al., 2012; Behringer et al., 2018), although other work suggests that the composition of diatom-associated bacterial assemblages shifts over weeks to months in culture (Sapp et al., 2007). Today, however, it remains unclear whether bacteria associated with diatom cells are species-specific (Grossart et al., 2005; Jasti et al., 2005; Rooney-Varga et al., 2005) or determined by bacterial source communities (Kaczmarska et al., 2005; Sapp et al., 2007).

Previous studies on the associations between bacteria and diatoms have mostly considered the bacteria at the population and community levels. The attachment of bacteria to algal cells represents, however, tight associations (Cole, 1982; Grossart et al., 2005). Indeed, Gärdes et al. (2011) demonstrated that attachment of specific bacteria to diatoms *Thalassiosira weissflogii* was required for transparent exopolymer particle formation and aggregation. Surprisingly, little is known regarding the interactions of bacterial assemblages attached to single host cells. The sole exceptions are a microscopy study documenting the abundance and mode of attachment of bacteria attached to individual diatoms (Kaczmarska et al., 2005) and a report evaluating the composition and variability of bacterial assemblages attached to individual diatoms (Baker and Kemp, 2014). More recently, Baker et al. (2016) examined the effect of abiotic and biotic factors on the composition of the attached bacteria associated to a *Chaetoceros* spp. culture.

In this study, our aim was to study tight associations between attached bacteria and diatom partners. For this, we focused on bacteria attached to single cells of the environmentally relevant diatom genera *Thalassiosira* and *Chaetoceros* in natural communities and in culture that were regarded as short- and long-term associations, respectively. These diatoms are ubiquitous and often numerically abundant phytoplankton species in marine systems (Leblanc et al., 2012) and they display the highest species diversity in the pelagic temperate phytoplankton community (Round et al., 1990; Hasle and Syvertsen, 1996). Based on a recent characterization of diatom diversity patterns on a global scale (Malviya et al., 2016), *Chaetoceros* and *Thalassiosira* represented the first and third most abundant ribotypes and were among the three most diverse genera. Although specific *Thalassiosira*–bacteria interactions have been studied (Gärdes et al., 2011; Durham et al., 2015; van Tol et al., 2017), the diversity of heterotrophic bacteria associated with both these globally significant phytoplankton genera is not well known. Furthermore, most past studies of the associations between phytoplankton and bacteria have used population or community-level approaches that may obscure cell-to-cell interactions. In this study, our major goal was to evaluate diatom-bacteria associations at an appropriate scale in focusing on the epibiotic microflora associated to *Chaetoceros* and *Thalassiosira* species. We evaluated the prevalence of attached bacteria to diatom cells and compared bacterial assemblages in both situations. We hypothesized that *in situ* bacterial associations differ from those in cultures and that the attachment of bacteria specific to each diatom was also favored in laboratory culture conditions.

MATERIALS AND METHODS

Diatom Cultures and Natural Samples

Clonal strains of *T. delicatula* RCC 2560 and *Chaetoceros danicus* RCC 2565 were obtained from the Roscoff Culture Collection (RCC). Both diatoms have been isolated from the same sample of surface seawater (1 m depth) collected in January 2011 offshore Roscoff at the Astan observatory site (60 m depth, 48°46′40″ N, 3°56′15″ W) using the RV Neomysis. The long-term maintenance of both strains in the RCC since their isolation is performed by regular subculturing at intervals of 2 weeks. Both strains are grown at 19°C in K medium for diatoms (Keller et al., 1987) with a 14:10 h light:dark cycle at 80 $\mu E.m^{-2}.s^{-1}$.

Natural surface seawater samples (1 m depth) were collected at the Astan and Estacade (48°43′56″ N, 3°58′58″ W) sites in March/April 2014 (molecular approach) and in July/August 2014 (culture approach) to isolate *Thalassiosira* and *Chaetoceros* cells. A recent analysis of the microphytoplankton abundance and diversity at Astan demonstrated that *Thalassiosira* and *Chaetoceros* are abundant (above 500 $cells.L^{-1}$ on average in all the 157 samples analyzed from 2000 to 2010) and able to become dominating at times (Guilloux et al., 2013). Diatom populations

in this system vary throughout the year in both species diversity and abundance of individual species.

Scanning Electron Microscopy

To visualize the epibionts attached on diatom cells, we roughly followed the protocol described by Kaczmarska et al. (2005). Diatom cultures (about 2 ml) were fixed for 2 h in 3% glutaraldehyde, filtered by gravity on 5 μm polycarbonate membranes (Isopore, Millipore) and washed three times with 10 ml of 0.22 μm filter-sterilized seawater. Samples were then dehydrated in a graded series of ethanol (two successive ethanol baths at 30, 50, 70, 90% and three at 100%) for at least 10 min at each grade. Ethanol solutions (3 ml) in the filtration tower were exchanged with gentle vacuum. After critical point drying (Bal-Ted CDP 030, Balzers, Liechtenstein), the samples were sputtered with gold and examined using a Phenom G2 Pro desktop scanning electron microscope (Phenom world). Only intact cells allowing visualization of one fully exposed side of the cingulum and valve or spine (according the diatom) at a time were analyzed. Only the bacteria that demonstrated clear evidence of attachment were counted (Kaczmarska et al., 2005).

Single Diatom Cell Isolation

Single diatom cells were isolated under sterile conditions in a laminar flow hood. To lower the number of free-living bacteria in the algal cultures and to concentrate microalgae from natural seawater samples, algal cells were first gently separated by gravity using a 47 mm diameter, 11 μm pore-size nylon filter (Millipore) and washed three times with 50 mL of autoclaved seawater. Single cells were picked with a sterile glass capillary micropipette and washed 3–4 times with filter-sterilized seawater for further bacterial epibiont culture or with sterile phosphate-buffered saline (PBS; 37 mM NaCl, 2.7 mM KCl, 10 mM Na_2HPO_4, 2 mM KH_2PO_4, pH 7.5) for further direct molecular identification of epibionts. We previously observed that replacement of sterile seawater by PBS as washing solution improved the PCR amplification success. Single cells were directly transferred in culture medium or kept on ice until further DNA extraction. For both approaches, controls were performed for each diatom cell isolated by checking the absence of bacteria in the last seawater or PBS drop used in the washing series (see below). Since these isolation steps were time-consuming, several independent late exponential cultures of both diatoms and seawater samples were needed to isolate a sufficient number of epibionts using both approaches.

Culture of Bacterial Epibionts

For cultivation of diatom epibionts, single isolated algal cells and controls were directly transferred in 48-well plates containing low-nutrient heterotrophic medium (LNHM) (Rappé et al., 2002) prepared by dissolving 35 g/L of commercial sea salts (Red Sea Europe) instead of using natural seawater. Bacterial cultures were incubated at 19°C for up to 6 weeks and growth was examined by flow cytometry using a BD Accuri C6 cytometer (BD Biosciences). For flow cytometry, 100 μl cultures were fixed with glutaraldehyde (0.25%, final concentration) and stained with SYBR Green (Life Technologies) as described by Marie et al. (1997). Cultures that contained bacteria were streaked on LNHM agar and selected colonies were purified by subculturing. Some of the isolates obtained in this study are available at the RCC.

Dereplication of Bacterial Isolates

In order to eliminate duplicates, bacterial isolates were dereplicated by matrix-assisted laser desorption ionization–time of flight mass spectrometry (MALDI-TOF MS) (Ghyselinck et al., 2011). Colonies were obtained by growing the isolates on marine agar medium (1:10; 0.5 g peptone, 0.1 g yeast extract, 35 g sea salts dissolved in 1 L of Milli-Q water) at room temperature for 4–7 days according to their growth rate. A small amount of colony was directly applied onto a polished steel MSP 96 target plate (Bruker Daltonics). After drying, the deposited bacteria were overlaid with 1 μl of HCCA matrix (a saturated α-cyano-4-hydroxycinnamic acid in 50% acetonitrile and 2.5% trifluoroacetic acid; Bruker Daltonics) and air dried at room temperature. Mass spectra were acquired on a microflex LT MALDI-TOF mass spectrometer (Bruker Daltonics) configured with Bruker flexControl software using the default settings. Mass spectra were obtained in t2d format and were converted to txt files using the Data Explorer 4.9 software (AB Sciex). The txt files were imported in BioNumerics 5.1 software (Applied Maths) and converted to fingerprints for further analyses. To obtain reliable data analysis, the spectra with extensive noise and/or insufficient signal intensities were excluded. The similarity between the spectra was expressed using Pearson's product moment correlation coefficient and the spectra were clustered using the UPGMA clustering algorithm.

Molecular Analysis of Epibiotic Microflora

DNA Extraction From Single Cells and Whole-Genome Amplification (WGA)

DNA from single diatom cells and their attached bacteria was extracted following chemical treatment and thermal shock. Cells were lysed using lysis and neutralization buffers prepared as described in Humily et al. (2014). After addition of 0.5 μL of lysis buffer, the mixture was incubated at 4°C for 10 min in a thermocycler. The lysate was further incubated at 95°C for 1 min, cooled at 4°C before adding 0.5 μL of neutralization buffer, and kept 3 min on ice until WGA.

Whole-Genome Amplification reactions were carried out under a HEPA/UV3 PCR Workstation (UVP) using the Genomiphi v2 kit (GE Healthcare). WGA reactions were carried out in 12 μL final volume by adding sample buffer (3.5 μL), reaction buffer (4.5 μL), and phi29 enzyme (0.5 μL) and then incubated for 4 h at 30°C before inactivating the enzyme for 5 min at 65°C. Positive controls consisting of 1–9 bacterial cells in 3 μL of PBS were performed to check the efficiency of WGA reaction. Blank controls with sterile PBS were also performed for each experiment. WGA products were stored at −20°C until processing.

PCR Amplification and Sequencing of rRNA Genes

Whole-Genome Amplification products were tested for the presence of bacteria with primer 1492R (Turner et al., 1999) in combination with primer 799F (Chelius and Triplett, 2001; Ghyselinck et al., 2013) that strongly discriminates against chloroplast 16S rDNA. Reaction mixtures (12.5 μL) contained 0.75 U of GoTaq G2 Flexi DNA polymerase (Promega), 1X polymerase buffer, 2.0 mM $MgCl_2$, 0.1 mM of each deoxynucleoside triphosphate, 0.2 μM of each primer, and 1 μL of WGA product. The program consisted of an initial denaturation step of 3 min at 95°C, followed by 35 cycles (20 s at 95°C, 40 s at 53°C, and 40 s at 72°C), and a final extension step of 10 min at 72°C. 16S rRNA genes from cultured epibionts were amplified with primers 8F (Turner et al., 1999) and 1492R using the conditions above. The program consisted of an initial denaturation step of 10 min at 94°C, followed by 35 cycles (30 s at 95°C, 1 min at 55°C, and 1 min at 72°C), and a final extension step of 10 min at 72°C.

In order to identify the diatom single cells isolated from the natural environment, the genes encoding their 18S rRNA gene and the large sub-unit (LSU) D1–D3 region were amplified using primers 63F and 1818R and D1R and D3Ca, respectively (Orsini et al., 2002). Reaction mixtures (15 μL) contained 0.75 U of GoTaq G2 Flexi DNA polymerase, 1X polymerase buffer, 2.0 mM $MgCl_2$, 0.2 μM of each primer, 0.1 mM of each deoxynucleoside triphosphate, and 1 μL of extracted DNA. The program consisted of an initial denaturation step of 5 min at 95°C, followed by 40 cycles (30 s at 95°C, 30 s at 50°C (for 18S rRNA amplification) or 30 s at 55°C (for LSU amplification), and 1 min at 72°C) and a final extension step of 10 min at 72°C.

Whole-Genome Amplification products that proved positive for 16S rRNA but negative for 18S rRNA were removed from further analysis. PCR products of 16S rRNA genes were cloned using TOPO TA Cloning Kit® (Invitrogen) as recommended by the manufacturer. Insert-containing clones were identified by agarose gel electrophoresis of PCR products amplified using M13F and M13R primers. Clones and PCR products were sequenced by Macrogen Europe (Amsterdam, Netherlands) or by the Biogenouest sequencing platform at the Station Biologique (Roscoff, France). Bacterial taxon for each sequence was identified and named by the homologous 16S sequence in Genbank using BLAST (Altschul et al., 1990). Phylogenetic analyses of 16S and 18S rRNA gene sequences were performed using the neighbor joining tree method implemented in MEGA6 software (Tamura et al., 2013).

Statistical Analyses of the Bacterial Communities

Each single algal cell was considered as an environment to which 16S rDNA sequences were assigned. We used the unweighted UniFrac distance measure (Lozupone and Knight, 2005; Hamady et al., 2010) to compare the presence or absence of taxa with the bacterial communities. To determine whether the cultured and natural bacterial communities in both diatoms were significantly different than random, we used the Unifrac significance test along with the principal coordinates analysis (PCoA) both run in Mothur (Schloss et al., 2009).

Nucleotide Sequence Accession Numbers

All nucleotide sequences obtained in this study are available in GenBank database under the accession numbers KX197296 to KX197383, and KU926270 (16S rRNA of cultured bacteria), KX197247 to KX197295 (16S rRNA of uncultured bacteria), and KX226392 to KX226398 (16S rRNA and LSU region of microalgae).

RESULTS AND DISCUSSION

Bacterial Colonization of Diatom Cells

In this study, we first compare the prevalence of bacterial cell attachment in both diatom species. It is well known that bacterial colonization may be influenced by the algal growth state in cultures and the bloom stage in natural samples (Grossart et al., 2005; Kaczmarska et al., 2005). To circumvent this issue, algal cultures used for single cell isolation were all in early stationary growth phase and the same natural samples were used to isolate *Chaetoceros* and *Thalassiosira* cells. A total of 296 and 469 cells were manually isolated from independent cultures and natural samples, respectively (**Table 1**). Both culture-based and molecular approaches yielded generally nearly identical proportions of *Chaetoceros* cells colonized by bacteria. However, both methods yielded different epibiont proportions in *Thalassiosira*. This was somewhat surprising because (i) the observed epibiont proportions were remarkably stable in the different *Thalassiosira* RCC 2560 cultures used for epibiont isolation whatever the approach used (see the section "Materials and Methods") and (ii) the high epibiont prevalences observed using the culture-based approach were consistent with that measured by scanning electron microsopy (**Supplementary Table 1**). From these results, a reasonable explanation is that the molecular approach is most prone to yield variable results. Epibiont proportions in diatom cells isolated from the environment were generally lower than that from the cultures as measured using the culture-based approach. This result makes sense because we observed a majority of diatom cells free of epibiotic bacteria (**Table 1**), with proportions exceeding 90% for *Chaetoceros* in natural waters. These observations are in agreement with early studies that led to the conclusion that living pelagic diatoms are not colonized by bacteria (Droop and Elson, 1966) and with more recent reports that showed high proportions of bacteria-free diatom cells in old cultures (Kaczmarska et al., 2005). They also support the hypothesis that the extent of algal colonization by bacteria are positively related to the densities of both free bacteria and microalgae (Vaqué et al., 1989). This may also explain the differential proportions of diatom cells colonized by bacteria we found in cultures and in natural samples. However, we can also assume that cells in culture are confined to uniform laboratory conditions favoring stable interactions between partners and colonization while a range of environmental factors can positively

TABLE 1 | Proportions of algal cells with bacterial epibionts in cultures and natural samples as evaluated by culture-based and molecular approaches and numbers of isolates and bacterial sequences obtained in this study.

	Cultures		Natural samples	
	***Chaetoceros* RCC 2565**	***Thalassiosira* RCC 2560**	***Chaetoceros* spp.**	***Thalassiosira* spp.**
Culture approach				
Algal cells isolated[a]	75	88	206	209
Algal cells with epibionts[b] (%)	27 (36)	69 (78)	19 (9)	68 (33)
Epibiont isolates[c]	38	63	12	64
Bacterial species[d]	5	14	7	38
Molecular approach				
Algal cells isolated[e]	20	113	28	26
Algal cells with epibionts[f] (%)	6 (30)	38 (34)	2 (7)	14 (54)
PCR libraries from positive WGAs	6	18	2	14
Bacterial phylotypes	9	19	3	14
Bacterial species[d]	7	4	3	10

[a]Cells for which no bacterial growth was obtained from controls. [b]Positive enrichments in LNHM as measured by flow cytometry. [c]Epibionts isolated on LNHM agar plates. [d]Defined at the 98% similarity level. [e]Cells for which no amplification products were obtained from controls. [f]Proportions of positive WGAs with negative controls.

or negatively influence temporary algal–bacterial relationships in natural conditions.

Only limited quantitative information exists on the interactions between attached bacteria and phytoplankton in pelagic aquatic environments. However, the actual view is that bacterial colonization of planktonic algae may vary with respect to algal species and physiological state (Grossart et al., 2005, 2006). Indeed, we found that *Thalassiosira* cells harbored significantly higher proportions of epibionts than *Chaetoceros* cells whatever the approach used (**Table 1**) and this was confirmed by SEM data (**Supplementary Table 1**). Two possibilities can bring out the difference observed. Since associations between bacteria and microalgae are known to change over the course of algal bloom cycles (Grossart et al., 2005, 2006; Mayali et al., 2011), one possibility is that the effect of temporal variation in algal hosts collections. However, it is not the case in our samples, because *Thalassiosira* and *Chaetoceros* cells were isolated from the same natural samples although there was a 4–5 month time difference between cell collections for both approaches. Since the epibiont proportions obtained by both approaches for each diatom showed the same trends, it is unlikely that the differences observed are linked to different physiological states. A likely possibility is that diatom hosts are quite distinct in their size and structure characteristics, their release of exopolymers and their production of inhibitory substances (Vaqué et al., 1989; Myklestad, 1995; Amin et al., 2012).

Using the cultivation and molecular data, we calculated the average number of species or OTUs attached to single diatoms cells. Interestingly, whatever the approach used, we found that each host cell harbored between 1 to 2.3 epibiotic species or OTUs, suggesting a rather low attachment. This average number is a minimum estimate of the number of bacterial cells that occurred on the host cell, but with the methods used it was not possible to evaluate how many bacterial cells were attached to the host cells examined. However, these numbers are close to that we obtained using SEM on late exponential cultures (0.8–3.8 bacterial epibionts on cingulum or spines/valve; **Supplementary Table 1**). These low numbers were generally in agreement with that reported by Baker and Kemp (2014) although these authors found also higher numbers of phylotypes (up to 11) per algal cell for some species or strains.

Microbial Community Comparisons Between Hosts in Short- and Long-Term Associations

Using the molecular method, a total of 45 bacterial phylotypes were obtained after WGA of 40 single diatom cells isolated from collection cultures and natural samples (**Tables 1**, **2**). When clustered at the 98% similarity level, 24 OTUs representing diverse lineages of bacterial phyla were identified and their distribution did not overlap among host species and between collection cultures and environmental samples. The identified OTUs were classified into the classes *Alpha-*, *Beta-* and *Gammaproteobacteria*, *Actinobacteria*, *Flavobacteriia*, *Bacilli*, *Cytophagia*, and *Sphingobacteria*. Bacterial cultivation using a low-nutrient organic medium and extended incubation periods of up to 6 weeks were used to increase the overall assessment of the species richness. Cultivation identified a total of 177 unique isolates (**Tables 1**, **3**, **4**). The isolated strains fell generally into the same bacterial classes than environmental clones but none belonged to the classes *Betaproteobacteria* and *Bacilli*.

In this study, we asked if microalgal species could influence the epibiont community structure in cultures and in natural communities. Unweighted UniFrac analyses, which takes into account only presence/absence data for OTUs/species, showed that the epibiotic bacterial communities associated with *T. delicatula* RCC 2560 and *C. danicus* RCC 2565 were significantly distinct ($P < 0.001$) as determined by the culture-based approach. Principal Coordinate Analysis

TABLE 2 | Epibiotic bacterial phylotypes recovered from diatom cells in culture and from natural waters and their closest cultivated relative identified by Blastn.

Diatom host	*n*[a]	Phylum/class	Order	Family	Species	16S rRNA similarity (%)
Cultures						
C. danicus RCC 2565	3	*Alphaproteobacteria*	*Rhodobacterales*	*Hyphomonadaceae*	*Algimonas* sp.	99.6
	1	*Betaproteobacteria*	*Burkholderiales*	*Burkholderiaceae*	*Limnobacter thiooxidans*	100
	1			*Comamonadaceae*	*Pelomonas* sp.	99.9
	1	*Gammaproteobacteria*	*Oceanospirillales*	*Halomonadaceae*	*Halomonas* sp	99.9
	1	*Flavobacteriia*	*Flavobacteriales*	*Cryomorphaceae*	*Brumimicrobium mesophilum*	93.5
	1	*Actinobacteria*	*Micrococcales*	*Micrococcaceae*	*Nesterenkonia flava*	99.4
	1	*Bacilli*	*Bacillales*	*Bacillaceae*	*Aeribacillus pallidus*	99.9
T. delicatula RCC 2560	1	*Alphaproteobacteria*	*Sphingomonadales*	*Erythrobacteraceae*	*Erythrobacter litoralis*	98.8
	1		*Rhodobacterales*	*Rhodobacteraceae*	*Maribius pelagius*	94.7
	1	*Bacilli*	*Bacillales*	*Bacillaceae*	*Aeribacillus pallidus*	100
	16	*Flavobacteriia*	*Flavobacteriales*	*Flavobacteriaceae*	*Tenacibaculum skagerrakense*	97.8
Environmental cells[b]						
Chaetoceros debilis	1	*Alphaproteobacteria*	*Rhodobacterales*	*Rhodobacteraceae*	*Marivita cryptomonadis*	98.5
	1				*Pseudoruegeria lutimaris*	97
Chaetoceros protuberans	1	*Gammaproteobacteria*	*Alteromonadales*	*Alteromonadaceae*	*Saccharophagus degradans*	95.1
Thalassiosira punctigera	1	*Alphaproteobacteria*	*Rhodobacterales*	*Rhodobacteraceae*	*Roseovarius nubinhibens*	97.9
	1	*Gammaproteobacteria*	*Alteromonadales*	*Colwelliaceae*	*Colwellia psychroerythraea*	99.3
	1		*Chromatiales*	*Ectothiorhodospiraceae*	*Ectothiorhodospira mobilis*	94.3
	1		*Cellvibrionales*	*Halieaceae*	*Chromatocurvus halotolerans*	95.7
	1			*Spongiibacteraceae*	*Dasania marina*	93
	1				*Oceanicoccus sagamiensis*	96.8
	1		*Pseudomonadales*	*Pseudomonadaceae*	*Pseudomonas trivialis*	90.7
	4	*Cytophagia*	*Cytophagales*	*Amoebophilaceae*	*Candidatus Amoebophilus asiaticus*	93
	2	*Flavobacteriia*	*Flavobacteriales*	*Cryomorphaceae*	*Salinirepens amamiensis*	94.4
	1	*Sphingobacteriia*	*Sphingobacteriales*	*Saprospiraceae*	*Lewinella cohaerens*	89.1

[a]*Number of individual diatom cell carrying the corresponding bacterial phylotype;* [b]*as identified by 18S rRNA sequencing.*

(PCoA) also separated the corresponding libraries (**Figure 1A**). No significant dissimilarities were shown between epibiont communities of the cultures as determined by the molecular approach (P = 0.124) (**Figure 1B**). Our results complement, however, earlier observations suggesting that microalgal cultures harbor specific bacterial communities (Schäfer et al., 2002; Grossart et al., 2005; Sapp et al., 2007; Guannel et al., 2011; Behringer et al., 2018). We also compared the culture-based and molecular bacterial diversity attached to *Thalassiosira* and *Chaetoceros* single cells isolated from natural samples and collection cultures, considered here as short- and long-term associations, respectively. Both methods indicated that epibiotic bacterial communities associated with cultures and environmental cells of *Thalassiosira* showed a highly significant difference ($P < 0.001$) (**Figures 1C,D**). Epibiont assemblages in cultured and environmental *Chaetoceros* cells also differed significantly as determined by culture-based approach ($P < 0.001$) while molecular libraries showed only marginally significant difference (P = 0.079) (**Figures 1E,F**). Since single cells isolated from natural waters belonged to two *Chateoceros* species, we enlarged the specificity of *in situ* associations to the genus level. Nevertheless, distinctness between *in situ* epibiotic communities of both diatom genera was observed in the same samples collected at the same place. This result is in line with previous findings showing that bacterial assemblages associated with phytoplankton cultures can be very different from the natural bacterial assemblages during blooms of the same species (Garcés et al., 2007). We acknowledge, however, that the diatom hosts isolated from natural waters differed at the species level from their cultured relatives.

Diversity of Diatom Epibionts

Although the molecular approach was designed and performed using necessary precautions (decontamination and cleaning procedures) to prevent contamination, the successive steps that include single cell isolation, whole genome and PCR amplification presented opportunities for the inclusion of non-host derived bacterial sequences. We also removed samples with any negative control amplification from further analysis. We didn't find sequences recognized as being commonly associated to human skin but a few phylotypes and strains were not typical of bacterial taxa found previously with algal cultures (**Tables 2–4**) Among them, we identified sequences of *Aeribacillus pallidus* (*Firmicutes*) that were abundantly found in skin-associated bacterial communities of marine fishes (Larsen et al., 2013). Like other Gram-positive bacteria frequently found in marine microalgal laboratory cultures, we suspect their presence is due to a contamination from handling (Nicolas et al., 2004). Although *Actinobacteria* are known to be rare in pelagic marine environments (Pommier et al., 2007), we obtained several actinobacterial strains and sequences attached to diatom cells in cultures

and natural samples (**Tables 2–4**). Interestingly, the isolates belong to genera with species obtained from diatom cultures (Le Chevanton et al., 2013) and from marine environments, most of them in association with invertebrates, algae and microalgae (Green et al., 2004; Pathom-aree et al., 2006; Menezes et al., 2010; Palomo et al., 2013). We therefore cannot exclude that these bacteria represent rare members in the diatom phycosphere.

Epibiotic bacteria isolated from natural diatom populations were highly diverse (**Table 3**) and only a few species overlapped in *Chaetoceros* and *Thalassiosira* cells. Interestingly, the overlapping bacterial species were also the most frequently

TABLE 3 | Epibiotic bacterial strains isolated from diatom cells in natural waters and their closest cultivated relative identified by Blastn.

Diatom host	Strain (n)	Phylum/class	Order	Family	Species	16S rRNA similarity (%)
Chaetoceros spp.	KC58 (2)	*Alphaproteobacteria*	*Rhizobiales*	*Phyllobacteriaceae*	*Hoeflea phototrophica*	97.9
	KC43 (1)	*Gammaproteobacteria*	*Alteromonadales*	*Alteromonadaceae*	*Glaciecola punicea*	96
	KC55B (4)			*Pseudoalteromonadaceae*	*Pseudoalteromonas undina/marina*	99
	KC57 (1)				*Pseudoalteromonas carrageenovora*	100
	KC61 (1)		*Vibrionales*	*Vibrionaceae*	*Photobacterium aquimaris*	99.9
	KC46A (1)	*Flavobacteriia*	*Flavobacteriales*	*Flavobacteriaceae*	*Tenacibaculum gallaicum*	97.7
	KC79A (2)	*Actinobacteria*	*Actinomycetales*	*Micrococcaceae*	*Arthrobacter subterraneus*	99.8
Thalassiosira spp.	KC76 (1)	*Alphaproteobacteria*	*Kiloniellales*	*Kiloniellaceae*	*Kiloniella laminariae*	96.3
	KC56 (1)		*Rhizobiales*	*Hyphomicrobiaceae*	*Hyphomicrobium nitrativorans*	95.3
	KC41B (1)			*Phyllobacteriaceae*	*Nitratireductor indicus*	95.2
	KC41A (1)				*Nitratireductor pacificus*	95.2
	KC45 (1)		*Rhodobacterales*	*Rhodobacteraceae*	*Jannaschia sp.*	98
	KC59 (1)				*Litoreibacter meonggei*	97.7
	KC77A (2)				*Loktanella maricola*	99.6
	KC68 (1)				*Loktanella vestfoldensis*	96
	KC75 (1)				*Nereida ignava*	97.3
	KC63A (3)				*Octadecabacter antarcticus*	98.1
	KC47 (1)				*Roseobacter litoralis*	98.8
	KC52A (2)				*Shimia marina*	98.2
	KC42A (2)		*Sphingomonadales*	*Erythrobacteraceae*	*Altererythrobacter luteolus*	97
	KC74 (1)				*Croceicoccus marinus*	97.3
	KC49 (1)				*Erythrobacter aquimaris*	99.6
	KC67 (1)			*Sphingomonadaceae*	*Sphingopyxis flavimaris*	98.8
	KC60 (1)	*Cytophagia*	*Cytophagales*	*Flammeovirgaceae*	*Roseivirga ehrenbergii*	93.2
	KC65A (2)	*Flavobacteriia*	*Flavobacteriales*	*Flavobacteriaceae*	*Croceitalea eckloniae*	97.3
	KC50A (2)				*Dokdonia genica*	99.7
	KC62 (1)				*Lacinutrix sp.*	97.3
	KC44 (1)				*Lutimonas vermicola*	100
	KC51B (2)				*Maribacter aquivivus*	97.7
	KC51A (1)				*Maribacter forsetii*	96
	KC81 (1)				*Maribacter ulvicola*	99.3
	KC73A (2)				*Olleya namhaensis*	97.3
	KC46B (2)				*Tenacibaculum gallaicum*	97.7
	KC48 (1)	*Gammaproteobacteria*	*Alteromonadales*	*Alteromonadaceae*	*Aestuariibacter litoralis*	97.8
	KC78 (1)				*Alteromonas tagae*	99
	KC72 (1)				*Pseudohaliea rubra*	98
	KC53A (5)			*Pseudoalteromonadaceae*	*Pseudoalteromonas undina/marina*	99.9
	KC66 (1)			*Shewanellaceae*	*Shewanella japonica*	99.3
	KC70 (1)			*Colwelliaceae*	*Thalassomonas agariperforans*	96.9
	KC64 (1)		*Chromatiales*	*Granulosicoccaceae*	*Granulosicoccus coccoides*	96.9
	KC80 (1)		*Vibrionales*	*Vibrionaceae*	*Vibrio breoganii*	100
	KC54 (1)				*Vibrio splendidus*	100
	KC71 (1)		Unclassified *Gammaproteobacteria*		*Chromatocurvus halotolerans*	97.3
	KC69 (1)	*Sphingobacteriia*	*Sphingobacteriales*	*Saprospiraceae*	*Portibacter lacus*	91.5
	KC79C (1)	*Actinobacteria*	*Actinomycetales*	*Micrococcaceae*	*Arthrobacter subterraneus*	99.8

[a]*Number of individual diatom cell carrying the corresponding bacterial isolate;* [b]*based on partial sequences >663 bp.*

TABLE 4 | Epibiotic bacterial strains isolated from diatom cells in culture and their closest cultivated relative identified by Blastn.

Diatom host	Strain (n)	Phylum/class	Order	Family	Species	16S rRNA similarity (%)
C. danicus RCC 2565	KC05A (17)	*Alphaproteobacteria*	*Caulobacterales*	*Hyphomonadaceae*	*Algimonas ampicilliniresistens*	98
	KC39 (2)		*Rhodobacterales*	*Rhodobacteraceae*	*Sulfitobacter dubius*	99.9
	KC25 (11)	*Gammaproteobacteria*	*Alteromonadales*	*Alteromonadaceae*	*Marinobacter sediminum*	99.8
	KC36 (1)				*Marinobacter lipolyticus*	99.8
	KC86 (1)				*Silicimonas algicola*	100
T. delicatula RCC 2560	KC04 (1)	*Alphaproteobacteria*	*Sphingomonadales*	*Erythrobacteraceae*	*Altererythrobacter ishigakiensis*	97.9
	KC12 (26)				*Erythrobacter gaetbuli*	98
	KC18 (1)				*Erythrobacter citreus*	98.3
	KC90 (15)		*Rhodobacterales*	*Rhodobacteraceae*	*Silicimonas algicola*	100
	KC10 (10)				*Paracoccus aminophilus*	96.7
	KC17B (1)				*Paracoccus stylophorae*	97.8
	KC38C (1)	*Gammaproteobacteria*	*Alteromonadales*	*Alteromonadaceae*	*Sulfitobacter dubius*	99.9
	KC16 (3)				*Marinobacter salarius*	99.9
	KC31 (3)				*Marinobacter sediminum*	100
	KC14 (3)	*Flavobacteriia*	*Flavobacteriales*	*Flavobacteriaceae*	*Tenacibaculum sp*	95
	KC02 (1)	*Actinobacteria*	*Actinomycetales*	*Micrococcaceae*	*Kocuria rosea*	99.7
	KC23 (1)				*Micrococcus yunnanensis*	99.4
	KC03 (1)			*Nocardioidaceae*	*Nocardioides furvisabuli*	99.6
	KC24 (1)			*Dermacoccaceae*	*Dermacoccus nishinomiyaensis*	98.8

[a]*Number of individual diatom cell carrying the corresponding bacterial isolate;* [b]*based on partial sequences >663 bp.*

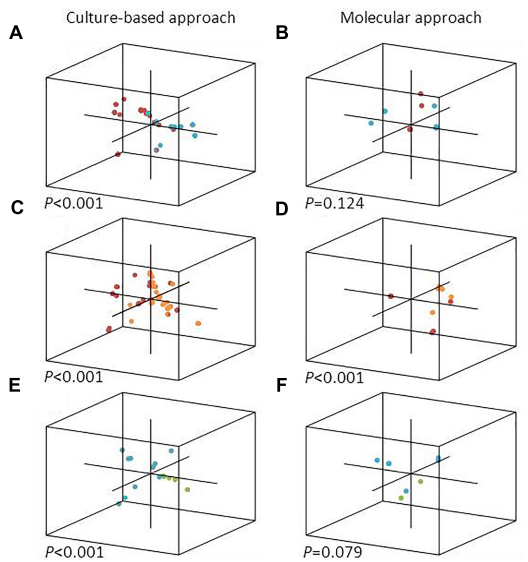

FIGURE 1 | PCoA representation of each single diatom cell analyzed in this study, with a 3D position depending on the composition of its epibiotic bacterial community. Culture-based (left) and molecular (right) bacterial diversity attached to diatoms isolated from collection cultures **(A,B)**, natural samples **(E,F)** and both **(C,D)** are shown. Diatom cells correspond to *T. delicatula* RCC 2560 (red), *C. danicus* RCC 2565 (blue), environmental *Thalassiosira* spp. (orange), and environmental *Chaetoceros* spp. (green).

isolated from both genera. They consisted in species of the genera *Pseudoalteromonas* and *Tenacibaculum*, the majority of which appear to be associated with eukaryotic hosts, including various marine algae (Akagawa-Matsushita et al., 1992; Egan et al., 2000, 2001; Suzuki et al., 2001). Strains and phylotypes of *Tenacibaculum* were also repeatedly isolated and amplified from cells of *T. delicatula* RCC 2560, suggesting a possible physiological adaptation to an epiphytic lifestyle. This hypothesis is in line with the ecology of *Tenacibaculum* species known to be often associated with surfaces of marine invertebrates, fishes and microalgae and responsible of skin lesions and algicidal activity (Piñeiro-Vidal et al., 2012; Li et al., 2013).

Alpha- and *Gammaproteobacteria* were the two main classes identified in the cultivable epibiotic communities associated with cultures (**Table 4** and **Supplementary Figure 1**). Interestingly, some epibionts were regularly isolated from both diatom cultures. Among them, strains belonging to the gammaproteobacterial genus *Marinobacter* are common inhabitants of phytoplankton cultures (Amin et al., 2009, 2015; Le Chevanton et al., 2013; Sison-Mangus et al., 2014; Green et al., 2015; Lupette et al., 2016). While investigating the bacterial community associated with dinoflagellates and coccolithophores, Amin et al. (2009) observed that members of the genus *Marinobacter* were present in over 80% of cultures. Further studies demonstrated that *Marinobacter* isolates formed specific beneficial associations with diverse phytoplankton that could require cell-to-cell adhesion (Amin et al., 2009; Bolch et al., 2011; Gärdes et al., 2011). Other frequently isolated epibiotic bacteria were affiliated with the *Rhodobacterales* and they differed with the algal species. *Rhodobacterales* appear also to be particularly well-adapted to close association with phytoplankton in general and have been shown to increase during phytoplankton blooms (Mayali et al., 2011; Teeling et al., 2012). Laboratory experiments involving specific co-culture experiments also indicate that widespread interactions may occur between phytoplankton and Roseobacters (Durham et al., 2015; Segev et al., 2016; Seymour et al., 2017). Cultivated attached microflora of *C. danicus* RCC 2565 were related to the genera *Algimonas* while *Erythrobacter*, *Paracoccus*

and a new genus within the family *Rhodobacteraceae*, recently described as *Silicimonas algicola* (Crenn et al., 2016), prevailed in *T. delicatula* RCC 2560. *Algimonas*, *Erythrobacter*, and *Paracoccus* are also reported for their common occurrence in algal cultures or as epibionts of macroalgae (Alavi et al., 2001; Schäfer et al., 2002; Jasti et al., 2005; Kaczmarska et al., 2005; Le Chevanton et al., 2013; Cruz-López and Maske, 2016).

Phylotypes recovered from diatom cells in culture and from natural waters were diverse and only a few of them were repeatedly obtained (**Table 2**). Similarly to *Tenacibaculum* species that were regularly amplified and isolated from cells of *T. delicatula* RCC 2560, sequences and strains of *Algimonas* were often obtained from cells of *C. danicus* RCC 2565, confirming the presence of members of this genus in *Chaetoceros* cultures (Le Chevanton et al., 2013). A phylotype distantly related to the obligate amoeba endosymbiont "*Candidatus* Amoebophilus asiaticus" was retrieved from environmental cells of *T. punctigera*. Although it was repeatedly amplified from single cells, it is impossible to draw any hypothesis on the possible relationships between these partners in natural waters.

A total of 56 unique isolates were obtained in this study (**Tables 3**, **4**). We used the 16S rRNA gene identity cut-off value of 98.7% to define isolates that may represent novel species (Stackebrandt and Ebers, 2006). Overall, 35 unique isolates (>60% of the total isolates) showed 16S rRNA gene identity below this threshold and therefore may be potential candidates of new taxa. Of the new taxa, 5 isolates may represent novel genera at the conservative 95–96% identity cut-off (Yarza et al., 2014). Although 16S rRNA gene identities are based on partial sequences and our study does not prove that these isolates represent novel species, it provides a framework for isolating large numbers of epibiotic bacteria for possible novel taxa that may be of ecological importance. Indeed, repeated isolation of particular bacterial species from microalgae could be indicative of niche specificity or even established mutualistic relationships (Amin et al., 2009, 2012).

Our data demonstrated that diversity of the cultured epibiotic microflora was lower in diatom culture than in natural waters. Furthermore, the most frequently isolated taxa from diatom cultures were unusually isolated or amplified from environmental cells (**Tables 2**, **3**). This is exemplified by *Marinobacter* species that we regularly grown from diatoms originally isolated from Roscoff coastal waters but were not found as diatom epibionts in natural waters off Roscoff, confirming the typically low annual relative abundance of these bacteria in the Western English Channel (Green et al., 2015). Together, our results provide some support to the hypothesis that, in uniform laboratory culture conditions, bacteria–bacteria and bacteria–diatom interactions selected for a simplified, but specific, epibiotic microbiota shaped and adapted for long-term associations. Since recent observations showed that cultivation in the laboratory for longer than 1 year resulted in only small changes in the bacteria composition suggesting robust associations between diatoms and their associated bacterial communities (Behringer et al., 2018), further work is needed to how these interactions can differ across algal species. Our findings reinforce also previous reports that showed that the amount and composition of the organic matter released by phytoplankton like polysaccharides, small amino acids, sugars, proteoglycans or glycoproteins, may act as selective agents for bacterial types (Myklestad, 1995; Sapp et al., 2007; Sarmento et al., 2013). We assume that bacterial groups able to develop an algal-attached lifestyle are probably more affected by this selection process.

Methodological Considerations

This study addressed the examination of interactions between attached bacteria and two environmentally relevant diatom genera. Most studies that tried to tackle specifically this question first separated free-living bacteria from diatom cells by filtration on membranes and examined the bacterial assemblages associated to the diatom cell fraction (Kaczmarska et al., 2005; Mayali et al., 2011). We assume that the issue of specific associations cannot be answered using this method because non-attached bacteria may also be retained by membranes, and remain on them even after extensive washing steps. The methods described in our study and that employed by Baker and Kemp (2014) ensure the epibiotic status of the bacterial communities analyzed. The main limitation of our approach is that the manual isolation of single cells is time-consuming and limits the number of analyzed cells. Future studies might apply different strategies to pursue this question further. Although they require an expensive and sophisticated equipment and special infrastructure such as a clean room (Baker and Kemp, 2014), flow cytometry cell sorting systems may represent powerful tools to facilitate the rapid and efficient isolation of microalgae. They could greatly improve the analysis of attached bacterial assemblages in multiple cultures and environmental cells.

CONCLUSION

Our observations complement previous studies which addressed the existence of algal-specific bacterial communities. The present analysis of the microflora attached to ubiquitous marine diatoms demonstrated conclusively that abundance and community composition of epibiotic bacteria may vary significantly with algal species. The dominance of certain epibiotic bacteria, either common or specific to algal species, together with the simplification of bacterial communities along regular algal subculturing indicate selection of bacteria highly adapted to long-term interactions with hosts.

In the context of finding bacteria that could have symbiotic interactions with diatoms, the bacterial strains we repeatedly isolated from cultures and environmental cells represent good candidates. Further co-cultures experiments with axenic cultures of *T. delicatula* RCC 2560 and *C. danicus* RCC 2565 evaluating the effect of bacteria on both microalgae could help us to determine the functional role of specific isolates.

AUTHOR CONTRIBUTIONS

KC designed and performed the experiments (diversity analysis) and wrote the manuscript. DD performed the experiments

(diversity analysis). CJ designed the experiments and wrote the manuscript.

FUNDING

This work was supported by the French national programme EC2CO-Microbien (project MICROMAR) and the MaCuMBA project funded by the European Union's Seventh Framework Programme (Grant agreement no. 311975). KC received a doctoral grant funded by Région Bretagne and CNRS.

ACKNOWLEDGMENTS

We greatly acknowledge Raffaele Siano and Diana Sarno for their help in the identification of both diatom cultures used in this study. We also thank Geneviève Héry-Arnaud and colleagues (Unité de Bactériologie, CHRU de la Cavale Blanche, Brest, France) for the use of their Microflex LT MALDI-TOF mass spectrometer (Bruker Daltonics). Many thanks to Biogenouest sequencing platform at the Station Biologique de Roscoff for help and advices. Camille Poirier, Mathilde Miossec, and Sophie Le Panse are warmly acknowledged for their help in sequencing and scanning electron microscopy.

SUPPLEMENTARY MATERIAL

The Supplementary Material for this article can be found online at: https://www.frontiersin.org/articles/10.3389/fmicb.2018.02879/full#supplementary-material

FIGURE S1 | Maximum-likelihood tree based on 16S rRNA gene sequences showing the position of bacterial epibionts isolated from *C. danicus* RCC 2565 and *T. delicatula* RCC 2560 (**Table 4**). Only bootstrap values (expressed as percentages of 1000 replications) of >80% are shown. Filled circles indicate that the corresponding nodes were also recovered using the neighbor-joining algorithm. *Thermococcus litoralis* JCM8560^T was used as outgroup. Bar, 0.05 substitutions per nucleotide position.

TABLE S1 | Attached bacteria on diatom cultures during late exponential (5 days) and late stationary (19 days) growth phases.

REFERENCES

Akagawa-Matsushita, M., Matsuo, M., Koga, Y., and Yamasato, K. (1992). Alteromonas atlantica sp. nov. and *Alteromonas carrageenovora* sp. nov., bacteria that decompose algal polysaccharides. *Int. J. Syst. Bacteriol.* 42, 621–627. doi: 10.1099/00207713-42-4-621

Alavi, M., Miller, T., Erlandson, K., Schneider, R., and Belas, R. (2001). Bacterial community associated with Pfesteria-like dinoflagellate cultures. *Environ. Microbiol.* 3, 380–396. doi: 10.1046/j.1462-2920.2001.00207.x

Altschul, S. F., Gish, W., Miller, W., Myers, E. W., and Lipman, D. J. (1990). Basic local alignment search tool. *J. Mol. Biol.* 215, 403–410. doi: 10.1016/S0022-2836(05)80360-2

Amin, S. A., Green, D. H., Hart, M. C., Küpper, F. C., Sunda, W. G., and Carrano, C. J. (2009). Photolysis of iron–siderophore chelates promotes bacterial–algal mutualism. *Proc. Natl. Acad. Sci. U.S.A.* 106, 17071–17076. doi: 10.1073/pnas.0905512106

Amin, S. A., Hmelo, L. R., van Tol, H. M., Durham, B. P., Carlson, L. T., Heal, K. R., et al. (2015). Interaction and signalling between a cosmopolitan phytoplankton and associated bacteria. *Nature* 522, 98–101. doi: 10.1038/nature14488

Amin, S. A., Parker, M. S., and Armbrust, E. V. (2012). Interactions between diatoms and bacteria. *Microbiol. Mol. Biol. Rev.* 76, 667–684. doi: 10.1128/MMBR.00007-12

Armbrust, E. V. (2009). The life of diatoms in the world's oceans. *Nature* 459, 185–192. doi: 10.1038/nature08057

Armbrust, E. V., Berges, J. A., Bowler, C., Green, B. R., Martinez, D., Putnam, N. H., et al. (2004). The genome of the diatom *Thalassiosira pseudonana*: ecology, evolution, and metabolism. *Science* 306, 79–86. doi: 10.1126/science.1101156

Azam, F., and Malfatti, F. (2007). Microbial structuring of marine ecosystems. *Nat. Rev. Microbiol.* 5, 782–791. doi: 10.1038/nrmicro1798

Baker, L., Alegado, R. A., and Kemp, P. (2016). Response of diatom-associated bacteria to host growth stage, nutrient concentrations, and viral host infection in a model system. *Environ. Microbiol. Rep.* 8, 917–927. doi: 10.1111/1758-2229.12456

Baker, L., and Kemp, P. (2014). Exploring bacteria–diatom associations using single-cell whole genome amplification. *Aquat. Microb. Ecol.* 72, 73–88. doi: 10.3354/ame01686

Behringer, G., Ochsenkühn, M. A., Fei, C., Fanning, J., Koester, J. A., and Amin, S. A. (2018). Bacterial communities of diatoms display strong conservation across strains and time. *Front. Microbiol.* 9:659. doi: 10.3389/fmicb.2018.00659

Bell, W., and Mitchell, R. (1972). Chemotactic and growth responses of marine bacteria to algal extracellular products. *Biol. Bull.* 143, 265–277. doi: 10.2307/1540052

Bolch, C. J. S., Subramanian, T. A., and Green, D. H. (2011). The toxic dinoflagellate gymnodinium catenatum (Dinophyceae) requires marine bacteria for growth. *J. Phycol.* 47, 1009–1022. doi: 10.1111/j.1529-8817.2011.01043.x

Bowler, C., Allen, A. E., Badger, J. H., Grimwood, J., Jabbari, K., Kuo, A., et al. (2008). The Phaeodactylum genome reveals the evolutionary history of diatom genomes. *Nature* 456, 239–244. doi: 10.1038/nature07410

Chelius, M. K., and Triplett, E. W. (2001). The diversity of archaea and bacteria in association with the roots of *Zea mays* L. *Microb. Ecol.* 41, 252–263. doi: 10.1007/s002480000087

Cole, J. J. (1982). Interactions between bacteria and algae in aquatic ecosystems. *Annu. Rev. Ecol. Syst.* 13, 291–314. doi: 10.1146/annurev.es.13.110182.001451

Cooper, M. B., and Smith, A. G. (2015). Exploring mutualistic interactions between microalgae and bacteria in the omics age. *Curr. Opin. Plant Biol.* 26, 147–153. doi: 10.1016/j.pbi.2015.07.003

Crenn, K., Serpin, D., Lepleux, C., Overmann, J., and Jeanthon, C. (2016). *Silicimonas algicola* gen. nov., sp. nov., a member of the *Roseobacter clade* isolated from the cell surface of the marine diatom *Thalassiosira delicatula*. *Int. J. Syst. Evol. Microbiol.* 66, 4580–4588. doi: 10.1099/ijsem.0.001394

Cruz-López, R., and Maske, H. (2016). The vitamin B1 and B12 required by the marine dinoflagellate *Lingulodinium polyedrum* can be provided by its associated bacterial community in culture. *Front. Microbiol.* 7:560. doi: 10.3389/fmicb.2016.00560

Droop, M. R., and Elson, K. G. R. (1966). Are pelagic diatoms free from bacteria? *Nature* 211, 1096–1097. doi: 10.1038/2111096a0

Durham, B. P., Sharma, S., Luo, H., Smith, C. B., Amin, S. A., Bender, S. J., et al. (2015). Cryptic carbon and sulfur cycling between surface ocean plankton. *Proc. Natl. Acad. Sci. U.S.A.* 112, 453–457. doi: 10.1073/pnas.1413137112

Egan, S., James, S., Holmstro, C., Holmström, C., and Kjelleberg, S. (2001). Inhibition of algal spore germination by the marine bacterium *Pseudoalteromonas tunicata*. *FEMS Microbiol. Ecol.* 35, 67–73. doi: 10.1111/j.1574-6941.2001.tb00789.x

Egan, S., Thomas, T., Holmström, C., and Kjelleberg, S. (2000). Phylogenetic relationship and antifouling activity of bacterial epiphytes from the marine alga Ulva lactuca. *Environ. Microbiol.* 2, 343–347. doi: 10.1046/j.1462-2920.2000.00107.x

Falkowski, P. G., Fenchel, T., and Delong, E. F. (2008). The microbial engines that drive Earth 's biogeochemical cycles. *Science* 320, 1034–1039. doi: 10.1126/science.1153213

Field, C. B., Behrenfeld, M. J., Randerson, J. T., and Falkowski, P. (1998). Primary production of the biosphere: integrating terrestrial and oceanic components. *Science* 281, 237–240. doi: 10.1126/science.281.5374.237

Garcés, E., Vila, M., Reñé, A., Alonso-Sáez, L., Anglès, S., Lugliè, A., et al. (2007). Natural bacterioplankton assemblage composition during blooms of Alexandrium spp. (Dinophyceae) in NW Mediterranean coastal waters. *Aquat. Microb. Ecol.* 46, 55–70. doi: 10.3354/ame046055

Gärdes, A., Iversen, M. H., Grossart, H. P., Passow, U., and Ullrich, M. S. (2011). Diatom-associated bacteria are required for aggregation of *Thalassiosira weissflogii*. *ISME J.* 5, 436–445. doi: 10.1038/ismej.2010.145

Ghyselinck, J., Pfeiffer, S., Heylen, K., Sessitsch, A., and De Vos, P. (2013). The effect of primer choice and short read sequences on the outcome of 16S rRNA gene based diversity studies. *PLoS One* 8:e71360. doi: 10.1371/journal.pone.0071360

Ghyselinck, J., Van Hoorde, K., Hoste, B., Heylen, K., and De Vos, P. (2011). Evaluation of MALDI-TOF MS as a tool for high-throughput dereplication. *J. Microbiol. Methods* 86, 327–336. doi: 10.1016/j.mimet.2011.06.004

Green, D. H., Echavarri-bravo, V., Brennan, D., and Hart, M. C. (2015). Bacterial diversity associated with the coccolithophorid algae *Emiliania huxleyi* and *Coccolithus pelagicus f. braarudii*. *Biomed. Res. Int.* 2015:194540. doi: 10.1155/2015/194540

Green, D. H., Llewellyn, L. E., Negri, A. P., Blackburn, S. I., and Bolch, C. J. S. (2004). Phylogenetic and functional diversity of the cultivable bacterial community associated with the paralytic shellfish poisoning dinoflagellate *Gymnodinium catenatum*. *FEMS Microbiol. Ecol.* 47, 345–357. doi: 10.1016/S0168-6496(03)00298-8

Grossart, H. P. (1999). Interactions between marine bacteria and axenic diatoms (*Cylindrotheca fusiformis*, *Nitzschia laevis*, and *Thalassiosira weissflogii*) incubated under various conditions in the lab. *Aquat. Microb. Ecol.* 19, 1–11. doi: 10.3354/ame019001

Grossart, H. P., Czub, G., and Simon, M. (2006). Algae-bacteria interactions and their effects on aggregation and organic matter flux in the sea. *Environ. Microbiol.* 8, 1074–1084. doi: 10.1111/j.1462-2920.2006.00999.x

Grossart, H. P., Levold, F., Allgaier, M., Simon, M., and Brinkhoff, T. (2005). Marine diatom species harbour distinct bacterial communities. *Environ. Microbiol.* 7, 860–873. doi: 10.1111/j.1462-2920.2005.00759.x

Grossart, H. P., and Simon, M. (2007). Interactions of planktonic algae and bacteria: effects on algal growth and organic matter dynamics. *Aquat. Microb. Ecol.* 47, 163–176. doi: 10.3354/ame047163

Guannel, M. L., Horner-Devine, M. C., and Rocap, G. (2011). Bacterial community composition differs with species and toxigenicity of the diatom *Pseudo-nitzschia*. *Aquat. Microb. Ecol.* 64, 117–133. doi: 10.3354/ame01513

Guilloux, L., Rigaut-Jalabert, F., Jouenne, F., Ristori, S., Viprey, M., Not, F., et al. (2013). An annotated checklist of marine phytoplankton taxa at the SOMLIT-Astan time series off Roscoff (Western English Channel, France): data collected from 2000 to 2010. *Cah. Biol. Mar.* 54, 247–256.

Hamady, M., Lozupone, C., and Knight, R. (2010). Fast UniFrac: facilitating high-throughput phylogenetic analyses of microbial communities including analysis of pyrosequencing and PhyloChip data. *ISME J.* 4, 17–27. doi: 10.1038/ismej.2009.97

Hasle, G. R., and Syvertsen, E. (1996). "Marine diatoms," in *Identifying Marine Diatoms and Dinoflagellates*, ed. C. R. Tomas (San Diego, CA: Academic Press, Inc), 5–385.

Humily, F., Farrant, G. K., Marie, D., Partensky, F., Mazard, S., Perennou, M., et al. (2014). Development of a targeted metagenomic approach to study a genomic region involved in light harvesting in marine *Synechococcus*. *FEMS Microbiol. Ecol.* 88, 231–249. doi: 10.1111/1574-6941.12285

Jasti, S., Sieracki, M. E., Poulton, N. J., Giewat, M. W., and Rooney-Varga, J. N. (2005). Phylogenetic diversity and specificity of bacteria closely associated with *Alexandrium* spp. and other phytoplankton. *Appl. Environ. Microbiol.* 71, 3483–3494. doi: 10.1128/AEM.71.7.3483-3494.2005

Kaczmarska, I., Ehrman, J. M., Bates, S. S., Green, D. H., Léger, C., and Harris, J. (2005). Diversity and distribution of epibiotic bacteria on *Pseudo-nitzschia* multiseries (Bacillariophyceae) in culture, and comparison with those on diatoms in native seawater. *Harmful Algae* 4, 725–741. doi: 10.1016/j.hal.2004.10.001

Keller, M. D., Seluin, R. C., Claus, W., and Guillard, R. R. L. (1987). Media for the culture of oceanic ultraphytoplankton. *J. Phycol.* 23, 633–638. doi: 10.1016/0198-0254(88)92621-0

Larsen, A., Tao, Z., Bullard, S. A., and Arias, C. R. (2013). Diversity of the skin microbiota of fishes: evidence for host species specificity. *FEMS Microbiol. Ecol.* 85, 483–494. doi: 10.1111/1574-6941.12136

Le Chevanton, M., Garnier, M., Bougaran, G., Schreibera, N., Lukomska, E., Beìrard, J.-B., et al. (2013). Screening and selection of growth-promoting bacteria for Dunaliella cultures. *Algal Res.* 2, 212–222. doi: 10.1016/j.algal.2013.05.003

Leblanc, K., Arístegui, J., Armand, L., Assmy, P., Beker, B., Bode, A., et al. (2012). A global diatom database – abundance, biovolume and biomass in the world ocean. *Earth Syst. Sci. Data* 4, 149–165. doi: 10.5194/essdd-5-147-2012

Li, Y., Wei, J., Yang, C., Lai, Q., Chen, Z., Li, D., et al. (2013). *Tenacibaculum xiamensense* sp. nov., an algicidal bacterium isolated from coastal seawater. *Int. J. Syst. Evol. Microbiol.* 63, 3481–3486. doi: 10.1099/ijs.0.050765-0

Lozupone, C., and Knight, R. (2005). UniFrac: a new phylogenetic method for comparing microbial communities. *Appl. Environ. Microbiol.* 71, 8228–8235. doi: 10.1128/AEM.71.12.8228-8235.2005

Lupette, J., Lami, R., Krasovec, M., Grimsley, N., Moreau, H., Piganeau, G., et al. (2016). *Marinobacter* dominates the bacterial community of the *Ostreococcus tauri* phycosphere in culture. *Front. Microbiol.* 7:1414. doi: 10.3389/fmicb.2016.01414

Malviya, S., Scalco, E., Audic, S., Vincent, F., Veluchamy, A., Bittner, L., et al. (2016). Insights into global diatom distribution and diversity in the world's ocean. *Proc. Natl. Acad. Sci. U.S.A.* 113, E1516–E1525. doi: 10.1073/pnas.1509523113

Marie, D., Partensky, F., Jacquet, S., and Vaulot, D. (1997). Enumeration and cell cycle analysis of natural populations of marine picoplankton by flow cytometry using the nucleic acid stain SYBR Green I. *Appl. Environ. Microbiol.* 63, 186–193. doi: 10.1111/j.1365-294X.2009.04480.x

Mayali, X., Franks, P. J. S., and Burton, R. S. (2011). Temporal attachment dynamics by distinct bacterial taxa during a dinoflagellate bloom. *Aquat. Microb. Ecol.* 63, 111–122. doi: 10.3354/ame01483

Menezes, C. B. A., Bonugli-Santos, R. C., Miqueletto, P. B., Passarini, M. R. Z., Silva, C. H. D., Justo, M. R., et al. (2010). Microbial diversity associated with algae, ascidians and sponges from the north coast of São Paulo state, Brazil. *Microbiol. Res.* 165, 466–482. doi: 10.1016/j.micres.2009.09.005

Myklestad, S. M. (1995). Release of extracellular products by phytoplankton with special emphasis on polysaccharides. *Sci. Total Environ.* 165, 155–164. doi: 10.1016/0048-9697(95)04549-G

Nelson, D. M., Tréguer, P., Brzezinski, M. A., Leynaert, A., and Quéguiner, B. (1995). Production and dissolution of biogenic silica in the ocean: revised global estimates, comparison with regional data and relationship to biogenic sedimentation. *Global Biogeochem. Cycles* 9, 359–372. doi: 10.1029/95GB01070 59

Nicolas, J.-L., Corre, S., and Cochard, J.-C. (2004). Bacterial population association with phytoplankton cultured in a bivalve hatchery. *Microb. Ecol.* 48, 400–413. doi: 10.1007/s00248-003-2031-6

Orsini, L., Sarno, D., Procaccini, G., Poletti, R., Dahlmann, J., and Montresor, M. (2002). Toxic *Pseudo-nitzschia* multistriata (Bacillariophyceae) from the Gulf of Naples: morphology, toxin analysis and phylogenetic relationships with other *Pseudo-nitzschia* species. *Eur. J. Phycol.* 37, 247–257. doi: 10.1017/S0967026202003608

Palomo, S., Gonzalez, I., De La Cruz, M., Martin, J., Tormo, J. R., Anderson, M., et al. (2013). Sponge-derived *Kocuria* and *Micrococcus* spp. as sources of the new thiazolyl peptide antibiotic kocurin. *Mar. Drugs* 11, 1071–1086. doi: 10.3390/md11041071

Pathom-aree, W., Stach, J. E. M., Ward, A. C., Horikoshi, K., Bull, A. T., and Goodfellow, M. (2006). Diversity of actinomycetes isolated from Challenger Deep sediment (10,898 m) from the Mariana Trench. *Extremophiles* 10, 181–189. doi: 10.1007/s00792-005-0482-z

Piñeiro-Vidal, M., Gijón, D., Zarza, C., and Santos, Y. (2012). *Tenacibaculum dicentrarchi* sp. nov., a marine bacterium of the familiy *Flavobacteriaceae* isolated from European sea bass. *Int. J. Syst. Evol. Microbiol.* 62(Pt 2), 425–429. doi: 10.1099/ijs.0.025122-0

Pommier, T., Canbäck, B., Riemann, L., Boström, K. H., Simu, K., Lundberg, P., et al. (2007). Global patterns of diversity and community structure in marine bacterioplankton. *Mol. Ecol.* 16, 867–880. doi: 10.1111/j.1365-294X.2006.03189.x

Rappé, M. S., Connon, S. A., Vergin, K. L., and Giovannoni, S. J. (2002). Cultivation of the ubiquitous SAR11 marine bacterioplankton clade. *Nature* 418, 630–633. doi: 10.1038/nature00917

Raven, J. A., and Waite, A. M. (2004). The evolution of silicification in diatoms: inescapable sinking and sinking as escape? *New Phytol.* 162, 45–61. doi: 10.1111/j.1469-8137.2004.01022.x

Rooney-Varga, J. N., Giewat, M. W., Savin, M. C., Sood, S., Legresley, M., and Martin, J. L. (2005). Links between phytoplankton and bacterial community dynamics in a coastal marine environment. *Microb. Ecol.* 49, 163–175. doi: 10.1007/s00248-003-1057-0

Round, F. E., Crawford, R. M., and Mann, D. G. (1990). *The Diatoms: Biology and Morphology of the Genera*. Cambridge: Cambridge University Press.

Sapp, M., Schwaderer, A. S., Wiltshire, K. H., Hoppe, H. G., Gerdts, G., and Wichels, A. (2007). Species-specific bacterial communities in the phycosphere of microalgae? *Microb. Ecol.* 53, 683–699. doi: 10.1007/s00248-006-9162-5

Sarmento, H., Romera-Castillo, C., Lindh, M., Pinhassi, J., Sala, M. M., Gasol, J. M., et al. (2013). Phytoplankton speciesspecific release of dissolved free amino acids and their selective consumption by bacteria. *Limnol. Oceanogr.* 58, 1123–1135. doi: 10.4319/lo.2013.58.3.1123

Schäfer, H., Abbas, B., Witte, H., and Muyzer, G. (2002). Genetic diversity of "satellite" bacteria present in cultures of marine diatoms. *FEMS Microbiol. Ecol.* 42, 25–35. doi: 10.1016/S0168-6496(02)00298-2

Schloss, P. D., Westcott, S. L., Ryabin, T., Hall, J. R., Hartmann, M., Hollister, E. B., et al. (2009). Introducing mothur: open-source, platform-independent, community-supported software for describing and comparing microbial communities. *Appl. Environ. Microbiol.* 75, 7537–7541. doi: 10.1128/AEM.01541-09

Segev, E., Wyche, T. P., Kim, K. H., Petersen, J., Ellebrandt, C., Vlamakis, H., et al. (2016). Dynamic metabolic exchange governs a marine algal-bacterial interaction. *Elife* 18:e17473. doi: 10.7554/eLife.17473

Seymour, J. R., Amin, S. A., Raina, J.-B., and Stocker, R. (2017). Zooming in on the phycosphere: the ecological interface for phytoplankton-bacteria relationships. *Nat. Microbiol.* 2:17065. doi: 10.1038/nmicrobiol.2017.65

Sison-Mangus, M. P., Jiang, S., Tran, K. N., and Kudela, R. M. (2014). Host-specific adaptation governs the interaction of the marine diatom, *Pseudo-nitzschia* and their microbiota. *ISME J.* 8, 63–76. doi: 10.1038/ismej.2013.138

Stackebrandt, E., and Ebers, J. (2006). Taxonomic parameters revisited: tarnished gold standards. *Microbiol. Today* 33, 152–155.

Suzuki, M., Nakagawa, Y., Harayama, S., and Yamamoto, S. (2001). Phylogenetic analysis and taxonomic study of marine *Cytophaga*-like bacteria: proposal for *Tenacibaculum* gen. nov. with *Tenacibaculum maritimum* comb. nov. and *Tenacibaculum ovolyticum* comb. nov., and description of *Tenacibaculum mesophilum* sp. nov. *Int. J. Syst. Evol. Microbiol.* 51, 1639–1652. doi: 10.1099/00207713-51-5-1639

Tamura, K., Stecher, G., Peterson, D., Filipski, A., and Kumar, S. (2013). MEGA6: molecular evolutionary genetics analysis version 6.0. *Mol. Biol. Evol.* 30, 2725–2729. doi: 10.1093/molbev/mst197

Teeling, H., Fuchs, B. M., Becher, D., Klockow, C., Gardebrecht, A., Bennke, C. M., et al. (2012). Substrate-controlled succession of marine bacterioplankton populations induced by a phytoplankton bloom. *Science* 336, 608–611. doi: 10.1126/science.1218344

Turner, S., Pryer, K. M., Miao, V. P., and Palmer, J. D. (1999). Investigating deep phylogenetic relationships among cyanobacteria and plastids by small subunit rRNA sequence analysis. *J. Eukaryot. Microbiol.* 46, 327–338. doi: 10.1111/j.1550-7408.1999.tb04612.x

van Tol, H. M., Amin, S. A., and Armbrust, E. V. (2017). Ubiquitous bacterium inhibits diatom celle division. *ISME J.* 11, 31–42. doi: 10.1038/ismej.2016.112

Vaqué, D., Duarte, C. M., and Marrasé, C. (1989). Phytoplankton colonization by bacteria: encounter probability as a limiting factor. *Mar. Ecol. Prog. Ser.* 54, 137–140. doi: 10.3354/meps054137

Yarza, P., Yilmaz, P., Pruesse, E., Glöckner, F. O., Ludwig, W., Schleifer, K. H., et al. (2014). Uniting the classification of cultured and uncultured bacteria and archaea using 16S rRNA gene sequences. *Nat. Rev. Microbiol.* 12, 635–645. doi: 10.1038/nrmicro3330

Conflict of Interest Statement: The authors declare that the research was conducted in the absence of any commercial or financial relationships that could be construed as a potential conflict of interest.

frontiers in Marine Science

ORIGINAL RESEARCH
published: 05 June 2018
doi: 10.3389/fmars.2018.00200

Identification of Bacterial Genes Expressed During Diatom-Bacteria Interactions Using an *in Vivo* Expression Technology Approach

*Ingrid Torres-Monroy and Matthias S. Ullrich**

Department of Life Sciences and Chemistry, Jacobs University Bremen, Bremen, Germany

OPEN ACCESS

Edited by:
Matthias Wietz,
University of Oldenburg, Germany

Reviewed by:
Irene Wagner-Doebler,
Helmholtz-Zentrum für Infektionsforschung (HZI), Germany
Shady A. Amin,
New York University Abu Dhabi, United Arab Emirates
Mary Ann Moran,
University of Georgia, United States

****Correspondence:***
Matthias S. Ullrich
m.ullrich@jacobs-university.de

Specialty section:
This article was submitted to Aquatic Microbiology, a section of the journal Frontiers in Marine Science

Received: *22 January 2018*
Accepted: *18 May 2018*
Published: *05 June 2018*

Citation:
Torres-Monroy I and Ullrich MS (2018) Identification of Bacterial Genes Expressed During Diatom-Bacteria Interactions Using an in Vivo Expression Technology Approach. Front. Mar. Sci. 5:200. doi: 10.3389/fmars.2018.00200

Diverse microalgae-bacteria interactions play important roles for nutrient exchange processes and marine aggregate formation leading to the cycling, mineralization, or sedimentation of organic carbon in the Oceans. The main goal of this study is to report an alternative way to assess a distinct diatom-bacteria interaction. To study this at the cellular scale, an *in vitro* interaction model system consisting of the diatom, *Thalassiosira weissflogii*, and the gamma-proteobacterium, *Marinobacter adhaerens* HP15, had previously been established. HP15 is able to attach to *T. weissflogii* cells, to induce transparent exopolymeric particle formation, and to increase marine aggregation formation. Several bacterial genes important during this interaction have been studied thus far, but genes specifically expressed *in co-culture* remained unknown. To identify such bacterial genes, an *in vivo* Expression Technology (IVET) screen was employed. For this, a promoter-trapping vector containing a fusion between a promoter-less selection marker gene and a promoterless reporter gene was constructed. Construction of a library of plasmids carrying genomic fragments upstream of the fusion and its subsequent transformation into a selection marker mutant allowed detection of 30 bacterial promoters specifically expressed during the interactions with *T. weissflogii*. Their sequence analyses revealed that the corresponding genes could be involved in many processes such as biochemical detection of diatom cells, bacterial attachment, metabolic exchange of nitrogen compounds, and resistance toward heavy metals. Identification of genes potentially involved in branched-chain amino acid uptake and utilization confirmed our previous results of a proteomics analysis. Since our current approach identified several additional genes to be induced in co-culture, use of IVET might be a valuable complementing strategy to proteomic or transcriptomic analysis of the diatom-bacteria crossplay. The current IVET approach demonstrated that the interaction between *M. adhaerens* HP15 and *T. weissflogii* is multifactorial and is likely to involve a complex network of physiological processes.

Keywords: *in vivo* expression technology, diatom-bacteria interactions, *Marinobacter adhaerens*, marine aggregate, carbon flux, *Thalassiosira weissflogii*

INTRODUCTION

In the Ocean, aggregate formation from organic matter, fecal pellets, detritus, and living cells is an important ecological mechanism that mediates settling of organic carbon to the depth (Alldredge and Silver, 1988). Aggregation in form of marine snow is fundamental for marine biogeochemical cycles since it greatly affects the efficiency of the biological pump (Fowler and Knauer, 1986; Jahnke, 1996). Initially mediated by either simple collision events or diverse chemical reactions, diatom-bacteria interactions initialize, or reinforce these processes by formation of extra-cellular polysaccharides affecting the stickiness and hence size of aggregates (Alldredge et al., 1993; Logan et al., 1995; Passow, 2002). In the last decade, considerable progress has been made in understanding algae-bacteria interactions at both, the ecological as well as the cellular and molecular levels (Wang et al., 2014; Amin et al., 2015; Durham et al., 2015, 2017; Needham et al., 2017; van Tol et al., 2017). In this way, different types of interactions were discovered, which were either microbial population driven or dictated by individual bacterial organisms. Recently, Behringer et al. (2018) demonstrated that bacterial communities on diatom surfaces displayed strong conservation across diatom strains. Seymour et al. (2017) elegantly summarized the main corresponding mechanisms and processes, which show an impressive array of diversity and complexity.

Irrespective of their origin, marine particles and aggregates represent surfaces for bacterial colonization (Dang and Lovell, 2016). These colonization processes have been studied intensively (Grossart et al., 2006b; Thiele et al., 2015; Busch et al., 2017). Interactions of bacteria with microalgae or detritus will result in a series of biochemical or physical events, which change the characteristics of the colonized particle, let it grow or shrink in size, and alter its density, porosity, stickiness, and sinking velocity (Alldredge and Youngbluth, 1985; Alldredge et al., 1986; Biddanda and Pomeroy, 1988; Kiørboe and Jackson, 2001; Kiørboe et al., 2002). The actual outcome of each individual aggregation event will depend on both, the biochemical properties of the particle(s) and the composition of the colonizing microbial populations (DeLong et al., 1993; Kiørboe et al., 2003; Bach et al., 2016), which in turn depend on each other making marine aggregate formation a highly dynamic event.

To contribute to a better understanding of the molecular basis of diatom-bacteria interactions and in particular to gain knowledge about the bacteria-mediated initial processes of diatom aggregation, we established an *in vitro* interaction model system consisting of the axenic diatom, *Thalassiosira weissflogii*, and the marine gamma-proteobacterium, *Marinobacter adhaerens* HP15 (Kaeppel et al., 2012), which belongs to a ubiquitously occurring marine bacterial genus. The two organisms are separately maintained and can be combined in co-culture. Strain HP15 was shown to preferentially attach to *T. weissflogii* cells as opposed to other bacteria, to induce transparent exopolymeric particle (TEPs) production in the diatom, and to increase aggregation during co-culture with *T. weissflogii* (Gärdes et al., 2011). This bacterial strain had initially been isolated from marine particles in the German Wadden Sea (Grossart et al., 2004), and its particular ability to interact with diatom cells had been screened from a pool of almost 90 different marine bacterial isolates (Gärdes et al., 2011). HP15's genome was sequenced and fully annotated (Gärdes et al., 2010). Furthermore, HP15 is genetically accessible and several genes potentially important for diatom-bacteria interactions have been investigated by mutagenesis (Sonnenschein et al., 2011). For instance, a variety of chemotaxis-deficient mutants were generated to study the chemotactic behavior of HP15 toward *T. weissflogii* in detail (Sonnenschein et al., 2012). The corresponding mutants showed a reduced attachment to live diatoms suggesting that chemotaxis is a substantial initial step for the interaction. The co-culture model system was further used to assess the impact of temperature and acidification on aggregate formation demonstrating that aggregation rates and sinking velocities decrease in warmer and more acidified seawater (Seebah et al., 2014). In order to get first hints on gene products potentially important for the interaction, a proteomics analysis of HP15 in response to the diatom was conducted (Stahl and Ullrich, 2016) suggesting a distinct nutrient supply for *M. adhaerens* during co-cultivation. The bacterium seemed to prefer amino acids as main carbon and nitrogen source but not polysaccharides or sugars as one would suspect from a TEP-consuming bacterial organism. Aside of this, other bacterial genes that are specifically and directly induced during the interaction remained unknown. The identification and characterization of such novel genes will in turn shed light on the nature of diatom-bacteria interaction and its underlying cellular and biogeochemical processes.

The *in vivo* expression technology (IVET) screen is a promoter-trapping technique that allows the selection of genes specifically expressed *in vivo* (Mahan et al., 1993). This technique has been applied to study gene expression in a wide range of microorganisms, providing new insights into the role of bacteria during various types of symbioses (Rediers et al., 2005; Dudley, 2008; Roberfroid et al., 2016). Although a comprehensive experimental comparison of IVET with other screening techniques such as transcriptomics or proteomics has not been done yet, IVET is unique in focusing on one of the two interacting partners thereby excluding signals from the other interaction partner. The approach is based on the principle that an auxotrophic bacterial mutant will only multiply and thus survive inside or in close proximity of a host organism if a host-inducible bacterial promoter drives a complementing essential growth factor gene provided on a separate plasmid (*in trans*). Thus, the method is qualitative and not quantitative as are screenings done with transcriptomics or proteomics. Herein, for the first time, an IVET screening was applied to identify bacterial genes relevant during diatom-bacteria interactions using the bacterial strain HP15 and *T. weissflogii* as an interaction model system.

In the present study and in order to complement and extend on our previous proteomics work with the diatom-bacteria co-culture system, an IVET screen was applied for co-cultured *M. adhaerens* and *T. weissflogii*. To this end, an IVET plasmid containing a promoterless essential growth factor

gene and an *in vitro* reporter gene was constructed and loaded with a genomic library of short DNA fragments, some of which contained promoters. The IVET library was inserted into an essential growth factor mutant, which was unable to survive in co-culture with the diatom, and transformants were screened for survival during co-culture. Surviving mutant transformants, which were not expressing the *in vitro* reporter gene after re-isolation from the co-culture, indicated presence of co-culture specific promoter sequences. The corresponding genes were analyzed with respect to homologies with data base entries in order to learn about their potential functions and to propose their putative roles during the diatom-bacteria interaction.

MATERIALS AND METHODS

Bacterial Strains, Plasmids, and Culture Conditions

Bacterial strains and plasmids used are listed in **Table 1**. HP15 was isolated from particles collected from surface waters of the German Bight (Grossart et al., 2004). The bacterium was grown in marine broth (MB) medium (ZoBell, 1941) using sterile North-Sea water at 28°C. MB medium was supplemented with uracil (5 μg ml^{-1}) as a pyrimidine source for growth of HP15 pyrimidine-deficient auxotrophs. During the *in vitro* screening, MB medium was supplemented with 5-bromo-4-chloro-3-indolyl-β-D-galactopyranoside (X-Gal) (50 μg ml^{-1}) allowing for blue/white colony selection. f/2 GLUT medium was made with f/2 medium (Guillard and Ryther, 1962) supplemented with 5 g l^{-1} glutamate and was used as minimal medium to confirm auxotrophy of the HP15 mutant Δ*pyrB*. f/2 medium was prepared with pre-filtered (0.2 μm pore size) and autoclaved North-Sea water. All herein reported CFU/ml values for bacteria were derived by determining the optical density at 600 nm (OD_{600}) and deducing CFU/ml from a previously established calibration curve of OD_{600} vs. CFU/ml derived from serial dilution platings.

Escherichia coli strains were maintained in Luria-Bertani (LB) agar medium supplemented with appropriate antibiotics. *E. coli*

TABLE 1 | Strains and plasmids used in this study.

Strain or plasmid	Genotype or relevant characteristics	Source or reference
E. coli		
DH5α	*Φ*80*dlacZ*ΔM15 Δ(*lacZYA- argF*) U169 *recA1 hsdR17 deoR thi-1 supE44 gyrA96 relA1/λpir*	(Miller and Mekalanos, 1988)
ST18	λpir Δ*hemA pro thi hsdR*$^+$ Trp Smr	(Thoma and Schobert, 2009)
HB101	Carrying helper plasmid pRK2013 Km^R	(Figurski and Helinski, 1979)
M. adhaerens		
HP15	Wild-type	(Grossart et al., 2004)
ΔpyrB	Δ*pyrB* Cm^R	This study
Plasmids		
pGEM®-T Easy	colE1 *lacZ* Amp^R	Promega, Mannheim, Germany
pGEM_pyrBup	pGEM®-T Easy containing 960 bp upstream *pyrB* flanking region of HP15 Amp^R	This study
pGEM_pyrBdown	pGEM®-T Easy containing 984 bp downstream *pyrB* flanking region of HP15 Amp^R	This study
pFCM1	Amp^R Cm^R	(Choi and Schweizer, 2005)
pGEM_pyrB_down_cm	Cm^R (1129 bp) from pFCM1 ligated into *Nde*I site of pGEM_pyrBdown Amp^R	This study
pGEM_pyrB_down_cm_up	Cm^R and downstream region (2168 bp) from pGEM_pyrB_down_cm ligated with *KpnI*/*Nhe*I into pGEM_pyrBup Amp^R	This study
pEX18Tc	pMB1 oriT *sacB* Tet^R	(Hoang et al., 1998)
pEX_pyrBcdu	Knock-out fragment (3134 bp) from pGEM_pyrB_down_cm_up ligated with *Hin*dIII into pEX18Tc	This study
pBBR1MCS-4	broad-host-range mob Amp^R	(Kovach et al., 1995)
pMC1871	*lacZ* Tet^R	(Shapira et al., 1983)
pITM3	derivative of pBBR1MCS-4 with insertion of *lacZ* by *Kpn*I in opposite direction to the lac promoter Amp^R	This study
pITM4	derivative of pBBR1MCS-4 with insertion of *lacZ* by *Kpn*I under control of the lac promotor Amp^R	This study
pITM3_pyrB	derivative of pITM3 with insertion of *pyrBC* of HP15 upstream *lacZ* Amp^R	This study
pITM1_Sau3A_3	pITM1 carrying a HP15 native promoter upstream *lacZ* Amp^R	This study
pITM3_pyrB_prom	derivative of pITM3_pyrB with insertion uppstream *pyrBC-kacZ* fussion of a promoter of HP15 Amp^R	This study
pITM1	derivative of pBBR1MCS with insertion of *lacZ* by *Kpn*I in opposite direction to the lac promoter Amp^R	(Sonnenschein et al., 2011)

DH5α was used for maintaining the HP15 genomic library generated in the IVET vector. *E. coli* ST18 (Thoma and Schobert, 2009) was used as a donor strain during bi-parental conjugation and grown in LB medium containing 50 μg/ml 5-aminolevulinic acid (ALA). *E. coli* HB101 (pRK2013) was used as a helper strain during tri-parental conjugation (Figurski and Helinski, 1979). The following antibiotics were added to media when needed (in μg ml^{-1}): chloramphenicol, 25; kanamycin, 50; and ampicillin, 50.

Diatom Culture Conditions

Axenic cultures of *T. weissflogii* (CCMP 1336) were obtained from the Provasoli-Guillard National Center for Culture of Marine Phytoplankton (Maine, USA). Diatom cultures were grown at 16°C in f/2 medium, with a 12-h photoperiod at 115 μmol photons m^{-2} s^{-1} and were checked regularly for bacterial contaminations by plating on LB agar medium plates and by frequent microscopic observations. Diatom cell numbers were determined by cell counts in a Sedgewick Rafter Counting Chamber S50 (SPI Supplies, West Chester, PA, USA).

DNA Techniques

Plasmid preparation, DNA extraction, PCR, and other standard DNA techniques were performed as previously described (Sambrook et al., 1989). Restriction enzymes and DNA-modifying enzymes were used as recommended by the manufacturer (Fermentas, St. Leon-Rot, Germany). Nucleotide sequencing was carried out at Eurofins MWG (Ebersberg, Germany). DNA sequences analysis and oligonucleotide primer design were done using Vector NTI® Software 10.3.0 (Invitrogen Corporation, Carlsbad, CA, USA). Nucleotide and amino acid sequences were compared using the Basic Local Alignment Search Tool BLAST provided by the National Center for Biotechnology Information (http://www.ncbi.nlm.nih.gov/BLAST/) (Altschul et al., 1990) and InterProScan Sequence Search provided by the European Bioinformatics Institute (http://www.ebi.ac.uk/Tools/pfa/iprscan/). The oligonucleotides used in this study are listed in **Table 2**.

IVET Vector Construction

The first step to implement the IVET strategy is the construction of an IVET vector (**Supplementary Figure 1**); the remaining steps in the strategy are summarized in **Figure 1**. The broad-host-range plasmid pBBR1MCS-4 (Kovach et al., 1995) was used as a backbone to construct the IVET vector (**Supplementary Figure 1**). The full-sized *E. coli* promoter-less *lacZ* gene was amplified from plasmid pMC1871 with the primers LacZF/LacZR (Smirnova and Ullrich, 2004). The resulting 3.1-kb PCR fragment was treated with *Kpn*I and ligated into *Kpn*I-treated pBBR1MCS-4 in opposite direction of the vector-borne lac promoter resulting in plasmid pITM3. A second plasmid, pITM4, was generated with the 3.1-kb PCR fragment containing *lacZ* cloned in the same orientation as that of the lac promoter of pBBR1MCS-4. Plasmids pITM3 and pITM4 were transformed into *E. coli* ST18 and subsequently transferred to HP15 by conjugation. For this, cells of donor and recipient ($\sim 10^9$ cell ml^{-1} each) were mixed in a ratio of 1:2, spotted on LB agar plates, and incubated for 24 h at 28°C. The cell mass was then scraped off and re-suspended in MB medium for subsequent dilution plating. Transconjugants were selected on MB agar supplemented with ampicillin and X-Gal after incubation at 28°C for 2–3 days. Presence of IVET plasmids in transconjugants was confirmed by plasmid DNA isolation using the Midi Prep Kit according to the manufacturer's recommendations (Macherey-Nagel, Düren, Germany) and agarose gel electrophoresis.

Primers pyrBF and pyrBR were designed to amplify the promoter-less *pyrBC* locus from HP15. This 2,285-bp PCR product was restricted with *Hin*dIII and *Xho*I and cloned into *Hin*dIII/*Xho*I-treated pITM3 to generate pITM3_pyrB. Plasmid pITM3_pyrB was transformed into HP15 wild-type and Δ*pyrB* mutant by bi-parental conjugation as described above. The

TABLE 2 | List of primers used in this study.

Primer	Sequence 5′-3′	Restriction enzyme
pyrBup-F	ATTGGGGTACCGCTAGCTCGTTCGCGGTCATGGGT	*Kpn*I, *Nhe*I
pyrBup-R	ATTGGAAGCTTCGCGTCATGGCGTTCGAT	*Hin*dIII
pyrB_Down2-F	ATTGGAAGCTTGGTACCCCTGCTTGGCGGCGGTAT	*Hin*dIII, *Kpn*I
pyrB_Down2-R	AGGGGCCAGGCATGAGCA	
Cm2 F	AGTGCCATATGGAGCTCGAATTGGGGATCTT	*Nde*I
Cm2 R	AGTGCCATATGGCTAGCGAGCTCGAATTAGCTTCAAA	*Nde*I, *Nhe*I
lacZF	AGT GGT ACC CGT CGT TTT ACA ACG TC	*Kpn*I
lacZR	AGT GGT ACC TAT TAT TTT TGA CAC CA	*Kpn*I
pyrB F	ATTGGCTCGAGCAGATTGCCGGCTTTGGC	*Xho*I
pyrB mutF	CGAATCAGCAGCGCGGTATT	
pyrB mutR	CCATCAACGCGTCAAACTGC	
pyrB out	CGAATCGTCAGCATATCC	
T7	TAATACGACTCACTATAGGG	

Underlined nucleotides represent endonuclease restriction enzyme recognition sites used for cloning steps.

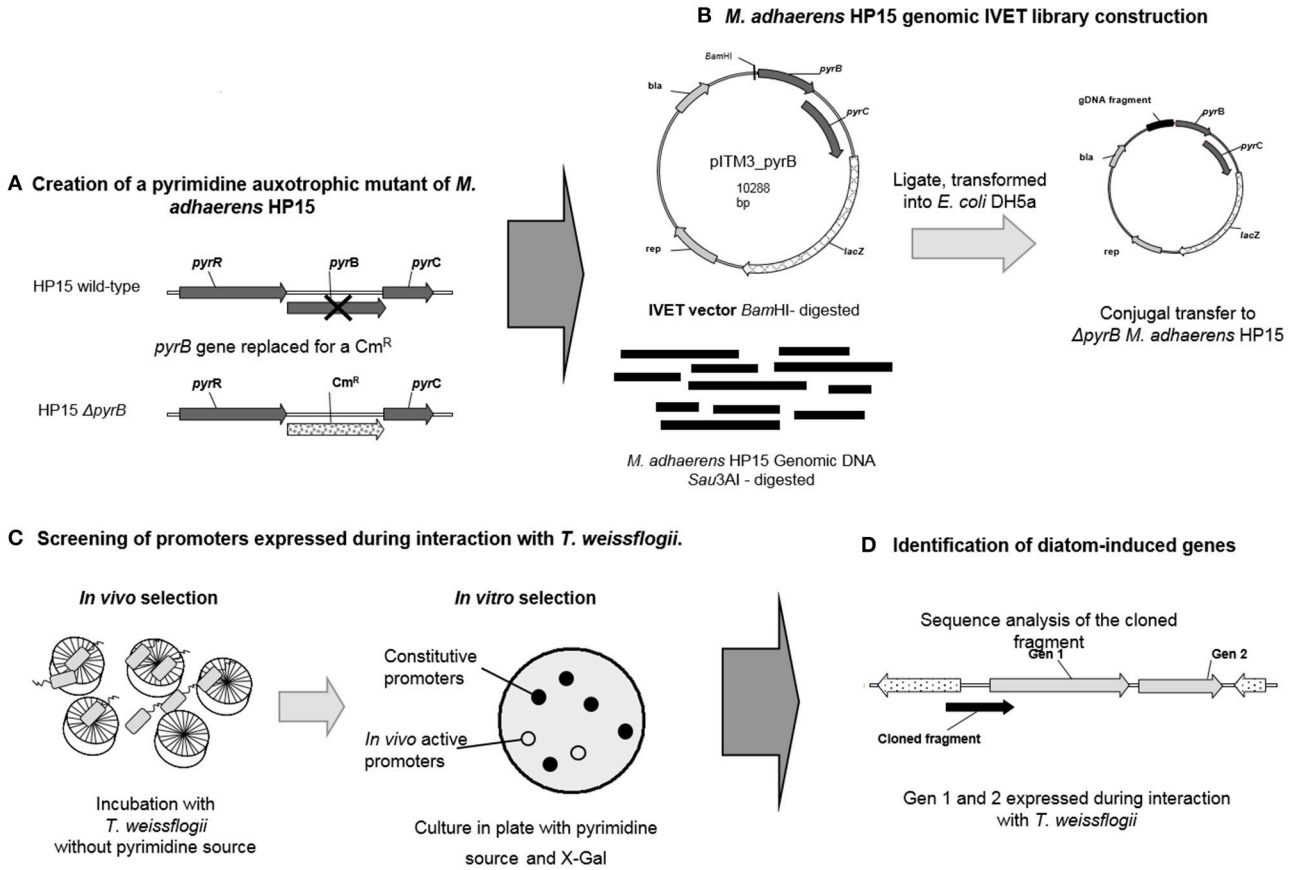

FIGURE 1 | Schematic representation of IVET strategy. **(A)** An auxotroph mutant in *M. adhaerens* HP15 was created by replacing the gene *pyrB* with a chloramphenicol resistant cassette (Cm^R). This mutant is unable to grow in the absence of a pyrimidine source; **(B)** A genomic library was generated in the pITM3-pyrB plasmid by digesting the genomic DNA of HP15 and cloning the resulting fragments into the *Bam*HI site of the plasmid. The resulting plasmids were transformed into HP15 by triparental conjugation; **(C)** For the selection of promoters active during the interaction the trasnconjugants of HP15 Δ*pyrB* carrying the genomic library in pITM3-pyrB were incubated with *T. weissflogii*, without the addition of a pyrimidine source. Then the survival trasnconjugants were plated in agar media supplemented with pyrimidine and X-Gal, the brownish (non-blue) colonies, which contain active *in co-culture* promoter, were selected; **(D)** The plasmid DNA was extracted from the positive colonies, the fragment upstream the fusion *pyrB-lacZ* was PCR amplified and sequenced. The genes under the control of the promoter found in the DNA fragment were identified.

transconjugants were selected in MB media containing X-Gal and ampicillin.

Generation of a Pyrimidine Auxotrophic Mutant of *M. adhaerens* HP15

A gene-specific mutagenesis based on homologous recombination was conducted to generate a Δ*pyrB* mutant in HP15 according to Hoang et al. (1998) (**Figure 1A**). A mutagenic plasmid was constructed in which a chloramphenicol resistance (Cm^R) cassette was flanked by DNA fragments obtained from upstream and downstream regions of the *pyrB* gene as follows: 960 bp upstream and 984 bp downstream of the *pyrB* gene were PCR-amplified using the primer pairs pyrB_upF/pyrB_upR and pyrB_down2F/pyrB_down2R, respectively. Both flanking fragments were sub-cloned into pGEM®-T Easy vector (Promega, Mannheim, Germany) resulting in plasmids, pGEM_pyrBup and pGEM_pyrBdown, respectively. A DNA fragment of 1,129 bp carrying a Cm^R cassette was amplified with the primers cm2R/cm2F from pFCM1. The fragment was treated with *Nde*I and sub-cloned into *Nde*I-treated pGEM_pyrBdown resulting in plasmid pGEM_pyrB_down_cm. From this plasmid, the 2,168-bp fragment containing the downstream region and the Cm^R cassette was restricted with *Kpn*I/*Nhe*I and ligated into *Kpn*I/*Nhe*I-treated pGEM_pyrB_up, resulting in plasmid pGEM_pyrB_down_cm_up. From this plasmid, a 3,134-bp fragment containing both flanking regions and the Cm^R cassette was excised with *Hind*III and ligated into the *Hind*III-treated vector pEX18Tc. The generated conjugable mutagenic construct pEX_pyrBcdu was then transformed into HP15 by bi-parental conjugation. Resulting mutants were selected on chloramphenicol-containing MB agar plates. A successful double cross-over event for the Δ*pyrB* mutant was confirmed by PCR using the primers mut_pyrBF/mut_pyrBR resulting in the expected 1,205 and 1,410-bp amplification fragments for the wild-type and the mutated *pyrB* gene, respectively.

To confirm the auxothrophy of mutant Δ*pyrB*, it was grown in f/2 GLUT medium with and without uracil. Subsequently, to determine whether the *pyrB* gene is a suitable selection marker for promoters expressed during the interaction with *T. weissflogii*, mutant Δ*pyrB* and the wild-type were separately co-cultivated with the diatom in the absence of uracil. Bacteria were grown overnight in MB liquid medium at 18°C and the cells were harvested by centrifugation at 4,000 rpm for 15 min. To avoid carrying over of nutrients from MB medium the cells were washed twice with f/2 medium. Cell numbers were adjusted to $\sim 10^5$ CFU ml^{-1} and mixed with $\sim 10^4$ cells ml^{-1} of *T. weissflogii* in exponential growth stage. The cultures were incubated for 6 days at 16°C, with a 2-h photoperiod at 115 μmol photons m^{-2} s^{-1}, and shaking at 50 rpm. Dilutions series were done daily in appropriate media, and CFU numbers were determined.

To complement the *pyrB* mutant, a functional native promoter from the HP15 genome was cloned upstream the *pyrBC-lacZ* fusion in pITM3_pyrB. Such a native promoter was selected by partial restriction of the genomic DNA of HP15 with *Sau*3AI and cloning of a pool of restriction fragments into *Bam*HI-treated plasmid pITM1 (Sonnenschein et al., 2011). The resulting genomic library was transformed into HP15 wild-type by bi-parental conjugation. Five blue colonies were selected and the region upstream the *pyrBC-lacZ* fusion from one of those clones (pITM1_Sau3A_3) was sequenced thereby identifying the native promoter. This DNA region was excised from pITM1_Sau3A_3 with *Xba*I and *Hin*dIII and cloned into *Xba*I/*Hin*dIII-treated pITM3_pyrB, resulting in the plasmid pITM3_pyrB_prom, which was transformed into Δ*pyrB* HP15 by bi-parental conjugation. Transconjugants were selected after incubation on f/2 GLUT agar supplemented with ampicillin and X-Gal without uracil at 28°C for 2–3 days.

M. adhaerens HP15 Genomic IVET Library Construction

A genomic IVET library of HP15 was constructed in pITM3_pyrB as follows (**Figure 1B**): Total genomic DNA of HP15 was partially digested with *Sau*3AI; DNA fragments with sizes ranging from 0.5 to 1.5 kb were selected, and ligated into the *Bam*HI site of pITM3_pyrB. The IVET library was then transformed into *E. coli* DH5α. To verify the randomness of inserts, 24 clones of *E. coli* DH5α were randomly picked and the region upstream the *pyrBC-lacZ* fusion was amplified with the primers T7 and PyrB_out by colony PCR. The IVET library was then transferred into the mutant Δ*pyrB* by tri-parental conjugation. Briefly, *E. coli* DH5α carrying the IVET library was used as a donor and *E. coli* HB101 (pRK2013) served as a helper strain. Cells of donor, helper, and recipient ($\sim 10^{10}$ cells ml^{-1}) were mixed in a ratio of 1:1:2, spotted on LB ALA agar plates, and incubated for 24 h at 28°C. Cell mass was scraped off and re-suspended in MB medium for subsequent dilution plating. The resulting transformants were selected on MB agar plates containing chloramphenicol, ampicillin, uracil, and X-Gal. To verify the randomness of plasmids transformed into mutant Δ*pyrB*, 24 clones were randomly picked and subjected to colony PCR as described above. Although, cloning by partial digestion using an enzyme with frequent recognition sites does not comprehensively cover the entire genome of *M. adhaerens*, the randomness of insert sizes allows to conclude that a genome-wide array of promoter sequences had been obtained.

Screening of Promoters Expressed During Interaction With *T. weissflogii*

For the *in co-culture* selection of promoters, co-cultivation of mutant Δ*pyrB* transconjugants carrying the IVET library with diatom cells was conducted (**Figure 1C**). Briefly, 10,000 cells ml^{-1} of *T. weissflogii* in exponential growth stage were mixed with the bacterial transconjugants (1×10^5 CFU ml^{-1}) in cell culture flasks with a final volume of 35 ml of f/2 media and incubated at room temperature and a 2-h photoperiod for 24 h. Next, 5 ml of the co-cultures were transferred to 30 ml fresh f/2 medium containing *T. weissflogii* in exponential growth stage (10,000 cells ml^{-1}) and incubated under the same conditions as above for additional 24 h. This procedure was repeated five times in order to enrich for positive clones. After 6 days of incubation, transconjugants were recovered and subjected to *in vitro* selection. For this, cultures initiated on day 4 and 5 were individually centrifuged at 4,000 rpm for 20 min and dilution series were performed with recovered cells in MB agar plates containing chloramphenicol, ampicillin, uracil and X-Gal at 28°C. After 3–4 days of incubation brownish colonies (non-blue) were selected and re-streaked.

A control experiment was performed to observe the growth pattern of the mutant Δ*pyrB* carrying plasmid pITM3_pyrB without any insertion upstream the *pyrBC-lacZ* fusion (empty IVET vector). 10,000 cells ml^{-1} of *T. weissflogii* in exponential growth stage were mixed with Δ*pyrB* transconjugants carrying pITM3_pyrB (1×10^5 CFU ml^{-1}) in cell culture flasks in f/2 medium and incubated at room temperature and a 2-h photoperiod for 5 days, which was used in all previous studies on this model interaction system (Gärdes et al., 2011) because the diatom aggregate formation was optimal under this light regime. Dilution series were carried out daily from the culture and the number of CFU was calculated.

Identification of Diatom-Induced Genes

Brownish colonies of Δ*pyrB* transconjugants were selected after co-inoculation with *T. weissflogii*, and subjected to colony PCR with the primers T7/pyrB_out to check for the presence of an insert upstream of the *pyrBC-lacZ* fusion in pITM3_pyrB. Transconjugants giving individually different PCR products of sizes larger than 570 bp were selected and their PCR product sequences determined. The obtained sequences were analyzed by BLAST and potential promoters regions as well as downstream located genes identified. The positive transconjugants were individually co-inoculated with *T. weissflogii* to confirm their survival in presence of diatoms. For this, bacteria were grown overnight in MB liquid cultures at 18°C, the cells were harvested by centrifugation at 4,000 rpm for 15 min, washed twice with f/2 medium, their concentration adjusted to 1×10^5 CFU ml^{-1}, and mixed with 10,000 cells ml^{-1} of *T. weissflogii* in exponential growth stage. The co-cultures were incubated for 8 days at 18°C,

with a 2 h photoperiod. Dilutions series were done in appropriate media and CFU numbers were determined.

RESULTS

Pyrimidine Auxotrophic Mutant of *M. adhaerens* HP15

For the identification of bacterial promoters, the gene *pyrB* was used as selection marker. *pyrB* is essential for survival encoding for aspartate transcarbamoylase (ATCase; EC 2.1.3.2), an enzyme that is necessary for biosynthesis of pyrimidines (Schurr et al., 1995). The availability of pyrimidines in many natural environments is limited, which renders *pyrB* a successful selection marker (Lee and Cooksey, 2000). To verify its potential as a selection marker in our system, a *pyrB* mutant in HP15 was created. This mutant should be unable to grow in the absence of a pyrimidine source. A mutagenic construct was transformed into HP15 wild-type and the *pyrB* gene was replaced by a Cm^R cassette via homologous recombination. A clone that had undergone a double crossover of the Cm^R cassette as demonstrated by PCR was selected. Subsequently, the auxotrophy of the *pyrB* deletion mutant was confirmed by testing its growth on agar minimal medium with or without uracil as the sole pyrimidine source. Mutant Δ*pyrB* was not able to grow without uracil thus proving its expected phenotype (data not shown). In addition, growth of mutant Δ*pyrB* and HP15 wild-type in liquid f/2 GLUT medium were indistinguishable from each other when uracil was supplemented indicating that the mutation did not affect bacterial growth in general (**Supplementary Figure 2**). However and as expected, mutant Δ*pyrB* did not grow without uracil.

To determine whether lack of *pyrB* expression is a suitable selection criterion during the interaction with *T. weissflogii* and to test whether the diatom provides any pyrimidines to functionally complement the mutant's genotype, mutant Δ*pyrB* was cultivated with diatoms in f/2 medium with and without any uracil. Mutant Δ*pyrB* cell numbers dramatically decrease during the incubation time when compared to the growth of the wild-type when no uracil was added to the medium (**Figure 2**). In accordance with the *in vitro* growth, mutant Δ*pyrB* grew similar to the wild type in presence of diatoms and uracil. These result clearly demonstrated that the diatom is not providing any pyrimidines proving *pyrB*'s suitability as a selection marker gene for this study.

Generation of the IVET Library

The suitability of *lacZ* as an *in vitro* reporter gene in HP15 had previously been described (Sonnenschein et al., 2011), thus this gene was used for the construction of the IVET vector. As an *in co-culture* selection marker the promoter-less *pyrBC* locus of HP15 was chosen since it had been previously shown that the gene *pyrB* alone was not able to complement *pyrB* deletion mutants and that the *pyrC* gene located downstream of *pyrB* was required for this purpose (Schurr et al., 1995; Lee and Cooksey, 2000). In order to be suitable tools, the Δ*pyrB* mutant must not grow unless provided by uracil while the IVET plasmid must not complement the Δ*pyrB* mutant as long as it does not carry a functional promoter sequence upstream of the *in co-culture* selection marker gene. The

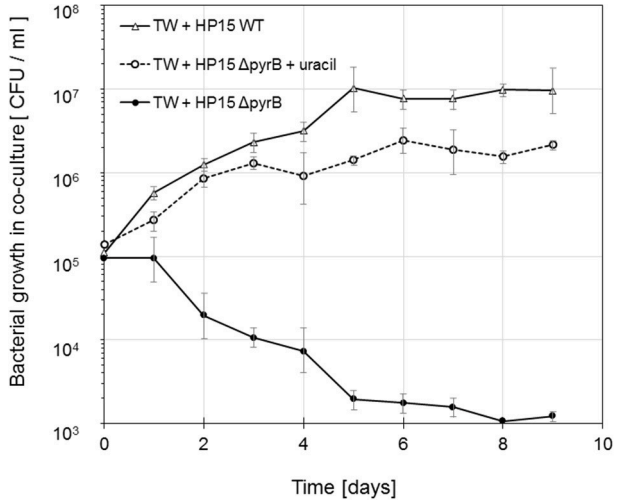

FIGURE 2 | Growth of *M. adhaerens* HP15 Δ*pyrB* in co-culture with *T. weissflogii* in F/2 media with and without uracil (5 μg ml^{-1}). *M. adhaerens* HP15 wild-type was used as a positive control. Experiment was conducted with three biological replicates, error bars represent standard deviation.

Δ*pyrB* mutant carrying the IVET plasmid pITM3_pyrB did not grow in f/2 GLUT medium without uracil. In contrast, this transconjugant grew well in form of brownish colonies in f/2 GLUT medium supplemented with uracil and X-Gal (data not shown) confirming that the *pyrBC-lacZ* fusion present in pITM3_pyrB is not expressed. Furthermore, the introduction of a functional promoter derived from the genome of HP15 into the IVET plasmid and its subsequent transformation into Δ*pyrB* mutant allowed its full complementation. Corresponding transformants grew on agar medium without uracil and formed LacZ-expressing (blue) colonies when X-Gal was provided (data not shown). In summary, these tested parameters demonstrated that the IVET plasmid and the Δ*pyrB* mutant were suitable tools for the identification of diatom contact-induced genes of HP15.

A genomic library of HP15 was constructed in pITM3_pyrB and transformed into *E. coli* DH5α plated on 50 agar plates each containing 200–300 colonies resulting in a total of roughly 10,000 to 15,000 clones. The randomness of inserts was confirmed by PCR with 190 randomyl chosen clones showing that 85% of the analyzed *E. coli* DH5α transformants had an insert in the IVET plasmid. Importantly, all of the insert sizes were different from each other (data not shown) demonstrating that the IVET library contained a random number of different DNA fragments. After conjugation of the IVET library into mutant Δ*pyrB*, a total of 4.5×10^6 CFU ml^{-1} were obtained, with roughly 40% of the transconjugants forming LacZ-positive blue colonies on X-Gal agar medium. To demonstrate the randomness of IVET plasmids in the transconjugant pool, a second round of PCR tests was done. In this case 82% of the analyzed 200 clones had an insert, and all inserts had different sizes (data not shown) suggesting that roughly one fifth of all transferred IVET plasmids did not contain an insert. In conclusion, there results hint at a randomness of DNA fragments inserted in the IVET plasmid but do not allow

speculations about the completeness of the screen since the very frequently occuring recognition sites of the used endonuclease *Sau3*A might have been used unevenly during the applied partial digest.

In Co-culture Selection of Promoters During Interaction With *T. weissflogii*

In order to test whether or not mutant transconjugants with empty IVET plasmids could survive the *in co-culture* selection, first a control experiment was conducted, in which a Δ*pyrB* transconjugant carrying an empty IVET plasmid was grown together with the diatom. From an initial inoculum of 1.2×10^5 CFU ml^{-1} only 395 CFU ml^{-1} were recovered after 2 days and 22 CFU ml^{-1} after 3 days. However, after day 4 no colonies were observed. These results showed that transconjugant Δ*pyrB* (pITM3_pyrB) is not able to survive for more than 4 days in the presence of the diatom. Consequently, the following diatom-bacteria co-cultures were performed in such a way that positive clones were enriched while negative clones or clones with empty IVET plasmids were eliminated. To frequently refresh potential diatom-borne selecting factors or signals, co-cultures of Δ*pyrB* mutants carrying the IVET library with diatom cells were diluted every 24 h by transferring 5 ml of the co-culture into f/2 medium containing fresh diatom cells. Co-cultures were repeated several times to increase the number of positive clones. Determination of CFUs was carried out daily (data not shown), and randomly chosen brownish colonies (non-blue) were selected while blue colonies, indicating a constitutive expression of *lacZ*, were discarded. Brownish colonies represented transconjugants with IVET plasmids carrying a promoter sequence inactive under *in vitro* conditions. However, since these transconjugants had survived several diatom co-cultures, their promoter sequences must have been active *in co-culture*. All obtained brownish colonies were checked for inserts by PCR. All analyzed colonies from 4- or 5-day-old cultures had an insert demonstrating the suitability of the selection regime.

Potential *in Co-culture* Induced Promoters

In total, 97 brownish colonies were obtained which carried a DNA insert (confirmed by PCR) upstream of the *pyrBC-lacZ* fusion in pITM3_pyrB. These transconjugants were subsequently cultivated in f/2 GLUT solid medium with or without uracil to confirm their auxotrophy in culture media. From these 97 transconjugants, 23 cultures did not show the expected lack of growth suggesting a false-positive result. The PCR products for the remaining 74 colonies were sequenced. Nucleotide sequence analysis indicated that almost one third of the sequences occurred in duplicates so that a total of 41 individual and unique insert DNAs could be obtained. The corresponding IVET plasmids were isolated from the transconjugants and used for further characterization.

Interestingly, from the 41 insert DNAs, 30 inserts were in the same 5′-3′ orientation in terms of their downstream reading frames and the *pyrBC-lacZ* fusion of the IVET plasmid, while 11 were found in the opposite orientation on the antisense strand of an annotated coding region. In addition to the *in co-culture* induced clones, a randomly chosen blue colony representing a constitutively expressed *pyrBC-lacZ* phenotype was sequenced and used as a control in the following experiments. The insert of this transconjugant showed sequence identities to the upstream sequence of a gene encoding aldehyde dehydrogenase (Locus tag: HP15_943).

To confirm that the 30 cloned insert sequences were specifically allowing expression of *pyrBC-lacZ* during the interaction with *T. weissflogii,* the growth patterns of 13 randomly chosen *in vitro* uracil-deficient brown transconjugants (colonies 1, 10, 15, 22, 26, 28, 30, 68, 90, 100, 161, 168, and 194), and the blue transconjugant were analyzed in individual co-cultures with the diatom in f/2 medium without uracil (**Figure 3**). A transconjugant carrying the empty IVET plasmid was used as a negative control. All 13 positive transconjugants were able to survive the diatom co-incubation reaching cell numbers comparable to that of the wild-type or the blue transconjugant, which harbors a constitutively expressed promoter sequence. After 4 days of incubation, there was a more than three orders of magnitude difference in viable cell numbers of the positive clones and the negative control demonstrating that the identified promoter sequences were induced and enabled the Δ*pyrB* mutant to survive during the interaction with *T. weissflogii*.

In order to rule out any possible genomic alterations in the 41 mutant transconjugants, re-isolated IVET plasmids were individually re-introduced to the Δ*pyrB* mutant for a second time. Novel transconjugants were again tested for growth in f/2 GLUT solid medium with or without uracil but with X-Gal: These novel transconjugants did not grow when uracil was missing but grew well on uracil-containing medium indicating that the corresponding promoter sequences were not active and that the mutant transconjugants remained auxotrophic *in vitro* (Data not shown). Colonies on agar plates with uracil were brownish in color just like those of the wild type of HP15. While this result was expected for the 30 IVET plasmids, which contained promoter sequences in the same orientation as the annotated downstream gene, the corrrspondingly positive results for the remaining 11 IVET plasmid with DNA sequences in opposite direction to annotated genes remained obscure. One can only speculate that the automatic annotation of the HP15 genome (accession no. CP001978.1) might still be partially incomplete or incorrect (Gärdes et al., 2010).

DNA Sequence Analysis

M. adhaerens HP15 genes under the control of the promoters identified as specifically induced during interaction with *T. weissflogii* are listed in **Table 3**. All accession numbers are from Genbank entries CP001978.1 (*M. adhaerens* HP15 genome) or CP001978.1 (*M. adhaerens* HP15 187-kb indigenous plasmid). The possible functions of the correspondingly downstream located genes were deduced by analyzing its amino acid sequences and determining the presence of conserved domains or similarities with reported proteins in the GenBank. Genes identified in the 11 transcriptional fusions orientated in the opposite direction to the *in vitro* reporter gene were not considered any further.

Detected genes were grouped depending on their potential ecological role during the interaction as follows: Genes that

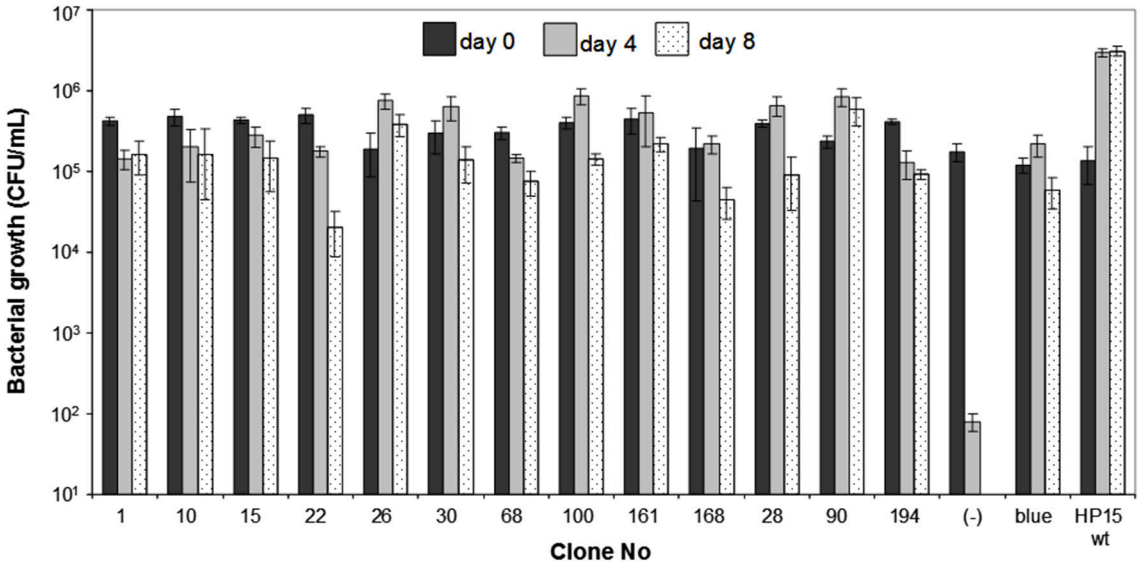

FIGURE 3 | Growth of individual clones of *M. adhaerens* HP15 Δ*pyrB* carrying potential *in co-culture* induced promoters and *T. weissflogii*. Wild-type and a blue colored mutant were used as a positive control. Δ*pyrB* HP15 (pITM3_pyrB) was used as a negative control.

encode enzymes required in (i) detection of diatom cells; (ii) attachment to the diatom cells; (iii) putative metabolic exchange with diatom cells; and (iv) unknown functions (**Table 3**). Their potential role(s) will be discussed below.

DISCUSSION

Identifying bacterial genes expressed during diatom-bacteria interactions is a fundamental pre-requisite for understanding the functional mechanisms governing bacteria-induced algal aggregation and bacterial organic matter transformation in the oceans. Therefore, an IVET strategy was employed to identify *M. adhaerens* HP15 genes specifically induced during its interaction with *T. weissflogii*. IVET is an economically feasible, cultivation-based approach, which allows the use of DNA and standard molecular techniques. DNA is generally more stable than RNA and thus less vulnerable to biasing differential signal degradation in course of multi-step procedures. In addition, IVET avoids some of the potential next-generation sequencing biases, such as problems associated with high-throughput cDNA generation and high-throughput nucleotide sequencing. Although IVET itself has biases such as being rather qualitative than quantitative and that the required absolute length of insert DNA in the IVET library or low level of expression from some promoters might exclude certain genes or groups of genes, the herein applied approach complements transcriptomics work of others (Durham et al., 2015, 2017) and our own proteomics work (Stahl and Ullrich, 2016). Others had shown previously that IVET can be used to identify novel genes important for the respective analyzed interactions (Rediers et al., 2005; Dudley, 2008). Naturally, those will differ from interaction to interaction. With our approach, for the first time we were able to evaluate the potential importance of key genes for diatom-bacteria interactions using a model system and promoter trapping. This strategy allowed the identification of HP15 genes coding for functions such as detection of diatom cells, attachment, and metabolic exchange. Additionally, six gene loci encoding conserved hypothetical proteins without known functions were identified, which were expressed during this interaction. Two of these were located in close proximity to other identified genes hits. In the current study, co-culture-inducible promoter activities were detected. Although it is widely accepted that promoters drive the expression of directly downstream located genes, our study did not detect the expression of those genes. However, finding active promoters for some genes, which code for proteins previously detected by a proteomics approach (Stahl and Ullrich, 2016) as well as finding gene homologs found by transcriptomics studies of others (Durham et al., 2017) are strong hints for a successful screening approach. In the next paragraphs, the possible ecological roles and importance of the identified genes are discussed.

Genes Involved in Detection of Diatom Cells

Chemotaxis is a mechanism that bacteria use to chemically sense their environment and move toward attractants or away from repellents (Baker et al., 2005). In this process, chemoreceptors interact with specific chemicals—often amino acids—and interact with key chemotaxis proteins to control flagellar or pilus-mediated motility (Eisenbach, 1996). Chemoreceptors have a methyl-accepting chemotaxis domain, a homolog of which was found in the putative HP15 protein encoded by the gene downstream of the promoter sequence found in col. 178 (**Table 3**). Therefore, our current results support the previous finding that chemotaxis of HP15 is important for the diatom-bacteria interaction (Sonnenschein et al., 2012). Another example

TABLE 3 | List of bacterial genes identified as being under control of the identified promoters during interaction with *T. weissflogii*.

Colony no.	Accession no.	Annotation	Possible role	Nucleotide number in the HP15 Genome position	
				From	To
GENES POTENTIALLY INVOLVED IN DETECTION OF DIATOM CELLS					
1	HP15_158	Transcriptional regulator MerR1	Regulation of heavy metal or oxygen stress	156071	156419
30	HP15_108	Outer membrane protein CzcC	Heavy metal efflux system CzcCBA	111322	112219
178	HP15_2157	Methyl-accepting chemotaxis protein	Chemotaxis	2265623	2264909
204	HP15_3664	Response regulator containing receiver domain	Two-component signal regulation	3862479	3861943
GENES POTENTIALLY INVOLVED IN ATTACHMENT					
32	HP15_313	Protein containing bacterial Ig-like domain	Adhesion/invasion	309868	309432
68	HP15_p187-g4	Type IVb fimbrial low-molecular-weight pilin	Tight adherence locus attachment	p178_2167	p178_2503
168	HP15_2444	PTS IIA-like nitrogen-regulatory protein PtsN	Sugar uptake regulation	2581782	2582236
GENES POTENTIALLY INVOLVED IN METABOLIC EXCHANGE					
10	HP15_2770	Cytosine permease	Uptake of nucelobases	2922464	2923177
15	HP15_3561	Haloacid dehalogenase, type II	Conversion of miscellaneous compounds	3752080	3751615
19	HP15_802	Glycerol-3-phosphate acyltransferase PlsB	Phospholipid metabolism	818997	818041
24	HP15_3716	Na(+)-translocating NADH-quinone reductase subunit B	Energy metabolism	3932302	3931766
26	HP15_3013	Family 3 extracellular solute-binding protein AotJ	Arginine/ornithine amino acid transporter	3155359	3155976
33	HP15_4087	Transcriptional regulator, GntR family	Transcriptional regulators	4320708	4319771
54	HP15_2599	3-isopropylmalate dehydratase, large subunit	Amino acid synthesis/leucine biosynthesis	2749214	2748780
65	HP15_3541	Spermidine/putrescine transporter, periplasmic binding protein	Uptake of diverse nitrogen compounds	3730124	3729560
100	HP15_4098	Amino acid-binding protein LivK	Branched-chain amino acid uptake	4332206	4332293
149	HP15_623	RNA methyltransferase	Protein synthesis / ribosomal structure	648235	648872
161	HP15_2039	Locus tol-pal	Cell envelope integrity/substance transport	2139374	2138565
165	HP15_480	3-dehydroquinate synthase AroB	Aromatic amino acid biosynthesis	490822	491054
205	HP15_4	Zinc-dependent alcohol dehydrogenase	Intermediary metabolism	5022	4348
211	HP15_3398	Major facilitator superfamily MFS_1	Transport of small solutes	3569976	3569854
238	HP15_910	3-hydroxyisobutyrate dehydrogenase MmsB	Amino acid degradation	922229	922747
239	HP15_1315	Leucyl aminopeptidase	Protein degradation	1377931	1377300
240	HP15_1623	Putative NADH dehydrogenase	Energy metabolism	1720224	1720570
GENES OF UNKNOWN FUNCTION					
13	HP15_1948	Hypothetical protein		2069088	2069846
45	HP15_2904	Conserved hypothetical protein		3043610	3043168
74	HP15_154	Hypothetical protein		154626	155331
166	HP15_2604	Conserved hypothetical protein		2755910	2755105
207	HP15_448	Conserved hypothetical protein		453802	453365
238	HP15_911	Conserved hypothetical protein		922887	923160

The exact position of the sequenced DNA fragments upstream the pyrBC-lacZ fusion in the different positive clones is shown by the nucleotide numbers in the HP15 genome and one of its indigenous plasmids (Accession Numbers: CP001978.1 and CP001980.1).

supporting this finding is col. 204 representing a genetic locus encoding a response regulator containing a receiver domain (HP15_3664) and a histidine kinase (HP15_3665). These proteins belong to the two-component signal transduction systems used by bacteria to respond to different stimuli and to regulate diverse cellular processes (Capra and Laub, 2012). They could be involved in chemotaxis since HP15_3664 shares similarities to chemotaxis-associated CheY-like response regulators (Stock et al., 1990). With new elegant technical approaches now available (Lambert et al., 2017) and our mutant arsenal in the model organism *M. adhaerens* HP15 (Sonnenschein et al., 2012), it is planned to investigate in depth the chemotactic behavior of HP15 in future studies.

An example of a regulatory gene potentially involved in sensing the diatom was found in col. 1 encoding the MerR1 transcriptional regulator (HP15_158) which has been described to mediate responses to environmental stimuli such as heavy metals, drugs, antibiotics, or oxidative stress (Brown et al., 2003). During the diatom's photosynthesis or photolysis of dissolved organic matter many reactive oxygen species are released (Asada,

2006). The ability to detoxify reactive oxygen species represents a selective advantage in the aquatic environment (Glaeser et al., 2010). Hünken et al. (2008) had shown that certain diatom-interacting bacteria protect the diatom by detoxifying oxygen species produced during the diatom's growth. However, it remains to be tested in future studies whether MerR1 is important for sensing reactive oxygen species or other potential threads such a heavy metals. The later possibility is supported by the IVET clone no. 30 containing the sequence of a genetic locus encoding the outer membrane component CzcC (HP15_108) of the heavy metal efflux pump CzcCBA (Nies, 2003). Interestingly, *M. adhaerens* HP15 possesses two highly homologous copies of fully functional *czcCBA* clusters prompting speculations about its pronounced role in detoxification processes (Stahl et al., 2015) and suggesting future studies on these clusters.

Genes Involved in Attachment

To initiate a close interaction, bacteria have to attach to diatom cells. The expression of genes, which change the adhesiveness of bacterial surface and promote adhesion has been previously observed in bacterial communities associated to algal blooms by meta-transcriptomics (Rinta-Kanto et al., 2012). In addition, proteins playing a role in biofilm formation have been identified in bacterial cultures growing with diatoms (Bruckner et al., 2011). Herein, we identified two genes and one operon that might be involved in the attachment of HP15 to *T. weissflogii*. Firstly, the gene associated with col. 32 was annotated to encode a protein with a putative conserved bacterial Ig-like domain. Proteins carrying this domain were found to be important in host-pathogen interactions (Kelly et al., 1999; Raman et al., 2010). For example, this domain is present in intimin, an outer membrane adhesion protein present in enteropathogenic or enterohaemorrhagic *E. coli* (Frankel et al., 2001). Secondly, the genetic locus identified in col. 168 encodes the phosphoenolpyruvate-carbohydrate phosphotransferase system (PTS) IIA-like nitrogen-regulatory protein (Cases et al., 2001). The PTS system consists of a group of phosphotransfer proteins involved in the transport of carbohydrates, in chemotaxis toward carbon sources, and in the regulation of other metabolic pathways (Postma et al., 1993). A similar PTS system, was previously identified by IVET in *Erwinia chrysanthemi* interacting with tomato plants (Yang et al., 2004). Mutation of this gene affected the systematic invasion capability of the plant pathogen suggesting that certain PTS systems might be pivotal for the attachment of bacteria with photosynthetic eukaryotic cells.

The third genetic locus associated with attachment is the most exciting finding: In col. 68, a plasmid-borne sequence located upstream of the gene encoding Type IV fimbrial low-molecular weight Flp pilin (Kachlany et al., 2000) was identified suggesting that expression of a corresponding pilus might be diatom-inducible. This gene is the first of the so-called tight adherence (*tad*) locus. The *tad* locus was described in a wide range of pathogenic and non-pathogenic bacteria as well as in archaea, where it plays an important role in the colonization of respective, surprisingly diverse environmental niches (Kachlany et al., 2001). In *Pseudomonas aeruginosa,* Flp pili contribute to adherence to abiotic surfaces and surfaces of eukaryotic cells (de Bentzmann et al., 2006). A homologous locus was also identified in *Caulobacter crescentus* and designated *cpa* (*Caulobacter* pilus assembly) (Bodenmiller et al., 2004). Due to its wide-spread distribution and presence on a mobile genomic island the *tad* locus was termed Widespread Colonization Island (WCI) (Planet et al., 2003). In the human peridontal pathogen, *Aggregatibacter actinomycetemcomitans* this locus is composed of the genes *flp1–flp2–tadV–rcpCAB–tadZABCDEFG* encoding proteins that constitute a fibril secretion system (Kachlany et al., 2000). This operon is responsible for tight adherence, autoaggregation, biofilm formation, and the production of bundled fimbria-like fibers of individual pili (Kachlany et al., 2001; Planet et al., 2003; Perez et al., 2006; Tomich et al., 2007). Interestingly, our model organism, HP15 possess the entire WCI allowing the cautious suggestion that this organism might employ similar mechanisms of attachment to diatom surfaces as pathogens use for their host cell surfaces. Future studies should focus, among others, on determining the specificity of the corresponding pili for a given attachment surface thus shedding light on role of the diatom cell wall for this interaction.

Genes Involved in Metabolic Exchange During the Interaction

Diatoms secrete organic compounds in the form of DOC or extracellular polymeric substances (Passow, 2002), which are taken up by heterotrophic bacteria (Grossart et al., 2006a). Gene expression analysis has identified an increase of transcripts involved in DOC uptake when bacteria interact with algae, e.g., transport systems for amino acid, carboxylic acids, carbohydrates (Poretsky et al., 2005, 2010; Rinta-Kanto et al., 2012; Teeling et al., 2012; Durham et al., 2017). In the current study, several promoters driving the expression of genes involved in the uptake of organic—mainly nitrogen-containing—compounds were identified. In col. 10 a genetic locus was identified which showed high sequence similarities to the *codBA* operon of *E. coli* previously described to have a putative role in a salvage pathway for nucleobases and being inducible by nucleobase starvation (Danielsen et al., 1992). Since the HP15 Δ*pyrB* mutant is deficient in pyrimidines biosynthesis and there is no pyrimidine available during its growth with *T. weissflogii*, the first explanation for the expression of this operon might be to allow the bacteria to survive under such conditions. However, DNA uptake by heterotrophic marine bacteria has been previously reported playing an important role as a supplement for nutrients or for new DNA synthesis (Jørgensen and Jacobsena, 1996).

The gene trapped in col. 211 encodes a protein containing a major facilitator superfamily (MFS) domain. Proteins containing this domain are secondary carriers that function as transporters for small solutes, such as monosaccharides, disaccharides, peptides, amino acids, and other molecules (Pao et al., 1998). Our result thus suggested that uptake of such compounds might be induced during the interaction. Similarly, gene *ybg*C (found in col. 161) encodes a homolog of the Tol-Pal system-associated acyl-CoA thioesterase, the first enzyme in the Tol-Pal system of *E. coli* (Godlewska et al., 2009). This system consists of five

proteins (TolQ, TolR, TolA, TolB, and Pal) forming a membrane associated complex, which maintains outer membrane integrity. In addition, the operon shows similarity to the TonB system, which is important for active transport of diverse substrates such as siderophores or vitamin B12 (Moeck and Coulton, 1998) indicating that HP15 might possibly use TonB-dependent outer membrane receptors for uptake of yet-to-be determined substances. In their seminal paper, Teeling et al. (2012) had pointed out that TonB-dependent transport mechanisms were instrumental for marine bacterial population during algal bloom in the German bight.

Once the yet-unknown organic compounds released by the diatom are transported into the bacterial cells, they may be (partially or fully) degraded. In this context, we identified six genetic loci, which unfortunately do not allow concluding anything directly in terms of increased catabolism or accelerated energy conservation during the co-culture (col. 15, 19, 24, 149, 205, and 240). However, these results confirmed previous metagenomic and transcriptomic studies in which genes for degradation of organic compounds and an increase in bacterial activity and cell division rates were identified during bacteria-algae interactions (Poretsky et al., 2010; Smith et al., 2013; Durham et al., 2017).

In seven of the identified transconjugants, the IVET plasmids contained upstream sequences of genes involved in amino acid uptake (col. 26, 65, and 100), amino acid or protein degradation (col. 238 and 239), or even amino acid biosynthesis (col. 54 and 165). Inserts of two additional clones physically clustered with those of col. 54 and 238 but indicated sequence similarities to conserved hypothetical proteins (col. 166 and 241). This over-proportional appearance of amino acid-associated gene products among *in co-culture* induced proteins prompts the assumption that HP15 might preferentially obtain and use amino acids or amino group containing substances derived from the diatom cells. A somewhat similar observation was made by Durham et al. (2017), who found that presence of *T. pseudonana* induced expression of uptake systems for organic nitrogen compounds in the marine bacterium *Ruegeria pomeroyi* DSS-3. Our previous proteomics approach combined with a functional metabolite analysis (Stahl and Ullrich, 2016) had also revealed that *M. adhaerens* HP15 utilizes amino acids but not sugars as preferred carbon sources.

While the co-occurrence of genetic loci encoding amino acid-degrading and amino acid-synthesizing enzymes is a bit puzzling to interpret, the simultaneous finding of three amino acid or amino compound uptake systems being required during the interaction seems to be promising: The genetic locus HP15_3541 (col. 65) encodes for the periplasmic portion of a spermidine/putrescine transporter. Diatom cell walls contain high amounts of long-chain polyamines, which are organic constituents of diatom bio-silica (Kröger et al., 2000; Kröger and Poulsen, 2008). Previously, a positive correlation was found between the concentrations of polyamines in seawater and the amount of transcripts from different groups of marine bacteria involved in the degradation of polyamines (Mou et al., 2011). Transcripts and genetic evidence involved in polyamines uptake were also found in bacteria associated to marine phytoplankton blooms (Moran et al., 2004; Poretsky et al., 2005, 2010) as well as in free-living freshwater bacteria (Garcia et al., 2013). Our data thus allowed us to speculate on a potential bacterial use of polyamines shed during diatom cell wall synthesis and prompts future experiments in this direction.

The IVET screen revealed two further genetic loci (col. 100 and 26), whose expression was associated with presence of *T. weissflogii*, and which encode for LivK (HP15_4098) and AotJ (HP15_3031), respectively. Interestingly, the gene product of *livK* was already found upregulated in our previous proteomics study (Stahl and Ullrich, 2016). LivK is part of a branched amino acid uptake system transporting leucine, isoleucine, and valine (Adams et al., 1990; Ribardo and Hendrixson, 2011). LivK's functional involvement in branched amino acid transport in *M. adhaerens* HP15 is supported by the close proximity of genes encoding the inner membrane translocators LivH and LivG as well as the ATP binding components LivM and LivF (Adams et al., 1990). Interestingly and in agreement with our finding, the RNAseq-based transcriptome analysis of *R. pomeroyi* DSS-3 revealed other branched amino acid uptake systems being upregulated in presence of diatom cells (Durham et al., 2017). Since the later study found several additional bacterial transport systems to be diatom-induced, the observed functional analogy of branched amino acid uptake systems in both organisms might reflect both, the multifactorial nature of the respective interactions and possible common metabolic interaction themes.

AotJ is an amino acid-binding protein, which belongs to the arginine/ornithine uptake system (Wissenbach et al., 1995; Nishijyo et al., 1998). AotJ's potential function is substantiated by presence of surrounding genes encoding the subunit of a histidine-lysine-arginine-ornithine transporter and two inner membrane permeases of arginine and histidine associated ABC transporters in the genome of HP15. Just like LivK, the AotJ gene product was found upregulated in *M. adhaerens* HP15 during exposure to *T. weissflogii* cells in our previous proteomics approach (Stahl and Ullrich, 2016). Both proteomics hits now substantiated by the IVET screen may hint at an important role of bacterial amino acid uptake during the bacteria-diatom interactions with a distinct focus on branched chain amino acids and arginine/ornithine, respectively.

CONCLUSIONS

This study revealed an exciting array of genes potentially important during diatom-bacteria interaction. The approach is innovative in the field and demonstrated that assessment of bacterial gene expression via determination of promoter activities without interference by mRNA degradation or protein instability is possible. From the identified genes, we can infer that chemotaxis might be important to detect diatom cells. Once the bacteria are in a close proximity, genes involved in pilus-associated attachment are expressed in order to start a cell-to-cell interaction. A benefit for the bacteria is observed by the expression of genes involved in uptake and utilization of nitrogen-containing compounds. These results are in agreement with results from the past 50 years of research and with those

from recent reports (Poretsky et al., 2005, 2010; Rinta-Kanto et al., 2012; Amin et al., 2015; Durham et al., 2017) that bacteria use the DOC produced by diatoms as nutrient source. A highly interesting but puzzling result remains the identification of a heavy metal efflux pump and the MerR1 transcriptional regulator as being encoded by *in co-culture* induced genes allowing multiple alternative speculations. Consequently, further experiments have to be carried out to confirm whether HP15 is actively provoking the diatom to produce or release metabolites thus participating in an active exchange of signals and compounds or is saprophytically living on non-specifically released compounds because of diatom cell lysis. Our findings indicate that HP15 might participate in the cycling of nitrogen-containing DOC in the ocean and could therefore be involved in the termination of phytoplankton blooms.

AUTHOR CONTRIBUTIONS

IT-M conducted all experiments, analyzed all data, and prepared the manuscript, all figures and tables. MU initiated this study, supervised and directed all experiments, wrote the manuscript, and submitted the manuscript.

ACKNOWLEDGMENTS

This work was supported by the Deutsche Forschungsgemeinschaft (UL169/6-1). Preliminary data and part of this manuscript have been included in the archived dissertation of the first author at Jacobs University Bremen (Torres-Monroy, 2013). The technical support by Nikki Atanasova was highly appreciated.

SUPPLEMENTARY MATERIAL

The Supplementary Material for this article can be found online at: https://www.frontiersin.org/articles/10.3389/fmars.2018.00200/full#supplementary-material

Supplementary Figure 1 | Construction of IVET vector pITM3_pyrB. A promoter-less copy of *lacZ* from *E. coli* was ligated into *Kpn*I-treated pBBR1MCS-4 resulting in plasmid pITM3. Then a promoter-less copy of the genes *pyrBC* from HP15 was cloned into *Hin*dIII/*Xho*I-treated pITM3 to generate pITM3_pyrB.

Supplementary Figure 2 | Bacterial *in vitro* growth curves of *M. adhaerens* HP15 wild type, HP15 ΔpyrB, and HP15 Δ*pyrB* complemented with 5 μg ml^{-1} of uracil in f/2 GLUT liquid medium and constant shaking at 250 rpm.

REFERENCES

Adams, M. D., Wagner, L., Graddis, T., Landick, R., Antonucci, T., Gibson, A., et al. (1990). Nucleotide sequence and genetic characterization reveal six essential genes for the LIV-I and LS transport systems of *Escherichia coli*. *J. Biol. Chem.* 265, 11436–11443.

Alldredge, A. L., Cole, J. J., and Caron, D. A. (1986). Production of heterotrophic bacteria inhabitating macroscopic organic aggregates (marine snow) from surface waters. *Limnol. Oceanogr.* 31, 68–78. doi: 10.4319/lo.1986.31.1.0068

Alldredge, A. L., Passow, U., and Logan, B. E. (1993). The abundance and significance of a class of large, transparent organic particles in the ocean. *Deep Sea Res. I* 40, 1131–1140. doi: 10.1016/0967-0637(93)90129-Q

Alldredge, A. L., and Silver, M. L. (1988). Characteristics, dynamics and significance of marine snow. *Prog. Oceanogr.* 20, 41–82. doi: 10.1016/0079-6611(88)90053-5

Alldredge, A. L., and Youngbluth, M. J. (1985). The significance of macroscopic aggregates (marine snow) as sites for heterotrophic bacterial production in the mesopelagic zone of the subtropical Atlantic. *Deep Sea Res* .32, 1445–1456. doi: 10.1016/0198-0149(85)90096-2

Altschul, S. F., Gish, W., Miller, W., Myers, E. W., and Lipman, D. J. (1990). Basic local alignment search tool. *J. Mol. Biol.* 215, 403–410. doi: 10.1016/S0022-2836(05)80360-2

Amin, S. A., Hmelo, L. R., van Tol, H. M., Durham, B. P., Carlson, L. T., Heal, K. R., et al. (2015). Interaction and signaling between a cosmopolitan phytoplankton and associated bacteria. *Nature* 522, 98–101. doi: 10.1038/nature14488

Asada, K. (2006). Production and scavenging of reactive oxygen species in chloroplasts and their functions. *Plant Physiol.* 141, 391–396. doi: 10.1104/pp.106.082040

Bach, L. T., Boxhammer, T., Larsen, A., Hildebrandt, N., Schulz, K. G., and Riebesell, U. (2016). Influence of plankton community structure on the sinking velocity of marine aggregates. *Global Biogeochem. Cycles* 30, 1145–1165. doi: 10.1002/2016GB005372

Baker, M. D., Wolanin, P. M., and Stock, J. B. (2005). Signal transduction in bacterial chemotaxis. *Bioessays* 28, 9–22. doi: 10.1002/bies.20343

Behringer, G., Ochsenkühn, M. A., Fei, C., Fanning, J., Koester, J. A., and Amin, S. A. (2018). Bacterial communities of diatoms display strong conservation across strains and time. *Front. Microbiol.* 9:659. doi: 10.3389/fmicb.2018.00659

Biddanda, B. A., and Pomeroy, L. R. (1988). Microbial aggregation and degradation of phytoplankton-derived detritus in seawater. I. Microbial. Succession. *Mar. Ecol. Prog. Ser.* 42, 79–88. doi: 10.3354/meps042079

Bodenmiller, D., Toh, E., and Brun, Y. V. (2004). Development of surface adhesion in *Caulobacter crescentus*. *J. Bacteriol.* 186, 1438–1447. doi: 10.1128/JB.186.5.1438-1447.2004

Brown, N. L., Stoyanov, J. V., Kidd, S. P., and Hobman, J. L. (2003). The MerR family of transcriptional regulators. *FEMS Microbiol. Rev.* 27, 145–163. doi: 10.1016/S0168-6445(03)00051-2

Bruckner, C. G., Rehm, C., Grossart, H. P., and Kroth, P. G. (2011). Growth and release of extracellular organic compounds by benthic diatoms depend on interactions with bacteria. *Environ. Microbiol.* 13, 1052–1063. doi: 10.1111/j.1462-2920.2010.02411.x

Busch, K., Endres, S., Iversen, M. H., Michels, J., Nöthig, E. M., and Engel, A. (2017). Bacterial colonization and vertical distribution of marine gel particles (TEP and CSP) in the Arctic Fram Street. *Front. Mar. Sci.* 4:166. doi: 10.3389/fmars.2017.00166

Capra, E. J., and Laub, M. T. (2012). Evolution of two-component signal transduction systems. *Annu. Rev. Microbiol.* 66, 325–347. doi: 10.1146/annurev-micro-092611-150039

Cases, I., Lopez, J. A., Albar, J. P., and De Lorenzo, V. (2001). Evidence of multiple regulatory functions for the PtsN (IIANtr) protein of *Pseudomonas putida*. *J. Bacteriol.* 183, 1032–1037. doi: 10.1128/JB.183.3.1032-1037.2001

Choi, K. H., and Schweizer, H. P. (2005). An improved method for rapid generation of unmarked *Pseudomonas aeruginosa* deletion mutants. *BMC Microbiol.* 5:30 doi: 10.1186/1471-2180-5-30

Dang, H., and Lovell, C. R. (2016). Microbial surface colonization and biofilm development in marine environments. *Microbiol. Mol. Biol. Rev.* 80, 91–138. doi: 10.1128/MMBR.00037-15

Danielsen, S., Kilstrup, M., Barilla, K., Jochimsen, B., and Neuhard, J. (1992). Characterization of the *Escherichia coli codBA* operon encoding cytosine permease and cytosine deaminase. *Mol. Microbiol.* 6, 1335–1344. doi: 10.1111/j.1365-2958.1992.tb00854.x

de Bentzmann, S., Aurouze, M., Ball, G., and Filloux, A. (2006). FppA, a novel *Pseudomonas aeruginosa* prepilin peptidase involved in assembly of type IVb pili. *J. Bacteriol.* 188, 4851–4860. doi: 10.1128/JB.00345-06

DeLong, E. F., Franks, D. G., and Alldredge, A. L. (1993). Phylogenetic diversity of aggregate-attached vs. free-living marine bacterial assemblages. *Limnol. Oceanogr.* 38, 924–934. doi: 10.4319/lo.1993.38.5.0924

Dudley, E. G. (2008). *In vivo* expression technology and signature-tagged mutagenesis screens for identifying mechanisms of survival of zoonotic foodborne pathogens. *Foodborne Pathog. Dis.* 5, 473–485. doi: 10.1089/fpd.2008.0104

Durham, B. P., Dearth, S. P., Sharma, S., Amin, S. A., Smith, C. B., Campagna, S. R., et al. (2017). Recognition cascade and metabolite transferrin a marine bacteria-phytoplankton model system. *Environ. Microbiol.* 19, 3500–3513. doi: 10.1111/1462-2920.13834

Durham, B. P., Sharma, S., Luo, H., Smith, C. B., Amin, S. A., Bender, S. J., et al. (2015). Cryptic carbon and sulfur cycling between surface ocean plankton. *Proc. Natl. Acad. Sci. U.S.A.* 112, 453–457. doi: 10.1073/pnas.1413137112

Eisenbach, M. (1996). Control of bacterial chemotaxis. *Mol. Microbiol.* 20, 903–910. doi: 10.1111/j.1365-2958.1996.tb02531.x

Figurski, D. H., and Helinski, D. R. (1979). Replication of an origin-containing derivative of plasmid RK2 dependent on a plasmid function provided in trans. *Proc. Natl. Acad. Sci. U.S.A.* 76, 1648–1652. doi: 10.1073/pnas.76.4.1648

Fowler, S. W., and Knauer, G. A. (1986). Role of large particles in the transport of elements and organic compounds through the oceanic water column. *Prog. Oceanogr.* 16, 147–194. doi: 10.1016/0079-6611(86)90032-7

Frankel, G., Phillips, A. D., Trabulsi, L. R., Knutton, S., Dougan, G., and Matthews, S. (2001). Intimin and the host cell – is it bound to end in Tir(s)? *Trends Microbiol.* 9, 214–218. doi: 10.1016/S0966-842X(01)02016-9

Garcia, S. L., McMahon, K. D., Martinez-Garcia, M., Srivastava, A., Sczyrba, A., Stepanauskas, R., et al. (2013). Metabolic potential of a single cell belonging to one of the most abundant lineages in freshwater bacterioplankton. *ISME J.* 7, 137–147. doi: 10.1038/ismej.2012.86

Gärdes, A., Iversen, M. H., Grossart, H.-P., Passow, U., and Ullrich, M. S. (2011). Diatom-associated bacteria are required for aggregation of *Thalassiosira weissflogii*. *ISME J.* 5, 436–445. doi: 10.1038/ismej.2010.145

Gärdes, A., Kaeppel, E., Shehzad, A., Seebah, S., Teeling, H., Yarza, P., et al. (2010). Complete genome sequence of *Marinobacter adhaerens* type strain (HP15), a diatom-interacting marine microorganism. *Stand. Genomic Sci.* 3, 97–107. doi: 10.4056/sigs.922139

Glaeser, S. P., Grossart, H. P., and Glaeser, J. (2010). Singlet oxygen, a neglected but important environmental factor, short-term and long-term effects on bacterioplankton composition in a humic lake. *Environ. Microbiol.* 12, 3124–3136. doi: 10.1111/j.1462-2920.2010.02285.x

Godlewska, R., Wiśniewska, K., Pietras, Z., and Jagusztyn-Krynicka, E. K. (2009). Peptidoglycan-associated lipoprotein (Pal) of Gram-negative bacteria, function, structure, role in pathogenesis and potential application in immunoprophylaxis. *FEMS Microbiol. Lett.* 298, 1–11. doi: 10.1111/j.1574-6968.2009.01659.x

Grossart, H. P., Czub, G., and Simon, M. (2006a). Algae-bacteria interactions and their effects on aggregation and organic matter flux in the sea. *Environ. Microbiol.* 8, 1074–1084. doi: 10.1111/j.1462-2920.2006.00999.x

Grossart, H. P., Kiørboe, T., Tang, K. W., Allgaier, M., Yam, E. M., and Ploug, H. (2006b). Interactions between marine snow and heterotrophic bacteria: aggregate formation and microbial dynamics. *Aquat. Microb. Ecol.* 42, 19–26. doi: 10.3354/ame042019

Grossart, H. P., Schlingloff, A., Bernhard, M., Simon, M., and Brinkhoff, T. (2004). Antagonistic activity of bacteria isolated from organic aggregates of the German Wadden Sea. *FEMS Microbiol. Ecol.* 47, 387–396 doi: 10.1016/S0168-6496(03)00305-2

Guillard, R. R., and Ryther, J. H. (1962). Studies of marine planktonic diatoms. I. *Cyclotella nana* Hustedt and *Detonula confervacea* Cleve. *Can. J. Microbiol.* 8, 229–239. doi: 10.1139/m62-029

Hoang, T. T., Karkhoff-Schweizer, R. A. R., Kutchma, A. J., and Schweizer, H. P. (1998). A broad-host-range Flp-FRT recombination system for site-specific excision of chromosomally-located DNA sequences: application for isolation of unmarked *Pseudomonas aeruginosa* mutants. *Gene* 212, 77–86. doi: 10.1016/S0378-1119(98)00130-9

Hünken, M., Harder, J., and Kirst, G. O. (2008). Epiphytic bacteria on the Antarctic ice diatom *Amphiprora kufferathii* manguin cleave hydrogen peroxide produced during algal photosynthesis. *Plant Biol.* 10, 519–526. doi: 10.1111/j.1438-8677.2008.00040.x

Jahnke, R. A. (1996). The global ocean flux of particulate organic carbon: areal distribution and magnitude. *Global Biogeochem. Cycles* 10, 71–88. doi: 10.1029/95GB03525

Jørgensen, N. G., and Jacobsena, C. S. (1996). Bacterial uptake and utilization of dissolved DNA. *Aquat. Microb. Ecol.* 11, 263–270. doi: 10.3354/ame011263

Kachlany, S. C., Planet, P. J., Bhattacharjee, M. K., Kollia, E., DeSalle, R., Fine, D. H., et al. (2000). Nonspecific adherence by *Actinobacillus actinomycetemcomitans* requires genes widespread in bacteria and archaea. *J. Bacteriol.* 182, 6169–6176. doi: 10.1128/JB.182.21.6169-6176.2000

Kachlany, S. C., Planet, P., and DeSalle, R. (2001). Genes for tight adherence of *Actinobacillus actinomycetemcomitans*: from plaque to plague to pond scum. *Trends Microbiol.* l9, 429–437. doi: 10.1016/S0966-842X(01)02161-8

Kaeppel, E. C., Gärdes, A., Seebah, S., Grossart, H. P., and Ullrich, M. S. (2012). *Marinobacter adhaerens* sp. nov., isolated from marine aggregates formed with the diatom *Thalassiosira weissflogii*. *Int. J. Syst. Evol. Microbiol.* 62, 124–128. doi: 10.1099/ijs.0.030189-0

Kelly, G., Prasannan, S., Daniell, S., Fleming, S., Frankel, G., Dougan, G., et al. (1999). Structure of the cell-adhesion fragment of intimin from enteropathogenic *Escherichia coli*. *Nat. Struct. Mol. Biol.* 6, 313–318.

Kiørboe, T., Grossart, H. P., Ploug, H., and Tang, K. (2002). Mechanisms and rates of bacterial colonization of sinking aggregates. *Appl. Environ. Microbiol.* 68, 3996–4006. doi: 10.1128/AEM.68.8.3996-4006.2002

Kiørboe, T., and Jackson, G. A. (2001). Marine snow, organic solute plumes, and optimal chemosensory behavior of bacteria. *Limnol. Oceanogr.* 46, 1309–1318. doi: 10.4319/lo.2001.46.6.1309

Kiørboe, T., Tang, K., Grossart, H. P., and Ploug, H. (2003). Dynamics of microbial communities on marine snow aggregates: colonization, growth, detachment, and grazing mortality of attached bacteria. *Appl. Environ. Microbiol.* 69, 3036–3047. doi: 10.1128/AEM.69.6.3036-3047.2003

Kovach, M. E., Elzer, P. H., Hill, D. S., Robertson, G. T., Farris, M. A., Roop, R. M., et al. (1995). 4 new derivatives of the broad-host-range cloning vector pBBR1MCS, carrying different antibiotic-resistance cassettes. *Gene* 166, 175–176. doi: 10.1016/0378-1119(95)00584-1

Kröger, N., Deutzmann, R., Bergsdorf, C., and Sumper, M. (2000). Species-specific polyamines from diatoms control silica morphology. *Proc. Natl. Acad. Sci. U.S.A.* 97, 14133–14138. doi: 10.1073/pnas.260496497

Kröger, N., and Poulsen, N. (2008). Diatoms-from cell wall biogenesis to nanotechnology. *Annu. Rev. Genet.* 42, 83–107. doi: 10.1146/annurev.genet.41.110306.130109

Lambert, B. S., Raina, J. B., Fernandez, V. I., Rinke, C., Siboni, N., Rubino, F., et al. (2017). A microfluidics-based *in situ* chemotaxis assay to study the behavior of aquatic microbial communities. *Nat. Microbiol.* 2, 1344–1349. doi: 10.1038/s41564-017-0010-9

Lee, S. W., and Cooksey, D. A. (2000). Genes Expressed in *Pseudomonas putida* during colonization of a plant-pathogenic fungus. *Appl. Environ. Microbiol.* 66, 2764–2772. doi: 10.1128/AEM.66.7.2764-2772.2000

Logan, B. E., Passow, U., Alldredge, A. L., Grossart, H. P., and Simon, M. (1995). Rapid formation and sedimentation of large aggregates is predictable from coagulation rates (half-lives) of transparent exopolymer particles (TEP). *Deep Sea Res. II* 42, 203–214. doi: 10.1016/0967-0645(95)00012-F

Mahan, M. J., Slauch, J. M., and Mekalanos, J. J. (1993). Selection of bacterial virulence genes that are specifically induced in host tissues. *Science* 259, 686–688. doi: 10.1126/science.8430319

Miller, V. L., and Mekalanos, J. J. (1988). A novel suicide vector and its use in construction of insertion mutations: osmoregulation of outer membrane proteins and virulence determinants in *Vibrio cholerae* requires toxR. *J. Bacteriol.* 170, 2575–2583.

Moeck, G. S., and Coulton, J. W. (1998). TonB-dependent iron acquisition: mechanisms of siderophore-mediated active transport. *Mol. Microbiol.* 28, 675–681. doi: 10.1046/j.1365-2958.1998.00817.x

Moran, M. A., Buchan, A., González, J. M., Heidelberg, J. F., Whitman, W. B., Kiene, R. P., et al. (2004). Genome sequence of *Silicibacter pomeroyi* reveals adaptations to the marine environment. *Nature* 432, 910–913. doi: 10.1038/nature03170

Mou, X., Vila-Costa, M., Sun, S., Zhao, W., Sharma, S., and Moran, M. A. (2011). Metatranscriptomic signature of exogenous polyamine utilization by coastal bacterioplankton. *Environ. Microbiol. Rep.* 3, 798–806. doi: 10.1111/j.1758-2229.2011.00289.x

Needham, D. M., Sachdeva, R., and Fuhrman, J. A. (2017). Ecological dynamicsand co-occurrence among phytoplankton, bacteria and myoviruses shows microdiversity matters. *ISME J.* 11, 1614–1629. doi: 10.1038/ismej.2017.29

Nies, D. (2003). Efflux-mediated heavy metal resistance in prokaryotes. *FEMS Microbiol. Rev.* 27, 313–339. doi: 10.1016/S0168-6445(03)00048-2

Nishijyo, T., Park, S., Lu, C., Itoh, Y., and Abdelal, A. (1998). Molecular characterization and regulation of an operon encoding a system for transport of arginine and ornithine and the ArgR regulatory protein in *Pseudomonas aeruginosa*. *J. Bacteriol.* 180, 5559–5566.

Pao, S. S., Paulsen, I. T., and Saier, M. H. (1998). Major facilitator superfamily. *Microbiol. Mol. Biol. Rev.* 62, 1–34.

Passow, U. (2002). Production of transparent exopolymer particles (TEP) by phyto- and bacterioplankton. *Mar. Ecol. Prog. Ser.* 236, 1–12. doi: 10.3354/meps236001

Perez, B. A., Planet, P., and Kachlany, S. (2006). Genetic analysis of the requirement for flp-2, tadV, and rcpB in *Actinobacillus actinomycetemcomitans* biofilm formation. *J. Bacteriol.* 188, 6361–6375. doi: 10.1128/JB.00496-06

Planet, P. J., Kachlany, S. C., Fine, D. H., DeSalle, R., and Figurski, D. H. (2003). The widespread colonization Island of *Actinobacillus actinomycetemcomitans*. *Nat. Genet.* 34, 193–198. doi: 10.1038/ng1154

Poretsky, R. S., Bano, N., Buchan, A., Lecleir, G., Kleikemper, J., Pickering, M., et al. (2005). Analysis of microbial gene transcripts in environmental samples. *Appl. Environ. Microbiol.* 71, 4121–4126. doi: 10.1128/AEM.71.7.4121-4126.2005

Poretsky, R. S., Sun, S., Mou, X., and Moran, M. A. (2010). Transporter genes expressed by coastal bacterioplankton in response to dissolved organic carbon. *Environ. Microbiol.* 12, 616–627. doi: 10.1111/j.1462-2920.2009.02102.x

Postma, P. W., Lengeler, J. W., and Jacobson, G. R. (1993). Phosphoenolpyruvate:carbohydrate phosphotransferase systems of bacteria. *Microbiol. Rev.* 57, 543–594.

Raman, R., Rajanikanth, V., Palaniappan, R. U. M., Lin, Y. P., and He, H. (2010). Big domains are novel Ca^{2+}-binding modules: evidences from big domains of *Leptospira* immunoglobulin-like (Lig) proteins. *PLoS ONE* 5:e14377. doi: 10.1371/journal.pone.0014377

Rediers, H., Rainey, P. B., Vanderleyden, J., and De Mot, R. (2005). Unraveling the secret lives of bacteria: use of *in vivo* expression technology and differential fluorescence induction promoter traps as tools for exploring niche-specific gene expression. *Microbiol. Mol. Biol. Rev.* 69, 217–261. doi: 10.1128/MMBR.69.2.217-261.2005

Ribardo, D. A., and Hendrixson, D. R. (2011). Analysis of the LIV system of *Campylobacter jejuni* reveals alternative roles for LivJ and LivK in commensalism beyond branched-chain amino acid transport. *J. Bacteriol.* 193, 6233–6243. doi: 10.1128/JB.05473-11

Rinta-Kanto, J. M., Sun, S., Sharma, S., Kiene, R. P., and Moran, M. A. (2012). Bacterial community transcription patterns during a marine phytoplankton bloom. *Environ. Microbiol.* 14, 228–239. doi: 10.1111/j.1462-2920.2011.02602.x

Roberfroid, S., Vanderleyden, J., and Steenackers, H. (2016). Gene expression variability in clonal populations: causes and consequences. *Crit. Rev. Microbiol.* 42, 969–984. doi: 10.3109/1040841X.2015.1122571

Sambrook, J., Fritsch, E., and Maniatis, T. (1989). *Molecular Cloning: a Laboratory Manual, 2nd Edn* Cold Spring Harbor, NY: Cold Spring Harbor Laboratory Press.

Schurr, M. J., Vickrey, J. F., Kumar, A. P., Campbell, A. L., Cunin, R., Benjamin, R. C., et al. (1995). Aspartate transcarbamoylase genes of *Pseudomonas putida*: requirement for an inactive dihydroorotase for assembly into the dodecameric holoenzyme. *J. Bacteriol.* 177, 1751–1759.

Seebah, S., Fairfield, C., Ullrich, M. S., and Passow, U. (2014). Aggregation and sedimentation of *Thalassiosira weissflogii* (diatom) in a warmer and more acidified future ocean. *PLoS ONE* 9:e112379. doi: 10.1371/journal.pone.0112379

Seymour, J. R., Amin, S. A., Raina, J. B., and Stocker, R. (2017). Zooming in on the phycosphere: the ecological interface for phytoplankton-bacteria relationships. *Nat. Microbiol.* 2:17065. doi: 10.1038/nmicrobiol.2017.65

Shapira, S. K., Chou, J., Richaud, F. V., and Casadaban, M. J. (1983). New versatile plasmid vectors for expression of hybrid proteins coded by a cloned gene fused to *lacA* gene sequences encoding an enzymatically active carboxy-terminal portion of β-galactosidase. *Gene* 25, 71–82. doi: 10.1016/0378-1119(83)90169-5

Smirnova, A. V., and Ullrich, M. S. (2004). Topological and deletion analysis of CorS, a *Pseudomonas syringae* sensor kinase. *Microbiology* 150, 2715–2726. doi: 10.1099/mic.0.27028-0

Smith, M. W., Zeigler Allen, L., Allen, A. E., Herfort, L., and Simon, H. M. (2013). Contrasting genomic properties of free-living and particle-attached microbial assemblages within a coastal ecosystem. *Front. Microbiol.* 4:120. doi: 10.3389/fmicb.2013.00120

Sonnenschein, E. C., Abebew Syit, D., Grossart, H. P., and Ullrich, M. S. (2012). Chemotaxis of *Marinobacter adhaerens* and its impact on attachment to the diatom *Thalassiosira weissflogii*. *Appl. Environ. Microbiol.* 78, 6900–6907. doi: 10.1128/AEM.01790-12

Sonnenschein, E. C., Gärdes, A., Seebah, S., Torres-Monroy, I., Grossart, H. P., and Ullrich, M. S. (2011). Development of a genetic system for *Marinobacter adhaerens* HP15 involved in marine aggregate formation by interacting with diatom cells. *J. Microbiol. Methods* 87, 176–183. doi: 10.1016/j.mimet.2011.08.008

Stahl, A., Pletzer, D., Mehmood, A., and Ullrich, M. S. (2015). *Marinobacter adhaerens* HP15 harbors two CzcCBA efflux pumps involved in zinc detoxification. *Antonie Van Leeuwenhoek* 108, 649–658. doi: 10.1007/s10482-015-0520-5

Stahl, A., and Ullrich, M. S. (2016). Proteomics analysis of the response of the marine bacterium *Marinobacter adhaerens* HP15 to the diatom *Thalassiosira weissflogii*. *Aquat. Microbial. Ecol.* 78, 65–79. doi: 10.3354/ame01804

Stock, J. B., Stock, A. M., and Mottonen, J. M. (1990). Signal transduction in bacteria. *Nature* 344, 395–400. doi: 10.1038/344395a0

Teeling, H., Fuchs, B. M., Becher, D., Klockow, C., Gardebrecht, A., Bennke, C. M., et al. (2012). Substrate-controlled succession of marine bacterioplankton populations induced by a phytoplankton bloom. *Science* 336, 608–611. doi: 10.1126/science.1218344

Thiele, S., Fuchs, B. M., Amann, R., and Iversen, M. H. (2015). Colonization in the photic zone and subsequent changes during sinking determine bacterial community composition in marine snow. *Appl. Environ. Microbiol.* 81, 1463–1471. doi: 10.1128/AEM.02570-14

Thoma, S., and Schobert, M. (2009). An improved *Escherichia coli* donor strain for diparental mating. *FEMS Microbiol. Lett.* 294, 127–132. doi: 10.1111/j.1574-6968.2009.01556.x

Tomich, M., Planet, P. J., and Figurski, D. H. (2007). The tad locus: postcards from the widespread colonization island. *Nat. Rev. Microbiol.* 5, 363–375. doi: 10.1038/nrmicro1636

Torres-Monroy, I. (2013). *Identification of Bacterial Genes Required for Diatom-Bacteria Interactions*. Dissertation, Jacobs University Bremen, Bremen.

van Tol, H. M., Amin, S. A., and Armbrust, E. V. (2017). Ubiquitous marine bacterium inhibits diatom cell division. *ISME J.* 11, 31–42. doi: 10.1038/ismej.2016.112

Wang, H., Tomasch, J., Jarek, M., and Wagner-Döbler, I. (2014). A dual-species co-cultivation system to study the interactions between *Roseobacters* and dinoflagellates. *Front. Microbiol.* 5:311. doi: 10.3389/fmicb.2014.00311

Wissenbach, U., Six, S., Bongaerts, J., Ternes, D., Steinwachs, S., and Unden, G. (1995). A 3rd periplasmic transport-system for L-arginine in *Escherichia coli* - molecular characterization of the *artPIQMJ* genes, arginine binding and transport. *Mol. Microbiol.* 17, 675–686. doi: 10.1111/j.1365-2958.1995.mmi_17040675.x

Yang, S., Perna, N. T., Cooksey, D. A., Okinaka, Y., Lindow, S. E., Mark Ibekwe, A., et al. (2004). Genome-wide identification of plant-upregulated genes of *Erwinia chrysanthemi* 3937 using a GFP-based IVET Leaf Array. *Mol. Plant Microbe Interact.* 17, 999–1008. doi: 10.1094/MPMI.2004.17.9.999

ZoBell, C. E. (1941). Studies on marine bacteria. I. The cultural requirements of heterotrophic aerobes. *J. Mar. Res.* 4, 42–75.

Conflict of Interest Statement: The authors declare that the research was conducted in the absence of any commercial or financial relationships that could be construed as a potential conflict of interest.

frontiers in Microbiology

ORIGINAL RESEARCH
published: 12 October 2017
doi: 10.3389/fmicb.2017.01985

The Exometabolome of Two Model Strains of the *Roseobacter* Group: A Marketplace of Microbial Metabolites

*Gerrit Wienhausen, Beatriz E. Noriega-Ortega, Jutta Niggemann, Thorsten Dittmar and Meinhard Simon**

Institute for Chemistry and Biology of the Marine Environment, University of Oldenburg, Oldenburg, Germany

Recent studies applying Fourier transform ion cyclotron resonance mass spectrometry (FT-ICR-MS) showed that the exometabolome of marine bacteria is composed of a surprisingly high molecular diversity. To shed more light on how this diversity is generated we examined the exometabolome of two model strains of the *Roseobacter* group, *Phaeobacter inhibens* and *Dinoroseobacter shibae*, grown on glutamate, glucose, acetate or succinate by FT-ICR-MS. We detected 2,767 and 3,354 molecular formulas in the exometabolome of each strain and 67 and 84 matched genome-predicted metabolites of *P. inhibens* and *D. shibae,* respectively. The annotated compounds include late precursors of biosynthetic pathways of vitamins B_1, B_2, B_5, B_6, B_7, B_{12}, amino acids, quorum sensing-related compounds, indole acetic acid and methyl-(indole-3-yl) acetic acid. Several formulas were also found in phytoplankton blooms. To shed more light on the effects of some of the precursors we supplemented two B_1 prototrophic diatoms with the detected precursor of vitamin B_1 HET (4-methyl-5-(β-hydroxyethyl)thiazole) and HMP (4-amino-5-hydroxymethyl-2-methylpyrimidine) and found that their growth was stimulated. Our findings indicate that both strains and other bacteria excreting a similar wealth of metabolites may function as important helpers to auxotrophic and prototrophic marine microbes by supplying growth factors and biosynthetic precursors.

Keywords: roseobacter, DOM, exometabolome, black queen hypothesis

OPEN ACCESS

Edited by:
Tilmann Harder,
University of Bremen, Germany

Reviewed by:
Rebecca Case,
University of Alberta, Canada
Torsten Thomas,
University of New South Wales, Australia

****Correspondence:***
Meinhard Simon
m.simon@icbm.de

Specialty section:
This article was submitted to Aquatic Microbiology, a section of the journal Frontiers in Microbiology

Received: *02 August 2017*
Accepted: *27 September 2017*
Published: *12 October 2017*

Citation:
Wienhausen G, Noriega-Ortega BE, Niggemann J, Dittmar T and Simon M (2017) The Exometabolome of Two Model Strains of the Roseobacter Group: A Marketplace of Microbial Metabolites. Front. Microbiol. 8:1985. doi: 10.3389/fmicb.2017.01985

INTRODUCTION

The biochemical processes in a living and active prokaryotic cell yield a highly complex blend of metabolites reflecting the catabolic, metabolic and anabolic properties of the organism. On the basis of available genomic information on the metabolic potential, metabolite patterns within the cell, endometabolomics, have been investigated during the recent past in various prokaryotes and as a function of substrate source and growth conditions (Rosselló-Mora et al., 2008; Zech et al., 2009; Frimmersdorf et al., 2010; Paczia et al., 2012; Drüppel et al., 2014). The exometabolome, i.e. the pool of metabolites released into the cell's environment, has also been investigated, showing species- or even ecotype-specific fingerprints as a function of growth stage and conditions (Kell et al., 2005; Villas-Bôas et al., 2006; Paul et al., 2009; Paczia et al., 2012; Romano et al., 2014; Fiore et al., 2015; Johnson et al., 2016).

Most of these studies applied targeted approaches mainly gas chromatography–mass spectrometry (GC–MS), searching for metabolites to be expected from predicted substrate use and metabolic pathways (Villas-Bôas et al., 2006; Zech et al., 2009; Drüppel et al., 2014). Several studies

have used Fourier transform ion cyclotron resonance mass spectrometry (FT-ICR-MS) applying non-targeted approaches and some combined both. They found that the diversity of the endo- and in particular the exometabolome is far higher than expected from targeted approaches, yielding several thousand molecular masses (Rosselló-Mora et al., 2008; Brito-Echeverría et al., 2011; Romano et al., 2014; Fiore et al., 2015; Johnson et al., 2016). Besides the expected metabolites, the metabolome obviously includes a surprisingly high proportion of compounds not expected from predicted metabolic pathways. In particular the exometabolome exhibited a wealth of metabolites, many with so far unknown molecular masses and elemental composition (Rosselló-Mora et al., 2008; Kujawinski et al., 2009; Romano et al., 2014; Fiore et al., 2015). There is some evidence that quite a few of these metabolites are released as a result of an overflow metabolism due to growth on an abundant carbon source (Paczia et al., 2012; Romano et al., 2014). However, under less excessive growth conditions, in addition to well-known exometabolites such as signaling compounds (Dickschat, 2010; Hartmann and Schikora, 2012), vitamins (Sañudo-Wilhelmy et al., 2014), siderophores (Mansson et al., 2011), many other unexpected metabolites are released into the environment. The bacterial secretion of several such microbial metabolites, including the plant hormone indole 3-acetic acid (IAA) and vitamin precursors, has been documented (Zhang et al., 2014; Amin et al., 2015; Fiore et al., 2015; Johnson et al., 2016; Paerl et al., 2017). Analyses of dissolved organic matter (DOM) from Sargasso Sea waters detected several compounds with molecular masses known to be released by a strain of the globally abundant SAR11 clade (Kujawinski et al., 2009). The thiamine (vitamin B_1) precursor 4-amino-5-hydroxymethyl-2-methylpyrimidine (HMP) was also detected. This precursor is essential for thiamine biosynthesis by members of the SAR11 clade because they lack the gene for its complete biosynthesis (Carini et al., 2014). Thiamine requirements by photoautotrophic eukaryotes can also be met when the phosphorylated form, thiamine diphosphate, is dephosphorylated by a partner. In a bioassay approach Paerl et al. (2015) showed that the thiamine-auxotrophic picoeukaryote *Ostreococcus* sp. could grow when supplied with thiamine diphosphate in the presence of an *Alteromonas* strain that exhibit phosphatase activity.

The exchange of metabolites and precursors between microbes appears to be more common because auxotrophy is much wider distributed among microbes than previously assumed (McRose et al., 2014; Garcia et al., 2015; Paerl et al., 2017). Growth of such organisms depends on mutualistic interactions and supply of metabolites by co-occurring microbes. The Black Queen hypothesis applied this phenomenon to explain genome streamlining of prokaryotes by deleting certain metabolic pathways or parts of it as a reaction to leaky metabolic pathways of other microbes, helpers, thus supplying metabolites or precursors as public goods to the auxotrophic prokaryotes (Morris et al., 2012). It has been proposed most recently that gene loss and niche partitioning may be major drivers in the co-evolution of auxotrophs and helpers (Mas et al., 2016). However, considering the metabolites found in the exometabolome of various microbes and the environment in recent studies it appears that exchange of metabolites has larger ramifications than just explaining genome streamlining of selected microbes (Zelezniak et al., 2015; Estrela et al., 2016). We hypothesize that the exometabolome of helpers includes multiple metabolites and precursors, not only vitamins and growth factors, which are beneficial for other microbes. This release may promote growth of auxotrophic organism and even enhance growth of prototrophic microbes because they may not need to allocate energy to synthesize these precursors.

In order to test this hypothesis we assessed the exometabolome of two model bacteria of the marine *Roseobacter* group, *Phaeobacter inhibens* DSM 17395 and *Dinoroseobacter shibae* DSM 16493, growing on either glucose, glutamate and acetate or succinate, by analysis on a 15 Tesla FT-ICR-MS. *Phaeobacter inhibens* DSM 17395 is a purely heterotrophic bacterium growing in biofilms (Thole et al., 2012; Gram et al., 2015). Strains of this species and the genus *Phaeobacter* have been found in various marine habitats, such as natural biofilms on solid surfaces and during a bloom of *Emiliana huxleyi* (Gifford et al., 2014; Gram et al., 2015; Segev et al., 2016; Breider et al., 2017). *Dinoroseobacter shibae* is photoheterotrophic, grows symbiotically with dinoflagellates (Wagner-Döbler et al., 2010), produces various signaling compounds (Neumann et al., 2013) and has also been found associated to algae in natural phytoplankton blooms (Gifford et al., 2014; Milici et al., 2016; Segev et al., 2016). In order to examine whether identified molecular masses, and more precisely formulas, are also relevant under natural conditions, we screened DOM samples analyzed by FT-ICR-MS from a mesocosm experiment (Osterholz et al., 2015) and the North Sea. It is the first application of such a powerful FT-ICR-MS for exometabolomic studies in combination with the search for molecular formulas in environmental samples thus greatly enhancing the sensitivity and resolution of metabolite identification.

MATERIALS AND METHODS

Growth Conditions

Phaeobacter inhibens DSM 17395 and *D. shibae* DSM 16493 were first grown on marine broth (MB; Difco MB 2216) medium and afterwards repeatedly (5x) transferred and cultivated in artificial seawater (ASW) medium with the addition of a single organic carbon source. Before every transfer and after centrifugation of the cultures the cell pellets were washed three times with ASW medium. All plastic and glass ware used were rinsed with acidified ultrapure water (MilliQ, pH 2) and all glassware additionally combusted for 3 h at 500°C.

The ASW-medium for the *P. inhibens* cultures was prepared as described by Zech et al. (2009) but slightly modified by excluding EDTA from the trace element solution. The cultures were supplemented with glucose (5 mM, 30 mM C; ultrapure brand), acetate (30 mM, 60 mM C; ultrapure brand) or glutamate (20 mM, 100 mM C; ultrapure brand). *Dinoroseobacter shibae* was cultivated in ASW-medium (Soora and Cypionka, 2013) with the same concentrations of glucose as for *P. inhibens* and of glutamate at 7.5 mM (37.5 mM C). Instead of acetate, succinate was used at an initial concentration of 10 mM (40 mM C;

ultrapure brand). Concentrations of the substrates were adjusted due to varying metabolic rate efficiencies to obtain rather equal growth yields as determined by optical density (OD_{600}). Bacteria were cultivated in 500 ml of medium in triplicate 2 liter baffled Erlenmeyer glass flasks at pH 8 at 28°C in the dark on a shaker (100 rpm) and growth was monitored by OD. A sterile flask with media and the respective single carbon source was run as control. Subsamples were withdrawn under laminar flow for the separate analysis of the replicates for dissolved organic carbon, exometabolome-DOM, dissolved free (DFAA) and dissolved combined amino acids (DCAA), dissolved free neutral monosaccharides (DFNCHO), and dissolved combined monosaccharides (DCNCHO) and fatty acids at the start, the lag phase, the mid-exponential and early stationary phase in order to recover the majority of exometabolites released at varying growth conditions. The growth patterns were assessed more precisely than by OD measurements by subsampling every 4–8 h depending on the growth phase patterns for bacterial cell enumeration. Cells were fixed with 2% glutaraldehyde and frozen at −20°C until further analysis.

In order to test the effect of the vitamin B_1 precursors HMP (AstaTech inc., Bristol, PA, USA) and HET [4-methyl-5-(β-hydroxyethyl)thiazole; Sigma Aldrich, Munich, Germany] on the growth of the diatoms *Thalassiosira pseudonana* (CCMP 1335) and *Leptocylindrus danicus* (CCMP 470) these diatoms were grown axenically in ASW medium in a 12:12 h light dark cycle and illuminated at 70 μE. Instead of B_1, the precursors were added at 100 nM final concentration together with vitamins B_7 and B_{12} (100 nM each) and growth was monitored as relative fluorescence against a positive control including all three vitamins at final concentrations of 100 nM each and a negative control including only B_7 and B_{12} at the same concentrations. Axenicity of the diatom cultures was checked microscopically.

Cell Abundance

Cells of the *D. shibae* cultures were enumerated by flow cytometry, those of the *P. inhibens* cultures by epifluorescence microscopy due to the formation of microaggregates. Flow cytometric analyses were done according to Osterholz et al. (2015). Cell aggregates of *P. inhibens* were dispersed by ultrasonication (5 × 10 s at 15 mV; Bandelin Sonopuls HD 200, Bandelin, Berlin, Germany), filtered onto a 0.2 μm polycarbonate membrane, stained for 30 min with SYBR® Green I and counted by epifluorescence microscopy as described (Lunau et al., 2005). At least 1,000 cells were enumerated per filter.

Amino Acids, Mono- and Polysaccharides and Fatty Acids

Aliquots of the cultures were centrifuged at 2,499 g in acid washed and combusted (3 h, 500°C) glass centrifuge tubes. The supernatant was filtered through a 0.22 μm polyethersulfone membrane (Minisart, Sartorius, Göttingen, Germany) and the filtrate stored in combusted 20 ml glass vials at −20°C until further analysis. Concentrations of DFAA and DCAA were analyzed by high performance liquid chromatography (HPLC) after precolumn derivatization with orthophtaldialdehyde (Lunau et al., 2006) and concentrations of DFNCHO and DCNCHO by HPLC and pulsed amperometric detection after desalting (Hahnke et al., 2013). Detection limits for DFAA and DFNCHO were 0.5 and 1.5 nM, respectively. Fatty acid concentrations in the treatments with additions of succinate and acetate were determined by HPLC (Sykam, Fürstenfeldbruck, Germany) equipped with an Aminex HPX-87H column (Biorad, München, Germany) (Graue et al., 2012).

DOM Analyses

Dissolved organic carbon in the filtrates of the bacterial cultures and of the solid-phase extracted DOM (see below) was quantified as described previously (Osterholz et al., 2014). For FT-ICR-MS analyses, filtrates were acidified to pH 2 (HCl 25% p.a., Carl Roth, Germany), extracted via PPL solid phase cartridges (100 mg; Agilent, Waldbronn, Germany) adapted to a concentration of 15 ppm carbon and analyzed by FT-ICR-MS according to Osterholz et al. (2015). The extraction efficiency increased from 2 to 31% on carbon basis in the course of the experiment, as result of the contrary running substrate availability. Extracted DOM was ionized by soft electrospray ionization (Bruker Apollo, Daltonics, Bremen, Germany) and analyzed in positive and negative mode with a 15 T Solarix FT-ICR-MS (Bruker, Daltonics, Bremen, Germany). For each spectrum 300 scans were accumulated in the mass window of 92 to 2,000 Da. An internal calibration list was generated using Bruker Daltonic Data Analysis software for the calibration of the spectra. FT-ICR-MS instrument performance was verified using a laboratory-internal deep ocean DOM reference sample. Detected mass to charge ratios were processed applying a customized routine Matlab script. Molecular formulas were assigned as described by Koch and Dittmar (2006) to molecular masses with a minimum signal-to-noise ratio of 5 (Koch et al., 2007). From the mass spectrograms of the single time points of each culture that of the respective sterile control was subtracted.

Exometabolite Fragmentation

To confirm structures of genome-predicted identified exometabolites, we performed fragmentation experiments using FT-ICR-MS. Therefore, both bacterial strains were cultured again at similar conditions as described above for the exometabolome experiments but the exometabolome was harvested at the time point of the peak concentration of the respective exometabolite. A total of 500 mL was extracted via PPL solid phase cartridges as described above. Extracts were redissolved in a 1:1 MilliQ water/methanol solution at a concentration of 29 ppm carbon and analyzed on the FT-ICR-MS as described above. We selected the exometabolites which were identified as precursors or products of biosynthetic pathways for fragmentation, i.e., 43 of the 107 exometabolites identified in total. However, only seven metabolites had sufficiently high signal intensities in the FT-ICR-MS to perform fragmentation experiments. Limitations to fragmentation experiments include the fact that fragments may not be ionizable and different fragments with rather similar masses may yield overlapping peaks. Exometabolites of interest were isolated in a 1 Da window using the quadrupole unit and collision with argon occurred in the hexapole unit of the FT-ICR-MS. Fragmentation parameters

were optimized for each mass with an isolation window ranging from 0.1 to 1 (m/z), collision energy adjusted by applying 10 to 15 mV and 300 to 700 broadband scans were accumulated per run.

Exometabolite Prediction from Genome Databases and Screening against Natural DOM Samples

Metabolites of *P. inhibens* and *D. shibae*, predicted by the genome database BioCyc (Caspi et al., 2012), were listed with their corresponding molecular masses and molecular formulae (MF). All MF calculated from FT-ICR-MS detected masses were scanned against the genome-based metabolite prediction list. Matches were analyzed in more detail, regarding intra and extracellular function identified by previous studies. Putatively identified MF of exometabolites were screened against MF of DOM data sets of naturally derived and North Sea phytoplankton blooms (Osterholz et al., 2015, 2016; Noriega-Ortega et al., in preparation).

RESULTS

Both model strains of the *Roseobacter* group were grown in batch culture on single carbon sources of three major substrate classes to examine the diversification of the exometabolome as a function of these different substrates. Here we focus on the identified exometabolites whereas the overall exometabolome and its diversity is dealt with in a different publication (Noriega-Ortega et al., in preparation)

Growth and Substrate Utilization

Phaeobacter inhibens reached highest growth with maximum ODs of 0.76, 1.04, and 1.96 on acetate, glucose and glutamate respectively, at 68, 56, and 20 h (**Figure 1**). Respective cell numbers at these time points were 1.4×10^9, 0.6×10^9, and 3.4×10^9 cells mL^{-1} (see supporting information Figure S1). Growth of *D. shibae* reached highest ODs of 1.11, 1.03, and 0.90 on succinate, glucose and glutamate respectively, at 23, 65, and 39 h (**Figure 1**) with corresponding cell numbers of 2.1×10^9, 0.8×10^9, and 3.3×10^9 cells mL^{-1} respectively (see supporting information Figure S1). Substrate concentrations decreased inversely to growth of both bacteria and went below detection limit in the stationary phase except for the culture of *D. shibae* growing on glucose (**Figure 1**).

Amino Acids in the Exometabolome

The analysis of dissolved amino acids within the exometabolome of both strains was biased in the glutamate treatments by the interfering large glutamate peak. Hence, concentrations could only be measured in the stationary phase when glutamate was completely utilized. In the *P. inhibens* cultures, concentrations of DFAA remained below the detection limit of the HPLC analysis at all growth phases but tryptophan, tyrosine and histidine were detected by the FT-ICR-MS analysis (see below). Concentrations of DCAA in the treatment with acetate remained below 4 μM during the exponential growth phase but reached 235.4 μM in the stationary phase (**Figure 2F**). In the treatment with glucose, DCAA concentrations increased continuously during the exponential and stationary phase but reached a final concentration of only 15.6 μM (**Figure 2E**). The glutamate treatment of this culture yielded a concentration of 684.9 μM in the stationary phase (**Figure 2D**). The substrate source had only a minor influence on the composition of the amino acid pool in the exometabolome. During the exponential and stationary phases aspartate, glutamate, glycine, and alanine constituted the highest mol% of DCAA and together at least 60 mol% (**Figure 2**, Table S1). The very high DCAA concentrations in the exometabolome may have been a result of cell lysis. To estimate the extent of potential lysis, we made a mass balance of carbon (C) in DCAA and in the bacterial biomass in the stationary phase. DCAA concentrations of 219.8 and 639.0 μM in the treatments with acetate and glutamate in the stationary phase translate into 11.5 and 32.8 mg C L^{-1}, respectively. On the basis of 50 fg C per cell of large bacteria (Simon and Azam, 1989), typical for fast growing cultures, the bacterial numbers of 1.39×10^9 and 3.44×10^9 cells mL^{-1} in the stationary phase in the acetate and glutamate treatments, respectively, equal 69.5 and 160.9 mg C L^{-1}. Hence, the C bound in DCAA comprises 17.1 and 20.6% of the C bound in bacterial biomass. Therefore, we conclude that at these two conditions, but neither at other conditions nor in the glucose treatments, protein released by lysed cells contributed to the high DCAA concentrations in the stationary phase of the *P. inhibens* culture. Consequently, these time points were not considered for further exometabolome analyses.

In the *D. shibae* cultures, DFAA concentrations were below the detection limit of the HPLC analyses at all growth phases, but tryptophan, tyrosine, phenylalanine and histidine were detected by FT-ICR-MS (see below). Concentrations of DCAA in the exometabolome of the *D. shibae* cultures continuously increased during the exponential growth phase and reached 12.0 and 14.7 μM in the glucose and succinate treatments in the stationary phase (**Figure 3**). The glutamate treatment yielded 23.0 μM in the stationary phase (**Figure 3D**). Glutamate, glycine and alanine dominated the DCAA pool at all substrate conditions and constituted >50 mol% (Table S2). A mass balance of carbon bound in DCAA and the bacterial biomass in the stationary phase of the three treatments showed that DCAA constituted always <1% of the C bound in the biomass of the *D. shibae* cultures. Hence, cell lysis was minimal in these cultures.

Mono- and Polysaccharides in the Exometabolome

The analysis of dissolved mono- and polysaccharides interfered with the addition of glucose as single substrate source. DFNCHO were not detected in the exometabolome at any growth stage of both strains. Concentrations of DCNCHO increased continuously during growth of both strains on glutamate and acetate or succinate with highest concentrations in the stationary phase (**Figures 2**, **3**). Released DCNCHO in the *P. inhibens* cultures were greatly dominated by glucose but galactose, rhamnose, and fucose constituted proportions of up to 22

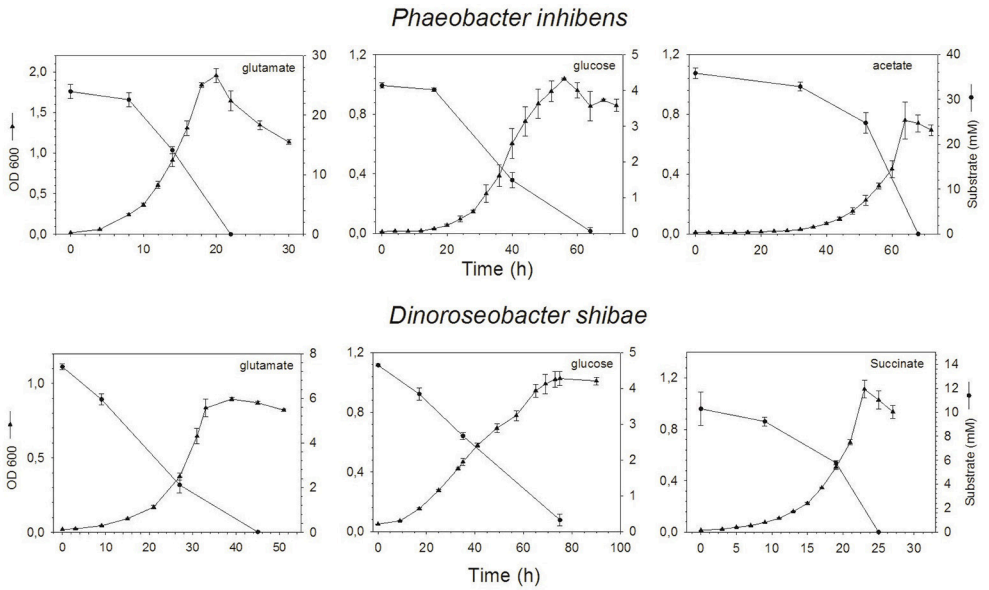

FIGURE 1 | Optical density and concentration of the substrates glutamate, glucose and acetate or succinate over time of *P. inhibens* **(upper)** and *D. shibae* **(lower)**. Note the different scales of the axes.

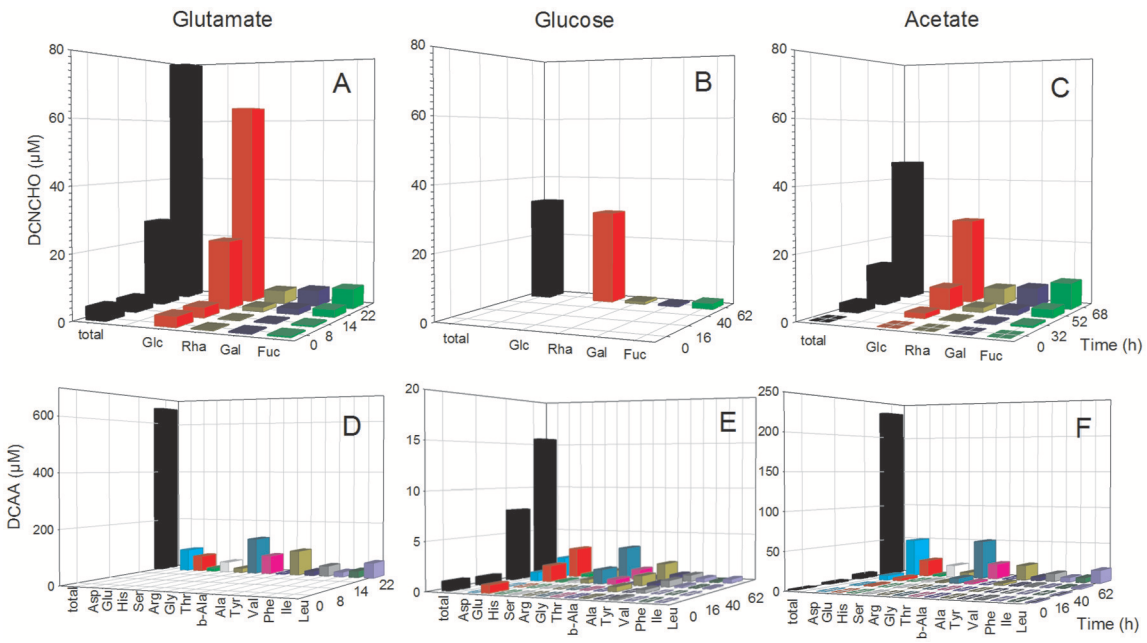

FIGURE 2 | Concentrations of individual neutral monosaccharides and amino acids (AA) bound in total dissolved combined neutral monosaccharides (DCNCHO) and total dissolved combined amino acids (DCAA), respectively, in the *P. inhibens* cultures. DCNCHO **(A–C)** and DCAA **(D–F)** right after inoculation, in the lag, exponential and stationary phase of *P. inhibens* growing on glutamate **(A,D)**, glucose **(B,E)** and acetate **(C,F)**. Note the different scales of the parameters in the different panels. Concentrations of DCNCHO in the treatment with glucose are not available until the stationary phase at 62 h due to interference with the HPLC analysis. Concentrations of AA in the glutamate treatment are only available for 22 h in the stationary phase because high glutamate concentrations until the exponential phase interfered with the HPLC analysis.

mol% in the treatment with acetate (**Figure 2**, Table S2). In the *D. shibae* cultures, DCNCHO concentrations remained lower than in those of *P. inhibens* (**Figure 3**). Only glucose, galactose and rhamnose were detected in the exometabolome. In the succinate treatment, rhamnose and galactose dominated whereas in the glutamate treatment galactose became the dominant

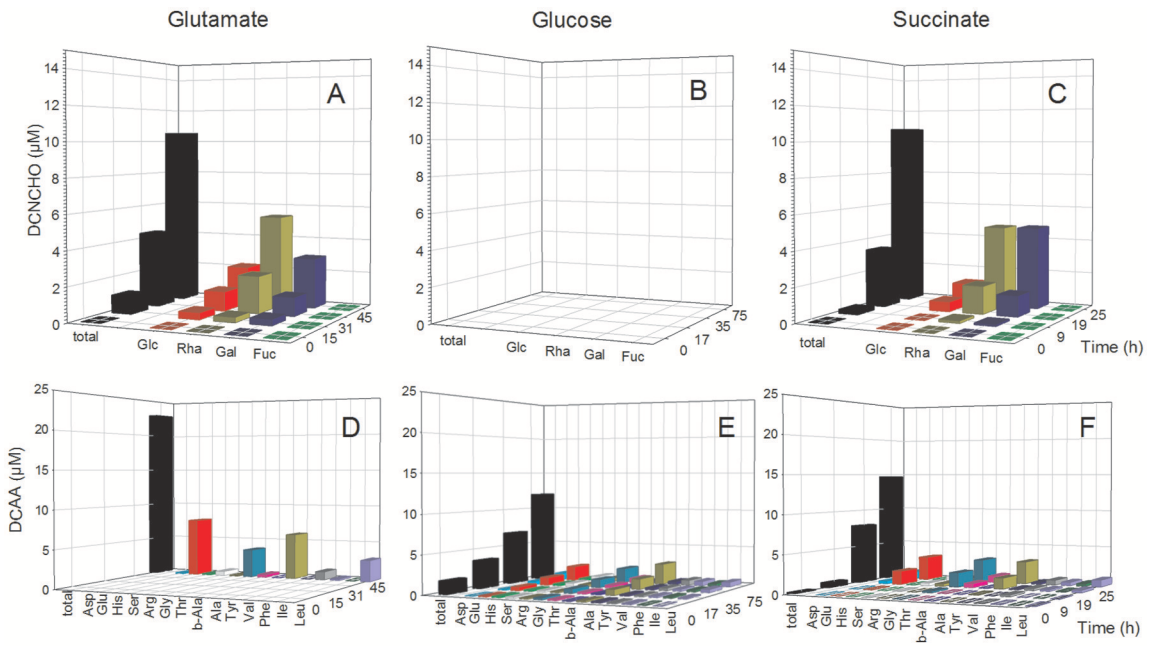

FIGURE 3 | Concentrations of individual neutral monosaccharides and amino acids (AA) bound in total dissolved combined neutral monosaccharides (DCNCHO) and total dissolved combined amino acids (DCAA), respectively, in the *D. shibae* cultures. DCNCHO **(A–C)** and DCAA **(D–F)** right after inoculation, in the lag, exponential and stationary phase of *D. shibae* growing on glutamate **(A,D)**, glucose **(B,E)** and succinate **(C,F)**. Concentrations of CHO in the treatment with glucose are not available due to interference with the HPLC analysis. Concentrations of DCAA in the glutamate treatment are only available for 45 h in the stationary phase because high glutamate concentrations until 31 h interfered with the HPLC analysis.

DCNCHO component in the exponential and stationary phase (Table S2).

Exometabolome Diversity and Exometabolite Identification

Applying the ultrahigh resolution FT-ICR-MS, we detected in total 2767 MF in the exometabolome of *P. inhibens* and 3,354 MF in that of *D. shibae* (**Figure 4**; Tables S3, S4). These numbers include all growth stages and all substrate treatments of both strains, except the stationary phase of *P. inhibens* grown on glutamate and acetate due to suspected cell lysis. The composition of the exometabolome, but not the exometabolites identified (see below) of both strains varied considerably as a function of the substrate utilized and growth stage (Noriega-Ortega et al., in preparation). Scanning all detected exometabolomic MF against the genome-predicted metabolites of *P. inhibens* and *D. shibae* by applying the BioCyc database revealed a match for 67 and 84 exometabolites, respectively (**Figure 4**). In addition, secondary metabolites known to be produced by *P. inhibens* and *D. shibae* were scanned against the exometabolomic MF obtained by FT-ICR-MS, yielding 4 identified compounds in the exometabolome of *P. inhibens* but none in that of *D. shibae* (**Table 1**). Identified exometabolites were further subdivided on the basis of their function and occurrence within the bacterial metabolism (**Figure 4**). For *D. shibae*, 35 metabolites were assigned to biosynthetic pathways (**Table 1**), 16 metabolites to degradation pathways (Table S5) and 33 metabolites originated from spontaneous non-enzymatic chemical-reactions (Table S6). For *P. inhibens*, 36 metabolites were assigned to biosynthetic pathways (**Table 1**), 15 to degradation pathways (Table S5), but only 16 derived from spontaneous non-enzymatic chemical reactions (Table S6). In total 43 different exometabolites of biosynthetic pathways were identified of which 28 were present in the exometabolome of both strains. In the *D. shibae* experiments 19 exametabolites assigned to biosynthetic pathways were detected in >50% of the time points sampled and in the experiments with *P. inhibens* 16 exometabolites. Alpha-ribazol was detected only at three time points in the exometabolome of *D. shibae* but in 88% of the time points of the *P. inhibens* experiments. Pyridoxal-P and histidine were detected only once in the exometabolome of the *D. shibae* experiments but in 43 and 55% of that of the *P. inhibens* experiments, respectively. HET was detected only once in the exometabolome of *P. inhibens* experiments but in 58% of that of the *D. shibae* experiments. All other exometabolites were detected in 10–50% of the samples analyzed in the experiments of both strains.

The detailed analysis showed that 12 (34%) and 10 (28%) of the annotated compounds linked to metabolic pathways of *D. shibae* and *P. inhibens*, respectively, were B vitamins and/or late precursors of biosynthetic pathways of vitamins B_1, B_2, B_5, B_6, B_7, and B_{12} (**Figure 5**, **Table 1**). Five (14%) and 6 (18%) of the annotated compounds were putatively quorum sensing-related metabolites and 10 (29%) and 9 (25%) amino acids and precursors of their biosynthetic pathways (**Figure 5**). Methyl-(indole-3-yl) acetate and tryptophan

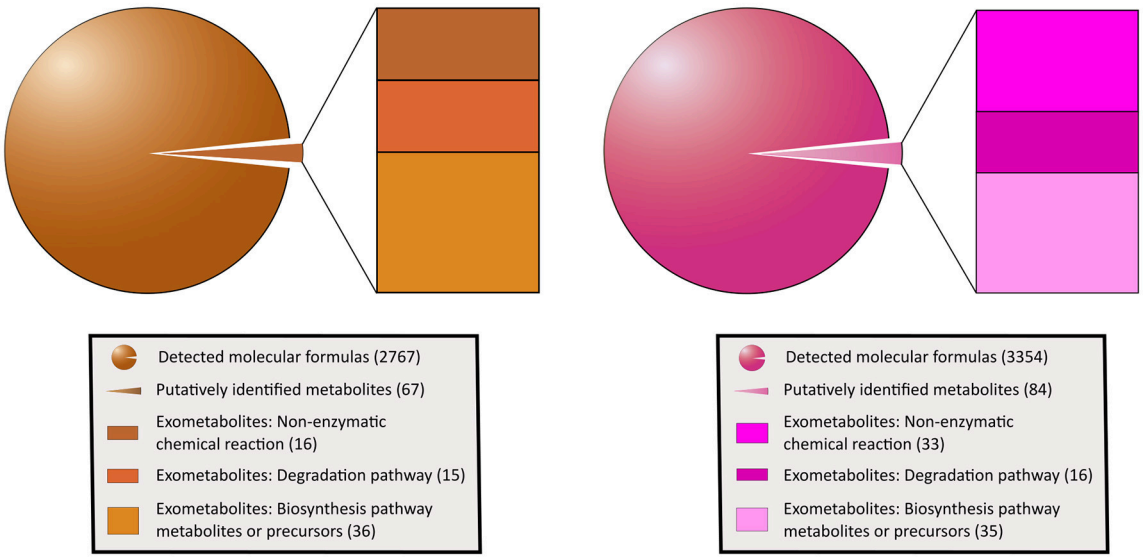

FIGURE 4 | Subdivision of all exometabolites released by *P. inhibens* and *D. shibae* during all growth phases. Given (in parenthesis) are total numbers of detected molecular formulas, putatively identified metabolites and those related to non-enzymatic chemical reactions, degradation and biosynthetic pathways and precursors.

as precursors in the biosynthetic pathways of IAA were annotated as exometabolites of both organisms whereas IAA was annotated only in that of *D. shibae*. Altogether, the complete set of annotated compounds was linked to 22 and 20 biosynthetic pathways in *D. shibae* and in *P. inhibens* respectively (**Table 1**).

To further validate the compounds annotated by the genome-based metabolite prediction approach, the respective molecular masses were isolated and fragmented via positive charge collision in the FT-ICR-MS. We confirmed the presence of 7 metabolites in the exometabolomes of *D. shibae* and *P. inhibens* respectively, including vitamins, vitamin precursors, acylated homoserine lactones (autoinducers) for quorum sensing and TDA (**Table 1**). Support for the correct annotation of the compounds was also provided by their detection in other studies applying similar experimental approaches (**Table 1**). Several identical metabolites were detected by Fiore et al. (2015), Johnson et al. (2016), annotated by Romano et al. (2014), or predicted to be needed exogenously because of lacking biosynthetic pathways in annotated bacterial genomes (Garcia et al., 2015).

Growth of Diatoms on Vitamin B1 and Precursors

In order to test the second part of our hypothesis whether identified precursors indeed enhance growth of prototrophic algae we selected two diatoms, *Thalassiosira pseudonana* and *Leptocylindrus danicus* and grew them with the supplementation of HET, HMP, HET, and HMP or B_1 and other vitamins they require (B_7, B_{12}). Supplementation of HET and HMP resulted in statistically significantly higher growth of both diatoms ($p < 0.01$; Student's *t*-test; Table S7). The growth rate and yield of *L. danicus* was enhanced by 17 and 35%, respectively, relative to a control, whereas the growth rate of *T. pseudonana* was enhanced by 22% but growth yield remained unaffected (**Figure 6**, Table S7). In both diatom cultures the growth stimulation differed among the various growth phases. The addition of vitamin B_1, surprisingly, resulted in a lower growth stimulation of both diatoms than that of the precursors and only for *T. pseudonana* the growth rate was significantly higher than that of the control (**Figure 6**, Table S7).

Identified Exometabolites in Marine DOM

To examine whether exometabolites produced by the two model strains of the *Roseobacter* group also occur in natural or naturally-derived DOM, we screened samples of a mesocosm experiment and from phytoplankton blooms in the North Sea. In the DOM of the mesocosm experiment in which a phytoplankton bloom was induced and various bacteria of the *Roseobacter* group were present (Osterholz et al., 2015), 19 MF were detected which matched those found also in the cultures of both strains. Sixteen and 15 MF were attributed to the cultures of *P. inhibens* and *D. shibae* respectively, and 14 occurred in both cultures. Eight MF included amino acids or biosynthetic precursors, three late biosynthetic precursors of vitamins and cofactors, three were autoinducers of quorum sensing and two the plant auxin IAA and its inactive form methyl-IAA (**Table 1**). In samples from in and outside phytoplankton blooms in the North Sea, 15 MF matched those found in the exometabolomes of both strains. Four of

TABLE 1 | Metabolites, their molecular formula, function, fragmentation results detected in the exometabolome of *D. shibae* and *P. inhibens*, in other studies, a mesocosm (Osterholz et al., 2015) and in a North Sea phytoplankton bloom (Noriega-Ortega et al., in preparation).

Metabolites	Molecular formula	Function	Fragmentation	*D. shibae*	*P. inhibens*	Other studies	Mesocosm	North Sea bloom
HET (4-methyl-5-(β-hydroxyethyl)thiazole)	C6H9NOS	vitamin B1 precursor		+	+			
Thiamine phosphate	C10H15N2O8P	vitamin B1		+	+	G, J		
Dimethyl-D-ribityl-lumazine	C13H18N4O6	vitamin B2 precursor	+	+	+	R		
Riboflavin	C17H20N4O6	vitamin B2	+	+	+	F, R, G, J		
Pantoate	C6H12O4	vitamin B5 precursor		+				
Pantothenate	C9H17NO5	vitamin B5		+	+	G, J		
Pyridoxal	C8H9NO3	vitamin B6 related		+	+		+	+
Pyridoxal phosphate	C8H10NO6P	vitamin B6		+	+			
Dethiobiotin	C10H17N2O3	vitamin B7 precursor			+			
Alpha-ribazole	C14H18N2O4	vitamin B12 precursor	+	+	+	R, J	+	+
Alpha-ribazole-5-phosphate	C14H19N2O7P	vitamin B12 precursor		+	+			+
Pyrroloquinoline quinone	C14H6N2O8	vit. B - cofactor	+	+				
6-(2-amino-2-carboxylatoethyl)−1,2,3,4-tetrahydroquinoline-2,4-dicarboxylate	C14H14N2O6	vit. B - cofactor		+			+	+
Methyl (indole-3-yl)acetate	C11H11NO2	IAA related		+	+		+	
Tryptophan	C11H12N2O2	IAA precursor		+	+	F, R, G	+	
Indole_acetate	C10H9NO2	IAA		+		F		
2,3-dihydroxybenzoate	C7H5O4	siderophore building block		+		F		
3-4-dihydroxybenzoate	C7H6O4	siderophore building block			+			
PAI-1 (N-(3-oxododecanoyl)-L-homoserine lactone)	C16H27NO4	quorum-sensing	+	+	+			
AAI	C12H19NO4	quorum-sensing		+	+		+	
VAI-2	C12H21NO3	quorum-sensing		+	+			
VAI-1	C10H15NO4	quorum-sensing		+	+		+	+
HAI-1	C8H13NO4	quorum-sensing		+	+		+	
N-3-hydroxydecanoyl-L-homoserine lactone	C14H25NO4	quorum-sensing	+		+	J		
Porphobilinogen	C10H14N2O4	AA derivate		+	+		+	+
Tyrosine	C9H11NO3	AA		+	+	R, G	+	+
Arogenate	C10H13NO5	AA precursor		+	+	R	+	+
4-Hydroxy-phenylpyruvate	C9H8O4	AA precursor		+	+		+	+
Phenylalanine	C9H11NO2	AA		+		F, R, G	+	+
L-SDAP	C11H18N2O7	AA precursor		+	+			
2-Isopropylmaleate	C7H10O4	AA precursor		+	+	R	+	
Delta-piperideine-2-6-dicarboxylate	C7H9NO4	AA precursor		+	+		+	+
O-Acetyl-L-homoserine	C6H11NO4	AA derivate		+	+		+	
Histidine	C6H9N3O2	AA		+	+	G, J		
Miraxanthin V	C17H18N2O6	betaxanthine			+		+	+
L-Dihydroxy-phenylalanine	C9H11NO4	betaxanthine			+		+	+
Glutathione	C10H17N3O6S	defense		+	+	R		
Tropodithietic acid	C8H4O3S2	antibiotic	+		+			
Inosine	C10H12N4O5	purin metabolism		+	+	F, R		
Thymidine	C10H14N2O5			+		R	+	+
Deoxycytidine	C9H13N3O4			+	+			
Phenylacetylcarbinol	C9H10O2				+			+
S-Methyl phenylethanethioate	C9H10OS				+	T		

F, Fiore et al. (2015); G, Garcia et al. (2015); J, Johnson et al. (2016); R, Romano et al. (2014); T, Thiel et al. (2010). Garcia et al. inferred the metabolites in cocultures on the basis of genomic information. +, Detected; AA, amino acid; IAA, indole acetic acid.

those were biosynthetic precursors of vitamins and cofactors including those detected in the mesocosm experiment, six were amino acids or biosynthetic precursors, matching those detected in the mesocosm experiment, and one was an autoinducer to quorum sensing found also in the mesocosm experiment (**Table 1**).

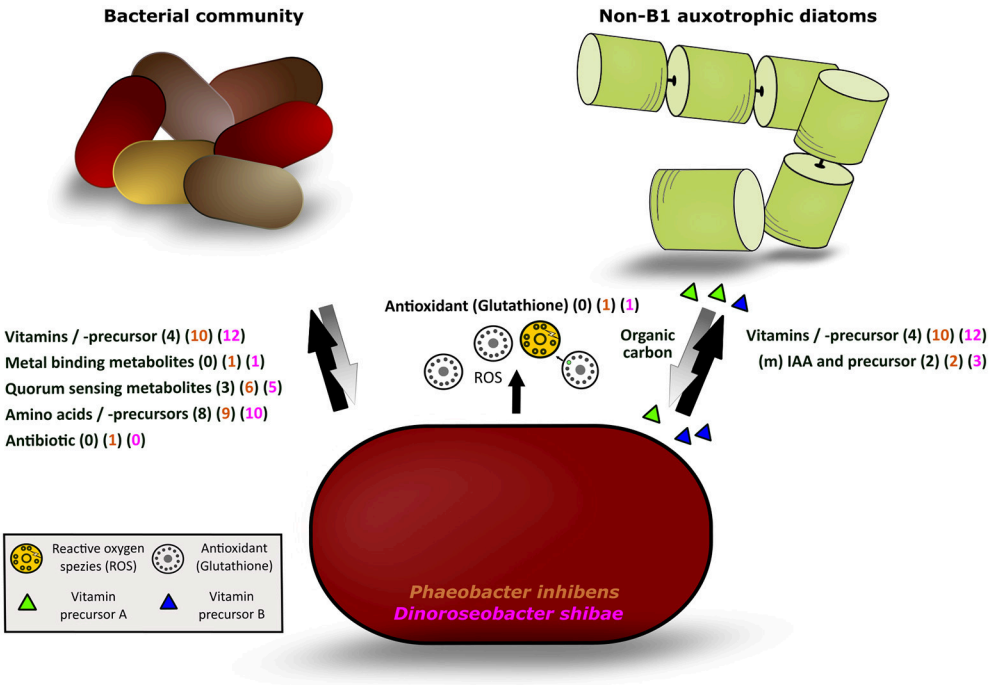

FIGURE 5 | Illustration of the different classes of exometabolites released by *P. inhibens* and *D. shibae* and mutualisms with other bacteria and phytoplankton algae. Black arrow: detected metabolites released by both strains; gray arrow: potential response of the bacterial or phytoplankton communities to the bacteria releasing metabolites; in parentheses, the number of exometabolites of each class detected in the natural phytoplankton bloom (black) and released by *P. inhibens* (brown) and *D. shibae* (pink) are given.

DISCUSSION

Our exometabolome analyses are based predominantly on an untargeted approach using FT-ICR-MS, which enables an ultrahigh resolution of individual molecular masses with a relative but no absolute quantification. The results show that *P. inhibens* and *D. shibae* both exhibit distinct exometabolite patterns consisting of 2,767 and 3,354 distinct MF and variations as a function of the carbon source. We were able to identify 2.3 and 2.6% of the exometabolites of *P. inhibens* and *D. shibae*, respectively, by comparing detected MF and genome-predicted metabolites. The observation that more than 97% of the MF consist of unknown chemical compounds, also reported in previous studies (Romano et al., 2014; Fiore et al., 2015; Johnson et al., 2016), is surprising and illustrates that the majority of MF comprises compounds is not predicted by genome annotated metabolites. There are indications that some of these compounds are metabolic waste (Fiore et al., 2015) but presumably other biological and physico-chemical reactions contribute to the formation of these compounds. The diversity of the exometabolome and implications for a better understanding of the bacterial processing of organic matter to shape the marine DOM pool are discussed elsewhere (Noriega-Ortega et al., in preparation). Here we focus on the identified exometabolites and the implications these findings have for the understanding of mutualistic interactions among bacteria and algae in marine ecosystems. The detection of seven exometabolites was further supported by fragmentation and we did not find a single case of mismatching fragments. We obtained further support of the correct MF by the genome-based exometabolite prediction. Hence our MF assignment is based on three independent methods and thus appears to be a solid base for discussing their significance in the interplay among marine microbes.

Significance of Identified Exometabolites

In both strains we identified MF identical to late biosynthetic precursors of and/or the vitamins B_1, B_2, B_5, B_6, B_7, and B_{12}, IAA and its methylated form, metal-acquisition growth factors, autoinducers for quorum sensing and biosynthetic precursors of several amino acids. Pyridoxal, the dephosphorylated form of vitamin B_6, alpha-ribazole, methyl-IAA and 3 autoinducers were also putatively detected in the DOM of a naturally-derived phytoplankton bloom (Osterholz et al., 2015) and the same vitamin precursors, alpha-ribazole-5 phosphate and one of the autoinducers also in the DOM of a North Sea phytoplankton bloom. Most MF identical to biosynthetic precursors of amino acids were also detected in the phytoplankton bloom samples. On the basis of genomic information of both strains and previous data, the vitamins and autoinducers were expected to be present in the exometabolome (Newton et al., 2010; Wagner-Döbler et al., 2010; Thole et al., 2012). However, the putative detection of late precursors of all B vitamins except one, methyl-IAA and five biosynthetic precursors of amino acids in the exometabolome of

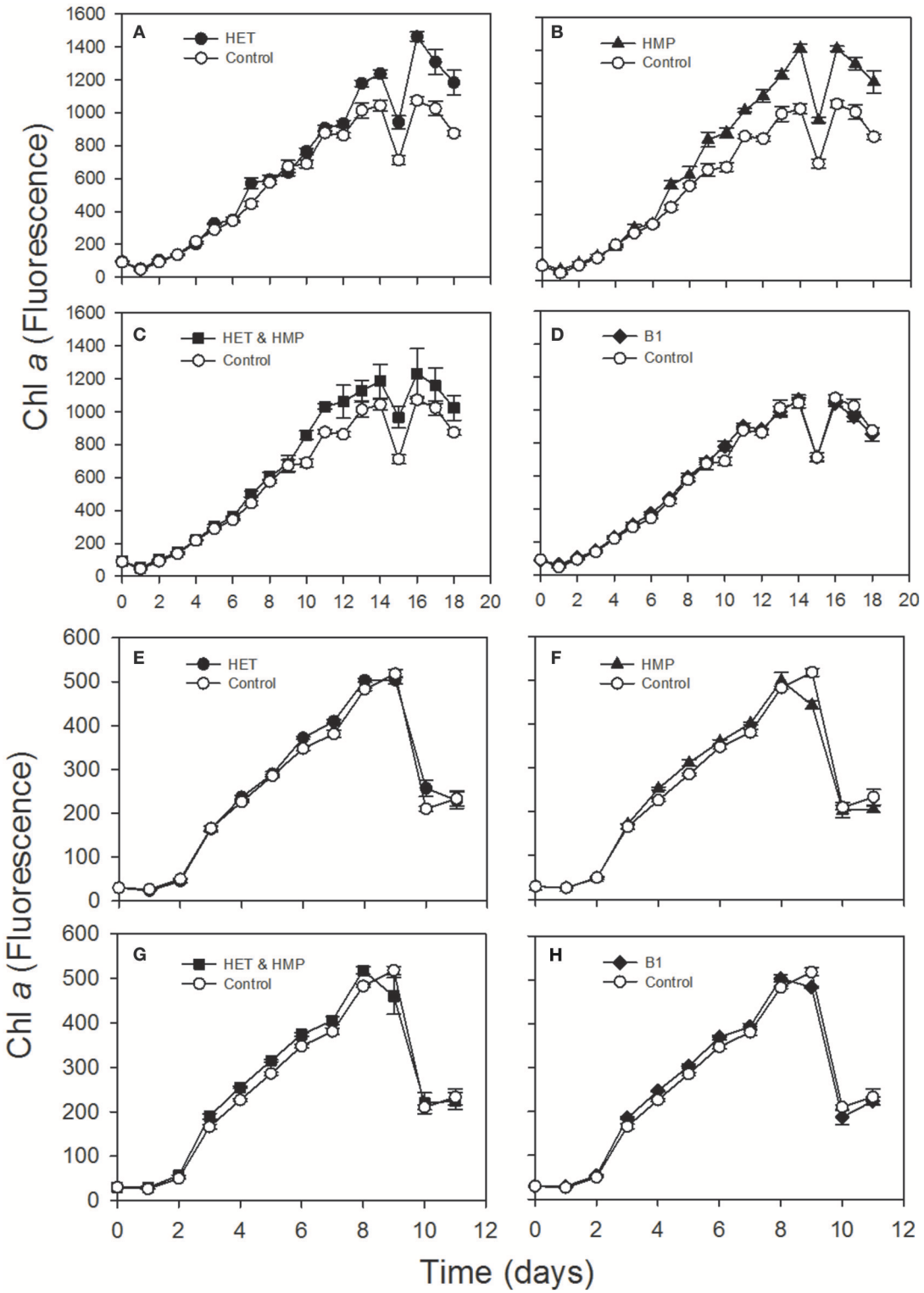

FIGURE 6 | Chlorophyll *a* fluorescence over time of an axenic culture of the diatoms *Leptocylindrus danicus* **(A–D)** and Thalassiosira pseudonana **(E–H)** supplemented with 4-methyl-5-(β-hydroxyethyl)thiazole (HET; **A,E**), 4-amino-5-hydroxymethyl-2-methylpyrimidine (HMP; **B,F**), HET & HMP **(C,G)** and vitamin B_1 **(D,H)** and a control without any of these supplements.

each strain and in the DOM of the phytoplankton bloom samples was surprising. It showed that these strains and presumably other microorganisms as well release a much greater variety of exometabolites than expected. Even though previous studies found a few of the precursors we detected, such a rich bouquet of biosynthetic precursors has neither been reported before in any bacterial exometabolome nor in the DOM of phytoplankton blooms.

The B_2 precursor dimethyl-D-ribityl-lumazine and/or the B_{12} precursor alpha-ribazole and two amino acid precursors were detected as exometabolites of a *Pseudovibrio* strain and *Ruegeria pomeroyi* (Romano et al., 2014; Johnson et al., 2016). The final precursor of the thiazole moiety of vitamin B_1, HET, we detected in both strains, is known to be used by several green algae, cryptophytes and dinoflagellates instead of B_1 (Lwoff, 1947; Droop, 1958; Turner, 1979). The pyrimidine moiety of vitamin B_1 which we did not detect, HMP, has been reported to be released by cyanobacteria, a marine betaproteobacterium and the alga *Dunaliella tertiolecta* (Carini et al., 2014). Results of previous research provides evidence that HMP and HET can be used in a salvage pathway for biosynthesis of thiamine by various B_1-auxotrophic eukaryotic algae and by Pelagibacterales (Turner, 1979; Carini et al., 2014; McRose et al., 2014; Paerl et al., 2015). There is most recent evidence, however, that HMP and unknown HET-related precursors can support growth of B_1-auxotrophic microeukaryotic marine algae via various bacteria and that these precursors are present in the open ocean (Paerl et al., 2017). Our results of the growth experiments with *T. pseudonana*, and *L. danicus* indicate that HMP and HET also stimulate growth of these vitamin B_1 prototrophic coastal diatoms. It was unexpected that the effect was even higher than that of the addition of B_1. This result is surprising and implies that *L. danicus* either lacks a vitamin B_1 transporter and/or that in both diatoms these precursors do not only compensate the lacking genetic capabilities of auxotrophic microbes but that HET and HMP have a so far unknown growth-promoting effect on vitamin B_1 prototrophic diatoms. If this stimulatory effect on vitamin B_1 prototrophic organisms is also true for other microorganisms the release of these precursors has even greater implications for controlling growth of these planktonic communities.

Pantoate as a precursor of vitamin B_5 was detected in the exometabolome of *D. shibae*. It is unknown whether this B_5 precursor can be used by marine algae or bacteria. An uptake system for pantoate, however, has been described for *Salmonella enterica* (Ernst and Downs, 2015) and thus is likely to exist in marine bacteria enabling them to use this precursor. Pyridoxal as the dephosphorylated form of vitamin B_6 was detected in the exometabolome of both strains and in the DOM of both phytoplankton blooms. Pyridoxal kinase (EC 2.7.1.35), the enzyme to phosphorylate this inactive form of vitamin B_6, is encoded in the genome of many bacteria as documented by a genomic search (https://img.jgi.doe.gov/cgi-bin/mer/main.cgi). If microbes can take up pyridoxal like *Sacharomyces cerevisiae* (Stolz and Vielreicher, 2003), this inactive form may be a so far neglected source of vitamin B_6.

Dethiobiotin, the last stage in the biosynthesis of vitamin B_7 (biotin), was detected in the exo-metabolome of *P. inhibens*. Extracellularly provided dethiobiotin has been demonstrated to cause diverging effects. Exogenous simultaneous supply of biotin and dethiobiotin caused a growth inhibition in several biotin-requiring fungi and bacteria including *Sacharomyces*, *Sordaria* and *Lactobacilli*, and was termed the anti-biotin effect (Dittmer et al., 1944; Lilly and Leonian, 1944). Contrary observations were reported for other fungi and Lactobacilli and a freshwater cyanobacterium, in which biotin auxotrophy was compensated by dethiobiotin addition (Dittmer et al., 1944; Lilly and Leonian, 1944; Bowman and DeMoll, 1993). Hence the significance of released dethiobiotin in marine microbial communities including the mycoplankton is still open and needs further studies.

Alpha-ribazole, a lower ligand building block of vitamin B_{12}, was released by both strains and detected in the phytoplankton bloom samples. The bioactive corrinoid cofactor vitamin B_{12} has been shown to be a controlling factor of primary production in pelagic ecosystems (Bertrand et al., 2007; Koch et al., 2011). Its cofactor binding, function and catalysis highly depends on the attached lower ligand (Lengyel et al., 1960; Stupperich et al., 1988; Renz, 1999; Yi et al., 2012). It has been shown, however, that the genome of *Listeria innocua*, lacking the genes for alpha-ribazole biosynthesis, encodes a transporter system of alpha-ribazole, cblT, and is able to synthesize B_{12} when this moiety is available as an exogenous source (Gray and Escalante-Semerena, 2010). Remodeling of corrinoids, such as vitamin B_{12}, by complementation of the lower ligand via uptake of exogenous compounds appears to be a common phenomenon within microbial communities (Gray and Escalante-Semerena, 2010; Keller et al., 2014; Men et al., 2014). Available 5,6-dimethylbenzimidazole (DMB), an alpha-ribazole precursor, allows major phytoplankton groups to remodel pseudocobalamin, commonly produced by cyanobacteria, into a usable corrinoid cofactor structure (Helliwell et al., 2016). Our results indicate that corrinoid building blocks are exchanged in marine ecosystems and that roseobacters such as *D. shibae* and *P. inhibens* may be providers of the most common and bioactive corrinoid cofactor lower ligand.

The auxin IAA has recently been identified to be secreted by various freshwater and marine bacteria and to be an important growth factor of various green algae and a diatom (Bagwell et al., 2014; Zhang et al., 2014; Amin et al., 2015, Fiore et al., 2015). It was also found in a phytoplankton bloom in the Pacific, in a eutrophic lake dominated by cyanobacteria and to be produced by *P. inhibens* (Zhang et al., 2014; Amin et al., 2015; Segev et al., 2016). We detected IAA in the exometabolome of *D. shibae* and its precursor tryptophan in the exometabolome of both strains and the naturally derived phytoplankton bloom. Tryptophan has been shown to enhance the production of IAA in *P. inhibens* (Segev et al., 2016) and also in the haptophyte *Emiliania huxleyi* (Labeeuw et al., 2016). It thus appears to be important in controlling the production of IAA in these roseobacters and the haptophyte. In both strains and in the naturally derived phytoplankton bloom, we also detected methyl-IAA, a related compound which was neither detected previously in the exometabolome of marine bacteria nor in marine DOM samples. It has been shown in *Arabidopsis* that methyl-IAA is an inactive form which can be taken up but needs to be demethylated

by an esterase to generate the active IAA (Yang et al., 2008). Because of the more hydrophobic form of methyl-IAA as compared to IAA, these authors suggest that it is more easily transported across the cell membrane, possibly even diffuses, thus enhancing the exploitation of the exogenous supply with the subsequent need to demethylate it intracellularly. Another aspect of hydrophobic compounds released into the water is that enhanced hydrophobicity results in a faster supply through this hydrophilic medium thus reducing the time of action and enhancing the accumulation at the target site, e.g. the cell surface (Maier et al., 1994). Hence it is conceivable that the methylated form of IAA in pelagic ecosystems leads to a more efficient use of this important auxin by phytoplankton.

The metal-binding 2,3-dihydroxybenzoate was detected in the exometabolome of *D. shibae*. This building block of the siderophore enterobactin is known to be secreted by heterotrophic and cyanobacteria under iron-limiting conditions (Young et al., 1967; Byers and Lankford, 1968; Fiore et al., 2015) and to enhance the expression of the 2,3-dihydroxybenzoate-AMP ligase, catalyzing an essential synthesis step toward the formation of enterobactin (Khalil and Pawelek, 2011). Other strains of the *Roseobacter* group are known to secrete enterobactin but not 2,3-dihydrobenzoate (Hogle et al., 2016). Hence, *D. shibae* appears to have the potential to provide 2,3-dihydroxybenzoate to marine bacterioplankton communities, thus inducing enterobactin synthesis and favoring iron uptake by itself and other bacteria. A building block of the siderophore petrobactin, 3,4-dihydroxybenzoate, was detected in the exometabolome of *P. inhibens* and not found before as a bacterial exometabolite. It has been shown that *P. inhibens* is able to produce enterobactin (Thole et al., 2012). Thus, 3,4-dihydroxybenzoate may have a similar role in metal acquisition as 2,3-dihydroxybenzoate (see above).

Glutathione was detected in the exometabolome of both strains and previously found also in that of a *Pseudovibrio* strain (Romano et al., 2014). Besides essential intracellular functions, glutathione is a fundamental extracellular protectant for bacteria, in particular as an antioxidant when reactive oxygen species (ROS) are present (Smirnova and Oktyabrsky, 2005; Montoya, 2013; Smirnova et al., 2015). One reason for the presence of glutathione in the exometabolome may be stress caused by the growth conditions and high cell densities and the possible protection against ROS. On the other hand, glutathione has been found in nanomolar concentrations in the oligotrophic north Pacific (Dupont et al., 2006) even though it is rapidly photooxidized (Moingt et al., 2010). Therefore, it is conceivable that bacteria such as our model strains actively excrete glutathione for protection against ROS produced by photochemical DOM oxidation.

Biosynthetic precursors of amino acids were previously reported in bacterial exometabolomes but interpreted as a result of an overflow metabolism (Paczia et al., 2012; Romano et al., 2014). As we found these precursors also in the DOM of phytoplankton blooms, we suggest that they are either actively secreted or released by dividing and growing cells or due to mortality by grazing or viral lysis of bacterial communities and are not a result of an overflow metabolism. They can potentially be used for amino acid biosynthesis by other bacteria but this pathway has yet to be shown. In support of this suggestion, it has recently been shown that bacterial mutants, missing biosynthetic genes in amino acid pathways, have a growth benefit over the wild type when supplied with the respective precursors or amino acids (D'Souza et al., 2014; Waschina et al., 2016). These authors consider amino acid cross-feeding as a specialized evolutionary mechanism of how bacterial subpopulations can receive mutual benefits by saving biosynthetic costs. Auxotrophy of essential amino acids can potentially be conquered by public amino acid goods and even facilitate metabolic interdependency or symbiosis (McCutcheon and Moran, 2007; Garcia et al., 2015). Our findings of several essential and non-essential amino acids and respective biosynthetic precursors in the exometabolome of both strains and in the DOM of the phytoplankton bloom samples suggests that beneficial amino acid cross-feeding also occurs in marine microbial communities.

The Exometabolome: A Market Place of Microbial Metabolites

The release of a wealth of exometabolites by the two model strains indicates that both of them may function as important suppliers of growth factors as well as of biosynthetic precursors, so-called public goods (Morris et al., 2012), to other pro- and eukaryotes in marine ecosystems. *Phaeobacter inhibens* dwells in biofilms (Gram et al., 2015) and both model strains live in association with microalgae and pelagic environments (Wagner-Döbler et al., 2010; Gifford et al., 2014; Segev et al., 2016) thus suggesting that these exometabolites are released as public goods in biofilm-associated as well as in pelagic marine communities. Biofilms with dense colonization of diverse bacterial communities may include surface-associated habitats but also marine aggregates which often form during phytoplankton blooms (Simon et al., 2002). Bacteria releasing public goods were recently termed Black Queen in the context of the Black Queen hypothesis (BQH; Morris et al., 2012; Morris, 2015), a scenario in which other bacteria benefit from losing genetic traits to synthesize certain growth factors such as vitamins or parts of their biosynthetic pathways when exogenous supply of these compounds is consistently available. Aggregate-associated bacteria acting as Black Queens may also supply free-living pelagic bacteria and phytoplankton algae in the surrounding water with public goods. Genome streamlining features were reported from various pelagic bacteria including *Pelagibacterales*, the SAR86 clade and *Prochlorococcus* (Dupont et al., 2012; Carini et al., 2014; Giovannoni et al., 2014) but also from free-living and symbiotic bacteria dwelling in nutrient-rich or constant environments (Van de Guchte et al., 2006; McCutcheon and Moran, 2007; D'Souza et al., 2014). Supply of released compounds as public goods to other microbes is part of a complex network of microbial interactions and there are quite a few public goods in this context, but also private metabolic goods not shared, which act beyond the concept of the BQH (Morris, 2015; Estrela et al., 2016). Our results in fact indicate that the two vitamin B_1 prototrophic diatoms benefit from supply by the B_1 precursors HET and HMP, a scenario not considered by the BQH. It

must also be kept in mind that in a microbial community mutual interactions exist between the primary producers secreting substrates to the (photo)heterotrophic microbes and that different microbes are distinct in their capabilities, e.g., in hydrolyzing polymers. For instance *Flavobacteria* exhibit a wealth of polysaccharide hydrolyzing enzymes (Teeling et al., 2012) whereas roseobacters are very limited in these polymer-degrading traits (Hahnke et al., 2013). Further, it has been shown that different bacteria, each missing distinct genomic metabolic traits and exhibiting streamlined genomic features, coexist by complementing each other with metabolites for which they are auxotrophic (Garcia et al., 2015). A microbial community with mutual interdependencies between two or among a group of microbes and no unidirectional flows of public and private goods among various bacteria and other microbes appears to be a more suitable model to describe this complex network, a marketplace of microbial metabolites (**Figure 5**; Zelezniak et al., 2015). Such scenarios presumably characterize the dynamic ecosystems in which both model strains dwell: In tighter or looser association with algae and other bacteria on biofilms or during phytoplankton blooms. Both scenarios exhibit many mutual interactions among a multitude of organisms with non-streamlined as well as streamlined genomes.

AUTHOR CONTRIBUTIONS

All authors designed the experiments. GW and BN carried out the experiments, GW identified the exometabolites and wrote the first draft of the manuscript. MS and GW wrote the final version of the manuscript. All authors critically reviewed and added aspects to the manuscript.

FUNDING

The study was supported by Deutsche Forschungsgemeinschaft within TRR51 Roseobacter.

ACKNOWLEDGMENTS

We thank Kathrin Klapproth, Birgit Kuerzel and Rolf Weinert for help with the sample analyses by FT-ICR-MS and HPLC.

SUPPLEMENTARY MATERIAL

The Supplementary Material for this article can be found online at: https://www.frontiersin.org/articles/10.3389/fmicb.2017.01985/full#supplementary-material

REFERENCES

Amin, S. A., Hmelo, L. R., van Tol, H. M., Durham, B. P., Carlson, L. T., Heal, K. R., et al. (2015). Interaction and signalling between a cosmopolitan phytoplankton and associated bacteria. *Nature* 522, 98–101. doi: 10.1038/nature14488

Bagwell, C. E., Piskorska, M., Soule, T., Petelos, A., and Yeager, C. M. (2014). A diverse assemblage of indole-3-acetic acid producing bacteria associate with unicellular green algae. *Appl. Biochem. Biotechnol.* 173, 1977–1984. doi: 10.1007/s12010-014-0980-5

Bertrand, E. M., Saito, M. A., Rose, J. M., Riesselman, C. R., Lohan, M. C., et al. (2007). Vitamin B12 and iron colimitation of phytoplankton growth in the Ross Sea. *Limnol. Oceanogr.* 52, 1079–1093. doi: 10.4319/lo.2007.52.3.1079

Bowman, W. C., and DeMoll, E. (1993). Biosynthesis of biotin from dethiobiotin by the biotin auxotroph *Lactobacillus plantarum*. *J. Bacteriol.* 175, 7702–7704. doi: 10.1128/jb.175.23.7702-7704.1993

Breider, S., Freese, H., Spröer, C., Simon, M., Overmann, J., and Brinkhoff, T. (2017). Phaeobacter porticola sp. nov., an antibiotic producing bacterium isolated from a harbor in the southern North Sea. *Int. J. System. Evol. Microbiol.* 67, 2153–2159. doi: 10.1099/ijsem.0.001879

Brito-Echeverría, J., Lucio, M., López-López, A., Antón, J., Schmitt-Kopplin, P., and Rosselló-Móra, R. (2011). Response to adverse conditions in two strains of the extremely halophilic species *Salinibacter ruber*. *Extremophiles* 15, 379–389. doi: 10.1007/s00792-011-0366-3

Byers, B. R., and Lankford, C. E. (1968). Regulation of synthesis of 2,3-dihydroxybenzoic acid in Bacillus subtilis by iron and a biological secondary hydroxamate. *Biochim. Biophys. Acta* 165, 563–566. doi: 10.1016/0304-4165(68)90244-4

Carini, P., Campbell, E. O., Morré, J., Sa-udo-Wilhelmy, S. A., Thrash, J. C., Bennett, S. E., et al. (2014). Discovery of a SAR11 growth requirement for thiamin's pyrimidine precursor and its distribution in the Sargasso Sea. *ISME J.* 8, 1727–1738. doi: 10.1038/ismej.2014.61

Caspi, R., Altman, T., Dreher, K., Fulcher, C. A., Subhraveti, P., Keseler, I. M., et al. (2012). The MetaCyc database of metabolic pathways and enzymes and the BioCyc collection of pathway/genome databases. *Nucleic Acids Res.* 40, D742–D753. doi: 10.1093/nar/gkr1014

Dickschat, J. S. (2010). Quorum sensing and bacterial biofilms. *Nat. Prod. Rep.* 27, 343–369. doi: 10.1039/b804469b

Dittmer, K., Melville, D. B., DU Vigneaud, V. (1944). The possible synthesis of biotin from desthiobiotin by yeast and the anti-biotin effect of desthiobiotin for *L. casei*. *Science* 99, 203–205. doi: 10.1126/science.99.2567.203

Droop, M. R. (1958). Requirement for thiamine among some marine and supra-littoral protista. *J. Mar. Biol. Assoc. UK* 37, 323–329. doi: 10.1017/S0025315400023729

Drüppel, K., Hensler, M., Trautwein, K., Koßmehl, S., Wöhlbrand, L., Schmidt-Hohagen, K., et al. (2014). Pathways and substrate-specific regulation of amino acid degradation in *Phaeobacter inhibens* DSM 17395 (archetype of the marine *Roseobacter clade*). *Environ. Microbiol.* 16, 218–238. doi: 10.1111/1462-2920.12276

D'Souza, G., Waschina, S., Pande, S., Bohl, K., Kaleta, C., and Kost, C. (2014). Less is more: selective advantage can explain the prevalent loss ob biosynthetic genes in bacteria. *Evolution* 68, 2559–2570. doi: 10.1111/evo.12468

Dupont, C. L., Moffett, J. W., and Ahner, B. A. (2006). Distributions of dissolved and particulate thiols in the sub-artic north Pacific. *Deep Sea Res. I* 57, 553–566. doi: 10.1016/j.dsr.2006.09.003

Dupont, C. L., Rusch, D. B., Yooseph, S., Lombardo, M. J., Richter, R. A., Valas, R., et al. (2012). Genomic insights to SAR86, an abundant and uncultivated marine bacterial lineage. *ISME J.* 6, 1186–1199. doi: 10.1038/ismej.2011.189

Ernst, D. C., and Downs, D. M. (2015). The STM4195 gene product (PanS) transports coenzyme A precursors in *Salmonella enterica*. *J. Bacteriol.* 197, 1368–1377. doi: 10.1128/JB.02506-14

Estrela, S., Moris, J. J., and Kerr, B. (2016). Private benefits and metabolic conflicts shape the emergence of microbial interdependencies. *Environ. Microbiol.* 18, 1415–1427. doi: 10.1111/1462-2920.13028

Fiore, C. L., Longnecker, K., Kido Soule, M. C., and Kujawinski, E. B. (2015). Release of ecologically relevant metabolites by the cyanobacterium *Synechococcus elongatus* CCMP 1631. *Environ. Microbiol.* 17, 3949–3963. doi: 10.1111/1462-2920.12899

Frimmersdorf, E., Horatzek, S., Pelnikevich, A., Wiehlmann, L., and Schomburg, D. (2010). How *Pseudomonas aeruginosa* adapts to various environments: a metabolomic approach. *Environ. Microbiol.* 12, 1734–1747. doi: 10.1111/j.1462-2920.2010.02253.x

Garcia, S. L., Buck, M., McMahon, K. D., Grossart, H. P., Eiler, A., and Warnecke, F. (2015). Auxotrophy and intrapopulation complementary in the "interactome" of a cultivated freshwater model community. *Mol. Ecol.* 2, 4449–4459. doi: 10.1111/mec.13319

Gifford, S. M., Sharma, S., and Moran, M. A. (2014). Linking activity and function to ecosystem dynamics in a coastal bacterioplankton community. *Front. Microbiol.* 5:185. doi: 10.3389/fmicb.2014.00185

Giovannoni, S. J., Cameron Thrash, J., and Temperton, B. (2014). Implications of streamlining theory for microbial ecology. *ISME J.* 8, 1553–1565. doi: 10.1038/ismej.2014.60

Gram, L., Rasmussen, B. B., Wemheuer, B., Bernbom, N., Hg, Y. Y., Porsby, C., et al. (2015). Phaeobacter inhibens from the *Roseobacter clade* has an environmental niche as a surface colonizer in harbors. *System. Appl. Microbiol.* 38, 483–493. doi: 10.1016/j.syapm.2015.07.006

Graue, J., Engelen, B., and Cypionka, H. (2012). Degradation of cyanobacterial biomass in anoxic tidal-flat sediments: a microcosm study of metabolic processes and community changes. *ISME J.* 6, 660–669. doi: 10.1038/ismej.2011.120

Gray, M. J., and Escalante-Semerena, J. C. (2010). A new pathway for the synthesis of α-ribazole-phosphate in *Listeria innocua*. *Mol. Microbiol.* 77, 1429–1438. doi: 10.1111/j.1365-2958.2010.07294.x

Hahnke, S., Brock, N. L., Zell, C., Simon, M., Dickschat, J. S., and Brinkhoff, T. (2013). Physiological diversity of *Roseobacter clade* bacteria co-occurring during a phytoplankton bloom in the North Sea. *Syst. Appl. Microbiol.* 36, 39–48. doi: 10.1016/j.syapm.2012.09.004

Hartmann, A., and Schikora, A. (2012). Quorum sensing of bacteria and trans-kingdom interactions of N-acyl homoserine lactones with eukaryotes. *J. Chem. Ecol.* 38, 704–713. doi: 10.1007/s10886-012-0141-7

Helliwell, K. E., Lawrence, A. D., Holzer, A., Kudahl, U. J., Sasso, S., Kräutler, B., et al. (2016). Cyanobacteria and eukaryotic algae use different chemical variants of vitamin B12. *Curr. Biol.* 26, 999–1008. doi: 10.1016/j.cub.2016.02.041

Hogle, S. L., Cameron, T. J., Dupont, C. L., Chris, L., and Barbeau, K. A. (2016). Trace metal acquisition by marine heterotrophic bacterioplankton with contrasting trophic strategies. *Appl. Environ. Microbiol.* 82, 1613–1624. doi: 10.1128/AEM.03128-15

Johnson, W. M., Kido Soule, M. C., and Kujawinski, E. B. (2016). Evidence for quorum sensing and differential metabolite production by a marine bacterium in response to DMSP. *ISME J.* 10, 2304–2316. doi: 10.1038/ismej.2016.6

Kell, D. B., Brown, M., Davey, H. M., Dunn, W. B., Spasic, I., and Oliver, S. G. (2005). Metabolic footprinting and systems biology: the medium is the message. *Nat. Rev. Microbiol.* 3, 557–565. doi: 10.1038/nrmicro1177

Keller, S., Ruetz, M., Kunze, C., Kräutler, B., Diekert, G., and Schubert, T. (2014). Exogenous 5,6-dimethylbenzimidazole caused production of a non-functional tetrachloroethene reductive dehalogenase in *Sulfurospirillum multivorans*. *Environ. Microbiol.* 16, 3361–3369. doi: 10.1111/1462-2920.12268

Khalil, S., and Pawelek, P. D. (2011). Enzymatic adenylation of 2,3-dihydroxybenzoate is enhanced by a protein-protein interaction between Escherichia coli 2,3-dihydro-2,3-dihydroxybenzoate dehydrogenase (EntA) and 2,3-dihydroxybenzoate-AMP ligase (EntE). *Biochemistry Mosc.* 50, 533–545. doi: 10.1021/bi101558v

Koch, B. P., and Dittmar, T. (2006). From mass to structure: an aromaticity index for highresolution mass data of natural organic matter. *Rapid Commun. Mass Spectrom.* 20, 926–932. doi: 10.1002/rcm.2386

Koch, B. P., Dittmar, T., Witt, M., and Kattner, G. (2007). Fundamentals of molecular formula assignment to ultrahigh resolution mass data of natural organic matter. *Anal. Chem.* 79, 1758–1763. doi: 10.1021/ac061949s

Koch, F., Marcoval, M. A., Panzeca, C., Bruland, K. W., Sa-udo-Wilhelmy, S. A., and Gobler, C. J. (2011). The effect of vitamin B12 on phytoplankton growth and community structure in the Gulf of Alaska. *Limnol. Oceanogr.* 56, 1023–1034. doi: 10.4319/lo.2011.56.3.1023

Kujawinski, E. B., Longkecker, K., Blough, N. V., Del Veccchio, R., Finlay, L., Kitner, J. B., et al. (2009). Identification of possible source markers in marine dissolved organic matter using ultrahigh resolution mass spectrometry. *Geochim. Cosmochim. Acta* 73, 4384–4399. doi: 10.1016/j.gca.2009.04.033

Labeeuw, L., Khey, J., Bramucci, A. R., Atwal, H., de la Mata, P., Harynuk, J., et al. (2016). Indole-3-acetic acid is produced by Emiliania huxleyi coccolith-bearing cells and triggers a physiological response in bald cells. *Front. Microbiol.* 7:828. doi: 10.3389/fmicb.2016.00828

Lengyel, P. L., Mazumder, R., and Ochoa, S. (1960). Mammalian methylmalonyl isomerase and vitamin B12 coenzymes. *Proc. Natl. Acad. Sci. U.S.A.* 46, 1312–1318.

Lilly, V. G., and Leonian, L. H. (1944). The anti-biotin effect of desthiobiotin. *Science* 99, 205–206. doi: 10.1126/science.99.2567.205

Lunau, M., Lemke, A., Dellwig, O., and Simon, M. (2006). Physical and biogeochemical controls of microaggregate dynamics in a tidally affected coastal ecosystem. *Limnol. Oceanogr.* 51, 847–859. doi: 10.4319/lo.2006.51.2.0847

Lunau, M., Lemke, A., Walther, K., Martens-Habbena, W., and Simon, M. (2005). An improved method for counting bacteria in samples with high proportions of particle-associated cells by epifluorescence microscopy: Environ. *Microbiol.* 7, 961–968. doi: 10.1111/j.1462-2920.2005.00767.x

Lwoff, A. (1947). Some aspects of the problem of growth factors for protista. *Ann. Rev. Microbiol.* 1, 101–114.

Maier, I., Müller, D. G., and Boland, W. (1994). Spermatozoid chemotaxis in *Laminaria digitata* (Phaeophyceae). III. Pheromone receptor specificity and threshold concentrations. *Z. Naturforschung* 49c, 601–606.

Mansson, M., Gram, L., and Larsen, T. O. (2011). Production of bioactive secondary metabolites by marine Vibrionaceae. *Mar. Drugs* 9, 1440–1468. doi: 10.3390/md9091440

Mas, A., Jamshidi, S., van Lagadeuc, Y., Eveillard, D., and Vandenkoornhuyse, P. (2016). Beyond the black queen hypothesis. *ISME J.* 10, 2085–2091. doi: 10.1038/ismej.2016.22

McCutcheon, J. P., and Moran, N. A. (2007). Parallel genomic evolution and metabolic interdependence in an ancient symbiosis. *Proc. Natl. Acad. Sci. U.S.A.* 104, 19392–19397. doi: 10.1073/pnas.0708855104

McRose, D., Guo, J., Monier, A., Sudek, S., Wilken, S., Yan, S., et al. (2014). Alternatives to vitamin B1 uptake revealed with discovery of riboswitches in multiple marine eukaryotic lineages. *ISME J.* 8, 2517–2529. doi: 10.1038/ismej.2014.146

Men, Y., Seth, E. C., Yi, S., Crofts, T. S., Allen, R. H., Taga, M. E., et al. (2014). Identification of specific corrinoids reveals corrinoid modification in dechlorinating microbial communities. *Environ. Microbiol.* 17, 4873–4884. doi: 10.1111/1462-2920.12500

Milici, M., Deng, Z. L., Tomasch, J., Decelle, J., Wos-Oxley, M., Wang, H., et al. (2016). Co-occurrence analysis of microbial taxa in the Atlantic Ocean reveals high connectivity in the free-living bacterioplankton. *Front. Microbiol.* 7:649. doi: 10.3389/fmicb.2016.00649

Moingt, M., Bresac, M., Belanger, D., and Amyot, M. (2010). Role of ultra-violet radiation, mercury and copper on the stability of dissolved glutathione in natural and artificial freshwater and saltwater. *Chemosphere* 80, 1314–1320. doi: 10.1016/j.chemosphere.2010.06.041

Montoya, M. (2013). Bacterial glutathione import. *Nat. Struct. Mol. Biol.* 20:775. doi: 10.1038/nsmb.2632

Morris, J. J. (2015). Black Queen evolution: the role of leakiness in structuring microbial communities. *Trends in Genetics* 31, 475–482. doi: 10.1016/j.tig.2015.05.004

Morris, J. J., Lenski, R. E., and Zinser, E. R. (2012). The black queen hypothesis: evolution of dependencies through adaptive gene loss. *MBio* 3, e00036–e00012. doi: 10.1128/mBio.00036-12

Neumann, A., Patzelt, D., Wagner-Döbler, I., and Schulz, S. (2013). Identification of new N-acylhomoserine lactone signalling compounds of Dinoroseobacter shibae DFL-12T by overexpression of luxI genes. *Chembiochem* 14, 2355–2361. doi: 10.1002/cbic.201300424

Newton, R. J., Griffin, L. E., Bowles, K. M., Meile, C., Gifford, S., Givens, C. E., et al. (2010). Genome characteristics of a generalist marine bacterial lineage. *ISME J.* 4, 784–798. doi: 10.1038/ismej.2009.150

Osterholz, H., Dittmar, T., and Niggemann, J. (2014). Molecular evidence for rapid dissolved organic matter turnover in Arctic fjords. *Mar. Chem.* 160, 1–10. doi: 10.1016/j.marchem.2014.01.002

Osterholz, H., Niggemann, J., Giebel, H. A., Simon, M., and Dittmar, T. (2015). Inefficient microbial production of refractory dissolved organic matter in the ocean. *Nat. Commun.* 6:7422. doi: 10.1038/ncomms8422

Osterholz, H., Singer, G., Wemheuer, B., Daniel, R., Simon, M., Niggemann, J., et al. (2016). Deciphering associations between dissolved organic molecules and bacterial communities in a pelagic marine system. *ISME J.* 7, 1717–1730. doi: 10.1038/ismej.2015.231

Paczia, N., Nilgen, A., Lehmann, T., Gätgens, J., Wiechert, W., and Noack, W. S. (2012). Extensive exometabolome analysis reveals extended overflow metabolism in various microorganisms. *Microb. Cell Fact.* 11:122. doi: 10.1186/1475-2859-11-122

Paerl, R., Bertrand, E., Allen, E., Palenik, B., and Azam, F. (2015). Vitamin B1 ecophysiology of marine picoeukaryotic algae: Strain-specific differences and a new role for bacteria in vitamin cycling. *Limnol. Oceanogr.* 60, 215–228. doi: 10.1002/lno.10009

Paerl, R. W., Bouget, F. Y., Lozano, J. C., Vergé, V., Schatt, P., Allen, E. E., et al. (2017). Use of plankton-derived vitamin B1 precursors, especially thiazole-related precursor, by key marine picoeukaryotic phytoplankton. *ISME J.* 11, 753–765. doi: 10.1038/ismej.2016.145

Paul, C., Barofsky, A., Vidoudez, C., and Pohnert, G. (2009). Diatom exudates influence metabolism and cell growth of co-cultured diatom species. *Mar. Ecol. Prog. Ser.* 389: 61–70. doi: 10.3354/meps08162

Renz, P. (1999). "Biosynthesis of the 5,6-dimethylbenzimidazole moiety of cobalamin and of the other bases found in natural corrinoids," in *Chemistry and Biochemistry of B12*, ed R. Banerjee (New York, NY: Wiley), 557–575.

Romano, S., Dittmar, T., Bondarev, V., Weber, R. J. M., Viant, M. R., and Schulz-Vogt, H. N. (2014). Exo-metabolome of *Pseudovibrio* sp. FO-BEG1 analyzed by ultra-high resolution mass spectrometry and the effect of phosphate limitation. *PLoS ONE* 9:e96038. doi: 10.1371/journal.pone.0096038

Rosselló-Mora, R., Pena, A., Brito-Echeverria, J., Lopez-Lopez, A., Valens-Vadell, M., Frommberger, M., et al. (2008). Metabolic evidence for biogeographic isolation of the extremophilic bacterium *Salinibacter ruber*. *ISME J.* 2, 242–253. doi: 10.1038/ismej.2007.93

Sañudo-Wilhelmy, S. A., Gómez-Consarnau, L., Suffridge, C., and Webb, E. A. (2014). The role of B vitamins in marine biogeochemistry. *Ann. Rev. Mar. Sci.* 6, 339–367. doi: 10.1146/annurev-marine-120710-100912

Segev, E., Wyche, T. E., Kim, K. H., Petersen, J., Ellebrandt, C., Vlamakis, H., Barteneva, N., et al. (2016). Dynamic metabolic exchange governs a marine algal-bacterial interaction. *Elife* 5:e17473. doi: 10.7554/eLife.17473

Simon, M., and Azam, F. (1989). Protein content and protein synthesis rates of planktonic marine bacteria. *Mar. Ecol. Prog. Ser.* 51, 201–213. doi: 10.3354/meps051201

Simon, M., Grossart, H. P., Schweitzer, B., and Ploug, H. (2002). Microbial ecology of organic aggregates in aquatic ecosystems. *Aquat. Microb. Ecol.* 28, 175–211. doi: 10.3354/ame028175

Smirnova, G. V., Muzyka, N. G., Ushakov, V. Y., Tyulenev, A. V., and Oktyabrsky, O. N. (2015). Extracellular superoxide provokes glutathione efflux from *Escherichia coli* cells. *Res. Microbiol.* 166, 609–617. doi: 10.1016/j.resmic.2015.07.007

Smirnova, G. V., and Oktyabrsky, O. N. (2005). Glutathione in bacteria. *Biochemistry* 70, 1199–1211. doi: 10.1007/s10541-005-0248-3

Soora, M., and Cypionka, H. (2013). Light enhances survival of *Dinoroseobacter shibae* during long-term starvation. *PLoS ONE* 8:e83960. doi: 10.1371/journal.pone.0083960

Stolz, J., and Vielreicher, M. (2003). Tpn1p, the plasma membrane vitamin B6 transporter of *Saccharomyces cerevisiae*. *J. Biol. Chem.* 278, 18990–18996. doi: 10.1074/jbc.M300949200

Stupperich, E., Eisiger, H. J., and Krautler, B. (1988). Diversity of corrinoids in acetogenic bacteria. P-cresolylcobamide from Sporomusa ovata, 5-methoxy-6-methylbenzimidazolylcobamide from *Clostridium formicoaceticum* and vitamin B12 from *Acetobacterium woodii*. *Eur. J. Biochem.* 172, 459–464.

Teeling, H., Fuchs, B. M., Becher, D., Klockow, C., Gardebrecht, A., Bennke, C. M., et al. (2012). Substrate-controlled succession of marine bacterioplankton populations induced by a phytoplankton bloom. *Science* 336, 608–611. doi: 10.1126/science.1218344

Thiel, V., Brinkhoff, T., Dickschat, J. S., Wickel, S., Grunenberg, J., Wagner-Döbler, I., et al. (2010). Identification and biosynthesis of tropone derivatives and sulfur volatiles produced by bacteria of the marine *Roseobacter clade*. *Org. Biomol. Chem.* 8, 234–246. doi: 10.1039/b909133e

Thole, S., Kalhoefer, D., Voget, S., Berger, M., Engelhardt, T., Liesegang, H., et al. (2012). Phaeobacter gallaeciensis genomes from globally opposite locations reveal high similarity of adaptation to surface life. *ISME J.* 6, 2229–2244. doi: 10.1038/ismej.2012.62

Turner, M. F. (1979). Nutrition of some marine microalgae with special reference to vitamin requirements and utilization of nitrogen and carbon sources. *J. Marine Biol. Assoc. UK* 59, 535–552. doi: 10.1017/S0025315400045550

Van de Guchte, M., Penaud, S., Grimaldi, C., Barbe, V., Bryson, K., Nicolas, P., et al. (2006). The complete genome sequence of *Lactobacillus bulgaricus* reveals extensive and ongoing reductive evolution. *Proc. Natl. Acad. Sci. U.S.A.* 103, 9274–9279. doi: 10.1073/pnas.0603024103

Villas-Bôas, S. G., Noel, S., Lane, G. A., Attwood, G., and Cookson, A. (2006). Extracellular metabolomics: a metabolic footprinting approach to assess fiber degradation in complex media. *Anal. Biochem.* 349, 297–305. doi: 10.1016/j.ab.2005.11.019

Wagner-Döbler, I., Baumgart, B., Brinkhoff, T., Buchholz, I., Bunk, B., Cypionka, H., et al. (2010). The complete genome sequence of the algal symbiont *Dinoroseobacter shibae* – a hitchhiker's guide to life in the sea. *ISME J.* 4, 61–77. doi: 10.1038/ismej.2009.94

Waschina, S., D'Souza, G., Kost, C., and Kaleta, C. (2016). Metabolic network architecture and carbon source determine metabolite production costs. *FEBS J.* 283, 2149–2163. doi: 10.1111/febs.13727

Yang, Y., Xu, R., Ma, C., Vlot, A. C., Klessig, D. F., and Pichersky, E. (2008). Inactive methyl indole-3-acetic acid ester can be hydrolyzed and activated by several esterases belonging to the AtMES esterase family of *Arabidopsis*. *Plant Physiol.* 147, 1034–1045. doi: 10.1104/pp.108.118224

Yi, S., Seth, E. C., Men, Y. J., Allen, R. H., Alvarez-Cohen, L., and Taga, M. E. (2012). Versatility in corrinoid salvaging and remodeling pathways supports the corrinoid-dependent metabolism of *Dehalococcoides mccartyi*. *Appl. Environ. Microbiol.* 78, 7745–7752. doi: 10.1128/AEM.02150-12

Young, I. G., Cox, G. B., and Gibson, F. (1967). 2,3-Dihydroxybenzoate as a bacterial growth factor and its route of biosynthesis. *Biochim. Biophys. Acta* 141, 319–331. doi: 10.1016/0304-4165(67)90106-7

Zech, H., Thole, S., Schreiber, K., Kalhöfer, D., Voget, S., Brinkhoff, T., et al. (2009). Growth phase-dependent global protein and metabolite profiles of Phaeobacter gallaeciensis strain DSM 17395, a member of the marine *Roseobacter-clade*. *Proteomics* 9, 3677–3697. doi: 10.1002/pmic.200900120

Zelezniak, A., Andrejev, S., Ponomarova, O. D., Mende, D. R., Bork, P., and Patil, K. R. (2015). Metabolic dependencies drive species co-occurrence in diverse microbial communities. *Proc. Natl. Acad. Sci. U.S.A.* 112, 6449–6454. doi: 10.1073/pnas.1421834112

Zhang, F., Harir, M., Moritz, F., Zhang, J., Witting, M., Wu, Y., et al. (2014). Molecular and structural characterization of dissolved organic matter during and post cyanobacterial bloom in Taihu by combination of NMR spectroscopy and FTICR mass spectrometry. *Water Res.* 57, 280–294. doi: 10.1016/j.watres.2014.02.051

Conflict of Interest Statement: The authors declare that the research was conducted in the absence of any commercial or financial relationships that could be construed as a potential conflict of interest.

frontiers in Marine Science

ORIGINAL RESEARCH
published: 28 August 2018
doi: 10.3389/fmars.2018.00274

The B-Vitamin Mutualism Between the Dinoflagellate *Lingulodinium polyedrum* and the Bacterium *Dinoroseobacter shibae*

Ricardo Cruz-López[1,2*†], *Helmut Maske*[1], *Kyoko Yarimizu*[2] *and Neal A. Holland*[2]

[1] Oceanografía Biológica, Centro de Investigación Científica y de Educación Superior de Ensenada (CICESE), Ensenada, Mexico, [2] Department of Chemistry and Biochemistry, San Diego State University, San Diego, CA, United States

OPEN ACCESS

Edited by:
Stanley Chun Kwan Lau,
Hong Kong University of Science and Technology, Hong Kong

Reviewed by:
Meinhard Simon,
University of Oldenburg, Germany
John Everett Parkinson,
Oregon State University, United States

***Correspondence:**
Ricardo Cruz-López
ricardo.crlp@gmail.com

†Present Address:
Ricardo Cruz-López,
Department of Chemistry and Biochemistry, San Diego State University, San Diego, CA, United States

Specialty section:
This article was submitted to Aquatic Microbiology, a section of the journal Frontiers in Marine Science

Received: 01 March 2018
Accepted: 20 July 2018
Published: 28 August 2018

Citation:
Cruz-López R, Maske H, Yarimizu K and Holland NA (2018) The B-Vitamin Mutualism Between the Dinoflagellate Lingulodinium polyedrum and the Bacterium Dinoroseobacter shibae. Front. Mar. Sci. 5:274. doi: 10.3389/fmars.2018.00274

Recent research has shown that in aquatic systems pairs of prokaryote and eukaryote species exercise symbiotic exchanges of metabolites that are essential for the proliferation of either species. Using dinoflagellate *Lingulodinium polyedrum* cultures and a factorial design, we examined its growth at different concentrations of vitamin B_1 (thiamine) and B_{12} (cobalamin). When both vitamins were at their lowest concentrations tested, 0.033 pM of B_1 and 0.053 pM of B_{12} the growth was limited. When axenic *L. polyedrum* was co-cultured with the bacterium *Dinoroseobacter shibae*, a known B_1 and B_{12} producer, then *L. polyedrum* grew at the same rate as in culture media supplemented with B_1 and B_{12}. In the *L. polyedrum* vitamin—limited culture (V-L), the abundance of attached and free-living *D. shibae* was higher than in the vitamin—replete (V-R) culture. In the V-R and V-L co-cultures the measured particulate B_{12} (pB_{12}) concentration of attached and free-living *D. shibae* were in the range of 4.7×10^{-19} to 3×10^{-18} and 8.4×10^{-21} to1.2×10^{-19} (mol cell^{-1}), respectively. Without B_{12} or B_7 (biotin) added to the culture medium of a co-culture of *L. polyedrum* and *D. shibae*, the measured dissolved B_{12} (dB_{12}) concentration was more than 60 pM higher than necessary for un-limited growth rates *of L. polyedrum*. In the same culture we measured B_7 in the *L. polyedrum* particulate fraction (pB_7; 4.7×10^{-19} to 9.4×10^{-19} mol cell^{-1}). We suggest that in response to the production of B_1 and B_{12} by *D. shibae* to supply *L. polyedrum* requeriments, the latter produced B_7, which is required by *D. shibae*, and in our culture was only produced by *L. polyedrum* when *D. shibae* was present. We propose that *D. shibae* can control *L. polyedrum* through the release of B_1 and B_{12}, and *L. polyedrum* can control *D. shibae* through the release of B_7. *D. shibae* is also auxotroph for niacin and 4-amino-benzoic acid, not provided by the culture medium. Therefore, *L. polyedrum* might affect a similar control through the release of these specific compounds and organic substrate necessary for the growth of *D. shibae*.

Keywords: B vitamin auxotrophy, growth limitation, Dinoflagellate-bacteria interactions, dissolved B_{12}, particulate B_{12}, particulate B_7

INTRODUCTION

Eukaryotic phytoplankton and bacteria have developed a number of interkingdom metabolic interactions. These include growth stimulators (Ferrier et al., 2002), potential toxin inducers (Green et al., 2004, 2006), cyst inducers (Adachi et al., 2003, 2004; Mayali et al., 2007), growth inhibitors (Hare et al., 2005), algicids (Doucette et al., 1999), and chemosensors (Miller et al., 2004). The interactions also include mutualistic trade-off of soluble factors, for example, iron siderophores (Amin et al., 2009) and vitamins (Croft et al., 2005; Wagner-Döbler et al., 2010; Kazamia et al., 2012; Cruz-López and Maske, 2016). B vitamins are essential growth factors for most marine eukaryotic phytoplankton because they are required for the activity of several enzymes in central metabolism. Vitamin B_{12} (cobalamin; hereafter B_{12}) is essential for the biosynthesis of deoxyriboses from riboses, the reduction and transfer of single carbon fragments in many biochemical pathways, porphyrin and methionine biosynthesis, which is dominant in eukaryotic phytoplankton (Tang et al., 2010; Sañudo-Wilhelmy et al., 2014). Vitamin B_1 (thiamin; hereafter B_1) plays a major role for enzymes involved in primary carbon metabolism like the Krebs and Calvin-Benson cycles, and for branch-chain amino acid metabolism, like alanine, leucine and valine (Sañudo-Wilhelmy et al., 2014). Vitamin B_7 (biotin; hereafter B_7) is essential for several carboxylase enzymes, including acetyl coenzyme A (CoA) carboxylase, which is involved in the fatty acid biosynthesis, and pyruvate carboxylase, which catalyzes the first step in gluconeogenesis by converting pyruvate to oxaloacetate, hence universally required (Croft et al., 2006; Tang et al., 2010; Sañudo-Wilhelmy et al., 2014). Many phytoplankton species are natural B vitamin auxotrophs, meaning they lack the biosynthetic pathways to produce B vitamins and thus must acquire them from exogenous sources. Of the phytoplankton surveyed to date, 54% are B12 auxotrophs, 27% are B1 auxotrophs, and 8% are B7 auxotrophs (Croft et al., 2005; Tang et al., 2010). Because these auxotrophs are common in natural waters, they are useful to study to determine the roles that niche partitioning and species succession play in phytoplankton blooms (Helliwell, 2017).

Although B vitamin auxotrophy is not systematically distributed across the algal lineages, in particular, dinoflagellates have evolved obligate dependence on vitamins (Croft et al., 2006; Tang et al., 2010; Helliwell et al., 2011). Dinoflagellates form part of the eukaryotic phytoplankton and contribute significantly to the primary production of coastal areas (Moustafa et al., 2010), many dinoflagellates form blooms that can represent a potential threat to coastal ecosystems, public health, economies, and fisheries (Tang et al., 2010). Tang et al. (2010) reported that of the surveyed dinoflagellate species that are involved in harmful algal bloom events, 100% required B_{12}, 78% required B_1 and 32% B_7.

Recent culture studies showed that for auxotrophic dinoflagellates a minimum of 2×10^{-5}-5×10^{-4} pM of B_{12} and from 1.4×10^{-11} to 0.55×10^{-6} nM of B_1 are required for growth (Tang et al., 2010). These concentrations are typically found in coastal waters where dinoflagellates thrive (Gobler et al., 2007; Panzeca et al., 2009; Sañudo-Wilhelmy et al., 2012). During bloom conditions, the B_1 and B_{12} concentrations are variable, from 5 to 20 pM for both vitamins; these concentrations should be sufficient to support dinoflagellate growth (Gobler et al., 2007; Koch et al., 2011).

Most experimental physiology studies related to vitamins have focused on single-vitamin limitation, for example, the role of B_{12} at different concentrations (reviewed in Droop, 2007; Tang et al., 2010). Droop (1974) found threshold type limitation for phosphate and B_{12} in phytoplankton cultures. Other authors have reported concurrent limitation of vitamins with nitrogen (Gobler et al., 2007; Koch et al., 2011; Bertrand and Allen, 2012), iron (Panzeca et al., 2006; Bertrand et al., 2007, 2011; Koch et al., 2011) or CO_2 (King et al., 2011). Although Panzeca et al. (2006), reported primary and secondary production limitation by Fe, B_1, and B_{12} in coastal communities off the Antarctic, they did not investigate the potential for co-limitation of B_{12} with other essential vitamins.

Heterotrophic bacteria, archaea, and marine cyanobacteria are the only known source of B vitamins (Bonnet et al., 2010; Sañudo-Wilhelmy et al., 2014; Doxey et al., 2015), although, in early studies, some phytoplankton species have also been reported to produce B vitamins (Bednar and Holm-Hansen, 1964; Carlucci and Bowes, 1970a,b; Aaronson et al., 1971, 1977). Hence dinoflagellates would have to acquire their B vitamin from the environment either through phagotrophy (Jeong et al., 2005), active uptake from the dissolved fraction (Bertrand et al., 2007; Tang et al., 2010; Kazamia et al., 2012), or episymbiosis (Croft et al., 2005; Wagner-Döbler et al., 2010; Kazamia et al., 2012; Kuo and Lin, 2013; Xie et al., 2013; Cruz-López and Maske, 2016). Little is known currently about the relative contribution of these different mechanisms to acquire the different vitamins by auxotrophic dinoflagellates.

Previously we reported *Lingulodinium polyedrum* vitamin auxotrophy for B_1 and B_{12} (Cruz-López and Maske, 2016), where a high concentration of one vitamin cannot overcome the lack of the other. This research left several questions open: At very low, ecologically relevant concentrations of both vitamins, can increasing the concentration of one support increased algal growth without an increase the in the other vitamin? Also, what is provided by the dinoflagellate to the bacteria in exchange for the necessary B-vitamins? Here we report the effect of vitamin B_1 and B_{12} under multiple vitamin concentrations on growth rate. We also report the B_7 and B_{12} cellular quotas for *L. polyedrum* in co-culture with the bacterium *Dinoroseobacter shibae*, a well-known B_1 and B_{12} producing bacterium. Differently from our previous work concerning a co-culture of *L. polyedrum* with a bacterial community, the present work did not include auxotrophic bacteria that could compete with *L. polyedrum* for B_1 and B_{12}.

MATERIALS AND METHODS

L. polyedrum Growth Conditions

Oceanic seawater was collected off Ensenada (31.671°N, 116.693°W; Ensenada, México) treated with activated charcoal, filtered through GF/F, and 0.22-mm pore-size cartridge filter (Pall Corporation) and stored in the dark at room temperature to age for at least 2 months. Aged seawater was sparged with CO_2 (5 min per 1 L of seawater), autoclaved for 15 min and

then equilibrated with air. *L. polyedrum* strain was isolated from Venice beach California and kindly provided by Avery Tatters (University of Southern California). Xenic *L. polyedrum* culture was grown in L1 medium (National Center for Marine Algae and Microbiota, NCMA, Maine, USA) prepared with aged oceanic water under 12:12 h light/dark cycle at an irradiance of 100 μmol m^2 s^{-1}, and a temperature of 20°C. To make the culture axenic, *L. polyedrum* culture was incubated with 1 mL of antibiotic solution (Penicillin, 5,000 U; Streptomycin, 5 mg mL^{-1}; Neomycin, 10 mg mL^{-1}. Sigma-Aldrich, P4083-100ML) for 50 mL of culture during 24 h, rinsed with the L1 medium, and repeated three times each step. Bacterial presence in the *L. polyedrum* culture was checked by staining with the nucleic acid-specific stain 4′,6-diamino-2-phenylindole (DAPI,1 μg mL^{-1}) and quantification using epifluorescence microscopy (Axioskope II plus, Carl Zeiss, Oberkochen, Germany) connected by liquid light guide to a 175W xenon arc lamp (Lambda LS, Sutter), with optical filtering (Excitation, 360 nm/Dichroic, 395 nm/Emission, >397 nm; Semrock & Zeiss) under X100 objective lens (Plan-Apochromat, Carl Zeiss). The axenic status was documented after three antibiotic rounds, and sterile medium washes when we could not detect bacteria in the culture using epifluorescence microscopy.

Assessment of *L. polyedrum* Vitamin B_1 and B_{12} Limiting Concentrations

To test the vitamin B_1 and B_{12} limiting concentrations of *L. polyedrum*, cultures were grown in 50 mL cell culture flasks (BD Falcon™). Cultures were acclimated by six semi-continuous transfers during 6 weeks with an initial cell concentration of 1,300 cell L^{-1}. The medium for *L. polyedrum* axenic cultures was supplemented with L1 and B_1, B_{12} vitamins (Sigma-Aldrich) using a factorial experimental design combining 1) two vitamins ($B_1 + B_{12}$) and five vitamin concentrations ranging from 3.33×10^{-2} to 3.33×10^{1} pM of B_1 and 5.25×10^{-2} to 5.25×10^{1} pM of B_{12} (**Table 1**). After acclimation, each culture and corresponding vitamin amendment were transferred and grown in 15 mL glass test tubes with silicon stoppers ($n = 3$) and placed randomly in transparent test tube holders to minimize bias in the data due to a heterogeneous light field in the incubator or shading by other cultures tubes. Cell growth rate was monitored by first mixing the cultures with an inclined rotating test tube holder (10 rpm) and then measuring *in vivo* Chlorophyll *a* (Chl *a*) fluorescence using a Turner Designs 10-000 fluorometer at the midpoint of the light phase. The specific growth rate (μ) was calculated according to the equation $\mu = \ln(N2/N1)/(t2-t1)$: where N1 and N2 was *in vivo* Chl *a* fluorescence in relative units (r. u.) at time 1 (t1) and time 2 (t2), respectively. To calculate μ, we used the data obtained during the exponential phase of each growth curve on days 8, 10 and 12 after inoculation. *in vivo* Chl *a* fluorescence and cell counts were well correlated (**Figure S1**, $r^2 = 0.98$). The specific growth rate was adjusted to a Monod-type model of specific growth rate vs. the initial B_1 and B_{12} concentrations in the bioassays. A least square estimate of a Michaelis-Menten type kinetic was calculated with the PRISM 6.07v software (GraphPad, CA, USA).

TABLE 1 | Half-saturation constants (*K*s) and maximum specific growth rates (μ) of *L. polyedrum* for B_1 and B_{12} amendments.

B_{12} (pM)	*K*max (B_1 pM)	K_s (B_1 pM)	μ max (d^{-1})	R^2
0.0526	3.3	0.60	0.17 ± 0.018	0.72
0.526	3.3	1.02	0.2 ± 0.016	0.88
5.26	3.3	0.14	0.11 ± 0.021	0.15
52.6	3.3	0.75	0.16 ± 0.017	0.75

Dinoflagellate-Bacterial Co-culture

The axenic bacterium culture *D. shibae* DFL-12^T (NCMA, Maine, USA) was grown in oceanic seawater supplemented with yeast extract (2 g L^{-1}) and peptone (1.25 g L^{-1}). The co-culture was started by inoculating *D. shibae* cells to a final concentration of 10^6 cells mL^{-1} of an axenic, early exponential phase *L. polyedrum* culture in the L1 medium that was $B_1B_7B_{12}$-supplemented (hereafter vitamin-replete, V-R) or $B_1B_7B_{12}$ non-supplemented (hereafter vitamin-limited, V-L) medium and incubated under 12:12 h light/dark cycle, irradiance of 100 μmol m^2 s^{-1}, and a temperature of 20°C. The cultures were transferred weekly to fresh L1 medium at a ratio of 1:10 during 4 weeks before the experiment.

Sampling and Cell Fixation

All cultures were monitored for 15 d, and sampled every 2 days for cell counting by light microscopy. One milliliter of *L. polyedrum* cells from V-R and V-L cultures were harvested at lag (d2), exponential (d8) and stationary (d15) phase and fixed with paraformaldehyde-PBS at a final concentration of 1% for 12 h at 4°C. For attached bacteria, fixed cells were immobilized onto an 8.0 μm pore size, 25 mm-diameter Nucleopore filters (Whatman International, Ltd., Maidstone, England), and rinsed with phosphate-buffered saline (PBS, 0.1 M NaCl, 2 mM KCl, 4 mM Na_2HPO_4, pH 8.1; Palacios and Marín, 2008). For free-living bacteria, the fraction which passed through an 8.0 μm pore size filter was collected on 0.2 μm pore size, 25 mm-diameter Nucleopore filters (Whatman International, Ltd., Maidstone, England) and rinsed with PBS. The cells collected on the 8.0 μm filter were covered with 13 μL of low-melting-point agarose (0.05%, LMA) (BioRad, 161-3111) at 55°C, dried for 15 min at 37°C, then LMA was added again and the filter dried as previously. For all filtration steps, the pressure difference was <3.3 kPa to minimize cell damage.

Visual Observations

To visualize *D. shibae* cells attached to *L. polyedrum* cells, we used an epifluorescence microscope (Axioskope II plus, Carl Zeiss, Oberkochen, Germany; oil immersion X100 objective, Plan-Apochromat, Carl Zeiss; 175W xenon arc lamp; Lambda LS, Sutter connected through a liquid light guide) with a triple Sedat filter, a dichroic filter with three transmission bands. Excitation and emission spectra were controlled by filter wheels (Lambda 10-3, Sutter). Images were captured with a cooled CCD camera (Clara E, Andor) with 10 ms integration time. Optical stacks,

2.0 μm focal distance between images, were acquired with a computer controlled focusing stage (Focus Drive, Ludl Electronic Products, Hawthorne, NY, USA) and Micro-Manager (version 1.3.40, Vale Lab, UCSF) that controlled the filter selection and the focusing stage. The images were processed in ImageJ (Schneider et al., 2012).

Quantification of Dissolved and Particulate B_{12} (dB_{12}, pB_{12})

For quantification of dB_{12} and pB_{12} we prepared four different fractions: 20 mL of *L. polyedrum* cells from V-R and V-L cultures were harvested at time zero, mid-exponential and stationary phase ($n = 3$). These samples were (a) pre-filtered (8.0 μm pore size, 25 mm-diameter Nuclepore filters) to harvest the fraction of pB_{12} of the *L. polyedrum* and attached *D. shibae*; (b) The filtrate of (a) was filtered again (0.4 μm pore size, 25 mm-diameter polycarbonate filter (Whatman International, Ltd., Maidstone, England) to recover the free-living *D. shibae* fraction. (c) The first filter (a) containing the *L. polyedrum* cells with attached *D. shibae* were treated with 10 mM N-acetyl cysteine (NAC; Sigma) (PBS−0.2 μM calcium chloride, 0.5 mM magnesium chloride, 15 mM glucose) for 1 h with agitation (70 rpm) at room temperature to detach adhered bacteria (Barr et al., 2013). Filtering this sample again with 0.8 μm collected *L. polyedrum*, cells without attached *D. shibae*. (d) The detached *D. shibae* cells were collected onto a 0.4 μm pore size, 25 mm-diameter polycarbonate filter.

Vitamin B_{12} was quantified by Enzyme-Linked Immunosorbent Assay, ELISA (Immunolab GmbH, B12-E01. Kassel, Germany) according to Zhu et al. (2011). These authors tested the ELISA with seawater samples and found close to 100 percent recovery of cyanocobalamin, methylcobalamin, hydroxycobalamin and coenzyme B_{12}, but the method cannot distinguish between these different forms of B_{12}.

For dB_{12}, the filtered sample (0.2 μm) was pre-concentrated by solid phase (RP-C18) extraction according to Okbamichael and Sañudo-Wilhelmy (2004); the column was eluted with 5 mL methanol, the methanol was evaporated at 60°C with low vacuum, the sediment dissolved in ddH_20 with a final volume of 1.5 mL, and 50 μL of the concentrate was injected into the ELISA well plate for quantification. Villegas-Mendoza et al. (in preparation) report a recovery efficiency of 85 percent using the above method for dissolved B_{12}.

For the pB_{12}, filters were cut for easier disintegration and transferred to bead beating tubes using 0.5 mm zirconia beads (biospec.com) with 1 mL of methanol (10:1 methanol:beads). Bead beating was conducted for 5 min followed by 5 min at −20°C, and repeated twice. The tubes were centrifuged at 5,000 rpm for 10 min and the supernatant transferred to a fresh tube. The methanol was evaporated at 60°C with vacuum, the sediment dissolved in ddH_20 with a final volume of 1.5 mL, and 50 μL of the concentrate was injected into the ELISA well plate for quantification.

Quantification of Particulate B_7 (pB_7)

The samples were prepared for the solid extraction method described in Suffridge et al. (2017), with a slight modification. One hundred milliliters of axenic *L. polyedrum* culture ($n = 3$) was harvested at exponential phase using 8.0 μm pore size, 25 mm-diameter Nuclepore filters (Whatman International, Ltd. Maidstone, England). 100 mL of *L. polyedrum* + *D. shibae* culture ($n = 3$) was harvested at mid-exponential phase, and pre-filtered (a) to harvest the fraction of particulate B_7 of the *L. polyedrum* and attached *D. shibae* using 8.0 μm pore size, 25 mm-diameter Nuclepore filter; (b) to collect the free-living *D. shibae* fraction the filtrate from (a) was filtered with 0.4 μm pore size, 25 mm-diameter polycarbonate filter (Whatman International, Ltd., Maidstone, England). The first filter (a) containing *L. polyedrum* cells with attached *D. shibae* was rinsed with 10 mL of Milli-Q water to detach adhered *D. shibae*. (c) Filtering this fraction again through 0.8 μm collected *L. polyedrum* cells without attached *D. shibae*. (d) The detached *D. shibae* cells passing through 8.0 μm filter were collected onto a 0.4 μm pore size, 25 mm-diameter polycarbonate filter.

Frozen filters containing the different fractions mentioned above were processed according to Suffridge et al. (2017) with slight modifications. In brief, frozen filters were placed in an autoclaved 1.5 mL Eppendorf tube with 1 mL of diluent (50% LC-MS grade acetonitrile, 50% water, 0.1% formic acid). The cells were lysed by repeated vortexing for 5 min followed by 1 min cooling on ice for a total period of 30 min. The cells were further sonicated for 5 min. The cell lysate was passed through 0.2 μm pore size, 25 mm-diameter polycarbonate filter (Whatman International, Ltd, Maidstone, England) to remove large particles and cell debris. The filters were washed with 0.5 mL of diluent to collect residual cell metabolites. An equal volume of chloroform was added to the filtrate; the mix was vigorously shaken for 1 min and then centrifuged for liquid phase extraction. The top aqueous phase was transferred to a new Eppendorf tube. The liquid phase extraction with chloroform was repeated twice. The residual aqueous phase was adjusted to 300–500 μL with the diluent, and then the sample was injected in triplicate in a LC-MS (Applied Biosystems API4000 SCIEX) for pB_7 quantification. To obtain the efficiency of recovery, 100 ng mL^{-1} of B_7 standard (Sigma-Aldrich-B4501) was added to three different samples.

D. shibae Frequency of Attachment on *L. polyedrum*

The frequency was established using the co-culture in exponential phase with modifications as follows: An initial V-R ($V\text{-}R_0$) culture was followed for 15 d, then, the culture was transferred weakly to fresh L1 medium under semi-continuous culture conditions during 4 weeks; each consecutive culture was termed $V\text{-}R_1$, $V\text{-}R_2$, and $V\text{-}R_3$. A parallel culture was started from the $V\text{-}R_0$ culture under V-L conditions, this was termed $V\text{-}L_0$, then the culture was transferred to a second V-L condition, and termed $V\text{-}L_1$, and for the next transferred, add-back to a V-R condition, and termed $V\text{-}L_1$ to $V\text{-}R_{1'}$. In each culture, a sample at mid-exponential phase was taken, and processed as described in *Sampling and cell fixation*, and *Visual observations*.

Statistical Analysis

One-way ANOVA was used to compare the specific growth rate during exponential phase at day 8 of *L. polyedrum* under V-R vs. V-L cultures, to compare the dB_{12} in V-R vs. V-L cultures,

and to compare pB_{12} from attached and free-living *D. shibae* at lag, exponential and stationary phase. Since the distribution of the number of attached *D. shibae* on *L. polyedrum* cell had no Gaussian distribution, we used a Mann–Whitney test to assess the significance of the number of attached bacteria on *L. polyedrum* during mid-exponential phase at day 8. All analysis were performed using STATISTICA 7.1v software (Stat Soft Inc., USA).

RESULTS

Quantitative Vitamin B_1 and B_{12} Requirements

L. polyedrum has recently been shown to be vitamin B_1 and B_{12} auxotroph but not to be B_7 auxotroph (Cruz-López and Maske, 2016), following the pattern of the majority of the examined dinoflagellate species requiring these two vitamins (Tang et al., 2010). In a new set of batch culture experiments, we explored the growth limiting concentrations for this species using a factorial design for both vitamins. In these experiments, cultures exhibited a μ_{max} of 0.18 ± 0.003 d^{-1} ($n = 3$) in the ranges of 0.33–3.3 pM for B_1, and 0.053–0.53 pM for B_{12} (**Figure 1**). Vitamin half-saturation constants (*Ks*) for μ_{max} were 3.3 pM for B_1, and 0.53 pM for B_{12} (**Table 1**). Growth rates and biomass were strongly dependent on both vitamins and did not grow at concentrations of 0.033 and 0.053 pM of B_1 and B_{12}, respectively (**Tables S1, S2**).

dB_{12} and Cell Quotas of *L. polyedrum* and *D. shibae*

Dissolved B_{12} varied between cultures. During the lag phase, in the V-R culture, dB_{12} was 42.7 (±1.8) pM, whereas in the V-L culture dB_{12} was 29.9 (±5.3) pM. In exponential phase, in the V-R culture the dB_{12} was 43.1 (±8.6) pM, and in the V-L 65.3 (±24.3) pM (**Table 1**). During stationary phase, in the V-R culture dB_{12} was 37.6 (±3.1) pM, and in the V-L culture 372 (±2.4) pM. The dB_{12} was higher during lag phase in the V-R than the V-L culture, dB_{12} concentration in the V-R and V-L cultures were similar during stationary phase, but unexpectedly during exponential phase, the dB_{12} in the V-R culture was much lower than in the V-L culture.

The B_{12} cell quotas (mol $cell^{-1}$) of *L. polyedrum*, attached and free-living *D. shibae* were calculated by dividing the pB_{12} concentration by cell abundance. Samples were taken at the lag, exponential and stationary phase of the V-R and V-L cultures. For *L. polyedrum*, during the lag phase, in the V-R and V-L culture, the pB_{12} were both the same, 2.7×10^{-17} mol $cell^{-1}$, respectively (**Table 2**). During the exponential phase, in the V-R and V-L cultures, the cell quotas were similar at 8.9×10^{-18} ($\pm 1.05 \times 10^{-18}$) and 9.9×10^{-18} ($\pm 1.1 \times 10^{-18}$) mol $cell^{-1}$, decreasing during the stationary phase to 5.8×10^{-18} ($\pm 5.6 \times 10^{-19}$) and 5.0×10^{-18} ($\pm 7.1 \times 10^{-19}$) mol $cell^{-1}$ in V-R and V-L cultures, respectively. The cell quotas of *L. polyedrum* in both types of culture were similar

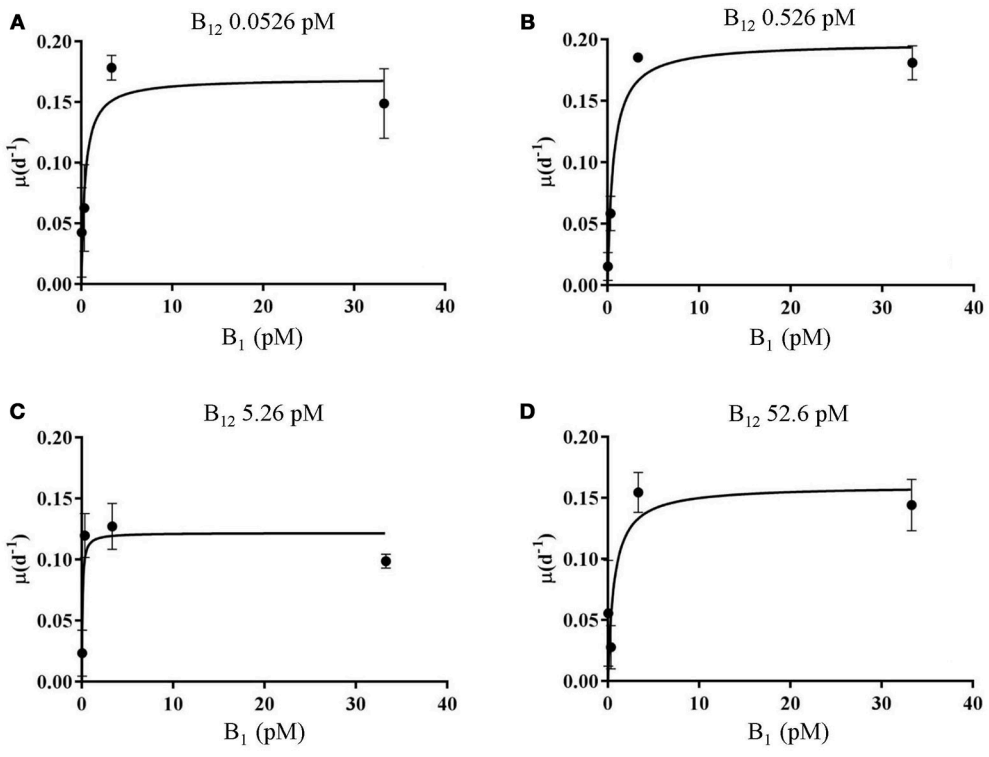

FIGURE 1 | Vitamin B_1 vs. B_{12} growth kinetics curve for *L. polyedrum*. The data plotted are from 16 ($n = 3$) independent experiments. *L. polyedrum* growth under **(A)** 0.0526, **(B)** 0.526, **(C)** 5.26, **(D)** 52.6 pM of B_{12}, and 0.0333, 0.333, 3.33, and 33.3 pM of B_1. Error bars represented one standard deviation ($n = 3$). A hyperbolic Michaelis–Menten model is plotted, *K*s and μmax are summarized in **Table 1**.

TABLE 2 | Dissolved and B_{12} quotas expressed per cell (mol cell^{-1}) for *L. polyedrum* and *D. shibae* in co-culture.

		B_{12} dissolved (pM)			B_{12} per cell (mol cell $^{-1}$)		
		Lag ($n = 4$)	Exp ($n = 4$)	Stat ($n = 4$)	Lag ($n = 1$)	Exp ($n = 3$)	Stat ($n = 3$)
L. polyedrum	V-R	62.9 (±40.4)	43 (±8.63)	37.6 (±3.15)	2.71×10^{-17}	8.9×10^{-18} ($\pm 1.05 \times 10^{-18}$)	5.8×10^{-18} ($\pm 5.6 \times 10^{-19}$)
	V-L	26.9 (±5.3)	65.3 (± 24.31)	37.2 (±2.43)	2.72×10^{-17}	10×10^{-18} ($\pm 1.06 \times 10^{-18}$)	5×10^{-18} ($\pm 7.1 \times 10^{-19}$)
D. shibae - free-living	V-R				1.2×10^{-19}	6.5×10^{-20} ($\pm 1.7 \times 10^{-20}$)	1.6×10^{-20} (2×10^{-21})
	V-L				9.7×10^{-20}	2.9×10^{-20} ($\pm 3.2 \times 10^{-21}$)	8.4×10^{-21} (3.3×10^{-22})
D. shibae - attached	V-R				3.1×10^{-18}	5.9×10^{-19} ($\pm 1.3 \times 10^{-19}$)	4.8×10^{-19} ($\pm 1.3 \times 10^{-20}$)
	V-L				3×10^{-18}	5.2×10^{-19} ($\pm 4.4 \times 10^{-20}$)	4.7×10^{-19} ($\pm 9.2 \times 10^{-22}$)

V-R,vitamin-replete; V-L, vitamin-limited. Lag, Lag phase; Exp, exponential phase; Stat, stationary phase.

TABLE 3 | B_7 quotas expressed per cell (mol cell^{-1}) for axenic *L. polyedrum* and with *D. shibae* in co-culture.

		B_7 per cell (mol cell^{-1})
		Exp
L. polyedrum	ax	b. l. d.
L. polyedrum	ax	b. l. d.
L. polyedrum	xe	4.74×10^{-19}
L. polyedrum	xe	9.41×10^{-19}
D. shibae—free-living	xe	b. l. d.
D. shibae—free-living	xe	b. l. d.
D. shibae—attached	xe	1.71×10^{-19}
D. shibae—attached	xe	1.89×10^{-19}

B_7 per cell (mol cell^{-1}). Axenic (ax), xenic (xe), below limit of detection (b. l. d.)

and showed maximum dB_{12} concentrations during exponential phase.

For free-living *D. shibae*, the estimates for the lag, exponential and stationary phase in the V-R culture, cell quotas were 1.2×10^{-19}, 6.5×10^{-20} ($\pm 1.7 \times 10^{-20}$) and 1.6×10^{-20} (2.1×10^{-21}), and for the V-L culture, they were 9.7×10^{-20}, 2.9×10^{-20} ($\pm 3.2 \times 10^{-21}$) and 8.5×10^{-21} (3.3×10^{-22}) mol cell^{-1}. For the attached *D. shibae*, the estimates for the lag, exponential and stationary phase in V-R culture were 3.1×10^{-18}, 5.9×10^{-19} ($\pm 1.3 \times 10^{-19}$) and 4.9×10^{-19} ($\pm 1.3 \times 10^{-20}$) mol cell^{-1}, and for the V-L culture were 3.0×10^{-18}, 5.3×10^{-19} ($\pm 4.4 \times 10^{-20}$), 4.7×10^{-19} ($\pm 9.2 \times 10^{-22}$) mol cell^{-1}. The *D. shibae* B_{12} cell quotas of attached *D. shibae* were always much higher than those for free-living *D. shibae* by a factor 10 to 55 (**Table 2**).

B_7 Cell Quotas of *L. polyedrum* and *D. shibae*

We could not detect pB_7 in *L. polyedrum* axenic cultures, while in the xenic culture; *L. polyedrum* contained an average of 7.07×10^{-19} mol cell^{-1} of B_7. As reported previously, *D. shibae* can thrive in two phenotypes, in attached mode or free-living; when we tried to quantify the free-living fraction, we could not detect any trace of pB_7, whereas, in the attached fraction, we quantified an average of 1.8×10^{-19} ($n = 2$) mol cell^{-1} (**Table 3**).

D. shibae Frequency of Attachment on *L. polyedrum*

We quantified the attachment of *D. shibae* to *L. polyedrum* cells by counting microscopically the number of attached bacteria to each *L. polyedrum* cell. Because 100 *L. polyedrum* cells were observed the frequency of bacteria per host cell in **Figure 2** gives the relative frequency in percent. **Figure 2** shows that in the V-R culture the average number of *D. shibae* bound to *L. polyedrum* was lower, compared with the V-L culture ($p < 0.05$, Mann-Whitney). In addition, the abundance of free-living *D. shibae* in the V-R culture was lower than in the V-L culture (**Figure 3**; $p < 0.05$, ANOVA).

DISCUSSION

Limiting Concentrations of B_1 and B_{12}

Our results show that B_1 and B_{12} at the lowest concentrations tested limited the growth rate of *L. polyedrum*. The *L. polyedrum* strain examined in this study must possess high-affinity uptake systems for B_1 and B_{12} to explain their low *K*s values (**Table 1**). Our *K*s estimate for B_{12} of 0.53 pM is in the range of values reported by Tang et al. (2010; **Table 2**) for six different phytoplankton species including two dinoflagellate species reported to have the lowest (0.02 pM) and highest *K*s values (13.1 pM) for B_{12} in the list. Our *K*s estimate for B_1 of 3.3 pM is lower than the values reported by Tang et al. (2010; **Table 2**) for five species. In their list, the values of the three dinoflagellates ranged from 86 to 131 pM.

The uptake of B_1 and B_{12} by phytoplankton communities has been documented in coastal areas (Gobler et al., 2007; Koch et al., 2011, 2012), but the potential for colimitation of B_1 and B_{12} has not been reported. Given the slow growth rate of dinoflagellates, it is difficult to imagine that traditional bioassay experiments with natural populations probing vitamin limitation would yield conclusive results for dinoflagellates. But concurrent limitation of vitamins with other compounds have been reported (Panzeca et al., 2006; Bertrand et al., 2007, 2011; Gobler et al., 2007; King et al., 2011; Koch et al., 2011; Bertrand and Allen, 2012).

The limiting concentrations of B_1 and B_{12} supporting maximum growth rates of *L. polyedrum* can be compared with measured *in situ* concentrations. In coastal systems dB_{12} ranges from undetectable to 87 pM (Sañudo-Wilhelmy et al., 2006, 2012; Panzeca et al., 2009) and for dB_1 from undetectable to 200 pM

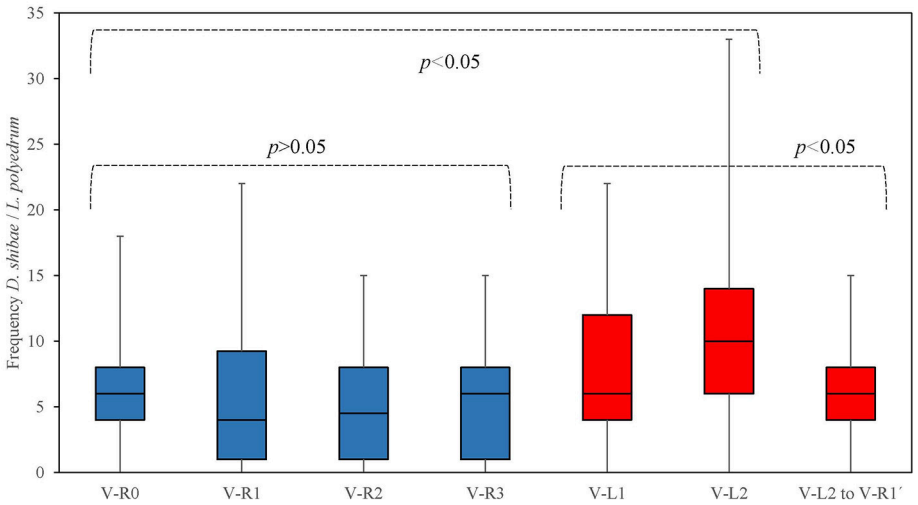

FIGURE 2 | Frequency of *D. shibae* cells attached to single *L. polyedrum* cell in semi-continuous culture conditions. *L. polyedrum* in V-R culture (■), and V-L culture (■).

(Gobler et al., 2007; Koch et al., 2012, 2013; Sañudo-Wilhelmy et al., 2012; Suffridge et al., 2017). This comparison suggests that B_1 or B_{12} might limit the growth rate of *L. polyedrum* during certain stages of bloom formation. Koch et al. (2014), measured dissolved B_1 and B_{12} concentrations inside and outside of dinoflagellate blooms, and found concentrations higher than the limiting concentrations reported in our study. They also reported that vitamin concentrations inside dinoflagellate blooms were lower than outside of blooms, which pointed to active uptake and the possibility of vitamin limitation. Further field data will have to show if the dinoflagellate bloom development can be limited by vitamin availability in coastal waters that are less eutrophic than their study area.

L. polyedrum and *D. shibae* Co-culture

Our experiments were planned after having shown B_1 and B_{12} auxotrophy of *L. polyedrum*, including experimental evidence that co-cultured bacterial communities could overcome the vitamin limitation without supplying the bacteria with additional organic substrate in the culture medium (Cruz-López and Maske, 2016). Our previous experimental approach could not separate the vitamin auxotrophy of part of the bacterial community from the auxotrophy of *L. polyedrum*. In a new set of experiments, we co-cultured *L. polyedrum* with *D. shibae*, a bacterium reported to produce B_1 and B_{12} (Wagner-Döbler et al., 2010). *D. shibae* has been shown to be B_7 auxotroph (Biebl et al., 2005; Wang et al., 2014a) which combined well with *L. polyedrum* that was shown not to be B_7 auxotroph (Cruz-López and Maske, 2016).

In the co-cultures, we calculated B_{12} cell quotas based on pB_{12} and cell abundances for *L. polyedrum* ranging from 5×10^{-18} to 2×10^{-17} mol cell^{-1} (**Table 2**). These cell quotas are comparable to 4×10^{-22} and 1.7×10^{-18}, the values reported for dinoflagellates by Tang et al. (2010; **Table 2**). Our measured cell quotas show between one and two orders higher cellular B_{12} content for *L. polyedrum* than for both types of *D. shibae* phenotypes, attached and free-living. In our results, *L. polyedrum* had lower *K*s but higher cell quotas compared with other dinoflagellate species (Tang et al., 2010); the former might provide an ecological advantage to *L. polyedrum* or partially compensate for the disadvantage of a high cell quota. The cell quota concentrations based on cell volumes are 2–3 orders of magnitude lower for *L. polyedrum* cells than for *D. shibae* cells (**Table 1**). Panzeca et al. (2009) quantified the concentration of B_{12} during a *L. polyedrum* bloom in a coastal, ranging from 2 to 61 pM, concentrations that should not be limiting for *L. polyedrum*. *L. polyedrum* abundance was not quantified at the time of B_{12} measurements, but at nearby locations at a later date the abundance was shown to be high, ranging from 1×10^6 to 6×10^6 (cell L^{-1}) (Peña-Manjarrez et al., 2009).

According to Croft et al. (2005), a minimum of 10 ng L^{-1} of B_{12} is required for growth in culture by most phytoplankton species, while Tang et al. (2010) showed that HAB species need higher concentrations than non-bloom forming species. Most of the B_{12} quantification in the field or in culture studies measured the dissolved form, and only few studies related to dinoflagellates in the field (Carlucci, 1970; Gobler et al., 2007; Panzeca et al., 2009) or in cultures (Croft et al., 2005; Tang et al., 2010; Cruz-López and Maske, 2016). Recently Suffridge et al. (2017), quantified the particulate fraction for several B-type vitamins in the field and cultured marine bacteria, given previous cell quotas for marine phytoplankton or heterotrophic bacteria are based on uptake rates (reviewed in Droop, 2003; Bonnet et al., 2010).

To quantify the B_{12} in the different fractions, we used a highly sensitive enzyme-linked immunosorbent assay (ELISA) able to recognize all B_{12} forms (cyanocobalamin, methylcobalamin, hydroxocobalamin, and coenzyme B_{12}), but unable to distinguish them individually. The cyanocobalamin produced by *D. shibae* can be used directly by the algal auxotroph without post-modifications (Helliwell et al., 2016). A likely explanation for our co-culture experimental results is that

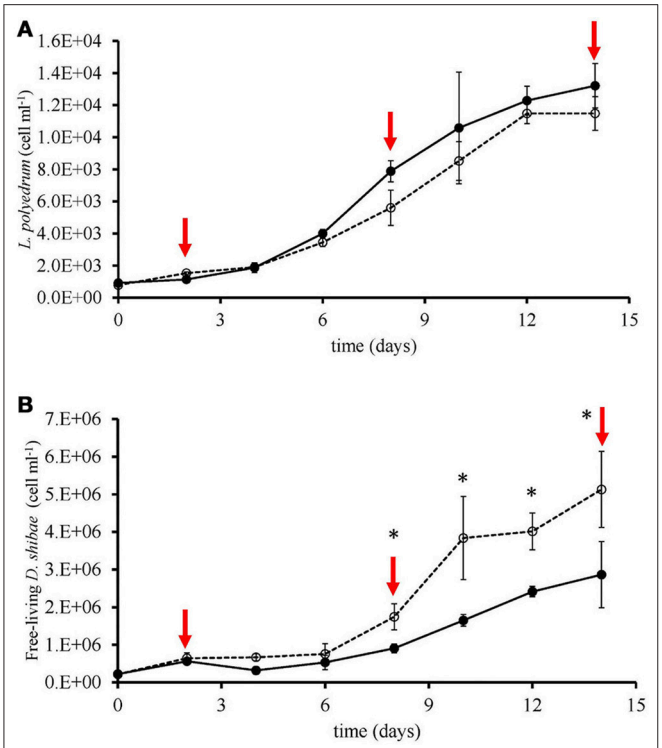

FIGURE 3 | Growth of *L. polyedrum* and *D. shibae* under V-R (-•-) and V-L (-○-) cultures. **(A)** *L. polyedrum* abundance; red arrows denoted time-points of sampling. **(B)** Free-living *D. shibae* abundance. *$p < 0.05$ (ANOVA).

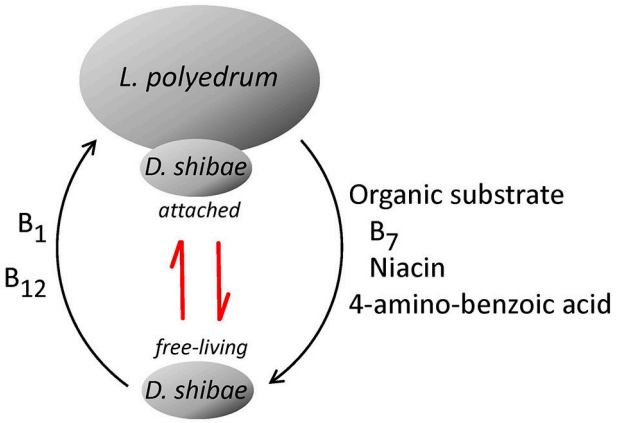

FIGURE 4 | Proposed mutualism of *L. polyedrum* and *D. shibae*. Depending on the degree of B_1 and B_{12} limitation *L. polyedrum* liberates growth promoters for *D. shibae*, for example, B_7, niacin and 4-amino-benzoic acid. *D. shibae* responds with an increased tendency to attach to *L. polyedrum* cells and to produce B_1 and B_{12}. The red arrows indicate the kinetic between free-living and attached lifestyle of *D. shibae* based on the dissolved pool of B_1 and B_{12}.

L. polyedrum acquired B_1 and B_{12} vitamins from *D. shibae* in sufficient quantity to sustain the maximum growth over many generations; however, it had not been shown what *D. shibae* receives in return from *L. polyedrum*. For *D. shibae* to grow together with *L. polyedrum*, it would need organic substrate for biomass formation but in addition also specific compounds because *D. shibae* is auxotroph for B_7, niacin and 4-amino-benzoic acid (Biebl et al., 2005). The production and release of niacin and 4-amino-benzoic acid by a dinoflagellate host was previously suggested by Wagner-Döbler et al. (2010) and Wang et al. (2014a) to explain their co-cultures of *Prorocentrum minimum* CCMP1329 with *D. shibae* in medium lacking B_{12} or any of the other essential vitamins mentioned above. However, the dinoflagellate *P. minimum* CCMP1329 is B_7 auxotroph (Wagner-Döbler et al., 2010) and therefore B_7 had to be supplied to the medium. In the case of *L. polyedrum*, B_7 is not required (Cruz-López and Maske, 2016) and the culture medium was not supplemented with B_7, niacin or 4-amino-benzoic acid. We assume that these organic growth factors could not be provided by the prepared seawater medium. We suggest that these three compounds were provided by *L. polyedrum* in the form of exudates in sufficient quantity to support the growth of the *D. shibae* population. In return, *L. polyedrum* thus promoted the production of B_1 and B_{12}. Due to technical limitations, we only measured B_7 in the particulate fraction, but not in the dissolved fraction. Future research should quantify B_7, niacin or 4-amino-benzoic acid in the dissolved fraction to better define the mutualistic relationship between *D. shibae* and *L. polyedrum* (**Figure 4**).

On the other hand, the release of B_7 from different phytoplankton species has been documented previously (Bednar and Holm-Hansen, 1964; Carlucci and Bowes, 1970a,b; Aaronson et al., 1971, 1977), cell quotas for dinoflagellates are based on uptake rates (Tang et al., 2010). Our pB_7 results showed no pB_7 in the *L. polyedrum* axenic culture, whereas in co-culture with *D. shibae*, *L. polyedrum* we found from 4.74×10^{-19} to 9.41×10^{-19} mol cell^{-1}. Adjusting to pmol cell^{-1}, our results are in the range (4.74×10^{-7} to 9.41×10^{-7}) for the cell quotas reported for *Gymnodinium instriatum* L3, and two orders of magnitude higher than those reported for *P. minimum* CCMP696 and *P. minimum* PB3 (Tang et al., 2010).

For marine heterotrophic bacteria, the B_7 production has been inferred, based on their available genomes, or *in situ* transcriptional studies (Luo and Moran, 2014; Sañudo-Wilhelmy et al., 2014; Gómez-Consarnau et al., 2018). Among the Roseobacter clade, of the 52 Roseobacter genomes analyzed by Luo and Moran (2014), 30 species were found to be auxotrophs for B_7, including *D. shibae* (Biebl et al., 2005; Wienhausen et al., 2017; Gómez-Consarnau et al., 2018). Of these 30 Roseobacter species, 13 produce B_1 and B_{12}, and 17 only B_{12} (**Table 4**). In the case of *D. shibae* in co-culture with *L. polyedrum*, we could only detect B_7 in the attached *D. shibae* phenotype, with cell quotas ranging from 1.72×10^{-7} to 1.9×10^{-7} pmol cell^{-1}.

In a recent study, Suffridge et al. (2017), developed a method to quantify B-type vitamins in the dissolved and particulate fraction using cultures of marine bacteria. They obtained cell quotas of B_7 for *Synechococcus* strain CC9311 ($9.9 \times 10^{-6} \pm 8.1 \times 10^{-6}$ mol cell^{-1}), and for *Vibrio* AND4 ($2.47 \times 10^{-6} \pm 1.36 \times 10^{-6}$ mol cell^{-1}). In our cultures, surprisingly the free-living

TABLE 4 | Select genes for B-vitamin biosynthesis in 30 B_7 auxotroph *Roseobacter* isolate genomes.

	B_{12}	B_1	Isolation
Rhodobacterales bacterium KLH11	√	√	n. a.
Oceanibulbus indolifex HEL45	√	√	Seawater 10 m depth
Roseobacter denitrificans Och 114	√	√	Coastal marine sediments
Roseobacter litoralis Och 149	√	√	Seaweed
Roseovarius nubinhibens ISM	√	√	Surface seawater
Roseobacter sp. AzwK-3b	√	√	n. a.
Roseovarius sp. 217	√	√	Surface seawater
Roseovarius sp. TM1035	√	√	**Dinoflagellate: *Pfiesteria piscicida***
Oceanicola batsensis HTCC2597	√	√	Seawater 10 m depth
Pelagibaca bermudensis HTCC2601	√	√	Seawater 10 m depth
Octadecabacter arcticus 238	√	√	n. a.
Octadecabacter antarcticus 307	√	√	n. a.
Dinoroseobacter shibae DFL 12	√	√	**Dinoflagellate: *Prorocentrum lima***
Ruegeria sp. TM1040	√	X	**Dinoflagellate: *Pfiesteria piscicida***
Roseobacter sp. GAI101	√	X	n. a.
Rhodobacterales bacterium HTCC2083	√	X	n. a.
Roseobacter sp. R2A57	√	X	Seawater
Sagittula stellata E-37	√	X	Coastal seawater
Thalassiobium sp. R2A62	√	X	n. a.
Loktanella sp. SE62	√	X	decaying *Spartina*
Roseobacter sp. CCS2	√	X	Coastal seawater
Loktanella vestfoldensis SKA53	√	X	Seawater 2–5 m depth
Loktanella vestfoldensis R-9477	√	X	Microbial mat
Oceanicola granulosus HTCC2516	√	X	Seawater 10 m depth
Wenxinia marina HY34	√	X	Marine sediments
Jannaschia sp. CCS1	√	X	Coastal seawater
Maritimibacter alkaliphilus HTCC2654	√	X	Seawater 10 m depth
Roseobacter sp. LE17	√	X	n. a.
Rhodobacterales bacterium HTCC2150	√	X	Coastal seawater
Rhodobacterales bacterium HTCC2255	√	X	Coastal seawater 10 m depth

Presence √, ■; absence X, ■.
B_7, biotin synthase; B_1, thiamine synthase; B_{12}, cobalamin synthase (extracted from Luo and Moran, 2014). Isolation source extracted from www.roseobase.org and https://genome.jgi.doe.gov. n. a., Not available.

D. shibae did not contain pB_7. As was shown by Luo and Moran (2014), the B_7 auxotrophy is a widespread phenomenon among the Roseobacter clade, although this auxotrophy is not always related to a symbiotic lifestyle with phytoplankton, which needs to be clarified with further culture and genomic studies.

D. shibae Frequency of Attachment on *L. polyedrum*

Eukaryotic phytoplankton and heterotrophic bacteria are interacting to fulfill the need for vitamins of the former and the need of excreted organic substrate of the latter. Different modes of exchange of vitamins and organic substrate are possible; vitamin-producing bacterial epibionts can be attached to the vitamin-auxotroph cells, or the vitamin-producing and consuming cells can be freely suspended, and the exchange of the dissolved compounds is maintained by turbulent and molecular diffusion at sufficiently high rates to supply the metabolic demand of the auxotrophs (Croft et al., 2005; Droop, 2007).

We used vitamin-replete and vitamin-limited cultures of *L. polyedrum* to produce contrasting host-bacterial culture conditions assuming that the V-L condition would promote the cellular attachment of bacteria and host. The frequency of *D. shibae* attached to *L. polyedrum* was higher under V-L condition compared to V-R condition (**Figure 2**; **Table S3**; Mann-Whitney, $p < 0.005$). When V-L cultures returned to V-R condition, the frequency of attachment reduced to average abundance. Higher attachment frequency under V-L condition suggests a more intense exchange of metabolites under growth culture conditions where this exchange would be essential to the growth of either population.

Because no carbon substrates were added to the culture medium that could have supported the growth of *D. shibae*, our results suggest that *D. shibae* was able to use dinoflagellate photosynthates as a carbon source in return for supplying the

host with vitamin B_1 and B_{12}. As pointed out above *L. polyedrum* might have provided more specific growth enhancing substrates to *D. shibae*. Although in media without added vitamin *D. shibae* was found to be attached more frequently to *L. polyedrum* cells suggesting a synergy between both species, it leaves the question open about the mechanism of delivery. Vitamin could have either been exchanged in the dissolved form originating from free-living partners or by a more direct exchange of metabolites when both cell types are physically attached. Interestingly, in similar experiments but with a natural community of microbes instead of *D. shibae*, the frequency of attachment of microbes to *L. polyedrum* did not increase but the abundance of free-living bacteria in the co-culture increased (Cruz-López and Maske, 2016). For co-cultures of *L. polyedrum* with bacterial communities, the vitamin exchange and balance is more difficult to analyze because an unknown part of the bacterial community is also B_{12} auxotroph.

During the co-culture of *L. polyedrum* and *D. shibae*, we quantified the free-living and attached *D. shibae* cells in V-R and V-L cultures, and observed that the abundance of free-living *D. shibae* in the V-R culture was lower than in V-L culture (**Figure 3B**; ANOVA, $p > 0.05$), and that *L. polyedrum* in the V-R culture was lightly colonized in comparison with the V-L culture (**Figure 2**; **Table S3**; Mann-Whitney, $p < 0.005$). These two alternative lifestyles of *D. shibae* have been documented before (Biebl et al., 2005; Wagner-Döbler et al., 2010; Wang et al., 2014a), and are controlled by quorum sensing (QS) *via* CtrA signal transduction protein (Patzel et al., 2013; Wang et al., 2014b). Note, however, that increased bacterial attachment frequency under vitamin limitation coincided with an increased abundance of free-living bacteria, further work will be required to confirm that this phenotype is driven by nutrient exchange requirements.

CONCLUSION

Our data show that the B_1 and B_{12} limiting concentrations for *L. polyedrum* growth are lower than typical concentrations found in coastal waters. In vitamin-depleted cultures of *L. polyedrum,* the limitation could be overcome by co-culture with *D. shibae*, because the bacterium was likely able to provide sufficient quantities of B_1 and B_{12} to support the growth of *L. polyedrum*. In return, *D. shibae* was likely provided sufficient exudates by *L. polyedrum* to support its growth. Also, the mutualism between both partners may have extended beyond the supply of B_1 and B_{12} and dissolved organic carbon. Since *D. shibae* is auxotrophic for B_7, niacin and 4-amino-benzoic acid, *L. polyedrum* needed to provide sufficient quantities of these compounds to overcome *D. shibae*'s auxotrophy. This mutualism was probably helped by the phenotypic ability of *D. shibae* to choose between a free-living or attached lifestyle, where the attached lifestyle could serve as a reservoir of B_7 within this isogenic population.

AUTHOR CONTRIBUTIONS

RC-L conceived, performed, and wrote the article. HM conceived and wrote the article. KY and NH performed and wrote the article.

ACKNOWLEDGMENTS

This work was partially supported by the National Council of Science and Technology (CONACyT-México) project CB-2008-01 106003 (to HM), a Ph.D. scholarship, and a Postdoctoral fellowship for overseas to RCL (CONACyT-México). Additionally, we would like to thank Avery O. Tatters (University of Southern California) for kindly providing the *L. polyedrum* strain and Prof. Carl J. Carrano (San Diego State University) for allowing us to use his laboratory to prepare samples. We would like to show our gratitude to Sharon and Christopher A. Rhodes, the owners of Drug Delivery Experts LLC., for allowing us to use their facility to generate LC-MS data. Finally, we would like to thank the reviewers for constructive comments and suggestions.

SUPPLEMENTARY MATERIAL

The Supplementary Material for this article can be found online at: https://www.frontiersin.org/articles/10.3389/fmars.2018.00274/full#supplementary-material

REFERENCES

Aaronson, S., DeAngelis, B., Frank, O., and Baker, H. (1971). Secretion of vitamins and amino acids into the environment by *Ochromonas danica*. *J. Phycol.* 7, 215–218.

Aaronson, S., Dhawale, S. W., and Patni, N. J. (1977). The cell content and secretion of water-soluble vitamins by several freshwater algae. *Arch. Microbiol.* 112, 57–59. doi: 10.1007/BF00446654

Adachi, M., Kanno, T., Okamoto, R., Itakura, S., Yamaguchi, M., and Nishijima, T. (2003). Population structure of *Alexandrium* (Dinophyceae) cyst formation-promoting bacteria in Hiroshima Bay, Japan. *Appl. Environ. Microbiol.* 69, 6560–6568. doi: 10.1128/AEM.69.11.6560-6568.2003

Adachi, M., Kanno, T., Okamoto, R., Shinozaki, A., Fujikawa-Adachi, K., and Nishijima, T. (2004). *Jannaschia cystaugens* sp. nov., an Alexandrium (Dinophyceae) cyst-formation-promoting bacterium from Hiroshima Bay, Japan. *Int. J. Syst. Evol. Microbiol.* 54, 1687–1692. doi: 10.1099/ijs.0.03029-0

Amin, S. A., Green, D. H., Hart, M. C., Küpper, F. C., Sunda, W. G., and Carrano, C. J. (2009). Photolysis of iron-siderophore chelates promotes bacterial-algal mutualism. *Proc. Natl. Acad. Sci. U.S.A.* 106, 17071–17076. doi: 10.1073/pnas.0905512106

Barr, J. J., Auro, R., Furlan, M., Whiteson, K. L., Erb, M. L., Pogliano, J., et al. (2013). Bacteriophage adhering to mucus provide a non-host-derived immunity. *Proc. Natl. Acad. Sci. U.S.A.* 110, 10771–10776. doi: 10.1073/pnas.1305923110

Bednar, T. W., and Holm-Hansen, O. (1964). Biotin liberation by the lichen *alga Coccomyxa* sp. and by *Chlorella pyrenoidosa*. *Plant Cell Physiol.* 5, 297–303.

Bertrand, E. M., and Allen, A. E. (2012). Influence of vitamin B auxotrophy on nitrogen metabolism in eukaryotic phytoplankton. *Front. Microbiol.* 3:375. doi: 10.3389/fmicb.2012.00375

Bertrand, E. M., Saito, M. A., Jeon, Y. J., and Neilan, B. A. (2011). Vitamin B_{12} biosynthesis gene diversity in the ross sea: the identification of a new group of putative polar B12 biosynthesizers. *Environ. Microbiol.* 13, 1285–1298. doi: 10.1111/j.1462-2920.2011.02428.x

Bertrand, E. M., Saito, M. A., Rose, J. M., Riesselman, C. R., Lohan, M. C., Noble, A. E., et al. (2007). Vitamin B_{12} and iron co-limitation of phytoplankton growth in the Ross Sea. *Limnol. Oceanogr.* 52, 1079–1093. doi: 10.4319/lo.2007.52.3.1079

Biebl, H., Allgaier, M., Tindall, B. J., Koblizek, M., Lünsdorf, H., Pukall, R., et al. (2005). *Dinoroseobacter shibae* gen. nov., sp. nov., a new aerobic phototrophic bacterium isolated from dinoflagellates. *Int. J. Syst. Evol. Microbiol.* 55, 1089–1096. doi: 10.1099/ijs.0.63511-0

Bonnet, S., Webb, E. A., Panzeca, C., Karl, D., Capone, D. G., and Sañudo-Wilhelmy, S. A. (2010). Vitamin B12 excretion by cultures of the marine cyanobacteria *Crocosphaera* and *Synechococcus*. *Limnol. Oceanogr.* 55, 1959–1964. doi: 10.4319/lo.2010.55.5.1959

Carlucci, A. F. (1970). "Part, I. I. Vitamin B_{12}, thiamine, biotin," in *The Ecology of the Phytoplankton Off La Jolla*, ed J. D. H. Strickland (Berkeley, CA: University of California Press), 23–31.

Carlucci, A. F., and Bowes, P. M. (1970a). Production of vitamin B_{12}, thiamine, and biotin by phytoplankton. *J. Phycol.* 6, 351–357.

Carlucci, A. F., and Bowes, P. M. (1970b). Vitamin production and utilization by phytoplankton in mixed culture. *J. Phycol.* 6, 393–400.

Croft, M. T., Lawrence, A. D., Raux-Deery, E., Warren, M. J., and Smith, A. G. (2005). Algae acquire vitamin B12 through a symbiotic relationship with bacteria. *Nature* 438, 90–93. doi: 10.1038/nature04056

Croft, M. T., Warren, M. J., and Smith, A. G. (2006). Algae need their vitamins. *Euk. Cell* 5, 1175–1183. doi: 10.1128/ec.00097-06

Cruz-López, R., and Maske, H. (2016). The vitamin B_1 and B_{12} required by the marine dinoflagellate *Lingulodinium polyedrum* can be provided by its associated bacterial community in culture. *Front. Microbiol.* 7:560. doi: 10.3389/fmicb.2016.00560

Doucette, G. J., McGovern, E. R., and Babinchak, J. A. (1999). Algicidal bacteria against *Gymnodinium breve* (Dynophyceae). I. Bacterial isolation and characterization of killing activity. *J. Phycol.* 35, 1447–1454. doi: 10.1046/j.1529-8817.1999.3561447.x

Doxey, A. C., Kurtz, D. A., Lynch, M. D. J., Sauder, L. A., and Neufeld, J. D. (2015). Aquatic metagenomes implicate *Thaumarchaeota* in global cobalamin production. *ISME J.* 9, 461–471. doi: 10.1038/ismej.2014.142

Droop, M. R. (1974). The nutrient status of algal cells in continuous culture. *J. Mar. Biol. Ass. U.K.* 54, 825–855. doi: 10.1017/S002531540005760X

Droop, M. R. (2003). In defence of the cell quota model of micro-algal growth. *J. Plankton Res.* 25, 103–107. doi: 10.1093/plankt/25.1.103

Droop, M. R. (2007). Vitamins, phytoplankton and bacteria: symbiosis or scavenging? *J. Plankton Res.* 29, 107–113. doi: 10.1093/plankt/fbm009

Ferrier, M., Martiny, J. L., and Rooney-Varga, J. N. (2002). Stimulation of *Alexandrium fundyense* growth by bacterial assemblages from the Bay of Fundy. *J. Appl. Microb.* 92, 706–716. doi: 10.1046/j.1365-2672.2002.01576.x

Gobler, C. J., Norman, C., Panzeca, C., Taylor, G. T., and Sañudo-Wilhelmy, S. A. (2007). Effect of B-vitamins (B1, B12) and inorganic nutrients on algal bloom dynamics in a coastal ecosystem. *Aquat. Microb. Ecol.* 49, 181–194. doi: 10.3354/ame01132

Gómez-Consarnau, L., Sachdeva, R., Gifford, S. M., Cutter, L. S., Fuhrman, J. A., Sañudo-Wilhelmy, S. A., et al. (2018). Mosaic patterns of B-vitamin synthesis and utilization in a natural marine microbial community. *Environ. Microbiol.* doi: 10.1111/1462-2920.14133. [Epub ahead of print].

Green, D. H., Bowman, J. P., Smith, E. A., Gutierrez, T., and Bolch, C. J. (2006). *Marinobacter algicola* sp. nov., isolated from laboratory cultures of paralytic shellfish toxin-producing dinoflagellates. *Int. J. Syst. Evol. Microbiol.* 56, 523–527. doi: 10.1099/ijs.0.63447-0

Green, D. H., Llewellyn, L. E., Negri, A. P., Blackburn, S. I., and Bolch, C. J. S. (2004). Phylogenetic and functional diversity of the cultivable bacterial community associated with the paralytic shellfish poisoning dinoflagellate *Gymnodinium catenatum*. *FEMS. Microbiol. Ecol.* 46, 345–357. doi: 10.1016/S0168-6496(03)00298-8

Hare, C. E., Demir, E., Coyne, K. J., Cary, S. C., Kirchman, D. L., and Hutchins, D. A. (2005). A bacterium that inhibits the growth of *Pfiesteria piscicida* and other dinoflagellates. *Harm. Alg.* 4, 221–234. doi: 10.1016/j.hal.2004.03.001

Helliwell, K. E. (2017). The roles of B vitamins in phytoplankton nutrition: new perspectives and prospects. *New Phytol.* 216, 62–68. doi: 10.1111/nph.14669

Helliwell, K. E., Lawrence, A. D., Holzer, A., Kudahl, U. J., Sasso, S., Kräutler, B., et al. (2016). Cyanobacteria and eukaryotic algae use different chemical variants of vitamin B12. *Curr. Biol.* 26, 999–1008. doi: 10.1016/j.cub.2016.02.041

Helliwell, K. E., Wheeler, G. L., Leptos, K. C., Goldsteins, R. E., and Smith, A. G. (2011). Insights into the evolution of vitamin B_{12} auxotrophy from sequenced algal genomes. *Mol. Biol. Evol.* 28, 2921–2933. doi: 10.1093/molbev/msr124

Jeong, H. J., Yoo, Y. D., Park, J. Y., Song, J. Y., Kim, S. T., Lee, S. H., et al. (2005). Feeding by phototrophic red-tide dinoflagellates: five species newly revealed and six species previously known to be mixotrophic. *Aquat. Microb. Ecol.* 40, 133–150. doi: 10.3354/ame040133

Kazamia, E., Czesnick, H., Nguyen, T. T., Croft, M. T., Sherwood, E., Sasso, S., et al. (2012). Mutualistic interactions between vitamin B(12)-dependent algae and heterotrophic bacteria exhibit regulation. *Environ. Microbiol.* 14, 1466–1476. doi: 10.1111/j.1462-2920.2012.02733.x

King, A. L., Sañudo-Wilhelmy, S. A., Leblanc, K., Hutchins, D. A., and Fu, F. (2011). CO_2 and vitamin B_{12} interactions determine bioactive trace metal requirements of a subarctic Pacific diatom. *ISME J.* 5, 1388–1396. doi: 10.1038/ismej.2010.211

Koch, F., Burson, A., Tang, Y. Z., Collier, J. L.., Fisher, N. S., Sañudo-Wilhelmy, S., et al. (2014). Alteration of plankton communities and biogeochemical cycles by harmful *Cochlodinium polykrikoides* (Dinophyceae) blooms. *Harm. Alg.* 33, 41–54. doi: 10.1016/j.hal.2014.01.003

Koch, F., Hattenrath-Lehmann, T. K., Goleski, J. A., Sañudo-Wilhelmy, S., Fisher, N. S., and Gobler, C. J. (2012). Vitamin B1 and B12 uptake and cycling by plankton communities in coastal ecosystems. *Front. Microbiol.* 3:363. doi: 10.3389/fmicb.2012.00363

Koch, F., Marcoval, A., Panzeca, C., Bruland, K. W., Sañudo-Wilhelmy, S. A., and Gobler, C. J. (2011). The effects of vitamin B12 on phytoplankton growth and community structure in the Gulf of Alaska. *Limnol. Oceanogr.* 3, 1023–1034. doi: 10.4319/lo.2011.56.3.1023

Koch, F., Sañudo-Wilhelmy, S. A., Fisher, N. S., and Gobler, C. J., (2013). Effect of vitamins B_1 and B_{12} on bloom dynamics of the harmful brown tide alga, *Aureococcus anophagefferens* (Pelagophyceae). *Limnol. Oceanogr.* 58, 1761–1774. doi: 10.4319/lo.2013.58.5.1761

Kuo, R. C., and Lin, S. (2013). Ectobiotic and endobiotic bacteria associated with *Eutreptiella* sp. isolated from Long Island sound. *Protist* 164, 60–74. doi: 10.1016/j.protis.2012.08.004

Luo, H., and Moran, M. A. (2014). Evolutionary ecology of the marine Roseobacter clade. *Microbiol. Mol. Biol. Biol. Rev.* 78, 573–587. doi: 10.1128/MMBR.00020-14

Mayali, X., Franks, P. J. S., and Azam, F. (2007). Bacterial induction of temporary cyst formation by the dinoflagellate *Lingulodinium polyedrum*. *Aquat. Microb. Ecol.* 50, 51–62. doi: 10.3354/ame01143

Miller, T. R., Hnilicka, K., Dziedzic, A., Desplats, P., and Belas, R. (2004). Chemotaxis of *Silicibacter* sp. strain TM1040 toward dinoflagellate products. *Appl. Environ. Microbiol.* 70, 4692–4701. doi: 10.1128/AEM.70.8.4692-4701.2004

Moustafa, A., Evans, A. N., Kulis, D. M., Hackett, J. D., Erdner, D. L., Anderson, D. M., et al. (2010). Transcriptome profiling of a toxic dinoflagellate reveals a gene-rich protist and a potential impact on gene expression due to bacterial presence. *PLoS ONE* 5:e9688. doi: 10.1371/journal.pone.0009688

Okbamichael, M., and Sañudo-Wilhelmy, S. A. (2004). A new method for the determination of vitamin B_{12} in seawater. *Anal. Chim. Acta* 517, 33–38. doi: 10.1016/j.aca.2004.05.020

Palacios, L., and Marín, M. (2008). Enzymatic permeabilization of the thecate dinoflagellate *Alexandrium minutum* (Dinophyceae) yields detection of intracellularly associated bacteria via catalyzed reporter deposition-fluorescence *in situ* hybridization. *Appl. Environ. Microbiol.* 74, 2244–2247. doi: 10.1128/AEM.01144-07

Panzeca, C., Beck, A. J., Tovar-Sanchez, A., Segovia-Zavala, J., Taylor, G. T., Gobler, C. J., et al. (2009). Distribution of dissolved vitamin B_{12} and Co in coastal and open-ocean environments. *Est. Coast. Shelf Sci.* 85, 223–230. doi: 10.1016/j.ecss.2009.08.016

Panzeca, C., Tovar-Sanchez, A., Agusti, S., Reche, I., Duarte, C. M., Taylor, G. T., et al. (2006). B vitamins as regulators of phytoplankton dynamics. *EOS Trans. Am. Geoph. Union* 87, 593–596. doi: 10.1029/2006EO520001

Patzel, D., Wang, H., Buchholz, I., Rohde, M., Gröbe, L., Pradella, S., et al. (2013). You are what you talk: quorum sensing induces individual morphologies

and cell division modes in *Dinoroseobacter shibae*. *ISME J.* 7, 2274–2286. doi: 10.1038/ismej.2013.107

Peña-Manjarrez, J. L., Gaxiola-Castro, G., and Helenes-Escamilla, J. (2009). Environmental factors influencing the variability of *Lingulodnium polyedrum* and *Scrippsiella trochoidea* (Dinophyceae) cyst production. *Ciencias Marinas* 35, 1–14. doi: 10.7773/cm.v35i1.1406

Sañudo-Wilhelmy, S. A., Cutter, L. S., Durazo, R., Smail, E. A., Gómez-Consarnau, L., Webb, E. A., et al. (2012). Multiple B-vitamin depletion in large areas of the coastal ocean. *Proc. Natl. Acad. Sci. U.S.A.* 109, 14041–14045. doi: 10.1073/pnas.1208755109

Sañudo-Wilhelmy, S. A., Gobler, C. J., Okbamichael, M., and Taylor, G. T., (2006). Regulation of phytoplankton dynamics by vitamin B12. *Geophys. Res. Lett.* 33:L04604. doi: 10.1029/2005GL025046

Sañudo-Wilhelmy, S. A., Gómez-Consarnau, L., Suffridge, C., and Webb, E. A. (2014). The role of B vitamins in marine biogeochemistry. *Annu. Rev. Mar. Sci.* 6, 339–367. doi: 10.1146/annurev-marine-120710-100912

Schneider, C. A., Rasband, W. S., and Eliceiri, K. W., (2012). NIH Image to ImageJ: 25 years of image analysis. *Nat. Methods* 9, 671–675. doi: 10.1038/nmeth.2089

Suffridge, C., Cutter, L., and Sañudo-Wilhelmy, S. A. (2017). A New analytical method for direct measurement of particulate and dissolved B-vitamins and their congeners in seawater. *Front. Mar. Sci.* 4:11. doi: 10.3389/fmars.2017.00011

Tang, Y. Z., Koch, F., and Gobler, C. J. (2010). Most harmful algal bloom species are vitamin B_1 and B_{12} auxotrophs. *Proc. Natl. Acad. Sci. U.S.A.* 107, 20756–20761. doi: 10.1073/pnas.1009566107

Wagner-Döbler, I., Ballhausen, B., Berger, M., Brinkhoff, T., Buchholz, I., Bunk, B., et al. (2010). The complete genome sequence of the algal symbiont *Dinoroseobacter shibae*: a hitchhiker's guide to life in the sea. *ISME J.* 4, 61–77. doi: 10.1038/ismej.2009.94

Wang, H., Tomasch, J., Jarek, M., and Wagner-Döbler, I. (2014a). A dual-species co-cultivation system to study the interactions between Roseobacters and dinoflagellates. *Front. Microbiol.* 5:311. doi: 10.3389/fmicb.2014.00311

Wang, H., Ziesche, L., Frank, O., Michael, V., Martin, M., Petersen, J., et al. (2014b). The CtrA phosphorelay integrates differentiation and communication in the marine alphaproteobacterium *Dinoroseobacter shibae*. *BMC Genomics* 15:130. doi: 10.1186/1471-2164-15-130

Wienhausen, G., Noriega-Ortega, B. E., Niggemann, J., Dittmar, T., and Simon, M. (2017). The exometabolome of two model strains of the roseobacter group: a marketplace of microbial metabolites. *Front. Microbiol.* 8:1985. doi: 10.3389/fmicb.2017.01985

Xie, B., Bishop, S., Stessman, D., Wright, D., Spalding, M. H., and Halverson, L. J. (2013). *Chlamydomonas reinhardtii* thermal tolerance enhancement mediated by a mutualistic interaction with vitamin B_{12}-producing bacteria. *ISME J.* 7, 1544–1555. doi: 10.1038/ismej.2013.43

Zhu, Q., Aller, R. C., and Kaushik, A. (2011). Analysis of vitamin B_{12} in seawater and marine sediment porewater using ELISA. *Limnol. Oceanogr. Methods* 9, 515–523. doi: 10.4319/lom.2011.9.515

Conflict of Interest Statement: The authors declare that the research was conducted in the absence of any commercial or financial relationships that could be construed as a potential conflict of interest.

frontiers in Marine Science

ORIGINAL RESEARCH
published: 05 June 2018
doi: 10.3389/fmars.2018.00180

Iron and Harmful Algae Blooms: Potential Algal-Bacterial Mutualism Between *Lingulodinium polyedrum* and *Marinobacter algicola*

Kyoko Yarimizu[1], *Ricardo Cruz-López*[1,2] *and Carl J. Carrano*[1]*

[1] *Department of Chemistry and Biochemistry, San Diego State University, San Diego, CA, United States,* [2] *Department of Biological Oceanography, Centro de Investigación Científica y de Educación Superior de Ensenada, Baja California, Mexico*

Phytoplankton blooms can cause acute effects on marine ecosystems either due to their production of endogenous toxins or due to their enormous biomass leading to major impacts on local economies and public health. Despite years of effort, the causes of harmful algal blooms (HAB) are still not fully understood. Our hypothesis is that bacteria that produce photoactive siderophores may provide a bioavailable form of iron to commensally associated phytoplankton, which could in turn affect algal growth and bloom dynamics. Here we report a laboratory-based study of binary cultures of the dinoflagellate *Lingulodinium polyedrum*, a major HAB species, with *Marinobacter algicola* DG893, a phytoplankton-associated bacterium that produces the photoactive siderophore vibrioferrin. Comparing binary cultures of *L. polyedrum* with both the wild type and the vibrioferrin minus mutant of *M. algicola* shows that bacteria are necessary to promote dinoflagellate growth and that this growth promotion effect is at least partially related to the ability of the bacterium to supply bioavailable iron via the siderophore vibrioferrin. These results support the notion of a carbon for iron mutualism in some bacterial-algal interactions.

Keywords: ***Lingulodinium polyedrum***, ***Marinobacter***, **iron, algal-bacterial interactions, binary culture**

OPEN ACCESS

Edited by:
Stanley Chun Kwan Lau,
Hong Kong University of Science and Technology, Hong Kong

Reviewed by:
Marius Nils Müller,
Universidade Federal de Pernambuco, Brazil
Simon M. Dittami,
UMR8227 Laboratoire de Biologie Intégrative des Modèles Marins, France

***Correspondence:**
Carl J. Carrano
ccarrano@mail.sdsu.edu

Specialty section:
This article was submitted to Aquatic Microbiology, a section of the journal Frontiers in Marine Science

Received: *27 February 2018*
Accepted: *07 May 2018*
Published: *05 June 2018*

Citation:
Yarimizu K, Cruz-López R and Carrano CJ (2018) Iron and Harmful Algae Blooms: Potential Algal-Bacterial Mutualism Between Lingulodinium polyedrum and Marinobacter algicola. Front. Mar. Sci. 5:180. doi: 10.3389/fmars.2018.00180

INTRODUCTION

Phytoplankton blooms are a frequent phenomenon in the coastal regions of every continent in the world. Certain phytoplankton algae occurring in mass proliferations produce toxins. Such harmful algal blooms (HABs) can, directly or indirectly, impact marine ecosystems with repercussions on local economies and public health (Lewitus et al., 2012). Direct effects on human health are often related to the consumption of shellfish that have ingested toxic phytoplankton, resulting in the accumulation of toxins and, consequently upon human consumption, paralytic, diarrheic, and neurotoxic poisoning which can sometimes be fatal (Anderson, 1994; Honner et al., 2012). HABs also have indirect impacts such as impairment of water quality leading to losses in the tourism and recreational sectors. Even phytoplankton blooms that do not produce toxins can be detrimental and lead to ecological impacts such as the displacement of indigenous species, habitat alteration, or oxygen depletion (Glibert et al., 2005). The economic effects caused by HABs in the U.S. alone were estimated at $82 million per year in 2006 (Hoagland and Scatasta, 2006). Current strategies to reduce health-related impacts due to HABs are based on frequent coastal monitoring and early

detection of HAB species and toxin levels. Nevertheless, the factors leading to the origins of HABs are still not well understood. Consequently, there is no strategy for their ultimate prevention.

There is an ongoing debate whether the factors leading to HABs are natural or anthropogenic. Oceanographic factors and global climate change including changes in upwelling and or relaxation and reversal of winds may be the major drivers initiating phytoplankton blooms (Roegner et al., 2002; Tweddle et al., 2010). HABs have also been proposed to be the consequence of human activities including eutrophication, changes in land use and agriculture, overfishing, and ballast water discharge (Glibert et al., 2005). Others consider that better analytics result in increased detection of HAB species (Burkholder, 1998). Nevertheless, HABs are a global threat to human health, fisheries, and aquaculture resources. While numerous studies concentrate on the causes of HABs, few have considered that bacterial species coexisting with microalgae could contribute to their development. However since Bell and Mitchell reported that specific bacterial communities occur and microbial activity was altered in the so-called phycosphere (Bell and Mitchell, 1972; Bell and Lang, 1974), more and more studies suggest that such algal-bacterial interactions are very specific and important (Azam and Malfatti, 2007; Amin et al., 2015; Bertrand et al., 2015; Ramanan et al., 2016; Seymour et al., 2017). A plausible hypothesis suggests that the mutualistic association of some phytoplankton and bacteria is based on nutrient exchange. Nitrogen and phosphorus are the best studied in this regard, although the molecular nature of interactions involving these nutrients is not well understood (Hallegraeff and Gollasch, 2006). Alternatively specific bacteria may affect algal growth and bloom dynamics by their control of iron, a trace element which is often growth limiting to phytoplankton in the marine environment (Maldonado et al., 2005; Miethke and Marahiel, 2007; Croot and Heller, 2012).

Iron is an essential element for all living organisms including phytoplankton and bacteria due to its involvement in photosynthesis and respiration. Despite iron being the fourth most abundant element on the Earth, its bioavailability in the marine environment is extremely low due to its poor solubility under the mildly alkaline aerobic conditions present in the ocean (Martin and Fitzwater, 1988; Wu and Luther, 1994). To overcome this low bioavailability, bacteria and fungi have evolved sophisticated systems to produce high-affinity iron-chelating compounds called siderophores to acquire, transport, and process this essential metal ion (Sandy and Butler, 2009). The major role of siderophores is to bind mineral phases of iron and to deliver the iron siderophore complex to specific outer membrane receptors on microbial cells. Several hundred siderophores have been isolated and extensively studied with respect to their synthesis, structures and transport mechanisms over the last three decades (Yamamoto et al., 1994; Challis, 2005; Sandy and Butler, 2009; Raymond et al., 2015). While much research has been done on terrestrial siderophores, the study of marine siderophores is less extensive and only a relatively few have been fully elucidated (Vraspir and Butler, 2009). Nevertheless one of the two major attributes that seem to distinguish marine siderophores from those of terrestrial origin is the tendency of the former to contain an α- and β-hydroxy acid group in their iron-binding domain (Barbeau et al., 2001, 2002; Küpper et al., 2006). The significance of the presence of these functional groups in siderophores is in their ability to make the iron-siderophore complex photoreactive. The chelated Fe(III) in such siderophores is reduced in the presence of sunlight via an internal redox process to release Fe(II), a more soluble form of iron (Amin et al., 2009b). It has been proposed that sunlight-driven reduction of the Fe(III) would transiently produce Fe(II) which might be utilized not only by the siderophore-producing bacteria themselves but also by non-siderophore producing bacteria and other organisms such as phytoplankton (Maldonado et al., 2005; Naito et al., 2008; Amin et al., 2009a, 2012a).

While iron acquisition by bacteria is well understood, that of phytoplankton remains less so. There are data to support the possibility of a variety of iron uptake mechanisms being operative simultaneously depending on the species involved. These include an iron-reductive route via a cell surface reductase, a direct xenosiderophore-mediated mechanism, and cell surface-enhanced processes (Sutak et al., 2012; McQuaid et al., 2018). However as of yet there are no well documented examples, with some exceptions among the cyanobacteria, where phytoplankton have been shown to produce their own siderophores for iron acquisition (Raven, 2013). Thus how phytoplankton effectively acquire this metal from the low concentration iron environment is still unclear.

Our hypothesis is that algal growth and bloom dynamics may be affected by the increased bioavailability of iron engendered by the presence of photoreactive siderophores produced by mutualistic bacteria. Previously, we studied a bloom of the dinoflagellate, *Lingulodinium polyedrum*, at the Scripps Pier (San Diego, CA, USA) in 2011. *L. polyedrum* is one of the HAB species known to produce Yessotoxins, a group of polyether toxins which can accumulate in shellfish and show high toxicity to mice via intraperitoneal injection (Tubaroa et al., 2004). As the first step to search for an association of phytoplankton with specific bacterial photoreactive siderophore producers (producing petrobactin, aerobactin, and vibrioferrin siderophores), we monitored both the population of *L. polyedrum* and the bacterial siderophore producers before, during, and after the 2011 bloom. The results showed that both *L. polyedrum* and the bacterial siderophore producers simultaneously increased and decreased during the bloom period (Yarimizu et al., 2014). At the *L. polyedrum* bloom maximum, the total number of bacterial producers of photoreactive siderophore reached their maximum accounting for roughly 9% of the total bacterial population suggesting that such high abundance of photoreactive siderophore producers could potentially provide bioavailable iron to the phytoplankton in this environment. Furthermore, when the PCR-derived amplicons were sequenced, a phylogenetic tree constructed from the sequencing results showed that the community of siderophore producers in pre-bloom was statistically significantly different than those found during and after the bloom by UniFrac analysis suggesting that this particular bacterial community could be involved in bloom initiation.

As a proof of concept, the present study was performed using laboratory culture data to correlate the association of

the vibrioferrin siderophore producing bacterium, *Marinobacter algicola DG893* and the dinoflagellate *L. polyedrum* with iron as a nutrient. It is hoped that finding an algal-bacterial mutualism based on iron availability may be useful for a more thorough understanding of the mechanisms of HAB formation.

MATERIALS AND METHODS

Trace Iron Cleaning Procedures

The container cleaning technique was adopted from Bruland and Franks (1979). All plastic and glass containers were washed with pure water and soaked in 3 N hydrochloric acid for at least 2 weeks at ambient temperature. The acid-washed containers were rinsed with Milli-Q water and dried in a laminar-flow air bench. For those experiments requiring sterile conditions, acid-washed containers were placed in pouches and autoclaved at 121°C for 30 min followed by a 45 min dry cycle. Alternatively, purchased sterile containers Nunc™ Cell Culture Treated Flasks with Filter Caps were used.

Growth Media

Of eight sources of natural waters screened, Pacific Ocean oligotrophic water was initially selected for our use due to its extremely low dissolved iron concentration (pM). This was replaced later by Scripps Pier seawater because of its easier accessibility and comparable *L. polyedrum* growth patterns observed in the two sources of seawater. Seawater from Scripps Pier (32.153°N, 117.115°W, San Diego, CA) was collected (pH 8.2–8.4, 980 mOsm/Kg H_2O, total *dissolved* iron 3–4 nM) and filtered immediately through 0.22 mm pore size membrane. The filtered seawater was mixed with approximately 0.005% metal free hydrochloric acid, autoclaved for 30 min, cooled at ambient temperature for a day, and stored in 5°C until use. The pH of the autoclaved seawater was ensured to be between 8.0 and 8.2 at ambient temperature. L1 nutrient was added to sterile seawater per manufacturer's instruction (L1 medium). For those cultures requiring controlled iron concentrations in media, L1 trace element solution without $FeCl_3$ and Na_2EDTA was prepared in house (Guillard and Hargraves, 1993) and added along with other L1 nutrients (nitrate, phosphate, silicate, vitamins) to sterile seawater (L1-Fe medium). Serial dilutions were made on L1 medium with L1-Fe medium to prepare growth medium with defined total iron concentrations, $[Fe]_T$.

Artificial Sea Water (ASW)

The component solutions were prepared in three separate containers, one with 15 g NaCl, 0.75 g KCl, 1 g NH_4Cl in approximately 500 mL water, one with 12.4 g $MgSO_4 \cdot 7H_2O$ in small volume of water, and one with 3.0 g of $CaCl_2 \cdot 2H_2O$ in a small volume of water. The three solutions were mixed and 0.1 g disodium ß-glycerol phosphate was added. The pH was adjusted to 8.0–8.2 and volume was adjusted to 1 L. The solution was autoclaved at 121°C for 30 min.

Algal Maintenance and Growth Monitoring

The *L. polyedrum* strain used in this study was isolated from Venice Beach, California, and kindly provided to us by Avery Tatters (University of Southern California). *L. polyedrum* cells were maintained in sterile 1L Erlenmeyer flasks containing L1 medium and capped with a ventilation sponge. Cultures were exposed to 100 μmol photons m^{-2} s^{-1} on a 12-h alternating light and dark cycle at a temperature of 20 ± 2°C (standard growth condition). The upper portion of a culture containing healthy cells was diluted 1/5 with L1 medium every 3 weeks. Algal growth was monitored by direct cell count using an inverted microscope (Nikon Eclipse TE2000-U, 4× objective). To prepare cells in controlled iron medium, cultures containing 10^4-10^5 cells per mL was placed in a 15-mL Falcon tubes and centrifuged for a few seconds to pellet cells which were gently washed three times and re-suspended to an appropriate volume with controlled iron medium.

"Axenic" *L. polyedrum* Preparation

Non-axenic *L. polyedrum* cells were grown to 10^5 cells/mL in L1 medium. Antibiotics 0.1% (v/v) (Penicillin 5 units/mL, Streptomycin 5 μg/mL, Neomycin 10 μg/mL) were added to a non-axenic culture and incubated for 24 h under the standard growth condition. Antibiotic-treated cultures were placed in 15 mL Falcon tubes and gently centrifuged for a few seconds. The pelleted cells were washed three times and re-suspended with L1 medium containing 0.05% (v/v) antibiotics in a sterile culture flask to appropriate volume. Antibiotics 0.05% (v/v) was added every 3 days to maintain the culture "axenic." The absence of cultureable bacteria in the antibiotic treated *L. polyedrum* was tested by spreading a 10 μL sample of the culture on a marine broth plate (5 g/L peptone, 1 g/L yeast extract, 15 g/L agar in 75% seawater) followed by incubation at 25°C for 2–3 days. The absence of any visible bacterial colonies was considered indicative of an "axenic" culture of *L. polyedrum*.

Bacteria Strains and Growth Monitoring

The model bacterium used was *Marinobacter algicola* DG893 (GenBank code NZ_ABCP00000000.1) since it has been isolated by Green et al. (2004) and well characterized as a producer of the photoactive siderophore vibrioferrin (Amin et al., 2007). The mutant Δ*pvsAB*-DG893 was made as described by Amin et al. (2012a) by 872 base pair deletion from the wild type to knock out two siderophore biosynthesis genes, *pvsA* and *pvsB*. To monitor bacterial growth, two methods were used: Optical density at 600 nm was applied to apparently turbid samples which generally contained $\geq 10^7$/mL of bacterial cells. Enumeration of bacteria by serial dilution was applied for samples containing lower numbers of bacteria cells ($<10^7$/mL). For enumeration techniques, serial dilution was made on those samples with sterile seawater, each diluted sample was spread on marine broth plates, and the number of colony forming units (CFU) recorded from the lowest diluted sample plate. CFU in original sample per mL was calculated by (CFU in diluted sample)/(volume plated in mL) × dilution factor.

Stock Bacteria Solution

One liter of marine broth was prepared (5 g/L peptone, 1 g/L yeast extract, 15 g/L agar in 75% seawater, pH 8.2, sterile) and dispensed into sterile tubes with a 5 mL volume. A few colonies

of bacteria picked from stock plates were transferred into the marine broth tubes and shaken at 25°C for 1–2 days until they reached log phase. The cells were collected by centrifugation, washed three times and re-suspended in sterile medium to an optical density (OD600) of 0.3 (stock bacteria solution).

CAS-Dye Assay

The method was adopted from Alexander and Zuberer (1991) to detect siderophore production by DG893. Using acid washed glassware, the following stock solutions were prepared: 10 mM HDTMA in water, 2 mM CAS in water, 1 mM $FeCl_3.6H_2O$ in water, 50 mM piperazine anhydrous buffer (pH 5.6), and 0.2 M 5-sulfosalicylic acid in water. CAS solution was prepared by pouring a mixture of 15 mL of CAS and 3 mL of $FeCl_3.6H_2O$ slowly into 12 mL of HDTMA followed by addition of 50 mL of piperazine. The final volume was adjusted to 200 mL with water. CAS shuttle solution was prepared by adding 20 μL of 5-sulfosalicylic acid to every mL of CAS solution (used within 1 day of preparation). Samples to be tested were centrifuged to remove particles and 0.5 mL supernatant was mixed with 0.5 mL of CAS shuttle solution followed by incubation in the dark at ambient temperature for 10 min. A color change from dark purple to clear red indicated siderophore production.

Materials and Reagents

The following materials were purchased from Sigma-Aldrich: Chrome azurol S (CAS, C-1018, MW605.28), antibiotics (Penicillin/Streptomycin/Neomycin, P4083-100 mL), peptone (P-1265), iron(III) chloride hexahydrate ($FeCl_3{\cdot}6H_2O$, 10025-77-1, MW270.30), manganese(II) chloride tetrahydrate ($MnCl_2{\cdot}4H_2O$, 13446-34-9, MW197.91), hexadecyltrimethylammonium bromide (HDTMA, H6269-100G, MW364.45), 1,4-diazacyclohexane, diethylenediamine (Piperazine, Sigma-Aldrich, P45907-100G, MW 86.14), 5-sulfosalicylic acid (390275, MW218. 18), zinc sulfate heptahydrate ($ZnSO_4{\cdot}7H_2O$, 1088830500, MW287.54), cobalt(II) chloride hexahydrate ($CoCl_2{\cdot}6H_2O$, 8025400010, MW129.83), copper(II) sulfate pentahydrate ($CuSO_4{\cdot}5H_2O$, 209198-5G, MW249.69), sodium molybdate dehydrate ($Na_2MoO_4{\cdot}2H_2O$, 331058-5G, MW241.95), selenous acid (H_2SeO_3, 211176-10G, MW128.97), nickel(II) sulfate hexahydrate ($NiSO_4{\cdot}6H_2O$, 227676-100G, MW262.85), sodium orthovanadate (Na_3VO_4, 450243-10G, MW183.91), potassium chromate (K_2CrO_4, 216615-100G, MW194.19), salicylaldoxime (SA, 84172-100G). The following materials were purchased from Fisher Scientific: trace metal-free hydrochloric acid (Optima, A466-250), yeast extract (BP9727-500), agar (BP1423-500), Casamino Acids (BP1424-500), Nunc™ Cell Culture Treated Flasks with Filter Caps (12-565-57), ethylenediaminetetraaceticacid, tetrasodium salt dihydrate ($Na_4EDTA{\cdot}2H_2O$, BP121-500, MW416.2), boric acid (AAJ67202A1). Other materials were purchased as follows: 0.22 μm filter membrane (Millipore, MillexGV, SLGV033RS), L1 medium kit (Bigelow, MKL150L), pure water (Barnstead water system, 18.2 mΩ). Vibrioferrin (VF, MW434.35) was isolated and purified in house according to Amin et al. (2007).

RESULTS

Bacterial Growth

The growth of DG893 and mutant Δ*pvsAB*-DG893 in L1 medium containing different total iron concentrations $[Fe]_T$ (1,000, 100, 10, and 0 nM) was monitored. All media were divided in two parts, one maintaining [EDTA] at 10,000 nM (L1 nutrient level) with variable $[Fe]_T$, and the other reducing [EDTA] along with $[Fe]_T$ to maintain molar ratio of Fe: EDTA of 1:1. All media were prepared with and without sterile Casamino Acids. In each medium, ca. 10^6 cells/mL of DG893 or mutant Δ*pvsAB*-DG893 were added and shaken in the dark at 30°C. The bacterial growth in each medium was monitored for 5 days by optical density at 600 nm. Neither WT DG893 nor the mutant grew in simple seawater or L1-Fe medium without a carbon source (**Figure 1A**). Addition of iron to seawater or L1-Fe medium also did not maintain growth (**Figure 1B**). However upon addition of Casamino Acids, both DG893 and the mutant grew and their growth increased with increasing $[Fe]_T$ in media (**Figure 1C**). There was no remarkable difference in growth pattern between DG893 and the mutant, consistent with the report by Amin et al. (2012a). In summary, both DG893 and the mutant require a carbon source to grow to a detectable level in seawater medium.

Siderophore Production and Total Iron Concentration $[Fe]_T$

The ability to produce the siderophore vibrioferrin (VF) by DG893 but not by the mutant was confirmed by the CAS-dye assay. Since siderophore biosynthesis is generally turned on under low iron concentrations and turned off under high concentrations (Braun, 1995; Braun et al., 1998; Miethke and Marahiel, 2007), WT was grown in L1 medium containing various $[Fe]_T$ with 0.3% Casamino Acids at 30°C in dark for 24 h to find the approximate $[Fe]_T$ under which DG893 produces VF. The WT did not produce VF in the media with $[Fe]_T \geq 10$ μM but did so with a $[Fe]_T$ of 1 μM or less. The mutant Δ*pvsAB*-DG893 did not show signs of siderophore production under any of the conditions tested. The results suggest that under normal seawater conditions, where $[Fe]_T$ is estimated to be nM to pM, that siderophore biosynthesis in DG893 is likely turned on.

Axenic Culture Preparation

The difficulty in preparing and maintaining axenic cultures of many marine algae has been reported in the past (Green et al., 2004; Jauzein et al., 2015; Liu et al., 2017). In fact, Lupette et al. (2016) noted that completely axenic cultures of a model green algal species could not be maintained despite the use of antibiotic treatment protocols. We were partially successful in our efforts to prepare axenic *L. polyedrum*. Initially, non-axenic *L. polyedrum* cultures containing 10^5 cells/mL were treated with antibiotics (1% v/v Penicillin 50 units/mL, Streptomycin 50 μg/mL, Neomycin 100 μg/mL) for 24 h under the normal growth conditions. The treated cells were washed and re-suspended with sterile L1 media and while the "axenicity" of the culture at this point was confirmed, bacterial colonies reappeared after only a few days. An attempt was made to keep 1% antibiotics in the culture longer than 24 h, however,

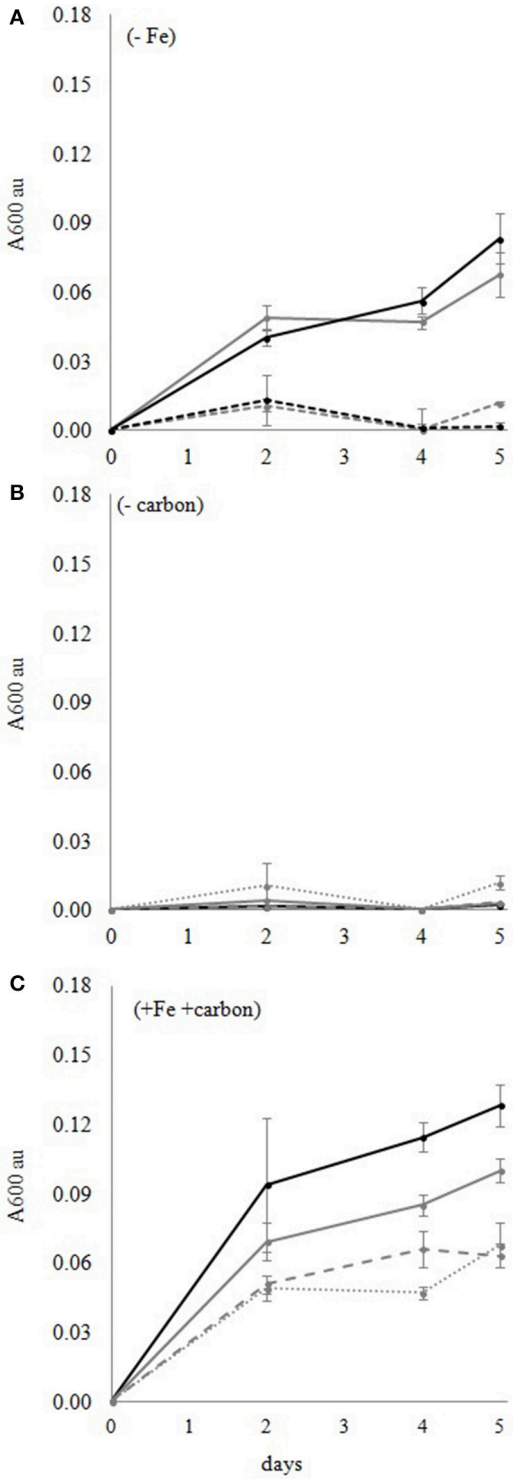

FIGURE 1 | DG893 growth in media with and without Fe and carbon. **(A)** DG893 growth in media without added Fe. The bold lines represent media containing 10 mg/mL Casamino Acids. The dotted lines represent media without Casamino Acids. The gray lines represent L1-Fe media. The black lines represent seawater. The VF null mutant of DG893 showed a similar pattern. **(B)** DG893 incubated in L1 media containing different $[Fe]_T$ but without an *(Continued)*

FIGURE 1 | added carbon source. The black bold line, gray bold line, gray wide dotted line, and gray narrow dotted line represent L1 media with 1,000, 100, 10, 0 nM $[Fe]_T$, respectively. The mutant DG893 showed a similar pattern. **(C)** DG893 incubated in L1 media containing 10 mg/mL Casamino Acids and different $[Fe]_T$. The black bold line, gray bold line, gray wide dotted line, and gray narrow dotted line represent L1 media with 1,000, 100, 10, 0 nM $[Fe]_T$, respectively.

dinoflagellate cells began to disintegrate after 2 days suggesting that 1% antibiotics must be removed from the culture within 24 h. The fact that the negative control and sterile L1 medium without phytoplankton cells remained bacteria-free for weeks ruled out a possibility of culture contamination. We believe that the antibiotics are most likely eliminating only free-living bacteria leaving attached bacteria unaffected. The next effort of preparing axenic cultures was made by immediate dilution of antibiotic-treated cultures. The rationale of this attempt was to minimize attached bacteria on *L. polyedrum* cells by dilution. The antibiotic treated *L. polyedrum* culture was diluted 200-fold with sterile L1 medium and incubated under standard growth conditions. The diluted culture remained bacteria-free for the first 10 days, however microbial growth was observed on the 12th day as the number of *L. polyedrum* cells also increased. Although this dilution method suggested that the culture stayed bacteria free for up to 10 days, the *L. polyedrum* cell count was too dilute to be useful for further study. The next attempt at axenic culture preparation was made with three sequential antibiotic treatments. The non-axenic culture was treated with 1% antibiotics for 24 h, washed three times, and re-suspended with sterile L1 medium. The cells were allowed to recover under normal growth conditions for a day and then again treated with 1% antibiotics. This procedure was repeated three times. This procedure also failed as the dinoflagellate cells began to disintegrate. Finally, using a similar procedure but reducing the concentration of antibiotics to 0.1% for the first treatment and adding 0.05% subsequently every 2–3 days resulted in *L. polyedrum* cultures without visible cell damage that appeared to be free of free-living bacteria for more than a month.

L. polyedrum Growth Screening

A matrix containing thirty cultures of *L. polyedrum* in L1 medium containing different numbers of DG893 cells in the initial inoculum (10^7, 10^6, 10^5, 10^4, 10^3, 0 CFU/mL) and different $[Fe]_T$ (10^4, 10^3, 10^2, 10^1, and 0 nM) was set up. The same matrix was set up with the mutant Δ*pvsAB*-DG893. Bacterial growth was monitored by enumeration of bacteria by serial dilution and phytoplankton growth was monitored by direct cell counts under the microscope. Regardless of the starting bacterial cell number, both DG893 wild type and mutant grew in all the binary culture matrices over 28 days to eventually reach a bacterial population of ca. 10^5 CFU/mL. The group of media containing 1,000 nM $[Fe]_T$ showed the greatest growth of *L. polyedrum* regardless of the starting bacterial inoculum (**Figure 2A**). The group of media containing ≤10 nM $[Fe]_T$ showed very slow *L. polyedrum*

growth regardless of starting bacterial inoculum. No significant differences in *L. polyedrum* growth co-cultured with DG893 or the mutant were observed, which left a question as to whether VF secreted by DG893 would have a significant effect on *L. polyedrum* growth. It was speculated that under these growth conditions, the amount of VF being produced by DG893 was insufficient to see detectable changes in *L. polyedrum* growth. This was later confirmed (*vide infra*) when excess VF artificially added to the culture produced pronounced *L. polyedrum* growth. Finally, the growth pattern of axenic *L. polyedrum* was similar to that of a non-axenic culture. This observation left open another question as to whether DG893 and *L. polyedrum* were commensally associated. However this also was confirmed by experiments described below where after subsequent culturing the "axenic" *L. polyedrum* ceased to grow while binary *L. polyedrum* DG893 kept growing exponentially (**Figure 3**).

Subsequent Batch Culture Growth of *L. polyedrum* in DG893 Binary Culture

L. polyedrum grown in L1 media containing various $[Fe]_T$ and DG893 (**Figure 2A**) for 28 days were diluted with appropriate media to adjust *L. polyedrum* to 10^2 cells/mL in the 2nd subsequent batch culture. The *L. polyedrum* growth in this 2nd subsequent culture was monitored for another 28 days under each growth condition. The result showed that the 2nd subsequent batch culture *L. polyedrum* in the higher two $[Fe]_T$ (10,000 and 1,000 nM) maintained their exponential growth while those in the lower three $[Fe]_T$ did not grow (**Figure 2B**). Although the cells under the latter conditions did not completely

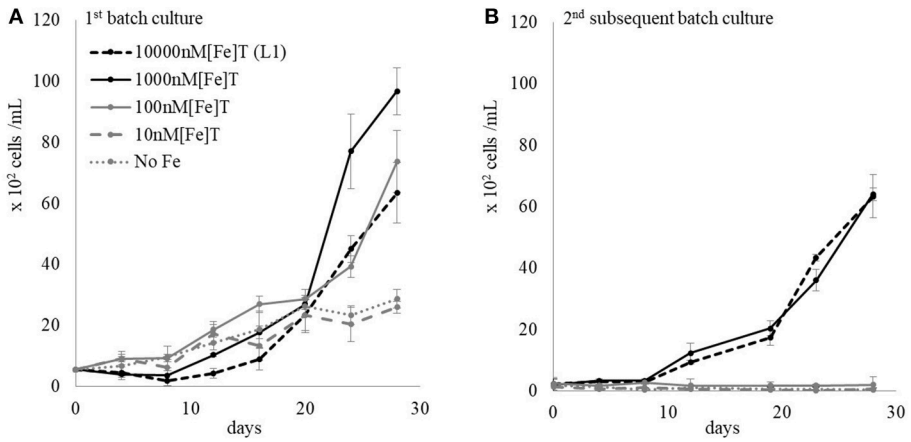

FIGURE 2 | *L. polydrum* co-cultured with a starting inoculum of DG893 at 10^3 cells/mL in media with various $[Fe]_T$. **(A)** First generation growth of *L. polyedrum* in the presence of DG893. The starting inoculum of DG893 was 10^3 cells/mL which reached 10^5 cells/mL after 28 days incubation under the standard growth conditions. A similar pattern was observed in all other groups: i.e., media containing a starting inoculum of DG893 of 10^7, 10^6, 10^5, 10^4, 10^3, 0 cells/mL and $[Fe]_T$ of 10^4, 10^3, 10^2, 10^1, or 0 nM. **(B)** Second generation growth of *L. polyedrum* in the presence of DG893. After 28 days the cultures in **(A)** were diluted to a *L. polyedrum* concentration of 10^2 cells/mL with appropriate media and incubated under the standard growth condition for an additional 28 days.

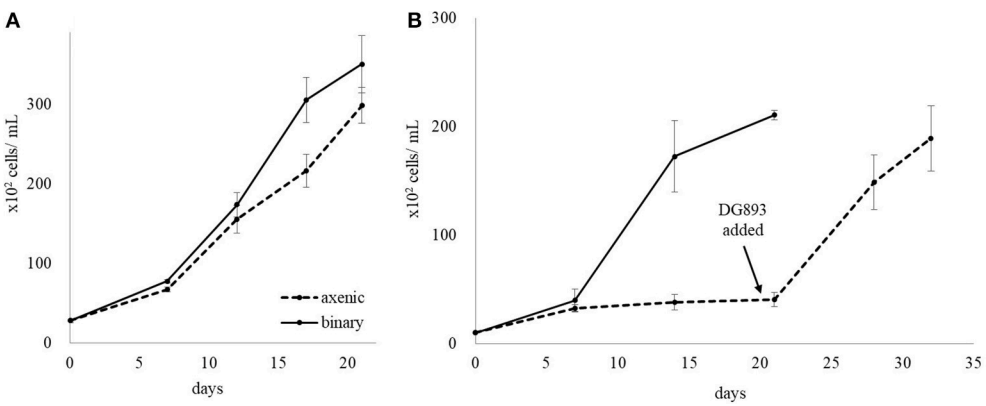

FIGURE 3 | Rescue of *L. polyedrum* by addition of DG893. **(A)** First generation of *L. polyedrum* growth maintained in L1 media either "axenic" or co-cultured with DG893. **(B)** Growth of *L. polyedrum* in the second subculture either "axenic" or co-cultured with DG893. After the second subculture of "axenic" *L. polyedrum* was incubated under the standard growth conditions for 21 days, an inoculum containing approximately 10^2 cells/mL of DG893 was added and incubation continued for an additional 14 days.

die out, the few cells that survived had their swimming activity under the microscope clearly reduced.

Axenic *L. polyedrum* Culture and Rescue

The growth of "axenic" and binary cultures of *L. polyedrum* with DG893 in L1 was compared over several subsequent batch cultures. No significant difference in growth was observed in the 1st culture, however, a clear difference was observed in the 2nd subsequent batch culture of *L. polyedrum* with and without DG893. While *L. polyedrum* with DG893 grew fully in both the 1st and 2nd subsequent batch cultures, "axenic" *L. polyedrum* ceased to grow (**Figure 3**). When DG893 was added to the 2nd subsequent "axenic" batch culture, *L. polyedrum* cells began to regrow exponentially demonstrating that DG893 could rescue "axenic" *L. polyedrum*.

Non-axenic *L. polyedrum* Growth and Rescue

The non-axenic *L. polyedrum* was maintained in L1 medium and assumed to contain not only siderophore-producing bacteria but also other unknown bacteria. The non-axenic culture was divided in two parts, one diluted to 1/5 with L1 medium and other diluted to 1/5 with L1-Fe medium (batch subculture 1). When the cell count reached approximately 10^4 cells/mL, both cultures were further diluted with appropriate medium. Therefore, one culture maintained $[Fe]_T$ at L1 level throughout the subsequent batch cultures while the other contained successively reduced $[Fe]_T$. The *L. polyedrum* growth was monitored for 28 days for each subculture. After the 6th subculture where $[Fe]_T$ in the medium was estimated to be 2 nM, *L. polyedrum* stopped growing completely (**Figure 4**). On 29th day of the 6th subculture, an iron supplement to give a $[Fe]_T$ of 5,850 nM was added to the culture and growth was continued to be monitored for additional 28 days. The results indicate that the *L. polyedrum* culture which stopped growing under 2 nM $[Fe]_T$, could be rescued by addition of iron after 28 days (**Figure 5**).

L. polyedrum Growth in DG893 Supernatant

Earlier it was stated that when *L. polyedrum* was co-cultured with either DG893 or the mutant Δ*pvsAB*-DG893, little difference was observed in its growth pattern. We speculated that this may have been due to the small amount of VF produced by the equilibrium population of DG893 in the binary culture. To test this idea, samples of the supernatant of the media from the WT DG893 grown under ideal conditions and containing detectable amounts of VF by CAS-dye assay, as well as the mutant Δ*pvsAB*-DG893 which did not, respectively, were added to *L. polyedrum* cultures and growth under these different conditions was compared. It should be noted that while we traditionally grow DG893 and the mutant in marine broth containing Casamino Acids, these were found to be toxic to *L. polyedrum* cells. In this experiment, we instead used ASW with succinic acid (at from 0.001 to 0.1%) as a carbon source (pH 8.2) to grow DG893 and the mutants prior to their supernatant being added to *L. polyedrum* cultures. *L. polyedrum* growth was enhanced the most by the addition of the DG893 supernatant. The mutant supernatant also showed a slightly positive effect on *L. polyedrum* growth compared to media without bacterial supernatant, however the degree of growth was not as large as that induced by the DG893 supernatant (**Figure 6**). These results suggest that VF has potential influence on *L. polyedrum* growth, but that other extracts from bacteria (vitamin B_{12}?) may also have a potential effect on their growth. Further experiments were performed using purified VF itself. When purified VF at 57 μM was directly added to a *L. polyedrum* culture in L1 media containing 100 nM $[Fe]_T$, *L. polyedrum* reached cell counts approximately 1.5 times as large as those in media without VF.

DG893 Growth in *L. polyedrum* Supernatant

"Axenic" *L. polyedrum* cells were resuspended in L1 media containing 100, 1,000, 10,000 nM $[Fe]_T$ and incubated under the standard growth conditions for 2 days to collect their organic extracts. The *L. polyedrum* cultures were divided in two parts, one of which was filtered through a 0.22 μm membrane to collect only organics and the other was kept without filtration to keep phytoplankton cell debris. The *L. polyedrum* supernatant with and without cells was added to the stock DG893 containing 0.3% Casamino Acids, and the mixture shaken at 30°C for several days. The control was prepared in the same manner without *L. polyedrum* supernatant and cells. In the media containing 1,000 and 10,000 nM $[Fe]_T$, DG893 growth was enhanced by the presence of *L. polyedrum* supernatant and was even more pronounced with the supernatant containing cell debris (**Figure 7**). In media with 100 nM $[Fe]_T$, only a subtle difference was observed in DG893 growth with and without *L. polyedrum* supernatant.

DISCUSSION

Before proceeding to a discussion of the results presented here it is important to operationally define what we mean by $[Fe]_T$ and "axenic" cultures. Here we used the term total iron concentrations $[Fe]_T$ to mean the total analytical amount of iron added to culture and includes all phases of iron present in the solution. This is different from the total dissolved iron concentration which we routinely measure for environmental seawater samples (and which is approximately 2–6 nM for Scripps Pier water for example) as determined by cathodic stripping voltammetry (CSV). Total dissolved iron in such environmental samples are processed by filtration through a 0.22 μm membrane followed by acidification. As a result, total dissolved iron in a sample is much lower than the total analytical iron concentration. We use this operational definition as it is not possible to measure total dissolved iron in culture media using the CSV method because equilibrium between the various iron oxo/hydroxo species potentially present in seawater at pH 8.2 is reached only extremely slowly and thus concentrations of total dissolved iron are constantly changing over the time course utilized in these experiments. Using a straight forward expression of total analytical iron concentration is thus a potentially more

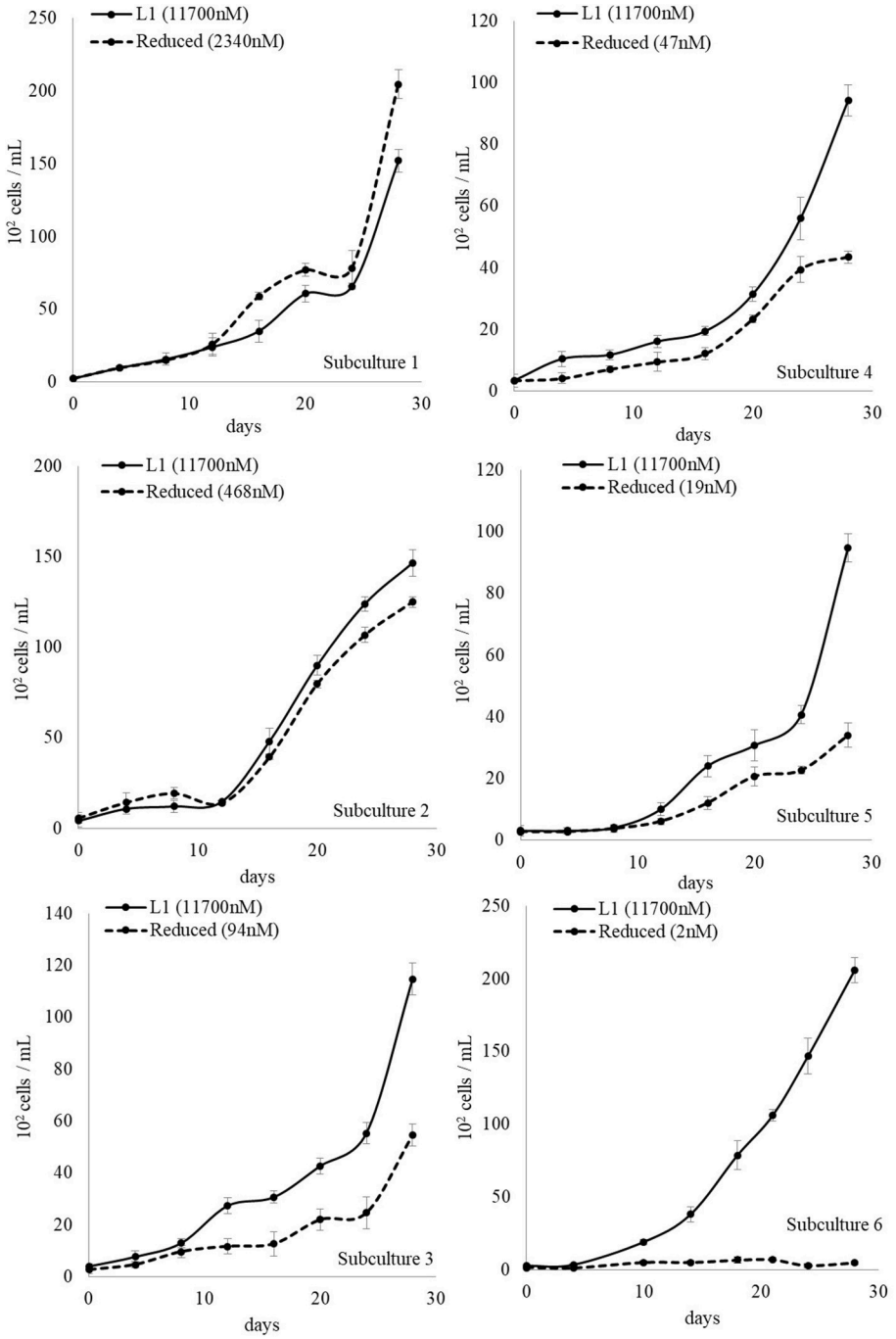

FIGURE 4 | Non-Axenic *L. polyedrum* growth in L1 media and reduced $[Fe]_T$ over 6 subculturings. Solid line: cultures maintained with a $[Fe]_T$ at the L1 level throughout the subculturing. Dotted line: cultures where the $[Fe]_T$ continually decreased over the subcultures due to dilution.

reproducible approach with which to compare the effects of iron on bacterial and algal growth in a laboratory setting.

Secondly we use the term "axenic" in quotation marks for describing cultures of *L. polyedrum*, to mean the absence of any observable *cultureable* bacteria based on the absence of visual bacterial colonies when cultures were placed on solid media and incubated for several days. We were only partially successful making the culture "axenic" by treating the culture with low concentration of antibiotics and sequential addition of the antibiotics to the culture over extended times. Using this method the culture appeared to remain bacteria free for at least a month. However when the sequential addition of antibiotics to

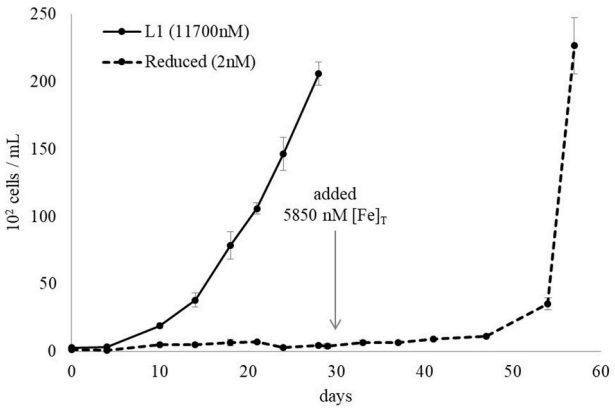

FIGURE 5 | Iron starved non-axenic *L. polyedrum* growth rescued by iron addition. The iron sufficient culture (solid black line) contained 11,700 nM $[Fe]_T$ while the iron deficient culture contained 2 nM (dotted black line). After 28 days 5,850 nM $[Fe]_T$ was added to the iron deficient culture which rescued *L. polyedrum* growth.

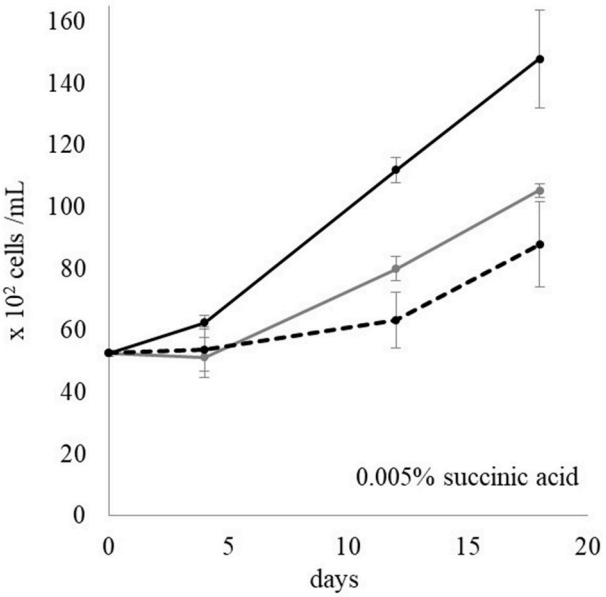

FIGURE 6 | *L. polyedrum* growth in media with DG893 supernatant, mutant supernatant, and without bacterial supernatant. The black lines, gray lines, and dotted lines represent *L. polyedrum* growth in media with added DG893 supernatant, with added VF null mutant supernatant, and without any bacterial supernatant, respectively.

the culture was stopped, bacteria growth was observed to return within a few days. Thus clearly the cultures were not truly axenic. Nevertheless our main concern was that the dominant species of bacteria growing in our binary culture should be DG893 and that "axenic" cultures should contain insignificant numbers of unknown bacteria. We confirmed the former by qPCR and the latter was further supported by presence of few if any bacteria seen via DAPI staining. To our knowledge, there is at present no general protocol for preparing a completely axenic culture *of L. polyedrum* hence our use of the operational definition of "axenic" described here.

We initially investigated conditions under which the bacterium *Marinobacter* DG893 and the dinoflagellate *L. polyedrum* could grow independently. As expected, in the absence of an added carbon source DG893 could not grow in natural unamended seawater or in L1 supplemented ASW irrespective of the iron concentration. In the presence of an adequate artificial source of carbon however bacterial growth was controlled by the available concentration of iron. Under idealized conditions, both DG893 and the VF null mutant reached a final concentration of around 10^5 CFU/mL independent of the initial inoculum. However even *without any externally added carbon source* DG893 grew well in the presence of *L. polyedrum* indicating that the dinoflagellate leaked enough dissolved organic carbon (DOC) to fully support the growth of the bacterium. The notion that DG893 could utilize *L. polyedrum* as a carbon source was further supported by the observation that growth of DG893 was stimulated when it was incubated in the media containing the supernatant from a filtered *L. polyedrum* culture which contains non-specific organics secreted from *L. polyedrum*. These may possibly include dimethylsulfoniopropionate (DMSP) a labile carbon and sulfur source known to "leaked" from dinoflagellates (Caruana and Malin, 2014).

In the case of both "axenic" and nonaxenic cultures of the photosynthetic dinoflagellate *L. polyedrum*, iron proved to be a growth limiting nutrient. Thus maximum growth occurred at total iron concentrations of 100–1,000 nM while higher concentrations proved toxic and lower concentrations (0–10 nM) were growth limiting. In the first culture, both "axenic" and non-axenic cultures grew equally well. However, their growth showed a remarkable difference in the second batch subculture. Here the non-axenic *L. polyedrum* culture continued to grow exponentially although now only at the higher $[Fe]_T$. When the iron concentrations were kept high, *L. polyedrum* cultures continued to thrive up to at least 6 subcultures. However when the iron concentrations were allowed to be reduced by dilution in subsequent subculturing, the growth gradually ceased. Poorly growing subcultures in low iron media could however be rescued by the addition of additional iron to the culture. Remarkably "axenic" *L. polyedrum* subcultures ceased to grow regardless of $[Fe]_T$ but could be rescued by the addition of DG893. These results emphasize the importance of both bacteria and iron to *L. polyedrum* growth.

Our results further suggest that the *L. polyedrum* growth promoting effects of the bacterium *Marinobacter* DG893 were in fact not unspecific but at least partially related to its production of the photoactive siderophore vibrioferrin. Thus only the supernatant of DG893 that contained sufficient amounts of vibrioferrin facilitated *L. polyedrum* growth. While the addition of the supernatant from a culture of the VF null mutant of DG893 also improved growth of *L. polyedrum* the effect was much less than that from the WT. This observation was further confirmed by direct addition of purified VF into

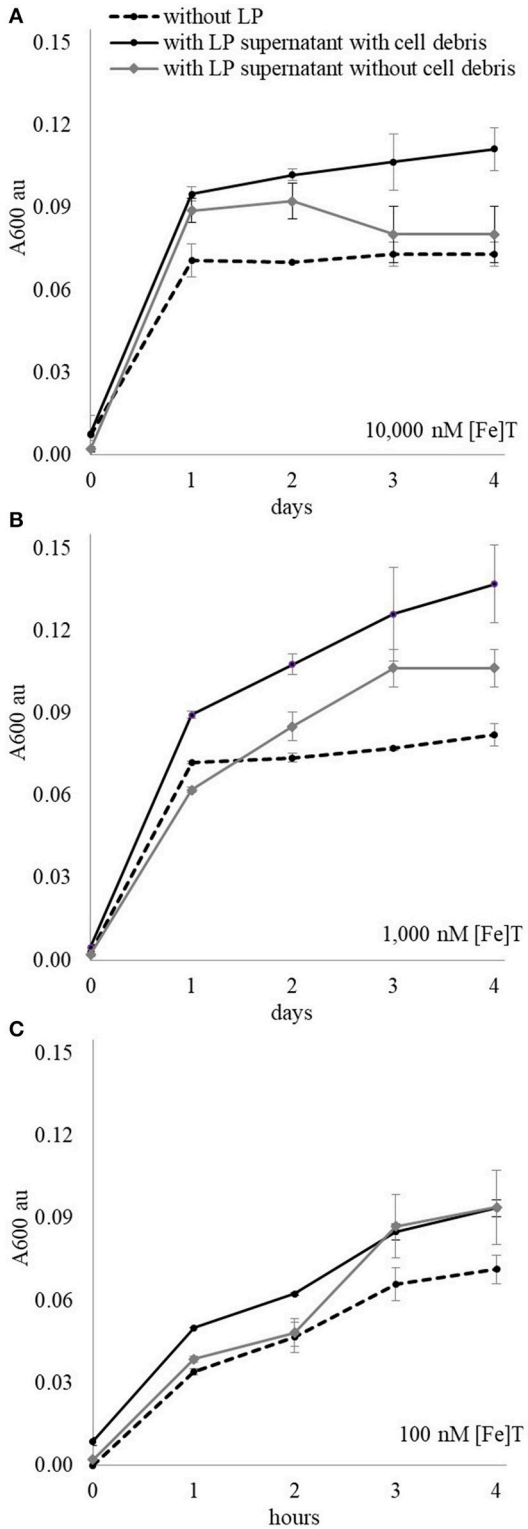

FIGURE 7 | DG893 growth in media containing different $[Fe]_T$ with and without presence of *L. polyedrum* supernatant and cell debris. The solid black lines represent growth of DG893 in the presence of *L. polyedrum* supernatant with their cell debris, the gray lines are DG893 growth in *L. polyedrum* supernatant without their cell debris, and the dotted lines are DG893 without any *L. polyedrum supernantant*. DG893 was grown in media containing **(A)** 10,000 nM $[Fe]_T$, **(B)** 1,000 nM $[Fe]_T$, and **(C)** 100 nM $[Fe]_T$.

the *L. polyedrum* culture which growth increased 1.5 times more than those without VF. These results imply that the presence of the siderophore vibrioferrin clearly influences *L. polyedrum* growth, but that other factors such as vitamin B12 (Cruz-Lopez and Maske, 2015) provided by bacteria may also be important in promoting this apparent bacterial-algal mutualism.

Here we have focused on a bacteria that produces the photoreactive siderophore, vibrioferrin. Vibrioferrin was chosen for more detailed study for a number of reasons. First vibrioferrin has been isolated from several different bacteria which are known to be closely associated with HAB species (Amin et al., 2007) and we found that bacteria that had the ability to synthesize vibrioferrin were by far the most numerous as compared to the producers of other photoreactive siderophores which we followed during the bloom of *L. polyedrum* at Scripps Pier in 2011 (Yarimizu et al., 2014). We initially supposed that vibrioferrin was a good candidate for a siderophore that could provide bioavailable iron for both the bacterial producers and their algal partners as it is the most rapidly photolyzed of the photoactive siderophores tested and that photolyzed vibrioferrin has no further affinity for iron. This feature is unusual in that most other photoactive siderophores retain the ability to strongly bind Fe(III) even after photolysis (Amin et al., 2009b). However we have recently shown that while vibrioferrin was the best source of iron for *L. polyedrum* of the ones we tested (Yarimizu et al., 2017), it was not due to its photolysis since iron uptake from VF was the same in the dark as in the light. We therefore attribute its ability to provide bioavailable iron to the dinoflagellate to its relatively weak iron binding properties (with respect to other more traditional siderophores) as it lacks the sixth donor group required to complete the octahedral coordination geometry preferred by Fe(III) (Amin et al., 2009b). This in turn leads to a less negative reduction potential (that falls within the biological range) so that the iron can readily be released from it by the cell surface reductases known to be present in *L. polyedrum*.

As a final note, while this laboratory study strongly supports a carbon for iron mutualism between the dinoflagellate *L. polyedrum* and *Marinobacter* DG893 as previously proposed (Amin et al., 2009a), it is unclear at present how, or indeed if, such a mutualism will operate in the field. To this end we have collected data from several field studies involving both HAB and non-HAB bloom events and are currently searching for relationships between phytoplankton, vibrioferrin producing bacteria, and available iron. We hope that both these laboratory and field studies will complement each other and advance our knowledge of the potential role of bacterial-algal interactions in understanding the mechanisms of HAB formation.

AUTHOR CONTRIBUTIONS

KY, RC-L, and CC designing the study, executing the experiments, analyzing the data, interpreting the data, reviewing the data for accuracy and integrity, drafting the work, and revising this report.

ACKNOWLEDGMENTS

We thank Avery Tatters (University of Southern California) for providing the *L. polyedrum* strain and helping us to set up an algal culture laboratory. We thank Professor Michael Latz (Scripps Institute of Oceanography) for providing us *L. polyedrum*. We also thank Professor Katharine Barbeau (Scripps Institute of Oceanography) for providing us Pacific Ocean oligotrophic water and advice on iron measurement techniques as well as Professor Frithjof C. Küpper (University of Aberdeen) for a critical reading of the manuscript. A National Science Foundation grant to CJC (CHE-1664657) is gratefully acknowledged for partial support of this work.

REFERENCES

Alexander, D. B., and Zuberer, D. A. (1991). Use of chrome azurol S reagents to evaluate siderophore production by rhizosphere bacteria. *Biol. Fertil. Soils* 12, 39–45. doi: 10.1007/BF00369386

Amin, S. A., Green, D. H., Al Waheeb, D., Gärdes, A., and Carrano, C. J. (2012a). Iron transport in the genus *Marinobacter*. *Biometals* 25, 135–147. doi: 10.1007/s10534-011-9491-9

Amin, S. A., Green, D. H., Gärdes, A., Romano, A., Trimble, L., and Carrano, C. J. (2012b). Siderophore-mediated iron uptake in two clades of *Marinobacter* spp. associated with phytoplankton: the role of light. *Biometals* 25, 181–192. doi: 10.1007/s10534-011-9495-5

Amin, S. A., Green, D. H., Hart, M. C., Küpper, F. C., Sunda, W. G., and Carrano, C. J. (2009a). Photolysis of iron–siderophore chelates promotes bacterial–algal mutualism. *Proc. Natl. Acad. Sci. U.S.A.* 106, 17071–17076. doi: 10.1073/pnas.0905512106

Amin, S. A., Green, D. H., Küpper, F. C., and Carrano, C. J. (2009b). Vibrioferrin, an unusual marine siderophore: iron binding, photochemistry, and biological implications. *Inorg. Chem.* 48, 11451–11458. doi: 10.1021/ic9016883

Amin, S. A., Hmelo, L. R., van Tol, H. M., Durham, B. P., Carlson, L. T., Heal, K. R., et al. (2015). Interaction and signalling between a cosmopolitan phytoplankton and associated bacteria. *Nature* 522, 98–101. doi: 10.1038/nature14488

Amin, S. A., Küpper, F. C., Green, D. H., Harris, W. R., and Carrano, C. J. (2007). Boron binding by a siderophore isolated from marine bacteria associated with the toxic dinoflagellate *Gymnodinium catenatum*. *J. Am. Chem. Soc.* 129, 478–479. doi: 10.1021/ja067369u

Anderson, D. M. (1994). Red tides. *Sci. Am.* 271, 52–58. doi: 10.1038/scientific american0894-62

Azam, F., and Malfatti, F. (2007). Microbial structuring of marine ecosystems. *Nat. Rev. Microbiol.* 5, 782–791. doi: 10.1038/nrmicro1747

Barbeau, K., Rue, E. L., Bruland, K. W., and Butler, A. (2001). Photochemical cycling of iron in the surface ocean mediated by microbial iron(iii)-binding ligands. *Nature* 413, 409–413. doi: 10.1038/35096545

Barbeau, K., Zhang, G., Live, D. H., and Butler, A. (2002). Petrobactin, a photoreactive siderophore produced by the oil-degrading marine bacterium *Marinobacter hydrocarbonoclasticus*. *J. Am. Chem. Soc.* 124, 378–379. doi: 10.1021/ja0119088

Bell, W. H., and Lang, J. M. (1974). Selective stimulation of marine bacteria by algal extracellular products. *Limnol. Oceanogr.* 19, 833–839. doi: 10.4319/lo.1974.19.5.0833

Bell, W., and Mitchell, R. (1972). Chemotactic and growth responses of marine bacteria to algal extracellular products. *Biol. Bull.* 143, 265–277. doi: 10.2307/1540052

Bertrand, E. M., McCrow, J. P., Moustafa, A., Zheng, H., McQuaid, J. B., Delmont, T. O., et al. (2015). Phytoplankton-bacterial interactions mediate micronutrient colimitation at the coastal Antarctic sea ice edge. *Proc. Natl. Acad. Sci. U.S.A.* 112, 9938–9943. doi: 10.1073/pnas.1501615112

Braun, V. (1995). Energy-coupled transport and signal transduction through the gram-negative outer membrane via TonB-ExbB-ExbD-dependent receptor proteins. *FEMS Microbiol. Rev.* 16, 295–307. doi: 10.1111/j.1574-6976.1995.tb00177.x

Braun, V., Hantke, K., and Köster, W. (1998). Bacterial iron transport: mechanisms, genetics, and regulation. *Met. Ions Biol. Syst.* 35, 67–145.

Bruland, K. W., and Franks, R. P. (1979). Sampling and analytical methods for the determination of copper, cadmium, zinc, and nickel at the nanogram per liter level in sea water. *Anal. Chim. Acta* 105, 233–245. doi: 10.1016/S0003-2670(01)83754-5

Burkholder, J. M. (1998). Implications of harmful microalgae and heterotrophic dinoflagellates in management of sustainable marine fisheries. *Ecol. Appl.* 8, S37–S62. doi: 10.1890/1051-0761(1998)8[S37:IOHMAH]2.0.CO;2

Caruana, A. M. N., and Malin, G. (2014). The variability in DMSP content and DMSP lyase activity in marine dinoflagellates. *Prog. Oceanogr.* 120, 410–424. doi: 10.1016/j.pocean.2013.10.014

Challis, G. L. (2005). A widely distributed bacterial pathway for siderophore biosynthesis independent of nonribosomal peptide synthetases. *Chembiochem* 6, 601–611. doi: 10.1002/cbic.200400283

Croot, P. L., and Heller, M. I. (2012). The importance of kinetics and redox in the biogeochemical cycling of iron in the surface ocean. *Front. Microbiol.* 3:219. doi: 10.3389/fmicb.2012.00219

Cruz-Lopez, R., and Maske, H. (2015). A non-amplified FISH protocol to identify simultaneously different bacterial groups attached to eukaryotic phytoplankton. *J. Appl. Phycol.* 27, 797–804. doi: 10.1007/s10811-014-0379-2

Glibert, P. M., Anderson, D. M., Gentien, P., Granéli, E., and Sellner, K. G. (2005). The global complex phenomena of harmful algae blooms. *Oceanography* 18, 130–141. doi: 10.5670/oceanog.2005.49

Green, D. H., Llewellyn, L. E., Negri, A. P., Blackburn, S. I., and Bolch, C. J. (2004). Phylogenetic and functional diversity of the cultivable bacterial community associated with the paralytic shellfish poisoning dinoflagellate *Gymnodinium catenatum*. *FEMS Microbiol. Ecol.* 47, 345–357. doi: 10.1016/S0168-6496(03)00298-8

Guillard, R. R. L., and Hargraves, P. E. (1993). Stichochrysis immobilis is a diatom, not a chrysophyte. *Phycologia* 32, 234–236. doi: 10.2216/i0031-8884-32-3-234.1

Hallegraeff, G., and Gollasch, S. (2006). "Ecological studies: ecology of harmful algae," in *Anthropogenic Introductions of Microalgae*, eds M. M. Caldwell, G. Heldmaier, R. B. Jackson, O. L. Lange, H. A. Mooney, E.-D. Schulze, and U. Sommer (Berlin; Heidelberg: Springer), 379–402.

Hoagland, P., and Scatasta, S. (2006). "Ecological studies: ecology of harmful algae," in *The Economic Effects of Harmful Algal Blooms*, eds M. M. Caldwell, G. Heldmaier, R. B. Jackson, O. L. Lange, H. A. Mooney, E.-D. Schulze, and U. Sommer (Berlin; Heidelberg: Springer), 391–402.

Honner, S., Kudela, R. M., and Handler, E. (2012). Bilateral mastoiditis from red tide exposure. *J. Emerg. Med.* 43, 663–666. doi: 10.1016/j.jemermed.2010.06.007

Jauzein, C., Evans, A. N., and Erdner, D. L. (2015). The impact of associated bacteria on morphology and physiology of the dinoflagellate *Alexandrium tamarense*. *Harmful Algae* 50, 65–75. doi: 10.1016/j.hal.2015.10.006

Küpper, F. C., Carrano, C. J., Kuhn, J.-U., and Butler, A. (2006). Photoreactivity of iron(III)-aerobactin: photoproduct structure and iron(III) coordination. *Inorgan. Chem.* 45, 6028–6033. doi: 10.1021/ic0604967

Lewitus, A. J., Horner, R. A., Caron, D. A., Garcia-Mendoza, E.,Hickey, B. M., Hunter, M., et al. (2012). Harmful algal blooms along the North American west coast region: history, trends, causes, and impacts. *Harmful Algae* 19, 133–159. doi: 10.1016/j.hal.2012.06.009

Liu, C. L., Place, A. R., and Jagus, R. (2017). Use of antibiotics for maintenance of axenic cultures of amphidinium carterae for the analysis of translation. *Marin Drugs* 15:242. doi: 10.3390/md15080242

Lupette, J., Lami, R., Krasovec, M., Grimsley, N., Moreau, H., Piganeau, G., et al. (2016). Marinobacter dominates the bacterial community of the *Ostreococcus tauri* phycosphere in culture. *Front. Microbiol.* 7:1414. doi: 10.3389/fmicb.2016.01414

Maldonado, M. T., Strzepek, R. F., Sander, S., and Boyd, P. W. (2005). Acquisition of iron bound to strong organic complexes, with different Fe binding groups and photochemical reactivities, by plankton communities in Fe-limited subantarctic waters. *Glob. Biogeochem. Cycles* 19:GB4S23. doi: 10.1029/2005GB002481

Martin, J. H., and Fitzwater, S. E. (1988). Iron deficiency limits phytoplankton growth in the north-east Pacific subarctic. *Nature* 331, 341–343. doi: 10.1038/331341a0

McQuaid, J. B., Kustka, A. B., Oborník, M., Horák, A., McCrow, J. P., Karas, B. J., et al. (2018). Carbonate-sensitive phytotransferrin controls high-affinity iron uptake in diatoms. *Nature* 555, 534–537. doi: 10.1038/nature25982

Miethke, M., and Marahiel, M. A. (2007). Siderophore-based iron acquisition and pathogen control. *Microbiol. Mol. Biol. Rev.* 71, 413–451. doi: 10.1128/MMBR.00012-07

Naito, K., Imai, I., and Nakahara, H. (2008). Complexation of iron by microbial siderophores and effects of iron chelates on the growth of marine microalgae causing red tides. *Phycol. Res.* 56, 58–67. doi: 10.1111/j.1440-1835.2008.00485.x

Ramanan, R., Kim, B. H., Cho, D. H., Oh, H. M., and Kim, H. S. (2016). Algae-bacteria interactions: evolution, ecology and emerging applications. *Biotechnol. Adv.* 34, 14–29. doi: 10.1016/j.biotechadv.2015.12.003

Raven, J. A. (2013). Iron acquisition and allocation in stramenopile algae. *J. Exp. Bot.* 64, 2119–2127. doi: 10.1093/jxb/ert121

Raymond, K. N., Allred, B. E., and Sia, A. K. (2015). Coordination chemistry of microbial iron transport. *Acc. Chem. Res.* 48, 2496–2505. doi: 10.1021/acs.accounts.5b00301

Roegner, G. C., Hickey, B. M., Newton, J. A., Shanks, A. L., and Armstrong, D. A. (2002). Wind-induced plume and bloom intrusions into Willapa Bay, Washington. *Limnol. Oceanogr.* 47, 1033–1042. doi: 10.4319/lo.2002.47.4.1033

Sandy, M., and Butler, A. (2009). Microbial iron acquisition: marine and terrestrial siderophores. *Chem. Rev.* 109, 4580–4595. doi: 10.1021/cr9002787

Seymour, J. R., Amin, S. A., Raina, J. B., and Stocker, R. (2017). Zooming in on the phycosphere: the ecological interface for phytoplankton-bacteria relationships. *Nat. Microbiol.* 2:17065. doi: 10.1038/nmicrobiol.2017.65

Sutak, R., Botebol, H., Blaiseau, P. L., Léger, T., Bouget, F. Y., Camadro, J. M., et al. (2012). A comparative study of iron uptake mechanisms in marine microalgae: iron binding at the cell surface is a critical step. *Plant Physiol.* 160, 2271–2284. doi: 10.1104/pp.112.204156

Tubaroa, A., Sosaa, S., Altiniera, G., Soranzob, M. R., Satakec, M., Loggiaa, R. D., et al. (2004). Short-term oral toxicity of homoyessotoxins, yessotoxin and okadaic acid in mice. *Toxicon* 43, 439–445. doi: 10.1016/j.toxicon.2004.02.015

Tweddle, J. F., Strutton, P. G., Foley, D. G., O'Higgins, L., Wood, A. M., Scott, B., et al. (2010). Relationships among upwelling, phytoplankton blooms, and phycotoxins in coastal Oregon shellfish. *Mar. Ecol. Prog. Ser.* 405, 131–145. doi: 10.3354/meps08497

Vraspir, J. M., and Butler, A. (2009). Chemistry of marine ligands and siderophores. *Ann. Rev. Mar. Sci.* 1, 43–63. doi: 10.1146/annurev.marine.010908.163712

Wu, J., and Luther, G. W. III. (1994). Size-fractionated iron concentrations in the water column of the western North Atlantic Ocean. *Limnol. Oceanogr.* 39, 1119–1129. doi: 10.4319/lo.1994.39.5.1119

Yamamoto, S., Okujo, N., Yoshida, T., Matsuura, S., and Shinoda, S. (1994). Structure and iron transport activity of vibrioferrin, a new siderophore of *Vibrio parahaemolyticus*. *J. Biochem.* 115, 868–874. doi: 10.1093/oxfordjournals.jbchem.a124432

Yarimizu, K., Cruz-López, R., Auerbach, H., Heimann, L., Schünemann, V., and Carrano, C. J. (2017). Iron uptake and storage in the HAB dinoflagellate Lingulodinium polyedrum. *Biometals*, 30, 945–953. doi: 10.1007/s10534-017-0061-7

Yarimizu, K., Polido, G., Gärdes, A., Carter, M. L., Hilbern, M., and Carrano, C. J. (2014). Evaluation of photo-reactive siderophore producing bacteria before, during and after a bloom of the dinoflagellate *Lingulodinium polyedrum*. *Metallomics* 6, 1156–1163. doi: 10.1039/C4MT00053F

Conflict of Interest Statement: The authors declare that the research was conducted in the absence of any commercial or financial relationships that could be construed as a potential conflict of interest.

frontiers in Marine Science

ORIGINAL RESEARCH
published: 29 May 2018
doi: 10.3389/fmars.2018.00188

The Bacterial Symbiont *Phaeobacter inhibens* Shapes the Life History of Its Algal Host *Emiliania huxleyi*

Anna R. Bramucci[1†], *Leen Labeeuw*[1†‡], *Fabini D. Orata*[1†], *Elizabeth M. Ryan*[2], *Rex R. Malmstrom*[2] *and Rebecca J. Case*[1*]

[1] Department of Biological Sciences, University of Alberta, Edmonton, AB, Canada, [2] Department of Energy Joint Genome Institute, Walnut Creek, CA, United States

OPEN ACCESS

Edited by:
Matthias Wietz,
University of Oldenburg, Germany

Reviewed by:
Rurun Wang,
Merck, United States
Hui Wang,
Helmholtz-Zentrum für Infektionsforschung (HZI), Germany

***Correspondence:**
Rebecca J. Case
rcase@ualberta.ca

[†] *These authors have contributed equally to this work.*

[‡] ***Present Address:***
Leen Labeeuw,
Plant Functional Biology and Climate Change Cluster (C3), University of Technology Sydney, Ultimo, NSW, Australia
Fabini D. Orata,
Department of Chemical and Materials Engineering, University of Alberta, Edmonton, AB, Canada

Specialty section:
This article was submitted to Microbial Symbioses, a section of the journal Frontiers in Marine Science

Received: *17 February 2018*
Accepted: *09 May 2018*
Published: *29 May 2018*

Citation:
Bramucci AR, Labeeuw L, Orata FD, Ryan EM, Malmstrom RR and Case RJ (2018) The Bacterial Symbiont Phaeobacter inhibens Shapes the Life History of Its Algal Host Emiliania huxleyi. Front. Mar. Sci. 5:188. doi: 10.3389/fmars.2018.00188

Marine microbes form host-associated biofilm communities that are shaped by complex interactions between bacteria and their host. The roseobacter *Phaeobacter inhibens* exploits both symbiotic and pathogenic niches while interacting with its microalgal host *Emiliania huxleyi*. During co-cultivation over extended periods with *E. huxleyi,* we show that *P. inhibens* selectively kills two host cell types, the diploid calcifying strain and the haploid flagellated strain. Meanwhile, various non-calcifying diploid strains are resistant to this pathogen or the pathogen is avirulent to this cell type. This differential pathogenesis has the potential of dramatically altering the composition of *E. huxleyi* blooms, which are typically dominated by the roseobacter-susceptible calcifying strain. This cell type makes calcite plates, which are an important sink in the marine carbon cycle and forms part of the marine paleobotanic record. *P. inhibens* kills the haploid cells, which have been proposed as critical to the survival of the algae, as they readily escape both eukaryotic predation and viral infection. Consequently, bacteria such as *P. inhibens* could influence *E. huxleyi's* life history by selective pathogenesis, thereby altering the composition of cell types within *E. huxleyi* populations and its bloom-bust lifestyle.

Keywords: coccolithophore, roseobacter, phytoplankton pathogen, marine pathogens, pathogen ecology, cell type, phytoplankton life history, bacterial–algal interactions

INTRODUCTION

On a microscopic scale, the marine environment is a heterogeneous mixture of nutrient "hotspots" formed by plankton and marine snow (Azam, 1998). Marine microbes take advantage of this aquatic array of nutrient gradients and "hotspots" by preferentially occupying specific niches (Hunt et al., 2008; Stocker, 2012). Motile microbes capable of directly associating with phytoplankton thereby expose themselves to a continuous stream of metabolites leaked from their algal hosts (Sapp et al., 2007; Geng and Belas, 2010; Sule and Belas, 2013). The concentrations of these metabolites are at their highest at the cell surface and within the phycosphere (Bell and Mitchell, 1972), the area immediately surrounding an algal cell, suggesting that algal-associated bacteria experience the greatest nutrient benefit and most likely to exchange communication and bioactive molecules.

While many bacteria directly benefit from algal metabolites exuding out of leaky or dying algae, some bacteria have fine-tuned their ability to sense and respond to host molecules by expressing symbiotic or pathogenic traits (Miller et al., 2004; Tripp et al., 2008; Seymour et al., 2010; Case et al., 2011; Wang et al., 2014; Amin et al., 2015) or releasing bioactive molecules that in turn

alter the host's behavior or survival (Seyedsayamdost et al., 2011b; Labeeuw et al., 2017). Some bacteria engage in symbiotic relationships with their algal host by producing small molecules, such as vitamins or growth hormones, that are beneficial or even required by the alga (Bolch et al., 2011). Other bacteria use bioactive molecules in pathogenesis to coordinate virulence or kill their host (Ashen et al., 1999; Fernandes et al., 2011; Seyedsayamdost et al., 2011b; Gardiner et al., 2017).

The haptophyte *Emiliania huxleyi*, which dominates coccolithophore blooms (Baumann et al., 2008), has recently been described as a host for bacteria in the marine environment (Seyedsayamdost et al., 2011b; Segev et al., 2016). It can quickly form dense populations ($>10^6$ cells·L^{-1}) (Rhodes et al., 1995; Tyrrell and Merico, 2004) over vast expanses of the upper ocean (>250,000 km^2) (Holligan et al., 1993). Its bloom-bust life cycle dramatically restructures the marine ecosystem, as it becomes a habitat-forming species for bacteria and viruses in the open ocean. Bloom formation has been associated with a variety of environmental factors (Tyrrell and Merico, 2004), while bloom collapse is frequently attributed to viral infection or microzooplankton grazing (Wolfe et al., 1994, 1997; Wilson et al., 2002). The ubiquity and abundance of *E. huxleyi* in the oceans, as well as its production of important intermediates in the carbon and sulfur biogeochemical cycles, have made it an important model phytoplankton species.

The *E. huxleyi* species complex, with an average diameter of 5–7 μm, has three distinct cell types: non-motile non-calcifying cells (N-type, diploid), non-motile coccolith-bearing cells (C-type, diploid), and motile scale-bearing cells (S-type, haploid) (Klaveness, 1972; Rhodes et al., 1995; Frada et al., 2012; von Dassow et al., 2015). *E. huxleyi* blooms are comprised of complex mixtures of C and S cells (Klaveness, 1972), though the fast growing calcifying C cells make up the majority of the bloom (Bidle et al., 2007; Baumann et al., 2008). It is not presently understood how these three cell types interact or alternate to shape the alga's life history, but each cell type is capable of asexual proliferation (Klaveness, 1972). However, the ways in which these different cell types impact the ecology, evolution, interactions, and metabolites of the *E. huxleyi* species complex is largely unknown, except for its interaction with viruses (EhVs). EhVs kill both diploid cell types (C and N) while S cells are resistant to infection (Wilson et al., 2002; Frada et al., 2008). Once an EhV infects a diploid cell, it proliferates and produces the viral glycosphingolipids that kill the algal cell (Vardi et al., 2009). Viral infection triggers caspase-like activity in *E. huxleyi* (associated with an upregulation of algal metacaspases), suggesting that the virus is hijacking algal programmed cell death (PCD) machinery to kill the host (Bidle et al., 2007).

Although viral infection and grazers have been studied (Wolfe et al., 1994; Wilson et al., 2002), the association of bacteria with *E. huxleyi* is largely unexplored (Seymour et al., 2010; Curson et al., 2011). We have investigated how *E. huxleyi* interacts with the marine α-proteobacteria *Phaeobacter inhibens* DSM 17395, previously named *Phaeobacter gallaeciensis* BS107 (Seyedsayamdost et al., 2011b). *P. inhibens* is a member of the roseobacter clade that is frequently identified within *E. huxleyi* blooms (González et al., 2000; Green et al., 2015; Segev et al., 2016). This bacterium produces a number of novel bioactives, including the antibiotic tropodithetic acid (TDA) (Geng et al., 2008; Berger et al., 2011; Thole et al., 2012) and potent algaecides called roseobacticides (Seyedsayamdost et al., 2011b, 2014) and roseochelins (Wang and Seyedsayamdost, 2017). These bioactives might allow *P. inhibens* to live a duplicitous lifestyle as both a beneficial symbiont and as a pathogen. TDA has been implicated in *P. inhibens*' chemical defense of various hosts (D'Alvise et al., 2012; Prol García et al., 2013; Beyersmann et al., 2017). Indeed, this bacterium is a symbiont of *Ulva australis*, chemically defending this ubiquitous seaweed from colonization (Rao et al., 2007). It can also act as a probiotic for turbot cod larvae, protecting it against *Vibrio anguillarum* infections (Planas et al., 2006). It also produces roseobacticides that could facilitate pathogenesis, as they have specific activity at very low concentrations against certain non-calcifying strains of *E. huxleyi*, causing these cells to lyse (Seyedsayamdost et al., 2011b). Additionally, a recent report suggested that *P. inhibens* uses the plant growth hormone indole-3-acetic acid (IAA) to kill calcifying (C-type) *E. huxleyi* (Segev et al., 2016), although the dynamics of this interaction have yet to be elucidated.

We co-cultured an axenic representative strain of the three *E. huxleyi* cell types (N diploid, C diploid, and S haploid) with *P. inhibens* and monitored photosynthetic health, as well as the cell dynamics of both the algae and bacterium. We demonstrate that *P. inhibens* selectively causes the precipitous population-wide death of aged *E. huxleyi* coccolith-bearing C cells as well as the motile scale-bearing S cells, while various non-calcifying diploid N populations were not killed. Algal death directly benefits the bacterium, which increases its own population size during its host's decline. Finally we utilized a *P. inhibens* mutant library to demonstrate that the potent roseobacticides produced by *P. inhibens*, which were previously shown to kill N cells at nanomolar concentrations (Seyedsayamdost et al., 2011b), are not required for *P. inhibens* pathogenesis of C or S cells. These findings suggest that alternative, as of yet unknown, pathogenicity factor(s) may play equally critical roles in the pathogenesis of *P. inhibens* toward *E. huxleyi*.

MATERIALS AND METHODS

Algal and Bacterial Strains

All *E. huxleyi* strains were obtained from the National Centre for Marine Algae and Microbiota (East Boothbay, ME, USA). This includes coccolith-producing (C-type) strain CCMP3266, scale-bearing haploid (S-type) strain CCMP3268, and non-calcifying diploid (N-type) strains CCMP370, CCMP372, CCMP374, CCMP379, and CCMP2090. The N-type strains are all from unique geographical locations spanning the biogeographical range of all available axenic *E. huxleyi* cultures (**Table 1**). They were maintained in L1-Si medium (Guillard and Hargraves, 1993) at 18°C in a diurnal incubator (8:16 h dark-light cycle) with 41.51 ± 11.15 μmol·m^{-2}·s^{-1} of light during the light period. Algal cultures and medium were checked for bacterial contamination by microscopic observations and by inoculation onto half-strength marine agar (½ MA) (18.7 g Difco Marine

TABLE 1 | Axenic *E. huxleyi* strains and their susceptibility to *P. inhibens* pathogenesis.

CCMP strain code	Isolation location	Cell type*	Killed by *P. inhibens*†
CCMP370	Oslo Fjord, Norway, North Atlantic	N	No
CCMP372	Sargasso Sea, North Atlantic	N	No
CCMP374	Gulf of Maine, North Atlantic	N	No
CCMP379	English Channel, North Atlantic	N	No
CCMP2090‡	Coast of South America, South Pacific	N	No
CCMP3266	Tasman Sea, South Pacific	C	Yes
CCMP3268	Clonal isolate from RCC1216	S	Yes

*Calcifying diploid (C), non-calcifying diploid (N), and scale-bearing haploid (S).
†Co-culture experiments were observed over 30 days without precipitous algal death.
‡The axenic form of the polymicrobial non-calcifying diploid strain CCMP1516.

Broth 2216 and 9 g NaCl, supplemented with 15 g Difco agar in 1 L) followed by incubation at 30°C for 2 days. *E. huxleyi* was inoculated with a 10^{-1} dilution, grown statically for 5 days to 10^5 cells·mL^{-1} (early-log) prior to all experiments.

The wild type *P. inhibens* DSM 17395 (Frank et al., 2014), was maintained at 30°C on ½ MA (see Supplementary Methods for identification of the bacterium). Colonies were then transferred to half-strength marine broth (18.7 g Difco Marine Broth 2216 and 9 g NaCl in 1 L). *P. inhibens* was grown to stationary phase in a shaking incubator at 30°C, 160 rpm, for 24 h and then subsequently re-cultured in the same conditions prior to experimentation. Transposon mutants of *P. inhibens* DSM 17395 (Wetmore et al., 2015) were grown under the same conditions with the addition of 200 μg·mL^{-1} kanamycin (Sigma-Aldrich).

P. inhibens Transposon Mutants

Transposon mutants in TDA biosynthesis have been identified previously as deficient in TDA and roseobacticide production and consequently have white colonies, as opposed to the typical brown colonies of the wild type (Wang et al., 2016). Mutants screened all produced white colonies and were in two genes in the *tda* gene cluster of a *P. inhibens* plasmid pPGA1_262: *tdaB* (PGA1_262p00970) and *paaZ2* (PGA1_262p00800); as well as two genes in the *paa* gene cluster encoded on the chromosome: *paaA* (PGA1_c04080) and *patB* (PGA1_c00860) (Wetmore et al., 2015; Wang et al., 2016).

Gene knockout strains of *P. inhibens* DSM 17395 were obtained from a previously generated library created through molecularly barcoded transposon mutagenesis (Wetmore et al., 2015; Price et al., 2016), and specific mutants were recovered following the approach outlined by Cole et al. (2017). Briefly, the *P. inhibens* mutant library was spread on MA plates with 50 μg·mL^{-1} kanamycin and incubated overnight at ∼22°C. Colonies were picked using Qpix460 (Molecular Devices), arrayed into 384-well plates containing half-strength YTSS media (2 g yeast, 1.25 g tryptone, and 20 g sea salts in 1 L) with 7.5% glycerol and 50 μg·mL^{-1} kanamycin, and incubated overnight at ∼22°C. Next, 25 nL of each well was collected using an Echo525 liquid handler (Labcyte) as part of a multiplexing strategy involving pooling of rows, columns, and plates. These pools were subject to PCR amplification and sequencing of the molecular barcodes that identified the transposon insertion site of each mutant strain (Wetmore et al., 2015). The well location of each mutant was determined from amplicon sequencing results using an in-house script. Successful interruption of the targeted genes was confirmed by sequencing over the mutation site. Genomic DNA was extracted using GeneJet Genomic DNA Purification Kit (Thermo Scientific). Gene-specific primers were designed, and PCR was performed using the Phusion High-Fidelity DNA polymerase (Thermo Scientific). PCR products were either column- or gel-purified using QIAquick PCR Purification Kit or MinElute Gel Extraction Kit (QIAGEN), respectively. Amplicon sequencing was performed using the Sanger dideoxy method (Applied Biosystems 3730 Genetic Analyzer).

Bacterial and Algal Co-cultivation

Bacterial-algal co-cultivation was performed as previously described (Bramucci et al., 2015). Briefly, stationary phase bacterial cultures were washed twice by centrifugation and re-suspended in L1-Si medium before further centrifugation and resuspension to the target cell concentration in colony forming units (CFU)·mL^{-1}. *E. huxleyi* and the bacteria were mixed 1:1 (volume:volume) with a final concentration in the co-culture of 10^2 CFU·mL^{-1} bacteria and 10^5 cells·mL^{-1} algae, then 1 mL of this co-culture was aliquoted in 48-well plates (Becton Dickinson). The same cell densities of the bacterium and the alga were inoculated as monocultures in L1-Si medium and aliquoted into the microtitre plate. All controls/co-cultures were performed in triplicate. The microtitre plates were incubated in a diurnal incubator (8:16 h dark-light cycle) at 18°C for all experiments.

Co-cultivation of CCMP3266 or CCMP3268 with *P. inhibens* transposon mutants were performed as described, with control and co-cultures amended with kanamycin to a final concentration of 100 μg·mL^{-1} to keep selective pressure for the mutants (Wetmore et al., 2015). *E. huxleyi* was grown with various concentrations of kanamycin (0, 10, 50, 100, 200 μg·mL^{-1}) to determine that 100 μg·mL^{-1} kanamycin did not adversely affect growth of photosynthetic yield (Supplementary Figure S1). The cell density of mutants was enumerated on ½ MA with and without 200 μg·mL^{-1} kanamycin throughout the co-cultivation with algae to ensure the transposon mutation had not been lost from *P. inhibens*.

Roseobacticide B Inhibition Assay

Roseobacticide B was obtained from Dr. Mohammad Seyedsayamdost (Princeton University, NJ, USA) and dissolved in methanol as previously described (Seyedsayamdost et al., 2011b). The compound was then added to senescent (i.e., cultures were declining after reaching their maximal cell fluorescence) *E. huxleyi* (CCMP3266 and CCMP3268) at half the maximal inhibitory concentration (IC_{50}) previously identified for the sensitive N strain (Seyedsayamdost et al., 2011b), as well as ten-fold lower and higher (final concentrations of 0.019, 0.19, and 1.9 μM). A final concentration of 2% methanol was added to experimental and control cultures. The samples were incubated in microtiter plates in the same conditions previously used for bacterial co-culture experiments for 24 h before

obtaining pulse-amplitude-modulation (PAM) fluorescence measurements.

Fluorescence Measurements

A PAM fluorometer (WATER-PAM, Heinz Walz) was used to measure chlorophyll fluorescence (Schreiber et al., 1986; Bramucci et al., 2015). All samples were taken at the midpoint of the dark cycle (4 h) and diluted in sterile L1-Si medium to within the detection range of the PAM fluorometer. Samples were maintained at 18°C throughout handling. A dark adaption period of 3 min was determined, after which a saturating pulse was applied and the fluorescence readings were taken in triplicate at intervals of 1 min 30 s to calculate the minimal dark fluorescence (F_0), the maximum dark fluorescence (F_m), and the photosystem II (PSII) maximum efficiency (F_v/F_m), $F_v/F_m = (F_m - F_0)/F_m$ (Schreiber et al., 1986; Baker, 2008). Triplicate readings of each sample were averaged and the three microtitre wells were treated as replicates to determine the maximum quantum efficiency.

Flow Cytometry

Subsamples from algal controls and co-cultures were fixed for flow cytometry, incubated in the dark for 10 min with 0.15% glutaraldehyde (Sigma-Aldrich), flash-frozen in liquid nitrogen, and stored at −80°C until flow cytometry was performed using a FACSCalibur (Becton Dickinson). A 488 nm laser was used for excitation. Samples were then run using chlorophyll fluorescence (emission = 670 nm) for detection and cell counting ($cells \cdot mL^{-1}$).

Bacterial Enumeration

Phaeobacter inhibens population density grown alone and in co-culture was enumerated by counting CFU on ½ MA after 2 days of incubation at 30°C. Five replicate counts from each well were averaged, and the triplicate wells were used as experimental replicates for analysis. Although *P. inhibens* attaches to *E. huxleyi* and itself, aggregated cells were not observed microscopically after 5 min of vigorous vortexing.

Microscopy

Brightfield images of algal controls and co-cultures were obtained using a 63× Axio Scope.A1 objective lens (Zeiss), equipped with an Optronics digital camera and PictureFrame software v2.3 (Zeiss). Epifluorescence images were obtained using a 100× Axio Imager.M2 microscope objective lens (Zeiss), equipped with a monochrome camera (AxioCam 506 mono). Epifluorescence microscopy was also used to assess algal chlorophyll auto-florescence and to visualize algal and bacterial DNA when stained with DAPI (4′,6-diamidino-2-phenylindole dihydrochloride) (DNA–DAPI complex: excitation = 364 nm; emission = 454 nm) (Life Technologies). Unfixed *E. huxleyi* control and co-culture aliquots were stained with DAPI according to manufacturer's instructions (30°C, 20 min) then immediately pelleted by centrifugation (5,000 × g, room temperature, 2 min). Cells were gently washed twice in sterile L1-Si medium and analyzed immediately on the epifluorescence microscope. Images were acquired simultaneously for three different channels and overlaid using Zen 2 Blue Edition software v2 (Zeiss). The differential interference contrast channel was overlaid with 1) algal chlorophyll auto-fluorescence (red: excitation = 610–650 nm; emission = 670–720 nm) and 2) DNA–DAPI complex fluorescence (blue: excitation = 350–400 nm; emission = 417–477 nm).

Data Processing and Statistical Analysis

Flow cytometry data were processed using FlowJo v9.2 (Tree Star Inc.). Quantitative data from all other experiments were processed using SigmaPlot 12.0 (Systat Software). Statistical significance was determined using a one-way ANOVA and Tukey HSD test.

RESULTS AND DISCUSSION

P. inhibens Kills Select *E. huxleyi* Cell Types

This study involves the bacterium previously identified as *P. gallaeciensis* BS107 that produces roseobacticides, which have a specific algaecidal effect on *E. huxleyi* (Seyedsayamdost et al., 2011b); however, there is evidence that there were differences in strains of the bacteria submitted to various repositories (Buddruhs et al., 2013). Therefore, we sequenced the genome of our strain and its identity was confirmed to be *P. inhibens* DSM 17395 (Frank et al., 2014) based on both 100% average nucleotide identity and percent (*in silico*) DNA–DNA hybridization to the published DSM 17395 genome (Thole et al., 2012; Supplementary Figure S2).

To determine if *P. inhibens* has a host cell type preference in its interactions with *E. huxleyi*, we co-cultured *P. inhibens* with five axenic N strains from distinct geographical locations, one axenic C strain (CCMP3266), and one axenic S strain (CCMP3268) (**Table 1**). The C and S strains were both killed by *P. inhibens,* and all tested N type strains survived, regardless of geographic origin (**Table 1**). To further investigate the differential pathogenesis of *P. inhibens* on various *E. huxleyi* cell types, an axenic N [CCMP2090, derived from the polymicrobial calcifying CCMP1516 (Orata et al., 2016; Zhang et al., 2016)], C (CCMP3266), and S [CCMP3268, derived from a single cell isolation from CCMP3266 (von Dassow et al., 2015)] strains (**Figure 1**) were investigated in more depth. Each strain was grown alone and in co-culture with *P. inhibens* for 14 days and monitored for PSII maximum quantum efficiency (F_v/F_m), which is affected by cellular stress and/or loss of functional PSII centers (**Figure 2**), as well as algal and bacterial cell density (**Figure 3**).

When grown alone, all three algal cell types had a stable PSII maximum quantum efficiency ($F_v/F_m > 0.5$) throughout the experiment, although they entered a senescent stage, represented by reduced fluorescent health after 6–10 days (**Figures 2A–C**). The algal cultures grown alone did not die in this experiment and have been shown to live for > 60 days in microtitre plates (Bramucci et al., 2015). Both C and S cultures grown alone reached their peak density between 6 and 10 days followed by a characteristic slow decline during senescence (**Figures 3B,C**), typified by gradual losses of cell numbers (Franklin et al., 2012). It has been suggested that *P. inhibens* stimulates *E. huxleyi's* growth rate in the early growth phases (Segev et al., 2016); however, no growth stimulation was detected for the N, C, or

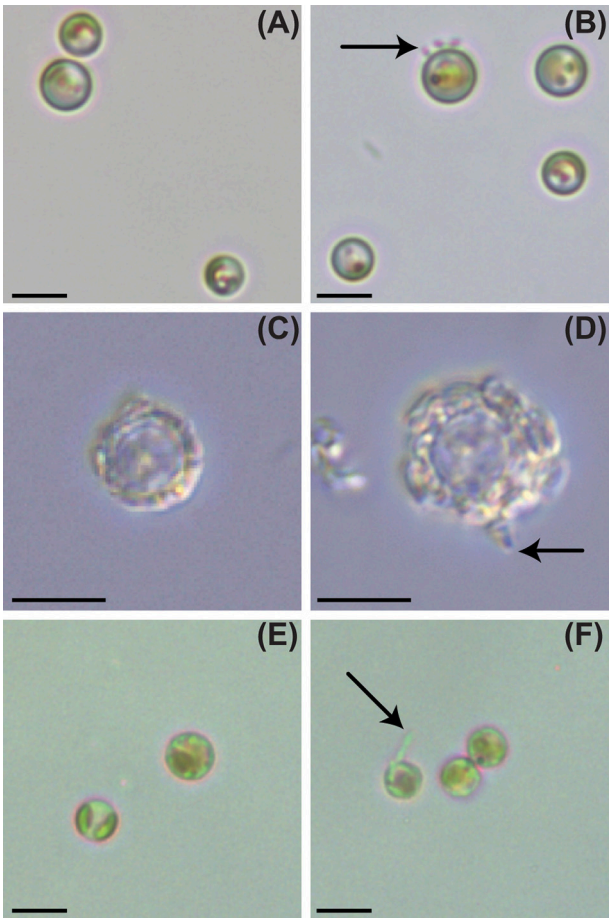

FIGURE 1 | Light and epifluorescence microscopy of *P. inhibens* attached to non-calcifying diploid N (CCMP2090), diploid calcifying C (CCMP3266), and haploid S (CCMP3268) *E. huxleyi* strains. Brightfield light microscopy of *E. huxleyi*, day 6: **(A)** control CCMP2090, **(B)** CCMP2090 co-culture with *P. inhibens*, **(C)** control CCMP3266, **(D)** CCMP3266 co-culture with *P. inhibens*, **(E)** control CCMP3268, **(F)** CCMP3268 co-culture with *P. inhibens*. *P. inhibens* cells attached to algal host are indicated by black arrows. The scale bar represents 5 μm.

S cell types in the co-cultures, with no significant difference between *E. huxleyi*'s cell density for any of the cell types in co-culture or the control in the first 6 days of the experiment (**Figure 3**).

The N strain grown in co-culture with the bacterial symbiont maintained chlorophyll health, functional PSII systems (**Figure 2A**), and cell density (**Figure 3A**) comparable to the axenic cultures throughout the experiment, despite *P. inhibens* being found attached to its surface (**Figures 2D,E**). This algal strain, alone or in co-culture with the bacterium, grows to a higher cell density than C- or S-type grown alone from 12 days onwards ($P < 0.05$) (**Figure 3**).

In contrast, the C and S cultures grown in co-culture with *P. inhibens* experienced an accelerated and premature decline in photosystem health (8–10 days) (**Figures 2B,C**). This population-wide decline is associated with a concurrent decrease in individual chlorophyll content in the algal cells co-cultured with the bacterium (**Figures 2F–I**). When co-cultured with *P. inhibens,* C-type cell densities are much lower than the control by 14 days ($P < 0.05$) compared to the axenic control (**Figure 3B**). A similar trend is observed for the S-type strain (**Figure 3C**). All S cells lost their photosynthetic ability in the co-culture with *P. inhibens* by day 12 with a detectible decrease in photosynthetic health initiated on day 8 (**Figure 2C**). This timing for rapid decline triggered by a bacterial pathogen coincides closely with the onset of senescence in the algal host.

The rapid decline of PSII efficiency when co-cultured with *P. inhibens* is intriguing, as it has not been observed in starved senescent *E. huxleyi* cells (Franklin et al., 2012), but occurs during viral infection and lysis of *E. huxleyi* cells by EhVs (Bidle et al., 2007). These findings suggest that the algaecidal activity of *P. inhibens* against its microalgal host, *E. huxleyi*, is dependent on algal cell type, and that the targeted cell types are different to EhVs which are only known to kill N- and C-type cells (Frada et al., 2008; Mordecai et al., 2017). Similarly, the closely related roseobacter pathogen, *Ruegeria* sp. R11 (Fernandes et al., 2011) (also known as *Nautella italica* R11; Vandecandelaere et al., 2009; Rodrigo-Torres et al., 2016), kills C and S cells and not N cells (Mayers et al., 2016). While the mechanism of *P. inhibens* pathogensis is not known, clues can be found in EhVs, which upregulate metacaspase activity in calcifying diploid cells, inducing alga PCD (Bidle et al., 2007). EhVs induce an autophagy-like PCD event in the algal host (Schatz et al., 2014). Autophagy, or the genetically programed lysosomal degradation of cellular constituents (Kroemer et al., 2009), is a vital part of the host immune response and can infer protection against bacterial pathogens by ensuring the rapid degradation of virulence factors (Cemma and Brumell, 2012). Because this viral-induced PCD response in *E. huxleyi* results in a loss of PSII function directly before death due to viral lysis (Bidle et al., 2007), it might follow that a similar mechanism is activated by the bacterial pathogen. Environmental stress is a factor in gradual loss of photosynthetic health, but the sudden complete loss of photosynthetic health has only so far been seen in the C cells undergoing viral-induced apoptosis. The activation of algal caspase-like molecules resulting in apoptosis-like PCD has already been described in the pathogenic interaction between *Ruegeria* sp. R11 and the C- and S-type culture CCMP3266 (Mayers et al., 2016).

This resistance of N-type cells to pathogenic roseobacters has been previously reported for the N-type strain, CCMP2090, cultured with *Ruegeria* sp. R11 (Mayers et al., 2016). Together, these findings suggest that, although the N cell used in the current study (CCMP2090) was recently derived from a polymicrobial calcifying parent strain (CCMP1516), calcifying and non-calcifying diploid strains have important biological differences, which might for instance confer widespread resistance to roseobacter pathogenesis. There are at least two possible explanations as to why *E. huxleyi* N cells are widely resistant to *P. inhibens* pathogenesis, or that *P. inhibens* does not interact with N cells. The first possibility is that N cells escape the pathogen, similar to the haploid escape from EhVs (Frada

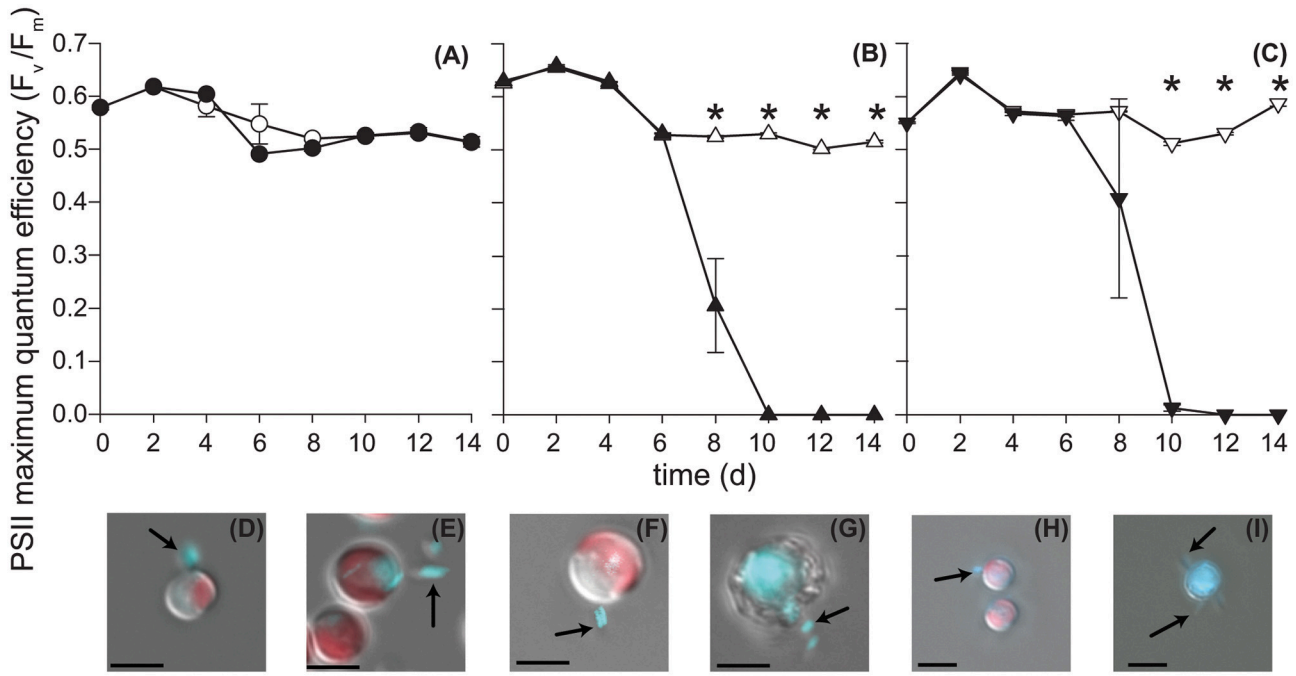

FIGURE 2 | *P. inhibens* effect on *E. huxleyi's* photosynthetic health. *P. inhibens* was co-cultured with non-calcifying diploid N cells (CCMP2090), diploid calcifying C cells (CCMP3266), and haploid S cells (CCMP3268) *E. huxleyi*. The maximum quantum efficiency (F_V/F_m) is shown for **(A)** CCMP2090 (circles), **(B)** CCMP3266 (triangles) and **(C)** CCMP3268 (upside down triangles). Data for axenic algal cultures are filled in white, whereas data from co-cultured experiments are solid black. Triplicate wells that represent independent experiments were sacrificially sampled at each time point; error bars represent ±1 standard error. An asterisk (*) at a time point indicates that it is significantly different to the control. Statistical significance was determined using a one-way ANOVA and Tukey HSD test. Differential interference contrast images of **(D)** CCMP2090 co-culture with *P. inhibens* healthy, day 6 and **(E)** healthy, day 10, **(F)** CCMP3266 co-culture with *P. inhibens* healthy, day 6 and **(G)** dying, day 10, **(H)** CCMP3268 co-culture with *P. inhibens* healthy, day 6 and **(I)** dying, day 10 . Images are shown overlaid with two fluorescent channels: chlorophyll auto-fluorescence (red: excitation 610–650 nm; emission 670–720 nm) and DNA–DAPI complex fluorescence (blue: excitation 350–400 nm; emission 417–477 nm). DAPI-stained *P. inhibens* cells attached to algal host and non-associated are indicated by black arrows. The scale bar represents 5 μm.

et al., 2008; Mordecai et al., 2017). The haploid S-type is thought to be resistant to viral lysis, and it was postulated that the haploid's scaly coverings or that gene loss or mutation might infer viral resistance to the haploid cell type (Frada et al., 2008). Supporting this theory, an increase in culture temperature confers temperature-induced resistance to EhVs by altering the outer sphingolipids of representative calcifying and non-calcifying diploid *E. huxleyi* strains, impeding viral recognition and infection of target cells (Kendrick et al., 2014). By analogy, it is possible that *P. inhibens* does not interact with *E. huxleyi* N cells due to differential recognition and/or attachment to the alga, as was suggested for *Ruegeria* sp. R11 (Mayers et al., 2016). However, *P. inhibens* does attach to N cells (**Figure 1B**) and so N cell resistance, or *P. inhibens* lack of virulence, must have another mechanism. A second possibility for N cell escape is that there might be genetic differences between C and N cells. There are two prevalent theories as to how N cells are generated: (1) through a series of mutations resulting in, among other differences, a malformed coccolith-forming vesicle (van der Wal et al., 1983) and (2) due to prolonged lab domestication (Zhang et al., 2016). To our knowledge, only one axenic C and S culture exist, and it is commonly reported that coccoliths were lost through subsequent culturing. For example, the polymicrobial CCMP1516 was a C-type culture that recently became an N-type culture; it was a C-type culture when it produced its axenic daughter strain CCMP2090, which is N-type (Zhang et al., 2016). Future genomic effort should focus on sequencing parent (C) and daughter (N) cultures to elucidate if a genetic basis for the phenotypic switch can be identified as it could elucidate resistance mechanisms to the bacterial pathogen and the molecular basis of coccolithogenesis.

P. inhibens Benefits From Growth With *E. huxleyi* Before and After its Death

Bacterial population dynamics when grown alone and in co-culture were monitored using CFU (**Figures 3D–F**). Under the experimental conditions used (algal medium L1-Si from seawater, with no additional carbon), *P. inhibens* was able to grow to a maximum cell density of 10^5 CFU·mL^{-1} without *E. huxleyi* at 2–4 days (**Figures 3D–F**), after which *P. inhibens* cell density declined. Prolonged monitoring of *P. inhibens* grown without a host showed that all bacteria died by 25 days. However, its growth was greatly enhanced by the presence of *E. huxleyi*, reaching

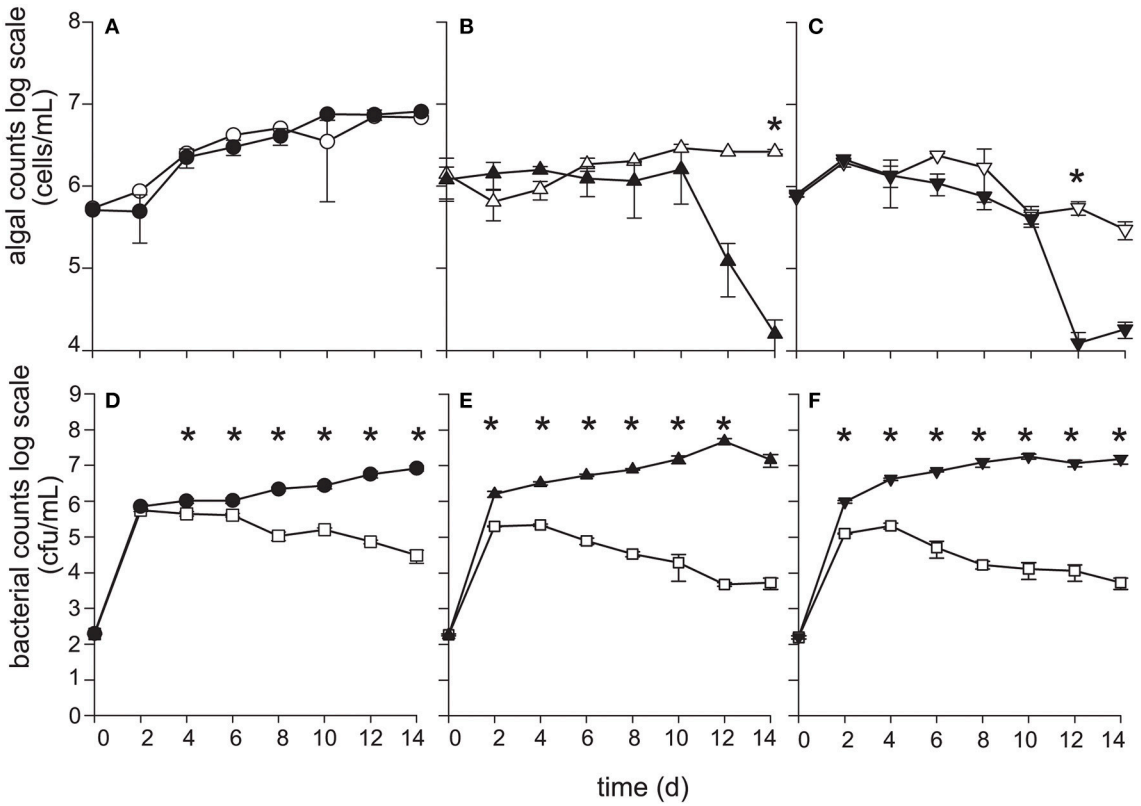

FIGURE 3 | *P. inhibens* kills diploid calcifying C (CCMP3266), and haploid S (CCMP3268) *E. huxleyi* while non-calcifying diploid N (CCMP2090) is resistant to *P. inhibens pathogenesis*. *E. huxleyi* cell density (cells·mL^{-1}) were enumerated using flow cytometry for **(A)** CCMP2090 (circles), **(B)** CCMP3266 (triangles), and **(C)** CCMP3268 (upside down triangles) for both axenic control (white) and grown in co-culture with *P. inhibens* (black). *P. inhibens* cell density (CFU·mL^{-1}) were enumerated for the control in L1-Si medium (white squares) and co-cultured with *E. huxleyi*: **(D)** CCMP2090 (black circles) **(E)** CCMP3266 (black triangles), and **(F)** CCMP3268 (black upside down triangles). Triplicate wells that represent independent experiments were sacrificially sampled at each time point; error bars represent ±1 standard error. An asterisk (*) at a time point indicates that it is significantly different to the control. Statistical significance was determined using a one-way ANOVA and Tukey HSD test.

100–1,000 times higher densities when grown with an algal host (**Figures 3D–F**).

The growth benefit conveyed to *P. inhibens* is greater in the short term (14 days and less) when grown with C- and S-type cells of *E. huxleyi* than the N-type (**Figures 3D–F**). The bacterial cell density in the C cell co-culture appears to benefit from 2 to 6 days ($P < 0.01$) and 10 days ($P < 0.05$) when compared to the N culture (**Figures 3D,E**). Directly after the C-type culture suffers a decline in both PSII health and numbers of chlorophyll containing cells (day 12), *P. inhibens* cell density increases 8.5-fold ($P < 0.01$), compared to those grown in co-culture with N-type, which does not die (day 12) (**Figures 3A,B,D,E**). *P. inhibens* co-cultured with S-type also has a significant ($P < 0.01$) benefit in terms of increased cell counts compared to the N-type co-culture between 4 and 10 days (**Figures 3D,F**), the time when the algae has reduced PSII maximum quantum efficiency as well as declining cells per mL in the co-culture (**Figures 2C**, **3C**). Additionally, the benefit to *P. inhibens* persisted after the death of the algal host (12–14 days). In fact, *P. inhibens* grown with C- and S-type maintained high cell counts until at least 30 days, when both co-cultures had 10^6 and 10^7 CFU·mL^{-1}, respectively, despite death of its host. *P. inhibens* grown in co-culture with N-type maintained high cell counts until at least 30 days (10^8 CFU·mL^{-1}).

This increased persistence and higher population density of *P. inhibens* when co-cultured with *E. huxleyi* is likely the result of nutrients made available by algal exudate (Borchard and Engel, 2012). Phytoplankton constantly leak sugars and oxygen from photosynthesis, as well as other chemicals such as dimethylsulfoniopropionate (DMSP) and amino acids, which are chemoattractants for roseobacters (Mitchell et al., 1985; Baines and Pace, 1991; Miller and Belas, 2004; Miller et al., 2004). Furthermore, DMSP-degrading microbes, such as *P. inhibens*, benefit directly from being able to efficiently assimilate the sulfur from DMSP directly into bacterial amino acids (Curson et al., 2011). These results demonstrate a population wide benefit for *P. inhibens* to being grown in co-culture with an algal host, regardless of host cell type. *P. inhibens* then increases its fecundity and persistence by killing certain cell types of its host, presumably because algal cell lysis could provide it with nutrients (Kolb et al., 2013). This interaction makes *P. inhibens* an opportunistic pathogen, not a parasite (Seyedsayamdost et al., 2011a), as

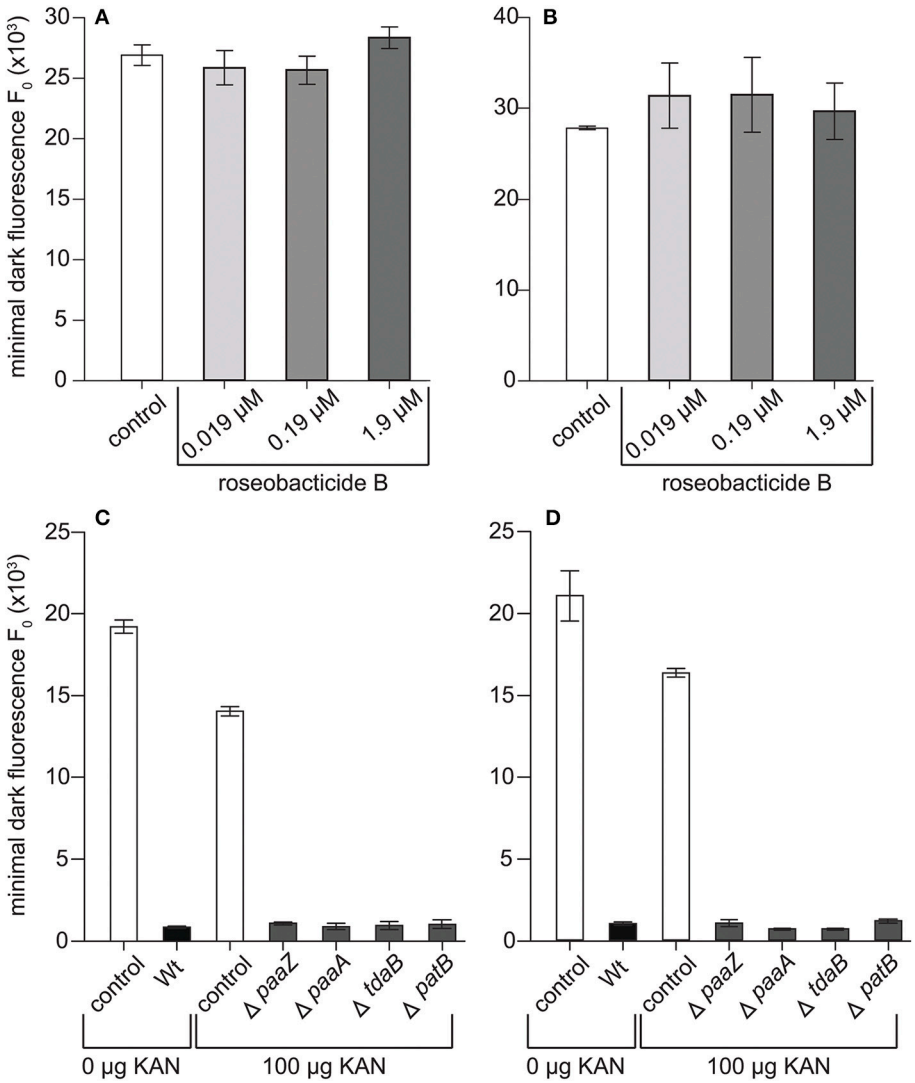

FIGURE 4 | *P. inhibens* has a roseobacticide-independent mechanism for killing diploid calcifying C cells (CCMP3266) and haploid S cells (CCMP3268). Minimal algal fluorescence of the population (F_0) is shown for **(A)** senescent CCMP3266 cells and **(B)** senescent CCMP3268 cells cultured with roseobacticide B. Both cell types were incubated for 24 h with methanol (white bar) and with 0.019 µM (lightest gray), 0.19 µM (gray), and 1.9 µM (darkest gray) roseobacticide B, dissolved in methanol. The final concentration of methanol solvent added to control and experimental cultures was 2% of the final volume. *P. inhibens* transposon mutants deficient in roseobacticide synthesis were co-cultured with **(C)** CCMP3266 and **(D)** CCMP3268. Minimal algal fluorescence of the population (F_0) was measured on day 10. Triplicate wells that represent independent experiments were sacrificially sampled; error bars represent ±1 standard error.

parasites reduce the health and fecundity of their host and benefit from prolonging the host's life, while *P. inhibens* causes C- and S-type cells to die prematurely.

Are Roseobacticides Responsible for Death of C- and S-Type Cells?

The rapid decline in maximum quantum yield and loss of chlorophyll observed in the C- and S-type cultures at 8–10 days (**Figure 2**) is consistent with the physiological response of *E. huxleyi* to roseobacticides, which causes cell membrane blebbing, chloroplast loss, and lysis of N-type cells (Seyedsayamdost et al., 2011b). Roseobacticides are produced by *P. inhibens* when supplied with *p*-coumaric acid (*p*CA) (Seyedsayamdost et al., 2011b) and other lignin precursors (Wang and Seyedsayamdost, 2017). *p*CA is produced by *E. huxleyi* and hypothesized to be made during senescence (Seyedsayamdost et al., 2011b) where it is an intermediary of the lignin and flavonoid pathways (Labeeuw et al., 2015). *P. inhibens* thereby produces the algaecidal roseobacticides to precipitously kill a dying host when it ages or is damaged. To determine if roseobacticides were responsible for decreases in quantum yield and chlorophyll loss, roseobacticide B was added to senescent C and S cultures of *E. huxleyi* on day 9—the day when those *E. huxleyi* cultures typically decline when grown with *P. inhibens*—at IC_{50} of 0.19 µM determined for

another N-type strain, CCMP372 (Seyedsayamdost et al., 2011b). Roseobacticide B concentrations 10-fold higher and lower than the IC50 were also tested. Surprisingly, no changes in PSII maximum quantum yield were observed at any roseobacticide concentrations (**Figures 4A,B**). Furthermore, the characteristic declines in C and S cultures were reproduced when co-cultured with four different *P. inhibens* mutants whose roseobacticide production genes had been disrupted (**Figures 4C,D**). These results suggest roseobacticides were not responsible for the death of C- and S-type cells, and that *P. inhibens* must be producing additional algaecidal compounds or virulence factors to kill *E. huxleyi*. In addition, non-calcifying diploid strains surviving co-culture with *P. inhibens* included CCMP372 (**Table 1**), which were previously shown to be killed by roseobacticides (Seyedsayamdost et al., 2011b).

Phaeobacter inhibens produces many different compounds with roles in microbe-microbe interactions. Segev et al. (2016) has proposed that *P. inhibens* uses IAA to kill *E. huxleyi*. This plant auxin is produced by various roseobacters (Fernandes et al., 2011; Wienhausen et al., 2017), including *P. inhibens*, and can kill the C-type culture, CCMP3266, at high concentrations (1,000 μM) (Labeeuw et al., 2016; Segev et al., 2016). However, Segev et al. (2016) also showed that *P. inhibens* did not produce IAA at high enough concentrations to kill *E. huxleyi* CCMP3266 (0.4–10 nM). In addition, *E. huxleyi* CCMP3266 produces IAA itself as a cell-cell signal at a higher concentration (200 μM) in the presence of tryptophan (Labeeuw et al., 2016). Finally, the N-type strain, CCMP2090, is susceptible to IAA when co-cultured at lower concentrations (10–100 μM), exhibiting morphological responses and reduced health similar to those seen in terrestrial plants (Labeeuw et al., 2016) that we did not observe in the *P. inhibens*–CCMP2090 co-culture. Taken together, these data show IAA is probably not the bioactive molecule causing *E. huxleyi's* decline when grown with *P. inhibens*, and that some other molecule or mechanism is responsible.

Tryptophan, the precursor to IAA, was also found to be lethal at the high concentration (1,000 μM) required to produce sufficient IAA to kill *E. huxleyi* (Labeeuw et al., 2016). Tryptophan was also shown to be released by CCMP3266, and the addition of exogenous tryptophan causes faster killing of CCMP3266 by both *P. inhibens* (Segev et al., 2016) and another roseobacter, *Ruegeria* sp. R11 (Labeeuw et al., 2016). This indicates that tryptophan may be a signal or metabolite for the bacteria to become virulent.

CONCLUSION

Phaeobacter inhibens interaction with *E. huxleyi* is dependent on the cell type of its algal host. This differential pathogenesis is also observed for EhVs, although the targeted cell types differ. Currently, N-type cells are heavily relied upon for cell biology studies of *E. huxleyi* because they are readily maintained axenically and avoid many of the problems associated with working with an autofluorescent mineral (i.e., coccoliths). However, our findings suggest that we should not assume that N-type cells will have similar biological interactions to their calcifying counterparts. The ability of *P. inhibens* to target coccolith-bearing (C) diploid cells and scale-bearing (S) haploid cells, while not killing non-calcifying diploid cells is a unique role, likely representing differentiation from EhVs, which kills both diploid cell types but not the haploid cell type (Frada et al., 2008). We have now shown two roseobacters, *P. inhibens* and *Ruegeria* sp. R11, can kill populations of C- and S-type cells (Mayers et al., 2016). This may have wide-reaching implications, as S cells are resistant to EhV lysis, which was postulated as a mechanism for the algal population to regenerate the dominant C cell population following viral-induced bloom collapse (Frada et al., 2008). Given the present findings, it is possible that the roseobacter's rapid pathogenesis of S cells could limit the alga's ability to reseed C cell populations. Additionally, roseobacter killing of C and S populations, while N populations evade bacterial induced death, could have important implications for the marine carbon cycle and formation of the paleobotanical record (Coolen, 2011), as well as the overall distribution of *E. huxleyi* blooms.

AUTHOR CONTRIBUTIONS

AB, LL, and RC conceived of the experiments. AB and LL carried out the experiments. FO carried out the whole-genome sequencing and analysis. ER and RM constructed the *P. inhibens* mutants. AB, LL, FO, and RC drafted the manuscript. All authors have read and approved the manuscript.

ACKNOWLEDGMENTS

We would like to thank Dr. Mohammad Seyedsayamdost (Princeton University) for providing the roseobacticide B and Albert Rosana (University of Alberta) for assistance with sequence confirmation of the barcoded transposon mutants. This work was supported by the Natural Sciences and Engineering Research Council of Canada (grant 402105) to RC. The work conducted by the U.S. Department of Energy Joint Genome Institute, a DOE Office of Science User Facility, is supported under Contract No. DE-AC02-05CH11231.

SUPPLEMENTARY MATERIAL

The Supplementary Material for this article can be found online at: https://www.frontiersin.org/articles/10.3389/fmars.2018.00188/full#supplementary-material

REFERENCES

Amin, S. A., Hmelo, L. R., van Tol, H. M., Durham, B. P., Carlson, L. T., Heal, K. R., et al. (2015). Interaction and signalling between a cosmopolitan phytoplankton and associated bacteria. *Nature* 522, 98–101. doi: 10.1038/nature14488

Ashen, J. B., Cohen, J. D., and Goff, L. J. (1999). GC-SIM-MS detection and quantification of free indole-3-acetic acid in bacterial galls on the marine alga *Prionitis lanceolata* (Rhodophyta). *J. Phycol.* 35, 493–500. doi: 10.1046/j.1529-8817.1999.3530493.x

Azam, F. (1998). Microbial control of oceanic carbon flux: the plot thickens. *Science* 280, 694–696. doi: 10.1126/science.280.5364.694

Baines, S. B., and Pace, M. L. (1991). The production of dissolved organic matter by phytoplankton and its importance to bacteria: patterns across marine and freshwater systems. *Limnol. Oceanogr.* 36, 1078–1090. doi: 10.4319/lo.1991.36.6.1078

Baker, N. R. (2008). Chlorophyll fluorescence: a probe of photosynthesis *in vivo*. *Annu. Rev. Plant Biol.* 59, 89–113. doi: 10.1146/annurev.arplant.59.032607.092759

Baumann, K., Boeckel, B., and Cepek, M. (2008). Spatial distribution of living coccolithophores along an east- west transect in the subtropical South Atlantic. *J. Nannoplankt. Res.* 30, 9–21.

Bell, W., and Mitchell, R. (1972). Chemotactic and growth responses of marine bacteria to algal extracellular products. *Mar. Biol. Lab.* 143, 265–277. doi: 10.2307/1540052

Berger, M., Neumann, A., Schulz, S., Simon, M., and Brinkhoff, T. (2011). Tropodithietic acid production in *Phaeobacter gallaeciensis* is regulated by N-acyl homoserine lactone-mediated quorum sensing. *J. Bacteriol.* 193, 6576–6585. doi: 10.1128/JB.05818-11

Beyersmann, P. G., Tomasch, J., Son, K., Stocker, R., Göker, M., Wagner-Döbler, I., et al. (2017). Dual function of tropodithietic acid as antibiotic and signaling molecule in global gene regulation of the probiotic bacterium *Phaeobacter inhibens*. *Sci. Rep.* 7, 1–9. doi: 10.1038/s41598-017-00784-7

Bidle, K. D., Haramaty, L., Barcelose Ramos, J., and Falkowski, P. (2007). Viral activation and recruitment of metacaspases in the unicellular coccolithophore, *Emiliania huxleyi*. *Proc. Natl. Acad. Sci. U.S.A.* 104, 6049–6054. doi: 10.1073/pnas.0701240104

Bolch, C. J., Subramanian, T. A., and Green, D. H. (2011). The toxic dinoflagellate *Gymnodinium catenatum* (Dinophyceae) requires marine bacteria for growth. *J. Phycol.* 47, 1009–1022. doi: 10.1111/j.1529-8817.2011.01043.x

Borchard, C., and Engel, A. (2012). Organic matter exudation by *Emiliania huxleyi* under simulated future ocean conditions. *Biogeosciences* 9, 3405–3423. doi: 10.5194/bg-9-3405-2012

Bramucci, A. R., Labeeuw, L., Mayers, T. J., Saby, J. A., and Case, R. J. (2015). A small volume bioassay to assess bacterial/phytoplankton co-culture using WATER-Pulse-Amplitude-Modulated (WATER-PAM) fluorometry. *J. Vis. Exp.* 97:e52455. doi: 10.3791/52455

Buddruhs, N., Pradella, S., Göker, M., Päuker, O., Pukall, R., Spröer, C., et al. (2013). Molecular and phenotypic analyses reveal the non-identity of the *Phaeobacter gallaeciensis* type strain deposits CIP 105210T and DSM 17395. *Int. J. Syst. Evol. Microbiol.* 63, 4340–4349. doi: 10.1099/ijs.0.053900-0

Case, R. J., Longford, S. R., Campbell, A. H., Low, A., Tujula, N., Steinberg, P. D., et al. (2011). Temperature induced bacterial virulence and bleaching disease in a chemically defended marine macroalga. *Environ. Microbiol.* 13, 529–537. doi: 10.1111/j.1462-2920.2010.02356.x

Cemma, M., and Brumell, J. H. (2012). Interactions of pathogenic bacteria with autophagy systems. *Curr. Biol.* 22, R540–R545. doi: 10.1016/j.cub.2012.06.001

Cole, B. J., Feltcher, M. E., Waters, R. J., Wetmore, K. M., Mucyn, T. S., Ryan, E. M., et al. (2017). Genome-wide identification of bacterial plant colonization genes. *PLoS Biol.* 15:e2002860. doi: 10.1371/journal.pbio.2002860

Coolen, M. J. (2011). 7000 years of *Emiliania huxleyi* viruses in the Black Sea. *Science* 333, 451–452. doi: 10.1126/science.1200072

Curson, A. R., Todd, J. D., Sullivan, M. J., and Johnston, A. W. (2011). Catabolism of dimethylsulphoniopropionate: microorganisms, enzymes and genes. *Nat. Rev. Microbiol.* 9, 849–859. doi: 10.1038/nrmicro2653

D'Alvise, P. W., Lillebø, S., Prol-Garcia, M. J., Wergeland, H. I., Nielsen, K. F., Bergh, Ø., et al. (2012). *Phaeobacter gallaeciensis* reduces *Vibrio anguillarum* in cultures of microalgae and rotifers, and prevents vibriosis in cod larvae. *PLoS ONE* 7:e43996. doi: 10.1371/journal.pone.0043996

Fernandes, N., Case, R. J., Longford, S. R., Seyedsayamdost, M. R., Steinberg, P. D., Kjelleberg, S., et al. (2011). Genomes and virulence factors of novel bacterial pathogens causing bleaching disease in the marine red alga *Delisea pulchra*. *PLoS ONE* 6:e27387. doi: 10.1371/journal.pone.0027387

Frada, M. J., Bidle, K. D., Probert, I., and de Vargas, C. (2012). *In situ* survey of life cycle phases of the coccolithophore *Emiliania huxleyi* (Haptophyta). *Environ. Microbiol.* 14, 1558–1569. doi: 10.1111/j.1462-2920.2012.02745.x

Frada, M., Probert, I., Allen, M. J., Wilson, W. H., and de Vargas, C. (2008). The "Cheshire Cat" escape strategy of the coccolithophore *Emiliania huxleyi* in response to viral infection. *Proc. Natl. Acad. Sci. U.S.A.* 105, 15944–15949. doi: 10.1073/pnas.0807707105

Frank, O., Pradella, S., Rohde, M., Scheuner, C., Klenk, H.-P., Göker, M., et al. (2014). Complete genome sequence of the *Phaeobacter gallaeciensis* type strain CIP 105210T (= DSM 26640T = BS107T). *Stand. Genomic Sci.* 9, 914–932. doi: 10.4056/sigs.5179110

Franklin, D. J., Airs, R. L., Fernandes, M., Bell, T. G., Bongaerts, R. J., Berges, J. A., et al. (2012). Identification of senescence and death in *Emiliania huxleyi* and *Thalassiosira pseudonana*: cell staining, chlorophyll alterations, and dimethylsulfoniopropionate (DMSP) metabolism. *Limnol. Oceanogr.* 57, 305–317. doi: 10.4319/lo.2012.57.1.0305

Gardiner, M., Bournazos, A. M., Maturana-Martinez, C., Zhong, L., and Egan, S. (2017). Exoproteome analysis of the seaweed pathogen *Nautella italica* R11 reveals temperature-dependent regulation of RTX-like proteins. *Front. Microbiol.* 8:1203. doi: 10.3389/fmicb.2017.01203

Geng, H., and Belas, R. (2010). Molecular mechanisms underlying roseobacter-phytoplankton symbioses. *Curr. Opin. Biotechnol.* 21, 332–338. doi: 10.1016/j.copbio.2010.03.013

Geng, H., Bruhn, J. B., Nielsen, K. F., Gram, L., and Belas, R. (2008). Genetic dissection of tropodithietic acid biosynthesis by marine roseobacters. *Appl. Environ. Microbiol.* 74, 1535–1545. doi: 10.1128/AEM.02339-07

González, J. M., Simó, R., Massana, R., Covert, J. S., Casamayor, E. O., Pedrós-Alió, C., et al. (2000). Bacterial community structure associated with a dimethylsulfoniopropionate-producing North Atlantic algal bloom. *Appl. Environ. Microbiol.* 66, 4237–4246. doi: 10.1128/AEM.66.10.4237-4246.2000

Green, D. H., Echavarri-Bravo, V., Brennan, D., and Hart, M. C. (2015). Bacterial diversity associated with the coccolithophorid algae *Emiliania huxleyi* and *Coccolithus pelagicus* f. *braarudii*. *Biomed. Res. Int.* 2015:194540. doi: 10.1155/2015/194540

Guillard, R. R. L., and Hargraves, P. E. (1993). *Stichochrysis immobilis* is a diatom, not a chrysophyte. *Phycologia* 32, 234–236. doi: 10.2216/i0031-8884-32-3-234.1

Holligan, P. M., Fernández, E., Aiken, J., Balch, W. M., Boyd, P., Burkill, P. H., et al. (1993). A biogeochemical study of the coccolithophore, *Emiliania huxleyi*, in the North Atlantic. *Global Biogeochem. Cycles* 7, 879–900. doi: 10.1029/93GB01731

Hunt, D. E., David, L. A., Gevers, D., Preheim, S. P., Alm, E. J., and Polz, M. F. (2008). Resource partitioning and sympatric differentiation among closely related bacterioplankton. *Science* 320, 1081–1085. doi: 10.1126/science.1157890

Kendrick, B. J., DiTullio, G. R., Cyronak, T. J., Fulton, J. M., Van Mooy, B. A. S., and Bidle, K. D. (2014). Temperature-induced viral resistance in *Emiliania huxleyi* (Prymnesiophyceae). *PLoS ONE* 9:e112134. doi: 10.1371/journal.pone.0112134

Klaveness, D. (1972). *Coccolithus huxleyi* (Lohm.) Kamptn. II. The flagellate cell, aberrant cell types, vegetative propagation and life cycles. *Br. Phycol. J.* 7, 309–318. doi: 10.1080/00071617200650321

Kolb, A., Strom, S., Center, S., and Anacortes, W. (2013). An inducible antipredatory defense in haploid cells of the marine microalga *Emiliania huxleyi* (Prymnesiophyceae). *Limnol. Oceanogr.* 58, 932–944. doi: 10.4319/lo.2013.58.3.0932

Kroemer, G., Galluzzi, L., Vandenabeele, P., Abrams, J., Alnemri, E. S., Baehrecke, E. H., et al. (2009). Classification of cell death: recommendations of the Nomenclature Committee on Cell Death 2009. *Cell Death Differ.* 16, 3–11. doi: 10.1038/cdd.2008.150

Labeeuw, L., Bramucci, A. R., and Case, R. J. (2017). "Bioactive small molecules mediate microalgal-bacterial interactions," in *Systems Biology of Marine Ecosystems*, eds M. Kumar and P. J. Ralph (Cham: Springer International Publishing), 279–300.

Labeeuw, L., Khey, J., Bramucci, A. R., Atwal, H., De La Mata, A. P., Harynuk, J., et al. (2016). Indole-3-acetic acid is produced by *Emiliania huxleyi* coccolith-bearing cells and triggers a physiological response in bald cells. *Front. Microbiol.* 7:828. doi: 10.3389/fmicb.2016.00828

Labeeuw, L., Martone, P. T., Boucher, Y., and Case, R. J. (2015). Ancient origin of the biosynthesis of lignin precursors. *Biol. Direct* 10:23. doi: 10.1186/s13062-015-0052-y

Mayers, T. J., Bramucci, A. R., Yakimovich, K. M., and Case, R. J. (2016). A bacterial pathogen displaying temperature-enhanced virulence of the microalga *Emiliania huxleyi*. *Front. Microbiol.* 7:892. doi: 10.3389/fmicb.2016.00892

Miller, T. R., and Belas, R. (2004). Dimethylsulfoniopropionate metabolism by *Pfiesteria*-associated *Roseobacter* spp. *Appl. Environ. Microbiol.* 70, 3383–3391. doi: 10.1128/AEM.70.6.3383-3391.2004

Miller, T. R., Hnilicka, K., Dziedzic, A., Desplats, P., and Belas, R. (2004). Chemotaxis of *Silicibacter* sp. strain TM1040 toward dinoflagellate products. *Appl. Environ. Microbiol.* 70, 4692–4701. doi: 10.1128/AEM.70.8.4692-4701.2004

Mitchell, J. G., Okubo, A., and Fuhrman, J. A. (1985). Microzones surrounding phytoplankton form the basis for a stratified marine microbial ecosystem. *Nature* 316, 58–59. doi: 10.1038/316058a0

Mordecai, G., Verret, F., Highfield, A., and Schroeder, D. (2017). Schrödinger's Cheshire Cat: Are haploid *Emiliania huxleyi* cells resistant to viral infection or not? *Viruses* 9:51. doi: 10.3390/v9030051

Orata, F. D., Rosana, A. R., Xu, Y., Simkus, D. N., Bramucci, A. R., Boucher, Y., et al. (2016). Draft genome sequences of four bacterial strains isolated from a polymicrobial culture of naked (N-type) *Emiliania huxleyi* CCMP1516. *Genome Announc.* 4, e00674–e00616. doi: 10.1128/genomeA.00674-16

Planas, M., Perez-Lorenzo, M., Hjelm, M., Gram, L., Fiksdal, I. U., Bergh, O., et al. (2006). Probiotic effect *in vivo* of *Roseobacter* strain 27-4 against *Vibrio* (*Listonella*) *anguillarum* infections in turbot (*Scophthalmus maximus* L.) larvae. *Aquaculture* 255, 323–333. doi: 10.1016/j.aquaculture.2005.11.039

Price, M. N., Wetmore, K. M., Deutschbauer, A. M., and Arkin, A. P. (2016). A comparison of the costs and benefits of bacterial gene expression. *PLoS ONE* 11:e0164314. doi: 10.1371/journal.pone.0164314

Prol García, M. J., D'Alvise, P. W., and Gram, L. (2013). Disruption of cell-to-cell signaling does not abolish the antagonism of *Phaeobacter gallaeciensis* toward the fish pathogen *Vibrio anguillarum* in algal systems. *Appl. Environ. Microbiol.* 79, 5414–5417. doi: 10.1128/AEM.01436-13

Rao, D., Webb, J. S., Holmström, C., Case, R. J., Low, A., Steinberg, P., et al. (2007). Low densities of epiphytic bacteria from the marine alga *Ulva australis* inhibit settlement of fouling organisms. *Appl. Environ. Microbiol.* 73, 7844–7852. doi: 10.1128/AEM.01543-07

Rhodes, L. L., Peake, B. M., MacKenzie, A. L., Simon, M., and Edwards, A. R. (1995). Coccolithophores *Gephyrocapsa oceanica* and *Emiliania huxleyi* (Prymnesiophyceae = Haptophyceae) in New Zealand's coastal waters: characteristics of blooms and growth in laboratory culture. *New Zeal. J. Mar. Freshw. Res.* 29, 345–357.

Rodrigo-Torres, L., Pujalte, M. J., and Arahal, D. R. (2016). Draft genomes of *Nautella italica* strains CECT 7645T and CECT 7321: two roseobacters with potential pathogenic and biotechnological traits. *Mar. Genomics* 26, 73–80. doi: 10.1016/j.margen.2016.01.001

Sapp, M., Schwaderer, A. S., Wiltshire, K. H., Hoppe, H. G., Gerdts, G., and Wichels, A. (2007). Species-specific bacterial communities in the phycosphere of microalgae? *Microb. Ecol.* 53, 683–699. doi: 10.1007/s00248-006-9162-5

Schatz, D., Shemi, A., Rosenwasser, S., Sabanay, H., Wolf, S. G., Ben-Dor, S., et al. (2014). Hijacking of an autophagy-like process is critical for the life cycle of a DNA virus infecting oceanic algal blooms. *New Phytol.* 204, 854–863. doi: 10.1111/nph.13008

Schreiber, U., Schliwa, U., and Bilger, W. (1986). Continuous recording of photochemical and non-photochemical chlorophyll fluorescence quenching with a new type of modulation fluorometer. *Photosyn. Res.* 10, 51–62. doi: 10.1007/BF00024185

Segev, E., Wyche, T. P., Kim, K. H., Petersen, J., Ellebrandt, C., Vlamakis, H., et al. (2016). Dynamic metabolic exchange governs a marine algal-bacterial interaction. *Elife* 5:e17473. doi: 10.7554/eLife.17473

Seyedsayamdost, M. R., Carr, G., Kolter, R., and Clardy, J. (2011a). Roseobacticides: small molecule modulators of an algal-bacterial symbiosis. *J. Am. Chem. Soc.* 133, 18343–18349. doi: 10.1021/ja207172s

Seyedsayamdost, M. R., Case, R. J., Kolter, R., and Clardy, J. (2011b). The Jekyll-and-Hyde chemistry of *Phaeobacter gallaeciensis*. *Nat. Chem.* 3, 331–335. doi: 10.1038/nchem.1002

Seyedsayamdost, M. R., Wang, R., Kolter, R., and Clardy, J. (2014). Hybrid biosynthesis of roseobacticides from algal and bacterial precursor molecules. *J. Am. Chem. Soc.* 136, 15150–15153. doi: 10.1021/ja508782y

Seymour, J. R., Simo, R., Ahmed, T., Stocker, R., Simó, R., Ahmed, T., et al. (2010). Chemoattraction to dimethylsulfoniopropionate throughout the marine microbial food web. *Science* 329, 342–345. doi: 10.1126/science.1188418

Stocker, R. (2012). Marine microbes see a sea of gradients. *Science* 338, 628–633. doi: 10.1126/science.1208929

Sule, P., and Belas, R. (2013). A novel inducer of Roseobacter motility is also a disruptor of algal symbiosis. *J. Bacteriol.* 195, 637–646. doi: 10.1128/JB.01777-12

Thole, S., Kalhoefer, D., Voget, S., Berger, M., Engelhardt, T., Liesegang, H., et al. (2012). *Phaeobacter gallaeciensis* genomes from globally opposite locations reveal high similarity of adaptation to surface life. *ISME J.* 6, 2229–2244. doi: 10.1038/ismej.2012.62

Tripp, H. J., Kitner, J. B., Schwalbach, M. S., Dacey, J. W. H., Wilhelm, L. J., and Giovannoni, S. J. (2008). SAR11 marine bacteria require exogenous reduced sulphur for growth. *Nature* 452, 741–744. doi: 10.1038/nature06776

Tyrrell, T., and Merico, A. (2004). "*Emiliania huxleyi*: bloom observation and the conditions that induce them," in *Coccolithophores: From Molecular Processes to Global Impact*, ed H. R. Thierstein and J. R. Young (Berlin; Heidelberg: Springer), 585–604.

Vandecandelaere, I., Nercessian, O., Segaert, E., Achouak, W., Mollica, A., Faimali, M., et al. (2009). *Nautella italica* gen. nov., sp. nov., isolated from a marine electroactive biofilm. *Int. J. Syst. Evol. Microbiol.* 59, 811–817. doi: 10.1099/ijs.0.002683-0

van der Wal, P., de Jong, E. W., Westbroek, P., de Bruijn, W. C., and Mulder-Stapel, A. A. (1983). Ultrastructural polysaccharide localization in calcifying and naked cells of the coccolithophorid *Emiliania huxleyi*. *Protoplasma* 118, 157–168. doi: 10.1007/BF01293073

Vardi, A., Van Mooy, B. A. S., Fredricks, H. F., Popendorf, K. J., Ossolinski, J. E., Haramaty, L., et al. (2009). Viral glycosphingolipids induce lytic infection and cell death in marine phytoplankton. *Science* 326, 861–865. doi: 10.1126/science.1177322

von Dassow, P., John, U., Ogata, H., Probert, I., Bendif, E. M., Kegel, J. U., et al. (2015). Life-cycle modification in open oceans accounts for genome variability in a cosmopolitan phytoplankton. *ISME J.* 9, 1–13. doi: 10.1038/ismej.2014.221

Wang, H., Tomasch, J., Jarek, M., and Wagner-Döbler, I. (2014). A dual-species co-cultivation system to study the interactions between Roseobacters and dinoflagellates. *Front. Microbiol.* 5:311. doi: 10.3389/fmicb.2014.00311

Wang, R., Gallant, É., and Seyedsayamdost, R. (2016). Investigation of the genetics and biochemistry of roseobacticide production in the Roseobacter clade bacterium *Phaeobacter inhibens*. *MBio* 7:e02118–e02115. doi: 10.1128/mBio.02118-15

Wang, R., and Seyedsayamdost, M. R. (2017). Roseochelin B, an algaecidal natural product synthesized by the roseobacter *Phaeobacter inhibens* in response to algal sinapic acid. *Org. Lett.* 19, 5138–5141. doi: 10.1021/acs.orglett.7b02424

Wetmore, K. M., Price, M. N., Waters, R. J., Lamson, J. S., He, J., Hoover, C. A., et al. (2015). Rapid quantification of mutant fitness in diverse bacteria by sequencing randomly bar-coded transposons. *MBio* 6, e00306–e00315. doi: 10.1128/mBio.00306-15

Wienhausen, G., Noriega-Ortega, B. E., Niggemann, J., Dittmar, T., and Simon, M. (2017). The exometabolome of two model strains of the *Roseobacter* group: a marketplace of microbial metabolites. *Front. Microbiol.* 8:1985. doi: 10.3389/fmicb.2017.01985

Wilson, W. H., Tarran, G., and Zubkov, M., V (2002). Virus dynamics in a coccolithophore-dominated bloom in the North Sea. *Deep Sea Res. II Top. Stud. Oceanogr.* 49, 2951–2963. doi: 10.1016/S0967-0645(02)00065-6

Wolfe, G. V., Sherr, E. B., and Sherr, B. F. (1994). Release and consumption of DMSP from *Emiliania huxleyi* during grazing by *Oxyrrhis marina*. *Mar. Ecol. Prog. Ser.* 111, 111–119. doi: 10.3354/meps111111

Wolfe, G. V., Steinke, M., and Kirst, G. O. (1997). Grazing-activated chemical defense in a unicellular marine alga. *Nature* 387, 894–897. doi: 10.1038/43168

Zhang, X., Gamarra, J., Castro, S., Carrasco, E., Hernandez, A., Mock, T., et al. (2016). Characterization of the small RNA transcriptome of the marine coccolithophorid, *Emiliania huxleyi*. *PLoS ONE* 11:e0154279. doi: 10.1371/journal.pone.0154279

Conflict of Interest Statement: The authors declare that the research was conducted in the absence of any commercial or financial relationships that could be construed as a potential conflict of interest.

frontiers in Marine Science

ORIGINAL RESEARCH
published: 12 January 2018
doi: 10.3389/fmars.2017.00441

Novel ssDNA Viruses Detected in the Virome of Bleached, Habitat-Forming Kelp *Ecklonia radiata*

Douglas T. Beattie[1]*, *Tim Lachnit*[1,2], *Elizabeth A. Dinsdale*[3], *Torsten Thomas*[1] and *Peter D. Steinberg*[1,4]

[1] Centre for Marine Bio-Innovation and School of Biological, Earth and Environmental Sciences, University of New South Wales, Sydney, NSW, Australia, [2] Zoological Institute, Christian-Albrechts-University Kiel, Kiel, Germany, [3] Department of Biology, San Diego State University, San Diego, CA, United States, [4] Sydney Institute of Marine Science, Mosman, NSW, Australia

Kelp forests provide essential habitats for organisms in temperate rocky shores. Loss of kelp forests has occurred over large areas in a number of temperate regions, including in Australia, where the dominant kelp *Ecklonia radiata* has been lost from substantial areas of the shoreline. Loss of *E. radiata* has been associated with environmental stressors, including increased temperature and anthropogenic contaminants, as well as biological factors, such as herbivory. Disease may also play a role, but there is little information on the role of disease in the loss of kelp from coastal ecosystems or on the potential role of pathogenic microorganisms, such as viruses. *E. radiata* across much of its distribution in Australia can develop a "bleached" phenotype, which may be a disease. To investigate whether the phenotype was associated with a potential viral agent, we shotgun sequenced viral particles that were isolated from kelp with normal (healthy) and bleached phenotypes. Each virome consisted of ∼380,000 reads, of which ∼25% were similar to known viruses. All samples were dominated by bacteriophages, but novel ssDNA virus sequences were detected that were almost exclusively in viromes from the bleached kelp phenotype. These ssDNA viruses are covered by 11 contigs that contained complete capsids and characteristic *rep* genes that were 30–60% similar to those of circular, Rep-encoding ssDNA viruses (CRESS-DNA viruses). CRESS-DNA viruses have not previously been described from macroalgae, and the *rep* genes were similar to CRESS-DNA viruses from marine water samples, snails, crabs, anemones, but also dragonflies. This raises the interesting possibility that the kelp could be a vector of the CRESS-DNA viruses to other organisms that are associated with the bleached state.

Keywords: circovirus, microbial ecology, virome, kelp, marine disease, metagenome, CRESS-DNA, viral ecology

OPEN ACCESS

Edited by:
Matthias Wietz,
University of Oldenburg, Germany

Reviewed by:
Karen Dawn Weynberg,
The University of Queensland, Australia
Simon M. Dittami,
UMR8227 Laboratoire De Biologie Intégrative Des Modèles Marins, France

***Correspondence:**
Douglas T. Beattie
d.beattie@student.unsw.edu.au

Specialty section:
This article was submitted to Microbial Symbioses, a section of the journal Frontiers in Marine Science

Received: *20 November 2017*
Accepted: *22 December 2017*
Published: *12 January 2018*

Citation:
Beattie DT, Lachnit T, Dinsdale EA, Thomas T and Steinberg PD (2018) Novel ssDNA Viruses Detected in the Virome of Bleached, Habitat-Forming Kelp Ecklonia radiata. Front. Mar. Sci. 4:441. doi: 10.3389/fmars.2017.00441

INTRODUCTION

Ecklonia radiata is a large, stipitate brown alga (class *Phaeophyceae*, order *Laminariales*, or commonly, kelp), and the dominant primary habitat-forming organism over 71,000 km^2 of the temperate rocky coastlines of Australia (Bennett et al., 2016). Kelps, such as *E. radiata,* provide habitat and nutrients that are essential to coastal food webs (Steneck et al., 2002), and the importance of *E. radiata* habitats in temperate Australia has led to them being described as

"The Great Southern Reef" (Bennett et al., 2016). Fisheries, tourism, and other industries taking place within these habitats are estimated to be worth AU$10 billion annually to the Australian economy (Bennett et al., 2016).

In recent years there has been a loss of kelp cover in temperate regions of Australia from locations across much of the range of *E. radiata*, from Perth on the West coast, along the Southern coast, up to the Solitary Islands on the East coast (Connell et al., 2008; Ling and Johnson, 2012; Vergés et al., 2016; Wernberg et al., 2016). Loss of kelp results in major losses in biodiversity, ecosystem function, and associated fisheries (Andrew and O'Neill, 2000; Bishop et al., 2010; Burge et al., 2014; Vergés et al., 2016; Wernberg et al., 2016), and in Australia loss of *E. radiata* has been associated with a number of environmental stressors. This includes stressors associated with urbanization, such as increased nutrients and sedimentation of the coastal region (Connell et al., 2008), and ocean warming, through both direct physiological effects of temperature as well as indirect effects through range extensions of herbivorous sea urchins or fishes, which consume large areas of kelp forests (Wernberg et al., 2011; Ling and Johnson, 2012; Vergés et al., 2016). Though relatively little studied in seaweed systems, microbial disease may also play a role in loss of habitat-forming seaweeds (Egan et al., 2014). Disease in marine systems appears to be increasing globally, including in communities that are dominated by primary habitat-forming organisms, such as coral reefs and kelp forests (Rosenberg et al., 2007; Vega Thurber et al., 2009; Krediet et al., 2013), and disease in seaweeds has been linked to anthropogenic stressors, such as ocean warming (Campbell et al., 2011; Case et al., 2011).

Microbial communities are integral to the health of all organisms, such that hosts and their associated microbial communities (microbiome) are increasingly being treated as a holistic system, or holobiont (Egan et al., 2013). This approach is now common for understanding the interaction between marine habitat-forming organisms, such as corals, seaweeds, or sponges (Bourne et al., 2009; Egan et al., 2013; Webster and Thomas, 2016). Disturbances to the microbiome of these organisms are associated with stress and disease of the host (Morris et al., 2016). For example, disruption of the microbiome of the Australian macroalga *Delisea pulchra* leads to bleaching and reduced reproductive capacity (Egan et al., 2013; Campbell et al., 2014; Wahl et al., 2015), and microbial pathogens cause bleaching of *D. pulchra* in both the field (Campbell et al., 2011) and in laboratory inoculation experiments (Kumar et al., 2016). Disruption of the holobiont and resultant disease is increasingly seen as critical for other marine habitat forming organisms.

We have recently identified a bleaching phenotype in *E. radiata*, which occurs widely across its biogeographic range and which is characterized by bleached areas of the thallus with reduced photosynthetic capacity (Marzinelli et al., 2015). The bacterial components of the microbiome of bleached vs. non-bleached *E. radiata* were distinct, suggesting that the microbiome of the algae undergoes a shift associated with the disruption of normal function (e.g., photosynthesis; Marzinelli et al., 2015). However, specific bacterial pathogens, which induce bleaching, have not yet been extensively characterized. Other components of the microbiome may also affect the health of hosts. In particular, viruses are likely ubiquitous components of marine holobionts and are now emerging as pathogens or potential pathogens in a diverse range of marine organisms, including archaea (Rohwer and Thurber, 2009), microalgae (Brussaard, 2004; Weynberg et al., 2017), sea stars (Hewson et al., 2014), and macroalgae (Lachnit et al., 2015).

Viruses consist of two major groups, bacteriophages that infect bacteria and viruses that infect eukaryotes. The tailed bacteriophages with dsDNA genomes, *Caudovirales,* include the families *Siphoviridae*, *Myoviridae*, and *Podoviridae*. Bacteriophages also include *Inoviridae*, which possess ssDNA genomes, and together these bacteriophages form a major component of marine viral assemblages (Mann, 2005; Dinsdale et al., 2008b; Roux et al., 2012; Xue et al., 2012). Abundant eukaryote viruses detected in algae are from the family *Phycodnaviridae*, which have a dsDNA genome of 100–550 kb and infect both unicellular and multicellular algae (Wilson et al., 2009). *Phycodnaviridae* have been investigated in the filamentous brown-alga *Ectocarpus siliculosus,* a model organism, and a few genomes have been sequenced (Van Etten et al., 1991; Müller and Frenzer, 1993; Easton et al., 1997; Kapp et al., 1997; Maier et al., 1998; Delaroque and Boland, 2008). However, few studies have been conducted on macroalgae from the field (e.g., viruses in *Laminaria digitata* McKeown et al., 2017) and none on *E. radiata*.

ssDNA viruses, which have small circular genomes (1–5 kb), are an emerging group of viruses that are implicated in marine disease and mass mortalities across a number of marine phyla, including fishes, molluscs, echinoderms, and crustaceans (Hasson et al., 1995; Friedman et al., 2005; McLoughlin and Graham, 2007; Lang et al., 2009). ssDNA viruses include a subgroup which possess circular genomes, and a particular replication initiation gene, *rep*. These are therefore called Circular Rep-Encoding ssDNA (CRESS-DNA) viruses (Rosario et al., 2009; Delwart and Li, 2012; Labonté and Suttle, 2013; Simmonds et al., 2017). These include the *Geminiviridae, Nanoviridae, Circoviridae,* and *Genomoviridae,* which employ rolling-circle replication (RCR), facilitated by the Rep protein (Rosario et al., 2012b). In addition to the Rep protein, CRESS-DNA viruses have a characteristic stem-and-loop secondary structure, which facilitates RCR. The loop region contains a conserved nonanucleotide motif, NANTATTAC (Labonté and Suttle, 2013). The *Circoviridae* and *Nanoviridae* are diverse in aquatic and marine environments, including ocean, freshwater, wastewater, deep-sea vents, Antarctic lakes and ponds, and hot springs (Angly et al., 2006; Rosario et al., 2009, 2012a; Cassman et al., 2012; Liu et al., 2012; Labonté and Suttle, 2013).

Here we investigate the viruses associated with bleached and non-bleached *E. radiata* from Sydney, Australia. First, virus particles were extracted from kelp tissue. DNA was extracted from these and amplified using whole-genome amplification (WGA), which is biased toward small and circular genomes (Sabina and Leamon, 2015), but thus aids in detection of potentially rare and small genomes in metagenomic samples (Kim et al., 2008; Cheval et al., 2011; Rosario et al., 2012a; Fahsbender et al., 2015). This was followed by shotgun

sequencing and metagenomic analysis. We describe the general features of the kelp virome, and test whether components of the virome differ between the non-bleached and bleached phenotype, in order to explore whether viral pathogens may be a possible cause of the bleaching phenotype. Our results show that circoviruses were nearly absent in the non-bleached kelp, but in high abundance in the bleached kelp, and we describe these novel viruses in detail.

METHODS

Sampling

Individual thalli of *E. radiata* were sampled from Long Bay in Sydney, Australia (−33.97, 151.26) during June 2014 at a depth of 3 m. The water temperature at the time of sampling was 16°C. Tissue samples of blades were taken from three bleached individuals and three non-bleached, healthy, thalli. These phentoypes are described in Marzinelli et al. (2015). Viral particles were isolated from kelp tissue as described in Lachnit et al. (2015).

DNA Extraction and Metagenomic Sequencing

Viral DNA was extracted from virus particles in SDS-extraction buffer (1% SDS, 200 mM Tris, 50 mM EDTA, pH 7.5) in the presence of 1% (w/v) polyvinylpyrrolidone (MW 40,000), 1% 2-mercaptoethanol and proteinase K (0.5 mg ml^{-1}) at 37°C for 30 min, followed by 56°C for 15 min. Double the volume of DNA-extraction buffer (2.6 M NaCl, 150 mM Tris, 75 mM EDTA, 2.5% cetyltrimethylammonium bromide (CTAB), 1% 2-mercaptoethanol, pH 7.5) was added and samples were incubated for another 15 min at 56°C. An equal volume of chloroform:isoamyl alcohol (24:1) was added to the solution, mixed and centrifuged at 12,000 RCF at room temperature for 5 min. The chloroform:isoamyl alcohol extraction of the supernatant was repeated three times to remove contaminating polysaccharides and proteins. The supernatant was transferred into a new tube and the nucleic acids were precipitated by the addition of 0.7 volume of isopropanol. After an incubation step at 20°C for 2 h nucleic acids were pelleted by centrifugation at 14,000 RCF at 4°C for 20 min. The pellet was washed with 75% (v/v) ethanol, air dried and dissolved in 30 µl molecular grade water.

All samples underwent whole genome amplification steps using a REPLI-g Mini Kit (QIAGEN), where the reaction was conducted using 20 µL of denatured DNA, incubating the reaction mix at 30°C for 16 h. DNA was frozen and submitted to the Ramaciotti Centre at UNSW for library preparation using a TruSeq Low Input kit (Illumina). Shotgun metagenomic sequencing was conducted using an Illumina MiSeq sequencer with 2 × 250 bp chemistry. A total of six viral metagenomes (or viromes) were sequenced, three from kelp with the bleached phenotype and three from the non-bleached phenotype. The reads were processed using Prinseq (Schmieder and Edwards, 2011) by trimming the ends where the quality score was below 20, and removing exact duplicates. The paired-end reads were assessed using default settings on PEAR (Zhang et al., 2014) to determine if they could be joined to form longer sequences.

Virome Profile Analysis

Several bioinformatics approaches were used to identify the types of phage and eukaryotic viruses in the kelp viromes. First, the reads were aligned against the NCBI non-redundant protein database (NR), downloaded on May 05 2017. Alignment was performed using BLASTx (Altschul et al., 1990) with an e-value of 10^{-5}. Alignment matches were screened to remove all non-viral similarities found. Alignment results were analyzed using MEGAN (Huson et al., 2016) to infer best taxonomic and/or functional assignments. The Least Common Ancestor (LCA) parameters was used with a minimum score of 50, max expected e-value 10^{-5}, top 10%, LCA 100%, minimum complexity 0. To detect significant differences in the relative abundances of assignments to each virus family, STAMP (Parks et al., 2014) was used to perform two tailed Welch's *t*-test ($\alpha = 0.05$) with Bonferroni correction to compare the bleached and non-bleached kelp viromes.

To assess possible contamination of the viromes by host genomic or bacterial DNA, the entire set of similarities found, including similarities to viruses and non-viruses, was considered. Sequences, which had higher alignment bitscores to non-viruses, were aligned against all the brown-alga sequences in NCBI (downloaded on May 05 2017), using BLASTn with an e-value of 10^{-5}. The sequences with <95% similarity to *Ecklonia spp.* suggested that they are not part of the brown algae. This threshold was chosen as essential genes (e.g., *rbcL*) of different species of *Eckonia*, and even some distally related members of the brown algae are >95% similar (Rothman et al., 2015). Decontamination programs (e.g., DeconSeq Schmieder and Edwards, 2011) were not employed to automate the removal of potential bacterial contamination, as genes are often shared between bacteriophage and their hosts. Instead, more information on the origin of the reads was obtained by assembly and assessment of the genomic content (see below), and contamination was retrospectively removed from the results and analyses.

The individual metagenomes were assembled to provide longer contigs using SPAdes 3.9.0 (using default parameters; Bankevich et al., 2012). SPAdes was chosen as it performs better than other assemblers on virome data (Hesse et al., 2017; Papudeshi et al., 2017; Vollmers et al., 2017). Reads were mapped to the contigs using Bowtie 2.2.5 (Langmead and Salzberg, 2012) and visualized using Tablet (Milne et al., 2009) to assess the evenness of read coverage and to identify possible chimeric assemblies, which were removed from further analysis. To investigate the distribution of viruses between the bleached and non-bleached kelp, the contigs were aligned to the NR database as described above. The contigs and their component reads were considered contamination and removed from the analysis and results if (a) the alignment bitscore to a virus reference was less than to a non-virus sequence, and (b) the alignment matches did not contain core

genes of the assigned virus taxon e.g., phage-tail genes of *Caudovirales*.

Viral Genome Reconstruction

All six metagenomes were pooled and cross-assembled with SPAdes 3.9.0 to obtain longer contigs and/or complete genomes. Assessment and alignments of the cross-assembled contigs were performed as described above. At this stage of the analysis, circoviruses were identified as the only part of the eukaryotic DNA virus community that varied in abundance between bleached and non-bleached kelp, and therefore were investigated in more detail. Open reading frames (ORFs) on the circoviral contigs were detected using Prodigal (Hyatt et al., 2010) with a length of > 50 amino acids. Predicted protein sequences were aligned against one another, and their reference sequences using the MUSCLE aligner with default settings (Edgar, 2004). To visualize the diversity of the ORFs a phylogenetic tree was produced using the Jukes-Cantor genetic distance model and the neighbor-joining algorithm with 100 bootstraps. *Circoviridae* contigs were submitted to Mfold (Zuker, 2003) to determine their stem-and-loop secondary structure. The loop motif was compared across the *Circoviridae* group through alignment using MUSCLE.

RESULTS

Overall Composition of the Virome of *Ecklonia radiata*

The six *E. radiata* viromes contained an average of 386,000 reads with an average length of 149 ± 2SD bp. (Supplementary information S1). No reads were removed through quality control, although 14% of the reads were trimmed up to 10 bp where the read quality was <20. Most paired reads could not be joined, and so forward-reads were only used in alignment searches. Analysis of alignment results found 81,256 ± 22,106 virus-like reads per metagenome (∼20% of the sequences were similar to the NR database). The majority (86–94%) of virus-like reads were assigned to bacteriophage in the order *Caudovirales* (**Figure 1**). In order of abundance, similarities were detected to the viral groups *Siphoviridae* (average of 48% of virus-assigned reads), *Myoviridae* (16%), unclassified bacteriophages (12%), *Inoviridae* (8%), *Podoviridae* (7%), followed by *Circoviridae* (7%). Within the *Caudovirales,* reads similar to *Siphoviridae* were more abundant (adjusted *p-value* = 0.003) in the non-bleached kelp phenotype, however the total number of bacteriophage reads within the *Caudovirales* did not significantly differ between non-bleached and bleached kelp viromes. In the eukaryotic viral fraction, reads similar to *Phycodnaviridae* and other large dsDNA viruses were lower in abundance (<2% of reads assigned) compared to the bacteriophages and did not differ in abundance between viromes of non-bleached and bleached kelp (adjusted *p-value* = 0.785). Sequences of ssDNA viruses belonging to the *Circoviridae* were rare overall (0.48% of total reads), but were almost exclusively in bleached kelp viromes. Six reads were assigned to *Circoviridae* from a single non-bleached kelp virome, whereas 6,403 reads were assigned from bleached kelp viromes.

Assembly of all reads per individual metagenome provided an average of 4,011 ± 351 contigs of 38,709 ± 6,392 bp length. The taxonomic assignment of the contigs mirrored that of the reads (Supplementary information S2). Bacteriophage possessed the greatest amount of read coverage in the contigs (60%), followed by the *Phycodnaviridae* (8%) and *Circoviridae* (6%). The *Circoviridae* contigs ($n = 42$) were assembled only in the bleached kelp viromes, with the exception of a single contig from one non-bleached kelp virome. Similar to the read data, *Circoviridae* contigs were the only eukaryotic viral group that varied in coverage between the bleached and non-bleached kelp phenotypes (adjusted *p-value* = 0.002).

Cross-assembly of all six metagenomes yielded 7,561 contigs, the longest being 246,893 bp (N_{50} 20,791 bp, N_{95} 246 bp). When aligned against an NCBI virus-only protein database, 847 contigs showed similarity to viruses (**Figure 2**). In descending order of abundance these were assigned to *Siphoviridae* (97 contigs), environmental viruses from metagenomes (92), *Myoviridae* (59), *Podoviridae* (48), unclassified bacteriophages (47), *Circoviridae* (26), *Phycodnaviridae* (21), *Mimiviridae* (15), *Inoviridae* (9) and other virus families with very low abundances (total of 434).

We assessed contamination by regarding the contig similarities to virus and non-viruses. Two thousand two hundred and sixty-seven contigs of the total 7,561 were given a taxonomic assignment through alignment to NR (Supplementary information S3). Eight hundred and forty-seven contigs had similarity to viruses. Of these, 146 contigs had no similarity to other references, 576 contigs were also similar to bacteria and 125 contigs were also similar to eukaryotes. The majority (36%) of contigs similar to both viruses and eukaryotes were similar to *E. siliculosus* Virus-1. Four contigs had both higher alignment bitscores to brown-alga sequences, and did not include characteristic virus genes or conserved domains and were thus assumed to be eukaryotic. The contigs with similarity to both viruses and bacteria (576) were examined further, finding 113 contigs with higher bitscores to bacterial references and no characteristic bacteriophage genes, and assumed to be from bacterial cells. Contigs and their constituent reads that were considered eukaryotic or bacterial contamination were removed from the analyses and results of virus abundances and gene content. Contigs that were assigned as circoviruses had no other similarities to references in NR, and as the circoviruses were the only eukaryotic virus that showed variation between kelp phenotypes, these were analysed in more detail.

Investigation of *Circoviridae*-Like Contigs

The *Circoviridae* contigs ($n = 26$) were 739–5,420 bp long, and contained up to two ORFs. The first ORF was 855 bp, and the only translated similarity between these and reference proteins were two ORFs with similarity to putative CRESS-DNA virus capsid genes from environmental metagenomes. These showed 30% pairwise identity to putative capsid genes of a circular virus associated with a sea anemone (Genbank accession: YP_009163900.1) and a circular ssDNA virus isolated from an Antarctic ice shelf pond (Genbank accession: YP_009047127.1).

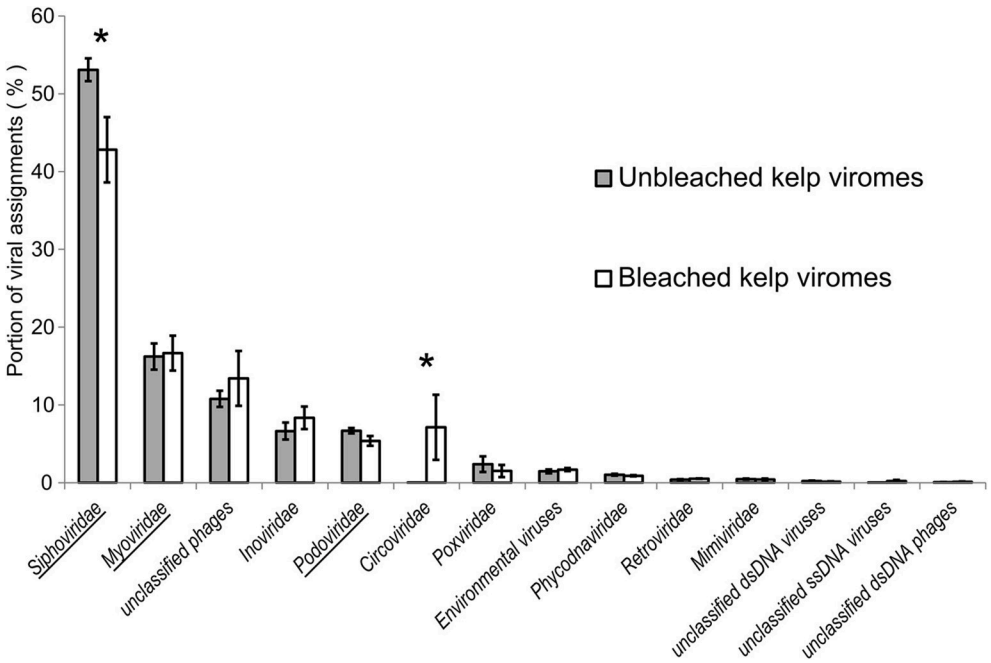

FIGURE 1 | Reads from viromes of bleached and unbleached kelps that were assigned to virus references. Bars are ±1 standard error. Asterisk denotes an adjusted *p-value* < 0.005. Underlined taxa belong to the *Caudovirales*. Environmental viruses are annotated sequences from environmental metagenomes.

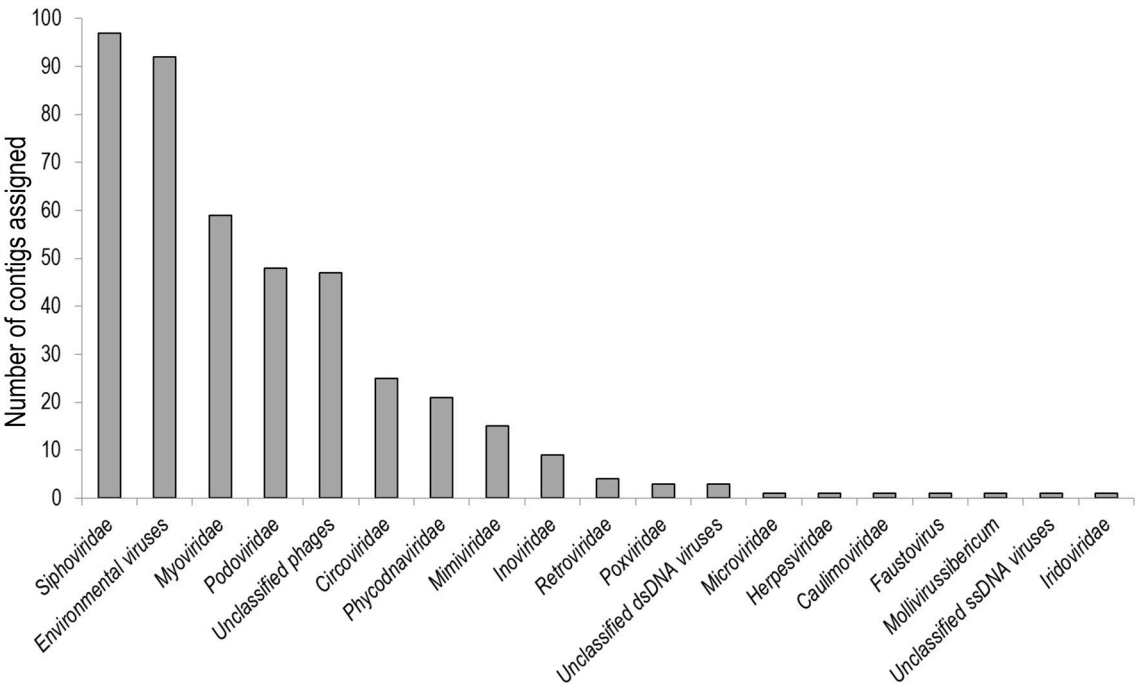

FIGURE 2 | Contigs from the cross-assembly of kelp viromes that were assigned to virus references.

The second ORF was 305–336 amino acids and was the characteristic *rep* genes of CRESS-DNA viruses. The *rep* genes were found in three different lengths (915 bp, 924 bp, and 1,008 bp) suggesting three genotypes, which we refer to from hereon as A-C. There were three contig configurations of the circovirus sequences: Type-A (8 contigs), Type-B (2 contigs)

and Type-C (single contig; **Figure 3**). Type-A contained both the capsid and *repA*, in reverse orientation with a conserved intergenic region (IR) between the two ORFs. The IR of the eight contigs shared a pairwise identity of 70%. Type-B contained *repB* and the IR. Type-C contained only *repC* and no capsid sequences or the IR. The origin of replication (*ori*), included the characteristic nonanucleotide stem and loop structures involved in rolling circle replication of CRESS-DNA viruses and was located upstream of the *rep* gene in all contigs (**Figure 3**). The nonanucleotide motif in each contig was TAGTATTAC. The other 15 of the 26 circovirus-like contigs that did not contain complete ORFs were found to contain fragments of *rep* and capsid genes of circoviruses, suggesting incomplete assembly.

The *rep* genes from the 11 contigs and the closest reference sequences in the database were aligned. The *rep* genes formed three clusters with each cluster showing >95% similarity. Between all *rep* genes in our dataset, and their most similar reference sequences, the *rep* sequences were 27–60% similar. The references with greatest similarity to the detected circoviruses were from viruses found in association with aquatic samples or invertebrates, including marine snails and hermit crabs, but also dragonflies (**Figure 4**).

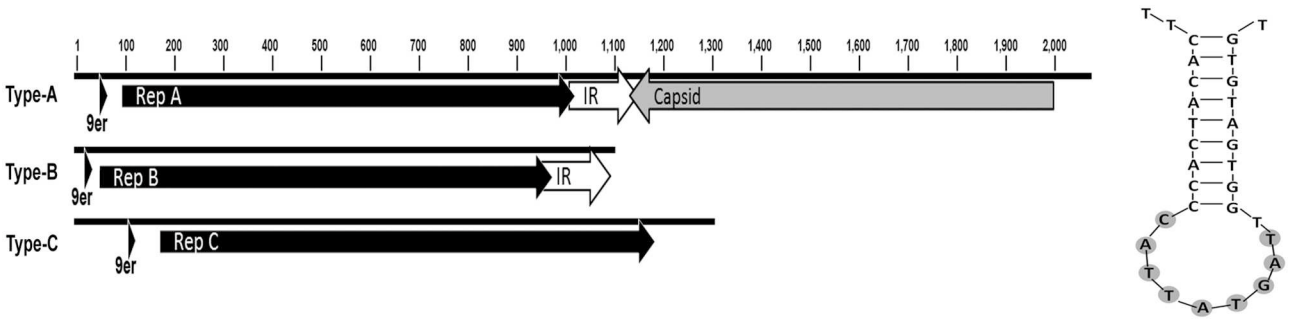

FIGURE 3 | Circovirus-like contig ORFs Appeared in three different configurations (L) *Rep* types were present on three types of contig. (R) Predicted stem-loop structures associated with the RCR initiation nonanuclotide motif (9er) is highlighted.

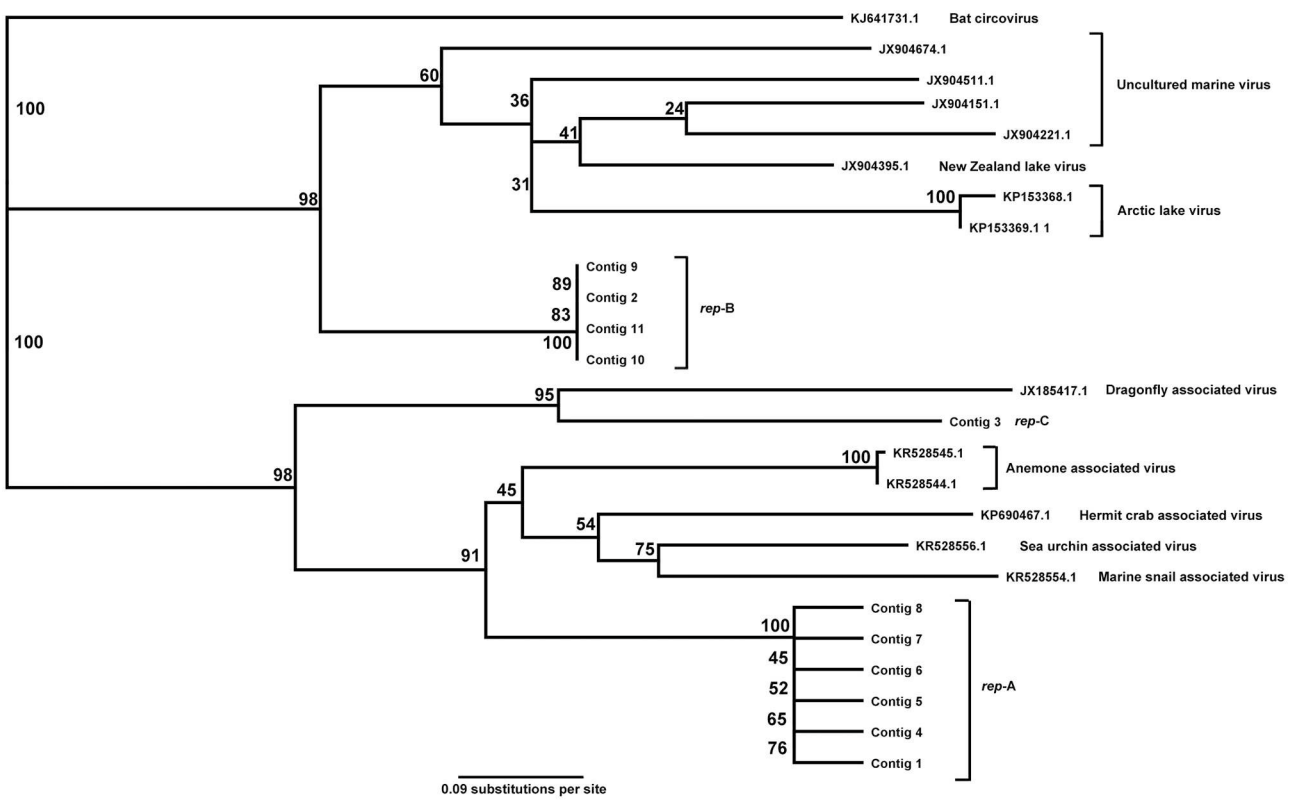

FIGURE 4 | Alignment tree of *rep* ORFs in circovirus-like contigs.

DISCUSSION

We characterized the virome of both bleached and non-bleached individuals of the kelp *E. radiata.* Sequences similar to bacteriophages in the *Siphoviridae* were detected in greatest abundance overall, followed by *Myoviridae*, unclassified phages, *Inoviridae*, and *Podoviridae*. For most viral taxa there was little difference in the relative abundance in reads between the two kelp phenotypes. However, eukaryote circovirus-like sequences differed significantly in abundance between bleached and non-bleached kelp, with bleached viromes containing the vast majority (>99%) of circovirus-like reads. The circoviruses sequences from *E. radiata* included three phylogenetic groups, which all contained the characteristic *rep* gene of CRESS-DNA viruses, and were most similar to recently described circoviruses from pelagic water samples and marine invertebrates.

Initial alignment of raw DNA reads of kelp-associated viromes against a non-redundant protein database showed that most sequences were unknown, which is often the case in environmental metagenomes, but especially in marine virome data (Dinsdale et al., 2008a,b; Willner et al., 2009; Cassman et al., 2012; Brussaard et al., 2016). The most abundant contigs with similarity to known viruses were the bacteriophage *Caudovirales* (**Figure 2**). While the overall abundance of bacteriophage-like contigs did not differ, contigs similar to *Siphoviridae* were more abundant in viromes of non-bleached kelp, perhaps as a cause or consequence of the differences in the bacterial community previously seen between bleached and non-bleached *E. radiata* (Marzinelli et al., 2015). Large dsDNA viruses, such as *Phycodnaviridae* and *Mimiviridae*, formed the second largest group of virus-like contigs detected, and found with similar relative read numbers in metagenomes of non-bleached and bleached kelp. The majority of similarities to *Phycodnaviridae* were to EsV-1, which only produces virus particles in the reproductive structures of its host. EsV-1 may share a similar life history to *Phycodnaviridae* present in *E. radiata*, in which case the virus particles likely originated from the sori on the sampled kelp thallus. This group of viruses may be part of a persistent and possibly stable viral assemblage of the kelp holobiont. In contrast, significantly more circovirus-like sequences were detected in bleached kelp viromes than in non-bleached ones.

The circovirus genomes assembled here were of 2–5 kb in length. The small size of ssDNA virus genomes means that their genetic material is predisposed to be relatively scarce when compared to other viruses that may have up to 100-fold larger genomes (e.g., *Phycodnaviridae)*. Whole genome amplification using multiple displacement amplification (MDA) of circular genomes has been used to sequence these viruses, even from very small amounts of DNA (Binga et al., 2008). MDA is known to create biases toward viruses with small genomes. Alternative methods, such as random priming-mediated sequence-independent single-primer amplification (RP-SISPA), could have been used, but this method can cause an overrepresentation in the datasets of viruses with large genomes (Adriaenssens et al., 2017). This bias away from small genomes has been noted by other authors (Karlsson et al., 2013; Weynberg et al., 2014).

The genome structures of the CRESS-DNA virus sequences are similar to Type I and II ssDNA viruses, where the reading frames of the *rep* and capsid genes are positioned 3′–5′ away from the stem-loop replication initiation structure. These viral types include *Circoviridae, Nanoviridae, Geminiviridae,* and other unclassified CRESS-DNA viruses from aquatic and marine metagenomes (Rosario et al., 2012b).

ssDNA (including CRESS-DNA) viruses have been characterized in medical and agricultural fields, due to their significance as human and agricultural pathogens (Roossinck, 2013). *Circoviridae, Anelloviridae, Genomoviridae,* and *Parvoviridae* are pathogens of humans and other vertebrates, such as pigs, poultry, and other domestic animals, but to date none have been identified in macroalgae. The circoviruses detected in the bleached kelp viromes were similar to a diverse subsection of marine viruses isolated from hermit crabs, sea anemones, but also had similarity to CRESS-DNA viruses detected in dragonflies (Rosario et al., 2012a). CRESS-DNA viruses are found in association with diverse habitats and host phyla (Rosario et al., 2012a,b; Eaglesham and Hewson, 2013; Fahsbender et al., 2015; Reavy et al., 2015), and circovirus-like proteins have been detected in a wide range of organisms, including mammals, birds, fish, cnidarians, as well as in a diverse range of aquatic and marine environments (Rosario et al., 2012b). Many circoviruses are important pathogens, or putative pathogens, and given their high relative abundance on the bleached phenotype it may be that they play a role in bleaching of *E. radiata*. Their increase may also be a secondary effect of bleaching, with the primary causative agent(s) being other microbes, or an interaction among multiple viruses, bacteria, fungi and others that are present in the kelp microbiome. Microbial agents can also interact with eukaryotic natural enemies, such as grazers to damage seaweeds (Campbell et al., 2014), which adds complexity when attempting to distinguish pathogens which cause disease from other secondary organisms (e.g., saprophytes such as fungi or bacteria) that arrive after disease onset to feed on compromised or decaying hosts (Burge et al., 2013; Egan and Gardiner, 2016). A more definitive resolution of the role of circoviruses in kelp bleaching thus awaits a more experimental approach, e.g., inoculation experiments, such as those conducted for *D. pulchra* and its bacterial pathogens (Campbell et al., 2015; Kumar et al., 2016). The circoviruses were the only eukaryotic DNA virus in the viromes that was overrepresented in the bleached compared with the non-bleached phenotypes, suggesting it may be associated with the bleached phenotype. However, ssDNA viruses have a ubiquitous presence in a wide range of eukaryotes and natural environments. The contigs we identified showed similarities to circoviruses found in hosts as broad as sea stars and crustaceans, raising the question of whether the circovirus was infecting the kelp host, or one of the herbivores associated with the kelp. Therefore, kelp could be infected with the circovirus, directly causing the phenotype, or the kelp could be acting as a vector to one of the herbivores or symbionts.

AUTHOR CONTRIBUTIONS

TL: performed isolation and sequencing of samples; DB: performed analysis onwards; Other authors are supervisors.

ACKNOWLEDGMENTS

Funding was provided by the University of New South Wales and the Centre for Marine Bio-Innovation, Sydney Australia and ARC Discovery Grant DP1401002776. TL acknowledges funding from the Deutsche Forschungsgemeinschaft (DFG-La297 8/1-1).

SUPPLEMENTARY MATERIAL

The Supplementary Material for this article can be found online at: https://www.frontiersin.org/articles/10.3389/fmars.2017.00441/full#supplementary-material

REFERENCES

Adriaenssens, E. M., Kramer, R., Van Goethem, M. W., Makhalanyane, T. P., Hogg, I., and Cowan, D. A. (2017). Environmental drivers of viral community composition in Antarctic soils identified by viromics. *Microbiome* 5:83. doi: 10.1186/s40168-017-0301-7

Altschul, S. F., Gish, W., Miller, W., Myers, E. W., and Lipman, D. J. (1990). Basic local alignment search tool. *J. Mol. Biol.* 215, 403–410. doi: 10.1016/S0022-2836(05)80360-2

Andrew, N. L., and O'Neill, A. L. (2000). Large-scale patterns in habitat structure on subtidal rocky reefs in New South Wales. *Mar. Freshw. Res.* 51, 255–263. doi: 10.1071/MF99008

Angly, F. E., Felts, B., Breitbart, M., Salamon, P., Edwards, R. A., Carlson, C., et al. (2006). The marine viromes of four oceanic regions. *PLoS Biol.* 4:e368. doi: 10.1371/journal.pbio.0040368

Bankevich, A., Nurk, S., Antipov, D., Gurevich, A. A., Dvorkin, M., Kulikov, A. S., et al. (2012). SPAdes: a new genome assembly algorithm and its applications to single-cell sequencing. *J. Comput. Biol.* 19, 455–477. doi: 10.1089/cmb.2012.0021

Bennett, S., Wernberg, T., Connell, S. D., Hobday, A. J., Johnson, C. R., and Poloczanska, E. S. (2016). The 'Great Southern Reef': social, ecological and economic value of Australia's neglected kelp forests. *Mar. Freshw. Res.* 67, 47–56. doi: 10.1071/MF15232

Binga, E. K., Lasken, R. S., and Neufeld, J. D. (2008). Something from (almost) nothing: the impact of multiple displacement amplification on microbial ecology. *ISME J.* 2, 233–241. doi: 10.1038/ismej.2008.10

Bishop, M. J., Coleman, M. A., and Kelaher, B. P. (2010). Cross-habitat impacts of species decline: response of estuarine sediment communities to changing detrital resources. *Oecologia* 163, 517–525. doi: 10.1007/s00442-009-1555-y

Bourne, D. G., Garren, M., Work, T. M., Rosenberg, E., Smith, G. W., and Harvell, C. D. (2009). Microbial disease and the coral holobiont. *Trends Microbiol.* 17, 554–562. doi: 10.1016/j.tim.2009.09.004

Brussaard, C. P. (2004). Viral control of phytoplankton populations—a review. *J. Eukaryot. Microbiol.* 51, 125–138. doi: 10.1111/j.1550-7408.2004.tb00537.x

Brussaard, C. P., Baudoux, A.-C., and Rodríguez-Valera, F. (2016). *The Marine Microbiome*. Cham: Springer.

Burge, C. A., Kim, C. J., Lyles, J. M., and Harvell, C. D. (2013). Special issue oceans and humans health: the ecology of marine opportunists. *Microb. Ecol.* 65, 869–879. doi: 10.1007/s00248-013-0190-7

Burge, C. A., Mark Eakin, C., Friedman, C. S., Froelich, B., Hershberger, P. K., Hofmann, E. E., et al. (2014). Climate change influences on marine infectious diseases: implications for management and society. *Ann. Rev. Mar. Sci.* 6, 249–277. doi: 10.1146/annurev-marine-010213-135029

Campbell, A. H., Harder, T., Nielsen, S., Kjelleberg, S., and Steinberg, P. D. (2011). Climate change and disease: bleaching of a chemically defended seaweed. *Glob. Change Biol.* 17, 2958–2970. doi: 10.1111/j.1365-2486.2011.02456.x

Campbell, A. H., Marzinelli, E. M., Gelber, J., and Steinberg, P. D. (2015). Spatial variability of microbial assemblages associated with a dominant habitat-forming seaweed. *Front. Microbiol.* 6:230. doi: 10.3389/fmicb.2015.00230

Campbell, A. H., Vergés, A., and Steinberg, P. D. (2014). Demographic consequences of disease in a habitat-forming seaweed and impacts on interactions between natural enemies. *Ecology* 95, 142–152. doi: 10.1890/13-0213.1

Case, R. J., Longford, S. R., Campbell, A. H., Low, A., Tujula, N., Steinberg, P. D., et al. (2011). Temperature induced bacterial virulence and bleaching disease in a chemically defended marine macroalga. *Environ. Microbiol.* 13, 529–537. doi: 10.1111/j.1462-2920.2010.02356.x

Cassman, N., Prieto-Davó, A., Walsh, K., Silva, G. G. Z., Angly, F., Akhter, S., et al. (2012). Oxygen minimum zones harbour novel viral communities with low diversity. *Environ. Microbiol.* 14, 3043–3065. doi: 10.1111/j.1462-2920.2012.02891.x

Cheval, J., Sauvage, V., Frangeul, L., Dacheux, L., Guigon, G., Dumey, N., et al. (2011). Evaluation of high-throughput sequencing for identifying known and unknown viruses in biological samples. *J. Clin. Microbiol.* 49, 3268–3275. doi: 10.1128/JCM.00850-11

Connell, S., Russell, B., Turner, D., Shepherd, A., Kildea, T., Miller, D., et al. (2008). *Recovering a lost* baseline: missing kelp forests from a metropolitan coast. *Mar. Ecol. Prog. Ser.* 360, 63–72. doi: 10.3354/meps07526

Delaroque, N., and Boland, W. (2008). The genome of the brown alga *Ectocarpus siliculosus* contains a series of viral DNA pieces, suggesting an ancient association with large dsDNA viruses. *BMC Evol. Biol.* 8:110. doi: 10.1186/1471-2148-8-110

Delwart, E., and Li, L. (2012). Rapidly expanding genetic diversity and host range of the Circoviridae viral family and other Rep encoding small circular ssDNA genomes. *Virus Res.* 164, 114–121. doi: 10.1016/j.virusres.2011.11.021

Dinsdale, E. A., Edwards, R. A., Hall, D., Angly, F., Breitbart, M., Brulc, J. M., et al. (2008a). Functional metagenomic profiling of nine biomes. *Nature* 452, 629–632. doi: 10.1038/nature06810

Dinsdale, E. A., Pantos, O., Smriga, S., Edwards, R. A., Angly, F., Wegley, L., et al. (2008b). Microbial ecology of four coral atolls in the Northern Line Islands. *PLoS ONE* 3:e1584. doi: 10.1371/journal.pone.0001584

Eaglesham, J. B., and Hewson, I. (2013). Widespread detection of circular replication initiator protein (rep)-encoding ssDNA viral genomes in estuarine, coastal and open ocean net plankton. *Mar. Ecol. Prog. Ser.* 494, 65–72. doi: 10.3354/meps10575

Easton, L. M., Lewis, G. D., and Pearson, M. N. (1997). Virus-like particles associated with dieback symptoms in the brown alga *Ecklonia radiata*. 30, 217–222.

Edgar, R. C. (2004). MUSCLE: multiple sequence alignment with high accuracy and high throughput. *Nucleic Acids Res.* 32, 1792–1797. doi: 10.1093/nar/gkh340

Egan, S., and Gardiner, M. (2016). Microbial dysbiosis: rethinking disease in marine ecosystems. *Front. Microbiol.* 7:991. doi: 10.3389/fmicb.2016.00991

Egan, S., Fernandes, N. D., Kumar, V., Gardiner, M., and Thomas, T. (2014). Bacterial pathogens, virulence mechanism and host defence in marine macroalgae. *Environ. Microbiol.* 16, 925–938. doi: 10.1111/1462-2920.12288

Egan, S., Harder, T., Burke, C., Steinberg, P., Kjelleberg, S., and Thomas, T. (2013). The seaweed holobiont: understanding seaweed–bacteria interactions. *FEMS Microbiol. Rev.* 37, 462–476. doi: 10.1111/1574-6976.12011

Fahsbender, E., Hewson, I., Rosario, K., Tuttle, A. D., Varsani, A., and Breitbart, M. (2015). Discovery of a novel circular DNA virus in the Forbes sea star, *Asterias forbesi*. *Arch. Virol.* 160, 2349–2351. doi: 10.1007/s00705-015-2503-2

Friedman, C. S., Estes, R. M., Stokes, N. A., Burge, C. A., Hargove, J. S., Barber, B. J., et al. (2005). Herpes virus in juvenile Pacific oysters *Crassostrea gigas* from Tomales Bay, California, coincides with summer mortality episodes. *Dis. Aquat. Org.* 63, 33–41. doi: 10.3354/dao063033

Hasson, K., Lightner, D. V., Poulos, B., Redman, R., White, B., Brock, J., et al. (1995). Taura syndrome in *Penaeus vannamei*: demonstration of a viral etiology. *Dis. Aquat. Org.* 23, 115–126. doi: 10.3354/dao023115

Hesse, U., van Heusden, P., Kirby, B. M., Olonade, I., van Zyl, L. J., and Trindade, M. (2017). Virome assembly and annotation: a surprise in the Namib Desert. *Front. Microbiol.* 8:13. doi: 10.3389/fmicb.2017.00013

Hewson, I., Button, J. B., Gudenkauf, B. M., Miner, B., Newton, A. L., Gaydos, J. K., et al. (2014). Densovirus associated with sea-star wasting disease and mass mortality. *Proc. Natl. Acad. Sci. U.S.A.* 111, 17278–17283. doi: 10.1073/pnas.1416625111

Huson, D. H., Beier, S., Flade, I., Górska, A., El-Hadidi, M., Mitra, S., et al. (2016). MEGAN community edition-interactive exploration and analysis of large-scale microbiome sequencing data. *PLoS Comput. Biol.* 12:e1004957. doi: 10.1371/journal.pcbi.1004957

Hyatt, D., Chen, G. L., LoCascio, P. F., Land, M. L., Larimer, F. W., and Hauser, L. J. (2010). Prodigal: prokaryotic gene recognition and translation initiation site identification. *BMC Bioinformatics* 11:119. doi: 10.1186/1471-2105-11-119

Kapp, M., Knippers, R., and Müller, D. G. (1997). New members of a group of DNA viruses infecting brown algae. *Phycological Res.* 45, 85–90. doi: 10.1111/j.1440-1835.1997.tb00067.x

Karlsson, O. E., Belák, S., and Granberg, F. (2013). The effect of preprocessing by sequence-independent, single-primer amplification (SISPA) on metagenomic detection of viruses. *Biosecur. Bioterror.* 11, S227–S234. doi: 10.1089/bsp.2013.0008

Kim, K. H., Chang, H. W., Nam, Y. D., Roh, S. W., Kim, M. S., Sung, Y., et al. (2008). Amplification of uncultured single-stranded DNA viruses from rice paddy soil. *Appl. Environ. Microbiol.* 74, 5975–5985. doi: 10.1128/AEM.01275-08

Krediet, C. J., Ritchie, K. B., Paul, V. J., and Teplitski, M. (2013). Coral-associated micro-organisms and their roles in promoting coral health and thwarting diseases. *Proc. R. Soc. Lond. B Biol. Sci.* 280:20122328. doi: 10.1098/rspb.2012.2328

Kumar, V., Zozaya-Valdes, E., Kjelleberg, S., Thomas, T., and Egan, S. (2016). Multiple opportunistic pathogens can cause a bleaching disease in the red seaweed *Delisea pulchra*. *Environ. Microbiol.* 18, 3962–3975. doi: 10.1111/1462-2920.13403

Labonté, J. M., and Suttle, C. A. (2013). Previously unknown and highly divergent ssDNA viruses populate the oceans. *ISME J.* 7, 2169–2177. doi: 10.1038/ismej.2013.110

Lachnit, T., Thomas, T., and Steinberg, P. (2015). Expanding our understanding of the seaweed Holobiont: RNA viruses of the red alga *Delisea pulchra*. *Front. Microbiol.* 6:1489. doi: 10.3389/fmicb.2015.01489

Lang, A. S., Rise, M. L., Culley, A. I., and Steward, G. F. (2009). RNA viruses in the sea. *FEMS Microbiol. Rev.* 33, 295–323. doi: 10.1111/j.1574-6976.2008.00132.x

Langmead, B., and Salzberg, S. L. (2012). Fast gapped-read alignment with Bowtie 2. *Nat. Methods* 9, 357–359. doi: 10.1038/nmeth.1923

Ling, S., and Johnson, C. R. (2012). Marine reserves reduce risk of climate-driven phase shift by reinstating size-and habitat-specific trophic interactions. *Ecol. Appl.* 22, 1232–1245. doi: 10.1890/11-1587.1

Liu, J., Wang, G., Wang, Q., Liu, J., Jin, J., and Liu, X. (2012). Phylogenetic diversity and assemblage of major capsid genes (g23) of T4-type bacteriophages in paddy field soils during rice growth season in Northeast China. *Soil Sci. Plant Nutr.* 58, 435–444. doi: 10.1080/00380768.2012.703610

Maier, I., Wolf, S., Delaroque, N., Müller, D., and Kawai, H. (1998). A DNA virus infecting the marine brown alga *Pilayella littoralis* (Ectocarpales, Phaeophyceae) in culture. *Eur. J. Phycol.* 33, 213–220. doi: 10.1080/09670269810001736713

Mann, N. H. (2005). The third age of phage. *PLoS Biol.* 3:e182. doi: 10.1371/journal.pbio.0030182

Marzinelli, E. M., Campbell, A. H., Zozaya Valdes, E., Vergés, A., Nielsen, S., Wernberg, T., et al. (2015). Continental-scale variation in seaweed host-associated bacterial communities is a function of host condition, not geography. *Environ. Microbiol.* 17, 4078–4088. doi: 10.1111/1462-2920.12972

McKeown, D. A., Stevens, K., Peters, A. F., Bond, P., Harper, G. M., Brownlee, C., et al. (2017). Phaeoviruses discovered in kelp (Laminariales). *ISME J.* 11, 2869–2873. doi: 10.1038/ismej.2017.130

McLoughlin, M. E., and Graham, D. A. (2007). Alphavirus infections in salmonids–a review. *J. Fish Dis.* 30, 511–531. doi: 10.1111/j.1365-2761.2007.00848.x

Milne, I., Bayer, M., Cardle, L., Shaw, P., Stephen, G., Wright, F., et al. (2009). Tablet—next generation sequence assembly visualization. *Bioinformatics* 26, 401–402. doi: 10.1093/bioinformatics/btp666

Morris, M. M., Haggerty, J. M., Papudeshi, B. N., Vega, A. A., Edwards, M. S., and Dinsdale, E. A. (2016). Nearshore pelagic microbial community abundance affects recruitment success of giant kelp, *Macrocystis pyrifera*. *Front. Microbiol.* 7:1800. doi: 10.3389/fmicb.2016.01800

Müller, D., and Frenzer, K. (1993). Virus infections in three marine brown algae: *Feldmannia irregularis*, F. simplex, and *Ectocarpus siliculosus*. *Hydrobiologia* 260, 37–44.

Papudeshi, B., Haggerty, J., Doane, M., Morris, M., Walsh, K., Beattie, D., et al. (2017). Optimizing the reconstruction of microbial population genomes from metagenomes. *BMC Genomics* 18:915. doi: 10.1186/s12864-017-4294-1

Parks, D. H., Tyson, G. W., Hugenholtz, P., and Beiko, R. G. (2014). STAMP: statistical analysis of taxonomic and functional profiles. *Bioinformatics* 30, 3123–3124. doi: 10.1093/bioinformatics/btu494

Reavy, B., Swanson, M. M., Cock, P. J. A., Dawson, L., Freitag, T. E., Singh, B. K., et al. (2015). Distinct circular single-stranded DNA viruses exist in different soil types. *Appl. Environ. Microbiol.* 81, 3934–3945. doi: 10.1128/AEM.03878-14

Rohwer, F., and Thurber, R. V. (2009). Viruses manipulate the marine environment. *Nature* 459, 207–212. doi: 10.1038/nature08060

Roossinck, M. J. (2013). Plant virus ecology. *PLoS Pathog.* 9:e1003304. doi: 10.1371/journal.ppat.1003304

Rosario, K., Dayaram, A., Marinov, M., Ware, J., Kraberger, S., Stainton, D., et al. (2012a). Diverse circular ssDNA viruses discovered in dragonflies (Odonata: Epiprocta). *J. Gen. Virol.* 93, 2668–2681. doi: 10.1099/vir.0.045948-0

Rosario, K., Duffy, S., and Breitbart, M. (2009). Diverse circovirus-like genome architectures revealed by environmental metagenomics. *J. Gen. Virol.* 90, 2418–2424. doi: 10.1099/vir.0.012955-0

Rosario, K., Duffy, S., and Breitbart, M. (2012b). A field guide to eukaryotic circular single-stranded DNA viruses: insights gained from metagenomics. *Arch. Virol.* 157, 1851–1871. doi: 10.1007/s00705-012-1391-y

Rosenberg, E., Koren, O., Reshef, L., Efrony, R., and Zilber-Rosenberg, I. (2007). The role of microorganisms in coral health, disease and evolution. *Nat. Rev. Microbiol.* 5, 355–362. doi: 10.1038/nrmicro1635

Rothman, M. D., Mattio, L., Wernberg, T., Anderson, R. J., Uwai, S., Mohring, M. B., et al. (2015). A molecular investigation of the genus Ecklonia (Phaeophyceae, Laminariales) with special focus on the Southern Hemisphere. *J. Phycol.* 51, 236–246. doi: 10.1111/jpy.12264

Roux, S., Krupovic, M., Poulet, A., Debroas, D., and Enault, F. (2012). Evolution and diversity of the microviridae viral family through a collection of 81 new complete genomes assembled from virome reads. *PLoS ONE* 7:e40418. doi: 10.1371/journal.pone.0040418

Sabina, J., and Leamon, J. H. (2015). Bias in whole genome amplification: causes and considerations. *Methods Mol. Biol.* 1347, 15–41. doi: 10.1007/978-1-4939-2990-0_2

Schmieder, R., and Edwards, R. (2011). Quality control and preprocessing of metagenomic datasets. *Bioinformatics* 27, 863–864. doi: 10.1093/bioinformatics/btr026

Simmonds, P., Adams, M. J., Benko, M., Breitbart, M., Brister, J. R., Carstens, E. B., et al. (2017). Consensus statement: virus taxonomy in the age of metagenomics. *Nat. Rev. Microbiol.* 15, 161–168. doi: 10.1038/nrmicro.2016.177

Steneck, R. S., Graham, M. H., Bourque, B. J., Corbett, D., Erlandson, J. M., Estes, J. A., et al. (2002). Kelp forest ecosystems: biodiversity, stability, resilience and future. *Environ. Conserv.* 29, 436–459. doi: 10.1017/S0376892902000322

Van Etten, J. L., Lane, L. C., and Meints, R. H. (1991). Viruses and viruslike particles of eukaryotic algae. *Microbiol. Rev.* 55, 586–620.

Vega Thurber, R., Willner-Hall, D., Rodriguez-Mueller, B., Desnues, C., Edwards, R. A., Angly, F., et al. (2009). Metagenomic analysis of stressed coral holobionts. *Environ. Microbiol.* 11, 2148–2163. doi: 10.1111/j.1462-2920.2009.01935.x

Vergés, A., Doropoulos, C., Malcolm, H. A., Skye, M., Garcia-Pizá, M., Marzinelli, E. M., et al. (2016). Long-term empirical evidence of ocean warming leading to tropicalization of fish communities, increased herbivory, and loss of kelp. *Proc. Natl. Acad. Sci. U.S.A.* 113, 13791–13796. doi: 10.1073/pnas.1610725113

Vollmers, J., Wiegand, S., and Kaster, A.-K. (2017). Comparing and evaluating metagenome assembly tools from a microbiologist's perspective-not only size matters! *PLoS ONE* 12:e0169662. doi: 10.1371/journal.pone.0169662

Wahl, M., Molis, M., Hobday, A. J., Dudgeon, S., Neumann, R., Steinberg, P., et al. (2015). The responses of brown macroalgae to environmental change from local to global scales: direct versus ecologically mediated effects. *Perspect. Phycol.* 2, 11–29. doi: 10.1127/pip/2015/0019

Webster, N. S., and Thomas, T. (2016). The sponge hologenome. *MBio* 7, e00135–e00116. doi: 10.1128/mBio.00135-16

Wernberg, T., Bennett, S., Babcock, R. C., de Bettignies, T., Cure, K., Depczynski, M., et al. (2016). Climate-driven regime shift of a temperate marine ecosystem. *Science* 353, 169–172. doi: 10.1126/science.aad8745

Wernberg, T., Russell, B. D., Thomsen, M. S., Gurgel, C. F. D., Bradshaw, C. J., Poloczanska, E. S., et al. (2011). Seaweed communities in retreat from ocean warming. *Current Biol.* 21, 1828–1832. doi: 10.1016/j.cub.2011.09.028

Weynberg, K. D., Allen, M. J., and Wilson, W. H. (2017). Marine prasinoviruses and their tiny plankton hosts: a review. *Viruses* 9:E43. doi: 10.3390/v9030043

Weynberg, K. D., Wood-Charlson, E. M., Suttle, C. A., and van Oppen, M. J. (2014). Generating viral metagenomes from the coral holobiont. *Front. Microbiol.* 5:206. doi: 10.3389/fmicb.2014.00206

Willner, D., Thurber, R. V., and Rohwer, F. (2009). Metagenomic signatures of 86 microbial and viral metagenomes. *Environ. Microbiol.* 11, 1752–1766. doi: 10.1111/j.1462-2920.2009.01901.x

Wilson, W., Van Etten, J. L., and Allen, M. (2009). *Lesser Known Large Dsdna Viruses*. Cham: Springer.

Xue, H., Xu, Y., Boucher, Y., and Polz, M. F. (2012). High frequency of a novel filamentous phage, VCYφ, within an environmental *Vibrio cholerae* population. *Appl. Environ. Microbiol.* 78, 28–33. doi: 10.1128/AEM.06297-11

Zhang, J., Kobert, K., Flouri, T., and Stamatakis, A. (2014). PEAR: a fast and accurate Illumina Paired-End reAd mergeR. *Bioinformatics* 30, 614–620. doi: 10.1093/bioinformatics/btt593

Zuker, M. (2003). Mfold web server for nucleic acid folding and hybridization prediction. *Nucleic Acids Res.* 31, 3406–3415. doi: 10.1093/nar/gkg595

Conflict of Interest Statement: The authors declare that the research was conducted in the absence of any commercial or financial relationships that could be construed as a potential conflict of interest.

frontiers in Microbiology

ORIGINAL RESEARCH
published: 11 December 2017
doi: 10.3389/fmicb.2017.02456

Exploring the Cultivable *Ectocarpus* Microbiome

Hetty KleinJan[1], Christian Jeanthon[2,3], Catherine Boyen[1] and Simon M. Dittami[1]**

[1] Sorbonne Universités, CNRS-UPMC, Station Biologique de Roscoff, UMR8227, Integrative Biology of Marine Models, Roscoff, France, [2] CNRS, Station Biologique de Roscoff, UMR7144, Adaptation et Diversité en Milieu Marin, Roscoff, France, [3] Sorbonne Universités, UPMC Univ Paris 06, Station Biologique de Roscoff, UMR7144, Adaptation et Diversité en Milieu Marin, Roscoff, France

Coastal areas form the major habitat of brown macroalgae, photosynthetic multicellular eukaryotes that have great ecological value and industrial potential. Macroalgal growth, development, and physiology are influenced by the microbial community they accommodate. Studying the algal microbiome should thus increase our fundamental understanding of algal biology and may help to improve culturing efforts. Currently, a freshwater strain of the brown macroalga *Ectocarpus subulatus* is being developed as a model organism for brown macroalgal physiology and algal microbiome studies. It can grow in high and low salinities depending on which microbes it hosts. However, the molecular mechanisms involved in this process are still unclear. Cultivation of *Ectocarpus*-associated bacteria is the first step toward the development of a model system for *in vitro* functional studies of brown macroalgal–bacterial interactions during abiotic stress. The main aim of the present study is thus to provide an extensive collection of cultivable *E. subulatus*-associated bacteria. To meet the variety of metabolic demands of *Ectocarpus*-associated bacteria, several isolation techniques were applied, i.e., direct plating and dilution-to-extinction cultivation techniques, each with chemically defined and undefined bacterial growth media. Algal tissue and algal growth media were directly used as inoculum, or they were pretreated with antibiotics, by filtration, or by digestion of algal cell walls. In total, 388 isolates were identified falling into 33 genera (46 distinct strains), of which *Halomonas* (*Gammaproteobacteria*), *Bosea* (*Alphaproteobacteria*), and *Limnobacter* (*Betaproteobacteria*) were the most abundant. Comparisons with 16S rRNA gene metabarcoding data showed that culturability in this study was remarkably high (~50%), although several cultivable strains were not detected or only present in extremely low abundance in the libraries. These undetected bacteria could be considered as part of the rare biosphere and they may form the basis for the temporal changes in the *Ectocarpus* microbiome.

Keywords: *Ectocarpus*, holobiont, bacterial cultivation, brown macroalgae, dilution-to-extinction, metabarcoding

OPEN ACCESS

Edited by:
Tilmann Harder,
University of Bremen, Germany

Reviewed by:
Meinhard Simon,
University of Oldenburg, Germany
Suhelen Egan,
University of New South Wales, Australia

****Correspondence:***
Hetty KleinJan
hetty.kleinjan@sb-roscoff.fr;
hettykleinjan@gmail.com
Simon M. Dittami
simon.dittami@sb-rocoff.fr;
simon.dittami@gmail.com

Specialty section:
This article was submitted to Microbial Symbioses, a section of the journal Frontiers in Microbiology

Received: *19 September 2017*
Accepted: *27 November 2017*
Published: *11 December 2017*

Citation:
KleinJan H, Jeanthon C, Boyen C and Dittami SM (2017) Exploring the Cultivable Ectocarpus Microbiome. Front. Microbiol. 8:2456. doi: 10.3389/fmicb.2017.02456

INTRODUCTION

Coastal areas form the major habitat of brown macroalgae, photosynthetic eukaryotic organisms that are important primary producers and form biodiversity hotspots for other marine (macro)organisms by providing them with food and shelter (Thornber et al., 2016). The seaweed surface is a highly attractive substrate for the settlement of marine microorganisms, due to the

fact that they actively excrete carbohydrates and other organic or growth-promoting substances (Salaün et al., 2012; Goecke et al., 2013b) that can be rapidly utilized by bacteria. Several stable relationships exist that have been shown to benefit brown macroalgal hosts (Goecke et al., 2010; Hollants et al., 2013; Singh and Reddy, 2016). Algae-associated (symbiotic) microbes can, for example, communicate on a chemical level through the provision of growth hormones (Pedersén, 1973), vitamins (Pedersén, 1969; Croft et al., 2005), or morphogens (Tapia et al., 2016), and some algal–bacterial interactions are known to affect biofouling and pathogenic invasion by other microorganisms (Singh and Reddy, 2014). Due to the tight relationships and functional co-dependencies between algae and their associated microbiomes, both can be seen as one functional entity or "holobiont" (Zilber-Rosenberg and Rosenberg, 2008; Egan et al., 2013).

Elucidating the functions and molecular mechanisms that shape the algal holobiont is of crucial importance, not only for the fundamental understanding of macroalgal functioning in marine ecosystems, but also to improve macroalgal culturing, an industry that has increased intensively over the last decade due to the growing interest in algae as a source for nutrients, chemicals, and bioactive compounds (Wells et al., 2017). *In vitro* studies of the commercially valuable and environmentally most relevant brown macroalgae (kelps, order *Laminariales*) remain challenging due to their size and complex life cycles (Peters et al., 2004). Model organisms, such as the filamentous brown alga *Ectocarpus* are therefore an essential tool to enable functional studies on algal–bacterial interactions in the laboratory. *Ectocarpus* is easily cultivable *in vitro*, has a short life cycle and a relatively small genome which has been sequenced several years ago (Peters et al., 2004; Cock et al., 2010).

Here, we study the microbiome of a freshwater strain of *Ectocarpus subulatus* (West and Kraft, 1996). The transition to fresh water is a rare event in brown algae that occurred in only a few species (Dittami et al., 2017). The examined strain is currently the only publicly available freshwater isolate within the Ectocarpales, and it is still able to grow in both seawater and freshwater (Dittami et al., 2012). This and other isolates of the same species are known for their particularly high tolerance to abiotic stressors (Bolton, 1983; Peters et al., 2015) and are being developed as a model to study brown algal adaptation and acclimation. These processes, and in particular algal growth in fresh water, have been shown to depend on interactions with symbiotic bacteria (Dittami et al., 2016).

The aim of the present study is to develop an extensive collection of cultivable *E. subulatus*-associated bacteria that can be used to study the functions of bacterial symbionts during abiotic stress in controllable and reproducible experimental settings, using the freshwater strain of *E. subulatus* as a model. Different bacterial isolation techniques were applied in parallel to increase the number and diversity of cultivable strains, i.e., direct plating and dilution-to-extinction cultivation techniques, each with chemically defined and undefined bacterial growth media. Algal tissue and algal growth media were directly used as inoculum, or they were pretreated with antibiotics, by filtration, or by digestion of algal cell walls. Our data show an overall high culturability of *Ectocarpus*-associated bacteria including a high number of low abundance taxa.

MATERIALS AND METHODS

Cultivation of Algae – Starting Material for Isolation of Bacterial Symbionts

All experiments were carried out using sporophytes of the *E. subulatus* freshwater strain (EC371, accession CCAP 1310/196, West and Kraft, 1996). This culture was obtained from Bezhin Rosko (Santec, France) in 2007 and maintained in our laboratory under the following conditions since then: cultures of EC371 were grown in Petri dishes (90 mm Ø) in natural seawater (NSW; collected in Roscoff 48°46′40″ N, 3°56′15″ W, 0.45 μm filtered, autoclaved at 120°C for 20 min), or in diluted seawater-based medium (DNSW; by 20-fold dilution of natural seawater with distilled water). Both media were enriched with Provasoli nutrients (Starr and Zeikus, 1993) and cultures kept at 13°C with a 12 h dark-light cycle (photon flux density 20 μmol m^{-2} s^{-1}).

Isolation and Characterization of Algae-Associated Bacteria

A range of cultivation strategies as well as bacterial growth media was exploited. The starting material for bacterial isolation was EC371 grown with its full microbial flora (direct plating and dilution-to-extinction cultivation) and EC371 with a reduced microbial flora (size-fractionation and antibiotic treatment), both originating from the same algal culture. Algal subcultures were sampled 5–10 days after the last change in medium. Algal growth medium and ground algal tissue, in NSW and DNSW were used. The isolation experiments took place from November 2013 to September 2016. Three selected cultivation experiments (dilution-to-extinction cultivation, direct plating with antibiotics; direct plating without pretreatment) were repeated under identical conditions after 6 months, 1 year, or 3 years, respectively, to assess reproducibility of the results over time. An overview of the isolation methods and cultivation strategies is provided in **Figure 1**.

Isolation of Bacteria from Algae with Their Full Microbial Flora

Direct plating techniques

To isolate bacteria, algal growth media, ground algal tissue, and algal protoplast digest product of EC371 grown in DNSW or NSW were directly plated (DP) on eight different growth media solidified with 1.5% agar. The eight bacterial growth media were: R2A prepared in distilled water (adapted from Reasoner and Geldreich, 1985); R2A prepared in natural seawater instead of distilled water; Zobell marine agar (Zobell, 1941); Zobell marine agar with 16-fold reduced salinity; *Ectocarpus*-based medium (ground *E. subulatus* 5 g DW·L^{-1}; Peptone 0.5 g L^{-1}, Provasoli nutrients 10 ml L^{-1}, 5% NSW); Peptone Yeast Glucose (PYG) agar (Peptone 0.5 g L^{-1}; Yeast Extract 0.5 g L^{-1}; Glucose 0.5 g L^{-1}); PYG with glucose replaced by mannitol (5 g L^{-1}) and Provasoli nutrients 10 ml L^{-1}; and LB with NaCl (2 g L^{-1}).

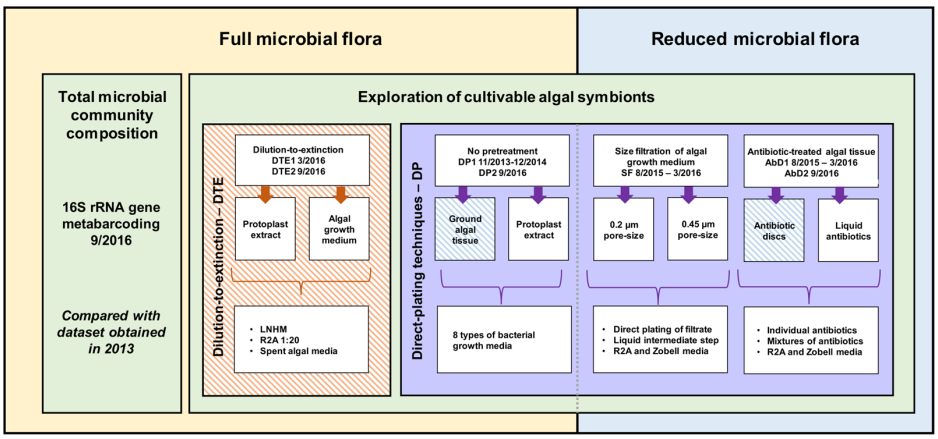

FIGURE 1 | Overview of the methodology and cultivation strategies used to cultivate algae-associated bacteria. On one hand, direct inoculation with algal tissue and/or algal growth medium was used (yellow), while on the other hand, the microbial community was reduced before inoculation (blue). Additionally, a distinction can be made between direct plating (DP, purple) with and without pretreatment, and dilution-to-extinction cultivation (orange). 16S rRNA gene metabarcoding of the total prokaryotic community was carried out in parallel. Striped boxes indicate experiments that have been repeated twice within a 6 months interval for DTE1–DTE2, a 1-year interval for AbD1–AbD2, and a 3-year interval for DP1–DP2 and META13–META16 (Dittami et al., 2016).

In some cases, a liquid intermediate step was applied, and in all cases non-inoculated media and plates were included as negative controls. The exact recipes of the media can be found in **Supplementary Table S1** and the detailed experimental treatments in **Supplementary Table S3**. The algal protoplast digest product (used in dilution-to-extinction cultivation as well) was produced using the protocol from Coelho et al. (2012) with an additional 2.0 µm size-filtration after complete cell wall digestion (step 5) and the filtrate was used for direct plating. After incubation for up to 45 days at either 4, 13, 30°C, or room temperature (RT), 1–10 single colonies were picked randomly. Furthermore, any colonies that differed with regard to their shape, size or color were also included. The colonies were grown in liquid growth media and identified by sequencing their 16S rRNA gene via Sanger sequencing (as described below). Direct plating of ground EC371 tissue grown in NSW was repeated after 3 years. Due to the variety of experiments colony counts were variable, ranging between one and several 100 per plate.

Dilution-to-extinction cultivation

As a strategy to reduce nutrient competition between the cultivable members of the EC371 microbiome, the high throughput dilution-to-extinction (DTE) cultivation approach was used as originally described by Connon and Giovannoni (2002): microbial communities from either algal growth medium or algal protoplast digest product (see the previous section) were 0.6 µm-filtered to remove microbial and carbohydrate aggregates, diluted to a predefined cell number, and distributed into 96-well deep well plates with low-nutrient media. Algal tissue may harbor cell-wall attached bacteria whose numbers cannot be determined with flow cytometry. In addition, the algal fragments block the flow cytometer which also prevents correct cell counting. Therefore, algal tissue could not be directly used in dilution-to-extinction experiments. Four liquid bacterial growth media were used to cultivate bacteria: 20-fold diluted R2A prepared in DNSW with starch replaced by alginate (0.025 g L^{-1}); Low Nutrient Heterotrophic Medium (LNHM) with 0.001 g L^{-1} mannitol (adapted from Cho and Giovannoni, 2004; Stingl et al., 2007, 2008; Carini et al., 2012; Jimenez-Infante et al., 2014) and 2 and 7 weeks old spent EC371 growth medium (5% NSW). Recipes can be found in **Supplementary Table S1**. For R2A and Zobell media, stock solutions of the individual components were prepared and autoclaved separately and the final bacterial growth medium was prepared on the day of the experiment. For LNHM, stock solutions were 0.2 µm filter-sterilized but not autoclaved. On the day of the experiment, individual components were mixed, the pH was adjusted to 7.3, and the bacterial growth media was filter-sterilized (0.1 µm) and divided into 96-well deep well plates before inoculation (0.5 ml/well). Preliminary tests of inoculations with 3, 1, and 0.5 cells/well, showed that 0.5 cells/well was the optimal inoculation density to limit the occurrence of bacterial mixtures and to obtain pure bacterial clones. Non-inoculated bacterial growth medium was used as a negative control. The experiment was performed twice within a 6 month interval (DTE1 in March 2016 and DTE2 in September 2016). Flow cytometry was used to obtain both the bacterial cell counts of the inocula and to monitor bacterial growth. After 4 weeks of incubation (16°C, 12:12 h dark:light cycle, 27 µmol s^{-1} m^{-2}), bacterial growth was screened by flow cytometry using a BD Accuri C6 cytometer (BD Biosciences): 100 µl of the cultures were fixed with glutaraldehyde (0.25%, final concentration) and stained with Sybr Green (Life Technologies) as described by Marie et al. (1997). Wells with cell densities of 10^4 cells/ml and higher were considered positive. The number of cultivable bacteria n_{cult} in the original inoculum was estimated based on the proportion of negative wells (p_{neg}) according to a Poisson distribution using the formula $n_{cult} = \ln(1/p_{neg})\cdot w$, where w is the total number of wells inoculated (Button et al., 1993). This allowed for the calculation of the ratio of cultivable to total bacteria (the latter

determined via flow cytometry) in these experiments (estimated culturability).

Isolation of Bacteria from Algae with a Reduced Microbial Flora

Size-fractionation of algal growth media

As a second strategy to reduce bacterial cell numbers before plating, size-fractionation (SF) was used to facilitate the growth of smaller and less abundant bacterial strains. EC371 culture medium was filtered with 0.2 (SF0.2), 0.45 (SF0.45), or 40 (SF40) μm pore-size, and 50 μl filtrate were directly plated on R2A or Zobell agar. At the same time, 100 μl filtrate were used to inoculate liquid R2A or Zobell as an intermediate to enhance bacterial growth before plating. After 5–8 days of incubation at RT, 50 μl of the liquid culture were plated on solidified R2A and/or Zobell. In both cases, plates were incubated until single colonies were visible (3–20 days) and the latter identified with 16S rRNA amplicon sequencing as described below.

Antibiotic-treatments of algal tissue and growth media

Antibiotics were used to reduce the abundance of dominant bacterial strains from the algal tissue and/or growth media, in our case especially *Halomonas* sp., and to facilitate the growth of other less abundant or slower-growing bacteria. Algal growth media and/or ground algal tissue was spread on R2A agar plates and incubated with two antibiotic disks (AbD1 and AbD2; Antimicrobial Susceptibility Disks, Bio-Rad Laboratories, Inc., France) for 5 days at RT, using antibiotics that were shown to be effective against *Ectocarpus*-derived *Halomonas*. Alternatively, algal subcultures of the same strain were treated with liquid antibiotics (AbL) for 3 days before plating on R2A or Zobell, whereafter 50 μl were plated on solidified R2A or Zobell. An overview of the antibiotics (disks and liquid) and their concentration can be found in **Supplementary Table S2**. Plates were incubated (3–20 days) until single colonies were visible and the latter identified with 16S rRNA amplicon sequencing as described below. Two experiments using antibiotic-treated algal tissue (AbD2 with chloramphenicol and erythromycin) were repeated after 1 year.

Bacterial Identification by 16S rRNA Gene Sequencing

To identify bacterial isolates, single colonies were grown in the corresponding liquid growth media until maximal density was reached. Approximately 50–100 μl of cultures were heated for 15 min at 95°C. Then the 16S rRNA gene was amplified using universal primers (8F 5′ AGAGTTTGATCCTGGCTCAG and 1492R 5′ GGTTACCTTGTTACGACTT from Weisburg et al., 1991) and the GoTaq polymerase in a PCR reaction with the following amplification conditions: 2 min 95°C; [1 min 95°C; 30 s 53°C; 3 min 72°C] 30 cycles; 5 min 72°C. In some cases a commercial kit was used to extract DNA (NucleoSpin® Tissue, Machery-Nagel; support protocol for bacteria). The PCR products were purified using ExoSAP (Affymetrix, Inc., Thermo Fisher Scientific) and sequenced with Sanger technology (BigDye Xterminator v3.1 cycle sequencing kit, Applied Biosystems®, Thermo Fisher Scientific). Only the forward primer 8F was used for the sequencing reaction. For classification and analyses of the sequences, RDP classifier (Wang et al., 2007) and BLAST[1] against the NCBI nr and 16S rRNA gene databases were used and sequences classified at the genus level if possible. Sequences were aligned[2] and checked manually to verify mismatches and to identify distinct strains within a genus (>99% identity). The 16S rRNA gene sequences from each distinct cultivable strain were aligned using MAFFT version 7 (Katoh et al., 2002) and the G-INS-i algorithm. Only well-aligned positions with less than 5% alignment gaps (492 positions) were retained. Phylogenetic trees were reconstructed using the Maximum-Likelihood method implemented in MEGA6.06 (Tamura et al., 2013), and the GTR+G+I model. Five hundred bootstrap replicates were tested to assess the robustness of the tree. The unique 16S rRNA gene sequences were submitted to the European Molecular Biology Laboratory (EMBL) database and are available under project accession number PRJEB22665. Stocks of bacterial isolates were preserved in 40% glycerol at −80°C.

The numbers of sequences obtained per taxa were normalized against the total number of sequences obtained within the complete cultivation study. To assess cultivation biases statistically, the absolute abundances of cultivable isolates were analyzed in R (RStudio Team, 2016) with the Fisher-exact test and Bonferroni *post hoc* correction for multiple testing ($\alpha = 0.05$, significant if $p < 0.0011$).

16S rRNA Gene Metabarcoding

To estimate the proportion of cultivable bacteria in our algal cultures, the collection of bacterial isolates was compared with 16S rRNA gene libraries from the same algal culture used for our isolation experiments. These libraries served as a reference to assess the total microbiome, including cultivated and non-cultivated bacteria; they were not used to infer diversity *per se*. EC371 cultures were grown for 9 weeks in seawater-based culture medium (changed on a monthly basis, last 1 week prior to sampling). Algal tissue was filtered with sterile coffee filters, dried on a paper-towel, and snap-frozen in liquid nitrogen. Four technical replicates were pooled two by two. Total DNA was isolated (NucleoSpin® Plant II, Machery-Nagel; standard protocol) and purified with Clontech CHROMA SPIN™-1000+DEPC-H2O Columns. The V3–V4 region of the 16S rRNA gene was amplified and sequenced with Illumina MiSeq technology by MWG Eurofins Biotech (Ebersberg, Germany) using their proprietary protocol. The first preliminary quality control was done with FastQC[3], and fastq_quality_trimmer from the FASTX Toolkit[4] was used to quality-trim and filter the 568,100 reads (quality threshold 25; minimum read length 200). The resulting 553,896 sequences (2.5% removed) were analyzed with Mothur (V.1.38.0) according to the MiSeq Standard Operating Procedures[5] (Kozich et al., 2013). Filtered reads were assembled into 270,522 contigs,

[1]https://blast.ncbi.nlm.nih.gov/Blast.cgi

[2]http://mafft.cbrc.jp/alignment/software

[3]https://www.bioinformatics.babraham.ac.uk/projects/fastqc/

[4]http://hannonlab.cshl.edu/fastx_toolkit/index.html

[5]https://www.mothur.org/wiki/MiSeq_SOP

preclustered (allowing for four mismatches), and aligned with the non-redundant Silva SSU reference database version 123 (Quast et al., 2013). Chimeric sequences were removed using the Uchime algorithm (Edgar et al., 2011) implemented in Mothur, and the remaining sequences classified taxonomically using the method of Wang et al. (2007). Non-bacterial sequences were removed. The sequences were then clustered into operational taxonomic units (OTUs) at a 97% identity level and each OTU was classified taxonomically. All OTUs with $n \leq 5$ sequences were removed (0.02%) resulting in a final data matrix with 217,923 sequences. The sequences obtained from cultivable isolates were compared with the 16S rRNA gene metabarcoding data using BLASTn searches against raw reads (99% identity) and consensus OTU sequences (97% identity). In addition, the current dataset (META2016-NSW) was compared to previous datasets (META2013-NSW, META2013-DNSW) obtained from the same algal strain 3 years earlier (Dittami et al., 2016). All counts for each individual OTU were normalized against the total number of sequences in the corresponding dataset. Raw Illumina reads were deposited at the European Nucleotide Archive under project accession number PRJEB22665. To compare the cultivable sequences and their abundance in the 16S metabarcoding data (META13-NSW and META16-NSW) a heatmap was created using the iTOL web application[6] (Letunic and Bork, 2016). Log(x+1)-transformed data was used for OTU sequence counts and cultivation abundances. All datasets (three for metabarcoding, 10 for cultivation) were grouped by hierarchical clustering using Euclidean distance calculations and the average linkage method implemented in the pvclust R-package[7] (Suzuki and Shimodaira, 2006). The resulting tree was tested using bootstrap analysis (500 replications). OTUs that did not correspond to cultivable strains are not shown in the graphical representation. In this manuscript, "isolate" refers to every bacterial culture for which a 16S rRNA sequence was obtained. All isolates with identical 16S rRNA sequences are considered to belong to the same "strain".

RESULTS

Isolation and Characterization of Algae-Associated Bacteria

Global Taxonomic Distribution of Cultivable Bacteria

16S rRNA gene sequences were obtained for 388 bacterial isolates and they were distributed among four phyla, 15 bacterial orders, 34 genera, and 46 taxonomically unique strains. Five genera encompassed more than one distinct strain (i.e., at least one verified mismatch in the 16S rRNA sequence): *Limnobacter* sp. (2), *Moraxella* sp. (2), *Sphingomonas* sp. (3), *Bacillus* sp. (8), and *Roseovarius* sp. (2). The most abundant phylum among the cultivable isolates was *Proteobacteria*, with 89% of all isolates and 26 unique strains belonging to this group. Within *Proteobacteria*, *Alpha-* and *Betaproteobacteria* accounted for 34 and 32% of the isolates, respectively. However, *Betaproteobacteria* comprised three unique strains, while *Alphaproteobacteria* comprised 16 unique strains in our experiments. 23% of proteobacterial isolates belonged to *Gammaproteobacteria*, covering seven unique strains. *Bacteroidetes* (4% of isolates), *Firmicutes* (4%), and *Actinobacteria* (3%) were cultivated less frequently compared to *Proteobacteria*. Despite their lower abundance, the three groups contribute considerably to the cultivable diversity, accounting for 20 out of 46 unique strains. The most abundant cultivable bacterial genera were *Limnobacter* (27% of all isolates), *Halomonas* (20%), and *Bosea* (9%). 80% of *Limnobacter* isolates were obtained from dilution-to-extinction cultivation experiments. *Halomonas* strains were predominantly cultivated using direct plating techniques and algae with full flora (84% of *Halomonas* isolates). For *Bosea*, most isolates (83%) originated from antibiotic-treated algae. An overview of all bacterial isolates characterized and their corresponding sequence abundances can be found in **Figure 2** and **Supplementary Table S3**.

Isolation of Bacteria from Algae with Their Full Microbial Flora

Direct plating of ground algae and algal protoplast extract (DP)

Direct plating of ground algal tissue and protoplast digest resulted in the isolation and characterization of 110 isolates corresponding to 17 strains of which seven were uniquely isolated with this method. The most frequently isolated strain was *Halomonas* sp., a gammaproteobacterium that makes up for 58% of isolates obtained with this method. Isolates of this strain originated predominantly from ground algal tissue rather than algal growth medium ($p = 1.92E\text{-}13$). After *Halomonas*, *Sphingopyxis* (10%), and *Hyphomonas* (8%) were the most frequently isolated taxa. Four isolates originated from protoplast extracts: *Imperialibacter* sp. (two isolates), *Sphingomonas* sp. (one isolate), and *Plantibacter* sp. (one isolate). Direct plating of algal tissue was repeated after 3 years and *Halomonas* sp. was again the most frequently isolated strain (9 out of 12 isolates). *Sphingomonas* 2, and *Plantibacter* sp. were two protoplast-specific strains obtained using DP, but they were only isolated once in the experiment.

Dilution-to-extinction cultivation (DTE)

One hundred and fifty isolates were identified and 16S rRNA gene sequences revealed eight unique strains. There were no isolates that were specific for the origin of the starting material used (protoplast extract or spent algal growth medium). The most abundant isolates belonged to the genus *Limnobacter* (55% of isolates), suggesting that they were the most abundant cultivable bacterium in the original algal cultures. Furthermore, five unique strains (*Brevundimonas*, *Erythrobacter*, *Hoeflea*, *Ahrensia*, and *Roseovarius 1*) were exclusively found with dilution-to-extinction cultivation. *Brevundimonas* sp. was significantly more isolated from algal growth media ($p = 0.00045$) compared to algal tissue/protoplast extract (**Supplementary Table S3**). In addition, some *Hyphomonas* sp. and *Undibacterium* sp. strains were isolated but they were not exclusive for this method. Experiments were performed twice in a 6-month interval (DTE1 and DTE2), and *Limnobacter* was, in both experiments, the most frequently

[6] http://itol.embl.de, version 3.5.3

[7] http://stat.sys.i.kyoto-u.ac.jp/prog/pvclust/

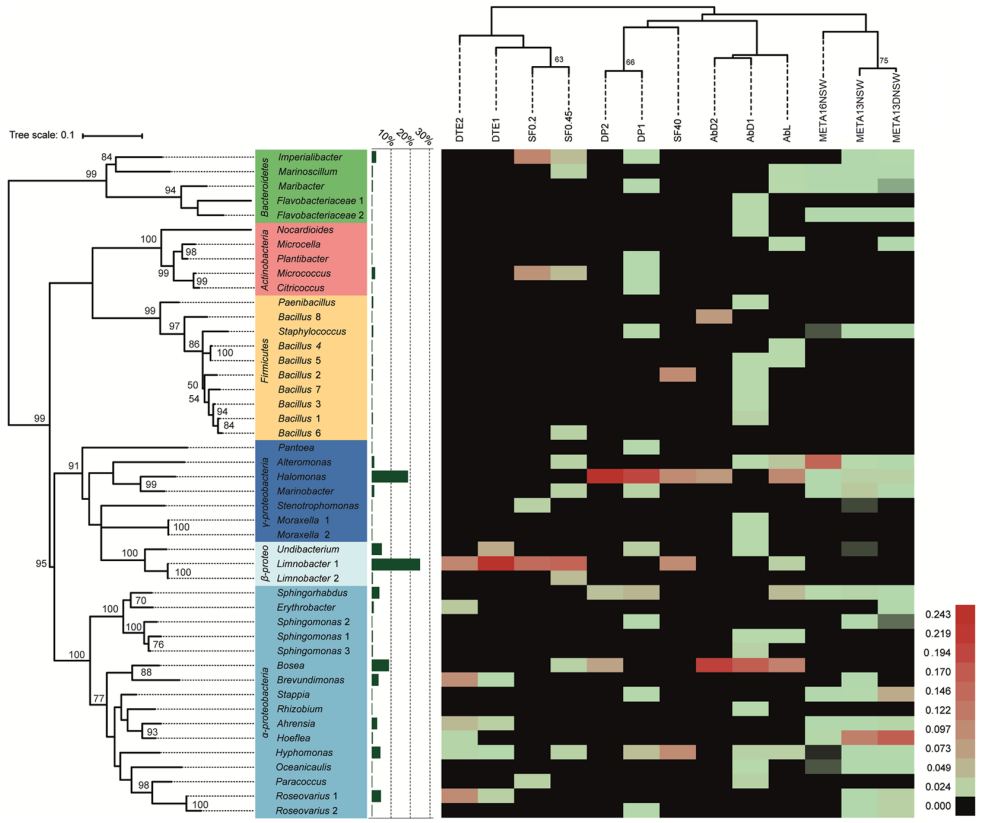

FIGURE 2 | Heat-map of cultivation and metabarcoding data. The number of sequences was normalized and log(x+1)-transformed for each unique cultivable strain and each experimental treatment (DP, direct plating without pretreatment; AbD, DP with pretreatment with antibiotic disks; AbL, DP with pretreatment with liquid antibiotics; SF, DP with pretreatment by size-fractionation; DTE, dilution-to-extinction cultivation). A comparison is made with molecular data from 16S rRNA metabarcoding (META16-NSW = this study; META13-NSW and META13-DNSW = previous study by Dittami et al., 2016; uncultured OTUs not shown). Red colors indicate high abundance, while green corresponds to relatively low abundance. Black color indicates taxa/strains that were not retrieved/isolated. Experimental treatments are grouped (top dendogram) using hierarchical clustering (Euclidean distance, average linkage method) and the phylogenetic tree (left) was calculated using the Maximum-Likelihood method and the GTR+G+I model. Bootstrap analysis for both trees was done using 500 replications. Only bootstrap values ≥ 50 are shown. The bar graph (green) shows the proportion of isolates per unique strain obtained in the whole cultivation dataset.

isolated taxon. The ratio of cultivable to total bacteria (estimated culturability) in the experiment varied from 44 to 68%, with different culturability dependent on the type of bacterial growth medium applied. DTE statistics and the Poisson calculations can be found in **Table 1**.

Isolation of Bacteria from Algae with Reduced Flora

Antibiotic-treated algae

The 16S rRNA gene sequences from 80 isolates revealed 27 unique strains, 16 of which were obtained only with this cultivation method. *Bosea* was the most abundant (44% of isolates) followed by *Halomonas* with 38%. Most others were only isolated once or twice. Unique strains isolated with this method were *Sphingomonas* sp. (strains 1, 3), *Bacillus* sp. (strains 1, 3–5, 7), *Nocardioides* sp., *Microcella* sp., *Moraxella* sp. (strains 1, 2), *Pantoea* sp., *Rhizobium* sp., two unclassified members of the *Flavobacteriaceae*, and *Oceanicaulis* sp. These were all (except *Microcella*) isolated from algal tissue that was exposed to 10 different antibiotics (**Supplementary Table S2**). The cultivation of bacteria from antibiotic-treated algae was performed twice within a 1-year interval and in both experiments *Bosea* was the most frequently isolated taxon.

Size-fractionation

The 16S rRNA gene sequences of the 43 isolates from this experiment cover 14 unique strains. Three of them were uniquely found using this method: *Bacillus* strain 6 (one isolate), *Limnobacter* strain 2, (two isolates), and *Stenotrophomonas* sp. (one isolate). Among the other strains cultivated, the most abundant one was *Limnobacter* strain 1 (40% of isolates), followed by *Imperialibacter* sp. (16% of isolates).

Estimating the Proportion of Cultivable Bacteria in *Ectocarpus* Cultures

16S metabarcoding experiments were carried out with the same algal culture also used for the isolation of bacteria and the libraries were used as a reference for the cultivated and non-cultivated microbiome as a whole. After cleaning

TABLE 1 | Estimation of the ratio of cultivable to total bacteria in the dilution-to-extinction cultivation experiments based on a Poisson distribution: $n_{cult} = \ln(1/p_{neg})*w$.

Experiment	Type of inoculation	Bacterial growth medium	# Bacterial cells inoculated (n_{total})	# Inoculated wells (w)	# Negative wells (P_{neg})	Theoretical # of cultivable cells (n_{cult})	Estimated culturability (n_{cult}/n_{total})
DTE1	P	ECM 2W	52	104	74	35.39	68%
DTE1	P	ECM 7W	52	104	83	23.46	45%
DTE1	M	ECM 7W	48	96	73	26.29	55%
DTE1	M	ECM 2W	48	96	77	21.17	44%
DTE1	M	LNHM	52	104	81	25.99	50%
DTE1	M	1:20 R2A	52	104	79	28.59	55%
DTE2	M	1:20 R2A	140	280	201	92.82	66%

P = protoplast digest product; M = low salinity algal growth medium; DTE1 = March 2016; DTE2 = September 2016; ECM = spent low salinity algal growth medium from 2 weeks (2W) or 7 weeks (7W) old cultures.

and filtering of the data, the sequences were clustered into 48 OTUs. The most abundant OTU belonged to the genus *Alteromonas* (OTU1) and accounted for 41.6% of the reads, which makes *Gammaproteobacteria* the most abundant class (42.3%). Other abundant OTUs corresponded to an unclassified *Rhodobacteraceae* (OTU3, 11%) and an unclassified *Bacteroidetes* (OTU4, 10%). Together these three OTUs correspond to 62% of all sequences (**Figure 3A**). *Alphaproteobacteria* make up 32.8% of the sequences and *Bacteroidetes* 15.3% (**Figure 3B**). Other phyla identified are *Actinobacteria* (2.1%) and *Deltaproteobacteria* (7.5%). Of the 48 OTUs, 10 corresponded to strains cultivated in our experiments. These 10 OTUs accounted for 47% of the reads in the metabarcoding data. Purely based on absence/presence of OTUs the culturability was 21%. Three additional cultivable strains corresponded to OTUs with sequence abundance below the threshold ($n \leq 5$, *Staphylococcus, Hyphomonas, Oceanicaulis;* **Figure 3**). Furthermore, taking into account all 16S rRNA gene libraries and rare reads, 22 of the 46 cultivable strains were detected. Among the 24 undetected strains that were not found in any of the barcoding libraries, 11 were isolated exclusively from DNSW and 8 exclusively from NSW. In the same vein, 11 strains were cultured exclusively from algal medium, and 7 only from algal tissue (**Supplementary Table S4**).

The 16S rRNA gene metabarcoding data obtained in this study (META2016-NSW) differed strongly from that obtained 3 years earlier (META2013-NSW) from the same *Ectocarpus* strain. Several OTUs that were present in the 2013 samples were no longer present in 2016 or declined in abundance below the detection limit. However, there were still 50 OTUs (corresponding to 90% of the sequences) shared between the 2013 and 2016 samples. The most abundant OTU in 2013 belonged to the genus *Hoeflea* (29% of reads) while the most abundant OTU in 2016 (*Alteromonas* sp.; 42% of reads) accounted for only 2.4% of the reads in 2013.

DISCUSSION

Global Taxonomic Distribution of Cultivable Bacteria

The main aim of this study was to establish a diverse collection of cultivable *Ectocarpus*-associated bacteria that can be used to perform functional studies of brown macroalgal–bacterial interactions in this model organism. We applied different cultivation strategies to facilitate the growth of less abundant or slow-growing bacteria and thus increased the variety of cultivable bacteria.

Among the cultivable taxa frequently found on brown macroalgal surfaces (such as *Laminaria*, *Saccharina*, *Fucus, Ascophyllum*) are *Proteobacteria*, *Firmicutes*, *Bacteroidetes*, and *Actinobacteria*, where the latter three phyla are generally less abundant (Ivanova et al., 2002; Wang et al., 2008; Wiese et al., 2009; Salaün et al., 2010; Dong et al., 2012; Goecke et al., 2013a,b; Hollants et al., 2013; Martin et al., 2015). Two cultivation studies in *Ectocarpus* species showed the presence of *Gammaproteobacteria*, *Actinobacteria,* and *Flavobacteria* (Kong and Kwong-yu, 1979; Tapia et al., 2016). The results of our study, with *Proteobacteria* being most abundant followed by *Bacteroidetes*, *Firmicutes*, and *Actinobacteria*, largely agree with these findings, except that *Alphaproteobacteria* were the most abundant proteobacteria in this study (**Figure 2** and **Supplementary Table S3**), compared to *Gammaproteobacteria* in the previous studies.

The three dominant genera obtained were *Limnobacter*, *Bosea,* and *Halomonas* (**Figure 2** and **Supplementary Table S3**). *Limnobacter* sp. are oligotrophic freshwater sulfur-oxidizing bacteria (Spring et al., 2001) that occur naturally in aquatic environments (Lu et al., 2011; Zhang et al., 2014) and drinking water reservoirs (Wu et al., 2014) and are generally considered rare in marine settings (Staufenberger et al., 2008; Wiese et al., 2009). The majority of the isolation experiments in this study were indeed carried out with low-salinity culture media, and the algal source also came from fresh water (West and Kraft, 1996), providing two possible explanations for the presence of *Limnobacter* in our experiments. As these experiments were always complemented with negative controls (i.e., non-inoculated bacterial growth media), a contamination with *Limnobacter* from the water source used to prepare the bacterial growth media is unlikely.

Members of the genus *Bosea* are known to be (multi)drug-resistant (Falcone-Dias et al., 2012; Zothanpuia et al., 2016). The results from our study agree with these observations since 92% of the *Bosea* isolates came from antibiotic-treated algae (**Figure 2** and **Supplementary Table S3**). In addition, several

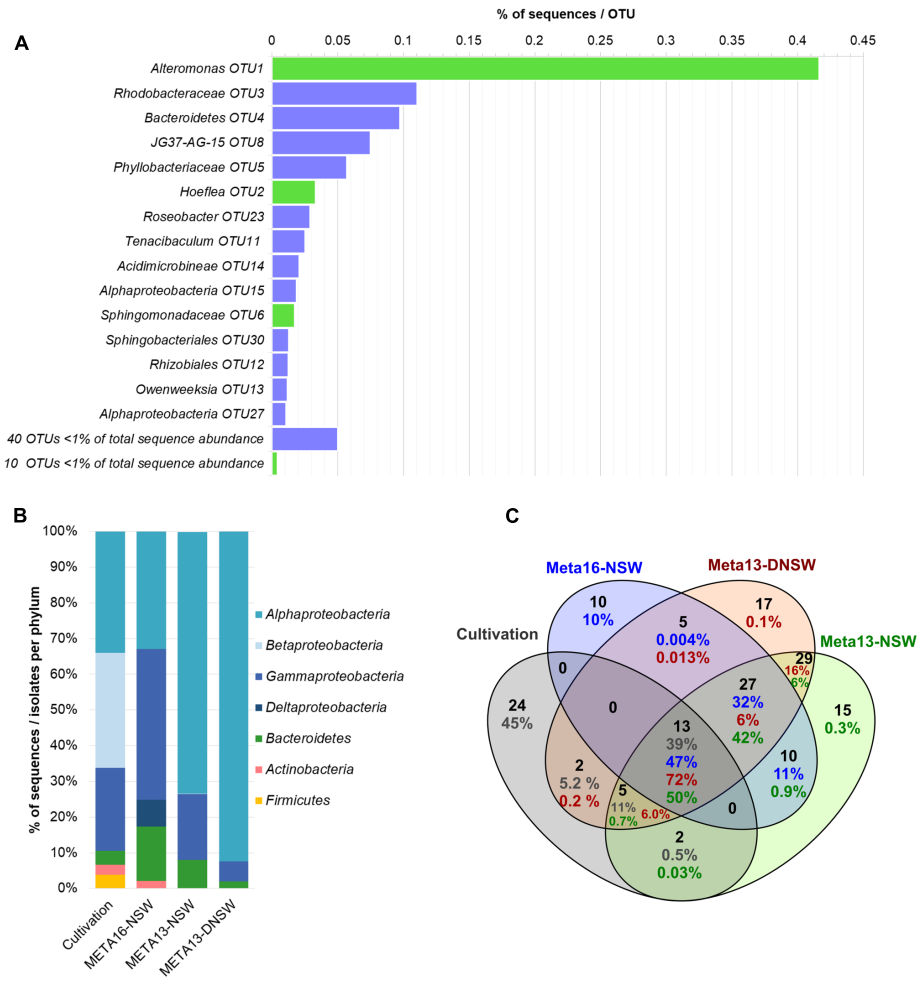

FIGURE 3 | Overview of metabarcoding data and comparison with cultivable isolates. **(A)** Shows the distribution of OTUs in the metabarcoding experiment (META16-NSW). OTUs with >1% of total sequence abundance are displayed separately: bars in green display OTUs that correspond to cultivable strains obtained in this study, while purple bars correspond to OTUs that were not cultivated; OTUs with <1% of total sequence abundance are combined and the sum of sequences is displayed. **(B)** Shows the distribution of 16S rRNA gene metabarcoding sequences per phylum compared to data obtained from the cultivation study. **(C)** Shows a Venn-diagram of the OTUs that are shared between the 2 metabarcoding datasets from 2013 to 2016 and the cultivable isolates. Numbers in blue correspond to META16-NSW, numbers in red correspond to META2013-NSW, numbers in green to META2013-DNSW, and numbers in gray correspond to the proportion of sequences for cultivable isolates.

other strains were uniquely isolated from antibiotic-treated algal tissue suggesting that part of the algae-associated microbiome is (multi)drug-resistant, or otherwise protected by the algal cell wall/inside the cell, where drug concentrations may be too low to be effective. In addition, some antibiotics employed in this study, such as chloramphenicol and erythromycin, may have had only temporal bacteriostatic effects.

The genus *Halomonas* comprises cultivable isolates from various saline environments (Eilers et al., 2000; Donachie et al., 2004; Arahal and Ventosa, 2006; Poli et al., 2009), including microalgal (Keshtacher-Liebson et al., 1995; Croft et al., 2005; Baggesen et al., 2014) and macroalgal surfaces (Ivanova et al., 2002; Wang et al., 2008; Hollants et al., 2013; Tapia et al., 2016). *Halomonas*-algae associations are potentially beneficial for the alga, since the bacteria may provide vitamins (Croft et al., 2005), release siderophores (Keshtacher-Liebson et al., 1995; Baggesen et al., 2014), or excrete morphogenetic compounds (Spoerner et al., 2012; Tapia et al., 2016) that are essential for algal growth. Symbiotic associations with algae may be linked to the capacity of *Halomonas* to degrade algal excreted polysaccharides and/or the presence of alginate lyases (Wong et al., 2000; Tang et al., 2008; Wang et al., 2008; Goecke et al., 2012) and indeed, bacterial cells can be closely attached to algal cell walls (Croft et al., 2005; Tapia et al., 2016). In this study, *Halomonas* was the most abundant isolate obtained with direct plating techniques without pretreatment (DP1 and DP2). More isolates were derived from tissue/protoplasts compared to algal growth medium ($p = 1.92E-13$), suggesting a close association between *Ectocarpus* and the *Halomonas* sp.

In summary, each cultivation strategy resulted in the cultivation of unique strains that were not cultivated with any of the other methods. For example, the application of antibiotics to eliminate *Halomonas* sp. reduced the competitive pressure between antibiotic resistant bacteria and led to the cultivation of 16 additional bacterial strains. Similar observations have been made in sponges (Sipkema et al., 2011; Lavy et al., 2014), lichens (Parrot et al., 2015), and tap water (Vaz-Moreira et al., 2013). Interestingly, direct plating without pretreatment, although dominated by *Halomonas* sp., also resulted in the isolation of seven unique strains.

The Cultivated vs. Uncultivated Microbiome

Marine pelagic bacteria often have complex growth and nutrient requirements (Stewart, 2012; Zengler, 2013). In addition, they are generally considered to be oligotrophs, since they inhabit a nutrient-poor environment and grow only very slowly, which might also compromise the cultivation process (Amann et al., 1995; Keller and Zengler, 2004; Zengler, 2013). Hence, a large part of the marine environmental microbiome has been considered non-cultivable using standard cultivation techniques (Amann et al., 1995; Morris et al., 2002; Giovannoni and Stingl, 2005).

Here, we aimed to cultivate bacteria that were associated with the algae/algal cell-walls, a carbohydrate-rich environment due to the accumulation of algal (poly)saccharides, i.e., alginates, fucans, and mannitol (Michel et al., 2010; Popper et al., 2011). The divergence in community structure between pelagic and algae-associated microbiomes is well-established (Kong and Kwong-yu, 1979; Staufenberger et al., 2008; Bengtsson et al., 2010; Burke et al., 2011; Wahl et al., 2012; Goecke et al., 2013b; Mancuso et al., 2016), and several algae-associated bacteria are able to digest/decompose algal cell material (Rieper-Kirchner, 1989; Goecke et al., 2013b; Groisillier et al., 2015; Martin et al., 2015), e.g., via the production of alginate lyases (Sawabe et al., 1997; Dong et al., 2012) and glycoside hydrolases/fucanases (Ficko-Blean et al., 2015). It is thus possible that algae-associated bacteria, contrary to pelagic bacteria, are well-adapted to grow on the laboratory cultivation media provided, resulting in relatively high numbers of cultivable bacteria.

Our data support this hypothesis since culturability was between 44 and 68% based on the dilution-to-extinction experiments (**Table 1**). For pelagic studies, culturability is usually below 15%, with some observation going as low as 0.05% (Connon and Giovannoni, 2002; Page et al., 2004; Stingl et al., 2007, 2008; Yang et al., 2016). In the same vein, dilution-to-extinction cultivation studies on pelagic bacteria generally apply between 1 and 25 bacterial cells/well as inoculum (Connon and Giovannoni, 2002; Stingl et al., 2007). In our study, however, concentrations as low as 0.5 cells/well were required to obtain pure cultures, further demonstrating that a relatively large part of the algae-associated microbiome is cultivable compared to pelagic bacteria.

Culturability was also assessed by comparing the distribution and abundance of taxa obtained in the cultivation study with taxa inferred from16S rRNA gene libraries. In a previous study on *Ectocarpus*, this type of comparison demonstrated an overall ratio of culturability of 11% based on the presence/absence of OTUs (Tapia et al., 2016). In the present study, this number was further increased with 21% of the OTUs and 47% of all 16S rRNA sequences corresponding to cultivable strains (**Figure 3C**).

To our knowledge, this is the first study to apply dilution-to-extinction cultivation to macroalgae-associated bacteria, and the standardized cultivation method (Connon and Giovannoni, 2002) was amended by adding the algal metabolites alginate and/or mannitol to the culture media. We assume that it was, therefore, well-adapted to the metabolic needs of the majority of *Ectocarpus*-associated bacteria, and indeed several bacteria known to be potential cell-wall digesters have representatives in our culture collection, e.g., *Alteromonas* (Sawabe et al., 1997), *Flavobacteria* (Groisillier et al., 2015), *Maribacter* (Martin et al., 2015), *Erythrobacter* (Goecke et al., 2013b), and *Halomonas* (Wong et al., 2000). Together these results validate the combination of cultivation approaches chosen to increase culturability in our system.

Cultivable Bacteria Not Detected by Metabarcoding

Of the 46 unique strains that were isolated in this study, 16 were isolated at least once from algal tissue grown in NSW, and could thus be directly compared to META2016-NSW metabarcoding data set generated in this study. Seven of them (44%) were represented in this gene library. To be able to compare also strains isolated only from low salinities with metabarcoding data, we included two further data sets obtained for the same strain in 2013. All data sets taken together, 22 of the 46 (48%) strains were found at least in one of the libraries, while 24 were undetectable or below the detection limit. Whether a strain was isolated directly from algal tissue or from the algal culture medium did not have a strong impact on these numbers (**Supplementary Table S4**).

There are several hypotheses to explain this observation. First, methodological flaws or biases including the inadequacy to extract DNA from certain bacterial cells due to species-specific characteristics (e.g., gram-positive are generally more difficult to extract than gram-negative cells), primers specificity, or PCR conditions (Suzuki and Giovannoni, 1996; Donachie et al., 2004, 2007). This may explain biases but, is unlikely to account for the complete absence of a taxon, because all cultivable taxa were detectable with standard primers and extraction methods in our cultures. A second explanation is that some "rare" microbes may be laboratory- or human-derived contaminants, e.g., *Staphylococcus*, sp., and *Bacillus* sp. All measures to avoid bacterial contamination of our algal/bacterial samples were taken and the controls were included in all cultivation experiments and generally negative for growth. Nevertheless, it is plausible that some of these "rare" bacteria were acquired during the monthly transfers of the algal cultures or during the bacteria cultivation procedures and growth of these bacteria might have been facilitated by the experimental treatments that were applied.

A third explanation is that the sequencing depth or the number of time points examined (one for DNSW two for NSW) may have been too low to identify members of the

microbiome that are "rare" (Zilber-Rosenberg and Rosenberg, 2008; Skopina et al., 2016). Bacteria might be present in low abundance in the natural environment but they can amplify rapidly under specific environmental conditions (Epstein, 2009; Buerger et al., 2012; Lindh et al., 2015). Rare bacteria might thus serve as a "seed bank" (Pedrós-Alió, 2012) that contributes to the microbial richness and may form the basis for temporal instability of the microbiome (Sogin et al., 2006; Shade and Gilbert, 2015; Jousset et al., 2017). Recently, it has been suggested that in particular marine macro-organisms, and possibly *Ectocarpus* as well, might serve as incubators for rare bacteria (Troussellier et al., 2017), since surface-associated microbiomes generally exhibit higher OTU diversity and harbor many rare OTUs compared to the surrounding seawater. In this scenario, the removal of competing microbes via the antibiotic treatments and our other measures to reduce competition during our cultivation experiments, have probably allowed them to increase in abundance. This explanation is supported by the variability of the microbiome observed in this study compared with the previous study of the same strain under the same conditions (Dittami et al., 2016), and by the fact that 4 of 46 cultured OTUs were found only among the rare ($n \leq 5$) reads in the available barcoding data.

Similar observations of cultivable isolates not being detected in corresponding gene libraries have been made in human stool samples (Lagier et al., 2012), sponges (Sipkema et al., 2011; Esteves et al., 2016), seawater (Eilers et al., 2000), and soil (Shade et al., 2012); more examples are discussed by Donachie et al. (2007). We put forward the hypothesis that, in analogy to "uncultivable" microbes that become cultivable by improving cultivation conditions, at least part of the undetected strains may, therefore, become "barcodable" merely by significantly increasing sequencing depths (Pedrós-Alió, 2012) and/or the temporal resolution of the study.

Perspectives: (Meta)genome-Guided Cultivation and Inference of Metabolic Networks

In this study, we show that a remarkably high number of bacterial cells (∼50%) associated with *Ectocarpus* was cultivable using a range of cultivation techniques. Each cultivation strategy resulted in another dominant genus or weed-species (*Bosea* for antibiotic-treated algae, *Limnobacter* for dilution-to-extinction cultivation) and each strategy also led to the cultivation of unique isolates that were not found with any other cultivation method. Our results thus emphasize the need to use samples from different environmental/abiotic conditions to obtain rare taxa and thus increase the overall cultivable diversity. To further improve these numbers, a metagenomics approach may be used to predict the specific cultivation requirements of yet uncultured taxa (Garza and Dutilh, 2015). One successful example of this approach is the cultivation of members of the SAR11 clade, for which genomic analysis revealed their requirement for exogenous reduced sulfur (Tripp et al., 2008). Such metagenomic analyses of the *Ectocarpus* holobiont are currently ongoing.

Regarding the cultivable isolates, genomic data currently in preparation for several strains may be used to predict their metabolic capacities and to generate hypotheses on how they may complement the metabolism of the alga (Dittami et al., 2014). Because the bacteria are cultivable it will be possible to experimentally verify the hypothesis generated using this approach. Sixty-two bacterial isolates and 12 artificial bacterial communities have already been experimentally tested in preliminary algal–bacterial co-culture experiments. They showed interactions ranging from weak beneficial effects on survival of *E. subulatus* in diluted natural seawater (29 isolates, 15 unique strains; three communities) to growth-inhibition (data not shown). These strains may serve as the first candidates to study the role of algal–bacterial interactions under abiotic stress.

The present bacterial culture collection constitutes a valuable tool to study the *Ectocarpus* holobiont *in vitro* and complements the genomic tools available for the model *Ectocarpus*. Together, they can be used to address fundamental questions regarding the functions of brown macroalgal holobionts during exposure to abiotic stressors, for instance during the acclimation to low salinity in *E. subulatus*.

AUTHOR CONTRIBUTIONS

All authors conceived the study. HK, CJ, and SD carried out experiments. HK wrote the manuscript with help from SD, CB, and CJ. All authors approved of the final manuscript.

FUNDING

This work has received funding from the European Union's Horizon 2020 research and innovation programme under the Marie Sklodowska-Curie grant agreement number 624575 (ALFF) and ANR project IDEALG (ANR-10-BTBR-04) "Investissements d'Avenir, Biotechnologies-Bioressources".

ACKNOWLEDGMENTS

The authors would like to thank Bernard Billoud for help with statistical analyses; Laurence Dartevelle for help with algal culturing; Akira Peters for providing the algal cultures; Dominique Marie for help with the flow cytometry; the Genomer platform (Station Biologique de Roscoff) for access to their sequencing equipment; the ABIMS Platform (Station Biologique de Roscoff) for technical support and server time; Laetitia Mest, Lolita Lecompte, and Maeva Harrivel for their participation in early isolation experiments; Christophe Destombe and Thomas Wichard for helpful discussions; and Angélique Gobet for critical reading of the manuscript.

SUPPLEMENTARY MATERIAL

The Supplementary Material for this article can be found online at: https://www.frontiersin.org/articles/10.3389/fmicb.2017.02456/full#supplementary-material

TABLE S1 | Bacterial growth media recipes for LB, R2A, Zobell, PYG, EC-based, and LNHM.

TABLE S2 | Antibiotics used to reduce the abundance of *Halomonas* sp.

TABLE S3 | Number of bacterial isolates obtained per experimental treatment.

TABLE S4 | Number of cultivable bacterial strains found in metabarcoding experiments depending on sample origin and sequencing library.

REFERENCES

Amann, R. I., Ludwig, W., and Schleifer, K. H. (1995). Phylogenetic identification and in situ detection of individual microbial cells without cultivation. *Microbiol. Rev.* 59, 143–169.

Arahal, D., and Ventosa, A. (2006). "The family Halomonadaceae," in *The Prokaryotes*, eds M. Dworkin, S. Falkow, E. Rosenberg, K.-H. Schleifer, and E. Stackebrandt (New York, NY: Springer), 811–835.

Baggesen, C., Gjermansen, C., and Brandt, A. B. (2014). *A Study of Microalgal Symbiotic Communities with the Aim to Increase Biomass and Biodiesel Production*. Ph.D. dissertation, DTU Chemical Engineering, Kongens Lyngby.

Bengtsson, M. M., Sjøtun, K., and Øvreås, L. (2010). Seasonal dynamics of bacterial biofilms on the kelp *Laminaria hyperborea*. *Aquat. Microb. Ecol.* 60, 71–83. doi: 10.3354/ame01409

Bolton, J. J. (1983). Ecoclinal variation in *Ectocarpus siliculosus* (Phaeophyceae) with respect to temperature growth optima and survival limits. *Mar. Biol.* 73, 131–138. doi: 10.1007/BF00406880

Buerger, S., Spoering, A., Gavrish, E., Leslin, C., Ling, L., and Epstein, S. S. (2012). Microbial scout hypothesis, stochastic exit from dormancy, and the nature of slow growers. *Appl. Environ. Microbiol.* 78, 3221–3228. doi: 10.1128/AEM.07307-11

Burke, C., Thomas, T., Lewis, M., Steinberg, P., and Kjelleberg, S. (2011). Composition, uniqueness and variability of the epiphytic bacterial community of the green alga *Ulva australis*. *ISME J.* 5, 590–600. doi: 10.1038/ismej.2010.164

Button, D. K., Schut, F., Quang, P., Martin, R., and Roberston, B. R. (1993). Viability and isolation of marine bacteria by dilution culture: theory, procedures, and initial results. *Appl. Environ. Microbiol.* 59, 881–891.

Carini, P., Steindler, L., Beszteri, S., and Giovannoni, S. J. (2012). Nutrient requirements for growth of the extreme oligotroph " Candidatus *Pelagibacter ubique* " HTCC1062 on a defined medium. *ISME J.* 7, 592–602. doi: 10.1038/ismej.2012.122

Cho, J. C., and Giovannoni, S. J. (2004). Cultivation and growth characteristics of a diverse group of oligotrophic marine Gammaproteobacteria. *Appl. Environ. Microbiol.* 70, 432–440. doi: 10.1128/AEM.70.1.432-440.2004

Cock, J. M., Sterck, L., Rouzé, P., Scornet, D., Allen, A. E., Amoutzias, G., et al. (2010). The *Ectocarpus* genome and the independent evolution of multicellularity in brown algae. *Nature* 465, 617–621. doi: 10.1038/nature09016

Coelho, S. M., Scornet, D., Rousvoal, S., Peters, N., Dartevelle, L., Peters, A. F., et al. (2012). Isolation and regeneration of protoplasts from *Ectocarpus*. *Cold Spring Harb. Protoc.* 7, 361–364. doi: 10.1101/pdb.prot067959

Connon, S. A., and Giovannoni, S. J. (2002). High-throughput methods for culturing microorganisms in very-low-nutrient media yield diverse new marine isolates. *Appl. Environ. Microbiol.* 68, 3878–3885. doi: 10.1128/AEM.68.8.3878-3885.2002

Croft, M. T., Lawrence, A. D., Raux-Deery, E., Warren, M. J., and Smith, A. G. (2005). Algae acquire vitamin B12 through a symbiotic relationship with bacteria. *Nature* 438, 90–93. doi: 10.1038/nature04056

Dittami, S. M., Duboscq-Bidot, L., Perennou, M., Gobet, A., Corre, E., Boyen, C., et al. (2016). Host-microbe interactions as a driver of acclimation to salinity gradients in brown algal cultures. *ISME J.* 10, 51–63. doi: 10.1038/ismej.2015.104

Dittami, S. M., Eveillard, D., and Tonon, T. (2014). A metabolic approach to study algal–bacterial interactions in changing environments. *Mol. Ecol.* 23, 1656–1660. doi: 10.1111/mec.12670

Dittami, S. M., Gravot, A., Goulitquer, S., Rousvoal, S., Peters, A. F., Bouchereau, A., et al. (2012). Towards deciphering dynamic changes and evolutionary mechanisms involved in the adaptation to low salinities in *Ectocarpus* (brown algae). *Plant J.* 71, 366–377. doi: 10.1111/j.1365-313X.2012.04982.x

Dittami, S. M., Heesch, S., Olsen, J. L., and Collén, J. (2017). Transitions between marine and freshwater environments provide new clues about the origins of multicellular plants and algae. *J. Phycol.* 53, 731–745. doi: 10.1111/jpy.12547

Donachie, S. P., Foster, J. S., and Brown, M. V. (2007). Culture clash: challenging the dogma of microbial diversity. *ISME J.* 1, 97–99. doi: 10.1038/ismej.2007.22

Donachie, S. P., Hou, S., Lee, K. S., Riley, C. W., Pikina, A., Belisle, C., et al. (2004). The hawaiian archipelago: a microbial diversity hotspot. *Microb. Ecol.* 48, 509–520. doi: 10.1007/s00248-004-0217-1

Dong, S., Yang, J., Zhang, X. Y., Shi, M., Song, X. Y., Chen, X. L., et al. (2012). Cultivable alginate lyase-excreting bacteria associated with the arctic brown alga *Laminaria*. *Mar. Drugs* 10, 2481–2491. doi: 10.3390/md10112481

Edgar, R. C., Haas, B. J., Clemente, J. C., Quince, C., and Knight, R. (2011). UCHIME improves sensitivity and speed of chimera detection. *Bioinformatics* 27, 2194–2200. doi: 10.1093/bioinformatics/btr381

Egan, S., Harder, T., Burke, C., Steinberg, P., Kjelleberg, S., and Thomas, T. (2013). The seaweed holobiont: understanding seaweed-bacteria interactions. *FEMS Microbiol. Rev.* 37, 462–476. doi: 10.1111/1574-6976.12011

Eilers, H., Pernthaler, J., Glöckner, F., and Amann, R. (2000). Culturability and in situ abundance of pelagic bacteria from the North Sea. *Appl. Environ. Microbiol.* 66, 3044–3051. doi: 10.1128/AEM.66.7.3044-3051.2000

Epstein, S. S. (2009). Microbial awakenings. *Nature* 457:1083. doi: 10.1038/4571083a

Esteves, A. I. S., Amer, N., Nguyen, M., and Thomas, T. (2016). Sample processing impacts the viability and cultivability of the sponge microbiome. *Front. Microbiol.* 7:499. doi: 10.3389/fmicb.2016.00499

Falcone-Dias, M. F., Vaz-Moreira, I., and Manaia, C. M. (2012). Bottled mineral water as a potential source of antibiotic resistant bacteria. *Water Res.* 46, 3612–3622. doi: 10.1016/j.watres.2012.04.007

Ficko-Blean, E., Hervé, C., and Michel, G. (2015). Sweet and sour sugars from the sea: the biosynthesis and remodeling of sulfated cell wall polysaccharides from marine macroalgae. *Perspect. Phycol.* 2, 51–64. doi: 10.1127/pip/2015/0028

Garza, D. R., and Dutilh, B. E. (2015). From cultured to uncultured genome sequences: metagenomics and modeling microbial ecosystems. *Cell. Mol. Life Sci.* 72, 4287–4308. doi: 10.1007/s00018-015-2004-1

Giovannoni, S. J., and Stingl, U. (2005). Molecular diversity and ecology of microbial plankton. *Nature* 437, 343–348. doi: 10.1038/nature04158

Goecke, F., Labes, A., Wiese, J., and Imhoff, J. F. (2010). Review chemical interactions between marine macroalgae and bacteria. *Mar. Ecol. Prog. Ser.* 409, 267–300. doi: 10.3354/meps08607

Goecke, F., Labes, A., Wiese, J., and Imhoff, J. F. (2012). Dual effect of macroalgal extracts on growth of bacteria in Western Baltic Sea. *Rev. Biol. Mar. Oceanogr.* 47, 75–86. doi: 10.4067/S0718-19572012000100007

Goecke, F., Labes, A., Wiese, J., and Imhoff, J. F. (2013a). Phylogenetic analysis and antibiotic activity of bacteria isolated from the surface of two co-occurring macroalgae from the Baltic Sea. *Eur. J. Phycol.* 48, 47–60. doi: 10.1080/09670262.2013.767944

Goecke, F., Thiel, V., Wiese, J., Labes, A., and Imhoff, J. F. (2013b). Algae as an important environment for bacteria - phylogenetic relationships among new bacterial species isolated from algae. *Phycologia* 52, 14–24. doi: 10.2216/12-24.1.s1

Groisillier, A., Labourel, A., Michel, G., and Tonon, T. (2015). The mannitol utilization system of the marine bacterium *Zobellia galactanovorans*. *Appl. Environ. Microbiol.* 81, 1799–1812. doi: 10.1128/AEM.02808-14

Hollants, J., Leliaert, F., De Clerck, O., and Willems, A. (2013). What we can learn from sushi: a review on seaweed-bacterial associations. *FEMS Microbiol. Ecol.* 83, 1–16. doi: 10.1111/j.1574-6941.2012.01446.x

Ivanova, E. P., Bakunina, I. Y., Sawabe, T., Hayashi, K., Alexeeva, Y. V., Zhukova, N. V., et al. (2002). Two species of culturable bacteria associated with degradation of brown algae *Fucus evanescens*. *Microb. Ecol.* 43, 242–249. doi: 10.1007/s00248-001-1011-y

Jimenez-Infante, F., Ngugi, D. K., Alam, I., Rashid, M., Baalawi, W., Kamau, A. A., et al. (2014). Genomic differentiation among two strains of the PS1 clade isolated from geographically separated marine habitats. *FEMS Microbiol. Ecol.* 89, 181–197. doi: 10.1111/1574-6941.12348

Jousset, A., Bienhold, C., Chatzinotas, A., Gallien, L., Gobet, A., Kurm, V., et al. (2017). Where less may be more: how the rare biosphere pulls ecosystems strings. *ISME J.* 11, 853–862. doi: 10.1038/ismej.2016.174

Katoh, K., Misawa, K., Kuma, K., and Miyata, T. (2002). MAFFT: a novel method for rapid multiple sequence alignment based on fast Fourier transform. *Nucleic Acids Res.* 30, 3059–3066. doi: 10.1093/nar/gkf436

Keller, M., and Zengler, K. (2004). Tapping into microbial diversity. *Nat. Rev. Microbiol.* 2, 141–150. doi: 10.1038/nrmicro819

Keshtacher-Liebson, E., Hadar, Y., and Chen, Y. (1995). Oligotrophic bacteria enhance algal growth under iron-deficient conditions. *Appl. Environ. Microbiol.* 61, 2439–2441.

Kong, M. K., and Kwong-yu, C. (1979). A study on the bacterial flora isolated from marine algae. *Bot. Mar.* 22, 65–82. doi: 10.1515/botm.1979.22.2.83

Kozich, J. J., Westcott, S. L., Baxter, N. T., Highlander, S. K., and Schloss, P. D. (2013). Development of a dual-index sequencing strategy and curation pipeline for analyzing amplicon sequence data on the miseq illumina sequencing platform. *Appl. Environ. Microbiol.* 79, 5112–5120. doi: 10.1128/AEM.01043-13

Lagier, J. C., Armougom, F., Million, M., Hugon, P., Pagnier, I., Robert, C., et al. (2012). Microbial culturomics: paradigm shift in the human gut microbiome study. *Clin. Microbiol. Infect.* 18, 1185–1193. doi: 10.1111/1469-0691.12023

Lavy, A., Keren, R., Haber, M., Schwartz, I., and Ilan, M. (2014). Implementing sponge physiological and genomic information to enhance the diversity of its culturable associated bacteria. *FEMS Microbiol. Ecol.* 87, 486–502. doi: 10.1111/1574-6941.12240

Letunic, I., and Bork, P. (2016). Interactive tree of life (iTOL) v3: an online tool for the display and annotation of phylogenetic and other trees. *Nucleic Acids Res.* 44, W242–W245. doi: 10.1093/nar/gkw290

Lindh, M. V., Figueroa, D., Sjöstedt, J., Baltar, F., Lundin, D., Andersson, A., et al. (2015). Transplant experiments uncover Baltic Sea basin-specific responses in bacterioplankton community composition and metabolic activities. *Front. Microbiol.* 6:223. doi: 10.3389/fmicb.2015.00223

Lu, H., Sato, Y., Fujimura, R., Nishizawa, T., Kamijo, T., and Ohta, H. (2011). Limnobacter litoralis sp. nov., a thiosulfate-oxidizing, heterotrophic bacterium isolated from a volcanic deposit, and emended description of the genus *Limnobacter*. *Int. J. Syst. Evol. Microbiol.* 61, 404–407. doi: 10.1099/ijs.0.020206-0

Mancuso, F. P., D'Hondt, S., Willems, A., Airoldi, L., and De Clerck, O. (2016). Diversity and temporal dynamics of the epiphytic bacterial communities associated with the canopy-forming seaweed *Cystoseira compressa* (Esper) Gerloff and Nizamuddin. *Front. Microbiol.* 7:476. doi: 10.3389/fmicb.2016.00476

Marie, D., Partensky, F., Jacquet, S., and Vaulot, D. (1997). Enumeration and cell cycle analysis of natural populations of marine picoplankton by flow cytometry using the nucleic acid stain SYBR Green I. *Appl. Environ. Microbiol.* 63, 186–193. doi: 10.1111/j.1365-294X.2009.04480.x

Martin, M., Barbeyron, T., Martin, R., Portetelle, D., Michel, G., and Vandenbol, M. (2015). The cultivable surface microbiota of the brown alga *Ascophyllum nodosum* is enriched in macroalgal-polysaccharide-degrading bacteria. *Front. Microbiol.* 6:1487. doi: 10.3389/fmicb.2015.01487

Michel, G., Tonon, T., Scornet, D., Cock, J. M., and Kloareg, B. (2010). Central and storage carbon metabolism of the brown alga *Ectocarpus siliculosus*: insights into the origin and evolution of storage carbohydrates in eukaryotes. *New Phytol.* 188, 67–81. doi: 10.1111/j.1469-8137.2010.03345.x

Morris, R. M., Rappé, M. S., Connon, S. A., Vergin, K. L., Siebold, W. A., Carlson, C. A., et al. (2002). SAR11 clade dominates ocean surface bacterioplankton communities. *Nature* 420, 806–810. doi: 10.1038/nature01240

Page, K. A., Connon, S. A., and Giovannoni, S. J. (2004). Representative freshwater bacterioplankton isolated from Crater Lake, Oregon. *Appl. Environ. Microbiol.* 70, 6542–6550. doi: 10.1128/AEM.70.11.6542-6550.2004

Parrot, D., Antony-Babu, S., Intertaglia, L., Grube, M., Tomasi, S., and Suzuki, M. T. (2015). Littoral lichens as a novel source of potentially bioactive *Actinobacteria*. *Sci. Rep.* 5:15839. doi: 10.1038/srep15839

Pedersén, M. (1969). Marine brown algae requiring vitamin B12. *Physiol. Plant.* 22, 977–983. doi: 10.1111/j.1399-3054.1969.tb07455.x

Pedersén, M. (1973). Identification of a Cytokinin, purine, in sea water and the effect of cytokinins on brown algae. *Physiol. Plant.* 28, 101–105. doi: 10.1111/j.1399-3054.1973.tb01158.x

Pedrós-Alió, C. (2012). The rare bacterial biosphere. *Annu. Rev. Mar. Sci.* 4, 449–466. doi: 10.1146/annurev-marine-120710-100948

Peters, A. F., Coucerio, L., Tsiamis, K., Küpper, F. C., and Valero, M. (2015). Barcoding of cryptic stages of marine brown algae isolated from incubated substratum reveals high diversity. *Cryptogam. Algol.* 36, 3–29.

Peters, A. F., Marie, D., Scornet, D., Kloareg, B., and Cock, J. M. (2004). Proposal of *Ectocarpus siliculosus* (Ectocarpales, Phaeophyceae) as a model organism for brown algal genetics and genomics. *J. Phycol.* 40, 1079–1088. doi: 10.1111/j.1529-8817.2004.04058.x

Poli, A., Kazak, H., Gürleyendağ, B., Tommonaro, G., Pieretti, G., Öner, E. T., et al. (2009). High level synthesis of levan by a novel *Halomonas* species growing on defined media. *Carbohydr. Polym.* 78, 651–657. doi: 10.1016/j.carbpol.2009.05.031

Popper, Z. A., Michel, G., Herve, C., Domozych, D. S., Willats, W. G. T., Tuohy, M. G., et al. (2011). Evolution and diversity of plant cell walls: from algae to flowering plants. *Annu. Rev. Plant Biol.* 62, 567–590. doi: 10.1146/annurev-arplant-042110-103809

Quast, C., Pruesse, E., Yilmaz, P., Gerken, J., Schweer, T., Yarza, P., et al. (2013). The SILVA ribosomal RNA gene database project: improved data processing and web-based tools. *Nucleic Acids Res.* 41, D590–D596. doi: 10.1093/nar/gks1219

Reasoner, D. J., and Geldreich, E. E. (1985). A new medium for the enumeration and subculture of bacteria from potable water. *Appl. Environ. Microbiol.* 49, 1–7.

Rieper-Kirchner, M. (1989). Microbial degradation of North Sea macroalgae: field and laboratory studies. *Bot. Mar.* 32, 241–252. doi: 10.1515/botm.1989.32.3.241

RStudio Team (2016). *RStudio: Integrated Development for R*. Boston, MA: RStudio, Inc.

Salaün, S., Kervarec, N., Potin, P., Haras, D., Piotto, M., and La Barre, S. (2010). Whole-cell spectroscopy is a convenient tool to assist molecular identification of cultivatable marine bacteria and to investigate their adaptive metabolism. *Talanta* 80, 1758–1770. doi: 10.1016/j.talanta.2009.10.020

Salaün, S., La Barre, S., Santos-Goncalvez, M., Dos Potin, P., Haras, D., and Bazire, A. (2012). Influence of exudates of the kelp *Laminaria digitata* on biofilm formation of associated and exogenous bacterial epiphytes. *Microb. Ecol.* 64, 359–369. doi: 10.1007/s00248-012-0048-4

Sawabe, T., Ohtsuka, M., and Ezura, Y. (1997). Novel alginate lyases from marine bacterium *Alteromonas* sp. strain H-4. *Carbohydr. Res.* 304, 69–76. doi: 10.1016/S0008-6215(97)00194-8

Shade, A., and Gilbert, J. A. (2015). Temporal patterns of rarity provide a more complete view of microbial diversity. *Trends Microbiol.* 23, 335–340. doi: 10.1016/j.tim.2015.01.007

Shade, A., Hogan, C. S., Klimowicz, A. K., Linske, M., Mcmanus, P. S., and Handelsman, J. (2012). Culturing captures members of the soil rare biosphere. *Environ. Microbiol.* 14, 2247–2252. doi: 10.1111/j.1462-2920.2012.02817.x

Singh, R. P., and Reddy, C. R. K. (2014). Seaweed-microbial interactions: key functions of seaweed-associated bacteria. *FEMS Microbiol. Ecol.* 88, 213–230. doi: 10.1111/1574-6941.12297

Singh, R. P., and Reddy, C. R. K. (2016). Unraveling the functions of the macroalgal microbiome. *Front. Microbiol.* 6:1488. doi: 10.3389/fmicb.2015.01488

Sipkema, D., Schippers, K., Maalcke, W. J., Yang, Y., Salim, S., and Blanch, H. W. (2011). Multiple approaches to enhance the cultivability of bacteria associated with the marine sponge *Haliclona* (*gellius*) sp. *Appl. Environ. Microbiol.* 77, 2130–2140. doi: 10.1128/AEM.01203-10

Skopina, M., Vasileva, A., Pershina, E., and Pinevich, A. (2016). Diversity at low abundance: the phenomenon of the rare bacterial biosphere. *Microbiology* 85, 272–282. doi: 10.1134/S0026261716030139

Sogin, M. L., Morrison, H. G., Huber, J. A., Welch, D. M., Huse, S. M., Neal, P. R., et al. (2006). Microbial diversity in the deep sea and the underexplored "rare biosphere". *Proc. Natl. Acad. Sci. U.S.A.* 103, 12115–12120. doi: 10.1073/pnas.0605127103

Spoerner, M., Wichard, T., Bachhuber, T., Stratmann, J., and Oertel, W. (2012). Growth and thallus morphogenesis of *Ulva mutabilis* (Chlorophyta) depends on a combination of two bacterial species excreting regulatory factors. *J. Phycol.* 48, 1433–1447. doi: 10.1111/j.1529-8817.2012.01231.x

Spring, S., Kämpfer, P., and Schleifer, K. H. (2001). Limnobacter thiooxidans gen. nov., sp. nov., a novel thiosulfate-oxidizing bacterium isolated from freshwater lake sediment. *Int. J. Syst. Evol. Microbiol.* 51, 1463–1470. doi: 10.1099/00207713-51-4-1463

Starr, R. C., and Zeikus, J. A. (1993). Utex – the culture collection of algae at the University of Texas at Austin 1993 List of Cultures. *J. Phycol.* 29, 1–106. doi: 10.1111/j.0022-3646.1993.00001.x

Staufenberger, T., Thiel, V., Wiese, J., Imhoff, J. F., Jf, I., Ep, I., et al. (2008). Phylogenetic analysis of bacteria associated with *Laminaria saccharina*. *FEMS Microbiol. Ecol.* 64, 65–77. doi: 10.1111/j.1574-6941.2008.00445.x

Stewart, E. J. (2012). Growing unculturable bacteria. *J. Bacteriol.* 194, 4151–4160. doi: 10.1128/JB.00345-12

Stingl, U., Cho, J. C., Foo, W., Vergin, K. L., Lanoil, B., and Giovannoni, S. J. (2008). Dilution-to-extinction culturing of psychrotolerant planktonic bacteria from permanently ice-covered lakes in the McMurdo Dry Valleys, Antarctica. *Microb. Ecol.* 55, 395–405. doi: 10.1007/s00248-007-9284-4

Stingl, U., Tripp, H. J., and Giovannoni, S. J. (2007). Improvements of high-throughput culturing yielded novel SAR11 strains and other abundant marine bacteria from the Oregon coast and the Bermuda Atlantic Time Series study site. *ISME J.* 1, 361–371. doi: 10.1038/ismej.2007.49

Suzuki, M. T., and Giovannoni, S. J. (1996). Bias caused by template annealing in the amplification of mixtures of 16S rRNA genes by PCR. *Appl. Environ. Microbiol.* 62, 625–630.

Suzuki, R., and Shimodaira, H. (2006). Pvclust: an R package for assessing the uncertainty in hierarchical clustering. *Bioinformatics* 22, 1540–1542. doi: 10.1093/bioinformatics/btl117

Tamura, K., Stecher, G., Peterson, D., Filipski, A., and Kumar, S. (2013). MEGA6: Molecular Evolutionary Genetics Analysis Version 6.0. *Mol. Biol. Evol.* 30, 2725–2729. doi: 10.1093/molbev/mst197

Tang, J., Xiao, Y., Oshima, A., Kawai, H., and Nagata, S. (2008). Disposal of seaweed wakame (*Undaria pinnatifida*) in composting process by marine bacterium *Halomonas* sp. AW4. *Int. J. Biotechnol.* 10, 73–85. doi: 10.1504/IJBT.2008.017970

Tapia, J. E., González, B., Goulitquer, S., Potin, P., and Correa, J. (2016). Microbiota influences morphology and reproduction of the brown alga *Ectocarpus* sp. *Front. Microbiol.* 7:197. doi: 10.3389/fmicb.2016.00197

Thornber, C., Jones, E., and Thomsen, M. (2016). "Epibiont-marine macrophyte assemblages," in *Marine Macrophytes As Foundation Species*, ed. E. Ólafsson (New York, NY: CRC Press), 43–65. doi: 10.4324/9781315370781-4

Tripp, H. J., Kitner, J. B., Schwalbach, M. S., Dacey, J. W. H., Wilhelm, L. J., and Giovannoni, S. J. (2008). SAR11 marine bacteria require exogenous reduced sulphur for growth. *Nature* 452, 741–744. doi: 10.1038/nature06776

Troussellier, M., Escalas, A., Bouvier, T., and Mouillot, D. (2017). Sustaining rare marine microorganisms: macroorganisms as repositories and dispersal agents of microbial diversity. *Front. Microbiol.* 8:947. doi: 10.3389/fmicb.2017.00947

Vaz-Moreira, I., Egas, C., Nunes, O. C., and Manaia, C. M. (2013). Bacterial diversity from the source to the tap: a comparative study based on 16S rRNA gene-DGGE and culture-dependent methods. *FEMS Microbiol. Ecol.* 83, 361–374. doi: 10.1111/1574-6941.12002

Wahl, M., Goecke, F., Labes, A., Dobretsov, S., and Weinberger, F. (2012). The second skin: ecological role of epibiotic biofilms on marine organisms. *Front. Microbiol.* 3:292. doi: 10.3389/fmicb.2012.00292

Wang, G., Shuai, L., Li, Y., Lin, W., Zhao, X., and Duan, D. (2008). Phylogenetic analysis of epiphytic marine bacteria on Hole-Rotten diseased sporophytes of *Laminaria japonica*. *J. Appl. Phycol.* 20, 403–409. doi: 10.1007/s10811-007-9274-4

Wang, Q., Garrity, G. M., Tiedje, J. M., and Cole, J. R. (2007). Naïve Bayesian classifier for rapid assignment of rRNA sequences into the new bacterial taxonomy. *Appl. Environ. Microbiol.* 73, 5261–5267. doi: 10.1128/AEM.00062-07

Weisburg, W. G., Barns, S. M., Pelletier, D. A., and Lane, D. J. (1991). 16S ribosomal DNA amplification for phylogenetic study. *J. Bacteriol.* 173, 697–703. doi: 10.1128/jb.173.2.697-703

Wells, M. L., Potin, P., Craigie, J. S., Raven, J. A., Merchant, S. S., Helliwell, K. E., et al. (2017). Algae as nutritional and functional food sources: revisiting our understanding. *J. Appl. Phycol.* 29, 949–982. doi: 10.1007/s10811-016-0974-5

West, J., and Kraft, G. (1996). *Ectocarpus siliculosus* (Dillwyn) Lyngb. from Hopkins River Falls, Victoria – the first record of a freshwater brown alga in Australia. *Muelleria* 9, 29–33.

Wiese, J., Thiel, V., Nagel, K., Staufenberger, T., and Imhoff, J. F. (2009). Diversity of antibiotic-active bacteria associated with the brown alga *Laminaria saccharina* from the baltic sea. *Mar. Biotechnol.* 11, 287–300. doi: 10.1007/s10126-008-9143-4

Wong, T. Y., Preston, L. A., and Schiller, N. L. (2000). Alginate lyase: review of major sources and enzyme characteristics, structure-function analysis, biological roles, and applications. *Annu. Rev. Microbiol.* 54, 289–340. doi: 10.1146/annurev.micro.54.1.289

Wu, H. T., Mi, Z. L., Zhang, J. X., Chen, C., and Xie, S. G. (2014). Bacterial communities associated with an occurrence of colored water in an urban drinking water distribution system. *Biomed. Environ. Sci.* 27, 646–650. doi: 10.3967/bes2014.099

Yang, S.-J., Kang, I., and Cho, J.-C. (2016). Expansion of cultured bacterial diversity by large-scale dilution-to-extinction culturing from a single seawater sample. *Microb. Ecol.* 71, 29–43. doi: 10.1007/s00248-015-0695-3

Zengler, K. (2013). "To grow or not to grow: isolation and cultivation procedures in the genomic age," in *The Human Microbiota*, ed. D. N. Fredricks (Hoboken, NJ: John Wiley & Sons, Inc.), 289–302. doi: 10.1002/9781118409855.ch12

Zhang, L., Gao, G., Tang, X., and Shao, K. (2014). Impacts of different salinities on bacterial biofilm communities in fresh water. *Can. J. Microbiol.* 60, 319–326. doi: 10.1139/cjm-2013-0808

Zilber-Rosenberg, I., and Rosenberg, E. (2008). Role of microorganisms in the evolution of animals and plants: the hologenome theory of evolution. *FEMS Microbiol. Rev.* 32, 723–735. doi: 10.1111/j.1574-6976.2008.00123.x

Zobell, C. (1941). Cultural requirements of marine heterotrophic aerobes. *J. Mar. Res.* 4, 42–75.

Zothanpuia, Passari, A. K., Gupta, V. K., and Singh, B. P. (2016). Detection of antibiotic-resistant bacteria endowed with antimicrobial activity from a freshwater lake and their phylogenetic affiliation. *PeerJ* 4:e2103. doi: 10.7717/peerj.2103

Conflict of Interest Statement: The authors declare that the research was conducted in the absence of any commercial or financial relationships that could be construed as a potential conflict of interest.

frontiers in Marine Science

PERSPECTIVE
published: 24 April 2018
doi: 10.3389/fmars.2018.00144

Multicellular Features of Phytoplankton

*Adi Abada and Einat Segev**

Department of Plant and Environmental Sciences, Weizmann Institute of Science, Rehovot, Israel

Microscopic marine phytoplankton drift freely in the ocean, harvesting sunlight through photosynthesis. These unicellular microorganisms account for half of the primary productivity on Earth and play pivotal roles in the biogeochemistry of our planet (Field et al., 1998). The major groups of microalgae that comprise the phytoplankton community are coccolithophores, diatoms and dinoflagellates. In present oceans, phytoplankton individuals and populations are forced to rapidly adjust, as key chemical and physical parameters defining marine habitats are changing globally. Here we propose that microalgal populations often display the characteristics of a multicellular-like community rather than a random collection of individuals. Evolution of multicellularity entails a continuum of events starting from single cells that go through aggregation or clonal divisions (Brunet and King, 2017). Phytoplankton may be an intermediate state between single cells and aggregates of physically attached cells that communicate and co-operate; perhaps an evolutionary snapshot toward multicellularity. In this opinion article, we journey through several studies conducted in two key phytoplankton groups, coccolithophores and diatoms, to demonstrate how observations in these studies could be interpreted in a multicellular context.

Keywords: phytoplankton, coccolithophore, *Emiliania huxleyi*, diatoms, multicellularity, programmed cell death, infochemical communication

OPEN ACCESS

Edited by:
Matthias Wietz,
University of Oldenburg, Germany

Reviewed by:
Nick A. Lyons,
Harvard Medical School, United States
Matthew' David Herron,
University of Montana, United States
Pierre Durand,
University of the Witwatersrand, South Africa

***Correspondence:**
Einat Segev
einat.segev@weizmann.ac.il

Specialty section:
This article was submitted to Aquatic Microbiology, a section of the journal Frontiers in Marine Science

Received: *30 January 2018*
Accepted: *10 April 2018*
Published: *24 April 2018*

Citation:
Abada A and Segev E (2018) Multicellular Features of Phytoplankton. Front. Mar. Sci. 5:144. doi: 10.3389/fmars.2018.00144

Emiliania huxleyi is the most widespread coccolithophore in modern oceans. Populations of this microalga form massive seasonal blooms that cover thousands of square kilometers and are easily detected by satellites (Holligan et al., 1983; Balch et al., 1991; Balch, 2018). The blooms exhibit unique dynamics whereby they form seasonally over several weeks and then suddenly collapse (Tyrrell and Merico, 2004; Behrenfeld and Boss, 2014; Lehahn et al., 2014). The sudden demise of these blooms is mostly attributed to viral infection (Bratbak et al., 1993; Vardi et al., 2012; Lehahn et al., 2014), and bacteria have also been shown to drive the sudden collapse of *E. huxleyi* populations (Segev et al., 2016). Algal death, whether due to biotic or abiotic factors, often bears much similarity to Programmed Cell Death (PCD), a process known from higher plants and animals (Bidle, 2016).

PCD has also been reported in diatoms, a key group of phytoplankton. Diatoms are responsible for 50% of the global phytoplankton productivity (Rousseaux and Gregg, 2014). Diatoms, similarly to coccolithophores, grow rapidly over wide areas of ocean, forming blooms that suddenly terminate with death of the vast majority of the population. Autocatalytic death in diatoms was initially reported in response to nutrient limitation (Brussaard et al., 1997; Berges and Falkowski, 1998). Numerous studies have since provided a comprehensive view of the environmental triggers and molecular mechanisms underlying various death mechanisms in diatoms (Bidle, 2015, 2016).

In multicellular organisms, PCD is a process that maintains proper growth and functionality of individuals (Hamburger and Levi-Montalcini, 1949; Glucksmann, 1951; Lockshin and Williams, 1964; Kerr et al., 1972; Milligan and Schwartz, 1996; Jones, 2001; Danial and Korsmeyer, 2004). PCD is an active and highly regulated process that can be undertaken by a subpopulation of cells that are infected or genetically perturbed, in order to eliminate the harmful influence and/or agent and save the other cells. It is considered to be an altruistic act executed by individual cells for the greater good of the entire organism (Glucksmann, 1951; Lockshin and Williams, 1964; Kerr et al., 1972; Milligan and Schwartz, 1996; Jones, 2001; Danial and Korsmeyer, 2004).

Much research has been conducted in recent years to elucidate the eco-physiology of PCD in phytoplankton (Franklin et al., 2006; Bidle, 2015, 2016). While knowledge about mechanisms driving and controlling PCD in phytoplankton expands, it remains unclear why a unicellular organism would execute a highly controlled death process. The paradox of PCD in single-celled organisms has been previously raised and discussed (Ameisen, 1996, 2002; Franklin et al., 2006; Nedelcu et al., 2011; Bayles, 2014; Durand et al., 2016). It has been posited that PCD in single-celled organisms has a different origin and nature than in multicellular organisms (Nedelcu et al., 2011). In addition, it has been proposed that PCD can increase biological complexity in microbial communities (Durand et al., 2016). Faced with the puzzling nature of unicellular PCD, we offer several observations and highlight reports from the literature that encourage a reconsideration of the multicellular features of phytoplankton. We provide several lines of evidence demonstrating multicellular traits of phytoplankton and subsequently discuss the benefits of phytoplankton PCD in analogy to this process in multicellular organisms.

To examine multicellular traits of phytoplankton, we sought to find a definition for multicellularity. Multicellularity has independently evolved at least 16 times within all domains of life (Bonner, 1998; King, 2004; Rokas, 2008; Knoll, 2011). Previous attempts to define multicellularity, especially in the microbial world, have delineated two essential parameters that must be met in a multicellular scenario: intercellular communication that leads to coordinated action, and cell-cell adhesion (Lyons and Kolter, 2015). In the next paragraphs we demonstrate modes of phytoplankton communication and cell-cell adhesion, and we discuss how phytoplankton PCD could be interpreted as a coordinated population action. While clearly phytoplankton cells exist as individual cells, we find ample reports suggesting that microalgae are frequently found as multicellular-like assemblages.

PHYTOPLANKTON COMMUNICATION AND COORDINATED BEHAVIOR

In diatoms, individual cells can communicate warning signals to the entire population, triggering either cell death or community-wide defense mechanisms. A diatom cell experiencing stress conditions will produce the lethal aldehyde (2E,4E/Z)-decadienal (DD) (Miralto et al., 1999; Pohnert, 2002). Diatoms that are exposed to high levels of DD will execute PCD through cellular events that are based on nitric oxide (NO) signaling (Vardi et al., 2006). At the same time, diatoms that are exposed to lower levels of DD initiate an intracellular signaling cascade culminating in resistance to lethal concentrations of DD (Vardi et al., 2006). The first diatoms that are exposed to stress, release DD to the environment before they die, and in their death the hazard is communicated to the rest of the population enabling a coordinated population-wide immunization. DD discharge by the dying diatoms has another benefit for the population; one of the common stresses experienced by diatoms is due to copepod feeders that graze on diatom communities. DD impairs normal development of copepods and other invertebrates (Miralto et al., 1999; Caldwell et al., 2002; Ianora et al., 2004).

Nitric oxide (NO) is another potent signaling molecule with potential roles in phytoplankton cell-cell communication. NO has an established cellular function as a pivotal signaling molecule during PCD in both diatoms and coccolithophores. Diatom cells produce NO under various stresses (Vardi et al., 2008). Production of NO is likely to lead to the formation of reactive oxygen species and ultimately PCD. Upon lysis of the cell and the release of its content, the produced NO may be a cue that triggers PCD in neighboring cells (Vardi, 2008). As a freely diffusing free radical gas, NO from lysing cells easily spreads through the diatom population acting as a signal (Vardi et al., 2006). NO, along with other signaling molecules, has been defined a phytoplankton "infochemical" (Vardi, 2008), due to its capacity to carry information between individual phytoplankton cells.

Significant production of NO was also observed in *E. huxleyi* populations, both in virus-infected cultures and in natural populations in the ocean (Bidle, 2015; Hirsh et al., 2016). Indeed it appears that phytoplankton communities share information in complex manners facilitating communication between cells. The release of signals from some cells, which are perceived by other cells, culminates in a variety of coordinated actions including death, resilience, and possibly additional modes of behavior yet to be explored. Physical proximity between individuals would facilitate efficient communication within the population, especially when using universal signals as NO.

PHYTOPLANKTON CELL-CELL ADHESION

We have found that *E. huxleyi* cultures regularly aggregate. While clumping seemed no more than a technical nuisance, a closer look revealed that algal aggregates are a complex structure of cells encased within an extracellular matrix (**Figure 1**). The algal aggregates are held together by at least two structural components: extracellular DNA (**Figure 2**) and Transparent Exopolymer Particles (TEP) (**Figure 2**). Recently, proteins were characterized as an additional structural component involved in phytoplankton aggregation (Thornton and Chen, 2017). Interestingly, TEP generation increases under stress conditions, however production of matrix proteins does not (Thornton and Chen, 2017). These observations suggest

that the production of the two polymers is differentially regulated, demonstrating the insufficiently studied complexity of phytoplankton aggregates. Further investigation both in the lab and in the environment is needed to determine the precise composition of the phytoplankton extracellular matrix. Current observations hold promise in providing a starting point for studying algal aggregation into multicellular-like assemblages. Both extracellular DNA and exopolysaccharides are structural component of bacterial biofilms (Watnick and Kolter, 2000; Whitchurch et al., 2002; Vlamakis et al., 2013). Bacterial biofilms are multicellular structures where, similar to *E. huxleyi* aggregates, individual bacterial cells rely on an extracellular matrix to act as a scaffold that holds the community together.

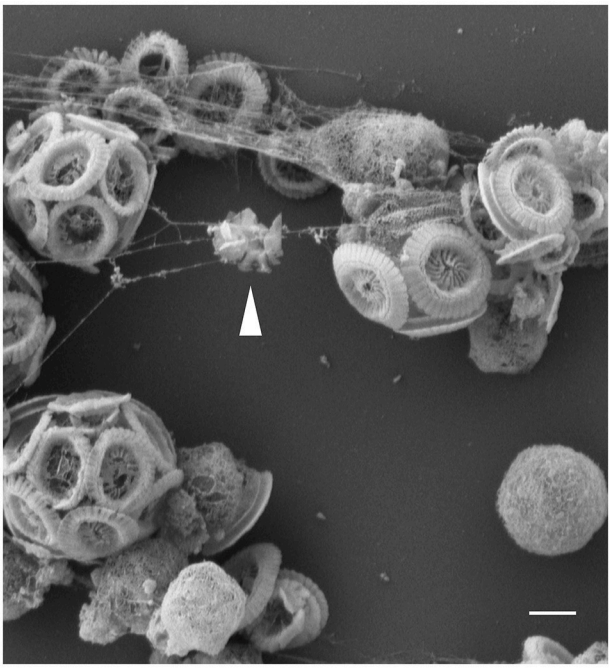

FIGURE 1 | Threads of extracellular matrix connect algal cells. Scanning Electron Microscopy (SEM) image of *E. huxleyi* cells with threads attaching individual calcified and naked cells. Coccoliths debris seen trapped in the threads (see arrow head), suggestive of the adhesive nature of the filaments. Scale bar corresponds to 1 μm. See Data Sheet 1 for Materials and Methods.

The phenomenon of phytoplankton aggregation through TEP has been widely explored. Most reports examined TEP-mediated aggregation as a mechanism facilitating the sinking of particles composed primarily of stressed and dying cells (Nissimov and Bidle, 2017). TEP production indeed increases under various stresses (Chow et al., 2015), but generation of the polymer is also seen in the absence of stress conditions. Diatom production of these polysaccharides was shown to be dynamic, influenced by various environmental conditions such as temperature, acidity and light (Ferreyra et al., 2006; Seebah et al., 2014). TEP formation in diatoms varies between species and was found to change during different growth phases (Passow, 2002; Kahl et al., 2008; Chen and Thornton, 2015). The formation of diatom TEP is increased under turbulent conditions that challenge cell-cell adhesion, and coagulation of TEP-precursors is enhanced (Schuster and Herndl, 1995; Stoderegger and Herndl, 1999; Passow, 2000).

TEP formation by natural *E. huxleyi* populations was monitored in mesocosm experiments in which TEP production was followed during the course of an induced *E. huxleyi* bloom (Vardi et al., 2012). In this work, two mesocosms exhibited high and constant basal levels of polysaccharide production. In a third mesocosm TEP increased significantly following viral infection. Microscopy images show algal

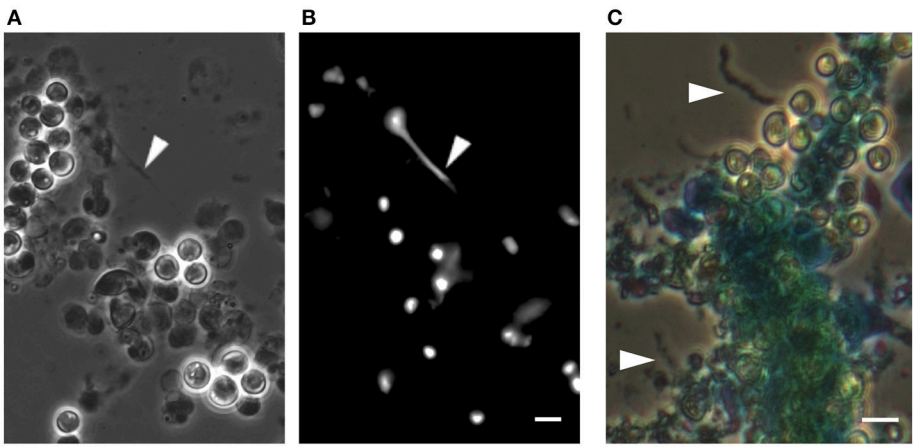

FIGURE 2 | DNA-like threads and polysaccharide fibers in algal aggregates. **(A)** Phase contrast microscopy of an algal aggregate reveals linear structures looking like extracellular DNA threads (see arrow head). **(B)** Fluorescence image of the same algal aggregate demonstrating a fluorescent signal from the threads following DNA staining with Sytox green, a dye that cannot penetrate the cell membrane and thus stains extracellular DNA as well as DNA in cells with perturebed membranes. Scale bar corresponds to 4 μm. **(C)** Image of an algal aggregate stained with the polysaccaride-binding stain alcian blue. Individual fiber-like structures are seen (indicated by arrow heads). The central mass of algal cells appears to be encased in a matrix that absorbed the stain, suggesting an exopolysaccharide composition similar to TEP. Scale bar corresponds to 4 μm. See Data Sheet 1 for Materials and Methods.

cells entangled in an extracellular matrix of TEP fibers (Vardi et al., 2012).

Taken together, cells in both coccolithophore and diatom communities appear to be joined together by components of structural and functional complexity. Interestingly, many genes that are necessary for animal multicellularity are involved in cell-cell adhesion and have evolved prior to animal origins (Brunet and King, 2017). Furthermore, clumping has been used as a trait to experimentally evolve multicellularity in yeast and algae (Ratcliff et al., 2012, 2013; Driscoll and Travisano, 2017). Following clumping, improved cooperation was evident resulting in better growth and enhanced ability to compete for resources (Koschwanez et al., 2011). In populations of the freshwater alga *Chlorella* as well as *Chlamydomonas*, a unicellular Volvocine alga, clumping occurred in response to predation as a defense mechanism (Sathe and Durand, 2016; Kapsetaki et al., 2017). Volvocine algae have been studied as a model system for the transition from unicellular to multicellular life (Kirk, 1999; Herron, 2016). This group includes species of clumping unicells such as *Chlamydomonas*, and the complex multicellular species of Volvox exhibiting division of labor into non-reproductive cells (Kirk, 1999; Hanschen et al., 2014; Herron, 2016). Genetic analysis of Volvocine algae revealed the key role of extracellular matrix in the transition to multicellularity (Merchant et al., 2007; Prochnik et al., 2010). It would therefore be fascinating to explore the genetics of phytoplankton exopolymers and modes of attachment and compare them to components with known functions in multicellularity such as cadherins, integrins, and extracellular matrix domains (Brunet and King, 2017). A better characterization of the phytoplankton extracellular polymers is crucial in determining whether these structural components are specific only toward the organisms that produce them, or whether the fibers are generally adhesive thereby promoting multi-species assemblages.

SEA SKIN

TEP have long been recognized as crucial components in the upper millimeter of the ocean, a region also known as the sea surface microlayer (SML) (Verdugo et al., 2004; Wurl and Holmes, 2008). In 1983, Sieburth first hypothesized that the SML is a continuous hydrated gelatinous layer formed by complex organic structures, and referred to it as the "sea's skin" (Sieburth, 1983). Later studies have confirmed and further discussed the role of TEP in the formation and gelatinous nature of the SML (Wurl and Holmes, 2008; Cunliffe and Murrell, 2009). The source of the TEP that accumulates and determines the SML properties are the phytoplankton communities beneath it that continuously produce and replenish the reservoir of oceanic extracellular polysaccharides (Cunliffe and Murrell, 2009). The fact that TEP are found at the sea surface, attests to the buoyant nature of these polymers. The floating capacity of TEP would be crucial in mediating multicellular-like assemblages without forcing them to sink. Indeed further study into the composition and structure of TEP in floating versus sinking particles is needed. Floating colonies of the phytoplankton *Phaeocystis* are composed of cells embedded in a polysaccharidic matrix (Schoemann et al., 2005). The matrix in these colonies maintains the buoyancy of the aggregated cells and keeps them afloat (Schoemann et al., 2005). One could think of the SML as a viscous scaffold holding together a global and probably diverse community of phytoplankton cells that comprise Sieburth's sea skin.

CONCLUDING REMARKS

Given the abundance of an oceanic gelatinous SML matrix, the ability of phytoplankton to aggregate, communicate and execute coordinated behaviors, perhaps we should think of the global phytoplankton population as an "oceanic tissue"? An ecosystem of multicellular units, each unit interconnected by an extracellular matrix, acting semi-coherently across kilometer scale. The basic multicellular unit would be of physically attached cells. But what are the physical dimensions of such multicellular units? How big are populations of physically attached phytoplankton cells? These questions should be the subject of further study. Furthermore, once attached through extracellular fibers, do cells keep dividing? This might be a key question in attempts to decipher the onset of phytoplankton aggregates; do individual cells converge or do cells undergo clonal divisions while attached? Both modes of multicellular-like assemblages occur in various microorganisms including choanoflagellates, ciliates, fungi, amoeba, and more (Brunet and King, 2017). Aggregation and clonal division are considered to be ancestral forms of current complex multicellularity, with clonal development being ancestral to all forms (Brunet and King, 2017). Regardless of its mode of formation, physical proximity between phytoplankton cells would make it easier for metabolites to diffuse among individuals, transferring information that enables coordinated behaviors.

The existence and evolution of PCD in unicells is controversial (Deponte, 2008). PCD in unicellular organisms could be explained from an evolutionary point of view using inclusive fitness theory, as long as cells are surrounded by genetic relatives (Hamilton, 1964). Adaptive explanations regarding the benefits conferred by PCD in a population of unicells have been discussed and supported by empirical work (Franklin et al., 2006; Vardi et al., 2007; Durand et al., 2014). Non-adaptive explanations discussing the different evolution and functions of phytoplankton PCD have also been raised and experimentally supported (Segovia et al., 2003; Jiménez et al., 2009; Nedelcu et al., 2011). Here we argue that phytoplankton populations have multicellular features that encourage examination of PCD in phytoplankton similarly to PCD in metazoans.

In analogy to the benefits of PCD in metazoans, a subset of the community members must survive the death of their siblings for a population-wide PCD to be beneficial in a multicellular-like community. Indeed, both coccolithophores and diatoms have such subpopulations with altered and durable phenotypes; in *E. huxleyi* a shift to a motile cell type occurs in a small part of the population following viral infection (Frada et al., 2017). The motile cells are resistant to the virus. Thus, while the virus triggers the spread of PCD in the population, the infection

gives rise to a resistant subpopulation. A similar phenotype-remodeling mechanism is seen in diatoms, where resting spores that are highly resilient cells that endure environmental stresses, can be formed (Sims et al., 2006). These survival strategies demonstrate how the context of multicellularity could facilitate a better understanding of phytoplankton PCD and phenotypic variations.

What areas of research would benefit from acknowledging the multicellular features of phytoplankton? We offer here two examples of testable hypotheses with the hope of sparking discussions that would lead to further ideas:

(i) **The algal microenvironment**- In *E. huxleyi*, chemical features of the algal cell and its mineralized shell are used as indicators of environmental and physiological conditions. Examples include boron concentrations and isotopic composition as pH indicators (Stoll et al., 2012) and carbon isotopes as CO_2 proxies (Pagani, 2002). In algal clumps, it is likely that the chemical features of microenvironments within aggregates differ from the ambient conditions due to respiration, calcification and altered diffusion imposed by the extracellular matrix. Therefore clumping, as a regular feature of multicellularity, should be considered in efforts to use algal derivatives as indicators of environmental conditions. In line with this idea, in blooms of the dinoflagellate *Peridinium gatunense*, the pH increases in dinoflagellate patches resulting in CO_2 limitation and oxidative stress (Vardi et al., 1999). Further, the chemical regime in the aggregate microenvironment would likely resemble a semi-closed system due to restricted diffusion. In comparison with the open ocean, nutrients would be exhausted more rapidly within aggregates and cells would become isotopically heavier (Kendall and Caldwell, 1998).

(ii) **Functional heterogeneity**- Phenotypic heterogeneity in isogenic phytoplankton communities is found in enzymatic activities (Dyhrman and Palenik, 2003), structural features (Godoi et al., 2009), biomineralization processes (Znachor et al., 2013), biosynthesis of secreted molecules (Hamilton and Lenton, 1998), motility (Frada et al., 2017) and more. In a multicellular context, the heterogeneity in these populations could be a manifestation of division of labor (Crespi, 2001). Whether disruption of algal aggregates influences the heterogeneity of algal populations should be further tested.

As our oceans change, phytoplankton populations are forced to quickly adapt. How phytoplankton cells adhere to each other, share information, and give rise to coordinated activity merits further study both in the laboratory and in the environment to allow a comprehensive understanding of these key populations under changing conditions.

AUTHOR CONTRIBUTIONS

AA and ES wrote the manuscript. ES conducted experiments and acquired images.

ACKNOWLEDGMENTS

We are grateful to Roberto Kolter for inspiring discussions and insightful comments. We thank Assaf Vardi, Daniella Schatz, Assaf Gal, and Or Eliason for thoroughly reading the manuscript and providing valuable input. We are thankful to Jonathan Gressel for his valuable assistance in editing the manuscript. The authors wish to thank Scott Chimileski and Nick Lyons for their feedback on earlier versions of this manuscript. We thank Estelle Kalfon-Cohen for her assistance with electron microscopy and the Harvard Center for Nanoscale Systems for use of its imaging facility. ES is supported by the Estate of Jacqueline Hodes and the Estate of Fannie Sherr.

SUPPLEMENTARY MATERIAL

The Supplementary Material for this article can be found online at: https://www.frontiersin.org/articles/10.3389/fmars.2018.00144/full#supplementary-material

REFERENCES

Ameisen, J. C. (1996). The origin of programmed cell death. *Science* 272, 1278–1279. doi: 10.1126/science.272.5266.1278

Ameisen, J. C. (2002). On the origin, evolution, and nature of programmed cell death: a timeline of four billion years. *Cell* 9, 367–393. doi: 10.1038/sj.cdd.4400950

Balch, W. M. (2018). The ecology, biogeochemistry, and optical properties of coccolithophores. *Ann. Rev. Mar. Sci.* 10, 71–98. doi: 10.1146/annurev-marine-121916-063319

Balch, W. M., Holligan, P. M., Ackleson, S. G., and Voss, K. J. (1991). Biological and optical-properties of mesoscale coccolithophore blooms in the gulf of Maine. *Limnol. Oceanogr.* 36, 629–643. doi: 10.4319/lo.1991.36.4.0629

Bayles, K. W. (2014). Bacterial programmed cell death: making sense of a paradox. *Nat. Rev. Microbiol.* 12, 63–69. doi: 10.1038/nrmicro3136

Behrenfeld, M. J., and Boss, E. S. (2014). Resurrecting the ecological underpinnings of ocean plankton blooms. *Ann. Rev. Mar. Sci.* 6, 167–194. doi: 10.1146/annurev-marine-052913-021325

Berges, J. A., and Falkowski, P. G. (1998). Physiological stress and cell death in marine phytoplankton: induction of proteases in response to nitrogen or light limitation. *Limnol. Oceanogr.* 43, 129–135. doi: 10.4319/lo.1998.43.1.0129

Bidle, K. D. (2015). The molecular ecophysiology of programmed cell death in marine phytoplankton. *Ann. Rev. Mar. Sci.* 7, 341–375. doi: 10.1146/annurev-marine-010213-135014

Bidle, K. D. (2016). Programmed cell death in unicellular phytoplankton. *Curr. Biol.* 26, R594–R607. doi: 10.1016/j.cub.2016.05.056

Bonner, J. T. (1998). The origins of multicellularity. *Integr. Biol.* 1, 27–36. doi: 10.1002/(SICI)1520-6602(1998)1:1<27::AID-INBI4>3.0.CO;2-6

Bratbak, G., Egge, J. K., and Heldal, M. (1993). Viral mortality of the marine alga *Emiliania huxleyi* (haptophyceae) and termination of algal blooms. *Mar. Ecol. Prog. Ser.* 93, 39–48. doi: 10.3354/meps093039

Brunet, T., and King, N. (2017). The origin of animal multicellularity and cell differentiation. *Dev. Cell* 43, 124–140. doi: 10.1016/j.devcel.2017.09.016

Brussaard, C. P. D., Noordeloos, A. A. M., and Riegman, R. (1997). Autolysis kinetics of the marine diatom *Ditylum brightwellii* (Bacillariophyceae) under nitrogen and phosphorus limitation and starvation. *J. Phycol.* 33, 980–987. doi: 10.1111/j.0022-3646.1997.00980.x

Caldwell, G. S., Olive, P. J., and Bentley, M. G. (2002). Inhibition of embryonic development and fertilization in broadcast spawning marine invertebrates by water soluble diatom extracts and the diatom toxin 2-trans,4-trans decadienal. *Aquat. Toxicol.* 60, 123–137. doi: 10.1016/S0166-445X(01)00277-6

Chen, J., and Thornton, D. C. (2015). Transparent exopolymer particle production and aggregation by a marine planktonic diatom (*Thalassiosira weissflogii*) at different growth rates. *J. Phycol.* 51, 381–393. doi: 10.1111/jpy.12285

Chow, J. S., Lee, C., and Engel, A. (2015). The influence of extracellular polysaccharides, growth rate, and free coccoliths on the coagulation efficiency of *Emiliania huxleyi*. *Mar. Chem.* 175, 5–17. doi: 10.1016/j.marchem.2015.04.010

Crespi, B. J. (2001). The evolution of social behavior in microorganisms. *Trends Ecol. Evol.* 16, 178–183. doi: 10.1016/S0169-5347(01)02115-2

Cunliffe, M., and Murrell, J. C. (2009). The sea-surface microlayer is a gelatinous biofilm. *Isme. J.* 3, 1001–1003. doi: 10.1038/ismej.2009.69

Danial, N. N., and Korsmeyer, S. J. (2004). Cell death: critical control points. *Cell* 116, 205–219. doi: 10.1016/S0092-8674(04)00046-7

Deponte, M. (2008). Programmed cell death in protists. *Biochim Biophys. Acta* 1783, 1396–1405. doi: 10.1016/j.bbamcr.2008.01.018

Driscoll, W. W., and Travisano, M. (2017). Synergistic cooperation promotes multicellular performance and unicellular free-rider persistence. *Nat. Commun.* 8:15707. doi: 10.1038/ncomms15707

Durand, P. M., Choudhury, R., Rashidi, A., and Michod, R. E. (2014). Programmed death in a unicellular organism has species-specific fitness effects. *Biol. Lett.* 10:20131088. doi: 10.1098/rsbl.2013.1088

Durand, P. M., Sym, S., and Michod, R. E. (2016). Programmed cell death and complexity in microbial systems. *Curr. Biol.* 26, R587–593. doi: 10.1016/j.cub.2016.05.057

Dyhrman, S. T., and Palenik, B. (2003). Characterization of ectoenzyme activity and phosphate-regulated proteins in the coccolithophorid *Emiliania huxleyi*. *J. Plankton Res.* 25, 1215–1225. doi: 10.1093/plankt/fbg086

Ferreyra, G. A., Mostajir, B., Schloss, I. R., Chatila, K., Ferrario, M. E., Sargian, P., et al. (2006). Ultraviolet-B radiation effects on the structure and function of lower trophic levels of the marine planktonic food web. *Photochem. Photobiol.* 82, 887–897. doi: 10.1562/2006-02-23-RA-810

Field, C. B., Behrenfeld, M. J., Randerson, J. T., and Falkowski, P. (1998). Primary production of the biosphere: integrating terrestrial and oceanic components. *Science* 281, 237–240. doi: 10.1126/science.281.5374.237

Frada, M. J., Rosenwasser, S., Ben-Dor, S., Shemi, A., Sabanay, H., and Vardi, A. (2017). Morphological switch to a resistant subpopulation in response to viral infection in the bloom-forming coccolithophore *Emiliania huxleyi*. *PLoS Pathog.* 13:e1006775. doi: 10.1371/journal.ppat.1006775

Franklin, D. J., Brussaard, C. P., and Berges, J. A. (2006). What is the role and nature of programmed cell death in phytoplankton ecology? *Eur. J. Phycol.* 41, 1–14. doi: 10.1080/09670260500505433

Glucksmann, A. (1951). Cell deaths in normal vertebrate ontogeny. *Biol. Rev. Camb. Philos. Soc.* 26, 59–86. doi: 10.1111/j.1469-185X.1951.tb00774.x

Godoi, R. H. M., Aerts, K., Harlay, J., Kaegi, R., Ro, C.-U., Chou, L., et al. (2009). Organic surface coating on Coccolithophores - *Emiliania huxleyi*: its determination and implication in the marine carbon cycle. *Microchem. J.* 91, 266–271. doi: 10.1016/j.microc.2008.12.009

Hamburger, V., and Levi-Montalcini, R. (1949). Proliferation, differentiation and degeneration in the spinal ganglia of the chick embryo under normal and experimental conditions. *J. Exp. Zool.* 111, 457–501. doi: 10.1002/jez.1401110308

Hamilton, W. D. (1964). The genetical evolution of social behaviour II. *J. Theor. Biol.* 7, 17–52. doi: 10.1016/0022-5193(64)90039-6

Hamilton, W. D., and Lenton, T. M. (1998). Spora and Gaia: how microbes fly with their clouds. *Ethol. Ecol. Evol.* 10, 1–16. doi: 10.1080/08927014.1998.9522867

Hanschen, E. R., Ferris, P. J., and Michod, R. E. (2014). Early evolution of the genetic basis for soma in the *Volvocaceae*. *Evolution* 68, 2014–2025. doi: 10.1111/evo.12416

Herron, M. D. (2016). Origins of multicellular complexity: volvox and the volvocine algae. *Mol. Ecol.* 25, 1213–1223. doi: 10.1111/mec.13551

Hirsh, D. J., Schieler, B. M., Fomchenko, K. M., Jordan, E. T., and Bidle, K. D. (2016). A liposome-encapsulated spin trap for the detection of nitric oxide. *Free Radic. Biol. Med.* 96, 199–210. doi: 10.1016/j.freeradbiomed.2016.04.026

Holligan, P. M., Viollier, M., Harbour, D. S., Camus, P., and Champagne-Phillippe, M. (1983). Satellite and ship studies of coccolithophore production along a continental shelf edge. *Nature* 304, 339–342. doi: 10.1038/304339a0

Ianora, A., Miralto, A., Poulet, S. A., Carotenuto, Y., Buttino, I., Romano, G., et al. (2004). Aldehyde suppression of copepod recruitment in blooms of a ubiquitous planktonic diatom. *Nature* 429, 403–407. doi: 10.1038/nature02526

Jiménez, C., Capasso, J. M., Edelstein, C. L., Rivard, C. J., Lucia, S., Breusegem, S., et al. (2009). Different ways to die: cell death modes of the unicellular chlorophyte *Dunaliella viridis* exposed to various environmental stresses are mediated by the caspase-like activity DEVDase. *J. Exp. Bot.* 60, 815–828. doi: 10.1093/jxb/ern330

Jones, A. M. (2001). Programmed cell death in development and defense. *Plant Physiol.* 125, 94–97. doi: 10.1104/pp.125.1.94

Kahl, L. A., Vardi, A., and Schofield, O. (2008). Effects of phytoplankton physiology on export flux. *Mar. Ecol. Prog. Ser.* 354, 3–19. doi: 10.3354/meps07333

Kapsetaki, S. E., Tep, A., and West, S. A. (2017). How do algae form multicellular groups? *Evol. Ecol. Res.* 18, 663–675.

Kendall, C., and Caldwell, E. A. (1998). *Isotope Tracers in Catchment Hydrology Place*. Amsterdam: Elsevier Science.

Kerr, J. F., Wyllie, A. H., and Currie, A. R. (1972). Apoptosis: a basic biological phenomenon with wide-ranging implications in tissue kinetics. *Br. J. Cancer* 26, 239–257. doi: 10.1038/bjc.1972.33

King, N. (2004). The unicellular ancestry of animal development. *Dev. Cell* 7, 313–325. doi: 10.1016/j.devcel.2004.08.010

Kirk, D. L. (1999). Evolution of multicellularity in the Volvocine algae. *Curr. Opin. Plant Biol.* 2, 496–501. doi: 10.1016/S1369-5266(99)00019-9

Knoll, A. H. (2011). The multiple origins of complex multicellularity. *Annu. Rev. Earth Planet. Sci.* 39, 217–239. doi: 10.1146/annurev.earth.031208.100209

Koschwanez, J. H., Foster, K. R., and Murray, A. W. (2011). Sucrose utilization in budding yeast as a model for the origin of undifferentiated multicellularity. *PLoS Biol.* 9:e1001122. doi: 10.1371/annotation/0b9bab0d-1d20-46ad-b318-d2229cde0f6f

Lehahn, Y., Koren, I., Schatz, D., Frada, M., Sheyn, U., Boss, E., et al. (2014). Decoupling physical from biological processes to assess the impact of viruses on a mesoscale algal bloom. *Curr. Biol.* 24, 2041–2046. doi: 10.1016/j.cub.2014.07.046

Lockshin, R. A., and Williams, C. M. (1964). Programmed cell death. II. Endocrine potentiation of the breakdown of the intersegmental muscles of silkmoths. *J. Insect Physiol.* 10, 643–649.

Lyons, N. A., and Kolter, R. (2015). On the evolution of bacterial multicellularity. *Curr. Opin. Microbiol.* 24, 21–28. doi: 10.1016/j.mib.2014.12.007

Merchant, S. S., Prochnik, S. E., Vallon, O., Harris, E. H., Karpowicz, S. J., Witman, G. B., et al. (2007). The Chlamydomonas genome reveals the evolution of key animal and plant functions. *Science* 318, 245–250. doi: 10.1126/science.1143609

Milligan, C. E., and Schwartz, L. M. (1996). "Programmed cell death during development of animals," in *Cellular Aging and Cell Death,* eds N. J. Holbrook, G. R. M. Martin, and R. A. Lockshin (New York, NY: Wiley-Liss), 181–208.

Miralto, A., Barone, G., Romano, G., Poulet, S. A., Ianora, A., Russo, G. L., et al. (1999). The insidious effect of diatoms on copepod reproduction. *Nature* 402, 173–176. doi: 10.1038/46023

Nedelcu, A. M., Driscoll, W. W., Durand, P. M., Herron, M. D., and Rashidi, A. (2011). On the paradigm of altruistic suicide in the unicellular world. *Evolution* 65, 3–20. doi: 10.1111/j.1558-5646.2010.01103.x

Nissimov, J. I., and Bidle, K. D. (2017). Stress, death, and the biological glue of sinking matter. *J. Phycol.* 53, 241–244. doi: 10.1111/jpy.12506

Pagani, M. (2002). The alkenone–CO_2 proxy and ancient atmospheric carbon dioxide. *Philos. Trans. A Math. Phys. Eng. Sci.* 360, 609–632. doi: 10.1098/rsta.2001.0959

Passow, U. (2000). Formation of transparent exopolymer particles, TEP, from dissolved precursor material. *Mar. Ecol. Prog. Ser.* 192, 1–11. doi: 10.3354/meps192001

Passow, U. (2002). Transparent exopolymer particles (TEP) in aquatic environments. *Prog. Oceanogr.* 55, 287–333. doi: 10.1016/S0079-6611(02)00138-6

Pohnert, G. (2002). Phospholipase A2 activity triggers the wound-activated chemical defense in the diatom *Thalassiosira rotula*. *Plant Physiol.* 129, 103–111. doi: 10.1104/pp.010974

Prochnik, S. E., Umen, J., Nedelcu, A. M., Hallmann, A., Miller, S. M., Nishii, I., et al. (2010). Genomic analysis of organismal complexity in the multicellular green alga *Volvox carteri*. *Science* 329, 223–226. doi: 10.1126/science.1188800

Ratcliff, W. C., Denison, R. F., Borrello, M., and Travisano, M. (2012). Experimental evolution of multicellularity. *Proc. Natl. Acad. Sci. U.S.A.* 109, 1595–1600. doi: 10.1073/pnas.1115323109

Ratcliff, W. C., Herron, M. D., Howell, K., Pentz, J. T., Rosenzweig, F., and Travisano, M. (2013). Experimental evolution of an alternating uni- and multicellular life cycle in *Chlamydomonas reinhardtii*. *Nat. Commun.* 4:2742. doi: 10.1038/ncomms3742

Rokas, A. (2008). The origins of multicellularity and the early history of the genetic toolkit for animal development. *Annu. Rev. Genet.* 42, 235–251. doi: 10.1146/annurev.genet.42.110807.091513

Rousseaux, S. C., and Gregg, W. W. (2014). Interannual variation in phytoplankton primary production at a global scale. *Remote Sens.* 6, 1–19. doi: 10.3390/rs6010001

Sathe, S., and Durand, P. M. (2016). Cellular aggregation in Chlamydomonas (Chlorophyceae) is chimaeric and depends on traits like cell size and motility. *Eur. J. Phycol.* 51, 129–138. doi: 10.1080/09670262.2015.1107759

Schoemann, V., Becquevort, S., Stefels, J., Rousseau, W., and Lancelot, C. (2005). Phaeocystis blooms in the global ocean and their controlling mechanisms: a review. *J. Sea Res.* 53, 43–66. doi: 10.1016/j.seares.2004.01.008

Schuster, S., and Herndl, G. J. (1995). Formation and significance of transparent exopolymeric particles in the northern adriatic sea. *Mar. Ecol. Prog. Ser.* 124, 227–236. doi: 10.3354/meps124227

Seebah, S., Fairfield, C., Ullrich, M. S., and Passow, U. (2014). Aggregation and sedimentation of *Thalassiosira weissflogii* (diatom) in a warmer and more acidified future ocean. *PLoS ONE* 9:e112379. doi: 10.1371/journal.pone.0112379

Segev, E., Wyche, T. P., Kim, K. H., Petersen, J., Ellebrandt, C., Vlamakis, H., et al. (2016). Dynamic metabolic exchange governs a marine algal-bacterial interaction. *Elife* 5:e17473. doi: 10.7554/eLife.17473

Segovia, M., Haramaty, L., Berges, J. A., and Falkowski, P. G. (2003). Cell death in the unicellular chlorophyte *Dunaliella tertiolecta*. A hypothesis on the evolution of apoptosis in higher plants and metazoans. *Plant Physiol.* 132, 99–105. doi: 10.1104/pp.102.017129

Sieburth, J. M. (1983). "Microbiological and organic–chemical processes in the surface and mixed layers," in *Air–Sea Exchange of Gases and Particles,* eds P. S. Liss and W. G. N. Slinn (Hingham, MA: Reidel Publishers Co.), 121–172.

Sims, P. A., Mann, D. G., and Medlin, L. K. (2006). Evolution of the diatoms: insights from fossil, biological and molecular data. *Phycologia* 45, 361–402. doi: 10.2216/05-22.1

Stoderegger, K. E., and Herndl, G. J. (1999). Production of exopolymer particles by marine bacterioplankton under contrasting turbulence conditions. *Mar. Ecol. Prog. Ser.* 189, 9–16. doi: 10.3354/meps189009

Stoll, H. M., Langer, G., Shimizu, N., and Kanamaru, K. (2012). B/Ca in coccoliths and relationship to calcification vesicle pH and dissolved inorganic carbon concentrations. *Geochim. Cosmochim. Ac.* 80, 143–157. doi: 10.1016/j.gca.2011.12.003

Thornton, D. C. O., and Chen, J. (2017). Exopolymer production as a function of cell permeability and death in a diatom (*Thalassiosira weissflogii*) and a cyanobacterium (*Synechococcus elongatus*). *J. Phycol.* 53, 245–260. doi: 10.1111/jpy.12470

Tyrrell, T., and Merico, A. (2004). "*Emiliania huxleyi*: bloom observations and the conditions that induce them," in *Coccolithophores: From Molecular Processes to Global Impact*, eds H. R. Thierstein and J. R. Young (Berlin; Heidelberg: Springer), 75–97.

Vardi, A. (2008). Cell signaling in marine diatoms. *Commun. Integr. Biol.* 1, 134–136. doi: 10.4161/cib.1.2.6867

Vardi, A., Berman-Frank, I., Rozenberg, T., Hadas, O., Kaplan, A., and Levine, A. (1999). Programmed cell death of the dinoflagellate *Peridinium gatunense* is mediated by CO_2 limitation and oxidative stress. *Curr. Biol.* 9, 1061–1064. doi: 10.1016/S0960-9822(99)80459-X

Vardi, A., Bidle, K. D., Kwityn, C., Hirsh, D. J., Thompson, S. M., Callow, J. A., et al. (2008). A diatom gene regulating nitric-oxide signaling and susceptibility to diatom-derived aldehydes. *Curr. Biol.* 18, 895–899. doi: 10.1016/j.cub.2008.05.037

Vardi, A., Eisenstadt, D., Murik, O., Berman-Frank, I., Zohary, T., Levine, A., et al. (2007). Synchronization of cell death in a dinoflagellate population is mediated by an excreted thiol protease. *Environ. Microbiol.* 9, 360–369. doi: 10.1111/j.1462-2920.2006.01146.x

Vardi, A., Formiggini, F., Casotti, R., De Martino, A., Ribalet, F., Miralto, A., et al. (2006). A stress surveillance system based on calcium and nitric oxide in marine diatoms. *PLoS Biol* 4:e60. doi: 10.1371/journal.pbio.0040060

Vardi, A., Haramaty, L., Van Mooy, B. A., Fredricks, H. F., Kimmance, S. A., Larsen, A., et al. (2012). Host-virus dynamics and subcellular controls of cell fate in a natural coccolithophore population. *Proc. Nat. Acad. Sci. U.S.A.* 109, 19327–19332. doi: 10.1073/pnas.1208895109

Verdugo, P., Alldredge, A. L., Azam, F., Kirchman, D. L., Passow, U., and Santschi, P. H. (2004). The oceanic gel phase: a bridge in the DOM-POM continuum. *Mar. Chem.* 92, 67–85. doi: 10.1016/j.marchem.2004.06.017

Vlamakis, H., Chai, Y., Beauregard, P., Losick, R., and Kolter, R. (2013). Sticking together: building a biofilm the *Bacillus subtilis* way. *Nat. Rev. Microbiol.* 11, 157–168. doi: 10.1038/nrmicro2960

Watnick, P., and Kolter, R. (2000). Biofilm, city of microbes. *J Bacteriol.* 182, 2675–2679. doi: 10.1128/JB.182.10.2675-2679.2000

Whitchurch, C. B., Tolker-Nielsen, T., Ragas, P. C., and Mattick, J. S. (2002). Extracellular DNA required for bacterial biofilm formation. *Science* 295:1487. doi: 10.1126/science.295.5559.1487

Wurl, O., and Holmes, M. (2008). The gelatinous nature of the sea-surface microlayer. *Mar. Chem.* 110, 89–97. doi: 10.1016/j.marchem.2008.02.009

Znachor, P., Visocká, V., Nedoma, J., and Rychtecký, P. (2013). Spatial heterogeneity of diatom silicification and growth in a eutrophic reservoir. *Freshwater Biol.* 58, 1889–1902. doi: 10.1111/fwb.12178

Conflict of Interest Statement: The authors declare that the research was conducted in the absence of any commercial or financial relationships that could be construed as a potential conflict of interest.

frontiers in Marine Science

REVIEW
published: 15 August 2017
doi: 10.3389/fmars.2017.00262

Responses of Coral-Associated Bacterial Communities to Local and Global Stressors

Jamie M. McDevitt-Irwin[1], Julia K. Baum[1], Melissa Garren[2] and Rebecca L. Vega Thurber[3]*

[1] Department of Biology, University of Victoria, Victoria, BC, Canada, [2] School of Natural Sciences, California State University Monterey Bay, Seaside, CA, United States, [3] Department of Microbiology, Oregon State University, Corvallis, OR, United States

The microbial contribution to ecological resilience is still largely overlooked in coral reef ecology. Coral-associated bacteria serve a wide variety of functional roles with reference to the coral host, and thus, the composition of the overall microbiome community can strongly influence coral health and survival. Here, we synthesize the findings of recent studies ($n = 45$) that evaluated the impacts of the top three stressors facing coral reefs (climate change, water pollution and overfishing) on coral microbiome community structure and diversity. Contrary to the species losses that are typical of many ecological communities under stress, here we show that microbial richness tends to be higher rather than lower for stressed corals (i.e., in ~60% of cases), regardless of the stressor. Microbial responses to stress were taxonomically consistent across stressors, with specific taxa typically increasing in abundance (e.g., *Vibrionales*, *Flavobacteriales*, *Rhodobacterales*, *Alteromonadales, Rhizobiales*, *Rhodospirillales,* and *Desulfovibrionales*) and others declining (e.g., *Oceanosprillales*). Emerging evidence also suggests that stress may increase the microbial beta diversity amongst coral colonies, potentially reflecting a reduced ability of the coral host to regulate its microbiome. Moving forward, studies will need to discern the implications of stress-induced shifts in microbiome diversity for the coral hosts and may be able to use microbiome community structure to identify resilient corals. The evidence we present here supports the hypothesis that microbial communities play important roles in ecological resilience, and we encourage a focus on the microbial contributions to resilience for future research.

Keywords: coral, bacteria, global change biology, environmental stress, symbiosis, global warming, pollution, overfishing

OPEN ACCESS

Edited by:
Matthias Wietz, University of Oldenburg, Germany

Reviewed by:
Amy Apprill, Woods Hole Oceanographic Institution, United States
Kathleen M. Morrow, University of New Hampshire, United States

****Correspondence:***
Jamie M. McDevitt-Irwin
jamie.mcirwin@gmail.com

Specialty section:
This article was submitted to Aquatic Microbiology, a section of the journal Frontiers in Marine Science

Received: *07 June 2017*
Accepted: *31 July 2017*
Published: *15 August 2017*

Citation:
McDevitt-Irwin JM, Baum JK, Garren M and Vega Thurber RL (2017) Responses of Coral-Associated Bacterial Communities to Local and Global Stressors. Front. Mar. Sci. 4:262. doi: 10.3389/fmars.2017.00262

INTRODUCTION

Corals are diverse meta-organisms that contain not only the conspicuous dinoflagellate partner *Symbiodinium* but also a microbiome assembled of bacterial, archaeal, viral, and other eukaryotic microorganisms (Rosenberg et al., 2007; Ainsworth et al., 2010; Thompson et al., 2014). Host specific differences in microbiome composition suggest that some bacterial members of the microbiome are mutualistic (Ainsworth et al., 2015); thus, many recent efforts have focused on identifying these bacteria and their specific metabolic roles in coral health (**Table 1**). These abundant coral-associated bacterial communities are distinct (**Box 1**) from the surrounding habitat, containing taxa that drastically differ from free-living seawater microbes (Rohwer et al., 2001; Carlos et al., 2013).

TABLE 1 | Overview of the proposed beneficial roles of different coral-associated bacteria.

Role	Description	Example taxa	References
Metabolism	Provide nitrogen to *Symbiodinium*	*Cyanobacteria* (potentially *Synenochocous* and *Prochlorococcous*)	Lesser et al., 2004
		Cyanobacteria	Lesser et al., 2007
	Provide nitrogen to coral larvae's *Symbiodinium*	*Altermonas* sp. and *Vibrio alginolyticus*	Ceh et al., 2013a
	Provide nitrogen to the coral larvae	*Rhizobiales*	Ceh et al., 2013a; Lema et al., 2014
	Provide nitrogen to *Symbiodinium* and the coral	*Gammaproteobacteria,* specifically *Vibrio* sp.	Olson et al., 2009
		Rhizobiales	Lema et al., 2012
	Provide nitrogen and sulphur to the holobiont	Unknown	Wegley et al., 2007
	Sulphur cycling	*Roseobacter, Spongiobacter, Vibrio, Altermonas*	Raina et al., 2009
	Cycling sulphur, carbon, nitrogen and phosphorous cycling to the holobiont, metal homeostasis, organic remediation, antibiotic resistance, secondary metabolism	Unknown	Zhang et al., 2015
Protection	20% of cultured bacteria had antibiotic activity against other strains and pathogens	*Photobacterium, Halomonas, Exiguobacterium, Bacillus, Altermonas*	Ritchie, 2006
	∼70% of culturable isolates from corals demonstrated inhibition to *Burkholder* agar diffusion assays	*Vibrionales, Alteromonadales* (e.g., *Pseudoaltermonas), Bacteroidetes*	Rypien et al., 2010
	Cultured isolates from corals demonstrated inhibition of four coral pathogens and three fungi	*Bacillus, Pseudomonas*	ElAhwany et al., 2013
	Opportunistic *Proteobacteria* increased when *Actinobacteria* were below ∼2.5% relative abundance	*Actinobacteria*	Zaneveld et al., 2016
	8% of coral commensals inhibited glycosidases (needed for growth) and of catabolic enzymes in a coral pathogen, *Serratia marcescens*	*Exiguobacterium*	Krediet et al., 2012
	Predatory bacteria consume the coral pathogens *Vibrio corallyticus* and *V. harveyii*	*Halobacteriovorax* sp.	Welsh et al., 2016
	Displayed antimicrobial activity against other coral cultured isolates	*Pseudoalteromonas*	Kvennefors et al., 2011
Recruitment	Cultures and filtrates significantly increased larval settlement suggesting an extracellular factor	*Roseivivax* sp. 46E8 (*Alphaproteobacterium*)	Sharp et al., 2015

Aspects of coral biology also influence microbiome structure and function. Similar to humans, compartmentalization of the microbiome generates distinct microbial communities in the coral animal, within the surface mucus layer, tissues, skeleton, and gut (Sweet et al., 2010; Ainsworth et al., 2015; Apprill et al., 2016) and some particularly associated with *Symbiodinium* (Ainsworth et al., 2015). Coral-associated bacteria can be transferred vertically from parent to larva (Sharp et al., 2012) or they can be horizontally acquired from the environment (Apprill et al., 2009; Sharp et al., 2010), including when adult corals release bacteria (e.g., *Altermonas* and *Roseobacter*) as a by-product of broadcast spawning (Ceh et al., 2013b). Although recent research has focused on the role of microbiomes in coral adaptation (Gilbert et al., 2012; Glasl et al., 2016), coral reef management still largely ignores the role of microbial communities, with the exception of *Symbiodinium*, in coral resilience (McClanahan et al., 2012). With rapid advances in DNA sequencing technologies, more studies are able to capture the influence of stressors on the coral microbiome, but no study to date has reviewed these impacts. Here, we conduct a synthesis of the results from 45 relevant studies that evaluated how three key stressors threatening coral reefs (i.e., climate change, water pollution and overfishing) altered coral microbiomes. In addition, we provide hypotheses as to how the microbiome may provide corals with resistance to these stressors.

Overview of the Beneficial Roles That Bacteria Play in Corals

Different coral-associated bacteria are hypothesized to play varying roles in coral health, nutrition and development (**Table 1**). Recent reviews have proposed the term "Beneficial Microorganisms for Corals" (BMC) to define microbial symbionts that maintain coral health (Peixoto et al., 2017), outlined microbiome roles in coral health and resilience (Bourne et al., 2016) and suggested that coral reef microbial communities serve as indicators of environmental stress and coral health (Glasl et al., 2017). Coral-associated microbial communities contribute to carbon cycling (Kimes et al., 2010), sulfur cycling (Wegley et al., 2007; Raina et al., 2009),

BOX 1 | Are coral microbiomes unusually diverse?

Corals are sometimes referred as "highly" diverse meta-organisms. Yet this is a somewhat subjective statement that likely has arisen when coral microbiomes are compared to other well studied mutualistic symbiotic model systems that are highly canalized (Dubilier et al., 2008). It is now well accepted that microorganisms colonize most marine species, yet a systematic comparison among marine organisms is currently lacking. For example, sponge tissues contain between 10 and 1,000 bacterial OTUs (Bourne and Webster, 2013), a species richness value well within the range for corals. A recent assessment of tropical reef algal microbiomes also demonstrate that algae contain even more diverse bacterial communities than corals (Barott et al., 2011). The number of bacterial OTU's in corals can range up to 10^2–10^4 compared to 10^1–10^3 for sponges and 10^2 for *Hydra* (Blackall et al., 2015), although as just discussed these richness estimates vary across species, habitat, and host compartment. With these context dependent numbers, it is thus difficult to say whether corals have a higher richness of microbial taxa than other marine species. For example, turf and CCA each exhibited overall higher numbers of OTUs (18,926 and 9,559) than the three coral species compared (*Acropora hyacinthus, A. rosaria,* and *Porites lutea*) (951, 2,331, 4,018) (Hester et al., 2016). Similarly, algal (i.e., *Dictyota bartayresiana, Halimeda opuntia,* turf algae, and CCA) microbiomes were generally more diverse overall [ranging from 6.22 to 7.82 (Shannon Index)] than those in corals (ranging from 2.84 to 4.51) (Barott et al., 2011). Therefore, more comparisons among coral species and marine meta-organisms are needed to determine if corals or certain coral species actually have highly diverse microbial communities.

Additionally, when comparing the composition and dynamics of the coral microbiome to other marine hosts, it is important to differentiate between stable and sporadic members of the community. It is likely that stable members play more important roles in promoting the health and longevity of the host while transient members might contribute to only the function of the host under explicit environmental conditions or alternatively play negative and antagonistic roles in the system (albeit, stable members could also act as opportunistic pathogens). Stable microbes should exhibit consistent relative abundances in the host vs. the sporadic members who will vary in their prevalence and relative abundance among individuals of the same host (Hester et al., 2016). Sporadic members may opportunistically associate with the coral and not play a beneficial role. In three coral species there was a high number of stable members to sporadic members: *A. hyacinthus* (stable = 902, sporadic = 49), *A. rosaria* (stable = 2,188, sporadic = 143), *P. lutea* (stable = 3,662, sporadic = 356) (Hester et al., 2016).

Another way to evaluate this is to conduct "core" microbiome analysis at various levels of stringency. This prevalence-based metric has been used to infer which members of a coral's microbiome are mutualistic or opportunistic. In an evaluation of the core coral microbiome (i.e., phylotype presence in 30% of the samples), *Acropora granulosa's* core microbiome consisted of 159 out of 1,508 phylotypes, *Leptoseris* spp. 204 out of 1,424, and *Montipora capitata* 350 out of 1,433 (Ainsworth et al., 2015). Importantly, most of these core microbiome members were highly diverse yet found in very low relative abundance compared to the entire community. Thus, it is important to consider rare microbiome members, as these may be the beneficial resident members researchers are interested in. In another longitudinal study from three coral species from South Florida, the core coral mucus microbiome consisted of 13 bacterial orders at a >95% prevalence score (Zaneveld et al., 2016). In this case, the "core" microbiome highly depends on the level of stringency used.

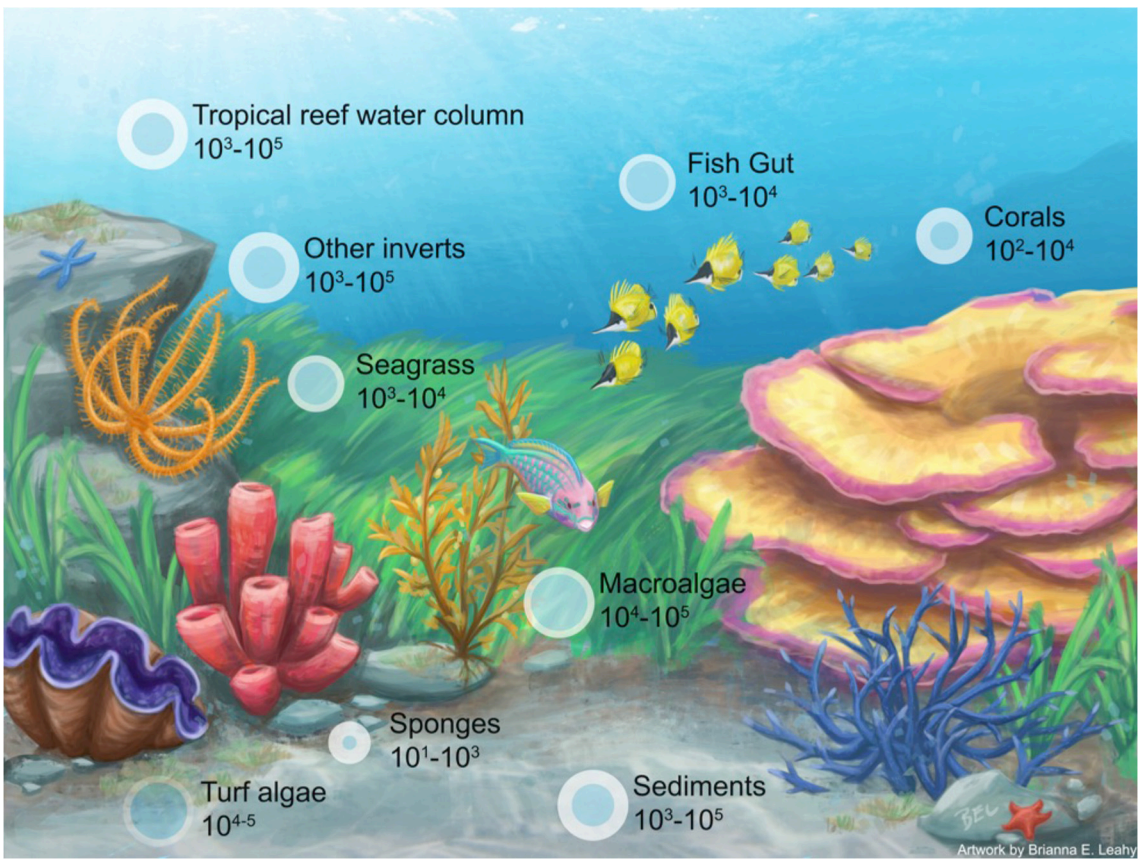

BOX FIGURE 1 | Depiction of a coral reef and associated microbiomes with organismal hosts [i.e., invertebrates (Bourne et al., 2013; Tianero et al., 2014; Hakim et al., 2016), seagrass (Ettinger et al., 2017; Fahimipour et al., 2017), fish (Ghanbari et al., 2015; Givens et al., 2015; Parris et al., 2016), corals (Barott et al., 2011; Blackall et al., 2015; Hester et al., 2016), macroalgae (Barott et al., 2011; Burke et al., 2011; Egan et al., 2013; Brodie et al., 2016), sponges (Bourne and Webster, 2013; Blackall et al., 2015), turf algae (Hester et al., 2016)] and environmental parameters [i.e., reef water (McCliment et al., 2012), sediment (Ettinger et al., 2017)]. The size of the bubble indicates a more species rich microbiome (based on OTUs).

phosphorous fixation, metal homeostasis, organic remediation (Zhang et al., 2015), production of antibiotics (Ritchie, 2006) and secondary metabolism (Zhang et al., 2015). For example, diazotrophs (i.e., nitrogen-fixing microbes) form species-specific associations with corals and may provide limiting fixed nitrogen to the algal partner of corals, *Symbiodinium,* and to the coral animal itself (Lesser et al., 2004, 2007; Lema et al., 2012). In the early coral life stages, bacteria provide nitrogen directly to larvae's *Symbiodinium* (Ceh et al., 2013a) and potentially to the coral larvae (Lema et al., 2014). Bacteria also play an important role in larval recruitment and settlement, for example, *Alphaproteobacterium*, *Roseivivax* sp. 46E8 significantly increases larval settlement of *Porites astreoides* (Sharp et al., 2015).

Many coral-associated bacteria defend the coral by exuding antimicrobial compounds to prevent invasions by pathogens or other exogenous bacteria (**Table 1**). For example, nearly 70% of cultivable isolates from *Montastrea annularis* inhibited the growth of other bacteria and 11.6% inhibited the growth of the known coral pathogen, *Vibrio shiloi* (Rypien et al., 2010). Approximately 20% of cultivable isolates from *Acropora palmata* demonstrated antibiotic activity against other strains and pathogens (Ritchie, 2006). Isolates from a soft coral, *Sarcophyton glaucum*, inhibited the growth of four coral pathogens and three fungi (ElAhwany et al., 2013). It was also found that under increased algal cover and temperatures, the relative abundances of *Actinobacteria* decreased while opportunistic *Proteobacteria* increased within the coral microbiome, suggesting that opportunists can take advantage of the absence of inhibition (Zaneveld et al., 2016). Eight percent of native coral bacteria inhibited the growth of the pathogen *Serratia marcescens*, with *Exiguobacterium* sp. inducing 10–100 fold reductions in growth within coral mucus (Krediet et al., 2012). Concurrently, the coral pathogen, *Vibrio corallilyticus*, has antimicrobial activity of its own, suggesting that it may use inhibition to colonize the coral (Kvennefors et al., 2011). There are also some resident bacteria that actively predate upon these pathogens within the coral mucus (Welsh et al., 2016). In summary, given the wide variety of roles vital to holobiont functioning that are played by coral-associated bacteria, any disruption or destabilization may influence host fitness and ecosystem functioning.

RESPONSES OF THE CORAL MICROBIOME TO STRESSORS THREATENING CORAL REEFS

Overview of Papers Synthesized

Here, we synthesized 45 relevant studies that each (1) were peer-reviewed (2) examined coral-associated bacteria and (3) measured how these bacteria were affected by climate change, water pollution or overfishing (**Table 2**). We included a broad range of methodologies as many researchers use different methods and we aimed to evaluate the field from a broad perspective. Over half of the studies focused on climate change ($n = 27$) and almost one quarter focused on water pollution ($n = 10$); only a small proportion addressed overfishing ($n = 4$) or more than one stressor at a time ($n = 4$) (**Figure 1**). The majority of the studies were published in the last 5 years (**Figure 1**). Geographically, almost all of the overfishing and water pollution studies occurred in the Caribbean compared with studies on climate change, which had a more global distribution of study sites (**Figure 1**).

The genera *Acropora* and *Porites* were the most represented corals within these studies, accounting for nearly 50% of all corals evaluated (**Figure 2A**). Massive *Porites* species may be "stress-tolerant" corals, as they are slow growing and may be able to survive harsher environments (Darling et al., 2012). *Acroporids* are considered "competitive" corals, meaning that they are fast-growing and dominate reefs in productive environments; they are also the most sensitive to environmental change (Darling et al., 2012). As a result, there was a bias toward studying climate change on competitive life history strategies, specifically *Acropora* in Australia (**Figure 2B**).

We note here that we report bacterial taxa at the levels of Phylum, Class and Order to provide consistency across the array of studies given that many of them reported their data in different ways and to different taxonomic levels. Additionally, researchers used varying metrics of community structure to evaluate the impact of stressors including: richness (i.e., total number of species), alpha diversity (i.e., the total number of species and their relative abundances, generally the Shannon and Simpson Index), evenness (i.e., distribution of species relative abundances) and beta diversity (i.e., difference in community composition).

Stressors Tend to Increase Coral Microbiome Richness/Alpha Diversity

While a consequence of human impacts on macro-scale communities is often species loss, the emerging evidence from our analysis suggests that similar impacts more commonly lead to an increase in bacterial richness or alpha diversity within coral-associated microbial communities (∼60% of the time, **Table 3**). Invasion is likely the mechanism underlying these increases, with stress events appearing to disrupt the functioning microbiome and facilitating an invasion of microbes not typically resident on corals, thus increasing the overall number of microbiome members (Welsh et al., 2015). For example, corals closer to human disturbance have been shown to harbor higher bacterial diversity than those farther from the disturbance (Morrow et al., 2012a). Similarly, corals in lowered pH had higher microbial diversity (Meron et al., 2011) and microbial diversity increased in overfishing and eutrophication treatments (Jessen et al., 2013). Lastly, it was found that upon algal contact, the coral microbiome increased in species richness (Zaneveld et al., 2016). These results also are contrary to the patterns found in the human gut microbiome, in which stress lowers microbial alpha diversity by allowing opportunistic and pathogenic taxa to dominate the community (Lozupone et al., 2012). This might be explained by the nature of the human gut microbiome being a more closed system compared with corals that are constantly bathed in the distinct microbial assemblages of seawater. We hypothesize that when corals are disturbed, their ability to regulate and/or exclude

TABLE 2 | Overview of the 45 papers that evaluated the influence of climate change, water pollution and overfishing on the coral microbiome, coral species evaluated, the method they used to capture effects on the microbial community (e.g., DGGE, denaturing gradient gel electrophoresis; TRFLP, terminal restriction fragment length polymorphism; PFGE, pulsed-field gel electrophoresis), and whether the paper had data that we included on changes in bacterial taxa (i.e., **Figure 3**) or microbial diversity (i.e., **Table 3**).

Author	Coral Species	Microbial community assessment method	Taxa changes?	Microbial diversity?
CLIMATE CHANGE				
Littman et al., 2010	*Acropora tenuis*	DGGE of 16S	y	n
Littman et al., 2011	*Acropora millepora*	Metagenomics	y	n
Salerno et al., 2011	*Porites compressa*	TRFLP of 16S	y	n
Meron et al., 2011	*Acropora eurystoma*	16S rRNA clones, DGGE of 16S	y	y
Webster et al., 2012	*Acropora millepora*	DGGE of 16S	y	n
Frydenborg et al., 2013	*Acropora palmata*	Culturing	y	n
Santos et al., 2014	*Mussismilia harttii*	DGGE of 16S, qPCR	y	y
Morrow et al., 2015	*Acropora millepora, Porites cylindrica*	454 16S rRNA amplicons	y	y
Tout et al., 2015	*Pocillopora damicornis*	454 16S rRNA amplicons, qPCR	y	y
Webster et al., 2016	*Acropora millepora, Seriatopora hystrix*	454 16S rRNA amplicons	y	n
Lee et al., 2016	*Acropora muricata*	454 16S rRNA amplicons	y	y
Tracy et al., 2015	*Gorgonia ventalina, Orbicella faveolata*	454 16S rRNA amplicons	y	y
Meron et al., 2012	*Balanophyllia europaea, Cladocora caespitosa*	16S rRNA clones	y	y
Banin et al., 2003	*Oculina patagonica*	Culturing	n	n
Ben-Haim et al., 2003	*Pocillopora damicornis*	Culturing	n	n
Ainsworth and Hoegh-Guldberg, 2009	*Acropora aspera, Stylophora pistillata*	FISH Microscopy	n	n
Bourne et al., 2007	*Acropora millepora*	RFLP of 16S, DGGE of 16S, colony blotting	y	y
Kushmaro et al., 1998	*Oculina patagonica*	Culturing	y	n
Ritchie, 2006	*Acropora palmata*	Culturing, 16S rRNA clones	y	n
Ben-Haim and Rosenburg, 2002	*Pocillopora damicornis, Acropora formasa, Acropora* sp., *Cycloseries* sp., *Fungiidae*	Culturing, 16S rRNA clones	n	n
Koren and Rosenberg, 2006	*Oculina patagonica*	16S rRNA clones	n	n
Koren and Rosenberg, 2008	*Oculina patagonica*	Culturing, 16S rRNA clones	n	n
Cardini et al., 2016	*Acropora hemprichii, Stylophora pistillata*	Measured microbial N_2 fixation	n	n
Ziegler et al., 2017	*Acropora hyacinthus*	Illumina 16S rRNA amplicons	y	n
Lee et al., 2017	*Acropora muricata*	Illumina 16S rRNA amplicons	y	n
Hadaidi et al., 2017	*Porites lobata*	Illumina 16S rRNA amplicons, qPCR	n	n
Gajigan et al., 2017	*Acropora digitifera*	Illumina 16S rRNA amplicons	y	y
CLIMATE CHANGE AND WATER POLLUTION				
Vega Thurber et al., 2009	*Porites compressa*	Metagenomics	y	n
Welsh et al., 2016	*Agaricia* sp., *Porites* sp., *Siderastraea siderea*	454 16S rRNA amplicons, culturing, microscopy, predation assays	n	n
WATER POLLUTION				
Sutherland et al., 2010	*Acropora palmata, Siderastrea siderea, Solenastrea bournoni*	PFGE of 16S	n	n
Looney et al., 2010	*Acropora palmata, Montastraea faveolata, Siderastrea siderea*	Culturing	n	n
Morrow et al., 2012a	*Montastraea faveolata, Porites astreoides*	DGGE of 16S, 454 16S rRNA amplicons	y	y
Röthig et al., 2016	*Fungia granulosa*	Illumina 16S rRNA amplicons	y	y
Kline et al., 2006	*Montastraea annularis*	Culturing	n	n
Klaus et al., 2007	*Montastraea annularis*	TRFLP of 16S	n	n
Garren et al., 2009	*Porites cylindrica*	16S rRNA clones, DGGE of 16S	n	n
Ziegler et al., 2016	*Pocillopora verrucosa, Acropora hemprichii*	Illumina 16S rRNA amplicons	y	y
Mitchell and Chet, 1975	*Platygyra*	Culturing	n	n
Al-Dahash and Mahmoud, 2013	*Porites compressa, Acropora clathrata*	DGGE of 16S, culturing	y	y
WATER POLLUTION AND OVERFISHING				
Jessen et al., 2013	*Acropora hemprichii*	454 16S rRNA amplicons	y	n

(Continued)

TABLE 2 | Continued

Author	Coral Species	Microbial community assessment method	Taxa changes?	Microbial diversity?
OVERFISHING				
Vega Thurber et al., 2012	*Porites astreoides*	TRFLP of 16S	y	y
Barott et al., 2012	*Montastraea annularis*	454 16S rRNA amplicons	y	y
Morrow et al., 2013	*Montastraea faveolata, Porites astreoides*	DGGE of 16S	n	n
Morrow et al., 2017	*Porites cylindrica*	Illumina 16S rRNA amplicons, culturing	y	y
OVERFISHING, WATER POLLUTION AND CLIMATE CHANGE				
Zaneveld et al., 2016	*Siderastrea siderea, Porites* sp., *Agaricia* sp.	454 16S rRNA amplicons	y	y

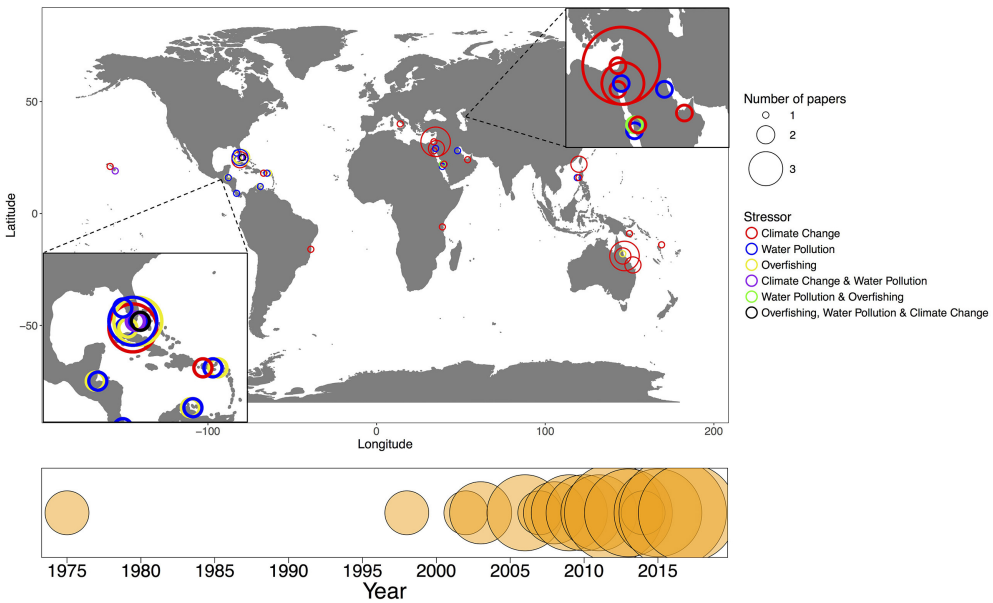

FIGURE 1 | A world map of studies evaluating the impact of stressors on the coral microbiome, climate change (red), water pollution (blue), overfishing (yellow), climate change and water pollution (purple), water pollution and overfishing (green), and overfishing, water pollution and climate change (black). The size of the bubble refers to the number of papers at that latitude/longitude. The timeline on the bottom represents the number of papers published each year from 1975 to 2017 that were included in the synthesis.

incoming microbial taxa from the surrounding environment may be reduced. However, this is not always the case, as other studies have demonstrated no significant change or a decrease in microbial diversity under these three stressors (Meron et al., 2012; Tracy et al., 2015; Morrow et al., 2017). These conflicting results likely are the result of variability in coral microbiome responses across coral host species, locations and stressors. Additionally, these diversity changes may reflect differences in experimental design.

Stressors Decrease the Stability and Increase Beta Diversity of Microbiome Community Structure

In addition to increased richness, there is mounting evidence that stressors induce changes to coral microbiome evenness and beta diversity. Changes in evenness indicates shifts in microbial species dominance, and evenness has been found to decrease in the rhizosphere with added disturbance (van der Voort et al., 2016). An increase in beta diversity in response to stress may indicate a destabilized microbiome in mammals (Moeller et al., 2013; Zaneveld et al., 2017) with the host being unable to regulate its microbiome. In corals, both temperature extremes and contact with macroalgae were shown to increase microbiome beta diversity (Zaneveld et al., 2016). Similarly, microbiome composition in shallow polluted sites was more variable from coral to coral than at the control sites (Klaus et al., 2007). Changes in salinity also impacted community evenness. For example it was found that the microbiome of hypersaline-treated corals shifted from a community dominated by a single OTU (*Rhodobacteraceae*) to a more even one in which *Pseudomonas veronii* was the most abundant taxon (Röthig et al., 2016).

Overfishing on reefs can lead to reduced grazing pressure, by decreasing herbivorous fish abundance, and increasing competition between corals and macroalgae for space (Morrow et al., 2013). Macroalgae are hypothesized to outcompete

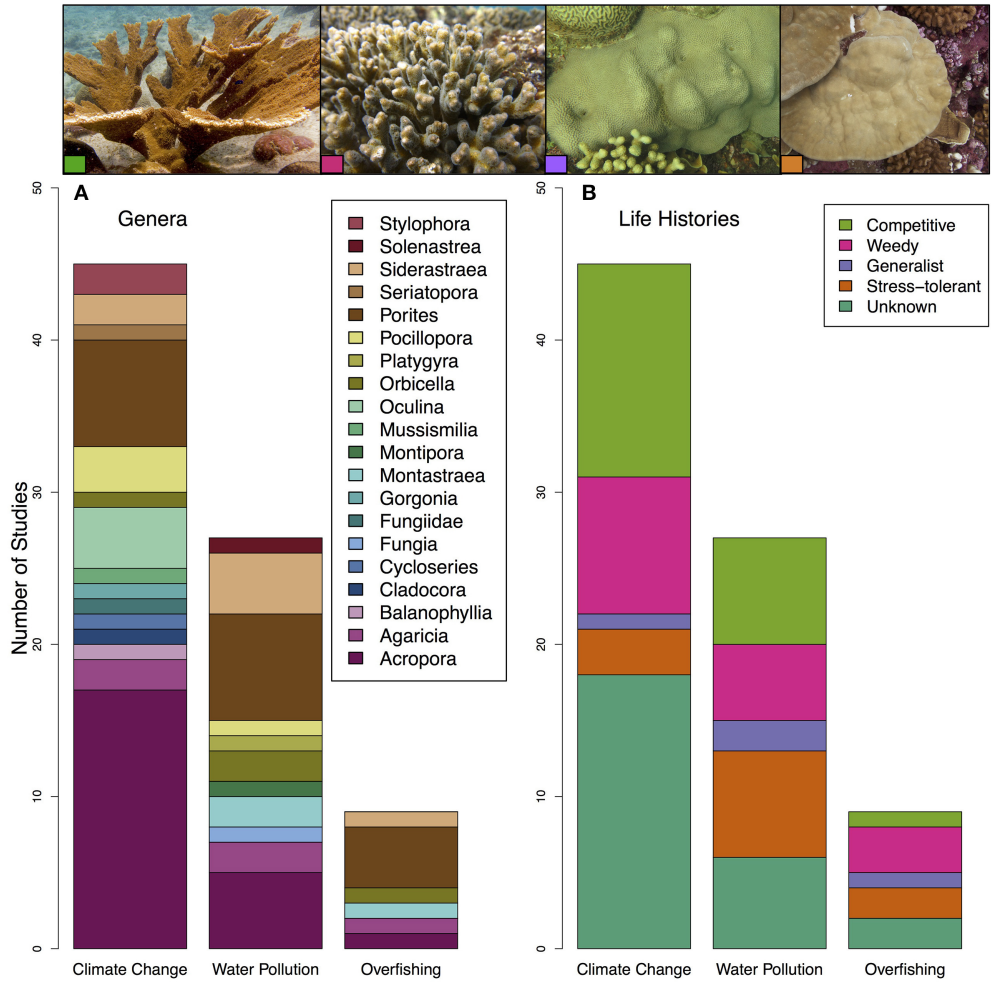

FIGURE 2 | Plot of **(A)** coral genera and **(B)** coral life-histories included in all studies on the impact of climate change, water pollution and overfishing on the coral microbiome. Coral life-histories are taken from Darling et al. (2012). Pictures on the top correspond to coral species and life history strategies included in these papers left to right: *Acropora palmata* (competitive) (photo by Ryan McMinds, Global Coral Microbiome Project, licensed under CC BY 2.0), *Pocillopora damicornis* (weedy) (photo by Joseph Pollock, Global Coral Microbiome Project, licensed under CC BY 2.0), *Orbicella faveolata* (generalist) (photo by Joseph Pollock, Global Coral Microbiome Project, licensed under CC BY 2.0), and *Porites lobata* (stress tolerant) (photo by Kristina Tietjen).

corals via a variety of mechanisms including alterations to the microbiome (Smith et al., 2006; Morrow et al., 2012b), faster growth rates, shading, allelopathic interactions (Rasher and Hay, 2010), and abrasion and preventing coral recruitment (Jompa and McCook, 2003). For example, macroalgal contact with the coral *Porites astreoides* caused multiple changes in the coral microbiome including increased dispersion (i.e., beta diversity), disappearance of a potentially mutualistic *Gammaproteobacteria,* changes in abundance for taxa already present, establishment of new taxa, and growth of algae-associated microbes within the coral (Vega Thurber et al., 2012). Macroalgal contact has also been shown to shift the coral microbiome to become more similar to the macroalgal microbiome (Morrow et al., 2013).

A counter example to the overall trend of stress-induced community shifts is provided by a study on *A. millepora* and *Seriatopora hystrix* microbiomes, which demonstrated stability in microbiome composition in the face of both lowered pH and increased temperatures. While *S. hystrix*'s microbiome did show some variability, the overarching conclusion was that corals demonstrated a more stable and robust microbiome compared to other key calcifying reef taxa such as foraminifera and crustose coralline algae (Webster et al., 2016).

Stressors Decrease the Abundance of the Proposed Bacterial Symbiont, Endozoicomonas

The studies we synthesized consistently found that the bacterial order, *Oceanospirillales,* especially the genus *Endozoicomonas,* was underrepresented in corals during stress events, particularly during climate anomalies (**Figure 3**). This may be problematic for corals as *Endozoicomonas* is a proposed beneficial symbiont to corals. Two studies used CARD-FISH and FISH probes, respectively, to reveal that *Endozoicomonas* was located deep

TABLE 3 | Changes in microbiome alpha diversity or richness due to stress from climate change, water pollution and overfishing (+, higher diversity; −, lower diversity; 0, no difference).

Stressor	Summary of findings	Coral species	Lab or field?	Overall	References
CLIMATE CHANGE					
Thermal Stress	Higher diversity (Shannon) within a coral colony during bleaching compared to pre- and post-bleaching	*Acropora millepora*	Field	+	Bourne et al., 2007
	Diazotroph diversity (Chao1, Shannon) and richness significantly increased 3-fold with +2.5° and +4°C increases	*Mussismilia harttii*	Lab	+	Santos et al., 2014
	Diversity (Chao1) was significantly higher under heat stress (31°C)	*Pocillopora damicornis*	Lab	+	Tout et al., 2015
	G. ventalina microbial diversity (Shannon) was significantly lower during the warming event comparing to pre-warming, *O. faveolata* was not significantly different to pre-warming	*Gorgonia ventalina, Orbicella faveolata*	Field	−0	Tracy et al., 2015
	Richness and diversity (Chao1, Simpson) increased with increasing temperatures	*Acropora muricata*	Lab	+	Lee et al., 2016
	Alpha diversity (Chao1, Inverse Simpson) decreased but richness stayed the same (32°C)	*Acropora digitifera*	Lab	−0	Gajigan et al., 2017
Ocean Acidification	Increase in alpha diversity (Shannon) at lower pH	*Acropora eurystoma*	Lab	+	Meron et al., 2011
	No significant changes except alpha diversity (Shannon) significantly decreased in *C. caespitosa* skeleton	*Cladocora caespitose, Balanophyllia europaea*	Field	− 0,0,0	Meron et al., 2012
	P. cylindrica had lower alpha diversity (Shannon, Chao1) at low pH while *A. millepora* showed no significant change	*Porites cylindrica, Acropora millepora*	Lab	−,0	Morrow et al., 2015
WATER POLLUTION					
Proximity to Humans	*P. astreoides* and *M. faveolata* had higher diversity (Shannon) at sites closer to shore (i.e., < 5km)	*Porites astreoides, Montastrea faveolata*	Field	+,+	Morrow et al., 2012a
	Alpha diversity (Chao1, Shannon, Simpson) and richness in *A. hemprichii* was significantly higher at sites impacted by sedimentation and sewage, *P. verrucosa* showed no significant difference. Both showed no significant difference at wastewater outfall	*Acropora hemprichii, Pocillopora verrucosa*	Field	+,0,0,0	Ziegler et al., 2016
High Salinity	Corals within the long-term salinity treatment increased in microbial diversity 3-fold (Chao1) and 10-fold (Inverse Simpson)	*Fungia granulosa*	Lab	+	Röthig et al., 2016
Oil Pollution	The number of bands increased after microcosm experiments exposed corals to 1 ml and 20 ul of crude oil	*Porites compressa, Acropora clathrata*	Field	+	Al-Dahash and Mahmoud, 2013
WATER POLLUTION AND OVERFISHING					
Eutrophication and Herbivore Exclusion	Diversity (Inverse Simpson, Chao1) increased over time in all stress treatments: herbivore exclusion, nutrient enrichment and herbivore exclusion * nutrient enrichment	*Acropora hemprichii*	Field	+,+,+	Jessen et al., 2013
OVERFISHING					
Macroalgae Contact	Richness increased next to all algae, and Chao1 was significantly higher in all treatments (i.e., corals touching *Dictyota menstrualis*, *Galaxuara obtusata, Halimeda tuna*, *Lobophora variegata, Sargassum polyceratium*)	*Porites astreoides*	Field	+,+,+,+,+	Vega Thurber et al., 2012
	Diversity (Shannon) increased next to CCA and *Dictyota bartayresiana*; Decreased next to *Halimeda opuntia* and turf algae	*Montastraea annularis*	Field	+, +, −, −	Barott et al., 2012

(Continued)

TABLE 3 | Continued

Stressor	Summary of findings	Coral species	Lab or field?	Overall	References
	Diversity (Shannon) was lower but not significantly different in coral fragments exposed to extracts from *Lobophora* sp.	*Porites cylindrica*	Lab	0	Morrow et al., 2017
OVERFISHING, POLLUTION, CLIMATE CHANGE					
Thermal Stress, Nutrients, Macroalgae Contact	Richness increased next to algae	*Siderastrea siderea, Porites* sp., *Agaricia* sp.	Field	+	Zaneveld et al., 2016

within the coral tissues, suggesting an intimate association with coral hosts (Bayer et al., 2013; Neave et al., 2016). Additionally, the first cultivable *Endozoicomonas* from corals suggests *Endozoicomonas montiporae* CL-33 helps corals under stress through preventing mitochondrial dysfunction and promoting gluconeogenesis (Ding et al., 2016). Additionally, researchers have proposed that *Endozoicomonas* plays a role in sulfur cycling (Raina et al., 2009), nutritional symbiosis (La Rivière et al., 2013) and protecting *Symbiodinium* from bleaching pathogens (Pantos et al., 2015). By comparing cultured and culture-independent genomes of Endozoicimonas, researchers demonstrated that *Endozoicimonas* likely plays a role in protein and carbohydrate transport for the host and may have diversified and adapted with their hosts (Neave et al., 2017). However, they also demonstrated that *Endozoicimonas* has a large genome, suggesting it has a free-living stage. Not only might the observed decrease in these potentially symbiotic taxa during stress events threaten coral resistance to stress, it also may influence coral resilience after the stress is alleviated if *Endozoicomonas* does not return to its original abundance and function. In a study of volcanic CO_2 seeps where the seawater has naturally reduced pH, researchers found that *Acropora millepora* and *Porites cylindrica* contained significantly different microbial communities compared to the same coral species at a control site (>500 m away); for *A. millepora* this was mainly due to a 50% decrease of this proposed mutualist *Endozoicomonas* (Morrow et al., 2015). These coral species were also less abundant at the volcanic seeps, potentially due to this loss of symbiont in their microbiomes. In a separate study, *Endozoicomonas* was significantly reduced at low pH in *A. millepora* showing that this stressor can cause loss of these symbionts (Webster et al., 2016). Other symbiotic taxa in addition to *Endozoicomonas* are likely to decline as well under stress. At anthropogenic impacted reefs (i.e., close to metropolitan cities), the main coral symbiotic taxon in *Pocillopora verrucosa* (*Endozoicomonaceae*) and *A. hemprichii* (*Alteromonadales*) declined in relative abundance (Ziegler et al., 2016).

Stressors Increase Opportunistic and Pathogenic Bacterial Taxa in the Coral Microbiome

Stressed corals may have a reduced ability to regulate their microbiomes and thus have reciprocal increases in potentially pathogenic and opportunistic microbial taxa (**Figure 3**). The overrepresented taxa during all three types of stressor we evaluated were: *Vibrionales*, *Flavobacteriales*, *Rhodobacterales*, *Alteromonadales*, *Rhizobiales*, *Rhodospirillales,* and *Desulfovibrionales* (**Figure 3**). The Order *Rhodobacterales,* for example, are fast growing opportunistic bacteria (Teeling et al., 2012) that have been found in both healthy and stressed corals (Meron et al., 2011; Sharp et al., 2012), potentially blooming under periods of stress when there is open niche space (Welsh et al., 2015). OTUs within the Order *Flavobacteriales* were shown to make up a large percentage of white band disease associated OTUs (Gignoux-Wolfsohn and Vollmer, 2015). Thus, these potentially pathogenic, opportunistic taxa may flourish when the coral is stressed and cannot regulate its microbiome.

In comparison, a meta-analysis of 16S sequences from 32 papers, showed that the microbiome of bleached corals differed from that of healthy corals primarily in having a higher proportion of two specific taxa: *Vibrios* and *Acidobacterias* (Mouchka et al., 2010). An increase in *Vibrionales* under climate change stress is unsurprising as the cultivable *Vibrio* strain AK-1 was shown to induce coral bleaching (Kushmaro et al., 1998) (albeit the coral, *Oculina patagonica,* may have developed resistance to this bacteria; Mills et al., 2013) and *Vibronales* are a common taxa to increase under conditions of thermal stress (Bourne et al., 2007; Frydenborg et al., 2013; Tout et al., 2015). Importantly, the coral microbiome may have a temperature tolerance threshold, as it was found that bacterial community structure only changes after an elevation of temperature greater than 1°C; all exposures at temperatures lower than this threshold showed no evidence of community alterations (Salerno et al., 2011). Thus, coral microbiomes may buffer thermal anomalies within that lower temperature range.

Bleached corals also exhibit different bacterial communities than "healthy" corals (Koren and Rosenberg, 2008). For example, during a bleaching event in Australia, the coral microbiome showed an increase in genes associated with virulence factors (Littman et al., 2011). Correspondingly, during heat stress experiments, the known pathogen *V. coralliilyticus* increased in abundance by four orders of magnitude (Tout et al., 2015). One likely mechanism for these observed changes are strong competition between native commensals and pathogenic bacteria (i.e., *V. shiloi* and *V. coralliilyticus*) on corals, with temperature stress mediating the growth of the foreigners. This has been supported by work within *Acropora palmata*, where high temperatures tend to select for pathogens in the coral microbiome (Frydenborg et al., 2013). Increased temperatures also correlated with increased expression of virulence genes (Banin et al., 2003), lysis of coral cells (Ben-Haim et al., 2003),

FIGURE 3 | Summary of the number of papers showing differences in bacterial taxa during stress events (climate change, water pollution or overfishing). The size of the bubble indicates the number of papers (although, some papers found both an increase and decrease in the taxonomic level (i.e., class or family) if a lower level was evaluated (i.e., genus or OTU) so the bubble size may be larger than the actual number of papers as both of these changes were plotted) and the color of the bubble shows the percent of papers that showed that taxa overrepresented under stress (red) or underrepresented under stress (blue). Bacteria were only plotted if they were represented by a paper in each of the three stressors.

and infection (Kushmaro et al., 1998; Ben-Haim and Rosenburg, 2002) by coral pathogenic bacteria. However, *Porites lobata* has been found to have a relatively stable microbiome between bleached and healthy colonies, suggesting its mucus microbiome plays a protective role within bleached corals (Hadaidi et al., 2017).

Furthermore, increased *Vibrio* and other taxa occur prior to visual bleaching signs (Bourne et al., 2007; Lee et al., 2016), suggesting some predictable changes in the bacterial community could forewarn which corals may bleach. The abundance of Vibrionales within the microbiome may also be regulated by factors other than temperature, including what strain of *Symbiodinium* is hosted by the coral (Littman et al., 2010).

Importantly, the increases in potentially pathogenic or opportunistic taxa found in our analysis (**Figure 3**) may be due to a variety of mechanisms such as the induction of temperature sensitive virulence cassettes found in pathogens, enhanced growth rates under higher temperatures, or altered microbial-host signals during stress. Thermally stressed corals often increase production of the metabolites like dimethylsulphoniopropionate (DMSP), which is normally exuded by corals (Raina et al., 2013) and their symbionts (Steinke et al., 2011). It is hypothesized that DMSP is used as a chemoattractant by bacterial pathogens to locate thermally stressed corals (Garren et al., 2014).

While in most cases stressors altered coral microbial community structure, shifts do not always occur. For example, *O. faveolata*'s microbiome did not significantly shift when the host bleached (Tracy et al., 2015). Furthermore, coral-associated microbial communities did not undergo major shifts when transplanted to a natural lower pH environment and did not harbor microbial pathogens (Meron et al., 2012). This study (Meron et al., 2012), suggests that for these two coral species (i.e., *Balanophyllia europaea* and *Cladocora caespitosa*), reduced pH does not pose a significant threat to coral health. Importantly, environmental conditions can buffer these microbiome changes, specifically with high water flow buffering coral microbiome changes under high temperatures (Lee et al., 2017).

Climate Change, Water Pollution and Overfishing Increase Disease Associated Bacteria

In addition to community structure changes, stressors can also increase disease on coral reefs (Brandt et al., 2013; Vega Thurber et al., 2013). For example, exposure of corals to lower pH resulted in microbiome communities reminiscent of those associated with diseased and stressed corals as they contained more *Vibrionaceae* and *Altermonadaceae* (Vega Thurber et al., 2009; Meron et al., 2011). Additionally, reduced pH significantly changed the microbial communities in *A. millepora* with the loss of *Proteobacteria* sequences typically associated with healthy corals while *Gammaproteobacteria*, which are often associated with diseased and stressed corals, increased (Webster et al., 2012).

Given that coral reefs occur in oligotrophic environments, added nutrients can dramatically influence ecosystem functioning and alter microbial communities in ways that appear to favor disease. In Florida, human sewage supplied a strain of *Serratia marcescens* (a common fecal enterobacterium) into reef water and corallivorous snails acted as a vector, therefore inducing white-pox like diseases in *Acropora palmata*, *Siderastrea siderea,* and *Solenastrea bournoni* (Sutherland et al., 2010). Furthermore, the addition of glucose or inorganic nutrients improved the survival of *S. marcescens* in *A. palmata* (Looney et al., 2010). Under this water pollution stress, as with thermal stress (Littman et al., 2011), the microbial communities shifted toward a higher prevalence of heterotrophic bacteria relative to autotrophic bacteria (Dinsdale et al., 2008). Microbiome taxa in polluted sites can be more pathogenic, as demonstrated by a study in which exposure to pollutants increased coral mortality except when antibiotics were added, suggesting a bacterially mediated cause of death (Mitchell and Chet, 1975). As the proximity and size of human populations increases adjacent to coral reefs, so does the likelihood of land-based runoff, and evidence continues to demonstrate that corals living closer to shore have higher abundances of disease-related bacteria (Morrow et al., 2012a), and coral disease correlates with poor water quality and high nutrient levels (Furby et al., 2014). Nevertheless, the coral microbiome also demonstrates resilience against water pollution, when coral fragments were transplanted under eutrophic aquaculture pens, the coral microbiome shifted toward known pathogens but then showed no physical signs of disease and after 22 days the communities shifted back to their original state (Garren et al., 2009).

Overfishing may alter coral microbiomes indirectly, with decreases in herbivorous fish populations being one means by which algal growth can be facilitated at the expense of corals. For example, overfishing in Jamaica, in concert with warming and hurricanes, caused coral cover to decrease from 50 to 5% and an increase to 90% macroalgae cover (Hughes, 1994). Shifts to an algae dominated state can influence the coral microbiome by changing the water column microbial composition, increasing algal interactions (Morrow et al., 2013) and triggering coral disease (Nugues et al., 2004). Increased coral interactions with turf algae have been associated with an increase in pathogens and virulence genes (Barott et al., 2011). These authors also proposed that fleshy algae can alter reefs by increasing both bacterial respiration and pathogenic invasion (Barott et al., 2012). Moreover, algae may act as reservoirs for coral pathogens (Sweet et al., 2013) and thus enhance disease events. Algae harbor distinctly different microbial communities than corals (Barott et al., 2011; Vega Thurber et al., 2012) and produce more carbon exudate that can stimulate heterotrophic microbial growth in reef waters (Haas et al., 2011). Algae also produce dissolved organic matter (DOM) that is enriched in dissolved neutral sugars (DNS). These sugars can spur the growth of fast-growing bacteria in the water column, the result of which is a community with less bacterial diversity and dominated by copiotrophic bacteria like *Vibrionaceae* and *Pseudoaltermonadaceae* that typically carry virulence factors (Nelson et al., 2013). Conversely, corals exude DOM that selects for high bacterial diversity in the water column dominated by *Alphaproteobacteria* and few representatives with virulence factors (e.g., *Hyphomonadaceae* and *Erythrobacteraceae*) (Nelson et al., 2013). Other stressors in addition to climate change can also increase virulence sequences, for example increased nutrients, DOC, temperature or pH can all increase the abundance of virulence genes in the coral holobiont (Vega Thurber et al., 2009).

Overfishing also alters fish populations and induces trophic cascades (Jackson et al., 2001), and changes in fish functional roles can influence the reef-associated microbial communities. For example, within the territory of the damselfishes, *Stegastes apicalis* and *S. nigricans*, there were 2–3-fold increases in coral pathogens in the microbiome and a higher prevalence of corals with signs of black band disease. These *Stegates* species normally exclude macroalgae and cultivate filamentous algae, thus providing a trophic link among fish behavior, coral pathogen reservoirs and coral disease (Casey et al., 2014). Other fishes (i.e., *Chaetodontidae*) may also act directly as disease vectors (Raymundo et al., 2009), however, functionally diverse fish communities have been suggested to alleviate coral disease (Raymundo et al., 2009) and five *Chaetodontidae* and one *Labridae* species actually slowed the progression of blackband disease (Cole et al., 2009). Furthermore, damage to corals from abandoned fishing lines, is correlated with a 4-fold increase in coral disease and thus can somewhat explain the reduction in coral disease prevalence between marine reserve and non-reserve areas (Lamb et al., 2015).

Biases within the Available Data

There are several caveats associated with the data synthesized here, specifically evaluating changes in bacterial composition from disparate studies. These biases stem from uneven sequence library sizes, the use of different primer sets, low DNA amplification, and most importantly the use of different methods for assessment of microbiome response (e.g., culturing, 16S amplicons, metagenomes). Researchers in microbiology use a wide array of methodologies, which can make it difficult to compare studies quantitatively. At the same time, studies often reported only bacterial composition through relative abundance measures, and are therefore not directly quantifying bacterial cells within the coral microbiome. For example, if a study

measures a decrease in a bacterial taxon, that taxon could be staying in consistent quantity while all other members of the microbiome are increasing. Thus, it is important to remember these biases when inferring from these data and keep in mind they are a broad qualitative overview of what happens to the coral microbiome under stress.

EVIDENCE THAT CORAL MICROBIOMES MEDIATE HOST RESISTANCE TO STRESSORS

Some of the strongest evidence in support of the hypothesis that coral microbes provide their hosts with resilience or resistance to stressors comes from studies using antibiotics. For example, antibiotic treatment of thermally stressed corals caused tissue loss, significant declines in photosynthetic efficiency (Gilbert et al., 2012) and increased coral susceptibility to *Vibrio shiloi* infection and bleaching (Mills et al., 2013; although see Bellantuono et al., 2012). Furthermore, when corals were subjected to antibiotics and subsequently transplanted back onto the reef, those corals bleached and eventually died compared with the control corals that did not receive antibiotics (Glasl et al., 2016).

Early investigations into the role of DSMP cycling suggest that the coral microbiome likely plays an important role in coral resistance to stress. Coral-associated bacteria implicated in sulfur cycling (e.g., *Endozoicomonas*, *Halomonas*) (Raina et al., 2009; Todd et al., 2010) may help corals acclimate to climate change by protecting *Symbiodinium* from photosynthesis derived oxidative stress, as sulfur compounds such as DMSP and its breakdown products can act as antioxidants for marine algae (Sunda et al., 2002). As such, in bleaching corals, it was shown that there is a strong negative correlation between the abundance of bacterial pathogens and the abundance of the proposed symbiont *Endozoicomonas* (Pantos et al., 2015).

Nitrogen fixation and regulation by coral microbiome residents may also play an important role in coral resistance to stress. *Symbiodinium* depend on nitrogen for growth (Béraud et al., 2013), diazotroph abundance increases with higher seawater temperatures (Santos et al., 2014), and nitrogen fixation within corals increases with higher temperatures (Cardini et al., 2016). However, the mechanism behind and outcome of this relationship remains an active area of research. For example, it was recently suggested that these bacterial diazotrophs may in fact harm corals during heat stress by increasing the N:P ratio within the cells, causing a destabilization of the host-*Symbiodinium* partnership and thus inducing or prolonging holobiont bleaching events above normal levels (Rädecker et al., 2015). Yet diazotrophs still may play an important role in buffering the coral holobiont under water pollution stress by fixing nitrogen. In eutrophication experiments, nitrogen fixing and denitrifying bacteria increased in abundance in the coral *Acropora hemprichii*, but there were no significant changes to holobiont physiology (Jessen et al., 2013).

Finally, coral-associated bacteria may support coral resistance to algal growth simulated by overfishing given that resident bacteria defend the coral from microbial invasions (Rypien et al., 2010; Shnit-Orland et al., 2012; Welsh et al., 2016), thus potentially providing protection from algae altering the coral microbiome (Vega Thurber et al., 2012). There are clearly multiple mechanisms that influence these microbial roles and, as demonstrated above, a conflicting base of evidence. Recent research further supports the hypothesis that the microbiome plays a role in coral resistance, with coral microbiomes adapting to environmental conditions during reciprocal transplants and microbiomes that were previously exposed to a more variable and warmer environment having higher resistance during heat stress experiments (Ziegler et al., 2017). Clarity into these dynamics will likely grow as evidence increases and we suggest that these are key research topics to better understand the roles played by microbes in coral resistance to stress.

CONCLUSIONS AND FUTURE DIRECTIONS

Our understanding of how the coral microbiome contributes to reef health is rapidly evolving, with the studies synthesized herein providing insight into how microbial communities respond to environmental change and hypotheses regarding the potential mechanisms underlying microbial support of coral resistance to stress. When stressors induce changes in coral-associated bacterial communities their beneficial functions to the coral holobiont can be lost. Thus, the composition of the coral microbiome could help to inform resource managers about which corals are most likely to successfully resist stressors, but this information has not yet been compiled. However, our results suggest that stressed corals have more taxonomically diverse microbiomes and increased beta diversity between coral colonies, potentially due to the stressed corals' inability to regulate incoming microbial members. At the same time, in stressed corals the opportunistic bacterial taxa *Flavobacteriales*, *Rhodobacterales* and *Vibrionales* are generally overrepresented, while the proposed coral symbiont, *Endozoicimonas* and related species, is underrepresented. Our results suggest metrics of microbiome diversity should be further investigated, especially beta diversity dispersion, which has only recently been applied to coral microbiome studies as a measure of microbiome stability between coral colonies (Zaneveld et al., 2016). Researchers should also utilize metrics of phylogenetic diversity through metrics like Faiths phylogenetic diversity, mean pairwise distance, and variation of pairwise distance (Tucker et al., 2017) to better understand the coral microbiome. In the future, resource managers may be able to identify stressed corals by the presence of opportunistic microbe taxa (Pollock et al., 2011) and by increased microbiome alpha and beta diversity, even if the coral has not yet shown physical signs of stress or deterioration.

To assist these trajectories, researchers need a better understanding of coral microbiome variability (e.g., temporal, spatial, seasonal, coral host species), to assemble databases of the microbiomes during different coral states (i.e., what is the normal microbiome for a coral species?), and determine the function of these bacteria for the coral host. With climate

projections predicting that future conditions will increase disease susceptibility, pathogen abundance and virulence on coral reefs (Maynard et al., 2015) and diverging predicted responses of marine microbes to anthropogenic change (Hutchins and Fu, 2017), it is critical that researchers continue to advance understanding of the relationships between corals and their microbiomes, and how these change under stress. Promisingly, ongoing research suggests that we may have the ability to increase coral adaptation to these stressors by modifying the coral-associated microbial community (van Oppen et al., 2015) or by using coral probiotics (Krediet et al., 2013). This review and an ever-growing body of evidence suggest that conservationists may be able to screen for corals with resilient microbiomes to determine where best to focus management priorities as threats to coral reefs continue to accumulate.

FUNDING

JMI acknowledges funding from a Natural Sciences and Engineering Research Council of Canada (NSERC) Canada Graduate Scholarship and Michael Smith Foreign Study Supplement, and from the University of Victoria; JB acknowledges funding from an NSERC Discovery Grant. This work was also supported by a National Science Foundation Dimensions of Biodiversity grant (#1442306) to RVT.

AUTHOR CONTRIBUTIONS

JMI wrote the first draft of the manuscript, synthesized the papers, and created the figures. All authors contributed to the writing and revisions of the manuscript.

REFERENCES

Ainsworth, T. D., and Hoegh-Guldberg, O. (2009). Bacterial communities closely associated with coral tissues vary under experimental and natural reef conditions and thermal stress. *Aquat. Biol.* 4, 289–296. doi: 10.3354/ab00102

Ainsworth, T. D., Thurber, R. V., and Gates, R. D. (2010). The future of coral reefs: a microbial perspective. *Trends Ecol. Evol.* 25, 233–240. doi: 10.1016/j.tree.2009.11.001

Ainsworth, T., Krause, L., Bridge, T., Torda, G., Raina, J.-B., Zakrzewski, M., et al. (2015). The coral core microbiome identifies rare bacterial taxa as ubiquitous endosymbionts. *ISME J.* 9, 2261–2274. doi: 10.1038/ismej.2015.39

Al-Dahash, L. M., and Mahmoud, H. M. (2013). Harboring oil-degrading bacteria: a potential mechanism of adaptation and survival in corals inhabiting oil-contaminated reefs. *Mar. Pollut. Bull.* 72, 364–374. doi: 10.1016/j.marpolbul.2012.08.029

Apprill, A., Marlow, H. Q., Martindale, M. Q., and Rappé, M. S. (2009). The onset of microbial associations in the coral *Pocillopora meandrina*. *ISME J.* 3, 685–699. doi: 10.1038/ismej.2009.3

Apprill, A., Weber, L. G., and Santoro, A. E. (2016). Distinguishing between microbial habitats unravels ecological complexity in coral microbiomes. *mSystems* 1:e00143–16. doi: 10.1128/mSystems.00143-16

Banin, E., Vassilakos, D., Orr, E., Martinez, R. J., and Rosenberg, E. (2003). Superoxide dismutase is a virulence factor produced by the coral bleaching pathogen *Vibrio shiloi*. *Curr. Microbiol.* 46, 418–422. doi: 10.1007/s00284-002-3912-5

Barott, K. L., Rodriguez-Brito, B., Janouškovec, J., Marhaver, K. L., Smith, J. E., Keeling, P., et al. (2011). Microbial diversity associated with four functional groups of benthic reef algae and the reef-building coral Montastraea annularis. *Environ. Microbiol.* 13, 1192–1204. doi: 10.1111/j.1462-2920.2010.02419.x

Barott, K. L., Rodriguez-Mueller, B., Youle, M., Marhaver, K. L., Vermeij, M. J. A., Smith, J. E., et al. (2012). Microbial to reef scale interactions between the reef-building coral *Montastraea annularis* and benthic algae. *Proc. R. Soc. Lond.* 279, 1655–1664. doi: 10.1098/rspb.2011.2155

Bayer, T., Neave, M. J., Alsheikh-Hussain, A., Aranda, M., Yum, L. K., Mincer, T., et al. (2013). The microbiome of the red sea coral stylophora pistillata is dominated by tissue-associated *Endozoicomonas* bacteria. *Appl. Environ. Microbiol.* 79, 4759–4762. doi: 10.1128/AEM.00695-13

Bellantuono, A. J., Hoegh-Guldberg, O., and Rodriguez-Lanetty, M. (2012). Resistance to thermal stress in corals without changes in symbiont composition. *Proc. R. Soc. Lond.* 279, 1100–1107. doi: 10.1098/rspb.2011.1780

Ben-Haim, Y., and Rosenburg, E. (2002). A novel *Vibrio* sp. pathogen of the coral *Pocillopora damicornis*. *Mar. Biol.* 141, 47–55. doi: 10.1007/s00227-002-0797-6

Ben-Haim, Y., Zicherman-Keren, M., and Rosenberg, E. (2003). Temperature-regulated bleaching and lysis of the coral *Pocillopora damicornis* by the novel pathogen *Vibrio coralliilyticus*. *Appl. Environ. Microbiol.* 69, 4236–4242. doi: 10.1128/AEM.69.7.4236-4242.2003

Béraud, E., Gevaert, F., Rottier, C., and Ferrier-Pagès, C. (2013). The response of the scleractinian coral *Turbinaria reniformis* to thermal stress depends on the nitrogen status of the coral holobiont. *J. Exp. Biol.* 216, 2665–2674. doi: 10.1242/jeb.085183

Blackall, L. L., Wilson, B., and van Oppen, M. J. H. (2015). Coral-the world's most diverse symbiotic ecosystem. *Mol. Ecol.* 24, 5330–5347. doi: 10.1111/mec.13400

Bourne, D. G., Dennis, P. G., Uthicke, S., Soo, R. M., Tyson, G. W., and Webster, N. (2013). Coral reef invertebrate microbiomes correlate with the presence of photosymbionts. *ISME J.* 7, 1452–1458. doi: 10.1038/ismej.2012.172

Bourne, D. G., Morrow, K. M., and Webster, N. S. (2016). Insights into the coral microbiome: underpinning the health and resilience of reef ecosystems. *Annu. Rev. Microbiol.* 70, 317–340. doi: 10.1146/annurev-micro-102215-095440

Bourne, D. G., and Webster, N. S. (2013). "Coral reef bacterial communities," in *The Prokaryotes,* eds E. Rosenberg, E. F. DeLong, S. Lory, E. Stackebrandt, and F. Thompson (Berlin, Heidelberg: Springer Berlin Heidelberg), 163–187.

Bourne, D., Iida, Y., Uthicke, S., and Smith-Keune, C. (2007). Changes in coral-associated microbial communities during a bleaching event. *ISME J.* 2, 350–363. doi: 10.1038/ismej.2007.112

Brandt, M. E., Smith, T. B., Correa, A. M. S., and Vega Thurber, R. (2013). Disturbance driven colony fragmentation as a driver of a coral disease outbreak. *PLoS ONE* 8:e57164. doi: 10.1371/journal.pone.0057164

Brodie, J., Williamson, C., Barker, G. L., Walker, R. H., Briscoe, A., and Yallop, M. (2016). Characterising the microbiome of Corallina officinalis, a dominant calcified intertidal red alga. *FEMS Microbiol. Ecol.* 92:fiw110. doi: 10.1093/femsec/fiw110

Burke, C., Thomas, T., Lewis, M., Steinberg, P., and Kjelleberg, S. (2011). Composition, uniqueness and variability of the epiphytic bacterial community of the green alga Ulva australis. *ISME J.* 5, 590–600. doi: 10.1038/ismej.2010.164

Cardini, U., van Hoytema, N., Bednarz, V. N., Rix, L., Foster, R. A., Al-Rshaidat, M. M. D., et al. (2016). Microbial dinitrogen fixation in coral holobionts exposed to thermal stress and bleaching. *Environ. Microbiol.* 18, 2620–2633. doi: 10.1111/1462-2920.13385

Carlos, C., Torres, T. T., and Ottoboni, L. M. M. (2013). Bacterial communities and species-specific associations with the mucus of Brazilian coral species. *Sci. Rep.* 3:1624. doi: 10.1038/srep01624

Casey, J. M., Ainsworth, T. D., Choat, J. H., and Connolly, S. R. (2014). Farming behaviour of reef fishes increases the prevalence of coral disease associated microbes and black band disease. *Proc. R. Soc. Lond.* 281:1788. doi: 10.1098/rspb.2014.1032

Ceh, J., Kilburn, M. R., Cliff, J. B., Raina, J.-B., van Keulen, M., and Bourne, D. G. (2013a). Nutrient cycling in early coral life stages: *Pocillopora damicornis* larvae provide their algal symbiont (*Symbiodinium*) with nitrogen acquired from bacterial associates. *Ecol. Evol.* 3, 2393–2400. doi: 10.1002/ece3.642

Ceh, J., van Keulen, M., and Bourne, D. G. (2013b). Intergenerational transfer of specific bacteria in corals and possible implications for offspring fitness. *Microb. Ecol.* 65, 227–231. doi: 10.1007/s00248-012-0105-z

Cole, A. J., Chong-Seng, K. M., Pratchett, M. S., and Jones, G. P. (2009). Coral-feeding fishes slow progression of black-band disease. *Coral Reefs* 28, 965–965. doi: 10.1007/s00338-009-0519-3

Darling, E. S., Alvarez-Filip, L., Oliver, T. A., McClanahan, T. R., and Côté, I. M. (2012). Evaluating life-history strategies of reef corals from species traits. *Ecol. Lett.* 15, 1378–1386. doi: 10.1111/j.1461-0248.2012.01861.x

Ding, J.-Y., Shiu, J.-H., Chen, W.-M., Chiang, Y.-R., and Tang, S.-L. (2016). Genomic insight into the host-endosymbiont relationship of *Endozoicomonas montiporae* CL-33(T) with its coral host. *Front. Microbiol.* 7:251. doi: 10.3389/fmicb.2016.00251

Dinsdale, E. A., Pantos, O., Smriga, S., Edwards, R. A., Angly, F., Wegley, L., et al. (2008). Microbial ecology of four coral atolls in the northern line islands. *PLoS ONE* 3:e1584. doi: 10.1371/journal.pone.0001584

Dubilier, N., Bergin, C., and Lott, C. (2008). Symbiotic diversity in marine animals: the art of harnessing chemosynthesis. *Nat. Rev. Microbiol.* 6, 725–740. doi: 10.1038/nrmicro1992

Egan, S., Harder, T., Burke, C., Steinberg, P., Kjelleberg, S., and Thomas, T. (2013). The seaweed holobiont: understanding seaweed-bacteria interactions. *FEMS Microbiol. Rev.* 37, 462–476. doi: 10.1111/1574-6976.12011

ElAhwany, A. M. D., Ghozlan, H. A., ElSharif, H. A., and Sabry, S. A. (2013). Phylogenetic diversity and antimicrobial activity of marine bacteria associated with the soft coral *Sarcophyton glaucum*. *J. Basic Microbiol.* 55, 2–10. doi: 10.1002/jobm.201300195

Ettinger, C. L., Voerman, S. E., Lang, J. M., Stachowicz, J. J., and Eisen, J. A. (2017). Microbial communities in sediment from *Zostera marina* patches, but not the *Z.* marina leaf or root microbiomes, vary in relation to distance from patch edge. *PeerJ* 5:e3246. doi: 10.7717/peerj.3246

Fahimipour, A. K., Kardish, M. R., Lang, J. M., Green, J. L., Eisen, J. A., and Stachowicz, J. J. (2017). Global-scale structure of the eelgrass microbiome. *Appl. Environ. Microbiol.* 83:12e03391–16. doi: 10.1128/AEM.03391-16

Frydenborg, B. R., Krediet, C. J., Teplitski, M., and Ritchie, K. B. (2013). Temperature-dependent inhibition of opportunistic *Vibrio* pathogens by native coral commensal bacteria. *Microb. Ecol.* 67, 392–401. doi: 10.1007/s00248-013-0334-9

Furby, K. A., Apprill, A., Cervino, J. M., Ossolinski, J. E., and Hughen, K. A. (2014). Incidence of lesions on Fungiidae corals in the eastern Red Sea is related to water temperature and coastal pollution. *Mar. Environ. Res.* 98, 29–38. doi: 10.1016/j.marenvres.2014.04.002

Gajigan, A. P., Diaz, L. A., and Conaco, C. (2017). Resilience of the prokaryotic microbial community of *Acropora digitifera* to elevated temperature. *Microbiologyopen* 72:e00478–11. doi: 10.1002/mbo3.478

Garren, M., Raymundo, L., Guest, J., Harvell, C. D., and Azam, F. (2009). Resilience of coral-associated bacterial communities exposed to fish farm effluent. *PLoS ONE* 4:e7319. doi: 10.1371/journal.pone.0007319

Garren, M., Son, K., Raina, J.-B., Rusconi, R., Menolascina, F., Shapiro, O. H., et al. (2014). A bacterial pathogen uses dimethylsulfoniopropionate as a cue to target heat-stressed corals. *ISME J.* 8, 999–1007. doi: 10.1038/ismej.2013.210

Ghanbari, M., Kneifel, W., and Domig, K. J. (2015). A new view of the fish gut microbiome: advances from next-generation sequencing. 448, 464–475. *Aquaculture.* doi: 10.1016/j.aquaculture.2015.06.033

Gignoux-Wolfsohn, S. A., and Vollmer, S. V. (2015). Identification of candidate coral pathogens on white band disease-infected staghorn coral. *PLoS ONE* 10:e0134416. doi: 10.1371/journal.pone.0134416

Gilbert, J. A., Hill, R., Doblin, M. A., and Ralph, P. J. (2012). Microbial consortia increase thermal tolerance of corals. *Mar. Biol.* 159, 1763–1771. doi: 10.1007/s00227-012-1967-9

Givens, C. E., Ransom, B., and Bano, N. (2015). Comparison of the gut microbiomes of 12 bony fish and 3 shark species. *Mar. Ecol. Prog. Ser.* 518, 209–223. doi: 10.3354/meps11034

Glasl, B., Herndl, G. J., and Frade, P. R. (2016). The microbiome of coral surface mucus has a key role in mediating holobiont health and survival upon disturbance. *ISME J.* 10, 2280–2292. doi: 10.1038/ismej.2016.9

Glasl, B., Webster, N. S., and Bourne, D. G. (2017). Microbial indicators as a diagnostic tool for assessing water quality and climate stress in coral reef ecosystems. *Mar. Biol.* 164, 1–18. doi: 10.1007/s00227-017-3097-x

Haas, A. F., Nelson, C. E., Wegley Kelly, L., Carlson, C. A., Rohwer, F., Leichter, J. J., et al. (2011). Effects of coral reef benthic primary producers on dissolved organic carbon and microbial activity. *PLoS ONE* 6:e27973. doi: 10.1371/journal.pone.0027973

Hadaidi, G., Röthig, T., Yum, L. K., Ziegler, M., Arif, C., Roder, C., et al. (2017). Stable mucus-associated bacterial communities in bleached and healthy corals of *Porites lobata* from the Arabian Seas. *Sci. Rep.* 7:45362. doi: 10.1038/srep45362

Hakim, J. A., Koo, H., Kumar, R., Lefkowitz, E. J., Morrow, C. D., Powell, M. L., et al. (2016). The gut microbiome of the sea urchin, *Lytechinus variegatus*, from its natural habitat demonstrates selective attributes of microbial taxa and predictive metabolic profiles. *FEMS Microbiol. Ecol.* 92:fiw146. doi: 10.1093/femsec/fiw146

Hester, E. R., Barott, K. L., Nulton, J., Vermeij, M. J., and Rohwer, F. L. (2016). Stable and sporadic symbiotic communities of coral and algal holobionts. *ISME J.* 10, 1157–1169. doi: 10.1038/ismej.2015.190

Hughes, T. P. (1994). Catastrophes, phase shifts, and large-scale degradation of a Caribbean coral reef. *Science* 265, 1547–1551. doi: 10.1126/science.265.5178.1547

Hutchins, D. A., and Fu, F. (2017). Microorganisms and ocean global change. *Nat. Microbiol.* 2:17058. doi: 10.1038/nmicrobiol.2017.58

Jackson, J., Kirby, M. X., Berger, W. H., and Bjorndal, K. A. (2001). Historical overfishing and the recent collapse of coastal ecosystems. *Science* 293, 629–638. doi: 10.1126/science.1059199

Jessen, C., Villa Lizcano, J. F., Bayer, T., Roder, C., Aranda, M., Wild, C., et al. (2013). *In-situ* effects of eutrophication and overfishing on physiology and bacterial diversity of the red sea coral *Acropora hemprichii*. *PLoS ONE* 8:e62091. doi: 10.1371/journal.pone.0062091

Jompa, J., and McCook, L. J. (2003). Coral-algal competition: macroalgae with different properties have different effects on corals. *Mar. Ecol. Prog. Ser.* 258, 87–95. doi: 10.3354/meps258087

Kimes, N. E., Van Nostrand, J. D., Weil, E., Zhou, J., and Morris, P. J. (2010). Microbial functional structure of *Montastraea faveolata*, an important Caribbean reef-building coral, differs between healthy and yellow-band diseased colonies. *Environ. Microbiol.* 12, 541–556. doi: 10.1111/j.1462-2920.2009.02113.x

Klaus, J. S., Janse, I., Heikoop, J. M., Sanford, R. A., and Fouke, B. W. (2007). Coral microbial communities, zooxanthellae and mucus along gradients of seawater depth and coastal pollution. *Environ. Microbiol.* 9, 1291–1305. doi: 10.1111/j.1462-2920.2007.01249.x

Kline, D. I., Kuntz, N. M., Breitbart, M., Knowlton, N., and Rohwer, F. (2006). Role of elevated organic carbon levels and microbial activity in coral mortality. *Mar. Ecol. Prog. Ser.* 314, 119–125. doi: 10.3354/meps314119

Koren, O., and Rosenberg, E. (2006). Bacteria associated with mucus and tissues of the coral *Oculina patagonica* in summer and winter. *Appl. Environ. Microbiol.* 72, 5254–5259. doi: 10.1128/AEM.00554-06

Koren, O., and Rosenberg, E. (2008). Bacteria associated with the bleached and cave coral *Oculina patagonica*. *Microb. Ecol.* 55, 523–529. doi: 10.1007/s00248-007-9297-z

Krediet, C. J., Ritchie, K. B., Alagely, A., and Teplitski, M. (2012). Members of native coral microbiota inhibit glycosidases and thwart colonization of coral mucus by an opportunistic pathogen. *ISME J.* 7, 980–990. doi: 10.1038/ismej.2012.164

Krediet, C. J., Ritchie, K. B., Paul, V. J., and Teplitski, M. (2013). Coral-associated micro-organisms and their roles in promoting coral health and thwarting diseases. *Proc. R. Soc. Lond.* 280:20122328. doi: 10.1098/rspb.2012.2328

Kushmaro, A., Rosenberg, E., Fine, M., Ben-Haim, Y., and Loya, Y. (1998). Effect of temperature on bleaching of the coral *Oculina patagonica* by *Vibrio AK-1*. *Mar. Ecol. Prog. Ser.* 171, 131–137. doi: 10.3354/meps171131

Kvennefors, E. C. E., Sampayo, E., Kerr, C., Vieira, G., Roff, G., and Barnes, A. C. (2011). Regulation of bacterial communities through antimicrobial activity by the coral holobiont. *Microb. Ecol.* 63, 605–618. doi: 10.1007/s00248-011-9946-0

Lamb, J. B., Williamson, D. H., Russ, G. R., and Willis, B. L. (2015). Protected areas mitigate diseases of reef-building corals by reducing damage from fishing. *Ecology* 96, 2555–2567. doi: 10.1890/14-1952.1

La Rivière, M., Roumagnac, M., Garrabou, J., and Bally, M. (2013). Transient shifts in bacterial communities associated with the temperate gorgonian *Paramuricea clavata* in the northwestern mediterranean sea. *PLoS ONE* 8:e57385. doi: 10.1371/journal.pone.0057385

Lee, S. T. M., Davy, S. K., Tang, S.-L., and Kench, P. S. (2016). Mucus Sugar Content Shapes the Bacterial Community Structure in Thermally Stressed *Acropora muricata*. *Front. Microbiol.* 7:371. doi: 10.3389/fmicb.2016.00371

Lee, S. T. M., Davy, S. K., Tang, S.-L., and Kench, P. S. (2017). Water flow buffers shifts in bacterial community structure in heat-stressed *Acropora muricata*. *Sci. Rep.* 7:43600. doi: 10.1038/srep43600

Lema, K. A., Bourne, D. G., and Willis, B. L. (2014). Onset and establishment of diazotrophs and other bacterial associates in the early life history stages of the coral *Acropora millepora*. *Mol. Ecol.* 23, 4682–4695. doi: 10.1111/mec.12899

Lema, K. A., Willis, B. L., and Bourne, D. G. (2012). Corals form characteristic associations with symbiotic nitrogen-fixing bacteria. *Appl. Environ. Microbiol.* 78, 3136–3144. doi: 10.1128/AEM.07800-11

Lesser, M. P., Falcón, L. I., Rodríguez-Román, A., Enríquez, S., Hoegh-Guldberg, O., and Iglesias-Prieto, R. (2007). Nitrogen fixation by symbiotic cyanobacteria provides a source of nitrogen for the scleractinian coral *Montastraea cavernosa*. *Mar. Ecol. Prog. Ser.* 346, 143–152. doi: 10.3354/meps07008

Lesser, M. P., Mazel, C. H., Gorbunov, M. Y., and Falkowski, P. G. (2004). Discovery of symbiotic nitrogen-fixing cyanobacteria in corals. *Science* 305, 997–1000. doi: 10.1126/science.1099128

Littman, R. A., Bourne, D. G., and Willis, B. L. (2010). Responses of coral-associated bacterial communities to heat stress differ with *Symbiodinium* type on the same coral host. *Mol. Ecol.* 19, 1978–1990. doi: 10.1111/j.1365-294X.2010.04620.x

Littman, R., Willis, B. L., and Bourne, D. G. (2011). Metagenomic analysis of the coral holobiont during a natural bleaching event on the Great Barrier Reef. *Environ. Microbiol. Rep.* 3, 651–660. doi: 10.1111/j.1758-2229.2010.00234.x

Looney, E. E., Sutherland, K. P., and Lipp, E. K. (2010). Effects of temperature, nutrients, organic matter and coral mucus on the survival of the coral pathogen, *Serratia marcescens* PDL100. *Environ. Microbiol.* 12, 2479–2485. doi: 10.1111/j.1462-2920.2010.02221.x

Lozupone, C. A., Stombaugh, J. I., Gordon, J. I., Jansson, J. K., and Knight, R. (2012). Diversity, stability and resilience of the human gut microbiota. *Nature* 489, 220–230. doi: 10.1038/nature11550

Maynard, J., Van Hooidonk, R., and Eakin, C. M. (2015). Projections of climate conditions that increase coral disease susceptibility and pathogen abundance and virulence. *Nat. Clim. Change* 5, 688–695. doi: 10.1038/nclimate2625

McClanahan, T. R., Donner, S. D., Maynard, J. A., MacNeil, M. A., Graham, N. A. J., Maina, J., et al. (2012). Prioritizing key resilience indicators to support coral reef management in a changing climate. *PLoS ONE* 7:e42884. doi: 10.1371/journal.pone.0042884

McCliment, E. A., Nelson, C. E., Carlson, C. A., Alldredge, A. L., Witting, J., and Amaral-Zettler, L. A. (2012). An all-taxon microbial inventory of the Moorea coral reef ecosystem. *ISME J.* 6, 309–319. doi: 10.1038/ismej.2011.108

Meron, D., Atias, E., Iasur Kruh, L., Elifantz, H., Minz, D., Fine, M., et al. (2011). The impact of reduced pH on the microbial community of the coral *Acropora eurystoma*. *ISME J.* 5, 51–60. doi: 10.1038/ismej.2010.102

Meron, D., Rodolfo-Metalpa, R., Cunning, R., Baker, A. C., Fine, M., and Banin, E. (2012). Changes in coral microbial communities in response to a natural pH gradient. *ISME J.* 6, 1775–1785. doi: 10.1038/ismej.2012.19

Mills, E., Shechtman, K., Loya, Y., and Rosenberg, E. (2013). Bacteria appear to play important roles in both causing and preventing the bleaching of the coral *Oculina patagonica*. *Mar. Ecol. Prog. Ser.* 489, 155–162. doi: 10.3354/meps10391

Mitchell, R., and Chet, I. (1975). Bacterial attack of corals in polluted seawater. *Microb. Ecol.* 2, 227–233. doi: 10.1007/BF02010442

Moeller, A. H., Shilts, M., Li, Y., Rudicell, R. S., Lonsdorf, E. V., Pusey, A. E., et al. (2013). SIV-induced instability of the chimpanzee gut microbiome. *Cell Host Microbe* 14, 340–345. doi: 10.1016/j.chom.2013.08.005

Morrow, K. M., Bourne, D. G., Humphrey, C., Botté, E. S., Laffy, P., Zaneveld, J., et al. (2015). Natural volcanic CO_2 seeps reveal future trajectories for host-microbial associations in corals and sponges. *ISME J.* 9, 894–908. doi: 10.1038/ismej.2014.188

Morrow, K. M., Bromhall, K., Motti, C. A., Munn, C. B., and Bourne, D. G. (2017). Allelochemicals produced by brown macroalgae of the lobophora genus are active against coral larvae and associated bacteria, supporting pathogenic shifts to vibrio dominance. *Appl. Environ. Microbiol.* 83:e02391–16. doi: 10.1128/AEM.02391-16.

Morrow, K. M., Liles, M. R., Paul, V. J., Moss, A., and Chadwick, N. E. (2013). Bacterial shifts associated with coral–macroalgal competition in the Caribbean Sea. *Mar. Ecol. Prog. Ser.* 488, 103–117. doi: 10.3354/meps10394

Morrow, K. M., Moss, A. G., Chadwick, N. E., and Liles, M. R. (2012a). Bacterial associates of two caribbean coral species reveal species-specific distribution and geographic variability. *Appl. Environ. Microbiol.* 78, 6438–6449. doi: 10.1128/AEM.01162-12

Morrow, K. M., Ritson-Williams, R., Ross, C., Liles, M. R., and Paul, V. J. (2012b). Macroalgal extracts induce bacterial assemblage shifts and sublethal tissue stress in caribbean corals. *PLoS ONE* 7:e44859. doi: 10.1371/journal.pone.0044859

Mouchka, M. E., Hewson, I., and Harvell, C. D. (2010). Coral-associated bacterial assemblages: current knowledge and the potential for climate-driven impacts. *Integr. Comp. Biol.* 50, 662–674. doi: 10.1093/icb/icq061

Neave, M. J., Michell, C. T., Apprill, A., and Voolstra, C. R. (2017). Endozoicomonas genomes reveal functional adaptation and plasticity in bacterial strains symbiotically associated with diverse marine hosts. *Sci. Rep.* 7:40579. doi: 10.1038/srep40579

Neave, M. J., Rachmawati, R., Xun, L., Michell, C. T., Bourne, D. G., Apprill, A., et al. (2016). Differential specificity between closely related corals and abundant *Endozoicomonas* endosymbionts across global scales. *ISME J.* 11, 186–200. doi: 10.1038/ismej.2016.95

Nelson, C. E., Goldberg, S. J., Kelly, L. W., Haas, A. F., Smith, J. E., Rohwer, F., et al. (2013). Coral and macroalgal exudates vary in neutral sugar composition and differentially enrich reef bacterioplankton lineages. *ISME J.* 7, 962–979. doi: 10.1038/ismej.2012.161

Nugues, M. M., Smith, G. W., and Hooidonk, R. J. (2004). Algal contact as a trigger for coral disease. *Ecology* 7, 919–923. doi: 10.1111/j.1461-0248.2004.00651.x

Olson, N. D., Ainsworth, T. D., Gates, R. D., and Takabayashi, M. (2009). Diazotrophic bacteria associated with Hawaiian *Montipora* corals: diversity and abundance in correlation with symbiotic dinoflagellates. *J. Exp. Mar. Biol. Ecol.* 371, 140–146. doi: 10.1016/j.jembe.2009.01.012

Pantos, O., Bongaerts, P., Dennis, P. G., Tyson, G. W., and Hoegh-Guldberg, O. (2015). Habitat-specific environmental conditions primarily control the microbiomes of the coral *Seriatopora hystrix*. *ISME J.* 9, 1916–1927. doi: 10.1038/ismej.2015.3

Parris, D. J., Brooker, R. M., Morgan, M. A., Dixson, D. L., and Stewart, F. J. (2016). Whole gut microbiome composition of damselfish and cardinalfish before and after reef settlement. *PeerJ* 4:e2412. doi: 10.7717/peerj.2412

Peixoto, R., Rosado, P., and Leite, D. (2017). Beneficial Microorganisms for Corals (BMC): proposed mechanisms for coral health and resilience. *Front. Microbiol.* 8:341. doi: 10.3389/fmicb.2017.00341

Pollock, F. J., Morris, P. J., Willis, B. L., and Bourne, D. G. (2011). The urgent need for robust coral disease diagnostics. *PLoS Pathog.* 7:e1002183. doi: 10.1371/journal.ppat.1002183

Rädecker, N., Pogoreutz, C., Voolstra, C. R., Wiedenmann, J., and Wild, C. (2015). Nitrogen cycling in corals: the key to understanding holobiont functioning? *Trends Microbiol.* 23, 490–497. doi: 10.1016/j.tim.2015.03.008

Raina, J.-B., Tapiolas, D. M., Forêt, S., Lutz, A., Abrego, D., Ceh, J., et al. (2013). DMSP biosynthesis by an animal and its role in coral thermal stress response. *Nature* 502, 677–680. doi: 10.1038/nature12677

Raina, J. B., Tapiolas, D., Willis, B. L., and Bourne, D. G. (2009). Coral-associated bacteria and their role in the biogeochemical cycling of sulfur. *Appl. Environ. Microbiol.* 75, 3492–3501. doi: 10.1128/AEM.02567-08

Rasher, D. B., and Hay, M. E. (2010). Chemically rich seaweeds poison corals when not controlled by herbivores. *Proc. Natl. Acad. Sci. U.S.A.* 107, 9683–9688. doi: 10.1073/pnas.0912095107

Raymundo, L. J., Halford, A. R., Maypa, A. P., and Kerr, A. M. (2009). Functionally diverse reef-fish communities ameliorate coral disease. *Proc. Natl. Acad. Sci. U.S.A.* 106, 17067–17070. doi: 10.1073/pnas.0900365106

Ritchie, K. B. (2006). Regulation of microbial populations by coral surface mucus and mucus-associated bacteria. *Mar. Ecol. Prog. Ser.* 322, 1–14. doi: 10.3354/meps322001

Rohwer, F., Breitbart, M., Jara, J., Azam, F., and Knowlton, N. (2001). Diversity of bacteria associated with the Caribbean coral *Montastraea franksi*. *Coral Reefs* 20, 85–91. doi: 10.1007/s003380100138

Rosenberg, E., Koren, O., Reshef, L., Efrony, R., and Zilber-Rosenberg, I. (2007). The role of microorganisms in coral health, disease and evolution. *Nat. Rev. Microbiol.* 5, 355–362. doi: 10.1038/nrmicro1635

Röthig, T., Ochsenkühn, M. A., Roik, A., van der Merwe, R., and Voolstra, C. R. (2016). Long-term salinity tolerance is accompanied by major restructuring of the coral bacterial microbiome. *Mol. Ecol.* 25, 1308–1323. doi: 10.1111/mec.13567

Rypien, K. L., Ward, J. R., and Azam, F. (2010). Antagonistic interactions among coral-associated bacteria. *Environ. Microbiol.* 12, 28–39. doi: 10.1111/j.1462-2920.2009.02027.x

Salerno, J. L., Reineman, D. R., Gates, R. D., and Rappé, M. S. (2011). The effect of a sublethal temperature elevation on the structure of bacterial communities associated with the coral *Porites compressa*. *J. Mar. Biol.* 2011, 1–9. doi: 10.1155/2011/969173

Santos, H. F., Carmo, F. L., Duarte, G., Dini-Andreote, F., Castro, C. B., Rosado, A. S., et al. (2014). Climate change affects key nitrogen-fixing bacterial populations on coral reefs. *ISME J.* 8, 2272–2279. doi: 10.1038/ismej.2014.70

Sharp, K. H., Distel, D., and Paul, V. J. (2012). Diversity and dynamics of bacterial communities in early life stages of the Caribbean coral *Porites astreoides*. *ISME J.* 6, 790–801. doi: 10.1038/ismej.2011.144

Sharp, K. H., Ritchie, K. B., Schupp, P. J., Ritson-Williams, R., and Paul, V. J. (2010). Bacterial acquisition in juveniles of several broadcast spawning coral species. *PLoS ONE* 5:e10898. doi: 10.1371/journal.pone.0010898

Sharp, K. H., Sneed, J. M., Ritchie, K. B., Mcdaniel, L., and Paul, V. J. (2015). Induction of larval settlement in the reef coral *Porites astreoides* by a cultivated marine *Roseobacter* strain. *Biol. Bull.* 228, 98–107. doi: 10.1086/BBLv228n2p98

Shnit-Orland, M., Sivan, A., and Kushmaro, A. (2012). Antibacterial activity of *Pseudoalteromonas* in the coral holobiont. *Microb. Ecol.* 64, 851–859. doi: 10.1007/s00248-012-0086-y

Smith, J. E., Shaw, M., Edwards, R. A., Obura, D., Pantos, O., Sala, E., et al. (2006). Indirect effects of algae on coral: algae-mediated, microbe-induced coral mortality. *Ecol. Lett.* 9, 835–845. doi: 10.1111/j.1461-0248.2006.00937.x

Steinke, M., Brading, P., Kerrison, P., Warner, M. E., and Suggett, D. J. (2011). Concentrations of Dimethylsulfoniopropionate and dimethyl sulfide are strain-specific in symbiotic dinoflagellates *(Symbiodinium* sp., *dinophyceae)*. *J. Phycol.* 47, 775–783. doi: 10.1111/j.1529-8817.2011.01011.x

Sunda, W., Kieber, D. J., Kiene, R. P., and Huntsman, S. (2002). An antioxidant function for DMSP and DMS in marine algae. *Nature* 418, 317–320. doi: 10.1038/nature00851

Sutherland, K. P., Porter, J. W., Turner, J. W., Thomas, B. J., Looney, E. E., Luna, T. P., et al. (2010). Human sewage identified as likely source of white pox disease of the threatened Caribbean elkhorn coral, *Acropora palmata*. *Environ. Microbiol.* 12, 1122–1131. doi: 10.1111/j.1462-2920.2010.02152.x

Sweet, M. J., Bythell, J. C., and Nugues, M. M. (2013). Algae as reservoirs for coral pathogens. *PLoS ONE* 8:e69717. doi: 10.1371/journal.pone.0069717

Sweet, M. J., Croquer, A., and Bythell, J. C. (2010). Bacterial assemblages differ between compartments within the coral holobiont. *Coral Reefs* 30, 39–52. doi: 10.1007/s00338-010-0695-1

Teeling, H., Fuchs, B. M., Becher, D., Klockow, C., Gardebrecht, A., Bennke, C. M., et al. (2012). Substrate-controlled succession of marine bacterioplankton populations induced by a phytoplankton bloom. *Science* 336, 608–611. doi: 10.1126/science.1218344

Thompson, J. R., Rivera, H. E., Closek, C. J., and Medina, M. (2014). Microbes in the coral holobiont: partners through evolution, development, and ecological interactions. *Front. Cell Infect. Microbiol.* 4:176. doi: 10.3389/fcimb.2014.00176

Tianero, M. D. B., Kwan, J. C., Wyche, T. P., Presson, A. P., Koch, M., Barrows, L. R., et al. (2014). Species specificity of symbiosis and secondary metabolism in ascidians. *ISME J.* 9, 615–628. doi: 10.1038/ismej.2014.152

Todd, J. D., Curson, A. R. J., Nikolaidou-Katsaraidou, N., Brearley, C. A., Watmough, N. J., Chan, Y., et al. (2010). Molecular dissection of bacterial acrylate catabolism–unexpected links with dimethylsulfoniopropionate catabolism and dimethyl sulfide production. *Environ. Microbiol.* 12, 327–343. doi: 10.1111/j.1462-2920.2009.02071.x

Tout, J., Siboni, N., Messer, L. F., Garren, M., Stocker, R., Webster, N. S., et al. (2015). Increased seawater temperature increases the abundance and alters the structure of natural *Vibrio* populations associated with the coral *Pocillopora damicornis*. *Front. Microbiol.* 6:432. doi: 10.3389/fmicb.2015.00432

Tracy, A. M., Koren, O., Douglas, N., Weil, E., and Harvell, C. D. (2015). Persistent shifts in Caribbean coral microbiota are linked to the 2010 warm thermal anomaly. *Environ. Microbiol. Rep.* 7, 471–479. doi: 10.1111/1758-2229.12274

Tucker, C. M., Cadotte, M. W., Carvalho, S. B., Davies, T. J., Ferrier, S., Fritz, S. A., et al. (2017). A guide to phylogenetic metrics for conservation, community ecology and macroecology. *Biol. Rev. Camb. Philos. Soc.* 92, 698–715. doi: 10.1111/brv.12252

van der Voort, M., Kempenaar, M., van Driel, M., Raaijmakers, J. M., and Mendes, R. (2016). Impact of soil heat on reassembly of bacterial communities in the rhizosphere microbiome and plant disease suppression. *Ecol. Lett.* 19, 375–382. doi: 10.1111/ele.12567

van Oppen, M. J. H., Oliver, J. K., Putnam, H. M., and Gates, R. D. (2015). Building coral reef resilience through assisted evolution. *Proc. Natl. Acad. Sci. U.S.A.* 112, 2307–2313. doi: 10.1073/pnas.1422301112

Vega Thurber, R., Burkepile, D. E., Correa, A. M. S., Thurber, A. R., Shantz, A. A., Welsh, R., et al. (2012). Macroalgae decrease growth and alter microbial community structure of the reef-building coral, *Porites astreoides*. *PLoS ONE* 7:e44246. doi: 10.1371/journal.pone.0044246

Vega Thurber, R. L., Burkepile, D. E., Fuchs, C., Shantz, A. A., McMinds, R., and Zaneveld, J. R. (2013). Chronic nutrient enrichment increases prevalence and severity of coral disease and bleaching. *Glob. Change Biol.* 20, 544–554. doi: 10.1111/gcb.12450

Vega Thurber, R., Willner-Hall, D., Rodriguez-Mueller, B., Desnues, C., Edwards, R. A., Angly, F., et al. (2009). Metagenomic analysis of stressed coral holobionts. *Environ. Microbiol.* 11, 2148–2163. doi: 10.1111/j.1462-2920.2009.01935.x

Webster, N. S., Negri, A. P., Botté, E. S., Laffy, P. W., Flores, F., Noonan, S., et al. (2016). Host-associated coral reef microbes respond to the cumulative pressures of ocean warming and ocean acidification. *Sci. Rep.* 6:19324. doi: 10.1038/srep19324

Webster, N. S., Negri, A. P., Flores, F., Humphrey, C., Soo, R., Botté, E. S., et al. (2012). Near-future ocean acidification causes differences in microbial associations within diverse coral reef taxa. *Environ. Microbiol. Rep.* 5, 243–251. doi: 10.1111/1758-2229.12006

Wegley, L., Edwards, R., Rodriguez-Brito, B., Liu, H., and Rohwer, F. (2007). Metagenomic analysis of the microbial community associated with the coral *Porites astreoides*. *Environ. Microbiol.* 9, 2707–2719. doi: 10.1111/j.1462-2920.2007.01383.x

Welsh, R. M., Rosales, S. M., Zaneveld, J., and Payet, J. P. (2015). Alien vs. Predator: pathogens open niche space for opportunists, unless controlled by predators. *PeerJ*. doi: 10.7287/peerj.preprints.1537v1

Welsh, R. M., Zaneveld, J. R., Rosales, S. M., Payet, J. P., Burkepile, D. E., and Thurber, R. V. (2016). Bacterial predation in a marine host-associated microbiome. *ISME J.* 10, 1540–1544. doi: 10.1038/ismej.2015.219

Zaneveld, J. R., McMinds, R., and Vega Thurber, R. (2017). An Anna Karenina Principle for Microbiomes: many stressors destabilize rather than predictably shift animal microbiomes. *Nat Microbiol.* 2:17121. doi: 10.1038/nmicrobiol.2017.121

Zaneveld, J. R., Shantz, A. A., Pritchard, C. E., McMinds, R., Payet, J. E. R. O. M. P., Welsh, R., et al. (2016). Overfishing and nutrient pollution interact with temperature to disrupt coral reefs down to microbial scales. *Nat. Commun.* 7:11833. doi: 10.1038/ncomms11833

Zhang, Y., Ling, J., Yang, Q., Wen, C., Yan, Q., Sun, H., et al. (2015). The functional gene composition and metabolic potential of coral-associated microbial communities. *Sci. Rep.* 5:16191. doi: 10.1038/srep16191

Ziegler, M., Roik, A., Porter, A., Zubier, K., Mudarris, M. S., Ormond, R., et al. (2016). Coral microbial community dynamics in response to anthropogenic impacts near a major city in the central Red Sea. *Mar. Pollut. Bull.* 105, 629–640. doi: 10.1016/j.marpolbul.2015.12.045

Ziegler, M., Seneca, F. O., Yum, L. K., Palumbi, S. R., and Voolstra, C. R. (2017). Bacterial community dynamics are linked to patterns of coral heat tolerance. *Nat. Commun.* 8, 1–8. doi: 10.1038/ncomms14213

Conflict of Interest Statement: The authors declare that the research was conducted in the absence of any commercial or financial relationships that could be construed as a potential conflict of interest.

frontiers in Marine Science

ORIGINAL RESEARCH
published: 06 June 2018
doi: 10.3389/fmars.2018.00198

Quorum Sensing Interference and Structural Variation of Quorum Sensing Mimics in Australian Soft Coral

Marnie L. Freckelton [1,2,3†], Lone Høj [2,3] and Bruce F. Bowden [1,3]*

[1] College of Science and Engineering, James Cook University, Townsville, QLD, Australia, [2] Australian Institute of Marine Science, Townsville, QLD, Australia, [3] AIMS@JCU, Division for Research and Innovation, James Cook University, Townsville, QLD, Australia

OPEN ACCESS

Edited by:
Stanley Chun Kwan Lau, Hong Kong University of Science and Technology, Hong Kong

Reviewed by:
Hauke Fabian Kegler, Leibniz Centre for Tropical Marine Research (LG), Germany
Fernando Reyes, Fundación Centro de Excelencia en Investigación de Medicamentos Innovadores en Andalucía, Spain

***Correspondence:**
Lone Høj
l.hoj@aims.gov.au

†Present Address:
Marnie L. Freckelton, Pacific Biosciences Research Center, University of Hawaii at Mānoa, Honolulu, HI, United States

Specialty section:
This article was submitted to Aquatic Microbiology, a section of the journal Frontiers in Marine Science

Received: *01 February 2018*
Accepted: *17 May 2018*
Published: *06 June 2018*

Citation:
Freckelton ML, Høj L and Bowden BF (2018) Quorum Sensing Interference and Structural Variation of Quorum Sensing Mimics in Australian Soft Coral. Front. Mar. Sci. 5:198. doi: 10.3389/fmars.2018.00198

Bacterial Quorum Sensing (QS), the indirect regulation of gene expression through production and detection of small diffusible molecules, has emerged as a point of interaction between eukaryotic host organisms and their associated microbial communities. The extracellular nature of QS molecules enables interference in QS systems, in many cases via mimicry. This study targeted QS induction and inhibition in soft coral holobionts, as many soft coral species commonly contain compounds with structural similarities to the well-studied bacterial QS molecules acyl homoserine lactones. Screening with two bacterial biosensors, *Agrobacterium tumefaciens* A136 and *Chromobacterium violaceum* CV026, demonstrated that QS interference differed between the two biosensor strains and extended across the soft coral families *Alcyoniidae*, *Clavulariidae, Nephtheidae*, and *Xeniidae*. Bioassay-guided fractionation revealed chemical activity patterns, particularly in the induction of QS. Cembranoid diterpenes from active fractions were purified and tested for QS interference activity. Interestingly, the type of QS activity (induction or inhibition) in *A. tumefaciens* A136 correlated with structural variability of the secondary oxygen ring; cembranoid diterpenes with a furan ring or five-membered lactone induced QS, while compounds with larger (six or seven membered) lactone rings inhibited QS. Addition of the dominant cembranoid diterpene in the soft coral *Lobophytum compactum*, isolobophytolide, to bacterial culture media increased the number and morphological diversity of bacteria recovered from the mucosal layer of this soft coral, demonstrating a selective effect on certain members of the soft coral bacterial community. The identity and QS activity of recovered isolates differed between the mucosal layers of *L. compactum* and *Sinularia flexibilis*. In conclusion, this study provides information on the complexity of the interaction between soft corals and their associated bacteria, as well as, a structural understanding of how QS mimic compounds are able to interfere with a bacterial communication system.

Keywords: quorum sensing, soft coral, bacterial isolates, cembrenolide, quorum sensing mimic

INTRODUCTION

Quorum Sensing (QS) is one form of cell to cell signaling employed by bacteria to coordinate gene expression across entire populations through release and detection of extracellular signal molecules (Miller and Bassler, 2001). The aspects of multicellularity gained through QS, enable bacteria to perform many important ecological functions such as the ability to interact with their physical and biological environment (Miller and Bassler, 2001), form biofilms (Rice et al., 2005), and secrete virulence factors (Zhu and Mekalanos, 2003). The extracellular nature of QS signaling molecules facilitates their disruption and mimicry (Chhabra et al., 2005). Consequently, many bacteria possess the ability to detect and respond to QS signals of other species (Joint et al., 2007). Indeed, QS systems are more prevalent amongst bacteria associated with mixed bacterial biofilms and macro-organisms, suggesting that possession of QS systems confers an advantage in these habitats (Dudler and Eberl, 2006).

QS mimics are extrinsic signals that can interfere directly with QS gene expression (Bauer and Robinson, 2002). To be effective, QS mimic compounds must specifically interfere with the target QS system. Multiple QS systems have been discovered; in Gram-negative bacteria (Papenfort and Bassler, 2016) the most well studied system is the Auto Inducer One system (AI-1), which utilizes acyl homoserine lactones (AHLs) as signal molecules. Studies into the structure and functions of AHLs suggest that the ɣ-lactone ring is required for QS activity and that the length and functionality of the acyl side chain provides specificity (Parsek and Greenberg, 2000; Watson et al., 2002; Geske et al., 2008). For this reason, it has been hypothesized that AI-1 QS mimics would also contain a ɣ lactone ring or homologous functionality such as the furanones of the red alga *Delisea pulchra*. The furanones are one of the few QS inhibitors to have been structurally elucidated and the presence of an oxygenated ring was demonstrated to be essential to their activity (Manefield et al., 1999).

Disruption and mimicry of QS signals are increasingly recognized as mechanisms that are commonly employed by macro-organisms to regulate and manipulate their associated microbial communities (Bauer and Robinson, 2002; González and Keshavan, 2006). QS interference by host organisms can confer the ability to respond to the presence of certain pathogenic or mutualistic bacteria quickly and reliably (Kjelleberg et al., 1997; Mathesius et al., 2003), render a pathogenic species of bacteria non-pathogenic (Dong et al., 2007; Swem et al., 2009), and enable manipulation of the abundance and composition of its associated bacterial assemblies (Givskov et al., 1996). A host's microbiota can be a first line of defense against pathogen invasion (McFall-Ngai et al., 2013), therefore manipulation of QS could strengthen the resilience of the holobiont (González and Keshavan, 2006; Teplitski and Ritchie, 2009).

The ability of some bacterial species to detect non-native QS molecules has allowed the development of bacterial biosensor strains. QS bacterial biosensor strains are genetically modified bacterial isolates that require external addition of QS signal molecules. Their expression of QS-regulated genes is linked to reporter genes, which typically produce a pigment or bioluminescence (Steindler and Venturi, 2007). Two of the most commonly used AI-1 bacterial biosensor strains are based on the species *Chromobacterium violaceum* and *Agrobacterium tumefaciens*. In *C. violaceum*, QS regulates the production of the secondary metabolite violacein, which is purple in color (McClean et al., 1997). Bacterial biosensors based on this species utilize the LuxI/LuxR homolog genes CivI/CivR and are sensitive to AHLs with C4–C8 carbon chains as well as 3-oxo-C6 and -C8 carbon chains (McClean et al., 1997; Steindler and Venturi, 2007). *A. tumefaciens* QS biosensors have a genetically modified QS plasmid such that QS by these strains results in an enzymatic breakdown of X-gal and the formation of an indigo colored product (Zhu et al., 1998; Farrand et al., 2002; Zhu and Mekalanos, 2003). *A. tumefaciens* QS biosensors often utilize the TraI/TraR genes that provide sensitivity to AHLs with C6–C14 acyl side chains as well their equivalent 3-oxo-acyl side chains and C6–C10 hydroxy acyl side chains (Zhu et al., 1998; Farrand et al., 2002; Zhu and Mekalanos, 2003; Steindler and Venturi, 2007). Despite the partly overlapping acyl chain lengths detected by these two sensors, previous studies have observed differences in their responses during screening of isolates (Chong et al., 2012).

Widespread QS inhibitory activity has been observed to occur in the marine benthos, particularly in sponges and soft corals (Taylor et al., 2004; Skindersoe et al., 2008; Hunt et al., 2012). Soft corals contain a number of secondary metabolites with the structural potential to mimic QS, including furanocembrenes (cembranoid diterpenes with fused 5-membered ether rings) and cembranolides (cembranoids that possess a fused second ring in the form of a lactone). Cembranoid diterpenes are most commonly, but not exclusively, found within the family *Alcyoniidae*. Furthermore, cembranoid diterpenes are inherently variable in the presence, position and size of oxygenated ring systems (Wahlberg and Eklund, 1992). Variation of substituents, direction of cyclisation and the corresponding position of the isoprenoid double bonds of different diterpenes from different species of soft coral are also encountered (Wahlberg and Eklund, 1992) making cembranoid diterpenes a natural pool of compounds to investigate QS mimic structure-activity relationships.

Soft corals have a high incidence of QS interference; however, so far all screened soft corals have been from a single family, *Alcyoniidae*, and the presence of QS induction has not yet been investigated. While QS and QS interference have been implicated in the regulation of mixed bacterial communities including those found in the surface mucosal layer (SML) of hard corals (Tait et al., 2010; Golberg et al., 2011, 2013), it is unknown whether these communities may be regulated by QS mimics. Currently very little known about bacterial communities that associate with soft corals. In hard corals, bacteria in the SML, the first and largest point of interaction between a coral and the environment, are considered important to the health and resilience of the holobiont (Reshef et al., 2006; Rosenberg et al., 2007; Zilber-Rosenberg and Rosenberg, 2008; Shnit-Orland and Kushmaro, 2009).

This study aims to assess the potential of soft corals to interact with their associated microbes via QS, with a focus on their associated secondary metabolites such as cembranolides and furanocembrenes. Crude extracts of 15 soft coral species, representing 4 families of soft corals, were tested for their

ability to induce or inhibit QS in 2 bacterial biosensors, *A. tumefaciens* A136 and *C. violaceum* CV026. Cembranolides and furanocembrenes were isolated from soft corals and the effect of their structural variability on QS interference was assessed. To gain a better understanding of the role that QS can play in regulating eukaryote associated bacterial communities, bacterial strains isolated from the surface mucosal layer (SML) of two soft corals, *Sinularia flexibilis* and *Lobophytum compactum* were similarly evaluated for QS activity. The possible role that isolobophytolide, the major secondary metabolite of *L. compactum*, might play in bacterial selection within the soft corals mucus was also assessed by supplementing culture media with this secondary metabolite.

MATERIALS AND METHODS

Soft Coral Collection

Twenty four specimens of soft coral, representing 15 species (Supplementary Tables 1–3), were collected at a depth of 1–3 m near Orpheus Island (Great Barrier Reef, Australia; latitude 18°36.878′S; longitude 146°29.990′E). All specimens except *Cespitularia* sp. were photographed (Supplementary Figure 1) and sampled underwater, with samples placed directly into plastic bags filled with seawater. Samples were frozen (−80°C) within 1 h of collection and stored until freeze drying. Additional colonies of *L. compactum*, *S. flexibilis*, and *Pachyclavularia violacea* were collected for fraction analysis and isolation of pure compounds (Supplementary Tables 2,3). ^{1}H NMR spectra of the crude extracts of all soft coral samples were compared between collections and with reference spectra from the Bowden laboratory to ensure consistency in the metabolites and species tested.

Soft Coral Extract Preparation

Dried soft coral tissue was weighed and homogenized before extraction. Three extracts of different polarity were generated for each soft coral sample. Solvents used for extraction were, in order, dichloromethane (DCM), methanol (MeOH), and water (H_2O). Each extract was the result of three successive applications of solvent. Extracts were concentrated by rotary evaporation before being dried under a stream of nitrogen (N_2) and stored at −20°C until analysis. The DCM and MeOH extracts were dissolved in ethanol and the aqueous extracts in H_2O to a concentration of 20 mg/ml. All soft coral extracts were tested at two concentrations (4 μg/well and 40 μg/well) three times for the presence of QS induction and QS inhibition activity in *A. tumefaciens* A136 and *C. violaceum* CV026 in at least two independent experiments.

Soft Coral Extract Fractionation

To further investigate the patterns of QS activity observed in crude extracts, nine soft coral species from five genera (three families) were chosen for further fractionation (Supplementary Table 2). The chosen species displayed five patterns of crude extract activity (Supplementary Table 4). In addition to four species with strong crude extract activities, five species were selected to investigate observed within genera variation in activity patterns or because they represent common genera on the Great Barrier Reef (GBR). Ten fractions of decreasing polarity were generated from the dichloromethane extracts of the chosen soft corals. Extracts were fractionated using flash column chromatography on RP-C18 silica cartridges (Phenomenex Strata C18-E 55 μm 70 Å, 1,000 mg) eluted with a stepwise 20–100% MeOH: H_2O gradient followed by a 1:1 DCM: MeOH wash. The resulting fractions were concentrated to dryness under a stream of N_2 gas and re-dissolved in ethanol for QS screening as described above. ^{1}H-NMR spectra (600 MHz) of active fractions were recorded with a Bruker 600 Avance spectrometer in deuterated chloroform ($CDCl_3$).

Isolation of Purified Metabolites From the Corals

Ten cembranoid diterpenes with variable secondary ring structures were assessed in this study (**Figure 1**, **Table 1**). Isoneocembrene A (**1**) represents the base cembrene backbone, without an additional ring (**Figure 1**, **Table 1**). Compounds **2**-**4** are ϒ-lactones (5-membered rings). Two δ-lactones (6-membered rings) and one ε-lactone (7-membered ring) are also included in compounds **6**-**8** respectively (**Figure 1**, **Table 1**). The final two compounds are furanocembrenes (**Figure 1**, **Table 1**). Pure samples of isoneocembrene A (**1**), lobolide (**4**) and sarcophine (**5**) were acquired from the Bowden Laboratory, Townsville Australia. Isolobophytolide (**2**), and isolobophytolide monoacetates (**3**) were isolated from freshly collected and extracted *L. compactum* (see below). Flexibilide (**6**), dihydroflexibilide (**7**) and sinulariolide (**8**) were isolated from freshly collected and extracted *S. flexibilis* (see below). The furanocembrenes, pachyclavulariadiol (**9**) and pachyclavulariadiol diacetate (**10**), were isolated from freshly collected and extracted *P. violacea.* Extracts of each species were generated as described previously (section Soft Coral Extract Preparation).

For the *L. compactum* extract, vacuum liquid chromatography of active crude DCM extract (2 g) was performed over reverse phase C18 silica gel (Phenomenex Luna 10 mm C18 silica gel) and 10 fractions (200 ml) were collected using MeOH: H_2O 0–100% stepwise gradient for each extract. Activity was identified in the 80% MeOH fraction and this fraction was subjected to RP-HPLC 60–100% MeOH gradient over 30 min (Phenomenex Gemini 3 μm NX-C18 110 Å, LC Column 30 × 4.6 mm). Isolobophytolide (**2**) eluted at 15 min and the two isomers of isolobophytolide monoacetate (**3**) eluted at 17 min.

For the *S. flexibilis* extract, flexibilide (**6**) and dihydroflexibilide (**7**) were isolated as reported by Kazlauskas et al. (1978). In brief, the DCM extract was subjected to normal phase flash column chromatography with combinations of hexane, DCM and EtOAc. Flexibilide was eluted by 6:1 DCM: EtOAc, 4:1 DCM: EtOAc yielded a mixture of **6** and **7** and 3:1 DCM: EtOAc afforded pure dihydroflexibilide. Sinulariolide (**8**) was isolated separately by a method adapted from Tursch et al. (1975) by direct crystallization of the DCM extract after dissolution in diethyl ether. Purification of compounds was performed by HPLC as described above.

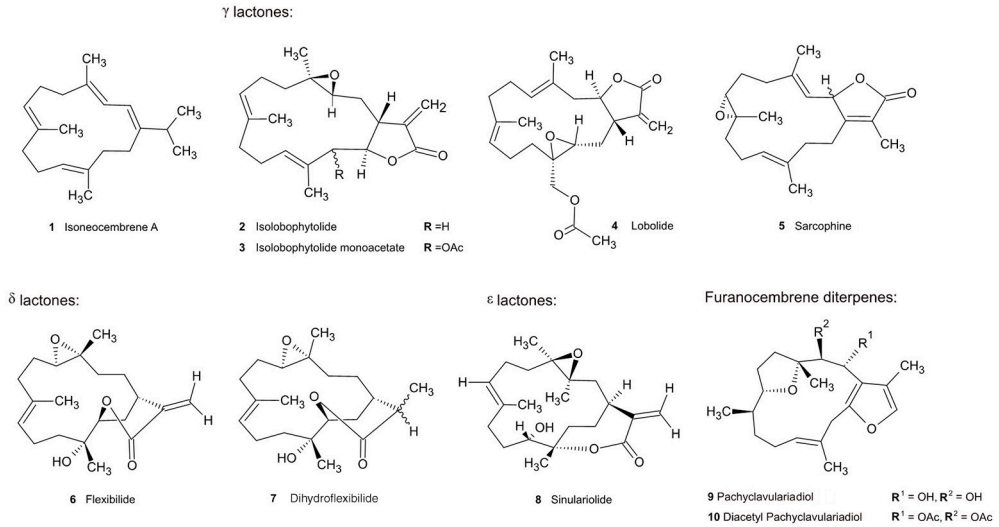

FIGURE 1 | Soft coral cembranoid diterpenes tested for QS interference capability.

TABLE 1 | Functional group analysis of tested soft coral metabolites.

#	Cembranoid diterpene	Secondary ring type	Secondary ring position	Other oxygenated functional groups	Double bonds	Exo methylene	-OH	Oxygenated side chain	Acetate
1	Isoneocembrene A	Absent	Absent	Absent	C4-C5, C8-C9, C12-C13, C14-C1	Absent	Absent	Absent	Absent
2	Isolobophytolide	ɤ lactone	C1-C2	C12-C13 (Epoxide)	C4-C5, C8-C9	Present	Absent	Absent	Absent
3	Isolobophytolide monoacetate	ɤ lactone	C1-C2	C12-C13 (Epoxide)	C4-C5, C8-C9	Present	Absent	Absent	Present
4	Lobolide	ɤ lactone	C1-C14	C3-C4 (Epoxide)	C7-C8, C11-C12	Present	Absent	On C4	C20
5	Sarcophine	α, β unsaturated ɤ lactone	C1-C14	C8-C9 (Epoxide)	C4-C5, C12-C13	Present	Absent	Absent	Absent
6	Flexibilide	δ-lactone	C1-C3	C11-C12 (Epoxide)	C7-C8	Present	C4	Absent	Absent
7	Dihydroflexibilide	δ-lactone	C1-C3	C11-C12 (Epoxide)	C7-C8	Absent	C4	Absent	Absent
8	Sinulariolide	ε-lactone	C1-C4	C12-C13 (Epoxide)	C8-C9	Present	C5	Absent	Absent
9	Pachyclavulariadiol	furan	C1-C2	C9-C12 (Ether)	C1-C2, C14-C15, C15-C16	Absent	Absent	Absent	Absent
10	Diacetyl Pachyclavulariadiol	Furan	C1-C2	C9-C12 (Ether)	C1-C2, C14-C15, C15-C16	Absent	Absent	Absent	C13, C14

Due to instability of the furanocembrenes from *P. violacea*, the pure compounds were generated semi-synthetically as per Bowden et al. (1979). In brief, the DCM extract was prepared at 4°C then partitioned between hexane and 10% aqueous MeOH. After removal of the solvent, the aqueous MeOH fraction was subjected to normal phase flash chromatography with a hexane: EtOAc gradient. All fractions containing (by TLC and ^{1}H NMR) pachyclavulariadiol, diacetyl pachyclavulariadiol and the two monoacetyl pachyclavulariadiols were combined and hydrolyzed to pachyclavulariadiol (**9**) by incubation for 24 h at room temperature with MeOH containing 1% (w/v) potassium hydroxide. Methanol was removed under vacuum and the residue was partitioned between diethyl ether and water. The ether fraction was evaporated and the residue was dissolved in hexane. Diacetyl pachyclavulariadiol (**10**) was acquired by acetylation of half of the obtained pachyclavuriadiol (**9**). Acetylation was affected by incubation for 24 h with 1:1 acetic anhydride in pyridine before evaporation of the solvent and retrieval via liquid a partition between hexane and water. The semi-synthesis of monoacetyl pachyclavulariadiols was not performed as both **9** and **10** exhibited similar activity, so it was considered unlikely that the activities of monoacetyl pachyclavulariadiols would be different.

Structure and purity of each extracted compound was confirmed by 1D and 2D NMR and comparison with literature values. ^{1}H-NMR (600 MHz) and ^{13}C -NMR (150 MHz) spectra were recorded with a Bruker 600 Avance spectrometer in $CDCl_3$, with tetramethylsilane (TMS) as internal standard. High

resolution mass spectra were collected using an unmodified Bruker BioAPEX 47e mass spectrometer equipped with an Analytica model 103426 (Branford, CT) electrospray ionization (ESI) source. Analytical thin layer chromatography (TLC) was performed on Merck Kieselgel 60. Spots were visualized by UV light or by spraying with a 1% vanillin in acidified ethanol solution. Pure compounds were re-solubilized in ethanol and serially diluted to generate five different concentration solutions (1×10^2 mM to 1×10^{-2} mM) for each compound.

Collection, Culture and Extraction of Bacterial Isolates From *S. flexibilis* and *L. compactum* Surface Mucosal Layer

Surface mucosal layer samples (SML) were collected from three healthy replicate colonies of *S. flexibilis* and *L. compactum* from the same depth and location. SML samples were collected underwater from the mid-capitulum region of the coral colony using 50 ml needleless sterile syringes. Samples were maintained at ambient temperatures and processed within 3 h of collection. At the same time as SML samples were retrieved, tissue samples of each replicate were collected and their metabolite ^{1}H NMR spectral profiles were compared with samples from *S. flexibilis* and *L. compactum* collected previously to ensure correct species identification.

SML samples were serially diluted (10^{-2}, 10^{-3}, 10^{-4}) using autoclaved artificial seawater (Instant Ocean; Spectrum Brands, Madison, WI, USA). One hundred microliters of each dilution were spread plated in triplicate on two types of media commonly used for studies of marine bacteria: 50% Marine Agar (50MA; BD) and Glycerol Artificial Seawater (GASW) agar (Smith and Hayasaka, 1982). Additionally, Thiosulfate Citrate Bile Salts (TCBS; BD) agar, which specifically selects for members of the family *Vibrionaceae*, was included. *L. compactum* SML dilutions were additionally plated onto 50MA and GASW agar supplemented with *L. compactum*'s major secondary metabolite, isolobophytolide. All plates were incubated at 28°C and sampled after 48 h, 72 h, 1, and 2 weeks. Representatives of each colony morphotype from each plate were sub-cultured to purity for identification.

Where possible, two representatives of each morphotype were selected for QS activity screening. Where bacteria had initially been isolated using media embedded with isolobophytolide, growth was attempted on the equivalent medium without isolobophytolide. Strains that could not be cultured without isolobophytolide were not included in the screening. Screening was performed on acidified ethyl acetate (EtOAc) extracts of the cell free supernatant of soft coral isolates. These were acquired by transferring single colonies from 50MA plates to liquid culture (10 ml 50% Marine broth culture, 28°C at 170 rpm) and grown to late exponential phase. Cultures were centrifuged for 10 min at 4°C at 10,000 *g* to obtain the cell free supernatant (CFS). Each CFS was subjected to exhaustive extraction with acidified EtOAc (1% acetic acid) and concentrated to dryness under a stream of N_2 gas. Extracts were then dissolved and diluted to a concentration of 20 mg/l with ethanol.

Bacterial QS Biosensor Strains and Culture Medium

The biosensor strains *A. tumefaciens* A136 (Fuqua and Winans, 1996) and *C. violaceum* CV026 (McClean et al., 1997) were used for detection of QS induction and inhibition in soft coral extracts. *A. tumefaciens* A136 was grown on ABt media (Clarrk and Maaloe, 1967) and *C. violaceum* CV026 was grown on Luria Bertani (LB) media (Bertani, 1951). In order to ensure that the QS plasmid was intact and functional, QS biosensor strains were grown in the presence of the appropriate antibiotic (Ravn et al., 2001). *A. tumefaciens* A136 was grown on media supplemented with 4.5 μg/ml of tetracycline and 50 μg/ml of spectinomycin, whereas, *C. violaceum* CV026 was grown on media supplemented with 20 μg/ml of kanamycin (Ravn et al., 2001).

QS Screening Assays

The presence of AHL type QS induction activity in soft coral extracts, fractions and pure compounds was detected by performing an agar diffusion assay as described in detail by Ravn et al. (2001). The QS biosensor strain, either *A. tumefaciens* A136 or *C. violaceum* CV026, was embedded within the agar and the sample being tested was added to a well cut or formed in the agar. For induction of QS, N-hexanoyl homoserine lactone was used as a positive control and extraction solvents were used as negative controls. Positive results were read as a blue coloration surrounding the wells of *A. tumefaciens* A136 and a purple coloration surrounding the wells of *C. violaceum* CV026 (see above and Supplementary Figure 2). The intensity of the response was measured as the diameter of the colored zone and normalized to the response of the positive control.

The agar diffusion assays described above were modified in order to detect QS inhibition. Briefly, as *A. tumefaciens* A136 and *C. violaceum* CV026 are not able to QS without the exogenous addition of AHLs, 8.5 μmol n-hexanoyl homoserine lactone was added into the agar embedded with the biosensor strain in order to test for QS inhibition. Two positive controls were chosen based on their previously reported ability to inhibit QS: n-dodecanoyl-DL-homoserine lactone (McClean et al., 1997) and vanillin (Choo et al., 2006). These controls proved effective for both biosensors. The extraction solvents were once again used as negative controls. Positive results in the inhibition assay were read as inhibition of blue or purple coloration of the plates containing *A. tumefaciens* A136 and *C. violaceum* CV026, respectively (Supplementary Figure 2). The intensity of the response was measured as the width of the inhibition zone surrounding the well and normalized to the positive control.

To generate dose response curves for pure compounds, agar containing the respective biosensor was poured into custom built molds with 28 preformed wells 4 mm in diameter. After solidification of the agar, 20 μl of sample was added to each well. Pure compounds were only tested with the *A. tumefaciens* A136 strain as it was the only strain to have both QS induction and inhibition activity.

Bacterial DNA Extraction, PCR and Sequencing

Genomic DNA of bacterial isolates was extracted using the Promega Wizard Genomic DNA Isolation kit (Promega, Madison WI USA) according to the manufacturer's directions. PCR amplification of 16S rRNA gene fragments was performed using the primers 27F and 1492R (Lane, 1991). The PCR reactions contained the following reagents: 0.4 mM of each primer, 1x MyTAQ buffer (Bioline, Australia), 1.25 U MyTAQ (Bioline, Australia), 1 μL DNA extract (final volume of 50 μL). Cycling conditions were an initial denaturing step of 94°C for 5 min, followed by 30 cycles at 95°C for 1 min, 56°C for 45 s, 72°C for 60 s, and a final elongation step at 72°C for 10 min. PCR products were verified by agarose gel electrophoresis and purified for sequencing using the Qiaquick PCR purification Kit (Qiagen, Valencia, CA) according to company supplied directions. Sanger sequencing was carried out at Macrogen (Seoul, South Korea) using both 27f and 1492R as sequencing primers.

Phylogenetic Analysis of Bacterial Isolates

Sequence fragments were assembled using Sequencher (Version 5, Gene Codes, Ann Arbour, USA). For each isolate, the 16S rRNA gene sequence was aligned with sequences in the nr and Ref_Seq database at the NCBI using the megablast tool (RRID:SCR_001598; Altschul et al., 1990) to identify closely related database sequences. Sequences of isolates and database matches were imported into MEGA6 (MEGA Software, RRID:SCR_000667) and aligned using ClustalW (Larkin et al., 2007). A Maximum Likelihood-based phylogenetic tree was constructed using the Maximum Parsimony algorithm for the starting tree, the Tamura-Nei model for nucleotide substitution, and 500 bootstrap replicates (Supplementary Figure 3). The 16S rRNA gene sequences for the 72 bacterial isolates were deposited into the NCBI Genbank database, under accession numbers KM360403-KM360473. Quantification and statistical analysis of CFUs and isolate morphotypes.

Colony forming unit (CFU) concentrations were estimated based on dilutions yielding between 30 and 300 colonies per plate. Differences in the number of CFUs between samples were determined based on three replicates for the corresponding dilution and media type. Statistical differences were determined using the non-parametric Kruskal-Wallis statistic, as the data violated both normality and homogeneity of variances required for ANOVA. Colony morphotype profile analysis was conducted on the variables color, size and texture and were compared using a nonmetric Multidimensional Scaling (nMDS) analysis in the vegan package (version 2.5-1; Oksanen et al., 2018) in R. The nMDS was chosen based on its suitability for spatial representation of complex data sets containing multiple variables, large numbers of zeroes and non-normal distributions (Rabinowitz, 1975). The statistical analyses were performed using Graphpad PRISM (GraphPad Prism, RRID:SCR_015807).

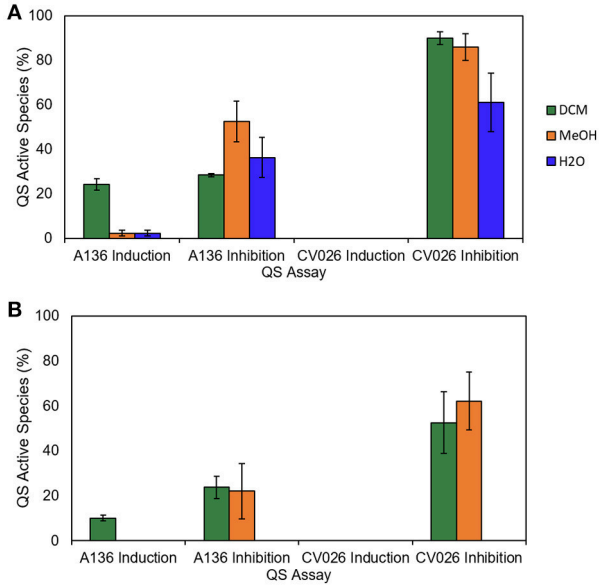

FIGURE 2 | Percentage of soft coral species displaying QS induction or inhibition against *A. tumefaciens* A136 and *C. violaceum* CV026 after addition of **(A)** 40 μg and **(B)** 4 μg extract. Error bars represent the standard error from three screening efforts.

RESULTS

Quorum Sensing Activities of Soft Coral Crude Extracts

Crude soft coral extracts demonstrated the ability to both induce and inhibit QS in the biosensors tested. While both induction and inhibition of QS were observed for the biosensor *A. tumefaciens* A136, none of the extracts, regardless of source coral species, polarity, or concentration, were able to induce QS in *C. violaceum* CV026 (**Figure 2A**). Inhibition of QS was more prevalent than induction across all polarity extracts (**Figure 2A**). For both biosensors, the number of active soft coral extracts was reduced at lower extract concentration, with none of the aqueous extracts retaining their activity at the lower dosage (**Figure 2B**).

Crude extracts of five species induced QS in *A. tumefaciens* A136; two species from the family *Alcyoniidae* (*L. compactum*, *Lobophytum sarcophytoides*), one from the family *Nephtheidae* (*Nephthea chabroli*), one from the family *Clavulariidae* (*P. violacea*), and one from the family *Xeniidae* (*Cespitularia* sp.) (**Figure 3**). The highest incidence and strength of induction activity was seen for DCM crude extracts, with the largest haloes of coloration produced by DCM extracts of *L. compactum* and *P. violacea* (**Figure 3**).

Low level QS inhibition of *A. tumefaciens* A136 was demonstrated for DCM crude extracts of most species, with the only exceptions being *L. microlobulatum*, *Sinularia polydactyla*, *P. violacea*, *Clavularia* sp., and *N. chabroli* (**Figure 4A**). The same trend was seen for MeOH crude extracts, with the additional exception of *Sarcophyton* sp. 2 (**Figure 4A**). Inhibition of QS in *C. violaceum* CV026 was present in DCM crude extracts of

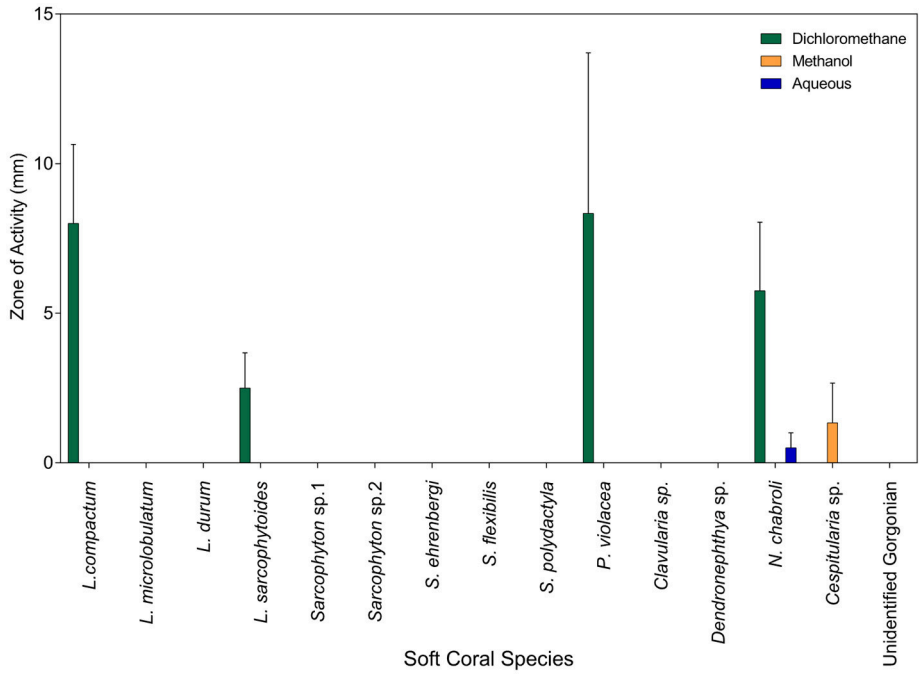

FIGURE 3 | Results of the *A. tumefaciens* A136 QS induction assay for the soft coral extracts from all polarity solvent extracts (dichloromethane, methanol and water). The bars represent positive responses, normalized to the response of the positive control (8.5 μmol N-hexanoyl-DL-homoserine lactone). Error bars represent the standard error from three screening efforts.

all species except *P. violacea* and *Clavularia* sp. (**Figure 4B**). Of the five species that induced QS in *A. tumefaciens* A136, three (*L. compactum*, *L. sarcophytoides* and *Cespitularia* sp.) also inhibited QS in both biosensors (**Figure 4**). This contrasted with the other two species capable of QS induction; *N. chabroli* extracts inhibited QS only in *C. violaceum* CV026 (**Figure 4**) while *P. violacea* demonstrated no QS inhibitory activity with either biosensor (**Figure 4**).

Quorum Sensing Activities of Soft Coral Fractions

For all fractionated species, at least two fractions induced QS in *A. tumefaciens* A136 (**Figure 5**), regardless of whether their corresponding crude extracts were active (**Figure 4**). All species produced fractions that induced QS and inhibited QS in at least one biosensor strain. The only exception was *P. violacea*, which did not inhibit QS in either strain (**Figure 5**) consistent with crude extract results (**Figure 4**). The two largest inductive haloes were observed for *N. chabroli* and *L. compactum*, which also retained their activity at the higher (1:10) dilution level (**Figure 4** The two major bands of induction activity seen in the *A. tumefaciens* A136 bioassay occurred for fractions eluted at 60% MeOH and at 80–90% MeOH (**Figure 5**). Many of the latter fractions (80–90% MeOH) also showed activity in the corresponding QS inhibition bioassay (**Figure 5**). The distinct patterns of QS activity observed for *A. tumefaciens* A136 contrasted strongly with the broad *C. violaceum* CV026 inhibition activity (**Figure 5**). The presence of cembrene diterpenes correlated well with the QS active fractions (data not shown).

Quorum Sensing Activities of Pure Compounds

The response to pure compounds also depended on the biosensor strain utilized. None of the tested cembranoid diterpenes induced QS in *C. violaceum* CV026. In contrast, both QS induction and inhibition activity was observed against *A. tumefaciens* A136 over three to four orders of magnitude, with a loss of activity at higher concentrations (**Figure 6**). No QS interference was observed for isoneocembrene A (Compound **1**; **Figure 6**). The strongest induction of QS in *A. tumefaciens* A136 was observed for pachyclavulariadiol and diacetyl pachyclavulariadiol (Compounds **9** and **10**; **Figure 6**). Induction was also observed in isolobophytolide (Compounds **2** and **3**), lobolide (Compound **4**), and sarcophine (Compound **5**). QS inhibition was strongest in the ε-lactone ring of sinulariolide (**Figure 6**). Peak QS interference for all compounds occurred at approximately 1×10^{-5} mM (or 3 ppm; **Figure 6**).

Culturable Bacteria

A significantly higher number of colony forming units (CFUs) were estimated for mucus of *S. flexibilis* as compared to *L. compactum* (Kruskal-Wallis, $H = 7.200$, 2 d.f., $P = 0.0036$; Supplementary Figure 4). Interestingly, when growth media for *L. compactum* were amended with isolobophytolide, the estimated number of CFUs increased for this species but

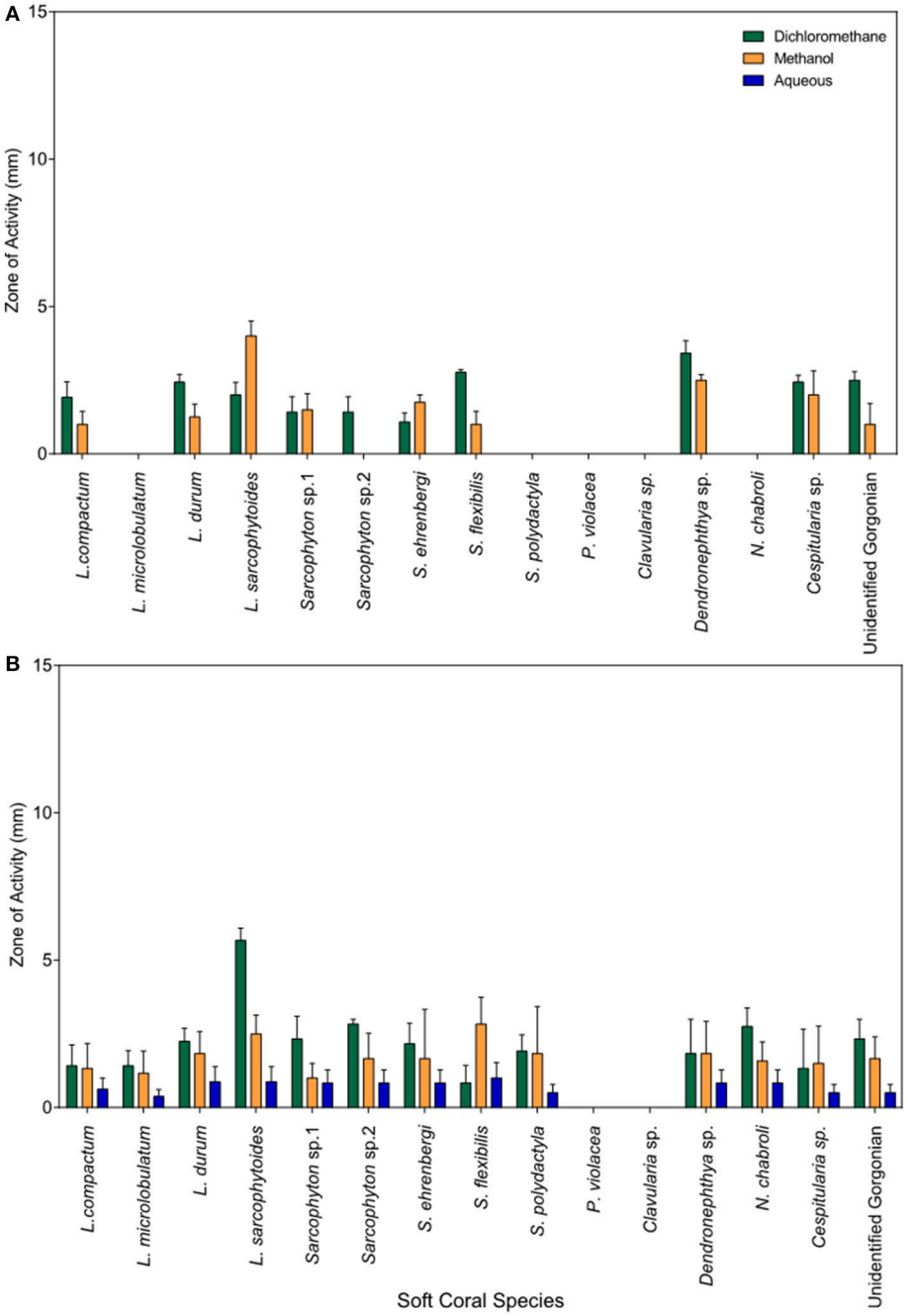

FIGURE 4 | Results of the QS inhibition assay for the soft coral extracts from all polarity solvent extracts (dichloromethane, methanol and water) **(A)** *A. tumefaciens* A136 and **(B)** *C. violaceum* CV026 QS inhibition assay for the soft coral extracts from all polarity solvent extracts (dichloromethane, methanol and water). The bars represent positive responses, normalized to the response of the positive control (vanillin). Error bars represent the standard error from three screening efforts.

remained lower than the estimates for *S. flexibilis* (Supplementary Figure 4). The number and type of colony morphotypes also differed between *L. compactum* and *S. flexibilis* (**Figure 7**). *S. flexibilis* showed little variation in the morphotype profiles of GASW or 50MA media, forming a tight cluster on the nMDS biplot (**Figure 7**). In comparison, the morphotype profiles generated from *L. compactum* showed higher variation in the same culture media. This trend was also consistent when isolobophytolide was added as a selection agent (**Figure 7**).

Sinularia flexibilis Bacterial Isolates

In total, 20 bacterial isolates from *S. flexibilis* were identified through 16S rRNA gene sequencing followed by BLAST searches and construction of phylogenetic trees (Supplementary

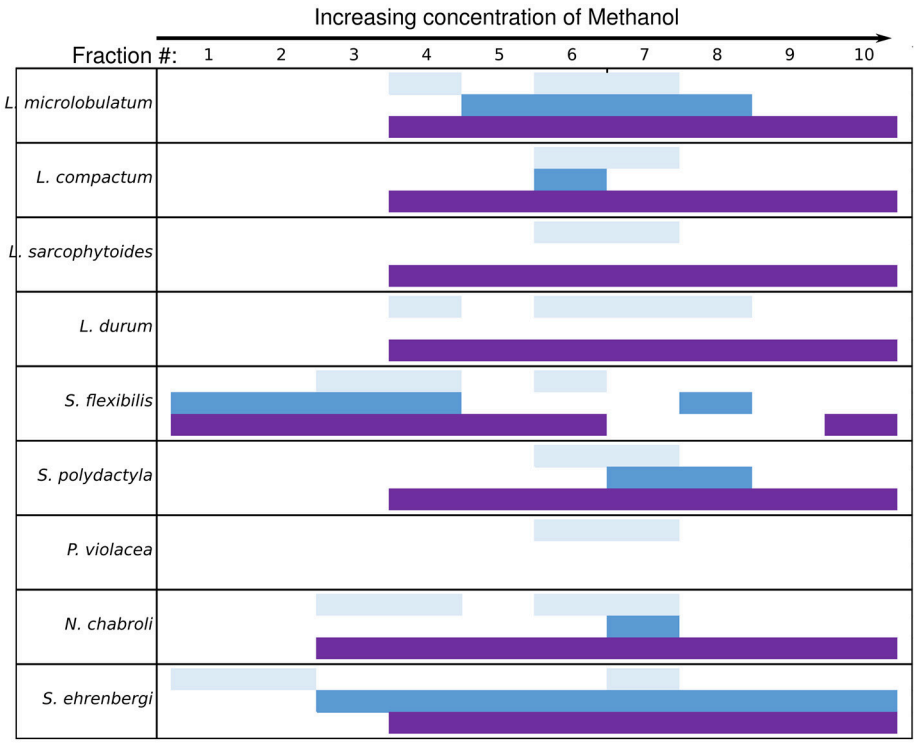

FIGURE 5 | Active soft coral fractions by QS biosensor assay. Fractions were generated using a C18 flash column with a stepwise MeOH:H_2O gradient. Fraction numbers reflect elution order with increasing MeOH percentage. Light blue bars represent the *A. tumefaciens* A136 induction assay, dark blue bars represent the *A. tumefaciens* A136 inhibition assay and the purple bars represent the *C. violaceum* CV026 inhibition assay.

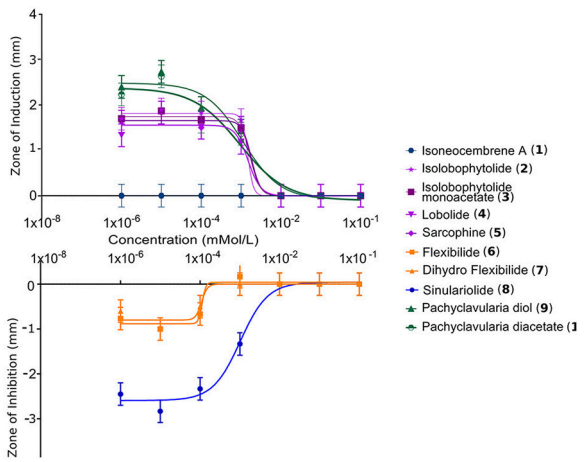

FIGURE 6 | Dose response patterns of QS in *A. tumefaciens* A136 in cembranoid diterpene compounds isolated from soft corals. Although all zones of activity had positive values, for clarity, the zone sizes depicted as positive represent induction of QS and those represented as negative represent inhibition of QS. A zone is defined as the size in mm of either pigment production or pigment inhibition. Concentration refers to the concentration of the compound that was present in the agar wells.

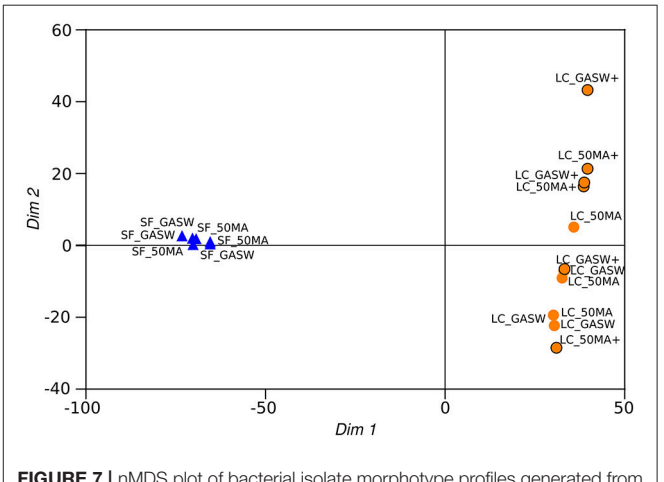

FIGURE 7 | nMDS plot of bacterial isolate morphotype profiles generated from *S. flexibilis* and *L. compactum*. Profiles generated from *S. flexibilis* are indicated by the prefix SF whereas profiles from *L. compactum* are indicated by the prefix LC. 50MA indicates a profile from a 50% marine agar plate, GASW indicates a profile from a Glycerol Artificial Seawater plate. The plus symbol indicates the presence of isolobophytolide in the isolation media.

Table 5, **Figures 8**, **9**). The isolates were dominated by Gammaproteobacteria belonging to the family *Vibrionaceae* both for the non-*Vibrionaceae* targeted media (GASW and 50MA) as well as the *Vibrionaceae* targeted medium (TCBS). Other Gammaproteobacteria included two isolates whose closest relative was "*Spongiobacter nickelotolerans*" (hereafter referred to

as *Endozoicomonas*, see below); and three *Alteromonas*-related strains. Finally, one isolate was identified with 99% sequence identity to *Bacillus megaterium* and *Bacillus aryabhattai* (phylum *Firmicutes*).

The potential of soft coral isolates from *S. flexibilis* to participate in AHL-type QS communication systems was investigated using the same reporter bioassays as used for coral extracts. Quorum sensing activity under the used test conditions was demonstrated for 52.4% of the tested *S. flexibilis* isolates. Both tested *Alteromonas* strains exhibited QS induction activity. The *Alteromonas* SFB10_2 strain triggered QS induction in both sensors strains, whereas, the *Alteromonas* YSF strain only triggered QS induction in *C. violaceum* CV026 (**Figure 8**). Both *Endozoicomonas*-related strains triggered QS induction in *C. violaceum* CV026 only. In addition, both strains triggered QS inhibition in *A. tumefaciens* A136, while QS inhibition in *C. violaceum* CV026 was only triggered by strain SF102 (**Figure 8**). We note that out of the 62 bacterial strains screened in this study, the two *Endozoicomonas*-related strains from *S. flexibilis* were the only strains with both induction and inhibition QS activity. Of the tested *Vibrionaceae* strains, 6 of 14 strains showed QS activity and this was evenly split between induction (3 strains) and inhibition (3 strains) activity.

Lobophytum compactum Bacterial Isolates

The isolates cultured from *L. compactum* demonstrated a number of similarities to the bacteria isolated from *S. flexibilis* (Supplementary Table 5, **Figures 10**, **11**). Firstly, the majority of *L. compactum* isolates were gammaproteobacteria of the genus *Vibrionaceae* (30/51). Secondly, strains related to the genera *Endozoicomonas* and *Bacillus*, and the order *Alteromonadales*, were isolated also from this soft coral species. In this instance, however, the diversity of *Alteromonadales*-related strains was higher with strains related not only to the genus *Alteromonas* (seven strains) but also to the genera *Pseudoalteromonas* (six strains), *Paramoritella*, *Ferrimonas*, and *Shewanella*. In contrast to the *S. flexibilis* isolates, the *L. compactum* isolates also included strains belonging to the genera *Psychrobacter* (class *Gammaproteobacteria*), *Erythrobacter* (class *Alphaprotebacteria*), and *Micrococcus* (class *Actinobacteria*).

The potential of soft coral isolates from *L. compactum* to participate in AHL-type QS communication systems was also investigated (**Figure 10**). Of the tested isolates from *L. compactum*, 47.5% demonstrated QS activity at the growth conditions tested and activity was mixed between induction and inhibition. Three of the tested *Vibrio* strains (LC111, LC103, and LC105) showed inhibitory activity against both biosensors. Of the strains that were initially isolated with media containing isolobophytolide, 41% were unable to be cultured in the absence of this compound and consequently were not tested for QS activity.

DISCUSSION

Soft Coral Extracts

This study has demonstrated that QS interference extends across at least four soft coral families (*Alcyoniidae*, *Clavulariidae*, *Nephtheidae*, and *Xeniidae*). Further, it was shown that both induction and inhibition QS activity extends across both polar and non-polar fractions, indicating that QS interference capability is widespread in soft corals from the central Great Barrier Reef, Australia.

Widespread activity, across not only species that are known to contain different metabolite types but also across a range polarities (indicated by the activities of extracts obtained by use of solvents with different polarities), is probably indicative of active compounds of more than one structural type. This is further supported by the finding that most (except *P. violacea*) of the soft coral species that induced QS in *A. tumefaciens* A136, also inhibited both biosensors. The widespread prevalence of QS inhibition as well as the presence of QS induction in the soft corals screened here is consistent with QS activity found across a range of marine invertebrates (Taylor et al., 2004; Skindersoe et al., 2008; Hunt et al., 2012). The dual presence of induction and inhibition of QS is similar to that found previously in gorgonian coral extracts (Hunt et al., 2012) but contrasts with the sole QS inhibition activity that was identified in *D. pulchra* (Kjelleberg et al., 1997). QS induction was also established in extracts of marine sponges and sponge associated bacteria (Taylor et al., 2004). Results from this study highlight the need to examine both induction and inhibition of QS to generate a realistic understanding of the complexity of ecological interactions between a host organism and its associated bacteria.

Soft Coral Fractions

In contrast with the initial crude extract testing, all the fractionated soft corals displayed at least one active fraction in the *A. tumefaciens* A136 QS induction assay. This may reflect an inherent increase in concentration of the active components or a decrease in complexity of the samples being tested. Soft coral extracts and fractions may be highly complex mixtures of compounds with contrasting QS regulatory activities. The potential for activity masking within extracts, a phenomenon previously observed in the QS screening of marine sponge extracts (Taylor et al., 2004), is high. This is particularly true if only one concentration or level of complexity is tested.

The QS induction pattern of the soft coral fractions was generally limited to one or two active fractions (80 and 90% methanol elution) for each species suggests that the inductive capability may be due to the presence of structurally similar compounds. Cembranoid diterpenes are well documented in eleven of the soft coral species tested (MarinLit Database, 2013) and correlated well to QS induction therefore could be responsible for the observed QS activity in these species. The same diterpene scaffolds, however, are not commonly known in the genera *Nephthea* (Amir et al., 2012a,b) *Cespitularia* (Elshamy et al., 2016) or in gorgonian corals (Changyun et al., 2008), so cembranoid diterpenes cannot fully explain the observed QS interference in these species. Isolation of cembranoid diterpenes was therefore required to understand the relative importance of these secondary metabolites to act as QS mimics.

A similarly discrete pattern was not reflected in the QS inhibition profile for these fractions. The broad QS inhibition profile of these fractions, might be due to multiple compounds,

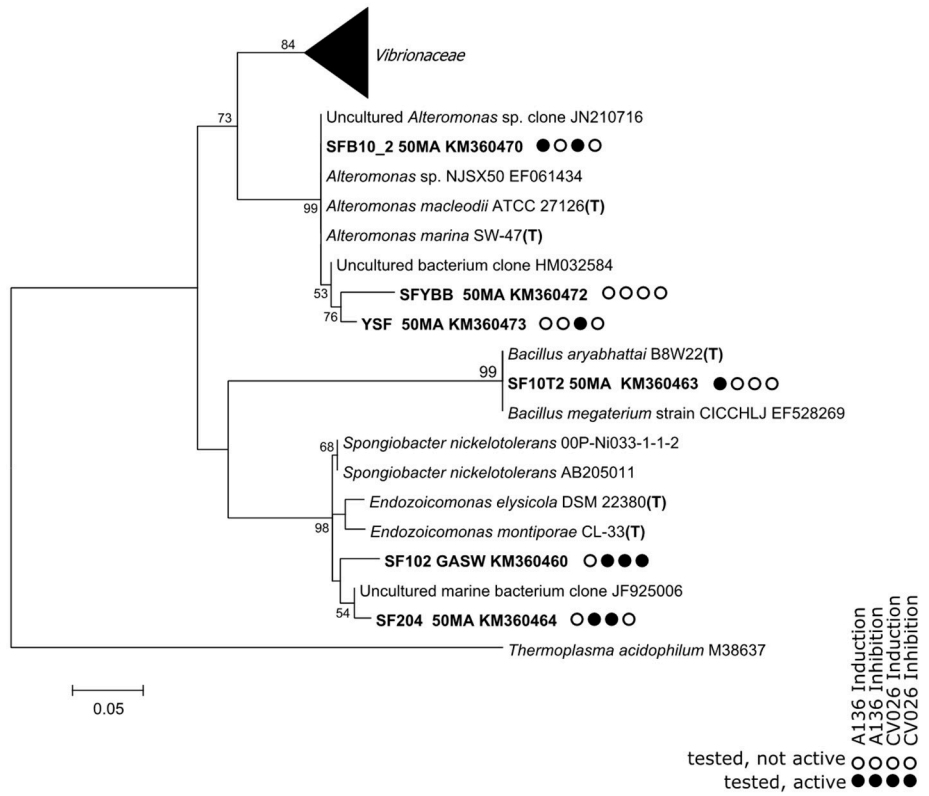

FIGURE 8 | A phylogenetic tree based on partial 16S rRNA gene sequences retrieved from bacterial isolates from the mucus of the soft coral *S. flexibilis*. Details of the *Vibrionaceae* are shown in **Figure 9**. The tree is based on maximum-likelihood analysis, using a 50% conservation filter. The scale bar indicates 5% estimated sequence divergence. *Thermoplasma acidophilum* was used as the outgroup for analysis. Isolated sequences and their accession numbers are indicated in bold type. The nearest matches from the NCBI databases are included. T indicates that the sequence originates in the species type strain.

or, the compound(s) responsible may not be suited to the method of fractionation used and the same compounds could be spread across several fractions. The presence of multiple QS compounds within a single holobiont would potentially enable a larger number of interactions with different bacterial strains and / or trigger different QS responses. This complexity may also reflect the capability of some bacteria to possess multiple QS systems (Reshef et al., 2006), with each system regulating a different process or interaction.

Pure Compounds

The strength and type of QS interference by cembranoid diterpenes was observed to correlate with the size of the oxygenated ring. Those cembranoid diterpenes that contained either a five membered furan or lactone ring were capable of inducing QS in *A. tumefaciens* A136, whereas the cembranoid diterpenes with larger lactone rings (six or seven membered) were seen to inhibit QS in *A. tumefaciens* A136. The type of oxygenated functional group also appears to impact the strength these QS mimics, with the furans tested (Compounds **9** and **10**) having higher activities than the ɣ lactones (Compounds **2**-**5**). In keeping with our current understanding of the QS mechanism, QS interference was only observed for cembranoid diterpenes possessing secondary oxygen rings (Fuqua et al., 2001; Watson et al., 2002; Geske et al., 2008). The presence of other minor functional groups (epoxides, acetates or level of saturation) had minimal discernible impact on the strength of QS interference observed and no obvious effect on the type of activity observed with respect to *A. tumefaciens* A136. QS mimics have previously been isolated that possess a ɣ lactone, however, these mimics (such as the furanones of *D. pulchra*) are often associated with QS inhibition rather than the inductive activity demonstrated here (Givskov et al., 1996; Defoirdt et al., 2013). In the case of the furanones from *D. pulchra*, bromine substituents are also present and may be influencing the type of activity. The presence of these metabolites in soft corals is strongly correlated to their taxonomy and may represent different strategies of interaction between species.

A common feature of QS mimic compounds previously identified from eukaryotic extracts is multiple forms of biological activity (Davies, 2006; Yim et al., 2007; Defoirdt et al., 2013). Cembranoid diterpenes appear to be no different with a number, including those identified in the current study, having previously been reported to demonstrate antibiotic (Aceret et al., 1995), cytotoxic (Maida et al., 1993) and algacidal properties. The antimicrobial activity identified in flexibilide (**7**) by Aceret et al. (1995), however, was exhibited at concentrations at least one order of magnitude higher than those that produced QS

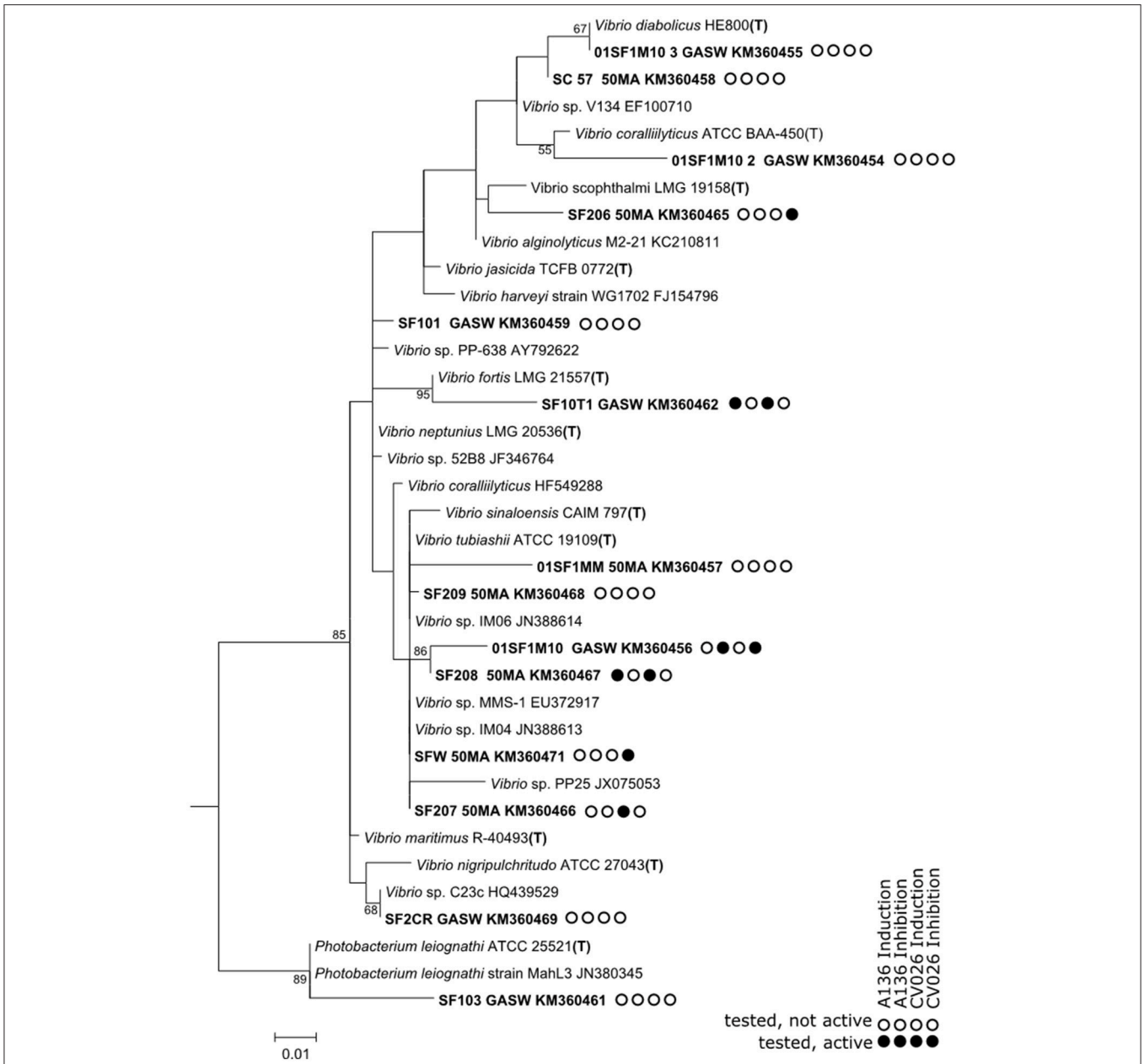

FIGURE 9 | *Vibrionaceae* sub-tree based on 16S rRNA gene sequences retrieved from an analysis of bacterial isolates from the mucus of the soft coral *S. flexibilis*. The tree is based on maximum-likelihood analysis, using a 50% conservation filter. The scale bar indicates 1% estimated sequence divergence. *Thermoplasma acidophilum* was used as the outgroup for analysis. Isolated sequences and their accession numbers are indicated in bold type. The nearest matches from the NCBI databases are included. T indicates that the sequence originates in the species type strain.

interference in this study. The peak QS active concentration occurred 1×10^{-5} mM (or 3 ppm), reflecting the concentrations of flexibilide and sarcophytoxide in the mucous and water column surrounding *S. flexibilis* and *S. crassocaule* detected by Coll et al. (1982). Rather than being incompatible, the contrasting activities could be evidence of a hormetic response. Hormetic relationships have been previously observed in the QS mimics from garlic (Persson et al., 2005) and some antibiotic compounds, whereby growth stimulation or cell signaling properties are exhibited at concentrations below their minimum growth inhibitory concentration (Davies, 2006; Yim et al., 2007). A hormetic response could be relevant in soft corals with loosely packed sclerites, where uptake or release of water from the tissue can lead to large changes in volume over a matter of hours (Freckelton, 2015). As a result, associated metabolites will show a correspondingly dramatic change in concentration in the tissues on a volumetric basis over the same time period. More research is required to understand the potential of hormetic relationships

FIGURE 10 | A phylogenetic tree based on 16S rRNA gene sequences retrieved from an analysis of bacterial isolates from the mucus of the soft coral *L. compactum*. Details of the *Vibrionaceae* are shown in **Figure 11**. The tree is based on maximum-likelihood analysis, using a 50% conservation filter. The scale bar indicates 10% estimated sequence divergence. *Thermoplasma acidophilum* was used as the outgroup for analysis. Isolated sequences and their accession numbers are indicated in bold type. The nearest matches from the NCBI databases are included. T indicates that the sequence originates in the species type strain.

in QS mimics and how such concentration changes could be manipulated in the defense of the coral.

Strong evidence for the ecological role of cembranolides and furanocembranoid diterpenes as QS mimics is further exhibited in the strong differences in the ability of the two biosensor strains to respond to QS mimics in the soft corals. The QS inductive compounds present within the soft corals were more readily detected by the *A. tumefaciens* A136 strain. In contrast, QS inhibition was observed more frequently for *C. violaceum* CV026. This could suggest that *C. violaceum* CV026 can be inhibited by a broader range of compounds or that it is more sensitive to a broader range of compound concentrations. This

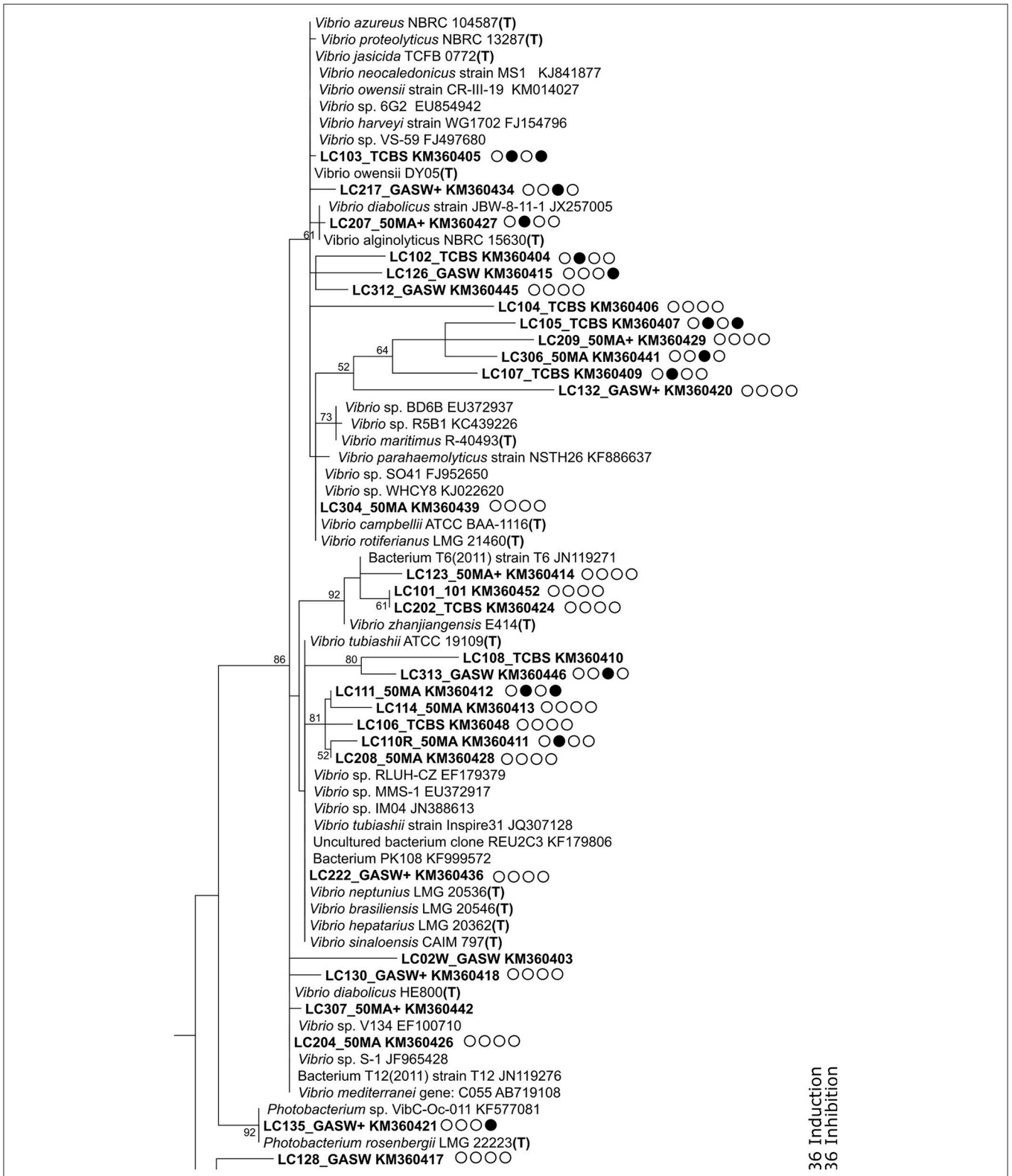

FIGURE 11 | *Vibrionaceae* sub-tree tree (part of tree presented in **Figure 10**) based on 16S rRNA gene sequences retrieved from an analysis of bacterial isolates from the mucus of the soft coral *L. compactum*. The tree is based on maximum-likelihood analysis, using a 50% conservation filter. The scale bar indicates 10% estimated sequence divergence. *Thermoplasma acidophilum* was used as the outgroup for analysis. Isolated sequences and their accession numbers are indicated in bold type. The nearest matches from the NCBI databases are included. T indicates that the sequence originates in the species type strain.

difference in sensitivity is despite an overlap of AHL acyl chain length detection by the two biosensor strains (Steindler and Venturi, 2007). *A. tumefaciens* A136 utilizes the TraR QS response regulator system and responds to a broad range of acyl chain lengths in AHL molecules (Steindler and Venturi, 2007). *C. violaceum* responds to a shorter range of acyl chain lengths in AHL molecules and utilizes the CivR QS response regulator (Steindler and Venturi, 2007). The differential responses of these two biosensors highlights the advantage of using multiple biosensors when screening for QS mimics where chain length sensitivities may have little applicability.

Isolated Bacteria

This study strongly suggests that isolobopytolide, the major secondary metabolite in *L. compactum*, is an important selection factor regulating the microbial community of this soft coral. Firstly, we demonstrated that isolobophytolide can interfere with the QS activity of sensor strains, and secondly we demonstrated that addition of isolobophytolide to culture media increased the number and morphological variation of colonies produced from *L. compactum*. Moreover, the latter result suggests that the inclusion of secondary metabolites in growth media can improve the success of culturing soft coral associated bacterial isolates.

Most isolates generated in this study had high sequence identity with bacterial sequences sourced from the marine environment, including marine invertebrate hosts (Supplementary Table 5). Many of the recovered genera have also previously been isolated from coral mucus samples including *Alteromonas*, *Bacillus*, *Endozoicomonas*, *Erythrobacter*, *Micrococcus*, *Pseudoalteromonas*, *Shewanella,* and *Vibrio* (Lampert et al., 2006; Nithyanand and Pandian, 2009; Pootakham et al., 2017). The isolates were dominated by gammaproteobacteria belonging to the family *Vibrionaceae*, a result that is consistent with previous observations in scleractinian corals (Kvennefors et al., 2010, 2012). For both coral species, several *Vibrio* strains were isolated whose sequences clustered together and separately from the most closely related database sequences and hence may represent novel species. Scleractinian corals have previously been recognized as harboring a number of novel bacterial taxa (Rohwer et al., 2002; Sunagawa et al., 2010). This situation still remains, with amplicon-based studies of coral microbiomes returning many unassigned OTUs (Blackall et al., 2015). The bacteria of alcyonacean corals are less well studied and it is reasonable to assume that a similar situation could exist.

Multiple strains capable of inducing and/or disrupting QS in the bacterial biosensors were isolated from *L. compactum* and *S. flexibilis* (57.5 and 57.8% of tested strains, respectively). The genera of all the bacteria isolated, regardless of activity detected in this study, have previously been reported to possess or interact with QS systems (Ansaldi et al., 2002; Long et al., 2003; Waters and Bassler, 2005; Case et al., 2008; Tait et al., 2009, 2010; Nithya et al., 2010; Albuquerque and Casadevall, 2012; Lade et al., 2014), providing support for the hypothesis that QS is one of the mechanisms regulating coral associated microbial communities.

There was no clear taxonomic pattern of QS activity within the *Vibrionaceae*, which is consistent with a previous study that assessed QS activity in 29 *Vibrionaceae* strains (Tait et al., 2010). It is well recognized that QS in *Vibrio* spp. is tightly regulated by environmental conditions including host-released cues and nutritional status (Waters and Bassler, 2005). *Vibrio* spp. are ubiquitous in the marine environment (Urakawa and Rivera, 2006), however many *Vibrio* strains have been implicated in disease either as primary or opportunistic pathogens (Urakawa and Rivera, 2006). Given that QS is involved in the regulation of a number of the genes involved in pathogenicity (de Kievit and Iglewski, 2000; LaSarre and Federle, 2013), the presence of a wide range of *Vibrio* spp. with QS capabilities in otherwise healthy corals warrants further investigation to elucidate which genes are under QS control in these species.

"*Spongiobacter,*" now recognized as belonging to the genus *Endozoicomonas* (Neave et al., 2016), was originally recovered from a marine sponge (Pike et al., 2013) but is also present in many gorgonian (Sunagawa et al., 2010; La Rivière et al., 2013) and scleractinian corals (Raina et al., 2009; Blackall et al., 2015; Bourne et al., 2016). "*Spongiobacter*" strains have been attributed a number of ecological roles; "*Spongiobacter*" strains from *A. millepora* demonstrated a dependence on DMSP and consequently a role in the biogeochemical sulfur cycle was postulated (Raina et al., 2009), whereas, "*Spongiobacter*" strains from the sponge *Suberites carnosus* demonstrated antibacterial activity (Flemer et al., 2012). Of greatest interest to this study is the QS activity detected in "*Spongiobacter*" strains from the sponges *Mycale laxissima* and *Ircinia strobilina* (Mohamed et al., 2008). The *Endozoiocomonas*-related strains SF102 and SF204 from *S. flexibilis* that were tested in this study induced QS activity in *C. violaceum* CV026 and not in *A. tumefaciens* A136, whereas Mohamed and coworkers found the opposite response (positive in *A. tumefaciens* and negative in *C. violaceum*).

In this study, QS activities were assessed for the culturable fraction of bacteria associated with the mucus of two soft coral species. In future, functional gene analysis and gene expression analysis may allow a more complete assessment of the genes that are responsible for and regulated by QS in these bacteria. Moreover, new –omics techniques will allow investigations of quorum sensing genes and their expression also in bacteria that cannot easily be cultured with standard methods. A combination of culture-independent studies and manipulative experiments using isolates holds great promise for further elucidation of QS mechanisms in soft coral holobiomes.

CONCLUSION

This research establishes a framework for the importance of QS and the identity of potential QS mimics within the soft coral holobiont, highlighting the potential value of soft corals as a model system for both structural and ecological investigations of QS mimics. The results presented here

clearly show that cembranolides and furanocembrenes are partially responsible for previously observed QS interference in soft coral extracts. Their QS interference translates to a potentially new structural backbone for QS mimic compounds. The size of the oxygenated ring had more bearing on the activity expressed than the presence or position of epoxides, double bonds or acetate groups, an observation which extends the structural understanding of QS mimics. QS interference extended however also to soft coral species not known to contain cembranolides and furanocembrenes, suggesting that new structural backbones with QS activity remain to be elucidated. The presence of both QS metabolites and QS bacteria within soft corals supports the role of QS as a way of mediating soft coral associated microbial communities. If the active compounds in these extracts are indeed produced by the soft coral, this interaction with QS could be important to the health and resilience of the host organism and may reflect a more widespread strategy of sessile marine invertebrates.

ETHICS STATEMENT

Soft coral samples were legally collected between 2009 and 2015 under Great Barrier Reef Marine Park Authority (GBRMPA) permits (G09/30327.1, G12/35236.1).

DATA AVAILABILITY STATEMENT

The raw data supporting the conclusions of this manuscript will be made available by the authors, without undue reservation, to any qualified researcher.

AUTHOR CONTRIBUTIONS

MF experimental design, sample collection, lab work, data analysis and write-up. LH experimental design, data analysis and write-up. BB experimental design, sample collection, data analysis and write-up.

ACKNOWLEDGMENTS

The authors would like to thank Dr. Cherie Motti at the Biomolecular Analysis Facility, Australian Institute of Marine Science, for her invaluable experience and technical expertise. We would also like to thank Dr. Linda Blackall (now University of Melbourne) for preliminary discussions on Quorum Sensing. Dr. Tilmann Harder and Dr. Nete Bernbom at the Centre for Marine *Biofouling* and Bio-Innovation, University of New South Wales, are thanked for giving access to and providing invaluable training in the use of quorum sensing assays. This research was funded by the Australian Institute of Marine Science Futures project and by the AIMS@JCU Joint Venture as part of MF's Ph.D. project. MF was supported by an Australian government research training program scholarship. The presented data have previously been published online as part of MF's doctoral dissertation (Freckelton, 2015).

SUPPLEMENTARY MATERIAL

The Supplementary Material for this article can be found online at: https://www.frontiersin.org/articles/10.3389/fmars.2018.00198/full#supplementary-material

REFERENCES

Aceret, T. L., Sammarco, P. W., and Coll, J. C. (1995). Toxic effects of alcyonacean diterpenes on scleractinian corals. *J. Expt. Mar. Biol. Ecol.* 188, 63–78. doi: 10.1016/0022-0981(94)00186-H

Albuquerque, P., and Casadevall, A. (2012). Quorum sensing in fungi-a review. *Med. Mycol.* 50, 337–345. doi: 10.3109/13693786.2011.652201

Altschul, S. F., Gish, W., Miller, W., Myers, E. W., and Lipman, D. J. (1990). Basic local alignment search tool. *J. Mol. Biol.* 215, 403–410. doi: 10.1016/S0022-2836(05)80360-2

Amir, F., Koay, Y. C., and Yam, W. S. (2012a). Chemical constituents and biological properties of the marine soft coral Nephthea: a review (Part 1). *Trop. J. Pharm. Res.* 11, 485–498.

Amir, F., Koay, Y. C., and Yam, W. S. (2012b). Chemical constituents and biological properties of the marine soft coral Nephthea: a review (Part 2). *Trop. J. Pharm. Res.* 11, 499–517.

Ansaldi, M., Marolt, D., Stebe, T., Mandic-Mulec, I., and Dubnau, D. (2002). Specific activation of the *Bacillus* quorum-sensing systems by isoprenylated pheromone variants. *Mol. Microbiol.* 44, 1561–1573. doi: 10.1046/j.1365-2958.2002.02977.x

Bauer, W. D., and Robinson, J. B. (2002). Disruption of bacterial quorum sensing by other organisms. *Curr Opin Biotechnol.* 13, 234–237 doi: 10.1016/S0958-1669(02)00310-5

Bertani, G. (1951). Studies on Lysogenesis. *J Bacteriol.* 62, 293–300

Blackall, L. L., Wilson, B., and Van Oppen, M. J. H. (2015). Coral—the world's most diverse symbiotic ecosystem. *Molec. Ecol.* 24, 5330–5347. doi: 10.1111/mec.13400

Bourne, D. G., Morrow, K. M., and Webster, N. S. (2016). Insights into the Coral Microbiome: Underpinning the Health and Resilience of Reef Ecosystems. *Annu. Rev. Microbiol.* 70:317–340 doi: 10.1146/annurev-micro-102215-095440

Bowden, B. F., Coll, J. C., Mitchell, S. J., Raston, C. L., Stokie, G. J., and White, A. H. (1979). Studies of Australian Soft Corals. XV. The structure of pachyclavulariadiol, a novel furano-diterpene from *Pachyclavularia violacea*. *Aust. J. Chem.* 32, 2265–2274. doi: 10.1071/CH9792265

Case, R. J., Labbate, M., and Kjelleberg, S. (2008). AHL-driven quorum-sensing circuits: their frequency and function among the Proteobacteria. *ISME J.* 2, 345-349. doi: 10.1038/ismej.2008.13

Changyun, W., Haiyan, L., Changlun, S., Yanan, W., Liang, L., and Huashi, G. (2008). Chemical defensive substances of soft corals and gorgonians. *Acta Ecol. Sin.* 28, 2320–2328.

Chhabra, S. R., Philipp, B., Eberl, L., Givskov, M., Williams, P., and Cámara, M. (2005). "Extracellular communication in bacteria," in *The Chemistry of Pheromones and Other Semiochemicals II,* ed S. Schultz (Berlin: Springer), 279–315.

Chong, G., Kimyon, O., Rice, S. A., Kjelleberg, S., and, M., Manefield (2012). The presence and role of bacterial quorum sensing in activated sludge *Microb. Biotechnol.* 5, 621–633

Choo, J. H., Rukayadi, Y., and Hwang, J.-K. (2006). Inhibition of bacterial quorum sensing by vanilla extract. *Lett. Appl. Microbiol.* 42, 637–641. doi: 10.1111/j.1472-765X.2006.01928.x

Clarrk, D., and Maaloe, O. (1967). DNA replication and division cycle in *Escherichia coli J Mol Biol.* 23, 99–112.

Coll, J. C., Bowden, B. F., Tapiolas, D. M., and Dunlap, W. C. (1982). *In situ* isolation of allelochemicals released from soft corals (Coelenterata:

Octocorallia): A totally submersible sampling apparatus. *J. Exp. Mar. Biol. Ecol.* 60, 293–299. doi: 10.1016/0022-0981(82)90166-6

Davies, J. (2006). Are antibiotics naturally antibiotics? *J Ind. Microbiol. Biotechnol.* 33, 496–499. doi: 10.1007/s10295-006-0112-5

Defoirdt, T., Brackman, G., and Coenye, T. (2013). Quorum sensing inhibitors: how strong is the evidence? *Trends Microbiol.* 21, 619–624.

de Kievit, T., and Iglewski, B. H. (2000). Bacterial quorum sensing in pathogenic relationships. *Infect. Immun.* 68, 4839–4849. doi: 10.1128/IAI.68.9.4839-4849.2000

Dong, Y. H., Wang, L. Y., and Zhang, L. H. (2007). Quorum-quenching microbial infections: mechanisms and implications. *Philos. Trans. R. Soc. Lond. B. Biol. Sci.* 362, 1201–1211. doi: 10.1098/rstb.2007.2045

Dudler, R., and Eberl, L. (2006). Interactions between bacteria and eukaryotes via small molecules. *Curr. Opin. Biotechnol.* 17, 268–273. doi: 10.1016/j.copbio.2006.04.004

Elshamy, A. I., Nassar, M. I., Mohamed, T. A., and Hegazy, M.-E. F. (2016). Chemical and biological profile of *Cespitularia* species: a mini review. *J. Adv. Res.* 7, 209–224. doi: 10.1016/j.jare.2015.07.003

Farrand, S., Qin, Y., and Oger, P. (2002). Quorum-sensing system of Agrobacterium plasmids: analysis and utility. *Meth. Enzymol.* 358, 452–484. doi: 10.1016/S0076-6879(02)58108-8

Flemer, B., Kennedy, J., Margassery, L., Morrissey, J., O'Gara, F., and Dobson, A. (2012). Diversity and antimicrobial activities of microbes from two Irish marine sponges, *Suberites carnosus* and *Leucosolenia* sp. *J. Appl. Microbiol.* 112, 289–301. doi: 10.1111/j.1365-2672.2011.05211.x

Freckelton, M. L. (2015). *Quorum Sensing in Australian Soft Corals*. Ph.D. thesis. Townsville, QLD: James Cook University. Available online at: http://researchonline.jcu.edu.au/41083

Fuqua, C., Parsek, M. R., and Greenberg, E. P. (2001). Regulation of gene expression by cell-to-cell communication: acyl-homoserine lactone quorum sensing. *Annu. Rev. Genet.* 35, 439–468. doi: 10.1146/annurev.genet.35.102401.090913

Fuqua, C., and Winans, S. C. (1996). Conserved cis-acting promoter elements are required for density-dependent transcription of *Agrobacterium tumefaciens* conjugal transfer genes. *J. Bacteriol.* 178, 435–440. doi: 10.1128/jb.178.2.435-440.1996

Geske, G. D., O'Neill, J. C., Miller, D. M., Wezeman, R. J., Mattmann, M. E., Lin, Q., et al. (2008). Comparative analyses of N-acylated homoserine lactones reveal unique structural features that dictate their ability to activate or inhibit quorum sensing. *Chembiochem.* 9, 389–400. doi: 10.1002/cbic.200700551

Givskov, M., de Nys, R., Manefield, M., Gram, L., Maximilien, R. I., Eberl, L., et al. (1996). Eukaryotic interference with homoserine lactone-mediated prokaryotic signalling. *J. Bacteriol.* 178, 6618–6622. doi: 10.1128/jb.178.22.6618-6622.1996

Golberg, K., Eltzov, E., Shnit-Orland, M., Marks, R. S., and Kushmaro, A. (2011). Characterization of quorum sensing signals in coral-associated bacteria. *Microb. Ecol.* 61, 783–792. doi: 10.1007/s00248-011-9848-1

Golberg, K., Pavlov, V., Marks, R. S., and Kushmaro, A. (2013). Coral-associated bacteria, quorum sensing disrupters, and the regulation of biofouling. *Biofouling.* 29, 669–682. doi: 10.1080/08927014.2013.796939

González, J. E., and Keshavan, N. D. (2006). Messing with bacterial quorum sensing. *Microbiol. Mol. Biol. Rev.* 70, 859–875. doi: 10.1128/MMBR.00002-06

Hunt, L. R., Smith, S. M., and Downum, K. R. (2012). Microbial regulation in gorgonian corals. *Mar. Drugs.* 10, 1225–1243. doi: 10.3390/md10061225

Joint, I., Downie, A. J., and Williams, P. (2007). Bacterial conversations: talking, listening and eavesdropping. *An introduction. Philos. Trans. R. Soc. Lond. B. Biol. Sci.* 362, 1115–1117. doi: 10.1098/rstb.2007.2038

Kazlauskas, R., Murphy, P. T., Wells, R. J., Schonholzer, P., and Coll, J. C. (1978). Cembranoid constituents from an Australian collection of the soft coral *Sinularia flexibilis*. *Aust. J. Chem.* 31, 1817–1824. doi: 10.1071/CH9781817

Kjelleberg, S., Steinberg, P., Givskov, M., Gram, L., Manefield, M., and de Nys, R. (1997). Do marine natural products interfere with prokaryotic AHL regulatory systems? *Aquat. Microb. Ecol.* 13, 85–93. doi: 10.3354/ame013085

Kvennefors, E. C. E., Sampayo, E., Kerr, C., Vieira, G., Ro,-, G., and Barnes, A. C. (2012). Regulation of bacterial communities through antimicrobial activity by the coral holobiont. *Microb. Ecol.* 63, 605–618. doi: 10.1007/s00248-011-9946-0

Kvennefors, E. C. E., Sampayo, E., Ridgway, T., Barnes, A. C., and Hoegh-Guldberg, O. (2010). Bacterial communities of two ubiquitous Great Barrier Reef corals reveals both site-and species-specificity of common bacterial associates. *PLoS ONE* 5:e10401. doi: 10.1371/journal.pone.0010401

Lade, H., Paul, D., and Kweon, J. H. (2014). Isolation and molecular characterization of biofouling bacteria and profiling of quorum sensing signal molecules from membrane bioreactor activated sludge. *Int. J Mol. Sci.* 15, 2255–2273. doi: 10.3390/ijms15022255

Lampert, Y., Kelman, D., Dubinsky, Z., Nitzan, Y., and Hill, R. T. (2006). Diversity of culturable bacteria in the mucus of the Red Sea coral *Fungia scutaria*. *FEMS. Microbiol. Ecol.* 58, 99–108. doi: 10.1111/j.1574-6941.2006.00136.x

Lane, D. (1991). "16S/23S rRNA sequencing", in *Nucleic Acid Techniques in Bacterial Systematic*, eds E. Stackebrandt, and M. Goodfellow (New York, NY: John Wiley and Sons), 115–175.

La Rivière, M., Roumagnac, M., Garrabou, J., and Bally, M. (2013). Transient shifts in bacterial communities associated with the temperate gorgonian *Paramuricea clavata* in the northwestern Mediterranean Sea. *PLoS ONE* 8:e57385. doi: 10.1371/journal.pone.0057385

Larkin, M. A., Blackshields, G., Brown, N., Chenna, R., McGettigan, P. A., McWilliam, H., et al. (2007). Clustal W and Clustal X version 2.0. *Bioinformatics.* 23, 2947–2948. doi: 10.1093/bioinformatics/btm404

LaSarre, B., and Federle, M. J. (2013). Exploiting quorum sensing to confuse bacterial pathogens. *Microbiol. Mol. Biol. Rev.* 77, 73–111. doi: 10.1128/MMBR.00046-12

Long, R. A., Qureshi, A., Faulkner, D. J., and Azam, F. (2003). 2-n-Pentyl-4- quinolinol produced by a marine *Alteromonas* sp. and its potential ecological and biogeochemical roles. *Appl. Environ. Microbiol.* 69, 568–576. doi: 10.1128/AEM.69.1.568-576.2003

Maida, M., Carroll, A. R., and Coll, J. C. (1993). Variability of terpene content in the soft coral *Sinularia flexibilis* (Coelenterata: Octocorallia), and its ecological implications. *J. Chem. Ecol.* 19, 2285–2296. doi: 10.1007/BF00979664

Manefield, M., de Nys, R., Kumar, N., Read, R., Givskov, M., Steinberg, P., et al. (1999). Evidence that halogenated furanones from *Delisea pulchra* inhibit acylated homoserine lactone (AHL)-mediated gene expression by displacing the AHL signal from its receptor protein. *Microbiology.* 145, 283–291

Mathesius, U., Mulders, S., Gao, M., Teplitski, M., Caetano-Anolles, G., Rolfe, B. G., et al. (2003). Extensive and specific responses of a eukaryote to bacterial quorum-sensing signals. *Proc. Natl. Acad. Sci. U.S.A.* 100, 1444–1449. doi: 10.1073/pnas.262672599

MarinLit Database (2013). *MarinLit Database*. Canterbury: Department of Chemistry, University of Canterbury.

McClean, K. H., Winson, M. K., Fish, L., Taylor, A., Chhabra, S. R., Camara, M., et al. (1997). Quorum sensing and Chromobacterium violaceum: exploitation of violacein production and inhibition for the detection of N-acyl homoserine lactones. *Microbiology.* 143, 3703–3711. doi: 10.1099/00221287-143-12-3703

McFall-Ngai, M., Hadfield, M. G., Bosch, T. C., Carey, H. V., Domazet-Lošo, T., Douglas, A. E., et al. (2013). Animals in a bacterial world, a new imperative for the life sciences. *Proc. Nat. Acad. Sci.* 110, 3229–3236. doi: 10.1073/pnas.1218525110

Miller, M. B., and Bassler, B. L. (2001). Quorum sensing in bacteria. *Ann Rev. Microbiol.* 55, 165–199. doi: 10.1146/annurev.micro.55.1.165

Mohamed, N. M., Cicirelli, E. M., Kan, J., Chen, F., Fuqua, C., and Hill, R. T. (2008). Diversity and quorum-sensing signal production of Proteobacteria associated with marine sponges. *Environ. Microbiol.* 10, 75–86. doi: 10.1111/j.1462-2920.2007.01431.x

Neave, M. J., Apprill, A., Ferrier-Pagès, C., and Voolstra, C. R. (2016). Diversity and function of prevalent symbiotic marine bacteria in the genus *Endozoicomonas*. *Appl. Microbiol. Biotechnol.* 100, 8315–8324 doi: 10.1007/s00253-016-7777-0

Nithya, C., Begum, M. F., and Pandian, S. K. (2010). Marine bacterial isolates inhibit biofilm formation and disrupt mature biofilms of *Pseudomonas aeruginosa* PAO1. *Appl. Microbiol. Biotechnol.* 88, 341–358. doi: 10.1007/s00253-010-2777-y

Nithyanand, P., and Pandian, S. K. (2009). Phylogenetic characterization of culturable bacterial diversity associated with the mucus and tissue of the coral *Acropora digitifera* from the Gulf of Mannar. *FEMS. Microbiol. Ecol.* 69, 384–394. doi: 10.1111/j.1574-6941.2009.00723.x

Oksanen, J., Blanchet, F. G., Friendly, M., Kindt, R., Legendre, P., McGlinn, D., et al. (2018). *vegan: Community Ecology Package*. R package version 2.5–1.

Papenfort, K., and Bassler, B. L. (2016). Quorum sensing signal–response systems in Gram-negative bacteria. *Nat. Rev. Microbiol.* 14, 576. doi: 10.1038/nrmicro.2016.89

Parsek, M. R., and Greenberg, E. P. (2000). Acyl-homoserine lactone quorum sensing in Gram-negative bacteria: a signaling mechanism involved in associations with higher organisms. *Proc. Natl. Acad. Sci. U.S.A.* 97, 8789–8793. doi: 10.1073/pnas.97.16.8789

Persson, T., Givskov, M., and Nielsen, J. (2005). Quorum sensing inhibition: targeting chemical communication in Gram-negative bacteria. *Curr. Med. Chem*. 12, 3103–3115.

Pike, R. E., Haltli, B., and Kerr, R. G. (2013). Endozoicomonas euniceicola sp. nov. and Endozoicomonas gorgoniicola sp. nov., bacteria isolated from the octocorals, *Eunicea fusca* and *Plexaura* sp. *Int. J. Syst. Evol. Microbiol.* 63, 4294–4302. doi: 10.1099/ijs.0.051490-0.

Pootakham, W., Mhuantong, W., Yoocha, T., Putchim, L., Sonthirod, C., Naktang, C., et al. (2017). High resolution profiling of coral associated bacterial communities using full-length 16S rRNA sequence data from PacBio SMRT sequencing system. *Sci. Rep.* 7:2774. doi: 10.1038/s41598-017-03139-4

Rabinowitz, G. B. (1975). An introduction to nonmetric multidimensional scaling. *Am J of Polit. Sci.* 19, 343–390. doi: 10.2307/2110441

Raina, J.-B., Tapiolas, D., Willis, B. L., and Bourne, D. G. (2009). Coral-associated bacteria and their role in the biogeochemical cycling of sulfur. *Appl. Environ. Microbiol*. 75, 3492–3501. doi: 10.1128/AEM.02567-08

Ravn, L., Christensen, A. B., Molin, S., Givskov, M., and Gram, L. (2001). Methods for detecting acylated homoserine lactones produced by Gram-negative bacteria and their application in studies of AHL-production kinetics. *J. Microbiol. Methods.* 44, 239–251. doi: 10.1016/S0167-7012(01)00217-2

Reshef, L., Koren, O., Loya, Y., Zilber-Rosenberg, I., and Rosenberg, E. (2006). The coral probiotic hypothesis. *Environ. Microbiol.* 8, 2068–2073. doi: 10.1111/j.1462-2920.2006.01148.x

Rice, S., Koh, K., Queck, S., Labbate, M., Lam, K., and Kjelleberg, S. (2005). Biofilm formation and sloughing in *Serratia marcescens* are controlled by quorum sensing and nutrient cues. *J. Bacteriol.* 187, 3477–3485. doi: 10.1128/JB.187.10.3477-3485.2005

Rohwer, F., Seguritan, V., Azam, F., and Knowlton, N. (2002). Diversity and distribution of coral-associated bacteria. *Mar. Ecol. Prog. Ser.* 243, 1–10. doi: 10.3354/meps243001

Rosenberg, E., Koren, O., Reshef, L., Efrony, R., and Zilber-Rosenberg, I. (2007). The role of microorganisms in coral health, disease and evolution. *Nat. Rev. Microbiol.* 5, 355–362. doi: 10.1038/nrmicro1635

Shnit-Orland, M., and Kushmaro, A. (2009). Coral mucus-associated bacteria: a possible first line of defense. *FEMS Microbiol. Ecol.* 67, 371–380. doi: 10.1111/j.1574-6941.2008.00644.x

Skindersoe, M. E., Ettinger-Epstein, P., Rasmussen, T. B., Bjarnsholt, T., de Nys, R., and Givskov, M. (2008). Quorum sensing antagonism from marine organisms. *Mar. Biotechnol. (N.Y.).* 10, 56–63. doi: 10.1007/s10126-007-9036-y

Smith, G. W., and Hayasaka, S. S. (1982). Nitrogenase activity associated with *Halodule wrightii Roots. Appl. Environ. Microbiol.* 143, 1244–1248.

Steindler, L., and Venturi, V. (2007). Detection of quorum-sensing N-acyl homoserine lactone signal molecules by bacterial biosensors. *FEMS Microbiol. Lett*. 266, 1–9. doi: 10.1111/j.1574-6968.2006.00501.x

Sunagawa, S., Woodley, C. M., and Medina, M. (2010). Threatened corals provide underexplored microbial habitats. *PLoS ONE* 5:e9554. doi: 10.1371/journal.pone.0009554

Swem, L. R., Swem, D. L., O'Loughlin, C. T., Gatmaitan, R., Zhao, B., Ulrich, S. M., et al. (2009). A quorum-sensing antagonist targets both membrane-bound and cytoplasmic receptors and controls bacterial pathogenicity. *Mol. Cell*. 35, 143–153. doi: 10.1016/j.molcel.2009.05.029

Tait, K., Hutchison, Z., Thompson, F. L., and Munn, C. B. (2010). Quorum sensing signal production and inhibition by coral-associated *Vibrios*. *Environ. Microbiol. Rep*. 2, 145–150. doi: 10.1111/j.1758-2229.2009.00122.x

Tait, K., Williamson, H., Atkinson, S., Williams, P., Cámara, M., and Joint, I. (2009). Turnover of quorum sensing signal molecules modulates cross-kingdom signalling. *Environ. Microbiol*. 11, 1792–1802. doi: 10.1111/j.1462-2920.2009.01904.x

Taylor, M. W., Schupp, P. J., Baillie, H. J., Charlton, T. S., de Nys, R., Kjelleberg, S., et al. (2004). Evidence for acyl homoserine lactone signal production in bacteria associated with marine sponges. *Appl. Environ. Microbiol*. 70, 4387–4389. doi: 10.1128/AEM.70.7.4387-4389.2004

Teplitski, M., and Ritchie, K. (2009). How feasible is the biological control of coral diseases? *Trends Ecol. Evol*. 24, 378–385. doi: 10.1016/j.tree.2009.02.008

Tursch, B., Braekman, J., Daloze, D., Herin, M., Karlsson, R., and Losman, D. (1975). Chemical studies of marine invertebrates XI. *Tetrahedron*. 31, 129–133. doi: 10.1016/0040-4020(75)85006-X

Urakawa, H., and Rivera, I. M. G. (2006). "Aquatic environment," in *The Biology of Vibrios*, eds F. L. Thompson and A. B. Swings (Washington DC: ASM Press), 175–189.

Wahlberg, I., and Eklund, A. M. (1992). "Cyclised cembranoids of natural occurrence," in *Progress in the Chemistry of Organic Natural Products*, Vol. 60, eds W. Herz, G. W. Kirby, R. E. Moore, W. Steglich, and C. Tamm (New York, NY: Springer), 1–141.

Waters, C. M., and Bassler, B. L. (2005). Quorum sensing: cell-to-cell communication in bacteria. *Annu. Rev. Cell Dev. Biol*. 21, 319–346. doi: 10.1146/annurev.cellbio.21.012704.131001

Watson, W. T., Minogue, T. D., Val, D. L., Beck von Bodman, S., and Churchill, M. E. A. (2002). Structural basis and specificity of acyl-homoserine lactone signal production in bacterial quorum sensing. *Mol. Cell.* 9, 685–694. doi: 10.1016/S1097-2765(02)00480-X

Yim, G., Wang, H. H., and Davies, J. (2007). Antibiotics as signalling molecules. *Philos. Trans. R. Soc. Lond. B. Biol. Sci.* 362, 1195–1200. doi: 10.1098/rstb.2007.2044

Zhu, J., Beaber, J., More, M., Fuqua, C., Eberhard, A., and Winans, S. (1998). Analogs of the autoinducer 3-oxooctanoyl-homoserine lactone strongly inhibit activity of the TraR protein of *Agrobacterium tumefaciens*. *J. Bacteriol*. 180, 5398–5405.

Zhu, J., and Mekalanos, J. J. (2003). Quorum sensing-dependent biofilms enhance colonization in *Vibrio cholerae*. *Dev. Cell.* 5, 647–656. doi: 10.1016/S1534-5807(03)00295-8

Zilber-Rosenberg, I., and Rosenberg, E. (2008). Role of microorganisms in the evolution of animals and plants: the hologenome theory of evolution. *FEMS Microbiol. Rev*. 32, 723–735. doi: 10.1111/j.1574-6976.2008.00123.x

Conflict of Interest Statement: The authors declare that the research was conducted in the absence of any commercial or financial relationships that could be construed as a potential conflict of interest.

frontiers in Microbiology

ORIGINAL RESEARCH
published: 24 April 2018
doi: 10.3389/fmicb.2018.00728

Predicted Bacterial Interactions Affect *in Vivo* Microbial Colonization Dynamics in *Nematostella*

Hanna Domin[1†], Yazmín H. Zurita-Gutiérrez[2†], Marco Scotti[3], Jann Buttlar[1], Ute Hentschel Humeida[2,4] and Sebastian Fraune[1]*

[1] Zoological Institute, Christian-Albrechts-Universität zu Kiel, Kiel, Germany, [2] RD3 Marine Microbiology, GEOMAR Helmholtz Centre for Ocean Research Kiel, Kiel, Germany, [3] RD3 Experimental Ecology, GEOMAR Helmholtz Centre for Ocean Research Kiel, Kiel, Germany, [4] Christian-Albrechts-Universität zu Kiel, Kiel, Germany

The maintenance and resilience of host-associated microbiota during development is a fundamental process influencing the fitness of many organisms. Several host properties were identified as influencing factors on bacterial colonization, including the innate immune system, mucus composition, and diet. In contrast, the importance of bacteria–bacteria interactions on host colonization is less understood. Here, we use bacterial abundance data of the marine model organism *Nematostella vectensis* to reconstruct potential bacteria–bacteria interactions through co-occurrence networks. The analysis indicates that bacteria–bacteria interactions are dynamic during host colonization and change according to the host's developmental stage. To assess the predictive power of inferred interactions, we tested bacterial isolates with predicted cooperative or competitive behavior for their ability to influence bacterial recolonization dynamics. Within 3 days of recolonization, all tested bacterial isolates affected bacterial community structure, while only competitive bacteria increased bacterial diversity. Only 1 week after recolonization, almost no differences in bacterial community structure could be observed between control and treatments. These results show that predicted competitive bacteria can influence community structure for a short period of time, verifying the *in silico* predictions. However, within 1 week, the effects of the bacterial isolates are neutralized, indicating a high degree of resilience of the bacterial community.

Keywords: correlation networks, bacteria–bacteria interactions, holobiont, host–microbe interactions, Cnidaria, metaorganism, resilience, community ecology

OPEN ACCESS

Edited by:
Matthias Wietz, University of Oldenburg, Germany

Reviewed by:
Rúben Martins Costa, King Abdullah University of Science and Technology, Saudi Arabia
Allison Helen Kerwin, University of Connecticut, United States

****Correspondence:***
Sebastian Fraune
sfraune@zoologie.uni-kiel.de

† These authors have contributed equally to this work.

Specialty section:
This article was submitted to Microbial Symbioses, a section of the journal Frontiers in Microbiology

Received: *02 February 2018*
Accepted: *28 March 2018*
Published: *24 April 2018*

Citation:
Domin H, Zurita-Gutiérrez YH, Scotti M, Buttlar J, Hentschel Humeida U and Fraune S (2018) Predicted Bacterial Interactions Affect in Vivo Microbial Colonization Dynamics in Nematostella. Front. Microbiol. 9:728. doi: 10.3389/fmicb.2018.00728

INTRODUCTION

Central for the ability to predict the rules determining the assemblage of host-associated microbial communities is the knowledge about the factors influencing their dynamics and stability. It is well established that extrinsic factors, like temperature (Fan et al., 2013; Mortzfeld et al., 2016), pH (Ribes et al., 2016), or pathogens (Agler et al., 2016), can influence the community membership. In addition, a number of studies describe host factors shaping the host-associated microbiota, e.g., the innate immune system (Vaishnava et al., 2008; Franzenburg et al., 2012, 2013), diet (David et al., 2014), or host mucus composition (Staubach et al., 2012; Kashyap et al., 2013). In contrast, less is known about how bacteria–bacteria interactions themselves affect the assemblage of host-associated bacterial communities. However, it is known that interactions within microbial

communities can be complex ranging from cooperation to competition (Deines and Bosch, 2016). They can be influenced by diverse factors, like bacterial metabolism (Grosskopf and Soyer, 2014; Zelezniak et al., 2015), environmental factors, or spatial organization (Kim et al., 2008; Mitri and Foster, 2013).

Until recently, it was assumed that cooperative interactions within host-associated bacterial communities are the driving force for stability and productivity (reviewed in Deines and Bosch, 2016). However, this view was challenged by theoretical work, which is based on ecological network analysis. While cooperative communities are predicted to be highly productive for the short term and unstable for the long term, competitive communities tend to be more diverse and stable over time (Coyte et al., 2015). Although much progress has been made in characterizing host-associated bacterial communities, few data are available on ecological interactions within these communities *in vivo* and their impact on community stability and dynamics.

The marine sea anemone *Nematostella vectensis* is characterized by a stable associated bacterial community, which is dynamic in response to host development (Mortzfeld et al., 2016). Host development is defined by several life stages. Upon fertilization, the embryos develop into free swimming planula larvae within 1–3 days. After roughly 1 week, the larvae metamorphose into sessile primary polyps. Sexual maturity is reached after 3–6 months (Hand and Uhlinger, 1994). In a previous study, the establishment of the bacterial community was monitored from the early developmental stages up to the reproductive adults over the time course of more than 1 year (Mortzfeld et al., 2016). Using this comprehensive dataset, we inferred theoretical bacteria–bacteria interactions (Faust and Raes, 2012; Weiss et al., 2016) to determine bacteria with a distinct predicted motif. Using bacterial isolates possessing predicted competitive or cooperative interactions, we tested their impacts on the assemblage of the microbiota in recolonization experiments in juvenile animals. Our results show that predicted competitive bacteria can influence community diversity for a short period of time, verifying the *in silico* predictions. With this study, we confirm the significance of the predictions of co-occurrence networks by experimentally testing the predicted ecological role of bacterial interactions.

MATERIALS AND METHODS

Inference of Bacteria–Bacteria Co-occurrence Networks

Network links were inferred using correlation analysis among 508 OTUs representing the relative bacterial abundance in *N. vectensis* (Mortzfeld et al., 2016). SparCC methodology (Friedman and Alm, 2012) was chosen as the inference method because it was explicitly designed for compositional (i.e., based on relative information) and sparse (with a small amount of non-zero values compared to the maximum possible) data, two key features displayed by the sequencing data used in our study. As the amount of significant correlations (pseudo p-value ≤ 0.05) was large, only the strongest correlations were considered for network construction and analysis (i.e., strong correlations are those exceeding 0.5 in absolute value).

Correlation Significance

SparCC methodology assigns a pseudo p-value to each correlation through a bootstrap approach. The pseudo p-value represents the proportion of times a correlation from permutated datasets is at least as extreme as the observed "real" one (Friedman and Alm, 2012). To calculate the pseudo p-values, 1,000 permutated datasets with a two-sided distribution were used.

Network Descriptors

The links in the co-occurrence networks can be either negative or positive. The value assigned to the interactions (i.e., interaction strength) ranges between -1 and $+1$, and the sign can provide proxies on the type of interaction (e.g., positive correlations can stand for cooperative activities, while negative correlations can indicate competition; see Shade et al., 2012). The number of nodes (the size of the network, which corresponds to the total number of OTUs; N), the number of links (the total number of significant correlations exceeding 0.5 in absolute value; L), the number of connected nodes (the OTUs with at least one interaction; N_C), the density [the ratio between L and the maximum number of links that an undirected network can have: $L_{max} = N\ (N-1)/2$; $D = L/L_{max}$], the numbers and proportions of positive (L_P, $\%L_P$) and negative (L_N, $\%L_N$) links, the mean correlation values based on total (m_t), positive (m_p), or negative (m_n) interactions, and the number of subnetworks (networks composed by isolated subsets of N, where the nodes of each subnetwork show no connections outside the subset; n_{sub}) were taken as network descriptors. The degree (d) of the nodes was used as an indicator of centrality to identify the most important OTUs in the network (Wasserman and Faust, 1994). Thus, an OTU i was considered to be important when it had a high degree (d_i is large if the node i is directly linked to several OTUs) and most connections of the same sign (i.e., to discriminate among cooperators or competitors). Also the mean ($\overline{d}$) and the maximum (d_{max}) degrees of the networks were calculated as global descriptors starting from single node values.

Animal Culture

All experiments were carried out with juvenile polyps of *N. vectensis*. The adult animals of the laboratory culture were F1 offspring of CH2XCH6 individuals collected from the Rhode River in Maryland, United States (Hand and Uhlinger, 1992; Fritzenwanker and Technau, 2002). They were kept under constant, artificial conditions without substrate or light in *Nematostella* Medium (NM), which was adjusted to 18°C and 16‰ salinity with Red Sea Salt® and Millipore H_2O. Polyps were fed 2–3 times a week with first instar nauplius larvae of *Artemia salina* as prey (Ocean Nutrition Micro *Artemia* Cysts 430–3500 g, Coralsands, Wiesbaden, Germany).

Antibiotic Treatment

The antibiotic treatment procedure was adapted after the protocol for germ-free (GF) *Hydra* polyps (Fraune et al., 2014).

The juveniles were incubated without food supply for 4 weeks in sterile NM with an antibiotic cocktail of ampicillin, neomycin, streptomycin, spectinomycin, and rifampicin in a final concentration of 50 μg/mL each. The medium was changed every 2–3 days. After the 4 weeks, the polyps were transferred into antibiotic-free medium. The absence of cultivatable bacteria was checked at the end of the antibiotic treatment by plating homogenized polyps on Marine Bouillon (MB) plates. While a weak band was detected using specific 16S rRNA gene primers (27F and 338R), no recovery of bacterial colonization was observed based on PCR signal intensity and plating on MB during the course of the experiment in non-colonized animals.

Recolonization

The bacterial load of larvae and juveniles was estimated by colony forming units (CFUs) of larvae and juveniles. Larvae (6 days old) and juveniles (8–10 tentacle stages) were homogenized and spread on MB plates. The plates were incubated at 18°C for 3 days before counting colonies. One smashed larva resulted in ∼200 colonies grown on MB plates and one smashed juvenile spread on an MB plate yielded ∼2,000 colonies. To ensure successful recolonization, the polyps were exposed to double the amount of their native microbiota (e.g., ∼4,000 colonies per juvenile). The bacterial isolates were grown to an OD600 of 0.2, spread out on MB plates, and counted in order to calculate the cell number.

Prior to recolonization, the juvenile polyps were treated with antibiotics for 4 weeks and remained in sterile antibiotic-free medium for 4 days before recolonization. The animals were starved during the whole experiment. For each recolonization treatment and replicate, 10 juvenile polyps were put into a 2 mL Eppendorf tube and filled up with 2 mL of one of the following solutions: (1) native larval bacteria; (2) native juvenile bacteria; or (3) a mix of native larval bacteria and one single bacterial isolate in overrepresentation. Complex bacterial mixtures were obtained by smashing whole larvae or juvenile polyps in sterile NM. The homogenates were centrifuged and the pellet washed twice in sterile NM. Samples were collected for the three types of treatments at two time points. Five replicates per treatment and time point were used and each replicate consisted of five pooled animals.

The juveniles were recolonized with a mix of native larval bacteria together with single isolates with the aim of adding the single isolates in a 1:3 ratio of larval bacteria to single isolates. By sequencing the 16S rRNA genes of inocula, we estimated the overrepresentation of all isolates. Although it was not possible to obtain any mix of larval bacteria and bacterial isolates with the 1:3 target ratio, the five selected OTUs were still overrepresented at the start of each treatment, i.e., at least 10-fold their initial abundance in the control. The fold change of each isolate was estimated by comparing the sequencing reads of control (bL) to treatment.

Cultivation and Identification of Bacterial Isolates

Bacteria were isolated from *Nematostella* polyps by smashing single polyps in sterile NM and plating them on MB, LB, and R2A agar plates. After incubation at 18°C for 5 days, single CFUs were isolated and cultivated in liquid MB, LB, or R2A medium. The bacteria were identified by Sanger sequencing of the 16S rRNA gene. Stocks were stored in Roti-Store cryo vials (Carl Roth, Karlsruhe, Germany) or in 50% glycerol at −80°C. Bacterial isolates were grown and isolated in the following media: OTU194 (*Ruegeria* sp.) and OTU1209 (*Vibrio* sp.) grew in MB medium, OTU1325 (*Aeromonas* sp.) and OTU941 (*Pseudomonas* sp.) in LB medium, and OTU670 (*Acinetobacter* sp.) in R2A medium.

DNA Extraction and 16S rRNA Sequencing

Before extraction, the animals were washed three times with 500 μL sterile filtered NM and frozen without liquid at −80°C until extraction. The gDNA was extracted from whole five animals per sample with the DNeasy® Blood & Tissue Kit (Qiagen, Hilden, Germany) as described in the manufacturer's protocol. DNA was eluted in 200 μL elution buffer. The eluate was frozen at −20°C until sequencing. For each sample, the hypervariable regions V1 and V2 of bacterial 16S rRNA genes were amplified. The forward primer (5′-AA TGATACGGCGACCACCGAGATCTACAC XXXXXXXX TAT GGTAATTGT AGAGTTTGATCCTGGCTCAG-3′) and reverse primer (5′-CAAGCAGAAGACGGCATACGAGAT XXXXXXXX AGTCAGTCAGCC TGCTGCCTCCCGTAGG AGT-3′) contained the Illumina Adaptor p5 (forward) and p7 (reverse). Both primers contain a unique 8 base index (index; designated as XXXXXXXX) to tag each PCR product. For the PCR, 100 ng of template DNA (measured with Qubit) were added to 25 μL PCR reactions, which were performed using Phusion® Hot Start II DNA Polymerase (Finnzymes, Espoo, Finland). All dilutions were carried out using certified DNA-free PCR water (JT Baker). PCRs were conducted with the following cycling conditions (98°C – 30 s, 30 × [98°C – 9 s, 55°C – 60 s, 72°C – 90 s], 72°C – 10 min) and checked on a 1.5% agarose gel. The concentration of the amplicons was estimated using a Gel Doc™ XR+ System coupled with Image Lab™ Software (BioRad, Hercules, CA, United States) with 3 μL of O'GeneRulerTM 100 bp Plus DNA Ladder (Thermo Fisher Scientific, Inc., Waltham, MA, United States) as the internal standard for band intensity measurement. The samples of individual gels were pooled into approximately equimolar subpools as indicated by band intensity and measured with the Qubit dsDNA br Assay Kit (Life Technologies GmbH, Darmstadt, Germany). Subpools were mixed in an equimolar fashion and stored at −20°C until sequencing. Sequencing was performed on the Illumina MiSeq platform with v3 chemistry (Rausch et al., 2016). The raw data are deposited at the Sequence Read Archive (SRA) and available under the project ID PRJNA433067.

Analyses of Bacterial Communities

The sequence analysis was conducted using the QIIME 1.9.0 package (Caporaso et al., 2010). Paired end reads were assembled using SeqPrep. Chimeric sequences were identified with Chimera Slayer (Haas et al., 2011). OTU picking was performed using the pick_open_reference_otus.py protocol with at least 97%

identity per OTU and annotation was conducted with the UCLUST algorithm (**RRID**:SCR_011921; Edgar, 2010) against the GreenGenes database v13.8 (**RRID**:SCR_002830; DeSantis et al., 2006) implemented in QIIME. OTUs with less than 50 reads were removed from the dataset to avoid false positive OTUs that may originate from sequencing errors (Faith et al., 2013). The number of reads was normalized to 10,000 reads for the analysis. Alpha-diversity was calculated with the Chao1 metric implemented in QIIME using ten replicates of rarefication per sample. Beta-diversity was depicted in a PCoA by 100 jackknifed replicates using Bray–Curtis and weighted UniFrac metrics. For statistical analysis of clustering the method ADONIS was used.

RESULTS

Bacteria–Bacteria Co-occurrence Networks During Host Development

To infer potential bacteria–bacteria interactions in the bacterial community of *N. vectensis*, network links were inferred using SparCC methodology (Friedman and Alm, 2012) to the relative abundance of 508 OTUs over the whole ontogeny (Mortzfeld et al., 2016). Using bacterial abundance data, network correlations were inferred from: (1) all sampling time points together, leading to the representation of the most important interactions along the whole development of the animal and (2) the three developmental stages separately, which characterize the most relevant correlations during each developmental stage. For the construction of the co-occurrence networks, the strongest significant interactions (i.e., those with pseudo p-value ≤ 0.05 and an absolute correlation value larger than 0.5) in each of the datasets were selected. A list of 66 nodes ($N = 66$), representing 66 bacterial OTUs, was obtained from the union of all OTUs that were found at least once in one of the four datasets of the significant and strong correlations. Using these 66 nodes, the four co-occurrence networks were constructed. **Figure 1** is the co-occurrence network along the whole developmental process of *N. vectensis*. **Figure 2** shows the co-occurrence networks for each developmental stage. The OTUs were arranged by taxonomy and relative abundance computed for the whole development (**Figure 1**) and the same order is preserved in **Figure 2** OTU numbers are provided in **Figure 1** and Supplementary Figure S1 but showing the relative abundance of OTUs at each developmental stage.

None of the constructed networks has more than 56 interactions ($L = 56$) or involves more than 29 OTUs ($N_C \leq 29$), resulting in a low density across all networks (**Table 1**). All networks have more positive than negative interactions ($L_P > L_N$), which is reflected in the mean correlation values calculated considering the total set of links (**Table 1**). All networks are composed of two or more subnetworks, but this could be a consequence of the chosen correlation cut-off rather than a biological property. The four networks together have 145 interactions and only one shared interaction between different

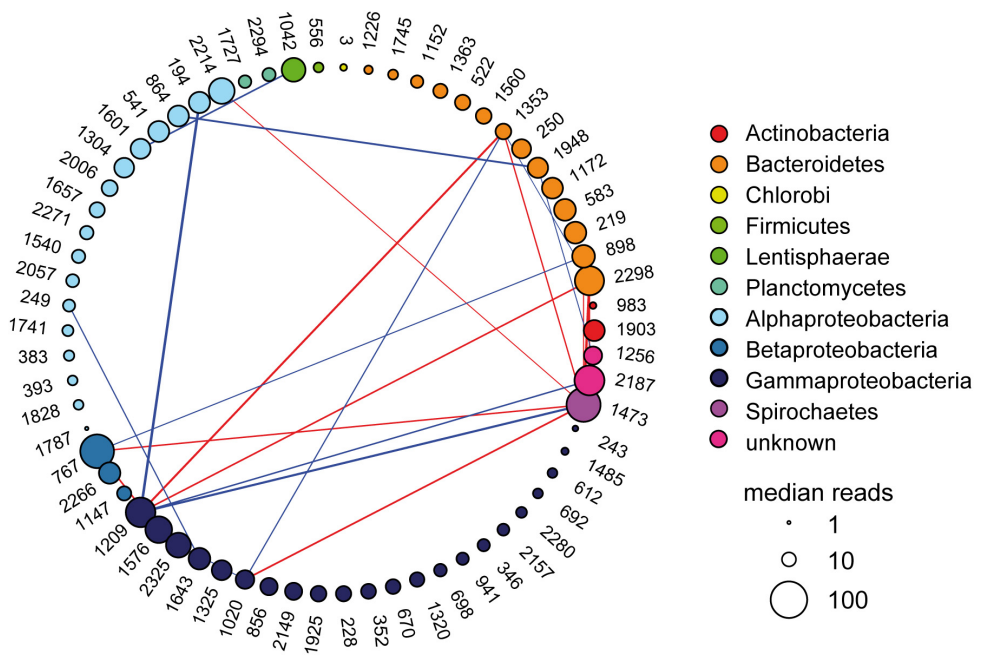

FIGURE 1 | Microbial co-occurrence network among OTUs during the whole development of *N. vectensis*. Nodes ($N = 66$) are the OTUs involved in at least one strong interaction during the whole development or the three developmental stages; their color reflects taxonomic affiliation. The size of the nodes is proportional to the $\log_{10}$ of the median reads (relative abundance of the OTUs) along the whole development. OTUs are arranged by taxonomy and relative abundance. Links represent the interactions (i.e., significant co-occurrences; pseudo p-value ≤ 0.05) with absolute correlation values above 0.5. Red links are negative interactions, while blue links stand for positive interactions; the thickness of the links is proportional to the strength of the interactions.

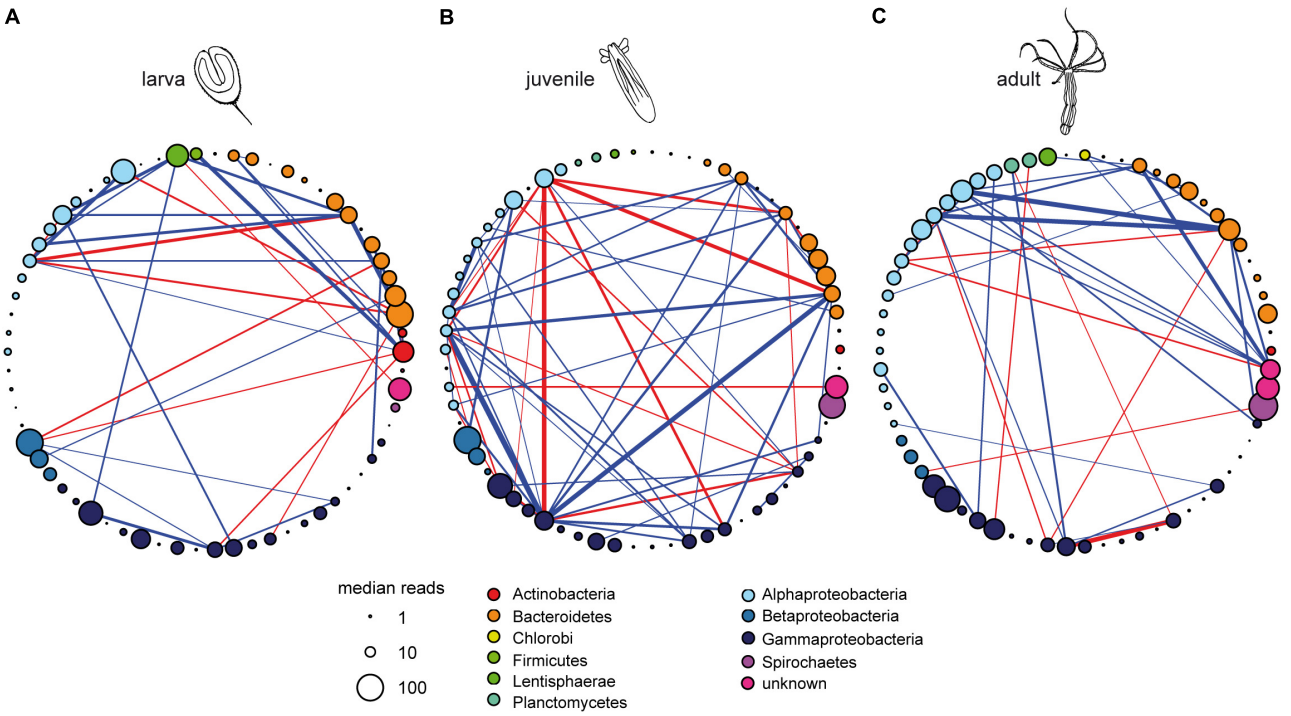

FIGURE 2 | Microbial co-occurrence networks for **(A)** larval stage, **(B)** juvenile stage, and **(C)** adult polyps of *N. vectensis*. Nodes (N = 66) are the same as in **Figure 1** and Supplementary Figure S1 their order in the circular arrangement was preserved. OTU numbers are provided in Supplementary Figure S1. The colors inform about the taxonomic affiliation of the nodes. The size of the nodes is proportional to the relative abundance of the OTUs (measured as $\log_{10}$ of median reads) in each developmental stage. Links are significant correlations (pseudo p-value ≤ 0.05) with absolute values above 0.5; their color allows distinguishing among negative (red) and positive (blue) interactions, while the thickness is proportional to the strength.

TABLE 1 | Network descriptors used to characterize the properties of the correlation networks. Indices were calculated for both the whole development network (i.e., based on all correlations among OTUs, irrespective of the various stages of polyp growth) and the networks that refer to three developmental stages (i.e., larva, juvenile, and adult). All networks are composed of the same 66 OTUs (N = 66).

Descriptors	Whole development	Larva	Juvenile	Adult
Number of links (L)	22	35	56	37
Number of connected nodes (N_C)	20	25	29	29
Density of the network (D)	0.010	0.016	0.026	0.017
Number of positive links (L_P)	12	25	39	27
Number of negative links (L_N)	10	10	17	10
Proportion of positive links (%L_P)	0.545	0.714	0.696	0.730
Proportion of negative links (%L_N)	0.455	0.286	0.304	0.270
Mean of total correlations (m_t)	0.045	0.250	0.218	0.260
Mean of positive correlations (m_p)	0.535	0.569	0.559	0.559
Mean of negative correlations (m_n)	−0.544	−0.548	−0.565	−0.547
Number of subnetworks (n_{sub})	4	2	6	5
Mean degree ($\overline{d}$)	2.200	2.800	3.862	2.552
Maximum degree (d_{max})	7	8	14	7
OTUs with maximum degree	1473	1903	1643	1948, 1601, 1256

developmental stages (i.e., the interaction OTU1601–OTU1657 is present in both larval and adult stages).

The co-occurrence network spanning the whole host development (**Figure 1**) has the lowest number of connected nodes (N_C = 20; **Table 1**). Here, a spirochaete bacterium (OTU1473) has the highest degree of links indicating a potential role as organizer along the whole development of *N. vectensis* (Supplementary Table S1 and **Figure 1**). Interestingly, when analyzing the different developmental phases separately, the structure of the interactions (**Figure 2**) and the degree of the nodes (Supplementary Table S1) vary during animal development. Thus, the set of nodes with

TABLE 2 | Bacterial strains cultivated from juvenile polyps of *N. vectensis*.

#OTU	Bacterium	Consensus lineage	Clone	Correlations in juvenile network	
				Positive	Negative
1304	*Kiloniella* sp.	Alphaproteobacteria; Kiloniellales; Kiloniellaceae	JB_90	1	0
194	*Ruegeria* sp.	Alphaproteobacteria; Rhodobacterales; Rhodobacteraceae	JB_30	1	6
1657	*Loktanella* sp.	Alphaproteobacteria; Rhodobacterales; Rhodobacteraceae	JB_36	0	0
2298	*Flavobacterium* sp.	Bacteroidetes; Flavobacteriia; Flavobacteriales; Flavobacteriaceae	JB_91	1	0
1325	*Aeromonas* sp.	Gammaproteobacteria; Aeromonadales	JB_15	0	0
2280	*Marinobacter* sp.	Gammaproteobacteria; Alteromonadales; Alteromonadaceae	JB_35	0	0
1320	*Alteromonas* sp.	Gammaproteobacteria; Alteromonadales; Alteromonadaceae	JB_27	0	0
670	*Acinetobacter* sp.	Gammaproteobacteria; Pseudomonadales; Moraxellaceae	JB_10	5	0
941	*Pseudomonas* sp.	Gammaproteobacteria; Pseudomonadales; Pseudomonadaceae	JB_53	0	0
1576	*Francisella* sp.	Gammaproteobacteria; Thiotrichales; Francisellaceae	JB_85	1	0
1209	*Vibrio* sp.	Gammaproteobacteria; Vibrionales	JB_14	1	3
243	*Vibrio* sp.	Gammaproteobacteria; Vibrionales; Vibrionaceae	JB_01	0	0
2325	*Vibrio* sp.	Gammaproteobacteria; Vibrionales; Vibrionaceae	JB_81	0	0

the highest degrees (i.e., OTUs with the higher number of direct links in the co-occurrence network; **Table 1**) is also modified, which reflects how the importance of the various phylogenetic groups changes through development. At the larval stage, the strongest correlations are mainly found between Actinobacteria, Bacteroidetes, Lentisphaerae, and Alphaproteobacteria (**Figure 2A**), but these links change during the onset of development. During the juvenile stage, Gammaproteobacteria become greatly important, interacting mainly with Alphaproteobacteria and Bacteroidetes (**Figure 2B**). However, at the adult stage, almost all interactions are between Alphaproteobacteria, Bacteroidetes, and an unknown taxon (**Figure 2C**). While at the larval stage, the bacterium with the highest degree belongs to Actinobacteria (OTU1903), at the juvenile stage, it is replaced by a Gammaproteobacterium (OTU1643). At the adult stage, three different bacteria are the most connected: one bacterium from the Bacteroidetes (OTU1948), one from the Alphaproteobacteria (OTU1601), and one unknown bacterium (OTU1256; Supplementary Table S1). Interestingly, the network constructed from the bacterial data of juvenile animals shows the highest number of links ($L = 56$; **Table 1**). This suggests that in this developmental phase of the animal, the bacteria–bacteria interactions may be of greater importance for shaping the bacterial community composition than during the two other developmental phases.

Experimental Testing of Predicted Bacteria–Bacteria Interactions

In order to test the role of predicted bacteria–bacteria interactions in the assemblage of the juvenile microbiota *in vivo*, a cultivation approach of bacteria colonizing juvenile polyps was performed. Of all isolates, 13 bacterial strains were present within the 66 OTUs of the co-occurrence networks (**Table 2**). Nine bacterial strains belong to the Gammaproteobacteria, three bacterial strains belong to the Alphaproteobacteria, and one belongs to the Bacteroidetes. Within these 13 bacterial isolates, only three strains have more than one correlation within the co-occurrence network of juvenile animals (**Table 2**) and form part of the same subnetwork (**Figure 3**). The bacterial isolates representing OTU194 *(Ruegeria* sp.) and OTU1209 (*Vibrio* sp.) are characterized by mainly negative correlations and therefore may act as competitive bacteria. Both isolates belong to the group of most abundant colonizers in juvenile polyps (**Figures 2**, **3**), while in the bacterial community of larvae, they are underrepresented (Mortzfeld et al., 2016). In contrast, the isolate representing OTU670 (*Acinetobacter* sp.) exerts mainly positive correlations, thus seeming to be a cooperative bacterium (**Figure 3** and **Table 2**).

Using these three bacterial isolates, it was tested if predicted bacteria–bacteria interactions influence the assemblage of the juvenile microbiota *in vivo*. Therefore, the experiments with antibiotic-treated juvenile polyps were conducted by recolonizing with: (1) larval bacteria; (2) juvenile bacteria; and (3) larval bacteria mixed with single bacterial isolates in excess (**Figure 4**). Two isolates without any correlations at the juvenile stage, OTU1325 (*Aeromonas* sp.) and OTU941 (*Pseudomonas* sp.), were selected as controls (Supplementary Table S1). The recolonization with larval bacteria was chosen as the tested bacterial isolates are not overrepresented in this bacterial community and this allows their overrepresentation in the recolonization experiments. All treatments were conducted with five independent replicates, sampled at 3- and 7-day post-recolonization (dpr) and analyzed by 16S rRNA gene profiling.

Recolonization of Juvenile Polyps With Larval and Juvenile Bacteria

Juvenile polyps which were inoculated with either juvenile (bJ) or larval bacteria (bL) showed a different community composition after 3dpr in comparison to the inocula and to each other (**Figure 5A**, ADONIS $R^2 = 0.95$, $p < 0.001$). After 7 days of recolonization, both bacterial communities shifted back in the direction of the native bacterial situation characterizing juvenile polyps. The animals recolonized with bacteria of

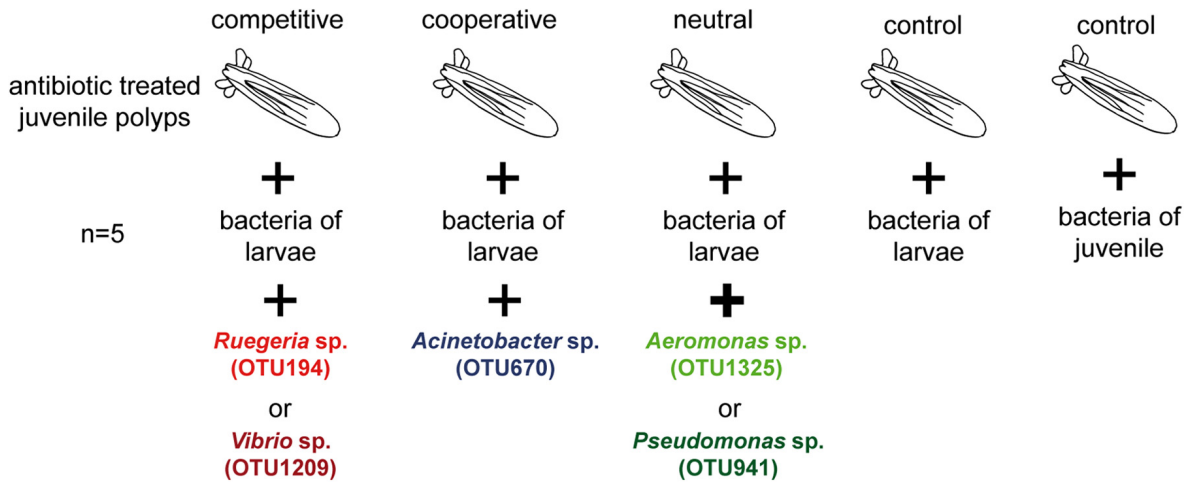

FIGURE 4 | Experimental setup for the recolonization experiments. For each treatment, juvenile polyps were treated with antibiotics and then recolonized with different bacterial inocula. For recolonizations with competitive, cooperative, or neutral bacteria, the selected OTUs were mixed with bacteria of larvae. For the two controls, antibiotic treated juveniles were recolonized with bacteria of larvae or juveniles alone.

juveniles resembled hereby the native situation significantly better than animals recolonized with bacteria from larvae (**Figure 5B**). Similar results were obtained when calculating weighted UniFrac distances instead of Bray-Curtis distances (Supplementary Figure S2). In contrast, the recolonized animals showed no difference in their bacterial alpha-diversity, even though they were recolonized with bacterial inocula that differed significantly in their alpha-diversity (**Figure 5C**).

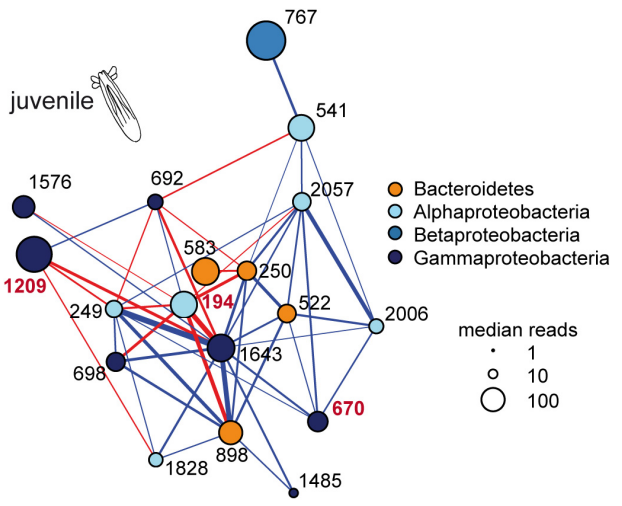

FIGURE 3 | Dominant microbial co-occurrence subnetwork in juvenile polyps. The colors inform about the taxonomic affiliation of the nodes. The size of the nodes is proportional to the relative abundance of the OTUs (measured as $\log_{10}$ of median reads) in juvenile polyps. Links are significant correlations (pseudo p-value ≤ 0.05) with absolute values above 0.5; their color allows distinguishing among negative (red) and positive (blue) interactions, while the thickness is proportional to the strength. OTUs with representative isolates available are labeled in red.

These results indicate that juvenile polyps can be recolonized with different source bacterial communities, but over time they develop back to the native juvenile community composition. However, only around 70% of the total bacterial diversity of juvenile polyps (bJ) could be restored within 7dpr (**Figure 5C**), independently of the alpha-diversity of the bacterial inoculum.

Influence of Bacterial Isolates on Colonization Process

Before testing the effect of bacterial isolates on the composition assemblage in juvenile polyps, it was first checked if the overrepresented bacterial isolates are able to colonize the polyp. Over the course of the experiment, all five isolates remained overrepresented (Supplementary Figure S3). At 3dpr, the isolates were overrepresented between 3- and 27-fold (Supplementary Figure S3B). While both competitive bacteria (OTU194; *Ruegeria* sp. and OTU1209; *Vibrio* sp.) showed the highest initial colonization efficiency, one of the neutral isolates (OTU1325; *Aeromonas* sp.) recolonized with the lowest efficiency (Supplementary Figure S3B). At 7dpr, all bacterial isolates showed a similar overrepresentation of two to fivefold compared to the control (Supplementary Figure S3C). Therefore, it was possible to recolonize the juvenile polyps with an overrepresentation of bacterial isolates.

To test for the effect of bacterial isolates on bacterial community assemblage in juvenile polyps, the colonization dynamics with isolates were compared to the control colonization without isolates. At 3dpr, the community composition was significantly affected by the addition of all five different isolates compared to the control (Supplementary Figure S4A). Surprisingly all isolates, cooperative (OTU670; *Acinetobacter* sp.), competitive (OTU194; *Ruegeria* sp. and OTU1209; *Vibrio* sp.), or neutral (OTU1325; *Aeromonas* sp. and OTU941; *Pseudomonas* sp.), shifted the community composition in

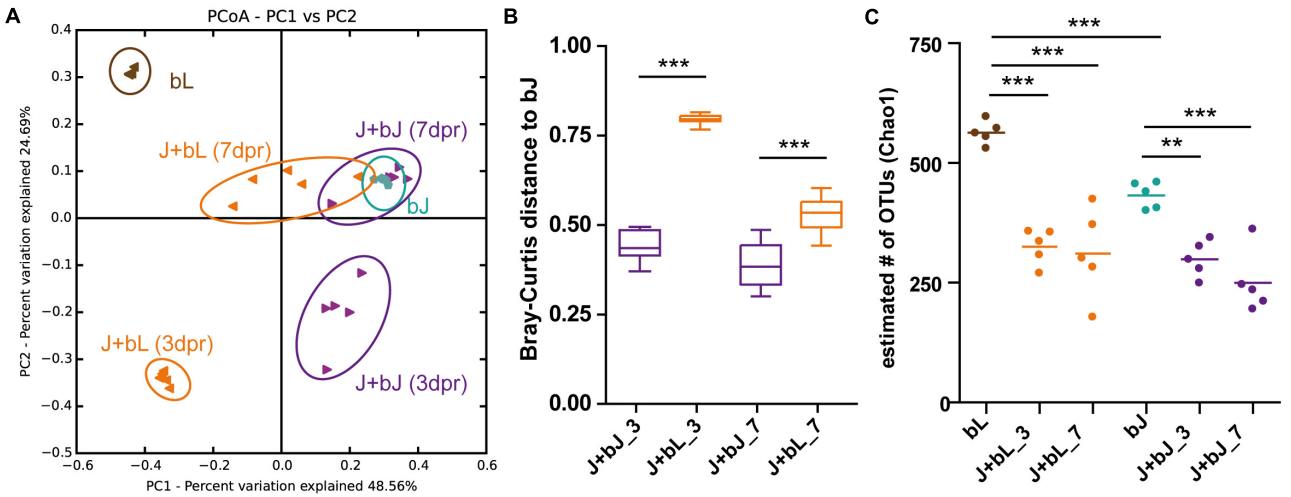

FIGURE 5 | Juvenile polyps recolonize differentially with larvae (bL) or juvenile bacteria (bJ). **(A)** Bacterial communities were clustered using PCoA of the Bray–Curtis distance matrix. The percent variation explained by the principal coordinates is indicated on the axes. bL, source bacteria of larvae; bJ, source bacteria of juvenile polyps; J+bL, bacterial community of polyps recolonized with bL after 3dpr and 7dpr; J+bJ, bacterial community of polyps recolonized with bJ after 3dpr and 7dpr. **(B)** Bray–Curtis distances to bJ after 3dpr and 7dpr. **(C)** Estimated number (Chao1) of OTUs of the source communities and recolonization communities. Statistical analysis was conducted using analysis of variance (ANOVA; $^{**}p < 0.01$, $^{***}p < 0.001$).

a similar pattern (**Figure 6A**). Additionally, the distances between juvenile bacteria and recolonized juvenile polyps became significantly smaller if bacterial isolates were added (Supplementary Figure S4A), indicating a slightly better reconstitution of the original juvenile microbiota in the presence of the isolates. Moreover, the competitive bacteria (OTU194; *Ruegeria* sp. and OTU1209; *Vibrio* sp.) caused a significantly greater alpha-diversity compared to the control; in contrast, cooperative and neutral isolates had no effect on the alpha-diversity of the bacterial community (**Figure 6B**).

However, the effect of the isolates on the Bray–Curtis distances (**Figure 6C** and Supplementary Figure S4B) and the alpha-diversity (**Figure 6D**) vanished after 7dpr. Therefore, all bacteria caused only temporary shifts in the community composition and only competitive bacteria were able to induce a significant but temporary increase in alpha-diversity.

DISCUSSION

Co-occurrence networks were constructed to quantify the importance of specific bacteria based on community-level interactions (Faust and Raes, 2012). The goal was to focus on the co-occurrence networks to infer the ecological role of the bacteria (i.e., cooperation and competition) and identify the hubs (i.e., bacteria with many direct connections of the same sign). The reestablishment of the whole bacterial community in the presence of cooperative, competitive, or neutral bacteria was tested with *in vivo* recolonization experiments. The bacteria with strongest predicted interactions changed the community composition during the early recolonization steps of *N. vectensis*, but only the communities inoculated with competitive bacteria exhibited a significant but temporary increase in alpha-diversity. Our study shows that co-occurrence network inference can be used to retrieve ecologically relevant interactions.

The network approach allows identifying the most important bacteria by their potential role in the community rather than solely relying on their relative abundance (e.g., Jordán et al., 2015). In our work, the degree of the nodes (OTUs) was used to study the direct effects of the bacteria in the community (Scotti and Jordán, 2010), under the assumption that co-occurrence networks can be informative of ecological processes. While at large phylogenetic levels, the abundance can still be a good descriptor of the microbial community associated to *N. vectensis* (Mortzfeld et al., 2016), the most abundant OTUs are not always those displaying the higher number of links (see **Figures 1**, **2**). Network analysis suggested potentially important bacteria and enabled designing *in vivo* experiments to test whether the predicted interactions are ecologically relevant.

Generalized Lotka–Volterra equations were previously applied to predict interactions in microbial communities, and the validity of model results was confirmed by culture experiments (Mounier et al., 2008). However, studies based on dynamical modeling routinely involve only a small number of species, and the validation of network inference (e.g., based on 16S rRNA sequencing data) with culture experiments is in its infancy (Faust and Raes, 2012). The novelty of our study stems from the ability to culture single bacterial isolates, representing certain OTUs, which allows experimental testing of their ecological roles predicted by analysis of co-occurrence networks.

The microbial networks, inferred using the bacterial data from larvae, juvenile, and adult polyps, demonstrate that bacterial interactions during host development are highly dynamic. On the one hand, aspects determining changes in the bacterial networks might be linked to physiological and immunological factors of the host that are remodeled during development as

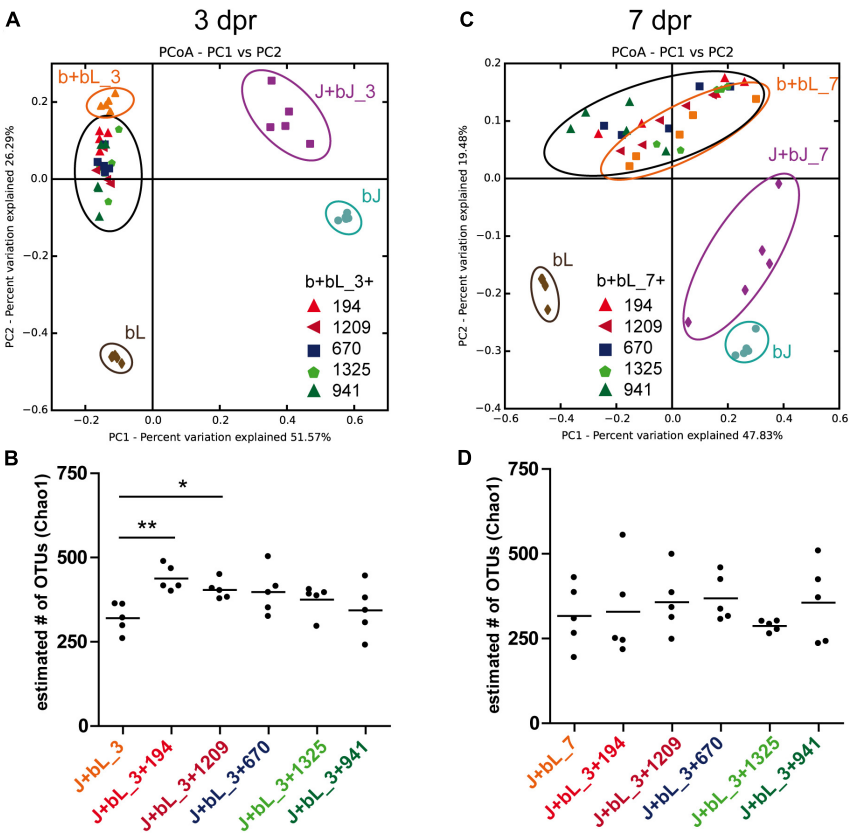

FIGURE 6 | Recolonization patterns in the presence of selected isolates. Bacterial communities at 3dpr **(A)** and 7dpr **(C)** were clustered using PCoA of the Bray–Curtis distance matrix. The percent variation explained by the principal coordinates is indicated at the axes. bL, source bacteria of larvae; bJ, source bacteria of juvenile polyps; J+bL, bacterial community of polyps recolonized with bL after 3dpr and 7dpr; J+bJ, bacterial community of polyps recolonized with bJ after 3dpr and 7dpr; b+bL+isolates, bacterial community of polyps recolonized with bL and one of the selected isolates. Estimated number (Chao1) of OTUs after 3dpr **(B)** and 7dpr **(D)**. Statistical analysis was conducted using analysis of variance (ANOVA; $*p < 0.05$, $**p < 0.01$, $n = 5$).

shown during metamorphosis in amphibians (Rollins-Smith, 1998; Faszewski et al., 2008) and insects (Vigneron et al., 2014). Especially, effector molecules of the innate immune system like AMPs (Salzman et al., 2010; Login et al., 2011; Franzenburg et al., 2013; Mukherjee et al., 2014) or the provision of selective nutrients by the host (Ley et al., 2006) may directly influence the bacterial interactions. In addition, the specific composition of complex carbohydrates on the boundary between epithelium and environment may have a huge impact on individual bacterial fitness and interactions between bacterial species (Kashyap et al., 2013; Pickard et al., 2014). On the other hand, observed changes within the bacterial interactions could be explained by successions driven by ecological bacterial interactions alone. Studying the succession of plant colonization of new habitats was part of ecological research for a long time already, but recently this approach also gained popularity to study successional patterns of microbial communities (Fierer et al., 2010). It was shown that microbial community successions in a host are accompanied by changes in the metabolic potential, adapting to environmental changes like diet (Koenig et al., 2011), but are also predictable after infection and recovery (David et al., 2014). However, the changes in microbial succession and metabolic potential also occur in the absence of a host, leaving these successions exclusively to ecological interactions between bacteria alone (Datta et al., 2016).

In the experiment, we show that the early recolonization dynamics depend on the initial bacterial inoculum, but after 7dpr all recolonizations result in a similar bacterial community composition (**Figures 5**, **6**). Three days after recolonization, the community composition observed for all treatments (i.e., those inoculated with cooperative, competitive, or neutral OTUs) was significantly different from both the native larval (bL) and the native juvenile (bJ) bacteria (**Figure 6**). Nevertheless, 7dpr all treatments resembled more the native microbiota of juveniles than the larval source used to assemble the communities (**Figure 5**). This process was more efficient when juveniles were recolonized with juvenile microbiota rather than with bacteria extracted from larvae. Even when starting from different initial conditions, all recolonization treatments that included isolates followed recolonization paths that were similar to that of native larval bacteria. Recolonization with competitive, cooperative, or neutral bacteria always developed toward attaining the native juvenile bacterial state, thus showing the resilience of the system to perturbations. One explanation, why even neutral bacteria

showed an effect on the assembly of the community, could be that the neutral bacteria were chosen based on network inference (e.g., the decision of considering strong correlations as those with absolute values above the 0.5 threshold, or the use of the SparCC algorithm for correlation detection). Although neutral bacteria do not present strong correlations in the larval and juvenile networks, they still have the potential to influence the community during initial establishment of the community or the later development of the host (**Figure 2**).

The convergence of all communities toward the native juvenile bacterial state shows that the initial composition is crucial for the stability of the system. The tested communities in our experiment showed resilience irrespective of the interaction strategy of the OTUs added in excess. Although the interaction mode of overrepresented OTUs does not alter the long-term equilibrium of the community, the competitors are the only OTUs challenging the stability of the system. As described in the literature (Czaran et al., 2002; Coyte et al., 2015), the addition of competitive OTUs significantly increased community diversity, even though such an effect was transient.

Competitive interactions between members of the bacterial community are expected to increase community diversity (Czaran et al., 2002; Coyte et al., 2015), spatial structure (Kim et al., 2008), stability (Kelsic et al., 2015), and functioning (Wei et al., 2015). After 7dpr, all communities have transited to a more stable composition, as the number of OTUs is almost the same among treatments (**Figure 6**) and overrepresented OTUs declined. In our recolonization experiment, mainly the spatial structure got abrogated by the antibiotic treatment and homogenization of the inocula. While with our experiment, we cannot assess the spatial structure or the functioning of the community, we can clearly see that only competitive bacteria increase community diversity, which is predicted by ecological theory (Coyte et al., 2015). The temporal increase in alpha-diversity could be explained by the fact that during the initial phase, the spatial structure of the bacterial community is not yet reestablished. In this initial phase bacteria can exert contact-dependent competition, which is particularly relevant in the treatments with overrepresented competitive bacteria, leading those communities to higher diversity. With the reestablishment of spatial structure, contact-dependent competition might be less pronounced. This is often described in literature as a real-life game of "rock-paper-scissors" (Kerr et al., 2002; Reichenbach et al., 2007), in which coexistence of competing communities is ensured by local interaction and dispersal (van Nouhuys and Hanski, 2005).

Neither the larval nor the juvenile bacterial communities are the final state of the system. Both are transient configurations from which the adult stable community develops (Fieth et al., 2016; Mortzfeld et al., 2016). Although stability has been described in marine ecosystems for microbial communities associated to various host taxa (Schmitt et al., 2012; Hester et al., 2016), there are examples (i.e., microbiota communities of corals) that do not present high resilience to perturbations (Rosenberg et al., 2009; Pogoreutz et al., 2018). Previous research has shown that environmental perturbations trigger slight changes in the composition of *N. vectensis* microbiota (Mortzfeld et al., 2016), but these effects were minor compared to the ones associated to the host development. Therefore, it is possible that the bacterial community associated to *N. vectensis* is able to buffer internal shifts such as the overrepresentation of single members of the community, as was simulated with our experiment.

Our study cannot exclude that host–bacteria interactions played a role in the succession of the microbial community, like the innate immune system (Franzenburg et al., 2012, 2013), spatial restriction (Kim et al., 2008; Mark Welch et al., 2017), or diet (David et al., 2014). Therefore, further investigations are needed to understand whether bacteria–bacteria interactions, host–bacteria interactions, or both modulate the resilience of the bacterial community. In the same way, we cannot discard that working with the strongest inferred correlations could mask some network properties (e.g., network connectivity and degree of each node) of particular relevance when choosing an OTU to implement an experiment. With the increasing number of isolates, exploration of other network properties or centrality measurements might be possible, and we could even gain the capacity to study only a few interactions at a time in a synthetic community approach (Bodenhausen et al., 2014).

CONCLUSION

The aim of this study was to experimentally show that co-occurrence networks infer ecologically relevant interactions. The recolonization treatments that included competitive bacteria resulted in increased alpha-diversity compared to treatments with cooperative or neutral OTUs and controls. Although the shift in community composition and diversity was short term (i.e., the effects vanished after 7 days), our results match the expectation of ecological theory for competitive players being able to increase the alpha-diversity (Coyte et al., 2015). This study provides experimental evidence about the ecological relevance of inferred correlations in microbial communities and is the first step to establish the marine sea anemone *N. vectensis* as an experimental model to test theoretical predictions in host-associated microbial communities.

AUTHOR CONTRIBUTIONS

HD, YZ-G, MS, UHH, and SF contributed to conception and design of the study. HD, YZ-G, and JB performed the research. HD, YZ-G, and SF performed the statistical analysis. HD, YZ-G, MS, and SF wrote the first draft of the manuscript. All authors contributed to manuscript revision and read and approved the submitted version.

FUNDING

This work was supported by the Deutsche Forschungsgemeinschaft (DFG; CRC1182 "Origin and function of Metaorganisms," Project B1). YZ-G was supported by a fellowship from the International Max Planck Research School for Evolutionary Biology.

ACKNOWLEDGMENTS

We are grateful to Thomas Bosch for his support and critical discussion. We thank Peter Deines and Benedikt Mortzfeld for their critical reading of the manuscript, the technicians Tanja Naujoks and Christopher Noack for the technical support. We also thank the Institute of Clinical Molecular Biology in Kiel for providing Sanger sequencing as supported in part by the DFG Cluster of Excellence "Inflammation at Interfaces" and "Future Ocean."

SUPPLEMENTARY MATERIAL

The Supplementary Material for this article can be found online at: https://www.frontiersin.org/articles/10.3389/fmicb.2018.00728/full#supplementary-material

REFERENCES

Agler, M. T., Ruhe, J., Kroll, S., Morhenn, C., Kim, S.-T., Weigel, D., et al. (2016). Microbial hub taxa link host and abiotic factors to plant microbiome variation. *PLoS Biol.* 14:e1002352. doi: 10.1371/journal.pbio.1002352

Bodenhausen, N., Bortfeld-Miller, M., Ackermann, M., and Vorholt, J. A. (2014). A synthetic community approach reveals plant genotypes affecting the phyllosphere microbiota. *PLoS Genet.* 10:e1004283. doi: 10.1371/journal.pgen.1004283

Caporaso, J. G., Kuczynski, J., Stombaugh, J., Bittinger, K., Bushman, F. D., Costello, E. K., et al. (2010). QIIME allows analysis of high-throughput community sequencing data. *Nat. Methods* 7, 335–336. doi: 10.1038/nmeth.f.303

Coyte, K. Z., Schluter, J., and Foster, K. R. (2015). The ecology of the microbiome: networks, competition, and stability. *Science* 350, 663–666. doi: 10.1126/science.aad2602

Czaran, T. L., Hoekstra, R. F., and Pagie, L. (2002). Chemical warfare between microbes promotes biodiversity. *Proc. Natl. Acad. Sci. U.S.A.* 99, 786–790. doi: 10.1073/pnas.012399899

Datta, M. S., Sliwerska, E., Gore, J., Polz, M. F., and Cordero, O. X. (2016). Microbial interactions lead to rapid micro-scale successions on model marine particles. *Nat. Commun.* 7:11965. doi: 10.1038/ncomms11965

David, L. A., Maurice, C. F., Carmody, R. N., Gootenberg, D. B., Button, J. E., Wolfe, B. E., et al. (2014). Diet rapidly and reproducibly alters the human gut microbiome. *Nature* 505, 559–563. doi: 10.1038/nature12820

Deines, P., and Bosch, T. C. G. (2016). Transitioning from microbiome composition to microbial community interactions: the potential of the metaorganism hydra as an experimental model. *Front. Microbiol.* 7:1610. doi: 10.3389/fmicb.2016.01610

DeSantis, T. Z., Hugenholtz, P., Larsen, N., Rojas, M., Brodie, E. L., Keller, K., et al. (2006). Greengenes, a chimera-checked 16S rRNA gene database and workbench compatible with ARB. *Appl. Environ. Microbiol.* 72, 5069–5072. doi: 10.1128/AEM.03006-05

Edgar, R. C. (2010). Search and clustering orders of magnitude faster than BLAST. *Bioinformatics* 26, 2460–2461. doi: 10.1093/bioinformatics/btq461

Faith, J. J., Guruge, J. L., Charbonneau, M., Subramanian, S., Seedorf, H., Goodman, A. L., et al. (2013). The long-term stability of the human gut microbiota. *Science* 341, 1237439. doi: 10.1126/science.1237439

Fan, L., Liu, M., Simister, R., Webster, N. S., and Thomas, T. (2013). Marine microbial symbiosis heats up: the phylogenetic and functional response of a sponge holobiont to thermal stress. *ISME J.* 7, 991–1002. doi: 10.1038/ismej.2012.165

Faszewski, E. E., Tyrell, A., Guin, S., and Kaltenbach, J. C. (2008). Metamorphic changes in localization of sugars in skin of the leopard frog, *Rana pipiens*. *J. Morphol.* 269, 998–1007. doi: 10.1002/jmor.10639

Faust, K., and Raes, J. (2012). Microbial interactions: from networks to models. *Nat. Rev. Microbiol.* 10, 538–550. doi: 10.1038/nrmicro2832

Fierer, N., Nemergut, D., Knight, R., and Craine, J. M. (2010). Changes through time: integrating microorganisms into the study of succession. *Res. Microbiol.* 161, 635–642. doi: 10.1016/j.resmic.2010.06.002

Fieth, R. A., Gauthier, M.-E. A., Bayes, J., Green, K. M., and Degnan, S. M. (2016). Ontogenetic changes in the bacterial symbiont community of the tropical demosponge amphimedon queenslandica: metamorphosis is a new beginning. *Front. Mar. Sci.* 3:228. doi: 10.3389/fmars.2016.00228

Franzenburg, S., Fraune, S., Künzel, S., Baines, J. F., Domazet-Lošo, T., and Bosch, T. C. G. (2012). MyD88-deficient Hydra reveal an ancient function of TLR signaling in sensing bacterial colonizers. *Proc. Natl. Acad. Sci. U.S.A* 109, 19374–19379. doi: 10.1073/pnas.1213110109

Franzenburg, S., Walter, J., Künzel, S., Wang, J., Baines, J. F., Bosch, T. C. G., et al. (2013). Distinct antimicrobial peptide expression determines host species-specific bacterial associations. *Proc. Natl. Acad. Sci. U.S.A.* 110, E3730–E3738. doi: 10.1073/pnas.1304960110

Fraune, S., Anton-Erxleben, F., Augustin, R., Franzenburg, S., Knop, M., Schröder, K., et al. (2014). Bacteria-bacteria interactions within the microbiota of the ancestral metazoan Hydra contribute to fungal resistance. *ISME J.* 9, 1543–1556. doi: 10.1038/ismej.2014.239

Friedman, J., and Alm, E. J. (2012). Inferring correlation networks from genomic survey data. *PLoS Comput. Biol.* 8:e1002687. doi: 10.1371/journal.pcbi.1002687

Fritzenwanker, J. H., and Technau, U. (2002). Induction of gametogenesis in the basal cnidarian *Nematostella vectensis* (Anthozoa). *Dev. Genes Evol.* 212, 99–103. doi: 10.1007/s00427-002-0214-7

Grosskopf, T., and Soyer, O. S. (2014). Synthetic microbial communities. *Curr. Opin. Microbiol.* 18, 72–77. doi: 10.1016/j.mib.2014.02.002

Haas, B. J., Gevers, D., Earl, A. M., Feldgarden, M., Ward, D. V., Giannoukos, G., et al. (2011). Chimeric 16S rRNA sequence formation and detection in Sanger and 454-pyrosequenced PCR amplicons. *Genome Res.* 21, 494–504. doi: 10.1101/gr.112730.110

Hand, C., and Uhlinger, K. R. (1992). The culture, sexual and asexual reproduction, and growth of the sea anemone *Nematostella vectensis*. *Biol. Bull.* 182, 169–176. doi: 10.2307/1542110

Hand, C., and Uhlinger, K. R. (1994). The unique, widely distributed, estuarine sea anemone, *Nematostella vectensis* stephenson: a review, new facts, and questions. *Estuaries* 17, 501–508. doi: 10.2307/1352679

Hester, E. R., Barott, K. L., Nulton, J., Vermeij, M. J., and Rohwer, F. L. (2016). Stable and sporadic symbiotic communities of coral and algal holobionts. *ISME J.* 10, 1157–1169. doi: 10.1038/ismej.2015.190

Jordán, F., Lauria, M., Scotti, M., Nguyen, T.-P., Praveen, P., Morine, M., et al. (2015). Diversity of key players in the microbial ecosystems of the human body. *Sci. Rep.* 5:15920. doi: 10.1038/srep15920

Kashyap, P. C., Marcobal, A., Ursell, L. K., Smits, S. A., Sonnenburg, E. D., Costello, E. K., et al. (2013). Genetically dictated change in host mucus carbohydrate landscape exerts a diet-dependent effect on the gut microbiota. *Proc. Natl. Acad. Sci. U.S.A.* 110, 17059–17064. doi: 10.1073/pnas.1306070110

Kelsic, E. D., Zhao, J., Vetsigian, K., and Kishony, R. (2015). Counteraction of antibiotic production and degradation stabilizes microbial communities. *Nature* 521, 516–519. doi: 10.1038/nature14485

Kerr, B., Riley, M. A., Feldman, M. W., and Bohannan, B. J. M. (2002). Local dispersal promotes biodiversity in a real-life game of rock-paper-scissors. *Nature* 418, 171–174. doi: 10.1038/nature00823

Kim, H. J., Boedicker, J. Q., Choi, J. W., and Ismagilov, R. F. (2008). Defined spatial structure stabilizes a synthetic multispecies bacterial community. *Proc. Natl. Acad. Sci. U.S.A.* 105, 18188–18193. doi: 10.1073/pnas.0807935105

Koenig, J. E., Spor, A., Scalfone, N., Fricker, A. D., Stombaugh, J., Knight, R., et al. (2011). Succession of microbial consortia in the developing infant gut microbiome. *Proc. Natl. Acad. Sci. U.S.A.* 108(Suppl.), 4578–4585. doi: 10.1073/pnas.1000081107

Ley, R. E., Peterson, D. A., and Gordon, J. I. (2006). Ecological and evolutionary forces shaping microbial diversity in the human intestine. *Cell* 124, 837–848. doi: 10.1016/j.cell.2006.02.017

Login, F. H., Balmand, S., Vallier, A., Vincent-Monégat, C., Vigneron, A., Weiss-Gayet, M., et al. (2011). Antimicrobial peptides keep insect endosymbionts under control. *Science* 334, 362–365. doi: 10.1126/science.1209728

Mark Welch, J. L., Hasegawa, Y., McNulty, N. P., Gordon, J. I., and Borisy, G. G. (2017). Spatial organization of a model 15-member human gut microbiota established in gnotobiotic mice. *Proc. Natl. Acad. Sci. U.S.A.* 114, E9105–E9114. doi: 10.1073/pnas.1711596114

Mitri, S., and Foster, K. R. (2013). The genotypic view of social interactions in microbial communities. *Annu. Rev. Genet.* 47, 247–273. doi: 10.1146/annurev-genet-111212-133307

Mortzfeld, B. M., Urbanski, S., Reitzel, A. M., Künzel, S., Technau, U., and Fraune, S. (2016). Response of bacterial colonization in *Nematostella vectensis* to development, environment and biogeography. *Environ. Microbiol.* 18, 1764–1781. doi: 10.1111/1462-2920.12926

Mounier, J., Monnet, C., Vallaeys, T., Arditi, R., Sarthou, A.-S., Helias, A., et al. (2008). Microbial interactions within a cheese microbial community. *Appl. Environ. Microbiol.* 74, 172–181. doi: 10.1128/AEM.01338-07

Mukherjee, S., Zheng, H., Derebe, M. G., Callenberg, K. M., Partch, C. L., Rollins, D., et al. (2014). Antibacterial membrane attack by a pore-forming intestinal C-type lectin. *Nature* 505, 103–107. doi: 10.1038/nature12729

Pickard, J. M., Maurice, C. F., Kinnebrew, M. A., Abt, M. C., Schenten, D., Golovkina, T. V., et al. (2014). Rapid fucosylation of intestinal epithelium sustains host–commensal symbiosis in sickness. *Nature* 514, 638–641. doi: 10.1038/nature13823

Pogoreutz, C., Rädecker, N., Cárdenas, A., Gärdes, A., Wild, C., and Voolstra, C. R. (2018). Dominance of *Endozoicomonas* bacteria throughout coral bleaching and mortality suggests structural inflexibility of the *Pocillopora verrucosa* microbiome. *Ecol. Evol.* 8, 2240–2252. doi: 10.1002/ece3.3830

Rausch, P., Basic, M., Batra, A., Bischoff, S. C., Blaut, M., Clavel, T., et al. (2016). Analysis of factors contributing to variation in the C57BL/6J fecal microbiota across German animal facilities. *Int. J. Med. Microbiol.* 306, 343–355. doi: 10.1016/j.ijmm.2016.03.004

Reichenbach, T., Mobilia, M., and Frey, E. (2007). Mobility promotes and jeopardizes biodiversity in rock-paper-scissors games. *Nature* 448, 1046–1049. doi: 10.1038/nature06095

Ribes, M., Calvo, E., Movilla, J., Logares, R., Coma, R., and Pelejero, C. (2016). Restructuring of the sponge microbiome favors tolerance to ocean acidification. *Environ. Microbiol. Rep.* 8, 536–544. doi: 10.1111/1758-2229.12430

Rollins-Smith, L. A. (1998). Metamorphosis and the amphibian immune system. *Immunol. Rev.* 166, 221–230. doi: 10.1111/j.1600-065X.1998.tb01265.x

Rosenberg, E., Kushmaro, A., Kramarsky-Winter, E., Banin, E., and Yossi, L. (2009). The role of microorganisms in coral bleaching. *ISME J.* 3, 139–146. doi: 10.1038/ismej.2008.104

Salzman, N. H., Hung, K., Haribhai, D., Chu, H., Karlsson-Sjoberg, J., Amir, E., et al. (2010). Enteric defensins are essential regulators of intestinal microbial ecology. *Nat. Immunol.* 11, 76–83. doi: 10.1038/ni.1825

Schmitt, S., Tsai, P., Bell, J., Fromont, J., Ilan, M., Lindquist, N., et al. (2012). Assessing the complex sponge microbiota: core, variable and species-specific bacterial communities in marine sponges. *ISME J.* 6, 564–576. doi: 10.1038/ismej.2011.116

Scotti, M., and Jordán, F. (2010). Relationships between centrality indices and trophic levels in food webs. *Community Ecol.* 11, 59–67. doi: 10.2307/24113632

Shade, A., Peter, H., Allison, S. D., Baho, D. L., Berga, M., Bürgmann, H., et al. (2012). Fundamentals of microbial community resistance and resilience. *Front. Microbiol.* 3:417. doi: 10.3389/fmicb.2012.00417

Staubach, F., Künzel, S., Baines, A. C., Yee, A., McGee, B. M., Bäckhed, F., et al. (2012). Expression of the blood-group-related glycosyltransferase B4galnt2 influences the intestinal microbiota in mice. *ISME J.* 6, 1345–1355. doi: 10.1038/ismej.2011.204

Vaishnava, S., Behrendt, C. L., Ismail, A. S., Eckmann, L., and Hooper, L. V. (2008). Paneth cells directly sense gut commensals and maintain homeostasis at the intestinal host-microbial interface. *Proc. Natl. Acad. Sci. U.S.A.* 105, 20858–20863. doi: 10.1073/pnas.0808723105

van Nouhuys, S., and Hanski, I. (2005). "Metacommunities of butterflies, their host plants and their parasitoids," in *Metacommunities - Spatial Dynamics and Ecological Communities*, eds R. D. H. M. Holyoak and M. A. Leibold (Chicago, IL: University of Chicago Press), 99–121.

Vigneron, A., Masson, F., Vallier, A., Balmand, S., Rey, M., Vincent-Monégat, C., et al. (2014). Insects recycle endosymbionts when the benefit is over. *Curr. Biol.* 24, 2267–2273. doi: 10.1016/j.cub.2014.07.065

Wasserman, S., and Faust, K. (1994). *Social Network Analysis?: Methods and Applications*. Cambridge: Cambridge University Press. doi: 10.1017/CBO9780511815478

Wei, Z., Yang, T., Friman, V.-P., Xu, Y., Shen, Q., and Jousset, A. (2015). Trophic network architecture of root-associated bacterial communities determines pathogen invasion and plant health. *Nat. Commun.* 6:8413. doi: 10.1038/ncomms9413

Weiss, S., Van Treuren, W., Lozupone, C., Faust, K., Friedman, J., Deng, Y., et al. (2016). Correlation detection strategies in microbial data sets vary widely in sensitivity and precision. *ISME J.* 10, 1669–1681. doi: 10.1038/ismej.2015.235

Zelezniak, A., Andrejev, S., Ponomarova, O., Mende, D. R., Bork, P., and Patil, K. R. (2015). Metabolic dependencies drive species co-occurrence in diverse microbial communities. *Proc. Natl. Acad. Sci. U.S.A.* 112, 6449–6454. doi: 10.1073/pnas.1421834112

Conflict of Interest Statement: The authors declare that the research was conducted in the absence of any commercial or financial relationships that could be construed as a potential conflict of interest.

frontiers in Marine Science

ORIGINAL RESEARCH
published: 15 August 2017
doi: 10.3389/fmars.2017.00267

Stimulated Respiration and Net Photosynthesis in *Cassiopeia* sp. during Glucose Enrichment Suggests *in hospite* CO_2 Limitation of Algal Endosymbionts

Nils Rädecker[1†], *Claudia Pogoreutz*[1†], *Christian Wild*[2] *and Christian R. Voolstra*[1*]

[1] *Biological and Environmental Sciences and Engineering Division, Red Sea Research Center, King Abdullah University of Science and Technology (KAUST), Thuwal, Saudi Arabia,* [2] *Marine Ecology Working Group, Faculty of Biology and Chemistry (FB 2), University of Bremen, Bremen, Germany*

OPEN ACCESS

Edited by:
Stanley Chun Kwan Lau, Hong Kong University of Science and Technology, Hong Kong

Reviewed by:
Luke Thompson, Southwest Fisheries Science Center (NOAA), United States
Adam Michael Reitzel, University of North Carolina at Charlotte, United States

***Correspondence:**
Christian R. Voolstra
christian.voolstra@kaust.edu.sa

[†] *These authors have contributed equally to this work.*

Specialty section:
This article was submitted to Marine Molecular Biology and Ecology, a section of the journal Frontiers in Marine Science

Received: *21 June 2017*
Accepted: *02 August 2017*
Published: *15 August 2017*

Citation:
Rädecker N, Pogoreutz C, Wild C and Voolstra CR (2017) Stimulated Respiration and Net Photosynthesis in Cassiopeia sp. during Glucose Enrichment Suggests in hospite CO_2 Limitation of Algal Endosymbionts. Front. Mar. Sci. 4:267. doi: 10.3389/fmars.2017.00267

The endosymbiosis between cnidarians and dinoflagellates of the genus *Symbiodinium* is key to the high productivity of tropical coral reefs. In this endosymbiosis, *Symbiodinium* translocate most of their photosynthates to their animal host in exchange for inorganic nutrients. Among these, carbon dioxide (CO_2) derived from host respiration helps to meet the carbon requirements to sustain photosynthesis of the dinoflagellates. Nonetheless, recent studies suggest that productivity in symbiotic cnidarians such as corals is CO_2-limited. Here we show that glucose enrichment stimulates respiration and gross photosynthesis rates by 80 and 140%, respectively, in the symbiotic upside-down jellyfish *Cassiopeia* sp. from the Central Red Sea. Our findings show that glucose was rapidly consumed and respired within the *Cassiopeia* sp. holobiont. The resulting increase of CO_2 availability *in hospite* in turn likely stimulated photosynthesis in *Symbiodinium*. Hence, the increase of photosynthesis under these conditions suggests that CO_2 limitation of *Symbiodinium* is a common feature of stable cnidarian holobionts and that the stimulation of holobiont metabolism may attenuate this CO_2 limitation.

Keywords: symbiosis, *Symbiodinium*, carbon limitation, heterotrophy, upside-down jellyfish

INTRODUCTION

Despite being surrounded by highly nutrient-poor (oligotrophic) waters, tropical coral reefs are among the most productive marine ecosystems (Hatcher, 1988). Reef ecosystems are sustained by an efficient uptake, retention, and reuse of nutrients on all levels of biological organization (Hatcher, 1990; Wild et al., 2004). In particular, the symbiosis between cnidarian hosts and endosymbiotic algae of the genus *Symbiodinium* facilitates the recycling of nutrients as it sustains primary productivity in the absence of major nutrient sources (Muscatine and Porter, 1977; Rädecker et al., 2015). In this symbiosis, *Symbiodinium* translocate most of their photosynthates to the cnidarian host that in turn provides inorganic nutrients derived from its metabolism (Muscatine et al., 1989). Thereby, this tight nutrient-exchange relationship, particularly in stony corals, is the functional basis for the ecological success of tropical coral reefs over millions of years.

Being surrounded by host membranes, *Symbiodinium* rely on their host to fulfill their photosynthetic carbon dioxide (CO_2) requirements. The supply of CO_2 to the symbiont

is controlled by two major processes: (1) CO_2 is produced during holobiont respiration (Muscatine et al., 1989). (2) Active carbon concentrating mechanisms (CCMs) by the host facilitate the uptake of dissolved inorganic carbon from surrounding seawater (Furla et al., 2000).

Despite these processes, several studies suggest that productivity in *Symbiodinium* may be carbon-limited even in stable symbiotic systems (Muscatine et al., 1989; Herfort et al., 2008; Klein et al., 2017). Hence, understanding the processes and environmental controls of *in hospite* CO_2 availability is crucial for our understanding of the cnidarian—alga symbiosis.

To address this issue, we experimentally tested whether photosynthesis of *Symbiodinium in hospite* is carbon-limited. Specifically, we investigated photosynthetic activity during glucose-stimulated holobiont respiration in the upside-down jellyfish *Cassiopeia* sp.. Unlike most other Scyphozoa, *Cassiopeia* spp. are mixotrophic, i.e. draw energy and nutrients from both heterotrophic and autotrophic sources (Rahav et al., 1989; Muscatine, 1990), as they form a close endosymbiotic relationship with *Symbiodinium*. Thereby, *Cassiopeia* spp. offer distinct advantages for the study of the cnidarian—alga symbiosis, similar to the Aiptasia model system (Baumgarten et al., 2015). For instance, they are easy to rear in aquaria cultures, are non-calcifying, have motile medusa stages and can be infected with various algal symbionts (Klein et al., 2017). Using this emerging cnidarian model system allowed us to tackle the issue of CO_2 limitation in the cnidarian—*Symbiodinium* symbiosis in a straightforward experiment.

METHODS

Collection and Maintenance

A total of 14 individuals of *Cassiopeia* sp. (mean bell diameter of 6.9 ± 0.3 cm) were collected with a dip net in the KAUST Harbor Lagoon, Saudi Arabia (N22°18′18.63″, E39°6′10.45″) in the Central Red Sea in September 2014. After collection, animals were immediately transferred to 2 recirculation aquaria (each filled with 20 L of ambient seawater) and acclimated to aquaria conditions for 7 days (salinity of 40, 28°C, 12:12 h light/dark cycle with ∼100 μmol m^{-2} s^{-1}). Stability of water parameters was ensured by exchanging 50% of aquaria seawater daily.

Incubations and Glucose Enrichment

Following acclimation, net photosynthesis and respiration rates of animals were directly assessed from oxygen (O_2) evolution/depletion measurements in 2 h light and dark incubations in 1 L gas-tight glass chambers, respectively. During these incubations, half of the animals were incubated in ambient seawater freshly enriched with glucose (500 mg L^{-1}). The other half of the animals served as a control and were incubated in ambient seawater. To correct jellyfish O_2 fluxes for planktonic background metabolism, two seawater controls (i.e., ambient seawater without jellyfish) were included for each treatment. Importantly, the dissolved organic carbon concentrations used here do not reflect naturally occurring ambient reef water conditions (Vaccaro et al., 1968; Kline et al., 2006). Rather, the level of enrichment was chosen to avoid glucose depletion over the course of the incubation and to ensure that effects of increased carbon availability were not buffered within the holobiont framework, in order to gain mechanistic insights into the cnidarian—alga symbiosis.

O_2 fluxes were assessed based on differences in O_2 concentrations before and after the incubation using an optical oxygen multiprobe (WTW, Germany). O_2 production/consumption rates were corrected for seawater controls and normalized to bell surface area of animals and incubation time. Gross photosynthesis rates were calculated based on differences in O_2 fluxes during light and dark incubations (gross photosynthesis = net photosynthesis + |respiration|). Differences between treatments for the individual response parameters were tested for significance using an unpaired Student's *t*-test with a significance level (α) of 0.05.

RESULTS AND DISCUSSION

Glucose enrichment stimulated respiration rates in seawater during both light and dark incubations (Supplementary Table S1). Still, seawater respiration rates were ∼5-fold below *Cassiopeia* sp. respiration rates at all times. Holobiont respiration rates of *Cassiopeia* sp. increased by ∼80% under glucose-enriched conditions compared to untreated controls [$t_{(13)} = 5.27$, $P < 0.001$, **Figure 1**]. Despite this increase in respiratory O_2 consumption, net photosynthesis rates during glucose-enriched conditions showed a significant increase of nearly 400% compared to controls [$t_{(13)} = 3.08$, $P = 0.008$]. Consequently, gross photosynthesis rates increased by ∼140% under glucose-enriched conditions compared to untreated controls [$t_{(13)} = 4.94$, $P < 0.001$].

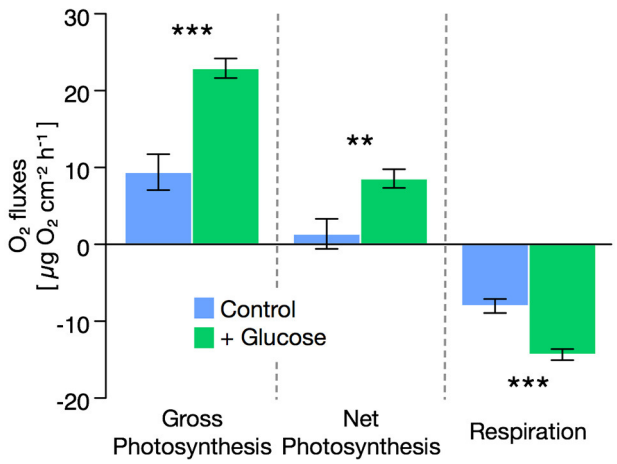

FIGURE 1 | Effect of glucose enrichment (500 mg L^{-1}) on gross and net photosynthesis as well as respiration rates in *Cassiopeia* sp. from the Central Red Sea. Net photosynthesis and respiration rates were derived from oxygen (O_2) flux measurements in light and dark incubations, respectively. Gross photosynthesis was calculated based on the differences in O_2 fluxes during light and dark incubations. All data are shown as mean ± SE. Asterisks indicate significant differences between groups (**$p < 0.01$; ***$p < 0.001$).

Glucose enrichment, hence, not only stimulated respiration rates but also caused a stark increase in photosynthetic activity in the mixotrophic cnidarian holobiont *Cassiopeia* sp.. The increase in respiration rates indicates that glucose was rapidly taken up and consumed (i.e., respired) within the holobiont (Pogoreutz et al., 2017). Given our current understanding of cnidarian holobionts, there is no reason to assume that glucose enrichment directly affected photosynthetic activity in *Symbiodinium*. Rather, the observed increase in net and gross photosynthesis can be attributed to an increase in CO_2 availability *in hospite*, stemming from increased respiration in the *Cassiopeia* holobiont and seawater planktonic communities within the incubation chamber. In the case of *Cassiopeia* sp. this CO_2 limitation may be potentially attenuated by their continuous pumping motion facilitating increased gas exchange with the surrounding seawater (Wild and Naumann, 2013).

On a broader scale, these results could have implications for our understanding of the mechanisms underlying the cnidarian—alga symbiosis. The observation of glucose-stimulated photosynthesis implies that productivity of *Symbiodinium in hospite* may be tightly limited by CO_2 derived from holobiont metabolism.

Wooldridge (2009) proposed that a failure of coral CCMs during heat stress may ultimately result in a CO_2 limitation of photosynthetic dark reactions in *Symbiodinium*, ultimately leading to coral bleaching. Direct empirical evidence for this theory is missing to date. Our results, therefore, add to a growing emerging body of work suggesting that *Symbiodinium* may be CO_2-limited even in stable symbiotic systems (Muscatine et al., 1989; Herfort et al., 2008; Buxton et al., 2009; Klein et al., 2017). Hence, environmental stressors which alter metabolic processes in the holobiont may indeed lead to severe CO_2 limitation as predicted by Wooldridge (2009). Furthermore, we could show that the stimulation of host heterotrophy may attenuate CO_2 limitation in *Symbiodinium*. In this context, several studies reported that increased heterotrophic feeding may mitigate the effects of thermal stress in reef-building corals, resulting in increased bleaching resilience (Grottoli et al., 2006; Baird et al., 2009; Houlbrèque and Ferrier-Pagès, 2009; Ezzat et al., 2016). While this effect was mostly attributed to a compensation of autotrophic with heterotrophic energy sources by the host, here we show that heterotrophy may also increase bleaching resilience by increasing CO_2 availability *in hospite*.

Taken together, our study highlights that the role of CO_2 availability within the cnidarian—algae symbiosis deserves further in-depth assessment. Further work will be necessary to understand the effects of environmental conditions on CO_2 availability *in hospite*, along with their implications for the cnidarian—alga symbiosis.

AUTHOR CONTRIBUTIONS

NR and CP designed and conducted the experiment. All authors analyzed the data and wrote and revised the manuscript.

FUNDING

Research reported in this publication was supported by KAUST baseline funding to CRV and grant Wi 2677/9-1 awarded to CW by German Research Foundation (DFG).

ACKNOWLEDGMENTS

The authors would like to thank Paul Müller and Zenon Batang for allocation of workspace and their assistance with the aquarium facilities at the Coastal and Marine Resources Core Lab (CMOR). We further thank the two reviewers for their constructive feedback and helpful comments.

SUPPLEMENTARY MATERIAL

The Supplementary Material for this article can be found online at: http://journal.frontiersin.org/article/10.3389/fmars.2017.00267/full#supplementary-material

REFERENCES

Baird, A. H., Bhagooli, R., Ralph, P. J., and Takahashi, S. (2009). Coral bleaching: the role of the host. *Trends Ecol. Evol.* 24, 16–20. doi: 10.1016/j.tree.2008.09.005

Baumgarten, S., Simakov, O., Esherick, L. Y., Jin, Y., Lehnert, E. M., Michell, C. T., et al. (2015). The genome of *Aiptasia*, a sea anemone model for coral symbiosis. *Proc. Natl. Acad. Sci. U.S.A.* 112, 11893–11898. doi: 10.1073/pnas.1513318112

Buxton, L., Badger, M., and Ralph, P. (2009). Effects of moderate heat stress and dissolved inorganic carbon concentration on photosynthesis and respiration of *Symbiodinium* sp. (Dinophycae) in culture and in symbiosis. *J. Phycol.* 45, 357–365. doi: 10.1111/j.1529-8817.2009.00659.x

Ezzat, L., Towle, E., Irisson, J.-O., Langdon, C., and Ferrier-Pagès, C. (2016). The relationship between heterotrophic feeding and inorganic nutrient availability in the scleractinian coral *T. reniformis* under a short-term temperature increase. *Limnol. Oceanogr.* 61, 89–102. doi: 10.1002/lno.10200

Furla, P., Allemand, D., and Orsenigo, M. N. (2000). Involvement of H^+-ATPase and carbonic anhydrase in inorganic carbon uptake for endosymbiont photosynthesis. *Am. J. Physiol. Regul. Integr. Comp. Physiol.* 278, 870–881.

Grottoli, A. G., Rodrigues, L. J., and Palardy, J. E. (2006). Heterotrophic plasticity and resilience in bleached corals. *Nature* 440, 1186–1189. doi: 10.1038/nature04565

Hatcher, B. G. (1988). Coral reef primary productivity: a beggar's banquet. *Trends Ecol. Evol.* 3, 106–111. doi: 10.1016/0169-5347(88)90117-6

Hatcher, B. G. (1990). Coral reef primary productivity. A hierarchy of pattern and process. *Trends Ecol. Evol.* 5, 149–155. doi: 10.1016/0169-5347(90)90221-X

Herfort, L., Thake, B., and Taubner, I. (2008). Bicarbonate stimulation of calcification and photosynthesis in two hermatypic corals. *J. Phycol.* 44, 91–98. doi: 10.1111/j.1529-8817.2007.00445.x

Houlbrèque, F., and Ferrier-Pagès, C. (2009). Heterotrophy in tropical scleractinian corals. *Biol. Rev. Camb. Philos. Soc.* 84, 1–17. doi: 10.1111/j.1469-185X.2008.00058.x

Klein, S. G., Pitt, K. A., Nitschke, M. R., Goyen, S., Welsh, D. T., Suggett, D. J., et al. (2017). *Symbiodinium* mitigate the combined effects of hypoxia and acidification on a non-calcifying organism. *Glob. Chang. Biol.* 23, 3690–3703. doi: 10.1111/gcb.13718

Kline, D. I., Kuntz, N. M., Breitbart, M., Knowlton, N., and Rohwer, F. (2006). Role of elevated organic carbon levels and microbial activity in coral mortality. *Mar. Ecol. Prog. Ser.* 314, 119–125. doi: 10.3354/meps314119

Muscatine, L. (1990). "The role of symbiotic algae in carbon and energy flux in reef corals," in *Ecosystems of the World*, *Coral Reefs*, ed Z. Dubinsky (Amsterdam: Elsevier), 75–87.

Muscatine, L., and Porter, J. W. (1977). Reef corals: mutualistic symbioses adapted to nutrient-poor environments. *Bioscience*, 27, 454–460. doi: 10.2307/1297526

Muscatine, L., Porter, J. W., and Kaplan, I. R. (1989). Resource partitioning by reef corals as determined from stable isotope composition. *Mar. Biol.* 100, 185–193. doi: 10.1007/BF00391957

Pogoreutz, C., Rädecker, N., Cárdenas, A., Gärdes, A., Voolstra, C. R., and Wild, C. (2017). Sugar enrichment provides evidence for a role of nitrogen fixation in coral bleaching. *Glob. Chang Biol.* 23, 3838–3848. doi: 10.1111/gcb.13695

Rädecker, N., Pogoreutz, C., Voolstra, C. R., Wiedenmann, J., and Wild, C. (2015). Nitrogen cycling in corals: the key to understanding holobiont functioning? *Trends Microbiol.* 23, 490–497. doi: 10.1016/j.tim.2015.03.008

Rahav, O., Dubinsky, Z., Achituv, Y., and Falkowski, P. G. (1989). Ammonium metabolism in the zooxanthellate coral, *Stylophora pistillata*. *Proc. R. Soc. B Biol. Sci.* 236, 325–337. doi: 10.1098/rspb.1989.0026

Vaccaro, R. F., Hicks, S. E., Jannasch, H. W., and Carey, F. G. (1968). The occurrence and role of glucose in seawater. *Limnol. Oceanogr.* 13, 356–360. doi: 10.4319/lo.1968.13.2.0356

Wild, C., Huettel, M., Klueter, A., Kremb, S. G., Rasheed, M. Y. M., and Jørgensen, B. B. (2004). Coral mucus functions as an energy carrier and particle trap in the reef ecosystem. *Nature* 428, 66–70. doi: 10.1038/nature02344

Wild, C., and Naumann, M. S. (2013). Effect of active water movement on energy and nutrient acquisition in coral reef-associated benthic organisms. *Proc. Natl. Acad. Sci. U.S.A.* 110, 8767–8768. doi: 10.1073/pnas.1306839110

Wooldridge, S. A. (2009). A new conceptual model for the warm-water breakdown of the coral – algae endosymbiosis. *Mar. Freshw. Res.* 60, 483–496. doi: 10.1071/MF08251

Conflict of Interest Statement: The authors declare that the research was conducted in the absence of any commercial or financial relationships that could be construed as a potential conflict of interest.

frontiers in Microbiology

ORIGINAL RESEARCH
published: 23 January 2018
doi: 10.3389/fmicb.2018.00024

Spatiotemporal Dynamics of Ammonia-Oxidizing Thaumarchaeota in Distinct Arctic Water Masses

Oliver Müller[1], Bryan Wilson[1], Maria L. Paulsen[1], Agnieszka Rumińska[1], Hilde R. Armo[1], Gunnar Bratbak[1] and Lise Øvreås[1,2]*

[1] Department of Microbiology, University of Bergen, Bergen, Norway, [2] University Center in Svalbard (UNIS), Longyearbyen, Norway

One of the most abundant archaeal groups on Earth is the Thaumarchaeota. They are recognized as major contributors to marine ammonia oxidation, a crucial step in the biogeochemical cycling of nitrogen. Their universal success is attributed to a high genomic flexibility and niche adaptability. Based on differences in the gene coding for ammonia monooxygenase subunit A (amoA), two different ecotypes with distinct distribution patterns in the water column have been identified. We used high-throughput sequencing of 16S rRNA genes combined with archaeal *amoA* functional gene clone libraries to investigate which environmental factors are driving the distribution of Thaumarchaeota ecotypes in the Atlantic gateway to the Arctic Ocean through an annual cycle in 2014. We observed the characteristic vertical pattern of Thaumarchaeota abundance with high values in the mesopelagic (>200 m) water throughout the entire year, but also in the epipelagic (<200 m) water during the dark winter months (January, March and November). The Thaumarchaeota community was dominated by three OTUs which on average comprised 76% ± 11 and varied in relative abundance according to water mass characteristics and not to depth or ammonium concentration, as suggested in previous studies. The ratios of the abundance of the different OTU types were similar to that of the functional *amoA* water cluster types. Together, this suggests a strong selection of ecotypes within different water masses, supporting the general idea of water mass characteristics as an important factor in defining microbial community structure. If indeed, as suggested in this study, Thaumarchaeota population dynamics are controlled by a set of factors, described here as water mass characteristics and not just depth alone, then changes in water mass flow will inevitably affect the distribution of the different ecotypes.

Keywords: thaumarchaeota, ammonia-oxidation, Arctic Ocean, water mass, ecotype, *amoA*, 16S rRNA gene sequencing

OPEN ACCESS

Edited by:
Stanley Chun Kwan Lau, Hong Kong University of Science and Technology, Hong Kong

Reviewed by:
Anne Bernhard, Connecticut College, United States
Yu Zhang, Shanghai Jiao Tong University, China

****Correspondence:***
Oliver Müller
oliver.muller@uib.no

Specialty section:
This article was submitted to Aquatic Microbiology, a section of the journal Frontiers in Microbiology

Received: *09 October 2017*
Accepted: *08 January 2018*
Published: *23 January 2018*

Citation:
Müller O, Wilson B, Paulsen ML, Rumińska A, Armo HR, Bratbak G and Øvreås L (2018) Spatiotemporal Dynamics of Ammonia-Oxidizing Thaumarchaeota in Distinct Arctic Water Masses. Front. Microbiol. 9:24. doi: 10.3389/fmicb.2018.00024

INTRODUCTION

The discovery of the high abundance of marine planktonic Archaea in 1992 was a revelation (DeLong, 1992; Fuhrman et al., 1992). Since then, numerous studies have confirmed both their high proportions and population dynamics, especially in deeper waters and from both polar oceans (Massana et al., 1998; Murray et al., 1998). In later studies the marine Archaea have been

found to play important roles in many biogeochemical processes (Ouverney and Fuhrman, 2000; Offre et al., 2013). When Craig Venter and colleagues discovered genes encoding for ammonia monooxygenase subunit A (amoA) in their metagenome analyses from the Sargasso Sea, new information regarding these processes was provided, leading to a particular interest in the marine Thaumarchaeota (Venter et al., 2004). This interest was further strengthened with the cultivation and characterization of the first marine archaeal isolate (*Candidatus Nitrosopumilus maritimus* SCM1) capable of ammonia oxidation (Könneke et al., 2005). Today, chemoautotrophic ammonia oxidizing Archaea (AOA) are recognized as the major contributors to marine microbial ammonia oxidation and thus driving nitrification processes, dominating these relative to their bacterial ammonia oxidizing (AOB) counterparts (Wuchter et al., 2006; Valentine, 2007).

Thaumarchaeota are widely distributed and may make up a significant part of marine microbial communities (Karner et al., 2001; Agogué et al., 2008; Beman et al., 2008). In the surface waters of polar regions there seem to be temporal changes in the relative abundance of Thaumarchaeota with an increase during winter and decline in summer (Massana et al., 1998; Murray et al., 1998; Church et al., 2003; Alonso-Sáez et al., 2008; Grzymski et al., 2012). Photoinhibition of ammonia oxidation has been hypothesized as an underlying cause for the seasonal disappearance of AOA (Guerrero and Jones, 1996; Murray et al., 1998; Mincer et al., 2007; Merbt et al., 2012). However, other factors, such as competition with an increasing abundance of phytoplankton and associated bacterial blooms (Massana et al., 1998; Church et al., 2003; Herfort et al., 2007) or nutrient limitations, including ammonium (Wuchter et al., 2006; Herfort et al., 2007; Kirchman et al., 2007), may also play important roles. Physical aspects such as deep water mixing have been suggested to resolve the winter increase of Thaumarchaeota abundance in the Southern Oceans (Kalanetra et al., 2009; Grzymski et al., 2012), but this could not explain the same trends in the Arctic, where the ocean remains relatively stratified during winter (Forest et al., 2011). Recent data have suggested that the increase in AOA is due to *in situ* growth at the surface and not to mixing with deeper water masses (Alonso-Sáez et al., 2012).

The surface Thaumarchaeota populations comprise predominantly one type of AOA, while the deep ocean is dominated by another type of AOA and have thus far, based on differences in their *amoA* genes, been divided into a surface (WCA) and a deep (WCB) type (Francis et al., 2005; Hallam et al., 2006; Beman et al., 2008; Sintes et al., 2013). Their depth-dependent distribution has been demonstrated in many different regions, including the Gulf of California (Beman et al., 2008), the Gulf of Mexico (Tolar et al., 2013), the Arctic Ocean (Pedneault et al., 2014), Monterey Bay (Smith et al., 2014) and throughout the entire Atlantic Ocean (Sintes et al., 2016). Taxonomically, *amoA* sequences can be divided into six main subclusters all branching to the *N. maritimus* cluster (Pester et al., 2012; Sintes et al., 2016). Two subclusters include only WCA sequences and the other four subclusters include exclusively WCB sequences.

The abundance of the different AOA types has also been correlated with ammonium concentrations and this has led to the introduction of high and low ammonium concentration AOA (HAC-AOA and LAC-AOA, respectively) (Herfort et al., 2007; Kirchman et al., 2007; Sintes et al., 2013). HAC-AOA dominate at depths with high ammonium concentrations while LAC-AOA are in higher abundance in deeper ocean regions where the ammonium concentration is low (Sintes et al., 2013). Overall, LAC-AOA corresponded taxonomically to WCB-types and HAC-AOA with WCA types. Ammonium concentrations (Woodward and Rees, 2001; Varela et al., 2007; Clark et al., 2008) measured for different oceanic regions could also support an observed macroecological AOA distribution in the Atlantic Ocean (Sintes et al., 2016). However, other environmental factors such as depth, temperature, dissolved oxygen, nitrite, and salinity have been previously identified as influences on the abundance and diversity of AOA (Francis et al., 2005; Herfort et al., 2007; Abell et al., 2010; Santoro et al., 2010; Biller et al., 2012; Pester et al., 2012; Sintes et al., 2015). Overall, the niche specification of the two ecotypes is best explained by depth in combination with geographic region and to a lesser extent with environmental factors, including ammonium concentration. However, it remains unclear whether these taxonomic definitions, both WCA/WCB and HAC/LAC, can be used to associate observed abundances with distinct biogeochemical niches, like water masses.

We have recently reported the high relative abundance and seasonal variation of Thaumarchaeota in waters around the western coast of Svalbard (Wilson et al., 2017). Here we extend the studies and investigate the Thaumarchaeota community in five different water masses, dominated by Atlantic and Arctic Water, using high throughput 16S rRNA gene sequencing aiming to identify different Thaumarchaeota populations and using *amoA* gene abundance to elucidate functional capabilities that may influence their distribution and dynamics.

MATERIALS AND METHODS

Study Site and Sampling

Samples were collected as part of the MicroPolar project (in cooperation with the project "CarbonBridge") during five cruises in 2014 north-west of Svalbard, following several transects along the West Spitsbergen Current (WSC) at the eastern part of the Fram Strait up to the Arctic Ocean (**Figure 1**). This area is hydrographically characterized by three Atlantic water masses, including Atlantic Water (AW), cold Atlantic Water (cAW) and Intermediate Water (IW), having salinity >34.9 and temperatures >2°C, 0–2°C and <0°C, respectively; and also, by two Arctic water masses, Surface Water (SW) and Arctic Water (ArW), having salinity <34.92 and density (σ_t) <27.7 and >27.7 respectively (Cokelet et al., 2008; de Steur et al., 2014; Randelhoff et al., 2015). An overview of the water mass characteristics is listed in Supplementary Table S3. The WSC at the eastern part of the Fram Strait transports Atlantic water into the Arctic Ocean. This Atlantic water can also be found in deeper mesopelagic zones as cAW and IW. The water masses classified as Arctic Water do not necessarily originate from the Arctic Ocean interior, but have undergone similar freshening and cooling processes and have the same physical characteristics as Arctic Ocean water masses.

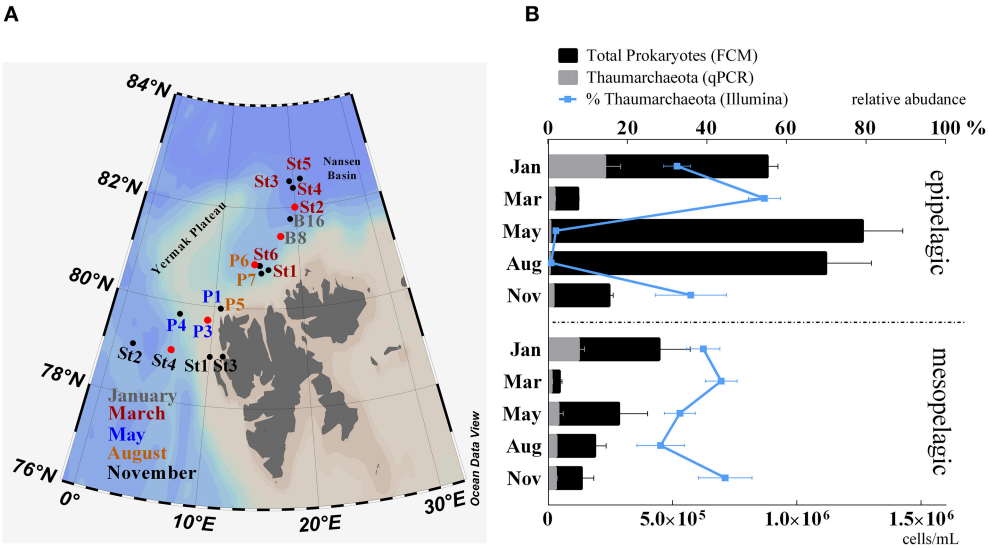

FIGURE 1 | (A) Study area Northwest of Svalbard. Stations are colored according to their time of sampling: gray, January; red, March; blue, May; yellow, August; black, November. Stations marked with a red circle were selected for *amoA* functional gene analyses. **(B)** Abundance of prokaryotes counted by flow cytometry (black bars) and superimposed abundance of Thaumarchaeota (gray bars) determined by qPCR of 16S rRNA genes. Relative abundance of Thaumarchaeota in relation to the total of 16S rRNA genes from Illumina sequencing data is shown by the blue line. Samples were grouped in epipelagic (0–200 m; $n = 28$) and mesopelagic (200–1,000 m; $n = 22$) zones and according to their sampling month. Standard errors were calculated for average values and are indicated as error bars.

Sampling periods extended over an entire polar year with cruises in January (06.01–15.01), March (05.03–10.03), May (15.05–02.06), August (07.08–18.08), and November (03.11–10.11). Depth profiles of temperature, salinity and fluorescence were recorded using a SBE 911plus CTD system (Sea-Bird Scientific, WA, USA) and used to identify water masses and to collect water for downstream analyses. Samples (25-50 L) for molecular analyses were taken between depths of 1 and 1,000 m (Supplementary Table S1), filtered onto 0.22 µm pore size Millipore® Sterivex filters (Merck-Millipore, MA, USA) and immediately frozen at −80°C. In total 50 samples (epipelagic zone; 0–200 m; $n = 28$ and mesopelagic zone; 200–1,000 m; $n = 22$) were used for molecular analysis. Further cruise and sampling details are described in Paulsen et al. (2016) and Wilson et al. (2017), respectively.

Flow Cytometry

The abundance of prokaryotes was detected from samples collected at 18 stations from 11 depths (1, 5, 10, 20, 30, 50, 100, 200, 500, 750, and 1,000 m) during 5 cruises using an Attune® Acoustic Focusing Flow Cytometer (Applied Biosystems by Life technologies, CA, USA) with a syringe-based fluidic system and a 20 mW 488 nm (blue) laser. First, samples were fixed with glutaraldehyde (0.5% final conc.) and incubated at 4°C for a minimum of 30 min, frozen in liquid nitrogen and stored at −80°C. For analysis, samples were diluted with 0.2 µm filtered TE buffer (Tris 10 mM, EDTA 1 mM, pH 8), stained with a green fluorescent nucleic acid dye (SYBR Green I; Molecular Probes, Eugene, Oregon, USA) and kept for 10 min at 80°C in a water bath (Marie et al., 1999). A minimum of 100 µL was counted at a low flow rate of 25 µL min^{-1} and prokaryotes were discriminated on a biparametric plot of green florescence vs. red florescence.

Ammonium Measurements

Concentrations of NH_4^+ were determined fluorometrically from frozen samples (4 mL) using orthophthadialdehyde according to the protocol by Holmes (1999). The method was adapted for microplate readings following (Poulin and Pelletier, 2007) and samples were analyzed on a 2300 EnSpire™ Multilabel Plate Reader (PerkinElmer, Finland). A 0.1 M ammonium chloride stock solution was used to prepare standard curves (0.1, 0.3, 0.6, 1, 2 µM) with correlation coefficients ≥0.986.

Nucleic Acids Extraction and Amplification for Amplicon Sequencing

DNA and RNA from Sterivex filters were extracted using the AllPrep DNA/RNA Mini Kit (Qiagen, Hilden, Germany). Details regarding RNA processing can be found in Wilson et al. (2017). In short, 10 ng RNA was treated with the DNA-free DNA Removal kit (Invitrogen, CA, USA) and subsequently reverse transcribed using the SuperScript III First-Strand Synthesis System for RT-PCR (Invitrogen), following the manufacturer's instructions. DNA was amplified using a two-step nested PCR approach with primers 519F and 806R (Supplementary Table S2) targeting both the archaeal and the bacterial 16S rRNA gene V4 hypervariable region. During the first step, triplicate samples were amplified in reaction volumes of 20 µL, comprising 10 ng DNA, 10 µL HotStarTaq Master Mix (Qiagen), 0.5 µM of each primer and nuclease-free water. PCR reaction conditions were as follows: initial denaturation of 15 min at 95°C, followed by 25 cycles of 95°C for 20 s, 55°C for 30 s and 72°C for 30 s and a final extension

step of 72°C for 7 min. Triplicate PCR products were pooled and purified using the DNA Clean & Concentrator-5 kit (Zymo Research Corporation, CA, USA). 10 ng of pooled PCR product was used for the second PCR step, in a reaction volume of 50 μL together with 25 μL HotStarTaq Master Mix, 0.5 μM of each nested primer (containing a unique eight-nucleotide barcode) and nuclease-free water. PCR reaction conditions were as follows: initial denaturation of 15 min at 95°C, followed by 15 cycles of 95°C for 20 s, 62°C for 30 s, 72°C for 30 s and a final extension step of 72°C for 7 min. Final PCR products were purified using Agencourt AMPure XP Beads (Beckman Coulter Inc., CA, USA) and prepared for sequencing by pooling the samples in equimolar amounts. The quality and concentration of the amplicon pool were assessed by agarose gel electrophoresis and a Qubit 3.0 Fluorometer, respectively. Libraries were sequenced at the Norwegian Sequencing Centre (Oslo, Norway) using their Illumina MiSeq platform (MiSeq Reagent Kit v2, Illumina, CA, USA). Sequencing data are available at the European Nucleotide Archive (ENA) under study accession number PRJEB23129. The primers (519F-806R) used in this study have been shown to have a low affinity for the SAR11 cluster, which can result in overestimation of other prokaryotic groups (Apprill et al., 2015).

16s rRNA Gene Sequence Analysis

Paired-end sequences were processed using various bioinformatic tools incorporated in the QIIME software environment (Caporaso et al., 2011), as described in Paulsen et al. (2016). Briefly, FASTQ files were quality end-trimmed, merged and prokaryotic OTUs were selected at a sequence similarity threshold of 97% and taxonomy assigned using the Silva 111 reference database (Quast et al., 2013). A total of 5,995,334 sequences were retrieved from high-throughput sequencing of the 16S rRNA gene V4 hypervariable region from DNA across fifty samples from five cruises. After removal of singletons, unassigned OTUs and chloroplast reads, sequences were rarefied to 10,000 reads per sample, with a total of 24,723 unique OTUs (63.1% singletons) at 97% sequence similarity. Bray–Curtis resemblance and ANOSIM statistical analysis were performed using PRIMER-E (Version 6; Quest Research Limited, Auckland, NZ).

Quantitative Real-Time PCR (qPCR)

All qPCR assays were run in triplicates on a C1000 Thermocycler (BioRad, CA, USA). The following qPCR reaction mixture was used: 10 μl Fast EvaGreen® qPCR Master Mix (Biotium, Inc., Hayward, CA, USA), 0.5 μM final concentration of each primer, 1 μL template DNA (corresponding to 1 ng of environmental DNA) and water were added to a final volume of 20 μL. All qPCR reactions were performed in white 96 well plates (BioRad). Thaumarchaeota 16S rRNA genes were quantified using the Thaumarchaeota specific forward primer Thaum-494F (Hong et al., 2015) and an archaeal universal primer ARC917R (Loy et al., 2002). This primer pair was suggested to better target the Thaumarchaeota and showed a higher affinity (96%) *in silico* to Marine Group I Archaea than previously used primer pairs (Hong et al., 2015). qPCR reaction conditions were as follows: initial activation for 2 min at 95°C, followed by 35 cycles of amplification, including denaturation at 95°C for 30 s, annealing at 55°C for 30 s, extension at 72°C for 30 s and a final extension step of 10 min at 72°C. The fluorescence was measured at the end of each cycle and a melting curve obtained from 65 to 95°C, with increments of 0.2°C. Ten-fold dilutions ranging from 1.1×10^8 to 1.1×10^3 copies of environmental Thaumarchaeota 16S rRNA gene were used as a quantification standard. Efficiencies for all qPCR reactions ranged from 83 to 84% with constant R^2-values of 0.998. To calculate gene copies per mL, the copy number per ng was multiplied by the DNA concentration per mL (based on flow cytometer counts and the assumption that one prokaryote contains 3 fg of DNA; Fuhrman and Azam, 1982; Jeffrey et al., 1996).

Phylogenetic Analysis of amoA and 16s rDNA Clone Libraries

A total of 10 MicroPolar samples from five stations representative of all five water masses were selected for *amoA* functional gene amplification. Each time point comprised both a surface and deep sample, excluding surface samples from the summer season (May and August), due to very low *amoA* abundances. Overall, eight DNA and two RNA samples were used for this analysis. The two RNA samples were from the same depths as the DNA samples from the November cruise and are included as an indicator of the active transcription of *amoA* mRNA. Amplification was performed using archaeal *amoA* primers (Supplementary Table S2) targeting a 635 bp gene fragment using the protocol of Francis et al. (2005) and 30 amplification cycles (iCycler, Bio-Rad, CA, USA). These primers have been widely used, but have been shown to underestimate *amoA* abundance in surface water samples (Tolar et al., 2013). PCR products were purified using the ExoSap-IT kit (Applied Biosystems) and subsequently cloned with the Qiagen PCR Cloning Kit (Qiagen) following manufacturer instructions. A total of 242 clones from all 10 samples were selected, and sequenced in-house at the sequencing facility of the University of Bergen (http://www.uib.no/en/seqlab). In order to obtain the 16S rRNA gene fragments for phylogenetic analysis, the same steps were followed as for the *amoA* genes; amplification was performed using an Archaea-specific forward primer in combination with a universal prokaryotic reverse primer resulting in amplicons of 1481 bp length (Supplementary Table S2). PCR reaction conditions were similar to those described before, with the exception of the annealing temperature, which was adjusted to 52°C. All *amoA* gene sequences from this study have been deposited at ENA under study accession number PRJEB23151. The three full length sequences of the 16S rRNA gene have been deposited at NCBI under GenBank accession numbers MG238502-MG238504.

Sequencing of *amoA* clones resulted in a total of 230 high quality sequences. This dataset was combined with an additional 254 *amoA* sequences (220 bp gene fragment) from a recent study on archaeal ammonia oxidizing ecotypes in the Atlantic Ocean (Sintes et al., 2016). This combined dataset was used to define OTUs at 97% sequence similarity using the *de novo* uclust (Edgar, 2010) OTU clustering method in QIIME, using

default parameters. In total, 189 OTUs were identified and used for phylogenetic analysis based on multiple alignments of *amoA* OTUs using MUSCLE (Edgar, 2004) with default parameters. The phylogenetic tree was inferred using the neighbor–joining method (Saitou and Nei, 1987) with 1000 bootstrap replicates. The retrieved tree was viewed using Evolview v2 (He et al., 2016).

The same strategy was implemented for Thaumarchaeota16S rRNA gene sequences. In order to include the Illumina amplicon reads, all sequences used (clonal or otherwise) for the phylogenetic analysis were trimmed to a size of 268 bp. A total of 1256 Thaumarchaeota sequences, including the three most abundant Thaumarchaeota OTUs from our amplicon data set, three full length 16S rRNA Sanger-sequenced reads and 1242 environmental sequences from the Arctic Ocean, the Atlantic Ocean, the Northeast Pacific, the North Sea and Gulf of Mexico were used to define OTUs at 97% similarity (Agogué et al., 2008; Bale et al., 2013; Tolar et al., 2013; Wright, 2013; Ijichi and Hamasaki unpublished). The resulting 23 OTUs were used for phylogenetic analysis as described above. We calculated the relative abundance of these OTUs in sets of samples from depths below or above 100 m.

RESULTS

Hydrography and Seasonal Thaumarchaeota Abundance

We used 16S rRNA gene sequencing and qPCR analyses to determine the relative and absolute abundance of Thaumarchaeota in samples taken during five cruises throughout the year in the Arctic Ocean off the western coast of Svalbard (**Figure 1**). Throughout the sampling period, Thaumarchaeota represented up to 73% (62% by qPCR) of the prokaryotic community. The relative abundance of Thaumarchaeota varied with both depth and season. Surface samples from the epipelagic (1–200 m) zone showed clear seasonal changes in Thaumarchaeota relative abundance. During the winter months relative abundance was high (44% ±15), while it was low during the summer season (1.4% ±1.4). In contrast, Thaumarchaeota relative abundance in the deep mesopelagic samples (200–1,000 m) was relatively high (38% ±11) throughout the entire year (**Figure 1B**).

Although total prokaryote abundance strongly increased during the summer months, absolute Thaumarchaeota abundance of up to 3.8×10^5 cells mL^{-1} (January, 1 m, station B8) was highest during the winter months (**Figures 1B**, **2**). Relative Thaumarchaeota abundance values from 16S rRNA gene sequencing and calculated values from qPCR were comparable, while the Illumina derived relative abundance was on average 14% higher (Supplementary Figure S3). We identified the three most abundant OTUs, which constituted on average 76% ±11 of the total Thaumarchaeota community in all samples. The same three OTUs were identified from 16S rRNA sequencing of reverse-transcribed total RNA, suggesting an active role in the prokaryotic community (Wilson et al., 2017).

Phylogenetic analysis of 16S rRNA genes, which included the three OTUs, and 1,242 environmental sequences from the Arctic Ocean, the Atlantic Ocean, the Northeast Pacific, the North Sea and Gulf of Mexico, showed that the three most abundant OTUs from our study are also represented in other environments. The OTUs representing our three most abundant Thaumarchaeota types comprise 92% of all sequences included in the analysis. The phylogenetic tree shows that all OTUs are related to the cultured strain *Nitrosopulimus maritimus* SCM1 and that they divide into two subgroups representing predominantly samples of either epipelagic or mesopelagic origin (Supplementary Figure S1). While OTUs affiliated to the surface group can be found in samples from both the epipelagic and mesopelagic zones, OTUs from the deep group were exclusively from mesopelagic samples indicating a depth-dependent distribution pattern as documented before.

Thaumarchaeota Abundance Patterns Correlated with Specific Water Masses

The profiles in **Figures 2A–D** illustrate the differences in abundance of Thaumarchaeota OTUs for the five cruises and in contrasting stations with varying water masses. Overall, similar presence/absence patterns of the three most abundant OTUs can be observed throughout all cruises, which are partly connected to depth (**Figure 2**). This includes OTU 81053 and OTU 201889 being most abundant in the surface and deep waters, respectively. In order to identify a distribution pattern for these OTUs, we separated all samples, according to their depth in epipelagic and mesopelagic groups, as has been done previously (**Figure 4A**). The OTU abundance pattern between the two water zones was significantly different, as shown by an ANOSIM analysis ($R = 0.32$; $p = 0.001$). Whilst OTU 81053 was most abundant in epipelagic waters (62–88%), it was found to be highly variable in samples from the mesopelagic zone (9.8–71%), thus referred to as "surface OTU". In contrast, OTU 201889 was barely detectable in epipelagic samples (<0.5%) and of varying abundance (0.2–51%) in mesopelagic samples, hence was referred to as "deep OTU". The third most abundant OTU (0.2–19%) was detected in variable abundance in both epipelagic and mesopelagic waters and is referred to as "middle OTU". All other Thaumarchaeota OTUs were grouped into those three OTU types, according to their abundance pattern.

In order to identify Thaumarchaeota distribution patterns throughout the entire sample set, a cluster analysis using Bray-Curtis similarities was performed (**Figure 3** and Supplementary Figure S4). The cluster analysis shows five groups, which are in co-occurrence with the five physical water masses observed in the study area (exceptions marked in red). This co-occurrence pattern was observed over the entire sampling period and the Thaumarchaeota abundance pattern in January in AW samples was highly similar to AW samples from March, May August and November (**Figure 3**). Therefore grouping the samples into the water mass groups revealed a more distinct distribution pattern of the three most abundant OTUs, shown to be significantly different by an ANOSIM analysis ($R = 0.63$; $p = 0.001$) (**Figure 4B**). The different water mass groups include samples from varying depths and some from both epipelagic and mesopelagic zones, as indicated in **Figure 4B**.

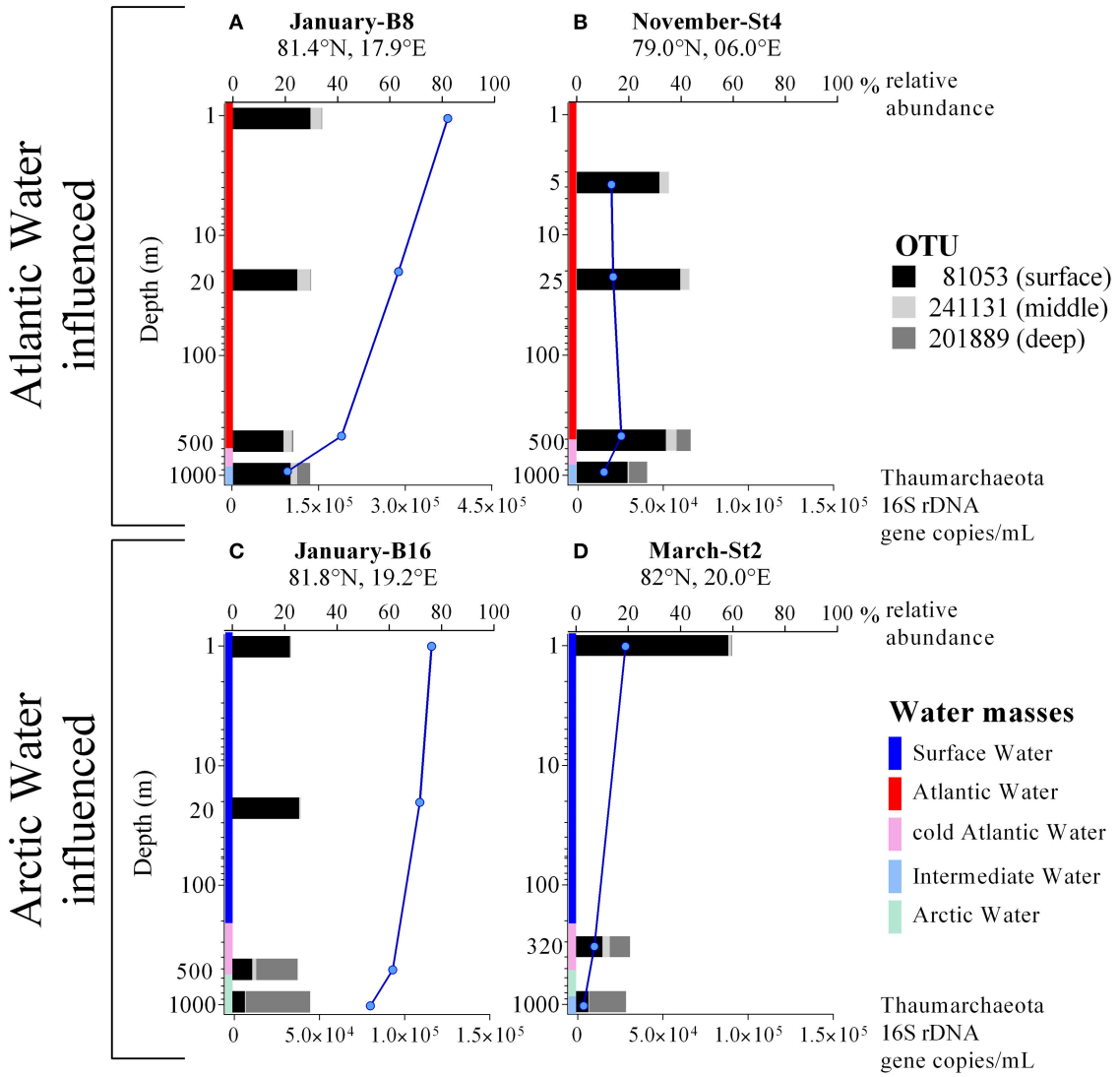

FIGURE 2 | (A–D) Profiles of Thaumarchaeota abundance (blue lines) determined by qPCR of 16S rRNA genes and Thaumarchaeota relative abundance (black, gray, light gray bars; in % of total 16S rRNA Illumina amplicons) from four different stations, where either Atlantic or Arctic water masses were dominating. Notice different scales on the x-axis (lower x-axis for qPCR derived Thaumarchaeota gene copies per mL; upper x-axis for Thaumarchaeota relative abundance from Illumina sequencing data). Colors indicate the water mass profile. Note that the y-axis is in logarithmic scale.

The influence between water mass and Thaumarchaeota OTU abundance was particularly noticeable at the two stations in January (**Figures 2A,C**). Only 43 km apart, the two stations showed very different Thaumarchaeota abundance patterns at comparable depths, connected to the discriminating water masses observed at the stations. These OTU abundance patterns seen in January were also observed at other stations during other sampling months. Over the entire sampling period, the three OTUs showed distinctive changes in abundance in the five water masses. The surface OTU showed highest abundance in SW (84% ± 3.1) and declined in the other water masses down to 14% ± 3.6 in ArW. An opposite trend was observed for the deep OTU with highest abundance in ArW (40%±10) declining in IW (23% ± 4.7), cAW (9.2% ± 2.5), AW (1.5% ± 1.7), and lowest in SW (0.2% ± 0.2). The highest abundance of the middle OTU was found in AW (11% ± 4.0) and declining in the other modified Atlantic water masses (cAW: 6.3% ± 0.2; IW: 4.0% ± 2.8). In the SW and ArW the middle OTU was underrepresented (1.7% ± 1.4; 1.3% ± 1.4).

We tested whether the changes in relative abundance of the three OTUs were significantly correlated with the different water masses and other environmental factors. The best fit for linear regressions was achieved when Thaumarchaeota abundance was plotted against water mass and not depth. All three OTUs showed distinct seasonally reoccurring abundance patterns that correlate with the distinct water masses in the area. OTU abundance either

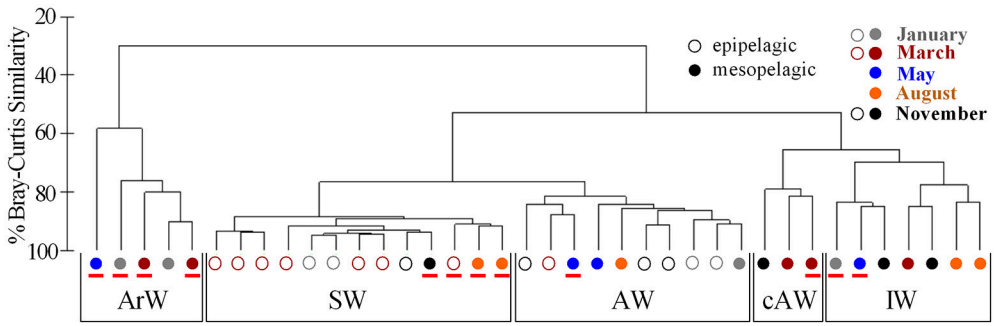

FIGURE 3 | Hierarchical cluster analysis of Bray-Curtis similarities, based on the diversity of Thaumarchaeota sequences from Illumina amplicon sequencing of 16S rRNA genes, illustrating the distribution of samples into five groups. These five groups are labeled according to water mass specificities of the samples within the groups (ArW, Arctic Water; SW, Surface Water; AW, Atlantic Water; cAW, cold Atlantic Water; IW, Intermediate Water). Samples with a mismatch between their associated water mass group and the physical water mass of their sampling origin are marked with a red line. The sampling month is given by colors. Samples were further distinguished according to depth, with open circles for epipelagic samples (0–200 m; $n = 16$) and filled circles for mesopelagic samples (200–1,000 m; $n = 22$).

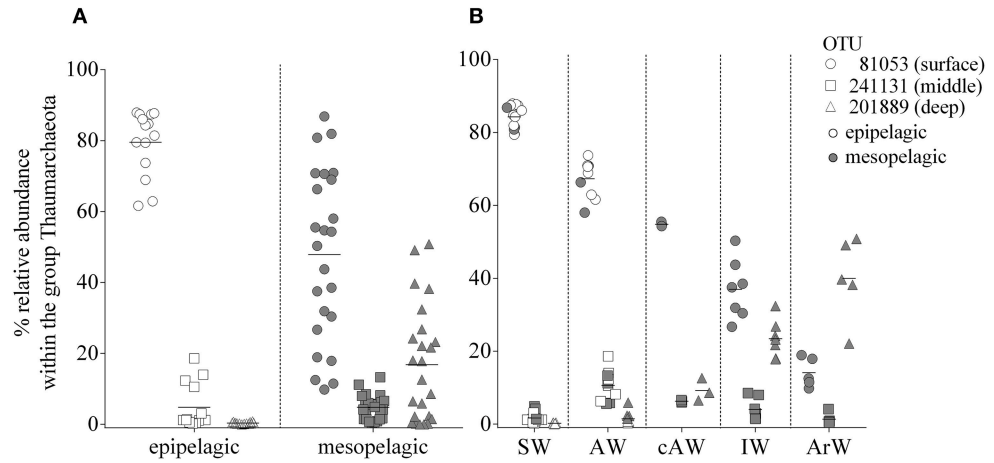

FIGURE 4 | (A) Relative abundance of the three most abundant Thaumarchaeota OTUs. Samples were divided according to their sampling origin in epipelagic (open symbols; 0–200 m; $n = 16$) and mesopelagic (filled symbols; 200–1,000 m; $n = 22$) zones. **(B)** Same data as in **(A)**, grouped according to assigned water masses based on sample similarities illustrated in **Figure 3**. ArW, Arctic Water; SW, Surface Water; AW, Atlantic Water; cAW, cold Atlantic Water; IW, Intermediate Water.

decreased (surface and middle OTU, $R^2 = 0.96$; $p < 0.0001$ and $R^2 = 0.6$; $p < 0.0001$) or increased (deep OTU, $R^2 = 0.84$; $p < 0.0001$) from SW or AW toward deeper water masses, such as cAW, IW, and ArW (**Figure 4B**). Environmental factors were correlated with some OTUs but not all three together. For example, both the middle OTU and surface OTU were positively (Pearson's r, $r = 0.51$; $p < 0.0014$) or negatively (Pearson's r, $r = -0.51$; $p < 0.0012$) correlated respectively to salinity, whilst the deep OTU was not correlated at all. Temperature was also correlated with abundance of the middle OTU (Pearson's r, $r = 0.69$; $p < 0.0001$), but not the other OTUs. None of the three OTUs was correlated with ammonium concentration or sampling month.

Analysis of amoA Gene Phylogeny

To answer whether there was a similar Thaumarchaeota distribution pattern on the functional gene level, we analyzed the distribution of the gene encoding for amoA. A single station for each sampling month (comprising both a surface and deep sampling point) was chosen, excluding summer season surface samples with the low Thaumarchaeota abundance. These eight samples represented all different water masses encountered during the five cruises and resulted in 230 *amoA* sequences. The genetic diversity of these MicroPolar sequences, combined with published sequences from the entire Atlantic, is illustrated in Supplementary Figure S2 and revealed the six main subclusters previously reported (Sintes et al., 2016). A simplified version of this phylogenetic tree is shown in **Figure 5**. MicroPolar sequences can be found both in subclusters 1 and 2 (representing sequences from WCA) and 3–6 (excluding 4; representing sequences from WCB). In total 15 (5 with >1 sequence) new *amoA* OTUs representing 50 MicroPolar sequences were identified. The majority of our Arctic *amoA* sequences affiliated to subclusters 2 and 6. The deep subcluster 6 represented sequences mostly from mesopelagic samples, while sequences from subcluster 2 were from both epipelagic and mesopelagic MicroPolar samples. The

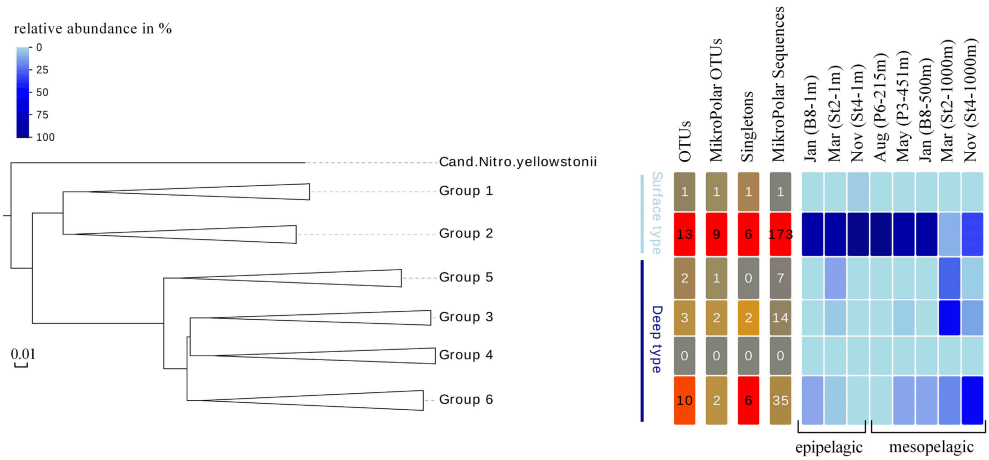

FIGURE 5 | Left panel Phylogenetic tree of 189 *amoA* OTUs at 97% sequence identity, representative of the genetic diversity of *amoA* clades 1-6 in reference samples (254 sequences) and in 10 MicroPolar samples (230 sequences). The colored lines indicates the grouping of the six *amoA* clusters in surface (light blue) and deep (dark blue) type. **Right panel** Distribution of OTUs, OTUs which only consist of MicroPolar sequences, OTUs that only consist of one sequence and MicroPolar sequences within the six *amoA* clusters. Heat map, in shades of blue, displaying the relative abundance of OTUs at each analyzed station and grouped by sampling depth.

heat map (illustrating the relative abundance pattern both of the WCA and WCB *amoA* sequences) shows only two samples (Mar-St2-1,000 m and Nov-St4-1,000 m) where *amoA* OTUs were more abundant in the deep WCB group than the surface WCA group (**Figure 5**). Other mesopelagic samples from January, May and August comprised mainly sequences from the WCA group. We compared the 10 samples from the *amoA* data set with our 16S rRNA gene Illumina amplicon data as we observed a similar pattern between the deep and surface OTU types (**Figure 6**). The different ratio of contrasting 16S rRNA gene surface/deep types was highly similar to *amoA* gene WCA/WCB types in all samples. For both genes the observed pattern was co-occurring with different water masses.

DISCUSSION

Thaumarchaeota are ubiquitous in marine environments, but a temporal pattern, where abundances decrease significantly during summer seasons, has been described for the polar regions (Massana et al., 1998; Murray et al., 1998; Church et al., 2003; Alonso-Sáez et al., 2008; Christman et al., 2011). We detected high Thaumarchaeota abundances in winter surface waters, contributing up to 38% to the total prokaryotic community. High Thaumarchaeota abundance in surface waters have been reported before, with maximum values of 64% in the Antarctic (Kalanetra et al., 2009) or up to 40% in the Northern Gulf of Mexico (Tolar et al., 2013). Measurements of absolute Thaumarchaeota abundance in other parts of the Arctic Ocean (Amundsen Gulf region) showed similar high gene copy numbers (10^5 16S rRNA gene copies mL^{-1}) in winter surface water as observed in our study. Our data confirmed a cyclical shift in Thaumarchaeota abundance in surface waters, showing a strong increase in winter months and a decline in summer months (**Figure 1B**). At the taxonomic level of OTUs, we observed a distinct distribution of different Thaumarchaeota ecotypes that were not directly correlated with their epipelagic or mesopelagic sampling origin. These ecotypes rather seemed to occur according to different water masses, representing a possibly important (yet often neglected) environmental factor as the main driver of Thaumarchaeota distribution. This study better defines how water masses may influence the abundance of Thaumarchaeota in the ocean. Water masses combine by definition a set of measurable environmental parameters, extending the three, including salinity, density and temperature used to define them, as well as factors like origin and history. Due to this complexity it remains unclear which environmental parameter is driving the distribution of Thaumarchaeota OTUs. However, the results of this study point toward a more complex mechanism of Thaumarchaeota distribution than, as previously reported, depth or ammonium concentration could explain.

Thaumarchaeota Abundance Patterns Correlated with Specific Water Masses

The 16S rRNA gene sequence data showed that the surface Thaumarchaeota group is dominated by a single OTU, which has previously been found both in the Arctic and Antarctic Oceans (Arctic 70%: Alonso-Sáez et al., 2012; Antarctic 83%: Kalanetra et al., 2009; Grzymski et al., 2012). The most abundant OTU in our data set was predominantly identified in surface samples, comprising up to 88% of the Thaumarchaeota population and sharing 98% identity with the same OTU from the Arctic and Antarctic studies. As a result of the repeated sampling campaigns of depth profiles over the entire polar year, we detected the reoccurrence of this OTU in the winter surface waters and decreasing abundance with depth. Interestingly, another single OTU outcompeted the surface OTU and was dominant in our

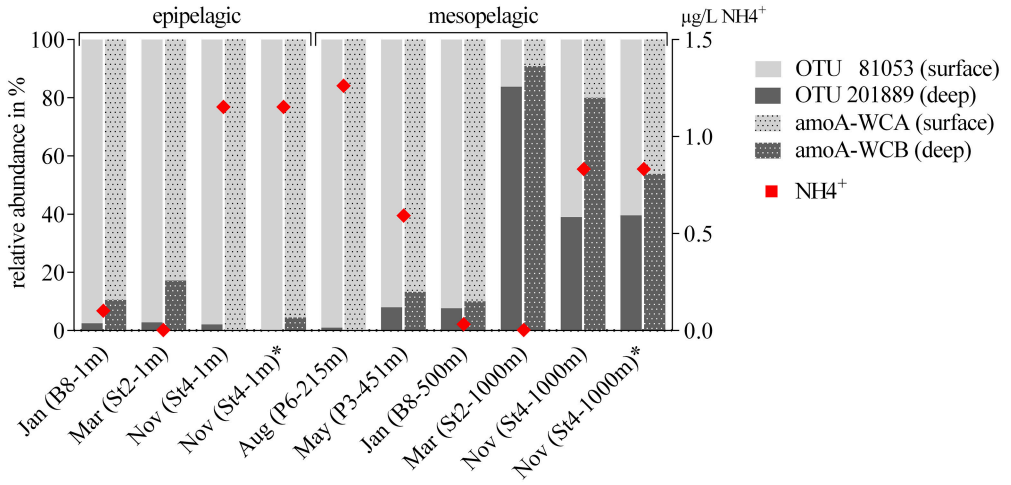

FIGURE 6 | Comparison of the relative abundance of Thaumarchaeota OTUs (16S rRNA gene) and the functional gene for ammonia oxidation (*amoA*). Thaumarchaeota OTUs are divided into the two most abundant sequences (OTU 81053 and OTU 201889), with highest relative abundance at the surface or the deep, respectively. *amoA* OTUs were divided into the two depth depending clusters WCA (surface) and WCB (deep). One station for each sampling month with a surface and deep sampling point were chosen (note, due to very low abundances, summer surface samples are not included), including all five water masses encountered during the five cruises. Ammonium concentrations at each sampling point are visualized as red diamonds (0 = below the detection limit).

mesopelagic samples. However, depth alone could not explain the abundance pattern. Our data indicates a clear distribution and hence niche diversification of Thaumarchaeota ecotypes according to discriminating water masses in this area (**Figure 4**). A distinct biogeography for Thaumarchaeota in the ocean has been described before, but abundance patterns of different Thaumarchaeota groups were only connected to depth-specific water profile characteristics (Francis et al., 2005; Beman et al., 2008; Sintes et al., 2013, 2016). However, there have been studies where shifts in marine microbial community composition were correlated to differences in physicochemical water mass parameters (Agogué et al., 2008; Galand et al., 2009; Baltar et al., 2016).

For the first time, we have made a causal link between the abundance patterns of different Thaumarchaeota ecotypes to water masses entering the Arctic Ocean. Thaumarchaeota OTUs group primarily into three clusters, with each group having one OTU being most abundant. These three OTUs, putatively defined as surface, middle and deep OTUs, seemingly exhibit a certain niche specificity, as they vary in abundance best explained by water mass distribution and not, as otherwise suggested, depth or ammonium concentration. By applying this principle to our data, twelve out of thirty-eight samples were revised with regard to their physicochemical water mass definition. These revisions however, can be used to explain the hydrographical system in our study area in a more concise way.

For example, according to the physicochemical water mass information, 1,000 m samples taken from stations in the Nansen Basin were different, either assigned to ArW or IW. However, the Thaumarchaeota abundance pattern was highly similar suggesting that they all originated from ArW, which is different from other deep water masses. Based on the molecular data, we therefore conclude that the water mass at 1,000 m throughout the Nansen Basin is ArW. We did not see this Thaumarchaeota pattern in all of our 1,000 m samples, but only from the stations closest to the deep Nansen Basin, indicating that this OTU was not depth-specific, but rather water mass-specific. Additionally, the absence of the surface OTU is indicative that this water mass did not result from mixing of SW or incoming AW, but rather originated from the deep central Arctic Ocean. Another, co-occurrence between an OTU abundance pattern and water mass was found for AW. By following the changes in abundance of the middle OTU (which correlated with higher salinity and warmer sea temperatures) in particular, we could trace the inflow and modification of AW. The surface OTU on the other hand had highest abundances in SW samples, which is influenced by ice melt. This suggests that the microbial assemblage can provide information on the origin of the water masses, in addition to the physical parameters. It further highlights the possibility that water mass definition can go beyond pure physical parameters and by including molecular microbiological data, such as OTU distribution patterns, presented in this study, explain better the origin and development of water masses (Fuhrman and Steele, 2008; Galand et al., 2009; Djurhuus et al., 2017).

The differences in Thaumarchaeota OTU abundance also reveal that water masses act as clearly separated boundaries for the distribution of marine prokaryotes, while we also defined water masses which seemed to be the result of mixing or dilution processes. On the one hand water masses can be considered barriers to microbial dispersal and on the other hand influencing community composition by physical processes like mixing (Agogué et al., 2011; Acha et al., 2015; Djurhuus et al., 2017). This was especially apparent in January, where two stations, just 43 km apart, showed a totally different abundance pattern for the three defined Thaumarchaeota ecotypes throughout the depth profile down to 1,000 m, while overall Thaumarchaeota abundance was

comparable at both stations (**Figures 2A,C**). This is similar to a phenomenon observed at the Subtropical Frontal zone, where community composition of surface water samples was highly different for samples taken only 7 km apart at an oceanic front (Baltar et al., 2016).

Oceanic frontal zones and ocean currents have been considered to be barriers of dispersal (Srivastava and Kratina, 2013). This affects to a high degree the biogeography of microbial communities and is adding a new element in contrast to the idea of strong regional environmental factors structuring the marine communities (Carr et al., 2003). Our data suggests a dual role of water masses in shaping Thaumarchaeota community composition. They both limit and facilitate dispersal of Thaumarchaeota OTUs, which dominate in specific water masses and are distributed when water mass are mixed.

16s rRNA and amoA Gene Phylogeny and Global Relevance

In our study, the deep OTU was highly abundant in samples up to 500 m, but not in shallower depths (**Figure 4**). The 16S rRNA gene sequence was the most abundant sequence (68%) of samples taken below 100 m, in a global dataset of 1256 marine Thaumarchaeota sequences (Supplementary Figure S1). The deep OTU sequence was not found in any samples collected above 100 m, whilst the middle OTU (phylogenetically in the same cluster as the deep OTU) was found both in epipelagic and mesopelagic samples. The surface OTU was found in highest abundance in the Arctic surface water in our data set. This same OTU has been recorded in high abundance in surface waters globally and seems to be universally successful under different conditions, having been found both at the Equator and in the Arctic. In fact, none of the three most abundant OTUs in our data set was Arctic-specific and all have been found in marine waters around the globe. Whether those three OTUs are indeed universally successful remains unclear, as the 16S rRNA gene with an OTU definition of 97% similarity might not be suitable to reveal functional ecotype variation.

The distribution of different *amoA* genes was investigated to see if we could identify a similar water mass-dependent pattern as for the 16S rRNA gene data. The relative distribution of the two AOA groups, WCA (surface) and WCB (deep), was found to correspond with the distribution of surface and deep OTUs based on 16S rRNA gene data. By using independent PCR approaches it is however not possible to directly associate the 16S rRNA and *amoA* genotypes, but their observed grouping, co-occurring with different water masses may indicate that the ecotypes defined by the 16S rRNA gene sequence could be functionally different. One hypothesis for this functional difference is the presence of urease genes (*ureC*) in the deep WCB clusters (Swan et al., 2011; Alonso-Sáez et al., 2012; Qin et al., 2014; Tolar et al., 2016). We did not measure the abundance of *ureC* genes in our samples, but it has been shown that Thaumarchaeota ecotypes from Arctic deep waters have a higher abundance of the *ureC* gene than surface groups (Alonso-Sáez et al., 2012). The genomic differences we observe between the surface and deep *amoA* types might be an indicator for evolutionarily different physiological strategies, including the utilization of urea by the deep WCB (**Figure 5**).

Identifying environmental drivers, which might explain the proportional abundances seen in this study as well as several other studies, will ultimately help understand the ecological role of the different AOA types. Our data indicated a distribution which corresponds to water masses rather than strict depth dependencies. We measured ammonium concentrations at the sampled stations and did not see a correlation between ammonium availability and WCA to WCB (HAC- to LAC-*amoA*) ratio, despite previous reports (Kirchman et al., 2007; Christman et al., 2011; Sintes et al., 2013, 2015, 2016; Santoro et al., 2017). Environmental parameters such as salinity (Francis et al., 2005; Abell et al., 2010), nitrite (Herfort et al., 2007), dissolved oxygen (Santoro et al., 2008), light (Mincer et al., 2007; Merbt et al., 2012), reactive oxygen species (Tolar et al., 2016), and temperature (Biller et al., 2012) have been suggested to regulate Thaumarchaeota community composition. It was further speculated that depth (Biller et al., 2012; Sintes et al., 2013, 2015), which is often correlated with Thaumarchaeota distribution, is a collection of other environmental factors following a gradient (Santoro et al., 2017). We expand that idea by highlighting that water masses, being by definition a set of several environmental parameters, are important for the distribution of Thaumarchaeota OTUs. Ultimately, it is therefore a challenge to comprehensively identify a single primary driver of AOA distribution.

CONCLUSION

We observed a co-occurrence of the three dominant Thaumarchaeota OTUs with water masses at the inflow to the Arctic Ocean. This supports the theory that water mass history to a great extent defines the mesopelagic microbial community structure (Galand et al., 2009; Reinthaler et al., 2010). The Thaumarchaeota pattern we observed was possibly a combination of several factors; water mass characteristics seemed to be a significant factor, influencing the distribution of the three most abundant OTUs; additionally, physical mixing or dilution of water masses might be another important factor explaining the differences in abundance of the three Thaumarchaeota ecotypes. Our study highlights the importance of water masses in influencing Thaumarchaeota population distributions. As water mass distributions will change in a future Arctic Ocean, due to processes such as increased sea ice melting (Comeau et al., 2011) or "Atlantification" (Polyakov et al., 2005; Holland et al., 2006; Walczowski and Piechura, 2006), so will the Thaumarchaeota distribution change. Further research is needed to investigate possible ecological implications of such scenarios.

AUTHOR CONTRIBUTIONS

LØ and GB: led the planning of the study; OM, HA, AR, and LØ: collected and processed samples; In addition, BW: assisted on designing bioinformatic analysis strategies and helped improving the language and grammar of the manuscript; MP: performed

flow cytometric analysis; OM, BW, AR and LØ: analyzed data, OM prepared figures and tables and wrote the paper; All authors contributed to discussion and interpretation of the data and writing the paper.

FUNDING

This study is part of the project "MicroPolar" (RCN 225956) funded by the Norwegian Research Council, which organized the cruises in March and November. The "CarbonBridge" project (RCN 226415) organized the cruises in January, May, and August where thankfully we could participate. Parts of the study were funded by the project "Microorganisms in the Arctic: Major drivers of biogeochemical cycles and climate change" (RCN 227062).

ACKNOWLEDGMENTS

We would like to thank crew members of the Norwegian Research Vessels RV Helmer Hanssen and RV Lance for their assistance in sampling expeditions and all colleagues in the UiB Marine Microbiology group and collaborators abroad who contributed to the research effort. A special thanks to Jean-Éric Tremblay for providing ammonium measurements.

SUPPLEMENTARY MATERIAL

The Supplementary Material for this article can be found online at: https://www.frontiersin.org/articles/10.3389/fmicb.2018.00024/full#supplementary-material

REFERENCES

Abell, G. C., Revill, A. T., Smith, C., Bissett, A. P., Volkman, J. K., and Robert, S. S. (2010). Archaeal ammonia oxidizers and nirS-type denitrifiers dominate sediment nitrifying and denitrifying populations in a subtropical macrotidal estuary. *ISME J.* 4, 286–300. doi: 10.1038/ismej.2009.105

Acha, E. M., Piola, A., Iribarne, O, and Mianzan, H. (2015). *Biology of Fronts.* Cham: Springer.

Agogué, H., Brink, M., Dinasquet, J., and Herndl, G. J. (2008). Major gradients in putatively nitrifying and non-nitrifying archaea in the deep North Atlantic. *Nature* 456, 788–791. doi: 10.1038/nature07535

Agogué, H., Lamy, D., Neal, P. R., Sogin, M. L., and Herndl, G. J. (2011). Water mass-specificity of bacterial communities in the North Atlantic revealed by massively parallel sequencing. *Mol. Ecol.* 20, 258–274. doi: 10.1111/j.1365-294X.2010.04932.x

Alonso-Sáez, L., Sánchez, O., Gasol, J. M., Balagué, V., and Pedrós-Alio, C. (2008). Winter-to-summer changes in the composition and single-cell activity of near-surface Arctic prokaryotes. *Environ. Microbiol.* 10, 2444–2454. doi: 10.1111/j.1462-2920.2008.01674.x

Alonso-Sáez, L., Waller, A. S., Mende, D. R., Bakker, K., Farnelid, H., Yager, P. L., et al. (2012). Role for urea in nitrification by Polar Marine *Archaea*. *Proc. Natl. Acad. Sci. U.S.A.* 109, 17989–17994. doi: 10.1073/pnas.1201914109

Apprill, A., McNally, S., Parsons, R., and Weber, L. (2015). Minor revision to V4 REgion SSU rRNA 806R gene primer greatly increases detection of SAR11 bacterioplankton. *Aq. Microb. Ecol.* 75, 129–137. doi: 10.3354/ame01753

Bale, N. J., Villanueva, L., Hopmans, E. C., Schouten, S., and Sinninghe Damsté, J. S. (2013). Different seasonality of pelagic and benthic thaumarchaeota in the North Sea. *Biogeosciences* 10, 7195–7206. doi: 10.5194/bg-10-7195-2013

Baltar, F., Currie, K., Stuck, E., Roosa, S., and Morales, S. E. (2016). Oceanic fronts: transition zones for bacterioplankton community composition. *Environ. Microbiol. Rep.* 8, 132–138. doi: 10.1111/1758-2229.12362

Beman, J. M., Popp, B. N., and Francis, C. A. (2008). Molecular and Biogeochemical evidence for ammonia oxidation by marine crenarchaeota in the gulf of California. *ISME J.* 2, 429–441. doi: 10.1038/ismej.2007.118

Biller, S. J., Mosier, A. C., Wells, G. F., and Francis, C. A. (2012). Global biodiversity of aquatic ammonia-oxidizing archaea is partitioned by habitat. *Front. Microbiol.* 3:252. doi: 10.3389/fmicb.2012.00252

Caporaso, J. G., Lauber, C. L., Walters, W. A., Berg-Lyons, D., Lozupone, C. A., and Turnbaugh, P. J., et al. (2011). Global patterns of 16S rRNA diversity at a depth of millions of sequences per sample. *Proc. Natl. Acad. Sci. U.S.A.* 108(Suppl. 1), 4516–4522. doi: 10.1073/pnas.1000080107

Carr, M. H., Neigel, J. E., Estes, J. A., Andelman, S., Warner, R. R., and Largier, J. L. (2003). Comparing marine and terrestrial ecosystems: implications for the design of coastal marine reserves. *Ecol. Appl.* 13, 90–107. doi: 10.1890/1051-0761(2003)013[0090:CMATEI]2.0.CO;2

Christman, G. D, Cottrell, M. T., Popp, B. N., Gier, E,., and Kirchman, D. L. (2011). Abundance, diversity, and activity of ammonia-oxidizing prokaryotes in the coastal Arctic Ocean in summer and winter. *Appl. Environ. Microbiol.* 77, 2026–2034. doi: 10.1128/AEM.01907-10

Church, M. J., DeLong, E. F., Ducklow, H. W., Karner, M. B., Preston, C. M., and Karl, D. M. (2003). Abundance and distribution of planktonic *Archaea* and *Bacteria* in the waters West of the Antarctic Peninsula. *Limnol. Oceanogr.* 48, 1893–1902. doi: 10.4319/lo.2003.48.5.1893

Clark, D. R., Rees, A. P., and Joint, I. (2008). Ammonium regeneration and nitrification rates in the oligotrophic Atlantic Ocean: implications for new production estimates. *Limnol. Oceanogr.* 53, 52–62. doi: 10.4319/lo.2008.53.1.0052

Cokelet, E. D., Tervalon, N., and Bellingham, J. G. (2008). Hydrography of the West spitsbergen current, svalbard branch: autumn 2001. *J. Geophys. Res.* 113, C01006. doi: 10.1029/2007JC004150

Comeau, A. M., Li, W. K. W., Tremblay, J.-É., Carmack, E. C., and Lovejoy, C. (2011). Arctic ocean microbial community structure before and after the 2007 record sea ice minimum. edited by jack anthony gilbert. *PLoS ONE* 6:e27492. doi: 10.1371/journal.pone.0027492

DeLong, E. F. (1992). *Archaea* in coastal marine environments. *Proc. Natl. Acad. Sci. U.S.A.* 89, 5685–5689. doi: 10.1073/pnas.89.12.5685

de Steur, L., Hansen, E., Mauritzen, C., Beszczynska-Möller, A., and Fahrbach, E. (2014). Impact of Recirculation on the east greenland current in fram strait: results from moored current meter measurements between 1997 and 2009. *Deep Sea Res.* 92, 26–40. doi: 10.1016/j.dsr.2014.05.018

Djurhuus, A., Boersch-Supan, P. H., Mikalsen, S.-O., and Rogers. A. D. (2017). Microbe biogeography tracks water masses in a dynamic oceanic frontal system. *Open Sci.* 4:170033. doi: 10.1098/rsos.170033.

Edgar, R. C. (2004). MUSCLE: multiple sequence alignment with high accuracy and high throughput. *Nucleic Acids Res.* 32, 1792–1797. doi: 10.1093/nar/gkh340

Edgar, R. C. (2010). Search and clustering orders of magnitude faster than BLAST. *Bioinformatics* 26, 2460–2461. doi: 10.1093/bioinformatics/btq461

Forest, A., Tremblay, J.-É., Gratton, Y., Martin, J., Gagnon, J., Darnis, G., et al. (2011). Biogenic Carbon flows through the planktonic food web of the amundsen gulf (Arctic Ocean): a synthesis of field measurements and inverse modeling analyses. *Prog. Oceanogr.* 91, 410–436. doi: 10.1016/j.pocean.2011.05.002

Francis, C. A., Roberts, K. J., Beman, J. M., Santoro, A. E., and Oakley, B. B. (2005). Ubiquity and diversity of ammonia-oxidizing *Archaea* in water columns and sediments of the Ocean. *Proc. Natl. Acad. Sci. U.S.A.* 102, 14683–14688. doi: 10.1073/pnas.0506625102

Fuhrman, J. A., and Azam, F. (1982). Thymidine incorporation as a measure of heterotrophic bacterioplankton production in marine surface waters: evaluation and field results. *Mar. Biol.* 66, 109–120. doi: 10.1007/BF00397184

Fuhrman, J. A., McCallum, K., and Davis, A. A. (1992). Novel major archaebacterial group from marine plankton. *Nature* 356, 148–149. doi: 10.1038/356148a0

Fuhrman, J. A., and Steele, J. A. (2008). Community structure of marine bacterioplankton: patterns, networks, and relationships to function. *Aq. Microb. Ecol.* 53, 69–81. doi: 10.3354/ame01222

Galand, P. E., Potvin,M., Casamayor, E. O., and Lovejoy, C. (2009). Hydrography shapes bacterial biogeography of the deep Arctic Ocean. *ISME J.* 4, 564–576. doi: 10.1038/ismej.2009.134

Grzymski, J. J, Riesenfeld, C. S., Williams, T. J., Dussaq, A. M., Ducklow, H., Erickson, M.,et al. (2012). A metagenomic assessment of winter and summer bacterioplankton from Antarctica peninsula coastal surface waters. *ISME J.* 6, 1901–1915. doi: 10.1038/ismej.2012.31

Guerrero, M. A., and Jones, R. D. (1996). Photoinhibition of marine nitrifying bacteria. I. Wavelength-dependent response. *Mar. Ecol. Prog. Ser.* 141, 183–192. doi: 10.3354/meps141183

Hallam, S. J, Mincer, T. J., Schleper, C., Preston, C. M., Roberts, K., Richardson, P. M., et al. (2006). Pathways of carbon assimilation and ammonia oxidation suggested by environmental genomic analyses of marine crenarchaeota. *PLoS Biol.* 4:e95. doi: 10.1371/journal.pbio.0040095

He, Z., Zhang, H., Gao, S., Lercher, M. J., Chen, W.-H., and Hu, S. (2016). Evolview v2: an online visualization and management tool for customized and annotated phylogenetic trees. *Nucleic Acids Res.* 44, W236–W241. doi: 10.1093/nar/gkw370

Herfort, L., Schouten, S., Abbas, B., Veldhuis, M. J. W., Coolen, M. J. L., Wuchter, C., et al. (2007). Variations in spatial and temporal distribution of archaea in the north sea in relation to environmental variables. *FEMS Microbiol. Ecol.* 62, 242–257. doi: 10.1111/j.1574-6941.2007.00397.x

Holland, M. M., Finnis, J., Serreze, M. C., Holland, M. M., Finnis, J., and Serreze, M. C. (2006). Simulated Arctic Ocean freshwater budgets in the twentieth and twenty-first centuries. *J. Clim.* 19, 6221–6242. doi: 10.1175/JCLI3967.1

Holmes, R. M. (1999). A simple and precise method for measuring ammonium in marine and freshwater ecosystems. *Can. J. Fish. Aquat. Sci.* 56, 1801–1808. doi: 10.1139/f99-128

Hong, J.-K., Cho, J.-C., Offre, P., Zumbragel, S., Haider, S., and Rychlik, N. (2015). Environmental variables shaping the ecological niche of thaumarchaeota in soil: direct and indirect causal effects. *PLoS ONE* 10:e0133763. doi: 10.1371/journal.pone.0133763

Jeffrey, W. H., Von Haven, R., Hoch, M. P., and Coffin, R. B. (1996). Bacterioplankton RNA, DNA, protein content and relationships to rates of thymidine and leucine incorporation. *Aq. Microb. Ecol.* 10, 87–95. doi: 10.3354/ame010087

Kalanetra, K. M., Bano, N., and Hollibaugh, J. T. (2009). Ammonia-Oxidizing *Archaea* in the Arctic Ocean and Antarctic coastal waters. *Environ. Microbiol.* 11, 2434–2445. doi: 10.1111/j.1462-2920.2009.01974.x

Karner, M. B., DeLong, E. F., and Karl, D. M. (2001). Archaeal dominance in the mesopelagic zone of the Pacific Ocean. *Nature* 409, 507–510. doi: 10.1038/35054051

Kirchman, D. L, Elifantz, H., Dittel, A. I., Malmstrom, R. R., and Cottrell, M. T. (2007). Standing stocks and activity of *Archaea* and bacteria in the western arctic ocean. *Limnol. Oceanogr.* 52, 495–507. doi: 10.4319/lo.2007.52.2.0495

Könneke, M., Bernhard, A. E., De La Torre, J. R., Walker, C. B., Waterbury, J. B., and Stahl, D. A. (2005). Isolation of an autotrophic ammonia-oxidizing marine Archaeon. *Nature* 437, 543–546. doi: 10.1038/nature03911

Loy, A., Lehner, A., Lee, N., Adamczyk, J., Meier, H., Ernst, J., et al. (2002). Oligonucleotide microarray for 16S rRNA gene-based detection of all recognized lineages of sulfate-reducing prokaryotes in the environment. *Appl. Environ. Microbiol.* 68, 5064–5081. doi: 10.1128/AEM.68.10.5064-5081.2002

Marie, D., Brussaard, C. P. D., Thyrhaug, R., Bratbak,G., , and Vaulot, D. (1999). Enumeration of marine viruses in culture and natural samples by flow cytometry. *Appl. Environ. Microbiol.* 65, 45–52.

Massana, R., Taylor, L. T., Murray, A. E., Wu, K. Y., Jeffrey, W. H., and DeLong, E. F. (1998). Vertical distribution and temporal variation of marine planktonic *Archaea* in the gerlache strait, Antarctica, during early spring. *Limnol. Oceanogr.* 43, 607–617. doi: 10.4319/lo.1998.43.4.0607

Merbt, S. N., Stahl, D. A., Casamayor, E. O., Martí, E., Nicol, G. W., and Prosser, J. I. (2012). Differential photoinhibition of bacterial and Archaeal ammonia oxidation. *FEMS Microbiol. Lett.* 327, 41–46. doi: 10.1111/j.1574-6968.2011.02457.x

Mincer, T. J., Church, M. J., Taylor, L. T., Preston, C., Karl, D. M., and DeLong, E. F. (2007). Quantitative distribution of presumptive archaeal and bacterial nitrifiers in monterey bay and the north pacific subtropical gyre. *Environ. Microbiol.* 9, 1162–1175. doi: 10.1111/j.1462-2920.2007.01239.x

Murray, A. E., Preston, C. M., Massana, R., Taylor, L. T., Blakis, A., Wu, K., et al. (1998). Seasonal and spatial variability of bacterial and archaeal assemblages in the coastal waters near Anvers Island, Antarctica. *Appl. Environ. Microbiol.* 64, 2585–2595.

Offre, P., Spang, A., and Schleper, C. (2013). *Archaea* in biogeochemical cycles. *Annu. Rev. Microbiol.* 67, 437–457. doi: 10.1146/annurev-micro-092412-155614

Ouverney, C. C., and Fuhrman, J. A. (2000). Marine planktonic *Archaea* take up amino acids. *Appl. Environ. Microbiol.* 66, 4829–4833. doi: 10.1128/AEM.66.11.4829-4833.2000

Paulsen, M., Doré, H., Garczarek, L., Seuthe, L., and Müller, O. (2016). Synechococcus in the Atlantic gateway to the Arctic Ocean. *Front. Mar. Sci.* 3:191. doi: 10.3389/fmars.2016.00191

Pedneault, E., Galand, P. E., Potvin, M., Tremblay, J.-É., and Lovejoy, C. (2014). Archaeal amoA and ureC genes and their transcriptional activity in the Arctic Ocean. *Sci. Rep.* 4:4661. doi: 10.1038/srep04661

Pester, M., Rattei, T., Flechl, S., Gröngröft, A., Richter, A., Overmann, J., et al. (2012). amoA-based consensus phylogeny of ammonia-oxidizing *Archaea* and deep sequencing of amoa genes from soils of four different geographic regions. *Environ. Microbiol.* 14, 525–539. doi: 10.1111/j.1462-2920.2011.02666.x

Polyakov, I. V., Beszczynska, A., Carmack, E. C., Dmitrenko, I. A., Fahrbach, E., Frolov, I. E., et al. (2005). One more step toward a warmer Arctic. *Geophys. Res. Lett.* 32:L17605. doi: 10.1029/2005GL023740

Poulin, P., and Pelletier, E. (2007). Determination of ammonium using a microplate-based fluorometric technique. *Talanta* 71, 1500–1506. doi: 10.1016/j.talanta.2006.07.024

Qin, W., Amin, S. A., Martens-Habbena, W., Walker, C. B., Urakawa, H., Devol, A. H., et al. (2014). Marine ammonia-oxidizing archaeal isolates display obligate mixotrophy and wide ecotypic variation. *Proc. Natl. Acad. Sci. U.S.A.* 111, 12504–12509. doi: 10.1073/pnas.1324115111

Quast, C., Pruesse, E., Yilmaz, P., Gerken, J., Schweer, T., Glo, F. O., et al. (2013). The SILVA Ribosomal RNA gene database project : improved data processing and web-based tools. *Nucleic Acid Res.* 41, 590–596. doi: 10.1093/nar/gks1219

Randelhoff, A., Sundfjord, A., and Reigstad, M. (2015). Seasonal variability and fluxes of nitrate in the surface waters over the Arctic shelf slope. *Geophys. Res. Lett.* 42, 3442–3449. doi: 10.1002/2015GL063655

Reinthaler, T., van Aken, H. M., and Herndl, G. J. (2010). Major contribution of autotrophy to microbial carbon cycling in the deep north Atlantic's interior. *Deep Sea Res.* 57, 1572–1580. doi: 10.1016/j.dsr2.2010.02.023

Saitou, N., and Nei, M. (1987). The neighbor-joining method: a new method for reconstructing phylogenetic trees. *Mol. Biol. Evol.* 4, 406–425.

Santoro, A. E., Casciotti, K. L., and Francis, C. A. (2010). Activity, abundance and diversity of nitrifying *Archaea* and *Bacteria* in the central California current. *Environ. Microbiol.* 12, 1989–2006. doi: 10.1111/j.1462-2920.2010.02205.x

Santoro, A. E., Francis, C. A., de Sieyes, N. R., and Boehm, A. B. (2008). Shifts in the relative abundance of ammonia-oxidizing *Bacteria* and *Archaea* across physicochemical gradients in a subterranean estuary. *Environ. Microbiol.* 10, 1068–1079. doi: 10.1111/j.1462-2920.2007.01547.x

Santoro, A. E., Saito, M. A., Goepfert, T. J., Lamborg, C. H., Dupont, C. L., and DiTullio, G. R. (2017). Thaumarchaeal ecotype distributions across the equatorial pacific Ocean and their potential roles in nitrification and sinking flux attenuation. *Limnol. Oceanogr.* 62, 1984–2003. doi: 10.1002/lno.10547

Sintes, E., Bergauer, K,., De Corte, D., Yokokawa, T., and Herndl, G. J. (2013). Archaeal *Amo* a gene diversity points to distinct biogeography of ammonia-oxidizing *Crenarchaeota* in the Ocean. *Environ. Microbiol.* 15, 1647–1658. doi: 10.1111/j.1462-2920.2012.02801.x

Sintes, E., De Corte, D., Haberleitner, E., and Herndl, G. J. (2016). Geographic distribution of archaeal ammonia oxidizing ecotypes in the Atlantic Ocean. *Front. Microbiol.* 7:77. doi: 10.3389/fmicb.2016.00077

Sintes, E., De Corte, D., Ouillon, N., and Herndl, G. J. (2015). Macroecological patterns of archaeal ammonia oxidizers in the Atlantic Ocean. *Mol. Ecol.* 24, 4931–4942. doi: 10.1111/mec.13365

Smith, J. M., Casciotti, K. L., Chavez, F. P., and Francis, C. A. (2014). Differential contributions of archaeal ammonia oxidizer ecotypes to nitrification in coastal surface waters. *ISME J.* 8, 1704–1714. doi: 10.1038/ismej.2014.11

Srivastava, D. S., and Kratina, P. (2013). Is dispersal limitation more prevalent in the ocean? *Oikos* 122, 298–300. doi: 10.1111/j.1600-0706.2012.21042.x

Swan, B. K., Martinez-Garcia, M., Preston, C. M., Sczyrba, A., Woyke, T., Lamy, D., et al. (2011). Potential for chemolithoautotrophy among ubiquitous bacteria lineages in the dark ocean. *Science* 333, 1296–1300. doi: 10.1126/science.1203690

Tolar, B. B., King, G. M., and Hollibaugh, J. T. (2013). An analysis of thaumarchaeota populations from the northern gulf of Mexico. *Front. Microbiol.* 4:72. doi: 10.3389/fmicb.2013.00072

Tolar, B. B., Powers, L. C., Miller, W. L., Wallsgrove, N. J., Popp, B. N., and Hollibaugh, J. T. (2016). Ammonia oxidation in the ocean can be inhibited by nanomolar concentrations of hydrogen peroxide. *Front. Mar. Sci.* 3:237. doi: 10.3389/fmars.2016.00237

Valentine, D. L. (2007). Adaptations to energy stress dictate the ecology and evolution of the *Archaea*. *Nat. Rev. Microbiol.* 5, 316–323. doi: 10.1038/nrmicro1619

Varela, M. M., van Aken, H. M., Sintes, E., and Herndl, G. J. (2007). Latitudinal trends of crenarchaeota and bacteria in the meso- and bathypelagic water masses of the Eastern North Atlantic. *Environ. Microbiol.* 10, 110–24. doi: 10.1111/j.1462-2920.2007.01437.x

Venter, J. C., Remington, K., Heidelberg, J. F., Halpern, A. L., Rusch, D., Eisen, J. A., et al. (2004). Environmental genome shotgun sequencing of the sargasso sea. *Science* 304, 66–74. doi: 10.1126/science.1093857

Walczowski, W., and Piechura, J. (2006). New evidence of warming propagating toward the Arctic Ocean. *Geophys. Res. Lett.* 33, L12601. doi: 10.1029/2006GL025872

Wilson, B., Müller, O., Nordmann, E.-L., Seuthe, L., Bratbak, G., and Øvreås, L. (2017). Changes in marine prokaryote composition with season and depth over an arctic polar year. *Front. Mar. Sci.* 4:95. doi: 10.3389/fmars.2017.00095

Woodward, E. M. S., and Rees, A. P. (2001). Nutrient distributions in an anticyclonic eddy in the Northeast Atlantic Ocean, with reference to nanomolar ammonium concentrations. *Deep Sea Res. Part II. Topical Stud. Oceanogr.* 48, 775–793. doi: 10.1016/S0967-0645(00)00097-7

Wright, J. J. (2013). *Microbial Community Structure and Ecology of Marine Group A Bacteria in the Oxygen Minimum Zone of the Northeast Subarctic Pacific Ocean, January*. Vancouver, BC: University of British Columbia.

Wuchter, C., Abbas, B., Coolen, M. J. L., Herfort, L., van Bleijswijk, J., Timmers, P., et al. (2006). Archaeal nitrification in the ocean. *Proc. Natl. Acad. Sci. U.S.A.* 103, 12317–12322. doi: 10.1073/pnas.0600756103

Conflict of Interest Statement: The authors declare that the research was conducted in the absence of any commercial or financial relationships that could be construed as a potential conflict of interest.

frontiers in Microbiology

ORIGINAL RESEARCH
published: 28 March 2018
doi: 10.3389/fmicb.2018.00584

Spatiotemporal Distribution and Assemblages of Planktonic Fungi in the Coastal Waters of the Bohai Sea

Yaqiong Wang[1,2†], Biswarup Sen[1†], Yaodong He[1], Ningdong Xie[1,3] and Guangyi Wang[1,4]*

[1] Center for Marine Environmental Ecology, School of Environment Science and Engineering, Tianjin University, Tianjin, China, [2] School of Ecology, Environment and Resources, Qinghai University for Nationalities, Xining, China, [3] Duke Marine Laboratory, Nicholas School of the Environment, Duke University, Durham, NC, United States, [4] Key Laboratory of Systems Bioengineering (Ministry of Education), Tianjin University, Tianjin, China

Fungi play a critical role in the nutrient cycling and ecological function in terrestrial and freshwater ecosystems. Yet, many ecological aspects of their counterparts in coastal ecosystems remain largely elusive. Using high-throughput sequencing, quantitative PCR, and environmental data analyses, we studied the spatiotemporal changes in the abundance and diversity of planktonic fungi and their abiotic and biotic interactions in the coastal waters of three transects along the Bohai Sea. A total of 4362 ITS OTUs were identified and more than 60% of which were unclassified Fungi. Of the classified OTUs three major fungal phyla, Ascomycota, Basidiomycota, and Chytridiomycota were predominant with episodic low dominance phyla Cryptomycota and Mucoromycota (Mortierellales). The estimated average Fungi-specific 18S rRNA gene qPCR abundances varied within 4.28×10^6 and 1.13×10^7 copies/L with significantly ($P < 0.05$) different abundances among the transects suggesting potential influence of the different riverine inputs. The spatiotemporal changes in the OTU abundance of Ascomycota and Basidiomycota phyla coincided significantly ($P < 0.05$) with nutrients traced to riverine inputs and phytoplankton detritus. Among the eight major fungal orders, the abundance of Hypocreales varied significantly ($P < 0.01$) across months while Capnodiales, Pleosporales, Eurotiales, and Sporidiobolales varied significantly ($P < 0.05$) across transects. In addition, our results likely suggest a tripartite interaction model for the association within members of Cryptomycota (hyperparasites), Chytridiomycota (both parasites and saprotrophs), and phytoplankton in the coastal waters. The fungal network featured several hubs and keystone OTUs besides the display of cooperative and competitive relationship within OTUs. These results support the notion that planktonic fungi, hitherto mostly undescribed, play diverse ecological roles in marine habitats and further outline niche processes, tripartite and co-occurrence interaction as the major drivers of their community structure and spatiotemporal distribution in the coastal water column.

Keywords: marine ecosystem, water column, abundance, diversity, quantitative PCR, high-throughput sequencing

OPEN ACCESS

Edited by:
Stanley Chun Kwan Lau, Hong Kong University of Science and Technology, Hong Kong

Reviewed by:
William D. Orsi, Ludwig-Maximilians-Universität München, Germany
Xin Wang, Miami University, United States

***Correspondence:**
Guangyi Wang
gywang@tju.edu.cn

† These authors have contributed equally to this work.

Specialty section:
This article was submitted to Aquatic Microbiology, a section of the journal Frontiers in Microbiology

Received: *10 November 2017*
Accepted: *14 March 2018*
Published: *28 March 2018*

Citation:
Wang Y, Sen B, He Y, Xie N and Wang G (2018) Spatiotemporal Distribution and Assemblages of Planktonic Fungi in the Coastal Waters of the Bohai Sea. Front. Microbiol. 9:584. doi: 10.3389/fmicb.2018.00584

INTRODUCTION

Microbial plankton governs the ecological function of the marine ecosystem by sustaining food webs and regulating global biogeochemical cycles (Rousk and Bengtson, 2014; Worden et al., 2015). Recently, molecular approaches have revealed the vast and complex diversity of microbial plankton groups (e.g., bacterioplankton and protist) and their intrinsic relationship with a wide range of environmental drivers (Caporaso et al., 2012; Logares et al., 2014; de Vargas et al., 2015). Fungi have long been known to be a key component of biosphere involved in a wide range of biogeochemical cycles, ecological functions across disparate terrestrial environments (Christensen, 1989; Carlile et al., 2001; Pang and Mitchell, 2005; Fischer et al., 2006; Gulis et al., 2006), and natural product research (Pang et al., 2016). Planktonic fungi, which include morphologically diverse zoosporic fungi, free-living filamentous and yeast forms or parasites of the other planktons (Richards et al., 2012; Wang et al., 2012), are known for several decades about their existence in ocean waters. The function of their planktonic forms in marine ecosystems only has been recognized recently (Gao et al., 2010; Wang et al., 2014; Taylor and Cunliffe, 2016), but evidence to support their function is still lacking.

As one of the most dynamic ecosystems, coastal waters are generally characterized with a high biodiversity and high primary production (Danovaro and Pusceddu, 2007). Planktonic fungi are considered to decompose detrital organic matter or phytoplankton-derived organic matters and utilize dissolved organic carbon with a noticeable contribution to secondary production in the coastal marine ecosystems (Kimura and Naganuma, 2001; Kimura et al., 2001; Gao et al., 2010; Gutiérrez et al., 2011). Nevertheless, these ecological roles are largely proposed based on the comparison with their counterparts in terrestrial and freshwater ecosystems (Richards et al., 2012; Taylor and Cunliffe, 2016). The recent discovery of fungal mycelia (i.e., metabolically active forms of fungi) to exist as individual filaments or aggregates in coastal ocean waters (Gutiérrez et al., 2010; Li Q. et al., 2016) support the hypothesis that planktonic fungi are active. Furthermore, high fungal biomass can be comparable to that of planktonic prokaryotes and have been noticed to relate with an increase in phytoplankton biomass and in extracellular enzymatic hydrolysis in coastal waters (Gutiérrez et al., 2011). The vertical distribution patterns (e.g., diversity and species richness) of planktonic fungi have also been consistent with those of phytoplankton (Gao et al., 2010; Gutiérrez et al., 2011; Wang et al., 2014). The above findings clearly suggest the important role of planktonic fungi in the coastal waters, and like other heterotrophic plankton groups, they are tightly linked with primary production and organic matter.

An enormous fungal diversity has been reported from terrestrial environments (Hawksworth, 2001; O'Brien et al., 2005; Hibbett et al., 2007; Mueller et al., 2007). Relative to other marine plankton groups and their counterparts in terrestrial and freshwater ecosystems, the diversity of marine planktonic fungi and their response to environmental gradients remain quite limited (Fell and Newell, 1998; Raghukumar, 2005; Gulis et al., 2006; Gessner et al., 2007; Gao et al., 2010; Wang et al., 2012, 2014). Molecular-based approaches have revealed high diversity of planktonic fungi with novel lineages in the coastal water columns, displaying interesting temporal and spatial (lateral and vertical) variations (Gao et al., 2010). This includes the higher diversity and a greater fungal abundance in the surface and coastal waters than in open-ocean and deep water samples (Gao et al., 2010). In addition, the diversity patterns of planktonic fungi have been related to major phytoplankton taxa and various nutrients in the oceanic waters (Wang et al., 2014). Time-series assessments have revealed several dominant planktonic fungi groups and their interesting relationship with environmental variables, including nitrogen availability and temperature at Coastal Station L4 in the Western English Channel, and suggested the significance of riverine inputs on their abundance and diversity in the coastal region (Taylor and Cunliffe, 2016). Together, previous studies show that planktonic fungi are molecularly diverse and that a variety of fungal phylotypes, regulated by nutrients, mediate multiple biological processes in the coastal waters.

In our previous studies, we reported novel lineages of planktonic fungi and their relationship with environmental variables in the Hawaiian coastal waters and the pelagic waters of the Pacific Warm Pool (Gao et al., 2010; Wang et al., 2014). In this study, we applied high-throughput sequencing and qPCR tools to investigate the diversity and abundance of planktonic fungi in the semi-closed shallow bay ecosystem on the coast of Bohai Sea influenced by different riverine inputs. The specific objective of the present study was to realize the local dominant planktonic fungal groups, their spatiotemporal dynamics and factors governing their distribution patterns.

MATERIALS AND METHODS

Characteristics of Sampling Area and Sample Collection

The 125.4 km long coastline of the Qinhuangdao Coast stretches from the mouth of the Luan River to the city of Qinhuangdao on the northwest side of the Bohai Sea (**Figure 1**). Additionally, the Bohai Sea has been under the impacts of two branches of Yellow Sea warm circulation: one is a clockwise gyre toward Liaodong Bay, and the other is a counterclockwise gyre toward Bohai Bay (Wei et al., 2004). The semi-enclosed character of the Bohai Sea restricts water exchange and leads to rapid accumulation of pollutants in the environment (Zhang et al., 2009). In the Qinhuangdao coastal area of Bohai Sea, the brown tide outbreak occurs recurrently every April to August since 2009 (Zhang et al., 2012; Wang et al., 2015; Ma et al., 2016), thus, it remains a typical coastal ecosystem largely influenced by human and terrigenous inputs.

We set three sampling transects along the estuaries in Qinhuangdao coastal area: Section A, vertical shorelines from Tang River estuary extension to the sea; Section B, vertical shorelines from Yang River estuary extension to the sea; and Section C, vertical shorelines from Dapu River estuary extension to the sea. The gradient distribution consisted about 37 km long monitoring stations from nearshore to offshore and for each

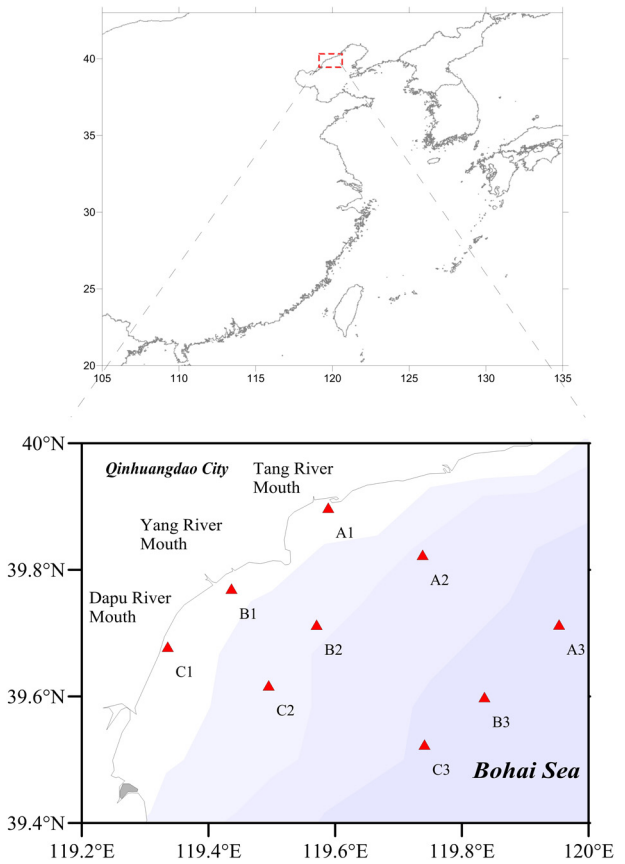

FIGURE 1 | Map of sampling sites in Qinhuangdao coastal area.

section, three sampling points were included (**Figure 1**). Seawater samples were collected with the standard sampling procedures from surface layer (0.5 m), bottom layer (the deepest depth of the station), and middle layer (5.0 m, when the depth of the station is more than 10 m) of nine locations (Station A1, Station A2, Station A3, Station B1, Station B2, Station B3, Station C1, Station C2, and Station C3) in the Qinhuangdao coastal area during November in 2014, April and July in 2015. Samples were designated 'S' (surface), 'M' (middle) and 'B' (bottom); 'S11' (November), 'S4' (April) and 'S7' (July), respectively in the following analysis. The information on sampling sites is shown in **Table 1**. We collected 2 L of water samples for each station, of which 500 mL was filtered through 0.22 μm polycarbonate filter membrane (Millipore, United States) for DNA extraction. The resulting filters for DNA extraction were stored at −80°C until further processing. The remaining seawater samples were used for environmental parameter determination. Water depth, temperature, salinity, dissolved oxygen (DO), and pH data were monitored at each sampling site using the corresponding sensors of YSI Pro Plus (Yellow Springs, OH 45387, United States). Water column samples were collected with polyvinyl chloride bottles. All water samples were stored in sterile containers at an *in situ* temperature and protected from direct sunlight until further processing in the laboratory.

Determination of Environmental Parameters

Ammonium (NH_4^+), nitrate (NO_3^-), nitrite (NO_2^-), phosphate (PO_4^{3-}), and silicate (SiO_4^{3-}) were measured using QuAAtro39 Continuous Segmented Flow Analyzer (SEAL Analytical, Inc.). Chlorophyll *a*, total and dissolved phosphorus and nitrogen (TP, DP, and DN) were measured following the methods described elsewhere (Zhou et al., 2016). For DN and DP, seawater sample was filtered through a 0.45 μm Millipore filter (Millipore, United States). Dissolved inorganic and organic N (DIN and DON), dissolved inorganic and organic phosphorus (DIP and DOP), particulate total N and P (PP and PN) were calculated from the measured parameters described above. The nutrient concentrations in the samples are provided in Supplementary Table S1.

DNA Extraction, PCR Amplification, and High-Throughput Sequencing

The total genomic DNA was extracted from the membrane filters using the E.N.Z.A.^{TM} Water DNA Kit (Omega Bio-tek, Inc., United States) and was used as a PCR template for the amplification of the ITS1 region and quantitative PCR. Fungal ITS gene primer ITS1F (F) (5′ CTTGGTCATT TAGAGGAAGTAA 3′) and primer ITS2(R) (5′ GCTGCGTTC TTCATCGATGC 3′) (White et al., 1990; Gardes and Bruns, 1993) were used in the PCR reaction. ITS1 and ITS2 primers yield similar results and are suitable as DNA metabarcoding markers (Blaalid et al., 2013). Barcode sequences (6-bases) were ligated to the 5′ end of the reverse and forward sequencing primers during the process of primer synthesis prior to PCR amplification. All PCR reactions were performed with the following conditions: an initial hot start incubation (5 min at 95°C) followed by 30 cycles of denaturation at 94°C for 30 s, annealing at 55°C for 35 s and extension at 72°C for 30 s, and a final elongation step at 72°C for 8 min. PCR products from three separate amplification reactions were pooled and then purified using TIANquick Midi Purification Kit (Tiangen Biotech Co., Ltd., Beijing, China). Amplicon libraries were then generated using NEB Next R Ultra TM DNA Library Prep Kit for Illumina (NEB, United States) following the manufacturer's recommendations. PCR reaction, amplicon library preparation, and high-throughput sequencing using the Illumina HiSeq 2500 platform (Illumina Inc., San Diego, CA, United States) following the manufacturer's instructions were performed by AuGCT Biotechnology Co., Inc., Beijing, China.

Fungi-Specific Quantitative PCR

Fungi-specific 18S rRNA gene quantitative PCR (qPCR) was performed using the method described by Taylor and Cunliffe (Taylor and Cunliffe, 2016). The primers FR1 5′-AICCAT TCAATCGGTAIT-3′ and FF390 5′-CGATAACGAACGAG ACCT-3′ (Vainio and Hantula, 2000; Prévost-Bouré et al., 2011) were used. A 10 μl reaction mixture contained 5 μl of 2X SybrGreen qPCR mix (GENE-BETTER^{TM}, Beijing, China), 0.25 μl of each primer (10 pmol μl^{-1}), 1 μl of DNA template (ca. 52–56 ng/μL) and 3.5 μl nuclease-free molecular-grade water.

TABLE 1 | Information of sampling sites.

Stations	Longitude (E)	Latitude (N)	Sampling time	Layer	Depth (m)
A1	119°35′341″	39°53′899″	November, April, July	S	0.5
				B	8.0
A2	119°44′282″	39°49′415″	November, April, July	S	0.5
				M	5.0
				B	13.6
A3	119°57′209″	39°42′813″	April	S	0.5
				M	5.0
				B	22.5
B1	119°26′178″	39°46′211″	November, April, July	S	0.5
				B	7.1
B2	119°34′243″	39°42′802″	November, April, July	S	0.5
				M	5.0
				B	12.0
B3	119°50′135″	39°35′944″	April	S	0.5
				M	5.0
				B	22.0
C1	119°20′145″	39°40′711″	November, April, July	S	0.5
				B	5.0
C2	119°29′697″	39°37′052″	November, April, July	S	0.5
				M	5.0
				B	11.4
C3	119°44′462″	39°31′430″	April	S	0.5
				M	5.0
				B	20.4

A CFX Connect™ Real-Time System (Bio-Rad Laboratories, Inc., Hercules, CA, United States) was used to perform qPCR. The following qPCR regime was used: denaturation at 94°C for 3 min, with 40 cycles at 94°C for 10 s, annealing at 50°C for 15 s, elongation and acquisition of fluorescence data at 72°C for 20 s. Standard curve was constructed using known amounts of target template generated by PCR amplification of the target gene from genomic DNA of *Rhodosporidium* sp. TJUWZ4 (CGMCC #2.5689, GenBank No: KT281890.1). The PCR product was purified by TIANquick Midi purification Kit (Tiangen Biotech (Beijing) Co., Ltd.) and its sequence was verified through sequencing (Beijing Genomics Institution, China). The target DNA fragment was then cloned into pTOPO-T Vector by Zero Background pTOPO-TA Cloning Kit following manufacturer's instructions (GENE-BETTER TM, Beijing). A E.Z.N.A.™ Plasmid Midi Kit (Omega Biotek, Inc., United States) was used to isolate the plasmid vector from the transformed *Escherichia coli* DH5α competent cells (Solarbio® LIFE SCIENCES, Beijing, China), and the concentration of extracted plasmid DNA was determined using the NanoDrop ND-1000 spectrophotometer (Nanodrop Technology, Thermo Fisher Scientific Inc.). The plasmid was linearized with HindIII [Takara Biomedical Technology (Beijing) Co., Ltd.] and the resulting plasmid was gel purified using TIANquick Midi Purification Kit (Tiangen Biotech Co., Ltd., Beijing, China) and its concentration was measured on a Nanodrop ND-1000 spectrophotometer. Appropriate dilutions of purified linear plasmid were done to obtain gene copy numbers ranging from 10^3 to 10^8 copies/L which were then stored at −20°C. A 1 μL template from each dilution was used to prepare standard curve for each qPCR assay. The average qPCR efficiency was 90.9%.

High-Throughput Sequence Analysis

The base call of each sequence read was inspected and filtered for quality control purpose. The raw reads were processed following the pipeline of Mothur (Schloss et al., 2009). All reads matching the barcodes (maximum mismatch = 1) were retained as well as reads with a maximum 3 bases mismatch to the primers. Reads were then trimmed by removing the sequencing adaptor, barcodes, and primer sequences. These reads were further screened by using the following thresholds: (i) minimum average quality score of 25; (ii) minimum read length of 200 bp; (iii) sequences containing no ambiguous bases; and (iv) maximum homopolymers of 8 bp (Liu et al., 2015). Sequence read pairs were merged using FLASH (Magoc and Salzberg, 2011) and compressed based on 97% similarity. Chimeric clusters were removed using *de novo* in USEARCH and unique clusters were subjected to BLAST analysis. The databases for fungal ITS sequences are not complete, so we added few more steps in the annotation of sequences. We used the BLASTn method with NT database (e < 1e-5, coverage > 80%) and the specialist fungal database, the UNITE database[1] (accessed in 2016) by classify.seqs() in Mothur with a similarity threshold of 0.8, to assign taxonomy to OTUs (Abarenkov et al., 2010).

[1]https://unite.ut.ee/repository.php

The search results were then mutually compared, and when the two databases results did not agree, the highest query coverage and percentage ID were chosen as a match. The other eukaryote sequences were removed using remove.lineage() in Mothur and those sequence which matched <100% to kingdom Fungi in UNITE database were removed from the dataset using perl script developed in-house. Sequences are available from the European Nucleotide Archive (Bioproject accession code: PRJNA341916).

Statistical Analysis

Normal distribution of the data was checked using Shapiro–Wilk test of normality. *Post hoc* tests according to Nemenyi-tests for multiple comparisons of (mean) rank sums of qPCR abundance of samples across each month were performed after a Kruskal–Wallis test. To explain the relationship between data (qPCR abundance, order abundance) and gradients (month, section, and depth) we conducted Kruskal-Wallis test. Correlation between OTU data at phyla level and environmental data was determined using Pearson's correlation test. A heatmap was generated with OTU relative abundance data and samples were clustered based on Bray-Curtis distance to visualize the β-diversity. Monte Carlo permutation test was performed followed by a constrained canonical correspondence analysis to estimate the correlation between OTU relative abundance and selected environmental factors. The above statistical tests were performed using vegan and status packages in R software (R version 3.3.1). Shannon diversity index for each sample was calculated at a 3% dissimilarity level using Mothur (Schloss et al., 2009) as the measure of α diversity. A network was constructed with CoNET (Faust et al., 2012) – a plugin in Cytoscape software following the method described elsewhere (Debroas et al., 2017). We employed an ensemble approach combining four different measures: two measures of dissimilarity (Bray–Curtis (BC) and Kullback–Leibler (KLD)) and two measures of correlation (Pearson and Spearman correlation). The dataset of 54 samples used in network analysis contained OTUs in rows and samples in columns. The rows were divided by their sum prior to computation of BC and KLD measures. The row minimum occurrence parameter was set at 20. To test the statistical significance of the edge scores, we computed measure- and edge-specific permutation and bootstrap score distributions with 1000 iterations each. The p-values were then computed by z-scoring the permuted null and bootstrap confidence interval using pooled variance. Edges with scores not within 95% confidence interval of the bootstrap distribution were removed.

RESULTS

Abundant and Dominant Planktonic Fungi in the Coastal Waters

We obtained high quality 6,072,738 reads with a read length of 200–440 base pairs from the Illumina HiSeq 2500 platform sequencing. The number of sequences from each sample ranged from 7,153 to 431,051 with an average number of 112,456 ± 96,784 (mean ± SD). The total sequences obtained after filtering were assigned to 4,362 OTUs. Among them, 1,483 OTUs (1,701,463 sequences) covered five known fungal phyla namely Ascomycota, Basidiomycota, Chytridiomycota, Mucoromycota, and Cryptomycota, 20 classes, 58 orders, 111 families, and 283 genera. Of these five known phyla, Ascomycota was the most abundant and accounted for 20.82% of the total 4,362 OTUs, covering 1,182,597 sequence reads (19.47% of total 6,072,738 reads). Basidiomycota, Chytridiomycota, Mucoromycota, and Cryptomycota represented 9.72, 2.64, 0.64, and 0.18% of the OTUs (4,362), respectively. Of particular interest, the phylum Cryptomycota and order Mortierellales of phylum Mucoromycota were detected first time in the coastal water column through high-throughput sequencing analysis where Mucoromycota was detected in 32 samples and only nine samples featured Cryptomycota. Within the most abundant top 50 OTUs, 12 OTUs (OTU3 OTU4, OTU7, OTU14, OTU16, OTU20, OTU21, OTU26, OTU32, OTU33, OTU38, and OTU40) were assigned to the Ascomycota, three OTUs (OTU6, OTU36, and OTU37) to the Basidiomycota and one OTU (OTU52) to the fungal parasite Chytridiomycota that were recently reported as important parasite of phytoplankton (Gutiérrez et al., 2011; Hassett and Gradinger, 2016; Jephcott et al., 2017). Nevertheless, more than 60% of the fungal sequences (4,371,275) could not be classified to any fungal phyla (**Figure 2**) based on the database information, likely suggesting undescribed fungal sequences in the coastal waters of Bohai Sea.

Within the five phyla, several taxa were present during the entire sampling period (**Figure 3**). Of these, several orders were frequently dominant with proportions in total sequences more than 1% (**Figure 3A**). Among these dominant orders, Hypocreales was found to be the most abundant (139 OTUs, 29.18% of fungal sequences), followed by Pleosporales (119 OTUs, 12.76%), Sporidiobolales (37 OTUs, 8.91%), Saccharomycetales (53 OTUs, 7.81%), Eurotiales (115 OTUs, 7.57%), Malasseziales (38 OTUs, 6.22%), Capnodiales (36 OTUs, 6.03%) and Cystofilobasidiales (11 OTUs, 2.84%). These eight dominant orders accounted for 81.32% of the total classified sequences that were generated within the five known phyla. Each dominant order composed of multiple OTUs was detected in the majority of the samples (Supplementary Figure S1). Notably, we found the order Mortierellales (phylum Mucoromycota) within the group of taxa with average relative abundance less than 0.1% (**Figure 3B**). The percent frequencies of Capnodiales, Pleosporales, Eurotiales, Saccharomycetales, Hypocreales were lowest (≤0.002%) in samples of section A2 in November while of Malasseziales, Sporidiobolales, and Cystofilobasidiales, the lowest were in the surface sample of section C2 in November, and mid-depth samples of section A2 in July, respectively. The peak percent frequencies (≥0.5%) of these orders were observed during November (C1B, C2B, C1B, C2M, C1B, C1S, and B1B, respectively), except Malasseziales which showed peak during July (B1S).

Abundance of Planktonic Fungi

The results of planktonic fungal abundance estimated using qPCR with the Fungi-specific 18S rRNA gene-specific primers are shown in **Figure 4**. The mean abundance of samples across the

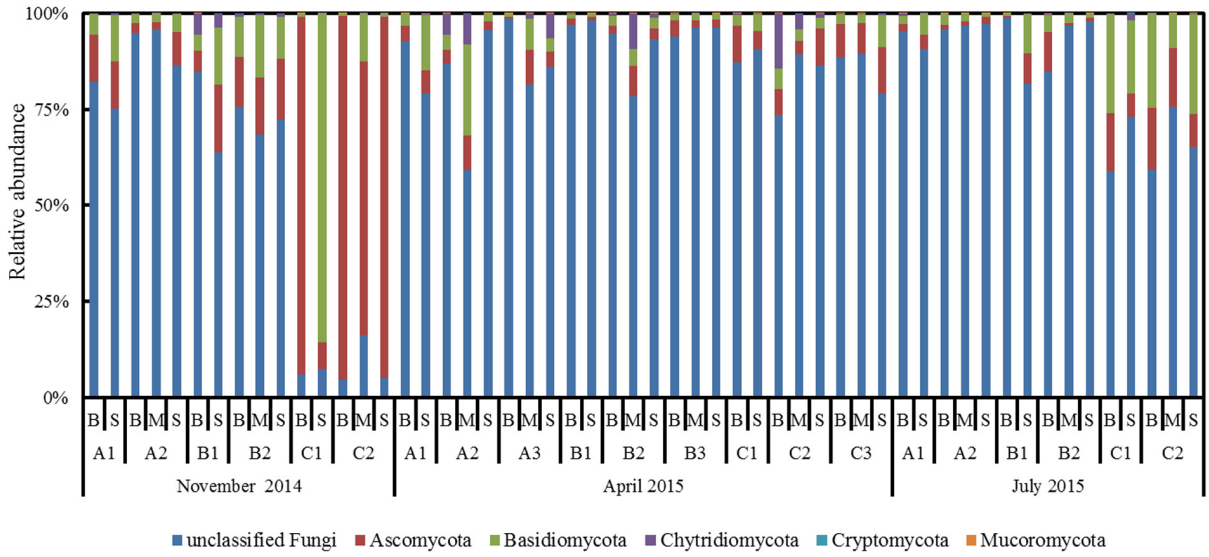

FIGURE 2 | Relative abundances of the planktonic fungal phyla across all samples collected from Qinhuangdao coastal area.

seasons in Qinhuangdao coastal areas was 8.20×10^6 copies/L. Of all samples, the lowest and the highest abundances were in November (B1S, 1.07×10^4 copies/L) and in April (A3B, 7.09×10^7 copies/L), respectively. Overall, the abundance varied significantly across sections ($P < 0.05$, Kruskal–Wallis test). Notably, the mean abundance in section A was higher than section C ($P < 0.05$, Nemenyi-tests) in July but not in November and April ($P > 0.05$, Nemenyi-tests). The results suggest the differential influence of riverine inputs and anthropogenic activities especially during the warm and wet season (July).

Spatiotemporal Dynamics and Drivers of Planktonic Fungi in Coastal Waters

Cluster analysis based on the relative abundance of top 50 OTUs (accounted for 66.04% of total sequences) revealed OTU composition dissimilarities across the samples in Qinhuangdao coastal area (**Figure 5**). Notably, the OTU composition within samples of July was distinctly different from other seasons. Most samples of section A and section B in April had a similar OTU composition to that of samples in July. All the samples of section C in April and November formed a separate cluster. Based on permutation tests of CCA results, the composition of the top 50 OTUs was significantly correlated with co-occurring concentrations of DIP ($P < 0.001$), silicate ($P < 0.001$), and DIN ($P < 0.005$) (**Table 2**).

The proportion of the unclassified fungi was the maximum in all the sections except for section C in November. Of the classified phyla, Ascomycota and Basidiomycota were dominant in all the three sections and seasons (**Figure 2**). Occasionally, Chytridiomycota exhibited higher proportion than Ascomycota and Basidiomycota in April (A3S, B2S, and C2B) (**Figure 2**). Focusing on the relative abundance of eight major orders revealed their dominance across time and space (lateral and vertical) (**Figure 6**). Of the eight orders, Hypocreales varied significantly ($P < 0.01$, Kruskal–Wallis test) across months while Capnodiales, Pleosporales, Eurotiales, and Sporidiobolales varied significantly ($P < 0.05$, Kruskal–Wallis test) across sections.

The changes in Ascomycota and Basidiomycota were closely linked to the changes in DP, PP, DIN, and silicate (**Table 3**). The OTU abundance of Ascomycota and Basidiomycota was greatest when the concentration of these nutrients increased. Additionally, Ascomycota abundance increased significantly ($P < 0.001$, Pearson's correlation test) when pH of seawater decreased. In contrast, Cryptomycota OTU abundance was greatest when the levels of Chlorophyll *a* increased ($P < 0.01$, Pearson's correlation test). Mucoromycota OTUs abundance increased when the salinity of seawater increased.

The α-diversity results of plankton fungi in Qinhuangdao coastal area are presented in **Table 4**. The Shannon index varied considerably across seasons and sections. Across all seasons and sections, the highest variance ($\sigma^2 = 0.99$) in the planktonic fungi Shannon index was noted in section A during April, while the lowest variance ($\sigma^2 = 0.04$) was in section B during November. The maximum Shannon index of 4.4 was observed in section A during April and November (Supplementary Table S2). No significant correlation of Shannon diversity with any of the environmental parameters was obtained (data not shown).

Overall, the results suggested the prominence of planktonic fungal phyla, Ascomycota and Basidiomycota, in the coastal waters of Qinhuangdao, with their abundance greatly influenced by some co-occurring nutrient levels. Distinct changes in the relative abundances of major orders across seasons and transects were evident.

Planktonic Fungi Assemblages

To identify the possible assemblages existing among planktonic fungal OTUs in the coastal water system, a network was

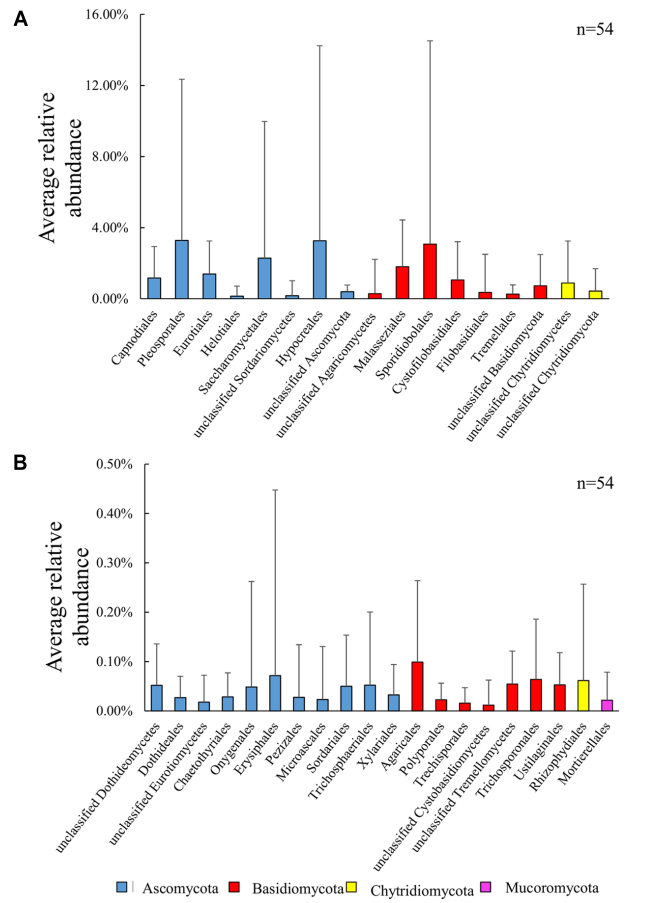

FIGURE 3 | Average relative abundance of planktonic fungal taxa in samples collected from Qinhuangdao coastal area from November 2014 to July 2015. Fungal taxon < 0.01% have been omitted from the figure. Average relative abundance was estimated for each fungal taxon by dividing the total relative abundance across all samples by the number of samples (n = 54). The error bars onto each of the columns show the standard deviation (calculation across 54 samples) for each average value. **(A)** Taxa with average relative abundance > 0.1% and **(B)** taxa with average relative abundance ≤ 0.1%.

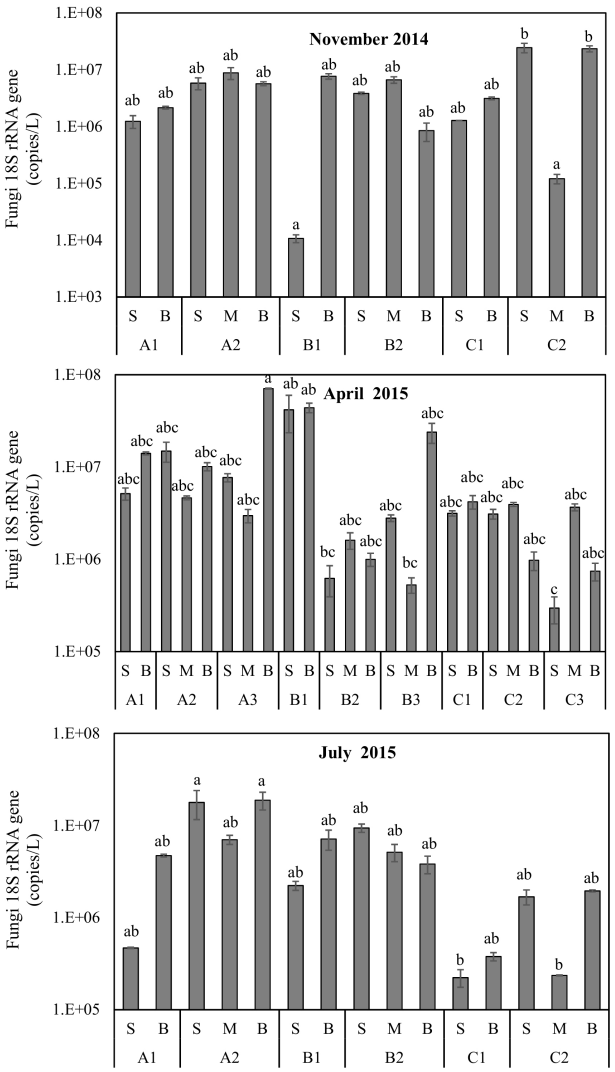

FIGURE 4 | Planktonic fungal abundance determined by Fungi-specific 18S rRNA gene qPCR of plankton DNA samples collected from Qinhuangdao coastal area from November 2014 to July 2015. Samples of each month with significant mean differences (P < 0.05) based on Kruskal–Wallis *post hoc* test (Nemenyi-tests) are marked in different letters (a, b, c). Thus, samples (bars) that are not significantly different are indicated with same letters (for e.g., 'abc') and sample pairs with significant differences will have different letters.

constructed and inferred. The resulting network (**Figure 7**) was composed of 117 nodes with clustering coefficient of 0.185 and 4.6 average number of neighbors. Analysis and visualization of the network revealed a planktonic fungal community consisting of three modules (A, B, and C) and several hubs (**Figure 7**). Two modules (A and C) were composed of co-occurring OTUs, while one module (B) relatively a larger sub-network than the other two clustered OTUs showed mostly mutual exclusion. Interestingly, the network also revealed several keystone species that were assigned to phyla Ascomycota (OTU152, OTU118, OTU4209, OTU77, OTU45, and OTU166), Basidiomycota (OTU1935) and Chytridiomycota (OTU59) at ≤0.8 identity threshold. Thus, species belonging to these phyla probably have roles in key metabolic steps within the fungal community and their further characterization would throw much information on their physiological and metabolic potential.

DISCUSSION

Diversity and Abundance of Planktonic Fungi

The present work explicates a high planktonic fungal diversity featured by the phyla Ascomycota and Basidiomycota and to a lesser extent the phyla Chytridiomycota, Cryptomycota, and Mucoromycota in the coastal waters. The dominance of Ascomycota, Basidiomycota, and Chytridiomycota phyla has been previously described in the coastal marine habitats (Gao et al., 2010; Taylor and Cunliffe, 2016; Picard, 2017). The overall

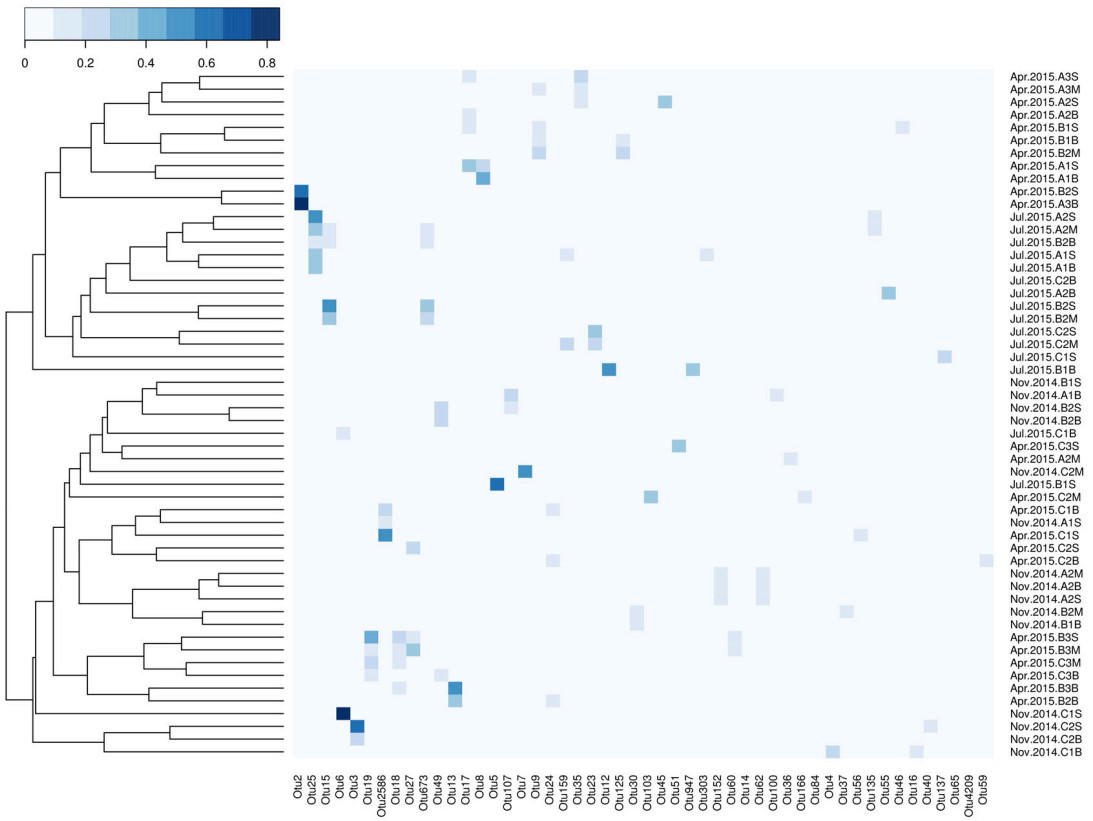

FIGURE 5 | Heatmap of the top 50 OTUs based on their relative abundance across samples from Qinhuangdao coastal area. Sample relationships are shown through clustering based on Bray–Curtis dissimilarity measure. Of these OTUs, the classified OTUs belonged to phyla Ascomycota (OTU# 3, 4, 7, 14, 16, 40, 73), Basidiomycota (OTU# 6, 36, 37, 65), and Chytridiomycota (OTU# 59). The color-key indicate the range of relative abundance of the OTUs.

diversity in fungal OTU composition in the Qinhuangdao coast of Bohai Sea was relatively higher compared to other studies, based on DNA sequencing, from different marine ecosystems (Richards et al., 2012; Manohar and Raghukumar, 2013), including coastal waters (Gao et al., 2010; Taylor and Cunliffe, 2016), surface open ocean (Wang et al., 2014), deep open ocean (Bass et al., 2007), and deep ocean sediments (Bass et al., 2007; Orsi et al., 2013; Orsi et al., 2017). Two fungal clades: Mortierellales (phylum Mucoromycota) and basal zoosporic fungi Cryptomycota are reported for the first time in the coastal waters. The members of Mortierellales are the most common Zygomycete fungi encountered in soil (Benny et al., 2016) and their presence in coastal waters perhaps implies their terrestrial-marine transition by terrestrial runoff or tidal action. Terrestrial forms of fungi have been found to be active in marine environment owing to physiological versatility (Raghukumar and Raghukumar, 1999). Our study, which revealed a high fungal diversity and OTU abundance, provides the basis of future studies on planktonic fungi that may challenge the historical view of fungi constituting a small fraction of total eukaryotes in coastal waters (Monchy et al., 2012).

The spatiotemporal changes in the planktonic fungi abundance estimated from Fungi-specific 18S rRNA gene based qPCR analysis suggested that their assemblages in the water column of the Qinhuangdao Coast of Bohai Sea are active and fluid. A similar feature of planktonic fungi abundance from the multi-year assessment was noted in the English Channel (Taylor and Cunliffe, 2016). The abundance of planktonic fungi, mostly higher in the coastal waters than in pelagic waters, is often attributed to the high carbon from autochthonous primary production and allochthonous (terrestrially derived) production in coastal region (Newell, 1982; Gao et al., 2010; Gutiérrez et al., 2011; Wang et al., 2014). In the nearshore water column of Qinhuangdao coastal area, the abundance was higher at the bottom than on the surface. Similarly, in the upwelling region

TABLE 2 | Correlations between selected environmental variables and planktonic fungi composition (OTU level) assessed by Monte Carlo permutation test (999 permutations) for canonical correspondence analysis.

Variables	CCA1	CCA2	r^2	*P*-value
Chlorophyll-a	−0.7756	0.6312	0.1055	0.085
DIP	0.1042	0.9945	0.8001	0.001 ***
silicate	−0.5200	0.8541	0.6989	0.001 ***
DIN	0.3508	0.9364	0.5888	0.001 ***

*$P < 0.05$, **$P < 0.01$, ***$P < 0.001$.

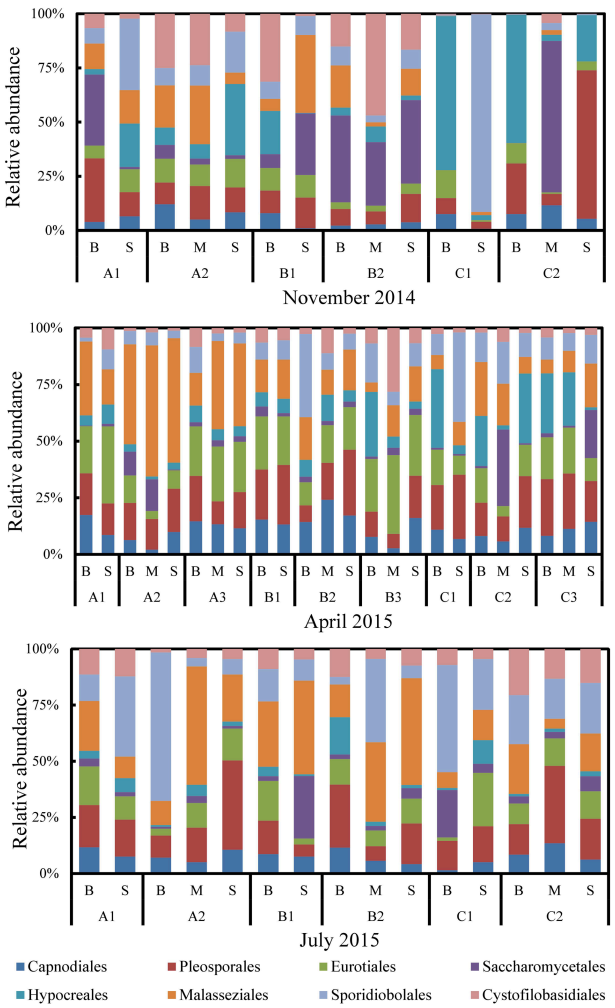

FIGURE 6 | Composition of dominant planktonic fungal orders across all samples collected from Qinhuangdao coastal area.

TABLE 3 | Correlations between environmental variables and normalized abundance of dominant planktonic fungi phyla.

Phyla	Significant correlations with environmental variable ($P < 0.05$)*
Ascomycota	pH ($P = 0.001$, $\rho = -0.485$)
	DIP ($P = 0.021$, $\rho = 0.314$)
	TP ($P = 0.001$, $\rho = 0.439$)
	DP ($P = 0.045$, $\rho = 0.274$)
	PP ($P = 0.000$, $\rho = 0.508$)
	Silicate ($P = 0.006$, $\rho = 0.368$)
	Nitrite ($P = 0.000$, $\rho = 0.607$)
	Nitrate ($P = 0.000$, $\rho = 0.467$)
	DIN ($P = 0.001$, $\rho = 0.426$)
	DN ($P = 0.000$, $\rho = 0.495$)
	DON ($P = 0.016$, $\rho = 0.328$)
Basidiomycota	DIP ($P = 0.000$, $\rho = 0.548$)
	TP ($P = 0.000$, $\rho = 0.502$)
	DP ($P = 0.000$, $\rho = 0.565$)
	PP ($P = 0.001$, $\rho = 0.426$)
	Silicate ($P = 0.003$, $\rho = 0.395$)
	Nitrate ($P = 0.029$, $\rho = 0.297$)
	DIN ($P = 0.043$, $\rho = 0.276$)
	DN ($P = 0.048$, $\rho = 0.271$)
Cryptomycota	Chlorophyll *a* ($P = 0.000$, $\rho = 0.501$)
Mucoromycota	Salinity ($P = 0.000$, $\rho = 0.513$)

**Based on Pearson's correlation analysis.*

of Chile, planktonic fungi biomass increased with depth in the top 15 m (Gutiérrez et al., 2011). Several lines of evidence suggested that fungi are relatively abundant in marine sediments (Orsi et al., 2013; Xu et al., 2014; Taylor and Cunliffe, 2015; Hassett and Gradinger, 2016; Li W. et al., 2016) than in the water column (Taylor and Cunliffe, 2016). An earlier study (Richards et al., 2012) provided the analogous explanation for the higher abundance at the nutrient rich bottom of the water column includes direct impact of the tidal action, releasing fungi from sediments into the water column, thus enabling these osmotrophs to populate therein.

The biomass (abundance) of fungi is an important indicator of its ecological role in marine habitats (Damare and Raghukumar, 2008). Previous studies have shown that fungal biomass in the coastal waters represent a considerable portion of microbial biomass and often of the similar order of magnitude to that of marine prokaryotes. For example, the planktonic fungi biomass was found to be comparable to prokaryotes biomass in the upwelling ecosystem off central-southern Chile (Gutiérrez et al., 2011). Likewise, in the West Pacific Warm Pool, Basidiomycota and bacterioplankton were in the similar order of the magnitude of DNA quantity (Wang et al., 2014). Similarly, the Fungi-specific 18S rRNA gene qPCR abundance (on average 8.20×10^6 copies/L) and bacterial cell numbers (on average 2×10^6 cells/L, data not shown) in the coastal waters of Qinhuangdao showed a roughly similar order. However, it should be noted that fungal cell numbers cannot be estimated from the Fungi-specific 18S rRNA gene qPCR abundance (Taylor and Cunliffe, 2016), and thus our comparison of fungal and bacterial abundances in the Qinhuangdao coastal waters is just an approximation and does not reflect an absolute interpretation. Moreover, Fungi-specific 18S rRNA gene qPCR abundance in our study only served as a proxy for planktonic fungi biomass because it is not possible to estimate the carbon biomass from qPCR abundance (Taylor and Cunliffe, 2016). Nevertheless, the planktonic fungi abundance changes, both over space and time, in the present study were quite pronounced (**Figure 4**) which likely indicated fungal carbon turnover in the Qinhuangdao coastal waters. Thus, we speculate that the dynamic planktonic fungi biomass is one of the significant components of the coastal carbon cycle, and like prokaryotes, fungi too have an important contribution to the coastal secondary production.

Forcing Factors and Prediction of Ecological Roles of Planktonic Fungi

As one of the most variable marine ecosystems, coastal waters are usually characterized by a high plankton diversity

TABLE 4 | Shannon diversity index for the planktonic fungi in the coastal waters of Qinhuangdao.

	November 2014			April 2015			July 2015		
Section	**A**	**B**	**C**	**A**	**B**	**C**	**A**	**B**	**C**
Mean	3.91	3.80	2.28	3.27	2.77	3.41	2.97	2.35	3.39
Min.	3.56	3.60	1.19	1.03	2.09	2.55	2.65	1.56	2.88
Max.	4.42	4.20	3.00	4.41	3.54	3.99	3.29	3.63	4.11
Variance (σ^2)	0.11	0.04	0.44	0.99	0.31	0.16	0.07	0.57	0.18

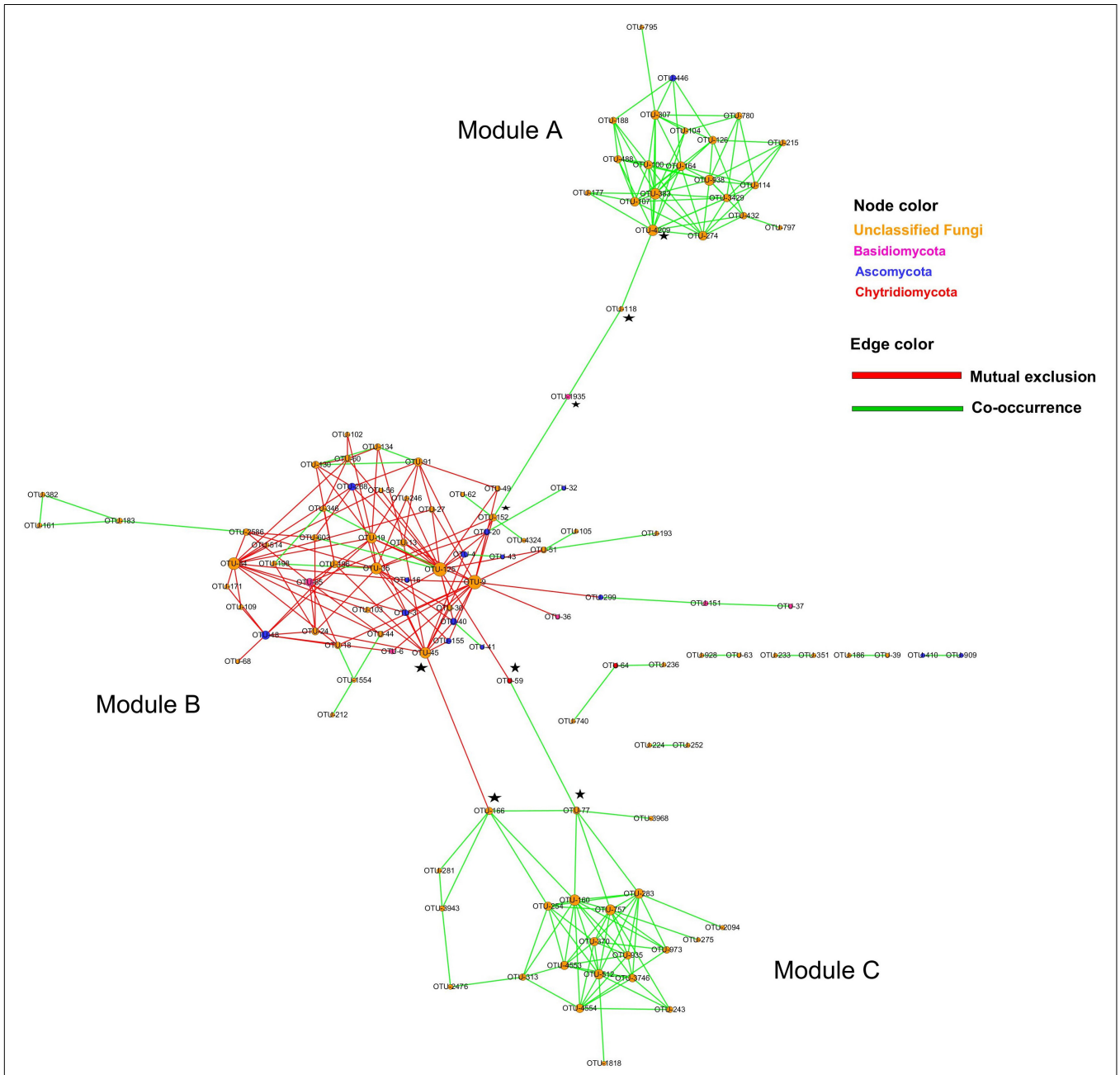

FIGURE 7 | Planktonic fungi network showing significant co-occurrence and mutual exclusion relationships among abundance of clades in the Qinhuangdao coastal waters. Circles indicate OTUs; circle width is a function of the degree of node. The keystone OTUs are indicated by a five pointed star in black.

and high primary production (Jickells, 1998; Danovaro and Pusceddu, 2007). Of particular notice, some pollutants that are washed off from upstream may lead to nutrient enrichments in both sediments and water column and may have detrimental effects on species abundance and fungal community composition. Die-off from dominant species resulting from eutrophication would stimulate the appearance of opportunistic species and may contribute to the increase of total diversity (Johnston and Roberts, 2009). In this study, the fungal OTU composition and the dominant phyla were closely linked with the co-occurring multiple nutrients (**Tables 2**, **3**); thus, we hypothesize that dominant species death probability rise when the nutrient concentration reduces, to allow the growth of the opportunistic species, eventually resulting in an increase in diversity.

The diversity and OTU abundance of planktonic fungi were largely regulated by the variations in the availability of several of potential growth substrates, for example, the changes in organic and inorganic nitrogen-rich substrates impacted the abundance and diversity at Station L4 of Western English Channel (Taylor and Cunliffe, 2016). In particular, Ascomycota diversity increased with the ammonia and phosphate concentrations, unlike Basidiomycota which did not link to changes in any of the co-occurring environmental parameters at Station L4 (Taylor and Cunliffe, 2016). However, in our study, both Ascomycota and Basidiomycota were impacted by the inorganic nitrogen and phosphorous sources (**Table 3**) which are key nutrients for phytoplankton growth. This suggests that these two phyla seem to be chiefly involved in processing phytoplankton detritus when substrate availability is high (phytoplankton bloom) in the water column of Qinhuangdao coastal area. Several studies have shown the direct involvement of fungi in nitrogen metabolism, including ammonia assimilation and nitrite ammonification (Wegley et al., 2007). Besides processing the phytoplankton detritus, planktonic fungi may also play a role in the water column nitrogen metabolism because of their significant relationship with nitrogen in this study (**Tables 2**, **3**). Thus, the ecological function of planktonic fungi should not be ignored in the process of the nitrogen cycle.

The sampling sites in our study were influenced by freshwater discharge from the Tang River, Yang River, and Dapu River, which may supply terrigenous organic matter to the coastal zone. These rivers together with the tides, rain, and the wind mostly affect the coastal ecosystem. With different mean diversity of planktonic fungi in each of the three different sections (**Table 4**) and significantly different qPCR abundance across sections, we speculate that Qinhuangdao coastal ecosystem is remarkably affected by different rivers and their inputs. Considering that fungi have been found to be responsible for degrading mainly terrigenous detritus in marine/terrestrial ecotones (Hyde et al., 1998; Pointing and Hyde, 2000; Kis-Papo, 2005), the relatively higher fungal diversity in the nearshore is most likely associated with the availability of terrestrial remnants from rivers. A similar trend of higher molecular richness nearshore than offshore was reported for sea waters of the Hawaiian coast and coastal upwelling ecosystem of central Chile (Gao et al., 2010; Gutiérrez et al., 2010; Wang et al., 2014).

The members of Chytridiomycota are zoosporic fungi that are either saprotrophs or parasites and are one of the important primary consumers in aquatic food-web (Frenken et al., 2017; Jephcott et al., 2017). Similarly, the members of phylum Cryptomycota (historically named as Rozellomycota), considered as the most basal clade of fungi, are also characterized as unicellular endoparasites of algae (Corsaro et al., 2014), and some reviews have suggested their role as hyperparasites of parasitic fungi Chytridiomycota (Gleason et al., 2012, 2014). Yet, both these groups of marine fungal parasites are poorly understood (Gleason et al., 2011), including their interactions with phytoplankton (Scholz et al., 2016). Although a tripartite interaction between the members of Chytridiomycota, Cryptomycota, and phytoplankton has been proposed (Gleason et al., 2014), such model has not been established in marine ecosystems so far. Based on this model, the presence of the members of Cryptomycota in the coastal waters would result in a reduction of the number of Chytridiomycota members eventually favoring phytoplankton bloom. We found a positive association of Cryptomycota OTU abundance and Chlorophyll *a* (**Table 3**) in our study but did not observe any relationship between Chytridiomycota and Chlorophyll *a*. Previous findings show that the cells of Cryptomycota are frequently found on diatoms and they acquire cell wall materials from their host (Jones et al., 2011). Thus, we hypothesize that some members of Chytridiomycota are playing a saprotrophic role, and members of Cryptomycota were either hyperparasites of the parasitic members Chytridiomycota or algal parasites. Previous studies have shown the frequent occurrence of the brown tide of picophytoplankton algae in Qinhuangdao coastal sea (Zhang et al., 2012; Yang et al., 2016; Qiao et al., 2017). We confirmed such brown tide outbreak in 2015 by comparing the color difference between brown tide water and non-brown tide water in the true color composite image of HJ-1 (data not shown). Moreover, the appearance of abnormal ocean color has been reported when Chlorophyll *a* was $\geq$2.5 mg/m^3 (Yang et al., 2016). In our study, the content of Chlorophyll *a* in the seawater reached 5.21 μg/L in July. These findings indirectly confirm the occurrence of phytoplankton bloom in the Qinhuangdao coastal water in 2015. We also noted high silicate content in seawater in July 2015, with concentration reaching up to 311.47 μg/L (Supplementary Table S1), perhaps resulting from the degradation of algal bloom detritus by saprotrophic members of Chytridiomycota leading to the release of silicates into the seawater. The positive association between Cryptomycota and Chlorophyll *a*, the occurrence of algal bloom, and release of silicate during an algal bloom, taken together suggest the regulation of the parasitic members of Chytridiomycota by the hyperparasitic members of Cryptomycota, ultimately favoring the algal bloom. Our findings provide a plausible evidence of the existence of a tripartite interaction in the Qinhuangdao coastal waters. Thus, we propose that the members of Chytridiomycota and Cryptomycota might play a significant role in the nutrient and energy flow in the water column food web through a tripartite interaction with phytoplankton.

Network Topology and Fungal Assemblages

Co-occurrence networks are essential for the understanding and management of the dynamics of the individual group members and of the entire ecosystem *per se* (Gaedke, 2007; Faust and Raes, 2012). Among the many topological indices, degree, closeness and redundancy in the networks provide information on the robustness of the community and its likely ability to resist change. Moreover, the highly connected phylotypes sometimes called hubs or keystones, characterized by their high degree, high closeness, and low betweenness, are predicted to perform key metabolic steps within the community (Mondav et al., 2017). In our planktonic fungi network at Qinhuangdao coastal waters, several hubs with high degree and high closeness but high betweenness were identified. Therefore, these hubs with their high betweenness and taxonomically close to adjacent OTUs exhibit qualities associated with redundancy or 'niche overlap.' The elimination of such hubs will have little or no effect on the community function and are unlikely the keystone species. Thus, keystone species are ecologically those that would cause (disproportionate) disruption to a network if lost, even though they are sometimes described statistically as hubs (Berry and Widder, 2014). Interestingly, we found several OTUs belonging to phyla Ascomycota, Basidiomycota, and Chytridiomycota that likely fit the description of keystone species in our network (putative keystones indicated in **Figure 7**). Although, these keystone fungal-OTUs could not be assigned to the genus and species levels because of limited fungal database information, we speculate that species within these phyla play crucial role in the fungal assemblages. The loss of these fungal OTUs would fragment the network and/or were the only phylotypes that have a critical metabolic function. Thus, the loss of any of the identified keystone fungal OTUs from the coastal water of Qinhuangdao could affect significant changes in nutrient cycling.

Statistically, none of the predicted keystone fungal OTUs in our network had a high degree, this means the high degree is a poor predictor of 'keystoneness' in coastal waters similar to soil microbial ecosystem (Mondav et al., 2017). Our networks also revealed both negative and positive interactions among the OTUs; and of the three modules, module B was relatively more complex and taxonomically diverse than modules A and B which displayed only positive interactions. Our co-occurrence fungal network reflected niche processes that drive coexistence and diversity maintenance within fungal communities in coastal waters, and showed co-occurring species pairs and assemblages that shared similar ecological characteristics, besides keystone species. The three modules and keystone species mostly consisted of unclassified Fungi (>0.8 sequence similarity threshold), which clearly suggest that further characterization and identification of these novel fungal OTUs are critical for providing a better knowledge of the fungal taxonomic groups and their cryptic role in coastal waters. Clearly, further studies are needed to identify the hubs and keystone fungal species and characterize their metabolic profiles to obtain a better insight into the coastal fungal community network. As per the knowledge of the authors, this is the first report of planktonic fungi network, which will form the basis of future studies on inferring ecological characteristics of poorly understood or non-culturable fungal taxa and their role in nutrient cycling in the marine ecosystems.

To conclude, the spatiotemporal analysis of Qinhuangdao coastal waters of the Bohai Sea has shown that planktonic fungi have a high diversity and abundance and thus they are speculated to play a significant role in the carbon and nitrogen cycling in the water column. The molecular diversity of dominant phyla exhibited a positive relationship with dissolved nitrogen, dissolved and particulate phosphorus, and silicate. We also proposed that riverine inputs have a potential influence on the diversity and abundance of the planktonic fungi, and reported the presence of Mortierellales, the common Mucoromycetes fungi, positively linked with salinity, in the coastal water column. This study provides the hypothesis of a tripartite interaction within members of Cryptomycota, Chytridiomycota, and phytoplankton, and suggests further studies for its validation. Furthermore, the co-occurrence analysis to the planktonic fungal system provided valuable information for characterizing the functional distribution, ecological interactions of fungi at the community scale, and identified ecological traits of poorly defined phylotypes that co-occur with well-characterized fungal taxa. Altogether, our findings clearly demonstrated the role of planktonic fungi in nutrient cycling as saprotrophs and parasites manifested by their high abundance, diversity, and co-occurrence in the water column and emphasize their ecological significance in the realm of the coastal ocean environment.

AUTHOR CONTRIBUTIONS

YW conceived the study, performed the molecular work, and statistical analysis. BS conceived the study, analyzed the data, performed the statistical analysis, and wrote the paper. YH and NX collected the field data and samples. GW conceived the study and revised the paper. All authors have approved the submission of the article.

FUNDING

The work was partially supported by NSFC (grant # 31670044 and 31602185) and National Marine Public Welfare Industry Special Scientific Research Project (201305022). The views expressed herein are those of the authors and do not represent the views of the funding agencies or any of its subagencies.

SUPPLEMENTARY MATERIAL

The Supplementary Material for this article can be found online at: https://www.frontiersin.org/articles/10.3389/fmicb.2018.00584/full#supplementary-material

REFERENCES

Abarenkov, K., Nilsson, R. H., Larsson, K. H., Alexander, I. J., Eberhardt, U., Erland, S., et al. (2010). The UNITE database for molecular identification of fungi – recent updates and future perspectives. *New Phytol.* 186, 281–285. doi: 10.1111/j.1469-8137.2009.03160.x

Bass, D., Howe, A., Brown, N., Barton, H., Demidova, M., Michelle, H., et al. (2007). Yeast forms dominate fungal diversity in the deep oceans. *Proc. R. Soc. B Biol. Sci.* 274, 3069–3077. doi: 10.1098/rspb.2007.1067

Benny, G. L., Smith, M. E., Kirk, P. M., Tretter, E. D., and White, M. M. (2016). "Challenges and future perspectives in the systematics of Kickxellomycotina, Mortierellomycotina, Mucoromycotina, and Zoopagomycotina," in *Biology of Microfungi*, ed. D.-W. Li (Cham: Springer International Publishing), 65–126.

Berry, D., and Widder, S. (2014). Deciphering microbial interactions and detecting keystone species with co-occurrence networks. *Front. Microbiol.* 5:219. doi: 10.3389/fmicb.2014.00219

Blaalid, R., Kumar, S., Nilsson, R. H., Abarenkov, K., Kirk, P. M., and Kauserud, H. (2013). ITS1 versus ITS2 as DNA metabarcodes for fungi. *Mol. Ecol. Resour.* 13, 218–224. doi: 10.1111/1755-0998.12065

Caporaso, J. G., Paszkiewicz, K., Field, D., Knight, R., and Gilbert, J. A. (2012). The Western English Channel contains a persistent microbial seed bank. *ISME J.* 6, 1089–1093. doi: 10.1038/ismej.2011.162

Carlile, M. J., Watkinson, S. C., and Gooday, G. W. (2001). *The Fungi*. San Diego, CA: Academic Press.

Christensen, M. (1989). A view of fungal ecology. *Mycologia* 81, 1–19. doi: 10.2307/3759446

Corsaro, D., Walochnik, J., Venditti, D., Steinmann, J., Muller, K. D., and Michel, R. (2014). Microsporidia-like parasites of amoebae belong to the early fungal lineage *Rozellomycota*. *Parasitol. Res.* 113, 1909–1918. doi: 10.1007/s00436-014-3838-4

Damare, S., and Raghukumar, C. (2008). Fungi and macroaggregation in deep-sea sediments. *Microb. Ecol.* 56, 168–177. doi: 10.1007/s00248-007-9334-y

Danovaro, R., and Pusceddu, A. (2007). Biodiversity and ecosystem functioning in coastal lagoons: Does microbial diversity play any role? *Estuar. Coast. Shelf Sci.* 75, 4–12. doi: 10.1016/j.ecss.2007.02.030

de Vargas, C., Audic, S., Henry, N., Decelle, J., Mahé, F., Logares, R., et al. (2015). Eukaryotic plankton diversity in the sunlit ocean. *Science* 348, 29223618–29223625. doi: 10.1126/science.1261605

Debroas, D., Domaizon, I., Humbert, J. F., Jardillier, L., Lepere, C., Oudart, A., et al. (2017). Overview of freshwater microbial eukaryotes diversity: a first analysis of publicly available metabarcoding data. *FEMS Microbiol. Ecol.* 93:fix023. doi: 10.1093/femsec/fix023

Faust, K., and Raes, J. (2012). Microbial interactions: from networks to models. *Nat. Rev. Microbiol.* 10, 538–550. doi: 10.1038/nrmicro2832

Faust, K., Sathirapongsasuti, J. F., Izard, J., Segata, N., Gevers, D., Raes, J., et al. (2012). Microbial co-occurrence relationships in the human microbiome. *PLoS Comput. Biol.* 8:e1002606. doi: 10.1371/journal.pcbi.1002606

Fell, J. W., and Newell, S. Y. (1998). "Biochemical and molecular methods for the study of marine fungi," in *Molecular Approaches to the Study of the Ocean*, ed. K. E. Cooksey (Dordrecht: Springer).

Fischer, H., Mille-Lindblom, C., Zwirnmann, E., and Tranvik, L. J. (2006). Contribution of fungi and bacteria to the formation of dissolved organic carbon from decaying common reed (*Phragmites australis*). *Arch. Hydrobiol.* 166, 79–97. doi: 10.1127/0003-9136/2006/0166-0079

Frenken, T., Alacid, E., Berger, S. A., Bourne, E. C., Gerphagnon, M., Grossart, H.-P., et al. (2017). Integrating chytrid fungal parasites into plankton ecology: research gaps and needs. *Environ. Microbiol.* 19, 3802–3822. doi: 10.1111/1462-2920.13827

Gaedke, U. (2007). "Ecological networks," in *Analysis of Biological Networks*, ed. F. Schreiber (Hoboken, NJ: John Wiley & Sons, Inc.), 283–304.

Gao, Z., Johnson, Z. I., and Wang, G. (2010). Molecular characterization of the spatial diversity and novel lineages of mycoplankton in Hawaiian coastal waters. *ISME J.* 4, 111–120. doi: 10.1038/ismej.2009.87

Gardes, M., and Bruns, T. D. (1993). ITS primers with enhanced specificity for basidiomycetes - application to the identification of mycorrhizae and rusts. *Mol. Ecol.* 2, 113–118. doi: 10.1111/j.1365-294X.1993.tb00005.x

Gessner, M. O., Gulis, V., Kuehn, K., Chauvet, E., and Suberkropp, K. (2007). "Fungal decomposer of plant litter in aquatic ecosystems," in *The Mycota*, eds C. P. Kubicek and I. S. Druzhinina (Berlin: Springer).

Gleason, F., Küpper, F., Amon, J., Picard, K., Gachon, C., Marano, A., et al. (2011). Zoosporic true fungi in marine ecosystems: a review. *Mar. Freshw. Res.* 62, 383–393. doi: 10.1071/MF10294

Gleason, F. H., Carney, L. T., Lilje, O., and Glockling, S. L. (2012). Ecological potentials of species of *Rozella* (Cryptomycota). *Fungal Ecol.* 5, 651–656. doi: 10.1016/j.funeco.2012.05.003

Gleason, F. H., Lilje, O., Marano, A. V., Sime-Ngando, T., Sullivan, B. K., Kirchmair, M., et al. (2014). Ecological functions of zoosporic hyperparasites. *Front. Microbiol.* 5:244. doi: 10.3389/fmicb.2014.00244

Gulis, V., Kuehn, K., and Suberkropp, K. (2006). "The role of fungi in carbon and nitrogen cycles in freshwater ecosystems," in *Fungi in Biogeochemical Cycles*, ed. G. M. Gadd (New York, NY: Cambridge University Press).

Gutiérrez, M. H., Pantoja, S., Quiñones, R. A., and González, R. R. (2010). First record of filamentous fungi in the coastal upwelling ecosystem off central Chile. *Gayana* 74, 66–73. doi: 10.4067/S0717-65382010000100010

Gutiérrez, M. H., Pantoja, S., Tejos, E., and Quiñones, R. A. (2011). The role of fungi in processing marine organic matter in the upwelling ecosystem off Chile. *Mar. Biol.* 158, 205–219. doi: 10.1007/s00227-010-1552-z

Hassett, B. T., and Gradinger, R. (2016). Chytrids dominate arctic marine fungal communities. *Environ. Microbiol.* 18, 2001–2009. doi: 10.1111/1462-2920.13216

Hawksworth, D. L. (2001). The magnitude of fungal diversity: the 1.5 million species estimate revisited. *Mycol. Res.* 105, 1422–1432. doi: 10.1017/s0953756201004725

Hibbett, D. S., Binder, M., Bischoff, J. F., Blackwell, M., Cannon, P. F., Eriksson, O. E., et al. (2007). A higher-level phylogenetic classification of the Fungi. *Mycol. Res.* 111(Pt 5), 509–547. doi: 10.1016/j.mycres.2007.03.004

Hyde, K. D., Jones, E. B. G., Leaño, E., Pointing, S. B., Poonyth, A. D., and Vrijmoed, L. L. P. (1998). Role of fungi in marine ecosystems. *Biodivers. Conserv.* 7, 1147–1161. doi: 10.1023/A:1008823515157

Jephcott, T. G., VanOgtrop, F. F., Gleason, F. H., Macarthur, D. J., and Scholz, B. (2017). "Chapter 16 the ecology of chytrid and aphelid parasites of phytoplankton," in *The Fungal Community*, eds J. Dighton, J. F. White, and P. Oudemans (Boca Raton, FL: CRC Press), 239–256. doi: 10.1201/9781315119496-17

Jickells, T. D. (1998). Nutrient biogeochemistry of the coastal zone. *Science* 281, 217–221. doi: 10.1126/science.281.5374.217

Johnston, E. L., and Roberts, D. A. (2009). Contaminants reduce the richness and evenness of marine communities: a review and meta-analysis. *Environ. Pollut.* 157, 1745–1752. doi: 10.1016/j.envpol.2009.02.017

Jones, M. D. M., Forn, I., Gadelha, C., Egan, M. J., Bass, D., Massana, R., et al. (2011). Discovery of novel intermediate forms redefines the fungal tree of life. *Nature* 474, 200–203. doi: 10.1038/nature09984

Kimura, H., and Naganuma, T. (2001). Thraustochytrids: a neglected agent of the marine microbial food chain. *Aquat. Ecosyst. Health Manage.* 4, 13–18. doi: 10.1080/146349801753569243

Kimura, H., Sato, M., Sugiyama, C., and Naganuma, T. (2001). Coupling of thraustochytrids and POM, and of bacterio- and phytoplankton in a semi-enclosed coastal area: implication for different substrate preference by the planktonic decomposers. *Aquat. Microb. Ecol.* 25, 293–300. doi: 10.3354/ame025293

Kis-Papo, T. (2005). "Marine fungal communities," in *The Fungal Community*, eds J. Dighton, J. F. White, and P. Oudemans (Boca Raton, FL: CRC Press), 61–92. doi: 10.1201/9781420027891.ch4

Li, Q., Wang, X., Liu, X., Jiao, N., and Wang, G. (2016). Diversity of parasitic fungi associated with phytoplankton in Hawaiian waters. *Mar. Biol. Res.* 12, 294–303. doi: 10.1080/17451000.2015.1088950

Li, W., Wang, M., Bian, X., Guo, J., and Cai, L. (2016). A high-level fungal diversity in the intertidal sediment of Chinese seas presents the spatial variation of community composition. *Front. Microbiol.* 7:2098. doi: 10.3389/fmicb.2016.02098

Liu, J., Fu, B., Yang, H., Zhao, M., He, B., Zhang, X. H., et al. (2015). Phylogenetic shifts of bacterioplankton community composition along the Pearl Estuary: the potential impact of hypoxia and nutrients. *Front. Microbiol.* 6:64. doi: 10.3389/fmicb.2015.00064

Logares, R., Audic, S., Bass, D., Bittner, L., Boutte, C., Christen, R., et al. (2014). Patterns of rare and abundant marine microbial eukaryotes. *Curr. Biol.* 24, 813–821. doi: 10.1016/j.cub.2014.02.050

Ma, Y., Wang, M., and Xia, J. (2016). Studies on abundance and diversity of microplankton during brown tide around Qinhuangdao area. *Period. Ocean Univ. China* 46, 142–150.

Magoc, T., and Salzberg, S. L. (2011). FLASH: fast length adjustment of short reads to improve genome assemblies. *Bioinformatics* 27, 2957–2963. doi: 10.1093/bioinformatics/btr507

Manohar, C. S., and Raghukumar, C. (2013). Fungal diversity from various marine habitats deduced through culture-independent studies. *FEMS Microbiol. Lett.* 341, 69–78. doi: 10.1111/1574-6968.12087

Monchy, S., Grattepanche, J.-D., Breton, E., Meloni, D., Sanciu, G., Chabé, M., et al. (2012). Microplanktonic community structure in a coastal system relative to a *Phaeocystis* bloom inferred from morphological and tag pyrosequencing methods. *PLoS One* 7:e39924. doi: 10.1371/journal.pone.0039924

Mondav, R., McCalley, C. K., Hodgkins, S. B., Frolking, S., Saleska, S. R., Rich, V. I., et al. (2017). Microbial network, phylogenetic diversity and community membership in the active layer across a permafrost thaw gradient. *Environ. Microbiol.* 19, 3201–3218. doi: 10.1111/1462-2920.13809

Mueller, G. M., Schmit, J. P., Leacock, P. R., Buyck, B., Cifuentes, J., Desjardin, D. E., et al. (2007). Global diversity and distribution of macrofungi. *Biodivers. Conserv.* 16, 37–48. doi: 10.1007/s10531-006-9108-8

Newell, R. C. (1982). The energetics of detritus utilisation in coastal lagoons and nearshore waters. *Oceanol. Acta* 4, 347–355.

O'Brien, H. E., Parrent, J. L., Jackson, J. A., Moncalvo, J. M., and Vilgalys, R. (2005). Fungal community analysis by large-scale sequencing of environmental samples. *Appl. Environ. Microbiol.* 71, 5544–5550. doi: 10.1128/AEM.71.9.5544-5550.2005

Orsi, W., Biddle, J. F., and Edgcomb, V. (2013). Deep sequencing of subseafloor eukaryotic rRNA reveals active Fungi across marine subsurface provinces. *PLoS One* 8:e56335. doi: 10.1371/journal.pone.0056335

Orsi, W. D., Richards, T. A., and Francis, W. R. (2017). Predicted microbial secretomes and their target substrates in marine sediment. *Nat. Microbiol.* 3, 32–37. doi: 10.1038/s41564-017-0047-9

Pang, K. L., and Mitchell, J. I. (2005). Molecular approaches for assessing fungal diversity in marine substrata. *Bot. Mar.* 48, 332–347. doi: 10.1515/bot.2005.046

Pang, K. L., Overy, D. P., Jones, E. B. G., Calado, M. D. L., Burgaud, G., Walker, A. K., et al. (2016). 'Marine fungi' and 'marine-derived fungi' in natural product chemistry research: toward a new consensual definition. *Fungal Biol. Rev.* 30, 163–175. doi: 10.1016/j.fbr.2016.08.001

Picard, K. T. (2017). Coastal marine habitats harbor novel early-diverging fungal diversity. *Fungal Ecol.* 25, 1–13. doi: 10.1016/j.funeco.2016.10.006

Pointing, S. B., and Hyde, K. D. (2000). Lignocellulose-degrading marine fungi. *Biofouling* 15, 221–229. doi: 10.1080/08927010009386312

Prévost-Bouré, C. N., Christen, R., Dequiedt, S., Mougel, C., Lelievre, M., Jolivet, C., et al. (2011). Validation and application of a PCR primer set to quantify fungal communities in the soil environment by real-time quantitative PCR. *PLoS One* 6:e24166. doi: 10.1371/journal.pone.0024166

Qiao, L., Chen, Y., Mi, T., Zhen, Y., Gao, Y., and Yu, Z. (2017). Quantitative PCR analysis of the spatiotemporal dynamics of *Aureococcus anophagefferens* and *Minutocellus polymorphus* and the relationship between brown tides and nutrients in the coastal waters of Qinhuangdao, China. *J. Appl. Phycol.* 29, 297–308. doi: 10.1007/s10811-016-0959-4

Raghukumar, S. (2005). "The role of fungi in marine detrital processes," in *Marine Microbiology: Facts and Opportunities*, ed. N. Ramaiah (Dona Paula: National Institute of Oceanography), 91–101.

Raghukumar, S., and Raghukumar, C. (1999). Marine fungi: a critique. *Aquat. Microbiol. Newsl.* 38, 26–27.

Richards, T. A., Jones, M. D., Leonard, G., and Bass, D. (2012). Marine fungi: their ecology and molecular diversity. *Annu. Rev. Mar. Sci.* 4, 495–522. doi: 10.1146/annurev-marine-120710-100802

Rousk, J., and Bengtson, P. (2014). Microbial regulation of global biogeochemical cycles. *Front. Microbiol.* 5:103. doi: 10.3389/fmicb.2014.00103

Schloss, P. D., Westcott, S. L., Ryabin, T., Hall, J. R., Hartmann, M., Hollister, E. B., et al. (2009). Introducing mothur: open-source, platform-independent, community-supported software for describing and comparing microbial communities. *Appl. Environ. Microbiol.* 75, 7537–7541. doi: 10.1128/AEM.01541-09

Scholz, B., Guillou, L., Marano, A. V., Neuhauser, S., Sullivan, B. K., Karsten, U., et al. (2016). Zoosporic parasites infecting marine diatoms – A black box that needs to be opened. *Fungal Ecol.* 19, 59–76. doi: 10.1016/j.funeco.2015.09.002

Taylor, J. D., and Cunliffe, M. (2015). Polychaete burrows harbour distinct microbial communities in oil-contaminated coastal sediments. *Environ. Microbiol. Rep.* 7, 606–613. doi: 10.1111/1758-2229.12292

Taylor, J. D., and Cunliffe, M. (2016). Multi-year assessment of coastal planktonic fungi reveals environmental drivers of diversity and abundance. *ISME J.* 10, 2118–2128. doi: 10.1038/ismej.2016.24

Vainio, E. J., and Hantula, J. (2000). Direct analysis of wood-inhabiting fungi using denaturing gradient gel electrophoresis of amplified ribosomal DNA. *Mycol. Res.* 104, 927–936. doi: 10.1017/S0953756200002471

Wang, G. Y., Wang, X., Liu, X., and Li, Q. (2012). "Diversity and biogeochemical function of planktonic fungi in the ocean," in *Biology of Marine Fungi*, ed. C. Raghukumar (Berlin: Springer), 71–88.

Wang, L., Nan, B., and Hu, P. (2015). Bacterial community characteristics in Qinhuangdao coastal area, Bohai Sea: a region with recurrent brown tide outbreaks. *Res. Environ. Sci.* 28, 899–906.

Wang, X., Singh, P., Gao, Z., Zhang, X., Johnson, Z. I., and Wang, G. Y. (2014). Distribution and diversity of planktonic fungi in the West Pacific Warm Pool. *PLoS One* 9:e101523. doi: 10.1371/journal.pone.0101523

Wegley, L., Edwards, R., Rodriguez-Brito, B., Liu, H., and Rohwer, F. (2007). Metagenomic analysis of the microbial community associated with the coral *Porites astreoides*. *Environ. Microbiol.* 9, 2707–2719. doi: 10.1111/j.1462-2920.2007.01383.x

Wei, H., Hainbucher, D., Pohlmann, T., Feng, S., and Suendermann, J. (2004). Tidal-induced Lagrangian and Eulerian mean circulation in the Bohai Sea. *J. Mar. Syst.* 44, 141–151. doi: 10.1016/j.jmarsys.2003.09.007

White, T. J., Bruns, T., Lee, S., and Taylor, J. (1990). "Amplification and direct sequencing of fungal ribosomal RNA genes for phylogenetics," in *PCR Protocols: A Guide to Methods and Applications*, eds M. A. Innis, D. H. Gelfand, J. J. Sninsky, and T. J. White (San Diego, CA: Academic Press), 315–322.

Worden, A. Z., Follows, M. J., Giovannoni, S. J., Wilken, S., Zimmerman, A. E., and Keeling, P. J. (2015). Environmental science. Rethinking the marine carbon cycle: factoring in the multifarious lifestyles of microbes. *Science* 347:1257594. doi: 10.1126/science.1257594

Xu, W., Pang, K. L., and Luo, Z. H. (2014). High fungal diversity and abundance recovered in the deep-sea sediments of the Pacific Ocean. *Microb. Ecol.* 68, 688–698. doi: 10.1007/s00248-014-0448-8

Yang, B., Shi, J., Tan, L., and Xu, W.-J. (2016). Preliminary study on brown tide of Picophytoplankton algal monitoring by remote sensing in Qinhuangdao coastal sea. *Mar. Environ. Sci.* 35, 605–610. doi: 10.13634/j.cnki.mes.2016.04.020

Zhang, P., Song, J., and Yuan, H. (2009). Persistent organic pollutant residues in the sediments and mollusks from the Bohai Sea coastal areas, North China: an overview. *Environ. Int.* 35, 632–646. doi: 10.1016/j.envint.2008.09.014

Zhang, Q.-C., Qiu, L.-M., Yu, R.-C., Kong, F.-Z., Wang, Y.-F., Yan, T., et al. (2012). Emergence of brown tides caused by *Aureococcus anophagefferens* Hargraves et Sieburth in China. *Harmful Algae* 19, 117–124. doi: 10.1016/j.hal.2012.06.007

Zhou, S.-Y., Chen, X.-N., Cui, L., Song, Z.-Q., Li, Z.-B., Zhang, S., et al. (2016). Impacts of environmental factors on bacterial diversity of Xinkai river estuary in the coastal area of Qinhuangdao. *Microbiol. China* 43, 2578–2593.

Conflict of Interest Statement: The authors declare that the research was conducted in the absence of any commercial or financial relationships that could be construed as a potential conflict of interest.

Advantages of publishing in Frontiers

OPEN ACCESS
Articles are free to read for greatest visibility and readership

FAST PUBLICATION
Around 90 days from submission to decision

HIGH QUALITY PEER-REVIEW
Rigorous, collaborative, and constructive peer-review

TRANSPARENT PEER-REVIEW
Editors and reviewers acknowledged by name on published articles

Frontiers
Avenue du Tribunal-Fédéral 34
1005 Lausanne | Switzerland

Visit us: www.frontiersin.org
Contact us: info@frontiersin.org | +41 21 510 17 00

REPRODUCIBILITY OF RESEARCH
Support open data and methods to enhance research reproducibility

DIGITAL PUBLISHING
Articles designed for optimal readership across devices

FOLLOW US
@frontiersin

IMPACT METRICS
Advanced article metrics track visibility across digital media

EXTENSIVE PROMOTION
Marketing and promotion of impactful research

LOOP RESEARCH NETWORK
Our network increases your article's readership